Cerium Dioxide Nanoparticle and Diesel Particulate Inhalation: Modifying Potential on Models of Asthma and Allergen Exposure.

Kirsty Meldrum

2020

A thesis submitted for the Degree of Doctor of Philosophy

Imperial College London

Faculty of Medicine

National Heart and Lung Institute

Declaration of originality

I declare that all work described within this thesis has been performed by myself, unless fully acknowledged.

Research was carried out in both the National Heart and Lung Institute, Imperial College London and Public Health England, Centre for Radiation, Chemical and Environmental Hazards (CRCE).

It is original research which has not been presented for the reward of any other degree in both this and any other institute.

Kirsty Meldrum

Copyright declaration

'The copyright of this thesis rests with the author. Unless otherwise indicated, its contents are licensed under a Creative Commons Attribution-Non Commercial 4.0 International Licence (CC BY-NC). Under this licence, you may copy and redistribute the material in any medium or format. You may also create and distribute modified versions of the work. This is on the condition that: you credit the author and do not use it, or any derivative works, for a commercial purpose. When reusing or sharing this work, ensure you make the licence terms clear to others by naming the licence and linking to the licence text. Where a work has been adapted, you should indicate that the work has been changed and describe those changes. Please seek permission from the copyright holder for uses of this work that are not included in this licence or permitted under UK Copyright Law.'

Abstract

Concerns have been raised regarding possible health effects due to constituents of air pollution, including increasing diesel use and addition of fuel catalysts such as cerium dioxide nanoparticles (CeO_2NPs). There is limited information on the potential hazards of this nanomaterial as part of diesel exhaust on respiratory conditions, including asthma and allergic airway disease (AAD).

We therefore aimed to identify the effects of diesel exhaust particles (DEP) alone and in combination with CeO_2NPs in both an *in vitro* lung epithelial model and an *in vivo* murine house dust mite (HDM) model of AAD.

Human primary bronchial epithelial cells (HPBECs) and Balb/c mice were exposed via a quasi-air liquid interface or intranasally to HDM alone or with DEP (50μg) alone or combined with low (50ng) or high (1.5μg) concentrations of CeO_2NPs in single and repeat dose protocols over 24 hours and 3 weeks.

HPBECs DEP exposure leads to increases in type II immune response mRNA expression when compared to co-exposure (CeO_2NPs/DEP), while IL-25 expression was significantly increased after CeO_2NPs/DEP exposure compared to particles alone and control.

Within the murine AAD model, the addition of DEP to HDM (over 3 weeks) caused an increase in the inflammatory cell counts (specifically lymphocytes, macrophages and neutrophils). Addition of CeO_2NPs to this combination resulted in a further significant increase in BAL cell counts, specifically lymphocytes and eosinophils. This was also paralleled by CeO_2NPs dependent alterations in inflammatory gene expression, as well as an increase in mucus production, airway remodelling and hyperresponsiveness when compared to DEP, CeO_2NPs alone and the HDM control.

This taken together suggests that the addition of CeO_2NPs has the potential to modify DEP effects and enhance an allergic response within a murine AAD model. This has the potential to have impacts within the asthmatic population as these catalysts increase in popularity.

Acknowledgments

Firstly, I must acknowledge my amazing supervisors – Terry Tetley and Martin Leonard. Thank you for allowing me to work in your labs, giving me support and advice (both professionally and personally), and thank you for not giving up on me. I'll never be able to repay you for taking a chance on me and for that I'll be forever grateful.

A second thanks goes to my funders, Public Health England, and everyone that supported me there. Rachel, Sarah, Tim, Emma, Chang, Michelle and Isabella – thank you for your help and wisdom! Liz, Alex and Nathan – thank you for keeping me sane and stopping me from drinking too much coffee!

To everyone at Imperial, my second home, thank you for taking me under your wing and teaching this country girl about the city. Lareb, Pat, Maryam, Rani, Alex and Alberto, your friendships mean the world to me and I'm glad I got to spend my time in London with you guys. Lareb especially deserves a special mention!

Thank you to everyone I have moaned to over the years. Claire and Eilidh, thank you for being there to listen to me regardless of when I called, and to Rachel, Alexa and Sophie.

Thank you to the "Wantage Girls" (Krissie, Lotte, Lucy, Molly, Coral, Ellie, Alice, and Tara) for taking me into the group and on holiday where all I really did was write a thesis! Carly and Andy for listening to numerous presentations where neither of us really knew what was going on.

This thesis would not have been possible in the first place without the love and support of my family. Mum and Dad – thank you for teaching me I could reach for the stars. Natalie, Hannah and Craig – thank you for putting me back in my place! Nanny and Ken and Nanny and Grandad, thank you for asking me what I do and encouraging me to keep going. My second family, Sandra, Dave and William, who have done nothing but support me regardless of where we have been (and at what stage of life I've been).

Martin, Shareen and Gareth, thank you for your understanding and support. Rachel, Steve, Mike and Sam, you guys need a massive box of doughnuts and buckets of coffee on me. I am incredibly lucky to have you guys in my life supporting me and bringing me biscuits. Thank you!

And finally, Philip and Theo. This thesis is for you. At my darkest days you were there for me, dragging me back to the light, listening regardless of whether it made sense or not, and pushing me to just keep going. I am glad it was you with whom I spent this chapter of my life. Here's to the future.

Contents

Abstract ii

Acknowledgments iii

Contents v

Chapter 1: General introduction 1

1 Overview 1

1.1 Air pollution 1

1.1.1 History 1

1.1.2 Air pollution components 3

1.1.2.1 Other gaseous components 6

1.1.2.2 Metals 6

1.1.2.3 Particulate matter (PM) 7

1.1.3 Air pollution sources 8

1.1.3.1 Man-made sources 9

1.1.3.1.1 Road and transport 9

1.1.3.1.2 Domestic 10

1.1.3.2 Natural sources 10

1.2 Engineered nanomaterials 11

1.2.1 Properties, characteristics, biological effects and safety concerns 12

1.2.1.1 Properties and characteristics of nanoparticulate objects 13

1.2.1.2 Biological effects of nanoparticles 14

1.2.1.2.1 Lungs 14

1.2.1.3 Deposition of particles in the lung 15

1.2.1.4 Translocation of nanoparticles 15

1.2.2 Cerium oxide (CeO_2) nanomaterials 18

1.2.2.1 Envirox 19

1.2.2.2 Biological effects of CeO_2 nanomaterials (CeO_2NPs) 20

1.2.2.3 Effects of CeO_2 nanomaterials in models of human disease 21

1.3 Asthma and allergic airway disease 22

1.3.1 Background 22

1.3.2 Cellular physiology 23
1.3.2.1 Epithelial barrier 23
1.3.2.2 Immune system activation 27
1.3.2.2.1 T cells 28
1.3.2.2.2 B cells 30
1.3.2.2.3 Type 2 Innate Lymphoid Cells (ILC2) 30
1.3.2.2.4 Eosinophils 31
1.3.2.2.5 Neutrophils 31
1.3.2.2.6 Macrophages 32
1.3.2.2.7 Mast cells 34
1.3.2.2.8 Dendritic cells 34
1.3.2.3 Airway remodelling and airway hyperresponsiveness 36
1.3.3 Aetiology and Pathophysiology 37
1.3.3.1 Asthma types 38
1.3.3.2 Genetics of asthma 39
1.3.3.3 Environmental considerations for development of asthma 40
1.3.3.3.1 Pest and pet exposure 41
1.3.3.3.2 Environmental tobacco smoke (ETS) exposure 42
1.3.3.3.3 Exercise and outdoor 42
1.3.3.3.4 Infections 43
1.3.3.3.5 Food and Obesity 43
1.3.3.3.6 Microbiome 44
1.4 Air pollution and burden of disease 45
1.4.1 Susceptible populations 45
1.4.1.1 Age 45
1.4.1.2 Cardiovascular patients 45
1.4.1.3 Cancer development 46
1.4.2 Effects of air pollutants on the respiratory system, including asthma and allergic airway disease 46
1.4.2.1 Particulate matter 48
1.4.2.2 Gases 48
1.4.2.3 Pollen and Moulds 49
1.4.3 Diesel exhaust particles (including ultrafines) and effects on asthma 49

1.5 Impact of nanomaterials on Asthma and Allergic airway disease 50
1.5.1 Impact of nanomaterials on human asthma (human exposure studies) 51
1.5.2 Adjuvant effects of nanomaterials on experimental models of allergic airway disease 51
1.5.3 Exacerbation effects of nanomaterials on experimental models of allergic airway disease 52
1.5.4 Impact of nanomaterials on asthma endpoints in non-allergic experimental models. 52
1.5.5 *In vitro* models for examination of allergic and asthma related endpoints 52
1.5.6 *In vivo* models for examination of allergic and asthma related endpoints 53
1.6 Overarching hypothesis 56
1.7 Specific aims of the thesis 56
2 Chapter 2: Experimental protocols 57
2.1 Particulates and nanomaterials 57
2.1.1 Preparation of particulate suspension 57
2.1.2 Characterisation of cerium dioxide (CeO_2) nanoparticles and diesel exhaust particles (DEP) alone and in combination. 57
2.1.2.1 Transmission Electron Microscopy (TEM) 58
2.1.2.2 Zeta potential 58
2.1.2.3 Size of particles 59
2.1.2.4 Endotoxin Assay 59
2.2 Laser ablation and inductively coupled plasma mass spectrometry (ICP-MS) 62
2.2.1 Elemental composition of DEP 62
2.2.2 Determining the concentration of cerium dioxide nanoparticles in the airways 63
2.2.3 Determining the location of cerium dioxide nanoparticles in the airways 64
2.3 RT-PCR (real time – polymerase chain reaction) 64
2.3.1 mRNA extraction 64
2.3.2 cDNA synthesis 65
2.3.3 Quantitative RT-PCR analysis 66
2.4 Enzyme-Linked Immunosorbent Assay (ELISA) 68

2.4.1 Human ELISAs 68
2.4.2 Mouse ELISAs 69
2.4.2.1 Plasma IgE by ELISA 69
2.4.2.2 Bronchial alveolar lavage (BAL) fluid ELISA analysis 70
2.4.2.3 Lung homogenate preparation and ELISA analysis 70
2.5 Human Primary Bronchial Airway Epithelial Cell (HPBECs) culture 71
2.5.1 Air liquid Interface culture media 71
2.5.1.1 Thawing and initial seeding of cells 71
2.5.1.2 Subculture of cells 72
2.5.1.3 Cell cryopreservation 72
2.5.1.4 Air-Liquid Interface (ALI) Cultures 73
2.5.1.5 Differentiation protocol 74
2.5.2 Characterisation of ALI cultures 75
2.5.2.1 Trans Epithelial Electrical Resistance (TEER) measurement 75
2.5.2.2 TEM of airway epithelial ALI cultures 75
2.5.3 *In vitro* particle exposures 76
2.5.3.1 Initial diesel exhaust particle exposure 76
2.5.3.2 24 hour exposure of diesel particles (DEPs), cerium dioxide nanoparticles (CeO_2NPs) and both particles together 77
2.5.3.3 Inflammatory priming and exposure protocols 77
2.5.4 Cytotoxicity measurement 77
2.5.4.1 Lactate assay 77
2.5.4.2 Lactate Dehydrogenase (LDH) assay 78
2.6 Murine model exposure and tissue collection 79
2.6.1 Rodent model of particulate exposure 79
2.6.2 Intranasal installation of HDM and particulates 79
2.6.2.1 HDM induced allergic airway disease 80
2.6.3 Blood and tissue collection 80
2.6.3.1 Blood processing for plasma isolation 80
2.6.4 Bronchoalveolar lavage (BAL) and inflammatory cell analysis 81
2.6.4.1 BAL collection 81

2.6.4.2 BAL processing 81
2.6.4.3 Cytospin and Inflammatory Cell Counts 81
2.7 Tissue processing and analysis 82
2.7.1 Bradford assay 82
2.7.2 Histochemistry and immunohistochemistry 82
2.7.2.1 Dehydration and embedding 83
2.7.2.2 Cutting and drying 83
2.7.2.3 Histochemistry staining 83
2.7.2.4 Haematoxylin and Eosin (H&E) staining 83
2.7.2.5 Periodic acid-Schiff (PAS) staining 84
2.7.2.5.1 PAS semi-quantification 84
2.7.2.6 Masson's trichrome staining (Sigma Aldrich, Cat# HT15-1KT) 84
2.7.2.7 Toluidine blue staining 85
2.7.2.8 Immunohistochemistry 85
2.7.2.8.1 Stains used 86
2.8 Airway mechanics measurement 87
2.8.1 Anaesthesia and tracheotomy 87
2.8.2 Airway mechanics protocols 87
2.9 Statistical analysis 89
Materials list 90
3 Chapter 3: The effect of CeO_2NP / DEP on human primary bronchial cell inflammatory responses *in vitro*. 93
3.1 Introduction 93
3.1.1 Hypothesis 97
3.1.2 Specific aims 97
3.2 Results 98
3.2.1 Characterisation of HPBECs ALI cultures 98
3.2.1.1 Measurement of cellular injury, metabolism and monolayer integrity 98
3.2.1.2 Alterations in epithelial mediator gene expression relevant to airway dysfunction. 99

3.2.2 Acute effects of exposure to CeO_2NPs alone, DEP alone and CeO_2NPs+DEP together on HPBECs (24hrs) 101
3.2.2.1 Measurement of cellular viability, metabolism and monolayer integrity 102
3.2.2.2 Alterations in epithelial expression of genes that mediate immune responses 104
3.2.2.3 Alteration in levels of epithelial protein mediators of allergic immune responses and inflammation. 110
3.2.3 Acute effects of exposure to particles in the presence of type II inflammatory signals (IL-4+IL-13) on the phenotype of HPBECs *in vitro* 113
3.2.3.1 Measurement of cellular viability, metabolism and monolayer integrity 114
3.2.3.2 Alterations in epithelial gene expression of genes that mediate immune responses 117
3.2.3.3 Alterations in epithelial expression of mediators of immune responses 124
3.2.4 Acute effects of CeO_2NPs and DEP and HDM allergen on HPBECs 126
3.2.4.1 Measurement of cellular viability, metabolism and monolayer integrity 126
3.2.4.2 Alterations in epithelial expression of mediators of immune responses 128
3.3 Summary 130
3.4 Discussion 132
3.4.1 Cellular differentiation 132
3.4.2 CeO_2NPs exposure 133
3.4.2.1 Acute effects of CeO_2NPs on HPBECs 133
3.4.3 DEP exposure 137
3.4.3.1 Acute effects of DEP alone on HPBECs 137
3.4.4 Effects of CeO_2NPs/DEP exposure 139
3.4.4.1 Acute effects of CeO_2NPs/DEPs alone on HPBECs 139
3.4.5 Examination of effects of co-exposure to cytokines on HPBECs 140
3.4.6 CeO_2NPs, DEPs and HDM exposures 141
3.4.7 Limitations and future direction 141
3.4.8 Conclusions 143
4 Chapter 4: Investigation of the effects of cerium dioxide nanoparticles in a murine model of allergen exposure 146
4.1 Introduction 146

4.1.1 Cerium dioxide 146

4.1.2 House Dust Mite (HDM) model of allergic airway disease 147

4.2 Hypothesis and aims 148

4.3 Methods 149

4.4 Results 150

4.4.1 Effect of single acute exposure to CeO_2 NPs ± HDM on airway inflammatory responses after 24 hours 150

4.4.1.1 Concentration and location of cerium oxide after acute exposures to CeO_2NPs±HDM and the effects on lung pathology. 150

4.4.1.2 Effect of CeO_2 NPs ± HDM on altered BAL Immune cells 154

4.4.1.3 Effect of CeO_2 NPs ± HDM on inflammatory markers in BAL fluid 155

4.4.2 Effect of single and repeat exposure (9 independent exposures over 3 weeks) to CeO2NPs (±HDM) on pulmonary responses 156

4.4.2.1 Concentration and location of cerium oxide after acute exposures to CeO_2NPs±HDM and the effects on lung pathology. 156

4.4.2.2 Effect of single and repeat CeO2NPs±HDM on altered BAL immune cell profile ... 158

4.4.2.3 Effect of single and repeat CeO2NPs±HDM on altered mast cell related markers 159

4.4.2.4 Effect of exposure to single and repeat CeO2NPs±HDM for 3 weeks on mediator gene expression in lung tissue 161

4.4.2.5 Effect of single and repeat exposure to CeO2NPs±HDM for 3 weeks on inflammatory markers levels in BAL fluid 167

4.4.2.6 Effect of single and repeat CeO2NPs±HDM for 3 weeks on airway mucin production 171

4.4.2.7 Effect of acute and chronic exposure to CeO2NPs±HDM on structure, remodelling and function of the lung 174

4.5 Discussion 177

4.5.1 Effect of acute, 24-hour exposure to CeO_2NPs in normal and allergic lungs 177

4.5.2 Effect of acute and chronic exposure to CeO_2NPs with or without 3 week HDM treatment 181

5 Chapter 5: Investigation of the effects of cerium dioxide nanoparticles and diesel exhaust particulates in a murine model of allergen exposure. 187

5.1 Introduction 187

5.1.1 Effects of diesel particulates in experimental models of asthma 187

5.1.2 Cerium modification of Diesel particulate effects in experimental models 188

5.2 Hypothesis and aims 189

5.3 Methods 190

5.4 Results 192

5.4.1 Effect of single acute exposure to DEP ± HDM on airway inflammatory responses after 24 hours 192

5.4.1.1 Effects on lung pathology after acute exposure to DEP±HDM 192

5.4.1.2 Effect of DEP ± HDM on altered BAL Immune cells 193

5.4.1.3 Effect of DEP ± HDM on inflammatory markers by ELISA of BAL fluid 194

5.4.2 Repeat co-exposure effects of DEP alone and DEP+HDM on pulmonary responses . 196

5.4.2.1 Effect of single and repeat DEP±HDM on altered BAL Immune cell counts 196

5.4.2.2 Effect of single and repeat DEP±HDM on altered mast cell related markers 196

5.4.2.3 Effect of single and repeat DEP±HDM on gene expression changes in lung tissue 199

5.4.2.4 Effect of single and repeat DEP±HDM on inflammatory markers assessed by ELISA of BAL fluid 202

5.4.2.5 Effect of single and repeat DEP±HDM on airway mucin production 203

5.4.2.6 Effect of single and repeat DEP±HDM on structure, remodelling and function of the lung 206

5.4.3 Acute respiratory effects of both (DEP+CeO_2NPs) and HDM on airway inflammatory responses (24hrs) 209

5.4.3.1 Effect of DEP, CeO2NP and HDM on BAL Immune cell counts 209

5.4.3.2 Effect of DEP, CeO_2NP and HDM on inflammatory markers within BAL fluid 209

5.4.3.3 Effect of DEP, CeO_2NP and HDM on lung cell structure assessed by histochemistry 211

5.4.4 Effects of CeO_2NPs+DEP±HDM on pulmonary responses 212

5.4.4.1 Effect of CeO_2NPs+DEP±HDM exposure on altered BAL Immune cell counts 212

5.4.4.2 Effect of single and repeat CeO_2NPs±HDM exposures on altered mast cell related markers 212

5.4.4.3 Effect of single and repeat CeO_2NPs±HDM exposure on gene expression changes in lung tissue 215

5.4.4.4 Effect of CeO2NPs+DEP±HDM exposure on inflammatory markers assessed by ELISA of BAL fluid 217

5.4.4.5 Effect of CeO_2NPs+DEP±HDM exposure on airway mucin production 219

5.4.4.6 Effect of CeO_2NPs+DEP±HDM exposure on structure, remodelling and function of the lung 222
5.5 Discussion 225
5.5.1 24 hour exposures 225
5.5.2 3 week exposures 226
6 Chapter 6: General Discussion 232
6.1 Summary 232
6.2 Limitations 234
6.3 Future work 238
7 Chapter 7: References 241
8 Appendix 8-I
8.1 Additional figures 8-I
8.2 Published papers 8-XIIIV

Table of figures

Figure 1-1. Daily air pollution and deaths. 2
Figure 1-2. Air pollution components. 3
Figure 1-3. Levels of specific air pollutant emissions from 1970-2016.. 4
Figure 1-4. Causes of CO poisoning deaths in 2015. 5
Figure 1-5. Examples of air pollution particulate matter. 7
Figure 1-6. Anthropogenic air pollution sources in England. 9
Figure 1-7. Number of papers published from 1997-2017 featuring "nanoparticle". 11
Figure 1-8. Size range from large down to the nanoscale. 12
Figure 1-9. Predicted deposition of inhaled particles. 15
Figure 1-10. Deposition and possible systemic translocation of inhaled nanoparticles.. 17
Figure 1-11. CeO_2 catalytic converter. 18
Figure 1-12. Consequences of addition of Envirox to diesel fuel on diesel engine emissions. 19
Figure 1-13. Various cells and their location within the lung 23
Figure 1-14. Subsets and differentiation of T cells. 28
Figure 1-15. Macrophage functions within an allergic asthmatic airway. 32
Figure 1-16. Asthmatic airway remodelling. 36
Figure 1-17 Animal models used to investigate asthma. 55

Figure 2-1 Characterisation of Particles. 61
Figure 2-2. Basic components of an ICP-MS. 62
Figure 2-3. Elemental Composition of DEPs 63
Figure 2-4. Culture Process to Air-Liquid Interface (ALI). 73
Figure 2-5 Various BAL fluid cells identified. 81
Figure 2-6. Cannulation and airway mechanic measurements. 87

Figure 3-1. Cell types of the epithelial layer within the lung. 94
Figure 3-2 Cell viability, cellular metabolism and monolayer integrity after 24 hours exposure to CeO_2NPs alone, DEP alone and CeO_2NPs/DEP combined 103
Figure 3-3 Changes in epithelial immune type II response gene expression after 24 hours exposure to CeO_2NPs alone, DEP alone and CeO_2NPs/DEP combined. 104
Figure 3-4 Changes in epithelial pro-inflammatory gene expression after 24 hours exposure to CeO_2NPs alone, DEP alone and CeO_2NPs/DEP combined. 105
Figure 3-5 Changes in gene expression of molecules that modulate asthma after 24 hours exposure to CeO_2NPs alone, DEP alone and CeO_2NPs/DEP combined exposures. 107
Figure 3-6 Gene expression changes related to induction of immune cell chemotaxis after 24 hours exposure to CeO_2NPs alone, DEP alone and CeO_2NPs/DEP combined. 109
Figure 3-7 Changes in immune type II apical mediator release after exposure for 24 hours to CeO_2NPs alone, DEP alone and CeO_2NPs/DEP combined 110
Figure 3-8 Changes in pro-inflammatory apical mediator release after exposure for 24 hours to CeO_2NPs alone, DEP alone and CeO_2NPs/DEP combined 111
Figure 3-9 Changes in lung defence (SLPI) apical mediator release after exposure for 24 hours to CeO_2NPs alone, DEP alone and CeO_2NPs/DEP combined 112
Figure 3-10. Cell viability, cellular metabolism and monolayer integrity after 24 hours exposure to CeO_2NPs alone, DEP alone and CeO_2NPs/DEP in the presence of type II immune response-related cytokines 116
Figure 3-11 Changes in epithelial type II response gene expression after exposure for 24 hours to CeO_2NPs alone, DEP alone and CeO_2NPs/DEP combined in the presence of type II immune response-related cytokines. 118

Figure 3-12 Changes in epithelial pro-inflammatory gene expression after exposure for 24 hours to CeO_2NPs alone, DEP alone and CeO_2NPs/DEP combined in the presence of type II immune response-related cytokines. 119
Figure 3-13 Changes in gene expression of molecules that modulate asthma after exposure for 24 hours to CeO_2NPs alone, DEP alone and CeO_2NPs/DEP combined in the presence of type II immune response-related cytokines. 120
Figure 3-14 Gene expression changes related to induction of immune cell chemotaxis after exposure for 24 hours to CeO_2NPs alone, DEP alone and CeO_2NPs/DEP combined in the presence of type II immune response-related cytokines. 123
Figure 3-15 Changes in immune type II and pro-inflammatory apical mediator release after exposure for 24 hours to CeO_2NPs alone, DEP alone and CeO_2NPs/DEP combined in the presence of type II immune response-related cytokines. 125
Figure 3-16 Cell viability, cellular metabolism and monolayer integrity after 24 hours exposure to CeO_2NPs alone, DEP alone and CeO_2NPs/DEP in the presence of HDM. 127
Figure 3-17 Changes in immune type II and pro-inflammatory apical mediator release after exposure for 24 hours to CeO_2NPs alone, DEP alone and CeO_2NPs/DEP combined in the presence of HDM. 129

Figure 4-1. Experimental protocol to determine the effect of CeO_2NPs in an animal model of allergic lung disease. 149
Figure 4-2. Concentration and location of CeO_2NPs after an acute exposure to CeO_2NPs±HDM 151
Figure 4-3 Lung sections stained 24 hours after exposure to high dose CeO_2NPs±HDM. 153
Figure 4-4 Inflammatory cell profile 24-hour after acute exposure to CeO_2NPs±HDM. 154
Figure 4-5. Cytokine release 24-hour after acute exposure to CeO_2NPs±HDM. 155
Figure 4-6. Concentration and location of CeO_2NPs after chronic exposures to CeO_2NPs±HDM. 157
Figure 4-7. Inflammatory cell response and plasma immunoglobulin E after acute and chronic exposure to CeO_2 ±HDM for 3 weeks 160
Figure 4-8 Changes in epithelial immune type II response gene expression in lung tissue following acute and chronic exposure to CeO_2 ±HDM for 3 weeks. 162
Figure 4-9 Changes in epithelial pro-inflammatory gene expression in lung tissue following acute and chronic exposure to CeO_2 ±HDM for 3 weeks. 163
Figure 4-10 Changes in gene expression of molecules that modulate asthma in lung tissue following acute and chronic exposure to CeO_2 ±HDM for 3 weeks 164
Figure 4-11 Gene expression changes related to induction of immune cell chemotaxis in lung tissue following acute and chronic exposure to CeO_2 ±HDM for 3 weeks 166
Figure 4-12 Immune type II markers, pro-inflammatory markers and molecules that modulate asthma protein levels in BAL fluid following acute and chronic exposure to CeO_2 ±HDM for 3 weeks. 169
Figure 4-13 Immune cell chemotaxis marker levels in BAL fluid following acute and chronic exposure to CeO_2 ±HDM for 3 weeks 170
Figure 4-14 Analysis of airway secretion-related molecules following acute and chronic exposure to CeO_2NPs±HDM for 3 weeks 172
Figure 4-15. Analysis of airway secretion-related molecules following acute and chronic exposure to CeO_2NPs±HDM for 3 weeks 173
Figure 4-16 Airway structure and remodelling after acute and chronic exposure to CeO_2NPs±HDM for 3 weeks. 175
Figure 4-17. Lung function analysis after acute and chronic exposure to CeO_2NPs±HDM for 3 weeks. 176

Figure 5-1. Experimental protocol to determine the effect of DEP alone and CeO_2NP/DEP in an animal model of allergic lung disease 191

Figure 5-2 Lung sections stained after 24 hours after exposure to DEP±HDM *193*
Figure 5-3 Inflammatory cell response and cytokine release after 24-hour exposure to DEP±HDM *195*
Figure 5-4 Inflammatory cell response and plasma immunoglobulin E after acute and chronic exposure to DEP±HDM for 3 weeks *198*
Figure 5-5 Inflammatory marker expression in lung tissue after various DEP±HDM exposures over 3 weeks ... *200*
Figure 5-6 Inflammatory marker expression in lung tissue after various DEP±HDM exposures over 3 weeks ... *201*
Figure 5-7 Inflammatory protein levels in BAL fluid following acute and chronic exposure to DEP±HDM for 3 weeks *202*
Figure 5-8 Analysis of airway secretion-related molecules following acute and chronic exposure to DEP±HDM for 3 weeks. *204*
Figure 5-9 Analysis of airway secretion-related molecules following acute and chronic exposure to DEP±HDM for 3 weeks. *205*
Figure 5-10 Airway structure and remodelling after DEP±HDM exposures over 3 weeks *207*
Figure 5-11 Lung function analysis after DEP±HDM exposures over 3 weeks. *208*
Figure 5-12 Inflammatory marker gene expression in lung tissue after various Both±HDM exposure combinations over 24 hours. *210*
Figure 5-13 Lung sections stained after 24 hours post-exposure to Both±HDM. *211*
Figure 5-14 Inflammatory cell response and plasma immunoglobulin E after acute and chronic exposure to Both±HDM for 3 weeks *214*
Figure 5-15 Inflammatory marker gene expression in lung tissue after various Both±HDM exposure combinations over 3 weeks *216*
Figure 5-16 Inflammatory cell response and cytokine release after various Both±HDM exposure combinations over 3 weeks *218*
Figure 5-17 Airway mucin analysis after various Both±HDM exposure combinations over 3 weeks. *220*
Figure 5-18 Airway mucin analysis after various Both±HDM exposure combinations over 3 weeks. *221*
Figure 5-19 Airway structure after Both±HDM exposures over 3 weeks. *223*
Figure 5-20. Airway lung function analysis after various Both±HDM exposure combinations over 3 weeks *224*

Figure 6-1. Particle transport rate in vitro. *236*

Figure 8-1. Time points for analysis of various characterisations. *8-I*
Figure 8-2. Confocal microscopy images showing HPBECs growing in the various differentiation media and TEM microscopy image of HPBECs grown in Gray medium *8-II*
Figure 8-3. Cellular injury and dysfunction measurements for the four differentiation medium types *8-III*
Figure 8-4. Basal protein expression changes after 24 hours of CeO_2NPs alone, DEP alone and CeO_2/DEP combined exposures *8-IV*
Figure 8-5. Basal protein expression changes after 24 hours of CeO_2NPs alone, DEP alone and CeO_2/DEP combined exposures *8-V*
Figure 8-6. Basal protein expression changes after 24 hours of CeO_2NPs alone, DEP alone and CeO_2/DEP combined exposures *8-VI*
Figure 8-7. Cell viability, cellular injury and membrane integrity after 24 hours of both CeO_2/DEP and cytokine co-exposure *8-VII*
Figure 8-8. Protein expression changes after 24 hour co-exposure of both CeO_2/DEP and cytokines *8-VIII*
Figure 8-9 Protein expression changes after 24 hour co-exposure of both CeO_2/DEP and cytokines. *8-IX*
Figure 8-10 Inflammatory cell profile after exposure to CeO_2NPs±HDM. BAL fluid was analysed for immune cell profile *8-X*
Figure 8-11 Inflammatory cell profile after exposure to DEP±HDM *8-XI*

Figure 8-12. Inflammatory cell profile after exposure to Both±HDM. BAL fluid was analysed for immune cell profile.....8-XII

Table of tables

Table 1-1 European emission standards for diesel and petrol engines. 5
Table 2-1. Example of PCR data analysis using one concentration of CeO_2NPs and control samples 67
Table 2-2. Details of and antibody and standard concentrations required for Human ELISAs kits 68
Table 2-3. Details of and antibody and standard concentrations required for Murine ELISAs kits 70
Table 2-4. Concentrations of the various components added to produce differentiation medium 74
Table 2-5. Various measured parameters 88
Table 3-1. Summary of PCR and ELISA data from Section 3.2.2 101
Table 3-2 Summary of PCR and ELISA data from Section 3.2.3 113

Chapter 1: General introduction

1 Overview

Air pollution is a worldwide problem which is thought to cause 7 million deaths each year (World Health Organisation (WHO)), with around 30 thousand of these in the UK (Committee on the Medical Effects of Air Pollutants). A major concern is diesel exhaust particles (DEPs) with high pollutant levels which have been linked to cardiovascular diseases, diabetes, reduced cognitive function and pulmonary diseases (such as Chronic Obstructive Pulmonary Disease (COPD) and asthma) (Kelly and Fussell, 2015b, Kaminsky, 2012). Inhaled engineered nanoparticles are also of concern as, like the ultrafine components of airborne particulate matter, they can reach the deep lung. Cerium oxide (CeO_2) is a rare metal that, amongst other applications, is used as a fuel catalyst added to diesel fuel to improve fuel economy, which is available commercially. Nothing is known about how the addition of CeO_2 to diesel might modify the behaviour of DEP within the lung. The focus of this work is to examine the bioreactivity of CeO_2 and DEP in relation to their impact on allergic lung disease and asthma. Each of these will be studied independently as well as in combination in the various models used within this thesis.

1.1 Air pollution

Air pollution has been present throughout human history; however, the composition and concentration of the pollutants have changed as civilisation proceeds. More recently, this has paralleled major advances in medicine and technology, leading to increased public involvement and focus. Indeed, indoor and outdoor air pollution, and air pollution tracking, have become independent fields of study, along with many other associated specialties.

1.1.1 History

Air pollution is not a new problem but a gradually changing one. The one thing that has without a doubt changed is the attitude towards pollution. Ironically, pollution was once considered a sign of growth and affluence - higher pollution indicated an industrial area and therefore more wealth being generated (Yang et al., 2014).

But air pollution has been a problem for as long as humans have burnt fossil fuels for heat and cooking and has been documented as far back as ancient Rome along with the realisation that clean air to breathe was important, and something had to be done to protect the clean air (Mosley, 2014). Other occupations (which will be discussed in section 1.1.2) also began to cause

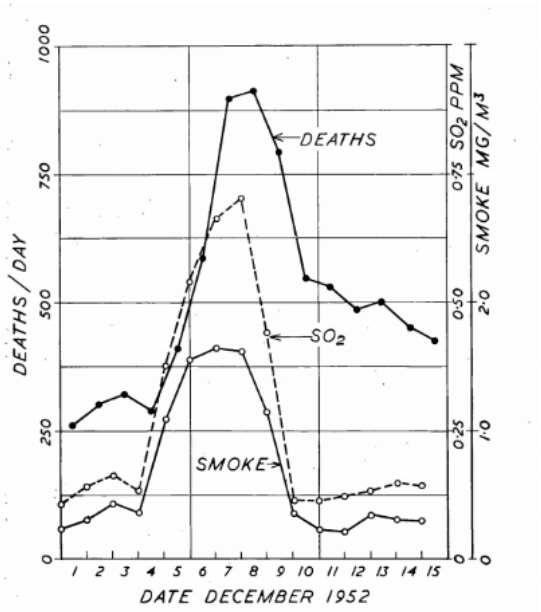


Figure 1-1. Daily air pollution and deaths. The levels of SO_2, smoke and deaths daily during the London Smog event of 1954 (Wilkins, 1954).

problems, such smelting and release of lead and copper particles (the evidence of which can be found in Arctic ice cores) (Mosley, 2014).

Even before the Industrial Revolution in Europe and the USA, there were rising concerns over the increasing amount of smoke in the cities as they switched from using the dwindling supply of wood, to the more abundant and smoky coal. So much so that Londoners were banned from using "sea-coal" in 1306 as the air quality in the city decreased (Mosley, 2014).

Smog (a mixture of smoke and fog, first coined by Dr. H.A. des Voeux (1905) affected many areas of the world including the UK, Europe and the USA. The most commonly used example of a "historic" pollution event, its connection to detrimental health and its legacy is the London Smog of 1952. This 4 day event occurred due to an assortment of different factors, starting with a slow anticyclone stopping above the city causing a cooling effect. This led to an increase in the amount of coal-derived heating required by the population and therefore an increase in domestic pollution. Every day of the 4 day event caused an increase of up to "1000 tonnes of smoke particles, 2000 tonnes of carbon dioxide, 140 tonnes of hydrochloric acid and 14 tonnes of fluorine compounds. 370 tonnes of sulphur dioxide were converted into 800 tonnes of sulphuric acid" (Fenger, 2009). This increase has been shown to be linked to thousands of deaths at the time of the incident (Figure 1-1) and a public outcry forced the government at the time to implement changes. This eventually resulted in the implementation of the 1st Clean Air Act of 1956, which aimed to control industrial as well as domestic air pollution sources by legally enforcing smoke free zones within cities, new regulations for burning furnaces, height of

chimneys, measurement of emitted materials from furnaces and the setup of a "Clean Air Council" (Akimoto, 2003).

1.1.2 Air pollution components

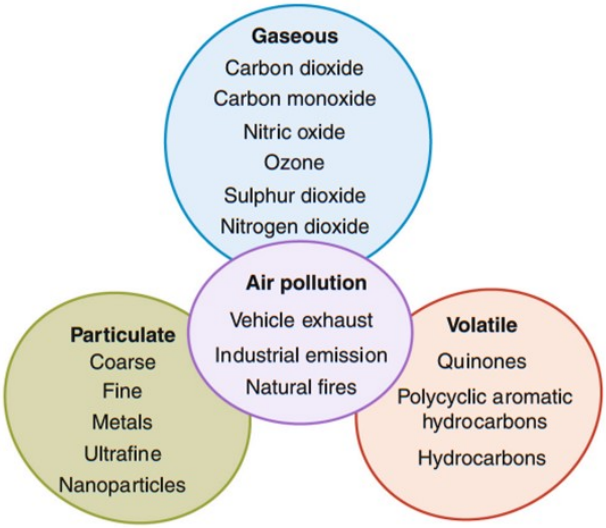


Figure 1-2. Air pollution components. Illustration of components of air pollution found in the atmospheric environment split into gaseous, particulate and volatile segments. Reproduced from Miller et al. (2012), (Kaminsky, 2012)

The composition of air pollution has dramatically changed throughout history. Air pollution can be made up of a variety of different components in varying proportions depending on location/source, weather and time of the year (Figure 1-2). This can be split into gaseous, volatile and particulate components. The air pollution segments that are of most interest are those that are predicted to affect human health; however, it is difficult to tease out exactly which component of these segments cause the observed health effects.

Since the 1970s, there has been a decrease in most fuel components (except ammonia; Figure 1-3.) which has had a number of impacts. One of the main causes for the steady decline of these components is the introduction of new European emission standards for both petrol and diesel cars. Burning of diesel or petrol produces different types of emissions and therefore they are subject to different regulations.

Furthermore, as different engines generate different emissions, it is important to have separate standards for them. These standards were originally introduced in 1992 and have steadily become more refined and restrictive in terms of the emissions that are produced by cars sold today (either petrol or diesel). The main focus of these standards was to initially lower the

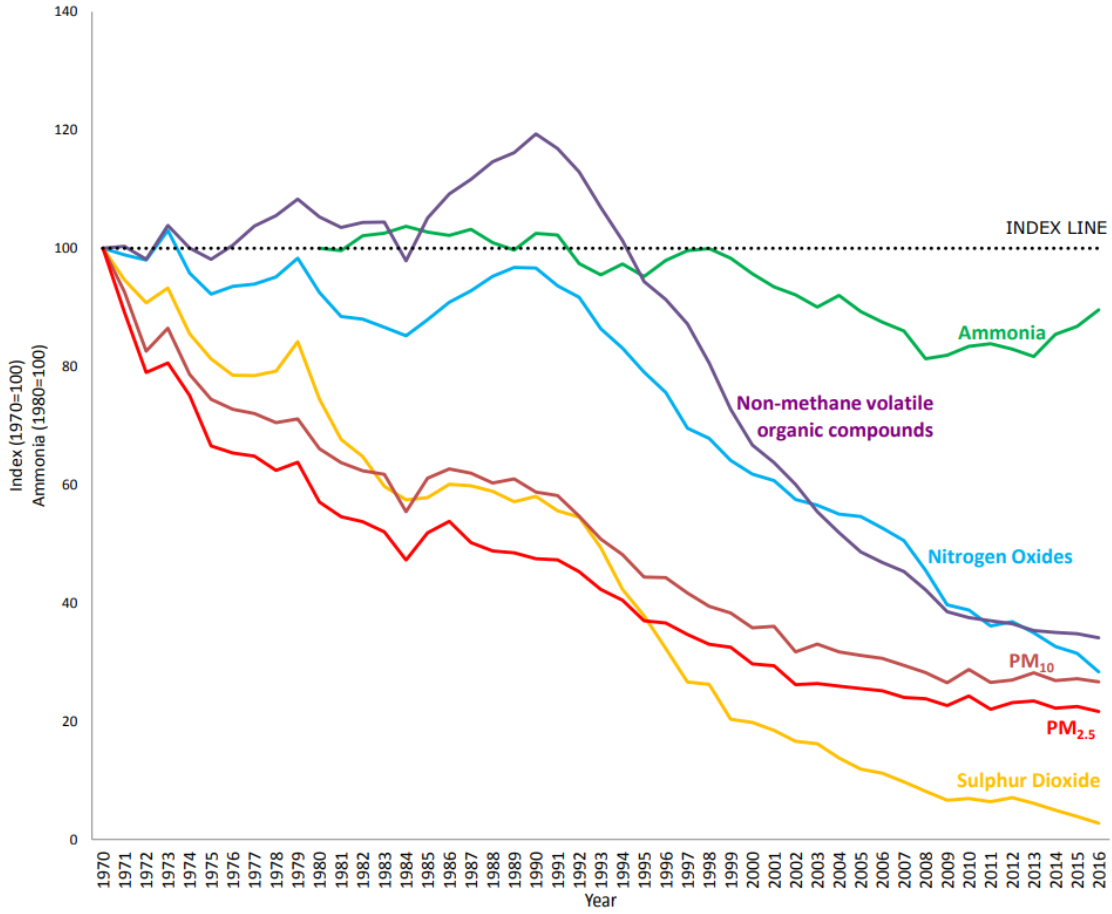


Figure 1-3. Levels of specific air pollutant emissions from 1970-2016. Levels of sulphur dioxides, non-methane volatile organic compounds, ammonia and particulate matter (PM10 and PM2.5). The index line is present to allow a comparison as a percent of original concentrations (Figure reproduced from Affairs, 2018).

carbon monoxide (CO) levels emitted in both engine types (with a slight focus on particulate matter from the diesel engines), this has now moved to a focus on reducing CO, nitrogen oxides (NO_x) and particulate matter (PM) regardless of engine type (Table 1.1). There is conflicting evidence with regards to the respiratory effects caused by NO_x, with some studies identifying a potential link between NO_x and respiratory disorders (Cesar et al., 2015, Amster et al., 2014, Nordling et al., 2008) and others debating this link (Sommar et al., 2014, Kelly et al., 2011).

The most recent of these standards is the Real Driving Emissions (RDE) test – which aims to tackle the ongoing problem of real-life emissions not reflecting what is measured in the laboratory environment. This test was implemented on all new cars from the 1st of September 2017 and will be applied to all cars by September 2019. However, this has led to manufacturers manipulating test situations and data in order for vehicles to pass laboratory tests but which will not necessarily pass real driving emission tests (Drive, air-quality.org.uk, 2018).

Table 1-1 European emission standards for diesel and petrol engines. The standards implemented from 1992 until the present day. These indicate the development of these standards and their requirements from newer engines. A recent focus has been NO_x from both diesel and petrol engines. The most recent aim is to decrease particulate matter generated by petrol engines (previously required of just diesel engines). Figure reproduced from http://www.autoexpress.co.uk/car-news/consumer-news/90816/euro-6-emissions-standards-what-do-they-mean-for-you and (Drive).

		CO (g/km)		NOx (g/km)		PM (g/km)	
Euro Standard	Date	Diesel	Petrol	Diesel	Petrol	Diesel	Petrol
Euro 1	Jul-92	2.72	2.72	n/a	n/a	0.14	n/a
Euro 2	Jan-96	1	2.2	n/a	n/a	0.08	n/a
Euro 3	Jan-00	0.64	2.3	0.5	0.15	0.05	n/a
Euro 4	Jan-05	0.5	1	0.25	0.08	0.025	n/a
Euro 5a	Sep-09	0.5	1	0.18	0.06	0.005	0.005
Euro 6	Sep-14	0.5	1	0.08	0.06	0.005	0.005
Euro 6 RDE	Sep-17	0.5	1	0.08	0.06	0.005	0.005

CO is a by-product of incomplete combustion, specifically the burning of organic compounds (such as diesel, petrol, domestic gas and solid fuels) with the largest source coming from vehicle emissions. Therefore, the highest concentrations of CO tend to be in urban areas where there are high levels of traffic (Board and Council, 2002). CO has an atmospheric half-life of 0.5-1 month, which means its potential effects can be long lasting (Akimoto, 2003). This being said, CO emissions have significantly declined since the requirement for vehicles to be fitted with a catalytic converter was introduced (Chen et al., 2007). Cigarette smoke is a source of carbon monoxide and there are also naturally occurring sources of CO, such as volcanoes,

Underlying cause	*Deaths (persons)* 2015
All accidental carbon monoxide poisonings	53
Accidental poisoning by other gases and vapours	25
Occurrence at home	24
Occurrence in residential institution	0
Occurrence at school other institution/public admin area	0
Occurrence at sports/athletics area	0
Occurrence on street/highway	0
Occurrence at trade/service area	0
Occurrence at industrial/construction area	0
Occurrence on farm	0
Occurrence at other specified place	1
Occurrence at unspecified place	0
Transport accident	1
Accidental exposure to smoke, fire and flames	27

Figure 1-4. Causes of CO poisoning deaths in 2015. Causes of death after CO poisoning in England and Wales in 2015. Cause of death was defined using the International Classification of Diseases, Tenth Revision (ICD 10). Only accidental deaths were included and where the secondary cause of death was due to CO effects. Taken from Office for National Statistics (2018).

photochemical reactions, forest fires and, in certain conditions, the ocean (Swinnerton et al., 1970). Indoor exposure is the most common route for CO poisoning due to incomplete combustion (cooking stoves, gas boilers, BBQs and open or accidental fires) and approximately 50% of reported cases in 2015 in England and Wales were due to indoor CO exposure (Figure 1-4).

CO is often used as an indicator for other pollutants that are released at the same time but cannot be measured as easily, such as $PM_{2.5}$ (as they are both produced through the same process)(Board and Council, 2002); however Carter et al. (2017) recently suggested that this was not the case and every exposure would need to be validated for different variables due to a variety of reasons and fuel burning methods.

1.1.2.1 Other gaseous components

Sulphur dioxide (SO_2) is produced from the combustion of sulphur-containing fuels such as oil and coal. SO_2 then dissolves in water droplets to form acid rain, and gasses in the environment to produce sulphates (air-quality.org.uk, 2018). In contrast to previously mentioned air pollution components, naturally produced nitrogen oxides far overshadow those that are manufactured by man. Sources include volcanoes, bacteria and lightning phenomena, as well as organic fuel combustion, and nitric acid production (air-quality.org.uk, 2018). Ozone (O_3) levels have gradually been increasing globally over the last 100 years and remote areas now have the same concentrations of ozone that were found in populated areas before the industrial times. This increase has been connected to the increase in NO_x production, which in turn is associated with fossil fuel burning, which has steadily increased with industrialisation (Finlayson-Pitts and Pitts, 1997).

1.1.2.2 Metals

Various metals are released into the atmosphere through chemical processes or from burning fuel. In early engines there were initially problems with "knocking", where the fuel was ignited too early. This was solved by the addition of lead to the fuel producing better fuel efficiency and economy, however causing lead to be released into the environment. Patterson (1965) highlighted the potential health effects of lead on the American public but this was not what caused the removal from petroleum. It was only removed when it became apparent it poisoned the catalytic converter in the engines (which were introduced to improve various gaseous emissions) (Mosley, 2014), and not due to the impact on public health.

1.1.2.3 Particulate matter (PM)

PM is defined as any particles (both solid and liquid) that are suspended in the air, which vary in size, configuration and origin (Pope, 2000). This category includes smoke, soot, combustion by-products, dust, salt, pollen and spores (Dockery, 2009).

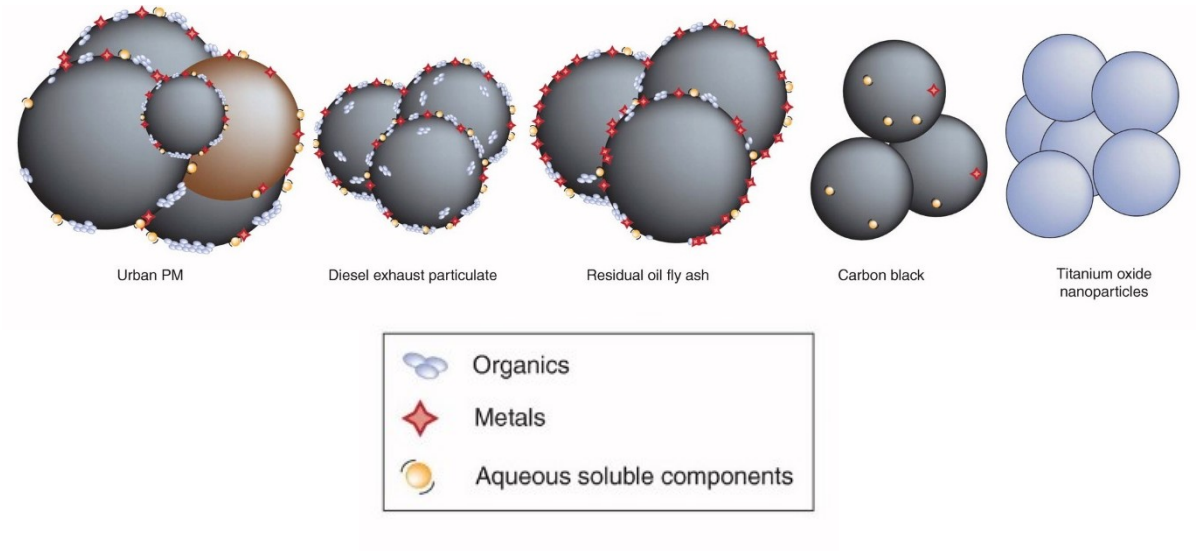


Figure 1-5. Examples of air pollution particulate matter. PM consists of a number of component sources and surface elements, including organics, metals and volatile elements. Reproduced from Miller et al. (2012).

Particles in the air are a mixture of sizes and can be categorised as follows, based on their aerodynamic diameter:

- Course Particles (PM_{10}, 2.5-10µm) – these are predominantly naturally occurring particles from soil and dust.
- Fine Particles ($PM_{2.5}$, <2.5µm) – these are generated from combustion in industry, vehicles, and power production (Pope, 2000).
- Ultrafine Particles (UF, $PM_{0.1}$, <100nm) – a significant component of this are DEP (Wichmann, 2007).

Currently only PM_{10} and $PM_{2.5}$ are systematically monitored and under regulation in the environment. The UFs cannot be consistently observed without using alternative measurement systems such as a particle number counter (Robertson and Miller, 2018b). As the UF are the smallest of all the environmental particles, these are the ones that could pose the highest potential risk to the general population as the smaller the particles the higher the potential to reach the deep lung and remain within the body. Different particle size leads to differential deposition at sites within the respiratory tract (Section 1.2.1.2) which will impact on their bioreactivity and fate.

PM is made up of many chemical and elemental constituents, as mentioned above (Figure 1-5), and is therefore both physically and chemically different with the potential to cause different responses. A critical factor is the geographical location of exposure and previous studies have sampled and characterised particles from across the world (Hoek et al., 2002, Marcazzan et al., 2001, Schmitz, 2005, Schäfer et al., 2006) in order to determine which physicochemical traits might relate to adverse health effects, as different fuels may alter the particle composition and therefore the health effects these particles may cause.

There have been numerous studies that have been completed identifying the potential health effects air pollution may have on various populations, with the majority of these being linked to the lung. However, after exposure to PM, studies have also found a link to cardiovascular diseases mortality and $PM_{2.5}$ (Hvidtfeldt et al., 2019, Hoek et al., 2013), increases in sleep disorders in an elderly population (Tang et al., 2019), a decrease in the lung function of children exposed to air pollution PM (Chen et al., 2019, Korten et al., 2017, Rice et al., 2016) and low birth weight and premature births if exposed *in utero* (Korten et al., 2017, Kim et al., 2018).

1.1.3 Air pollution sources

As noted earlier, air pollution is the result of a variety of processes, from both manmade and natural sources. The composition of air pollution and its effects can depend on other factors, such as the weather (including temperature fluctuations, humidity, sunlight, rain and windy conditions) and the time of the year. In terms of individual exposure and exposure limits, it is important to note that these sources will vary in importance in terms of the impact of exposure on health, depending on the location of the subject and whether they are indoors or outdoors.

1.1.3.1 Man-made sources

There are multiple anthropogenic sources of air pollution that can either be exclusively produced by man, or also have some natural sources. Man-made sources make up most of air pollution components. Most man-made pollutants are produced from transport (Figure 1-6), where this source is the highest contributor to carbon monoxide, nitrogen oxides and PM (Cichowicz et al., 2017).

Source	Pollutant (source contribution as a percentage of the total)			
	Carbon monoxide	Nitrogen oxides (NO_x)	Particulate matter (PM_{10})	Sulphur dioxide
Power stations	4	26	7	60
Transport	42	46	26	4
Burning of fuels (industries)	25	17	10	20
Burning of fuels (commercial)	7	4	10	2
Burning of fuels (residential)	12	3	13	7
Other industry	8	1	15	7
Farming	0	0	9	0
Waste	0	0	0	0
Other	2	3	10	4
Total	**100**	**100**	**100**	**100**

Figure 1-6. Anthropogenic air pollution sources in England. Percentages of the four major air pollution components and the source of their production in 2013. Taken from the National Atmospheric Emissions Inventory database (NAEI). The most recent NAEI report (Defra 2013).

Man-made sources of air pollution can be broadly divided and described as follows:

1.1.3.1.1 Road and transport

Road and traffic pollution are the main sources of particulate air pollution released into the environment and consist of both vehicle exhaust emissions and wear particles (such as brake disks, tyres and other abrasive mechanisms) (Pallavi Pant, 2013). If an engine is cold, then the engine operates less efficiently, and emission control systems do not work as they should. Combustion is not complete, and catalysts are not fully operational until the engine is hot (Board and Council, 2002). This effect can also be enhanced by low environmental temperatures. This incomplete combustion leads to more particulate matter and CO produced and can contribute up to 80% of the pollution level for 3-4 mins after engine ignition (the problem of cold starts).

As alluded to above, the amount of harmful emissions a vehicle produces varies, particularly in relation to the age of the vehicle; the greater these are the greater the road tax that is paid. This is an incentive by government to persuade the public to buy newer and “cleaner” vehicles.

1.1.3.1.2 Domestic

Domestic and indoor air pollution has become of more concern over the last few years. There is a realisation that the public are also exposed to the gaseous and particulate matter inside the home that has previously been described in outdoor air pollution.

The producer of the most gas and particulate matter is the wood burning stove (Hawkes, 2015). This has become a popular item in the home in the last 10 years, along with the fire pits and chimaeras now found in many gardens and communal spaces. Whether they have been installed for functional (cooking and heating) or for decorative appeal, they still produce pollutants, and these concentrations have been identified as being higher when there is a high or low throughput of material and vary depending on what is burned in the stove (Friederike Fachinger 2017).

1.1.3.2 Natural sources

There are multiple natural sources of air pollution that have not yet been mentioned. These can be formed during everyday processes or during extreme weather events. Sand and dust have been shown to travel thousands of miles in the air before settling and causing potential problems in completely different continents to that of their origin (Wilkening et al., 2000). There are also now strong indications that, in fact, sea salt ameliorates the effect of the pollution particles that are blown over the oceans (Rosenfeld et al., 2002). Volcanos, once erupted, can release a massive amount of particulate and gaseous material into the air which goes on to spread throughout the atmosphere. Clouds of volcanic gases contain sulphur dioxide, hydrogen chloride, hydrogen fluoride and toxic metal (Curtis et al., 2006), which can fall as acid rain once they interact with the moisture in the atmosphere. The ash emitted from volcanoes contains rock, silt and particles of silica, which all contribute to the particulate matter in the atmosphere (Beach, 2017).

1.2 Engineered nanomaterials

The synthesis and use of engineered nanomaterials has expanded rapidly over the last 40 years (Kessler, 2011), with the number of papers published increasing over 175-fold since 1997 (Figure 1-7). This indicates both an increased interest in a growing field and an increase in the number of types of particles being produced and used industrially, domestically, medically, environmentally and commercially (Khan et al., 2017).



Figure 1-7. Number of papers published from 1997-2017 featuring "nanoparticle". Data extracted from PubMed on the number of papers published containing the word "nanoparticle" over a twenty year period.

Nanoparticles (NPs) have incredibly wide and diverse uses, both inside and outside the laboratory, and have been used as fuel additives, in cosmetics and sun creams, and as industrial catalysts. In medicine they are being developed and used for a wide range of purposes, including targeted drug delivery, localisation and diagnosis of cancer (due to their light scattering abilities) (Tolstik et al., 2016), as antimicrobials in the environment and therapeutically (water and package disinfection; treatment of drug resistant bacterial infection (Malekkhaiat Haffner and Malmsten, 2017, Bhawana et al., 2011, Hoseinnejad et al., 2018)). In engineering, their applications include use as semiconductors, as coatings, lubricants and adhesives (Khan et al., 2017). Nanoparticulate materials have been used for centuries due to their novel properties, before the realisation that their nanosized properties conferred the unique qualities observed.

1.2.1 Properties, characteristics, biological effects and safety concerns

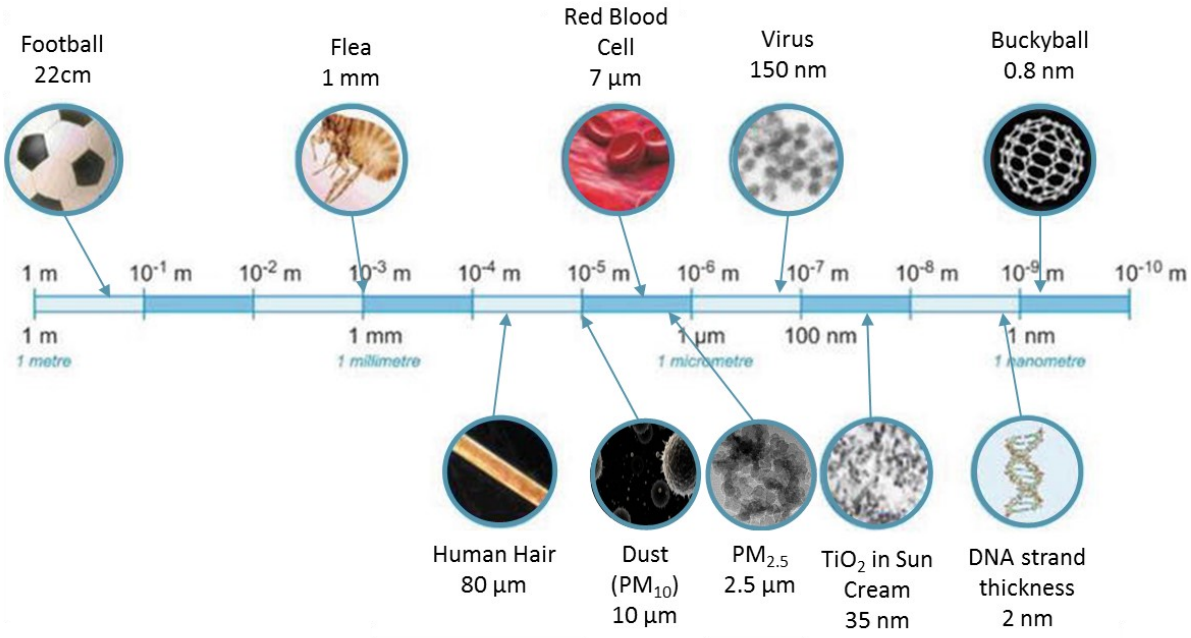


Figure 1-8. Size range from large down to the nanoscale. Nanoparticles are in the nanometer range (0.1µm range) and make up some of the smallest particles found in the air. The average diameter of a human hair equals 80 µm and is used as an easy comparison as something that can be seen but is still small. Figure adapted from Ahmed (2019), White et al. (2011), (Hartney and Robichaud, 2013)

A nanomaterial is defined as being 100nm or less in at least one dimension (Sambandam et al., 2014, Horie et al., 2011). A nanoparticle is, strictly speaking, a spheroid and hence has a diameter of 100nm or less (Figure 1-8). These nanoparticles are therefore perceived/recognised by eukaryotic cells as natural objects; this feature could potentially allow the particles to enter the cell passively, or by normal endosomal processes for nanosized molecules, without being prevented by the normal cellular mechanisms that would control them (Sambandam et al., 2014). Nanoparticles inhaled into the respiratory system have the potential to be bioreactive within the lung and therefore induce the release of various mediators that act locally. These mediators may also be accountable for the systemic effects associated with the inhalation of PM, but the exact mechanisms of this still needs to be established (Mostovenko et al., 2019, Yang et al., 2017). It has been shown that a proportion of inhaled nanoparticles are capable of reaching both the lung and the gastrointestinal tract (through swallowing mucus that is driven to the throat), but their translocation into secondary organs via translocation from the lung into the blood is very low, but is still possible (Raftis and Miller, 2019, Miller et al., 2017). A proportion of inhaled nanoparticles which are engulfed by macrophages within the lung secretions are cleared following swallowing of mucus and excreted in faeces (Krug, 2014).

1.2.1.1 Properties and characteristics of nanoparticulate objects

The smaller size of a nanoparticle results in a higher surface area per unit volume/mass when compared to particles greater than 100nm (Hackenberg et al., 2011). A larger surface area confers greater surface reactivity and potential to react with cellular membranes and components at a molecular level, possibly impacting the organ and systemic systems upon exposure. In addition, with significantly greater particle numbers per unit mass, inhalation and dispersion of even very small amounts by weight of nanoparticles could result in targeting large areas of the lung.

There are multiple other ways that a nanosized object can be defined including its shape (rod, tube, sphere, hexagon, cube, triangle, etc), chemistry, surface composition, surface electric charge and method of synthesis (Sukhanova et al., 2018). Due to the almost limitless combination of physicochemical possibilities, engineered nanoparticles have diverse characteristics that lend themselves to a wide range of applications. Where a property may be beneficial in one scenario it may be completely inappropriate in a different one. These various characteristics can cause problems for those interested in putative toxicological effects (an important consideration, as discussed below), as it is not always clear which properties might be responsible for any adverse effects seen in the models used. These characteristics (both physical and chemical) are vital in determining the mechanisms of toxicology of a specific nanoparticle and it is therefore crucial to work with fully characterised materials in any toxicological investigation.

Nevertheless, there is a distinct lack of sufficient characterisation of nanoparticles (both physical and chemical) in many nanotoxicology studies which hinders interpretation and significance of the data (Krug, 2014). It is important to know the conditions in which the nanomaterials have been characterised, and to characterise the nanoparticles under the conditions in which they are prepared/studied. For example, the pH of the diluent, or the addition of serum (found in cell culture medium) has the potential to impact the size of the particles (Cho et al., 2013), by forming a corona, or by initiating agglomeration/aggregation of the particles. Some fluids, such as pulmonary surfactant, have been shown to both disperse (General Strategies for Nanoparticle Dispersion) and enhance agglomeration (Kendall et al., 2015), depending on the particles under investigation. Furthermore, the modified characteristics and variable properties of the nanoparticles can have a striking influence on particle bioreactivity, uptake, translocation and the cellular responses (Kuhn et al., 2014).

1.2.1.2 Biological effects of nanoparticles

With the increased uses of engineered nanoparticles within a number of different applications, there is more potential for exposure and possible health effects. Just like their bulk particle counterparts, some nanoparticles potentially have more health implications than others and therefore an increase of their concentration in the air is of concern to many, including government agencies, health professionals, the public, and industry. Those who engineer nanomaterials focus on their mechanistic effects and the practical applications of these particles and not the toxicological effects (Krug, 2014).

Cells can internalise particles in various ways much depending on the size, but also membrane interactions, via phagocytosis (macrophage engulfment of larger particles, between 2 and 10μm), micropinocytosis (uptake of fluids or particles in small vesicles) or endocytosis via clathrin-mediated mechanisms (a receptor is activated and the particle, <300nm, is engulfed and taken into the cell) and caveolae (caveolin-mediated for molecules less than 100nm; e.g. this process is utilised for cholesterol translocation and homeostasis) (Cho et al., 2013, Kuhn et al., 2014). Not all cells internalise extracellular objects, and not every cell is capable of each uptake method, and therefore not every cell will be affected by every nanoparticle it is exposed to (Kuhn et al., 2014). For example, previous work within the group has demonstrated that TT1 cells (type I alveolar cells) take up significantly more nanoparticles (polystyrene) than ATII cells (type II alveolar cells) regardless of size or surface modification. 50nm particles were found to be distributed throughout the cytoplasm, involving passive uptake, while the 100nm particles were mostly found in the intracellular vesicles, indicating active uptake mechanisms. Transepithelial electrical resistance (TEER) values remained unchanged after particular exposure, indicating that there was no disruption to the tight junctions between the cells and therefore no translocation (Thorley et al., 2014). Thus, a combination of uptake mechanisms contribute to cellular internalisation of nanoparticles (Kuhn et al., 2014, Novak et al., 2014).

1.2.1.2.1 Lungs

Clearance of particles from the respiratory alveolar region of the lung is slower than that of the ciliated airways, where the mucociliatory escalator drives particles and particle-containing cells towards the throat where they are swallowed or expectorated. Instead, as there are no cilia and far fewer secretions, clearance of unwanted material in the alveolar region is dependent on macrophage phagocytotic elimination; however, nanoparticles may be so small that they evade detection and phagocytosis by macrophages and remain at the gas-liquid interface of the alveolae and can interact with the airway epithelium (Maynard et al., 2013).

1.2.1.3 Deposition of particles in the lung

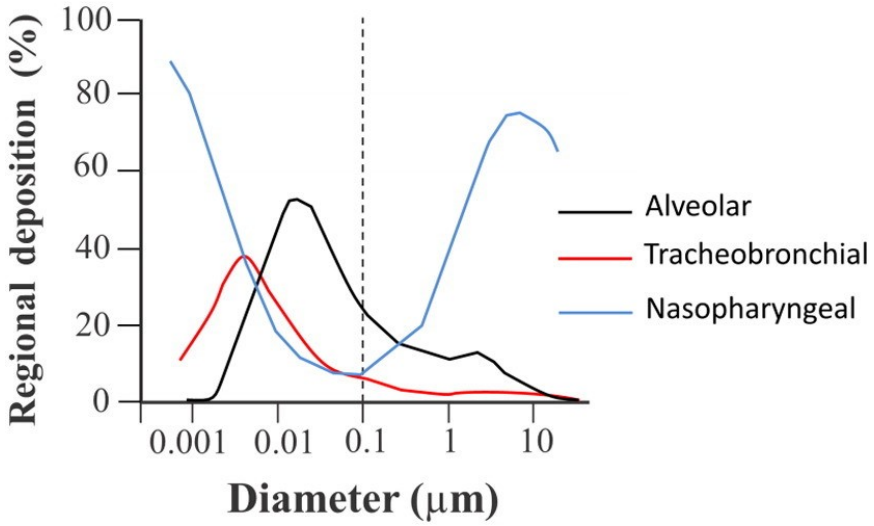


Figure 1-9. Predicted deposition of inhaled particles. Percentage of deposition of particle up to 10μm into the alveolar, tracheobronchial and nasopharyngeal regions of the respiratory tract. Only nanosized particles deposit in the alveolar region. Adapted from Chen et al. (2016), (Fulcher and Randell, 2013), originally from ICRP (1994), (Xu and Qu, 2014).

The deposition pattern of aerosolised particles within the lung needs to be taken into consideration when investigating a nanoparticle, particularly *in vivo*. Different sized particles will deposit into different regions of the lung (see Figure 1-9), with smaller particles getting deeper than the larger particles (Fulcher and Randell, 2013). There are a number of characteristics that have the potential to impact on how the particles are deposited and where. The particle size, size distribution (monodispersed or polydispersed samples), density, shape, atmospheric pressure in the environment in which they are suspended matter. The size of the respiratory tract (depending on age and gender of the person, species differences if comparing across animals), wind speed, type of breather (does the subject breathe from both the mouth and the nose at an equal rate or are they using one or the other) and the breathing rate of the subject (the higher the rate, the more particles that will be taken into the lung) are also important factors (Klumpp and Bertelli, 2017).

1.2.1.4 Translocation of nanoparticles

Nanoparticles after inhalation can translocate through the air-blood barrier and can be discovered in additional organs throughout the body (Kreyling et al., 2010), despite being a low proportion of that deposited. There have been several different studies that track the fate of nanoparticles after inhalation/pulmonary deposition that illustrate that translocation to other organs throughout the body (Figure 1-10) is reliant on the size of the particles that have been inhaled. Small particles (smaller than ~6nm) can enter the bloodstream and are cleared via the kidneys. Particles that are ~34nm or smaller can be found in the lymph nodes, while the particles that are larger are mostly retained within the lung (Choi et al., 2010). Uptake by alveolar

macrophages of these particles is the main clearance mechanism, which then have the potential to translocate into the lymphatics system and influence the immune system from there (Geiser, 2010). The size and the material of the particle is an important factor in the translocation of particles, along with exposure routes (Nakane, 2012). Once a particle has entered the bloodstream and circulation, there is the potential for it to translocate to any area of the body, via the blood or the lymph and accumulate there if the relevant clearance mechanisms are not present. NP surface charge influences the translocation potential as well as the uptake of the particle. This is easily modified within the microenvironment and is hard to predict (Chen et al., 2018, Choi et al., 2010). Human volunteers have been used to determine the deposition of particles with known characteristics within the lung and potentially analyse the translocation of these particles. One such study utilised radiolabelled carbon nanoparticles (diameter of 100nm) and tracked their location 6 hours after inhalation. It was found that the majority remained within the lung but a small percentage (3.2±0.7%) was detected within the blood immediately after inhalation and was cleared via the kidneys (observed 60 mins after inhalation) (Mills et al., 2006). Another study of gold nanoparticles (2 hour exposure during intermittent exercise), found that the gold was present in the blood within 15 mins of exposure and remained 3 months post-exposure. This study used particles of different sizes (5 and 30nm) and discovered that the smaller particles were at a higher concentration in the fluids analysed and were also present in the urine, while the larger particles were not (Miller et al., 2017).

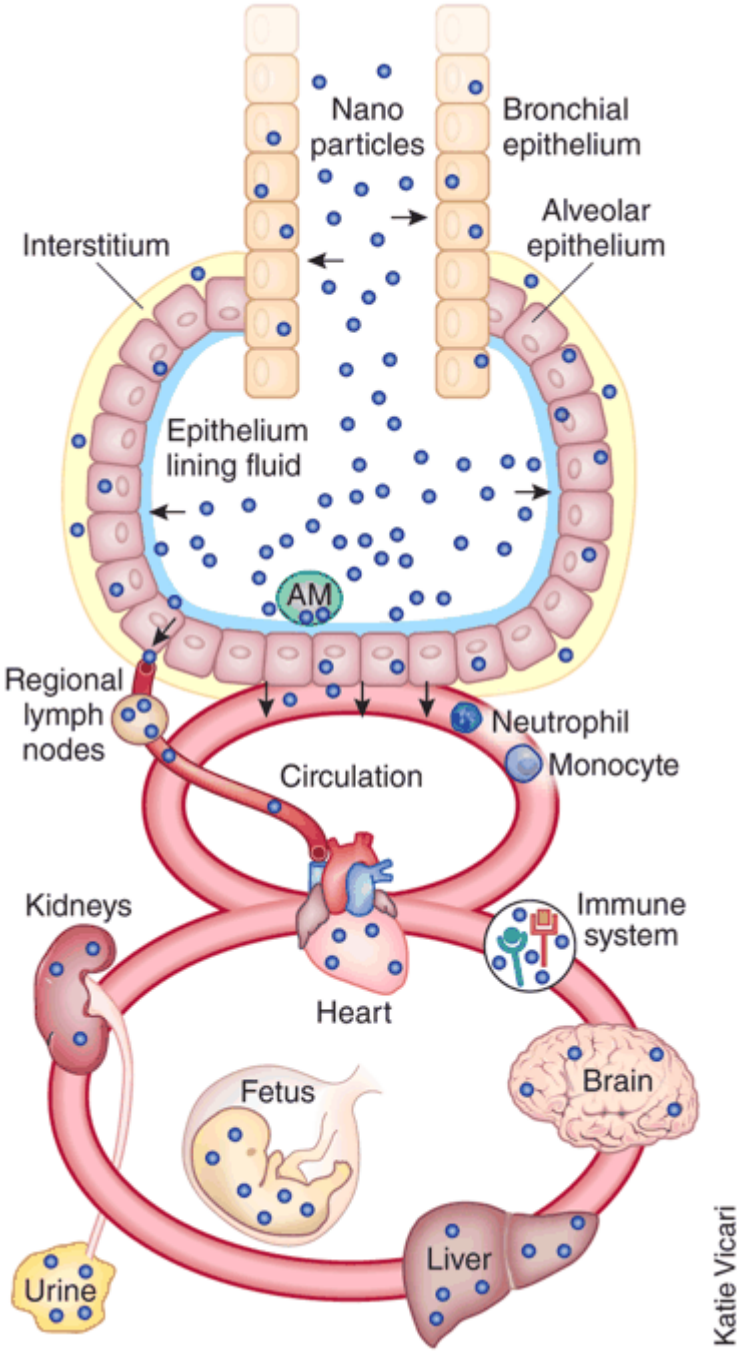


Figure 1-10. Deposition and possible systemic translocation of inhaled nanoparticles. Once nanoparticles have been inhaled, it has been shown that a small percentage of some types of particles are able to translocate via the blood and the lymph to other secondary organs. Reproduced from Kreyling et al. (2010).

1.2.2 Cerium oxide (CeO_2) nanomaterials

Cerium oxide (CeO_2) is an oxide of the rare metal cerium, and is one of the most abundant precious metals (Yokel et al., 2014). It has a high affinity for both oxygen and sulphur (Lin et al., 2006). Nanoceria (CeO_2 nano particles) has been used as a fuel catalyst in diesel engines, and is being used as a polishing agent, as a component of solar panels and is used in glass and ceramics production (Lin et al., 2006). The nano form is not found in nature commonly; importantly, it is becoming increasingly used within industry and industrial processes. CeO_2 has been used as a catalyst since 1999 (Cassee et al., 2011). With the increase in the number of diesel engines and the regular change of laws within the European Union to lower the emissions from these engines, new methods are being deployed to decrease the levels from older engines. These

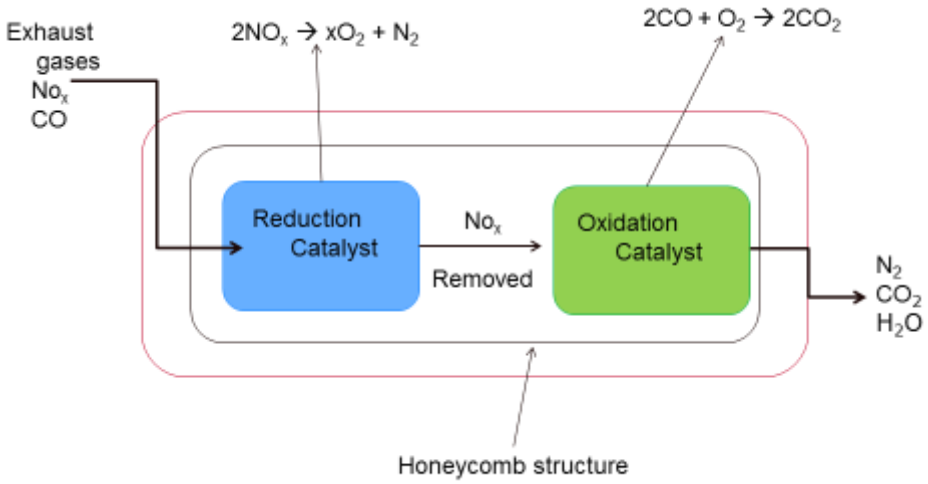


Figure 1-11. CeO_2 catalytic converter. Illustration of how CeO_2 catalysts work in increasing efficacy in diesel fuel consumption within the engine and the end products of combustion. CeO_2 is able to act as both a reduction and an oxidation catalyst depending on the burning conditions (Vivier and Duprez, 2010).

methods include the production of better catalytic converters and the introduction of chemical catalysts into the fuel tanks. These catalysts can contain a number of different components, including urea (AdBlue – which is injected and acts as a reductant within the catalyst system) and CeO_2 (Eolys and Envirox). These catalysts are added to a tank of fuel with the aim to increase fuel efficacy by making the engine more efficient, thus saving expenditure. A by-product of this is a reduction of emissions produced by that engine.

The catalytic nature of CeO_2 is due to its chemical properties (Figure 1-11). It donates oxygen molecules for the oxidation of CO and causes a reduction effect on the NO_x molecules (Arul Mozhi Selvan et al., 2014). The addition of CeO_2 to the fuel lowers the temperature that the soot requires to be burnt off (the "light off" temperature). Thus more of the soot is burnt away from

the inside of the engine causing the engine to run more efficiently and cleanly (Zhang et al., 2013, Cassee et al., 2011, Jung et al., 2005).

1.2.2.1 Envirox

Envirox is a fluid that is manually added to the tank of diesel by the consumer. Before the release of Envirox onto the market, a number of safety tests were carried out in order to ensure the additional amount of CeO_2 released from the exhaust did not cause harm to humans. The initial study (Park et al., 2007), determined that there were no adverse effects from the cerium based on full characterisation of the particles, *in vitro* and *in vivo* assays. Adding the Envirox



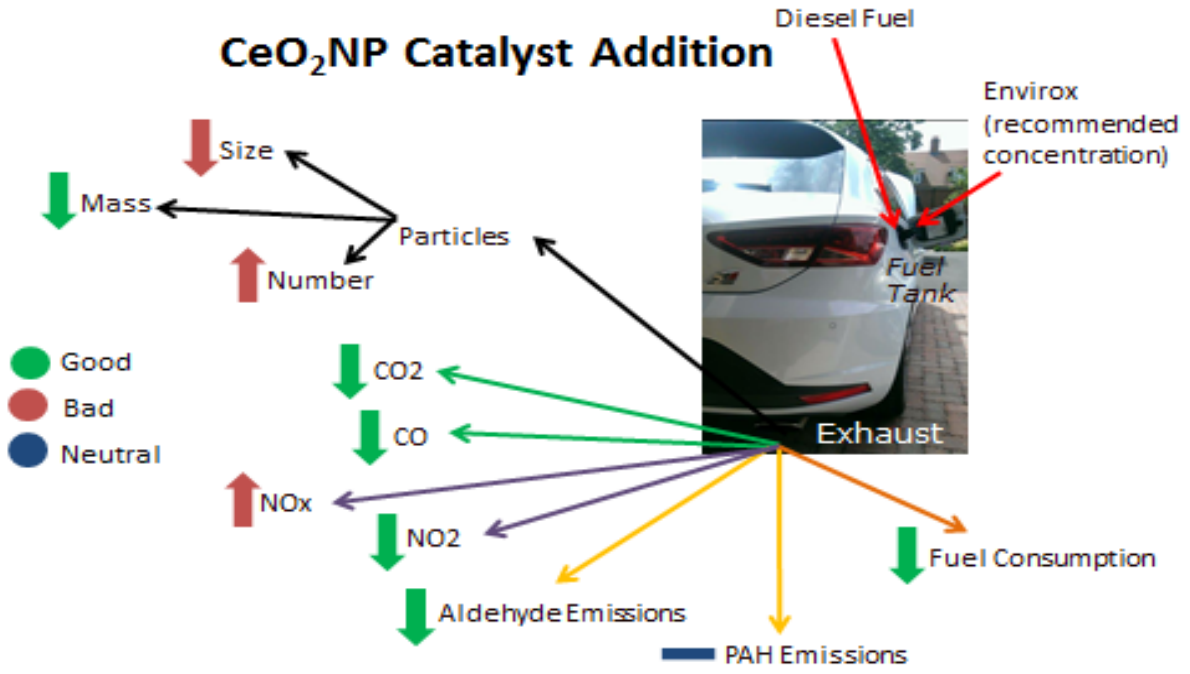


Figure 1-12. Consequences of addition of Envirox to diesel fuel on diesel engine emissions. This figure shows some of the changes in engine exhaust emissions when the CeO_2 nanoparticle catalyst, Envirox, is added to diesel engine fuel at the recommended concentration. Green arrows show decreased emissions, red arrows show unwanted increased emissions or changes (reduced particle size) and blue bars show no change, indicated as good, bad or neutral effects. Reproduced from Zhang et al. (2013).

catalyst to the diesel at the manufacture's recommended concentration of 0.5ml of Envirox to one litre of diesel fuel and above, decreases the fuel consumption of the engine, the volume of CO_2 produced and the particulate mass (Figure 1-12). With an increase in the concentration of Envirox there is also an increase in the volume of NO_x produced and the total number of particles produced (Zhang et al., 2013). This can also cause a change in the physical properties of the particles emitted from the engine, which are smaller, and might therefore lead to an increase in the toxicity of these particles. In conclusion, this catalyst does do the job for which it is intended, but the health consequences of the Envirox needs to be further investigated. In

summary, as the concentration of Envirox in the fuel increases, so does the concentration of NO_x and particulate cerium found in the emissions, while the size of the particles decreases. However, the particle zeta potential remains consistent regardless of volume of Envirox added to the fuel. The carbon content of the particles and the oxidative potential are reduced, and the concentration of cerium and nitrogen are increased. The structure of the particles is also changed. This could cause changes in the clearance of these particles from the lung, as well as the biological responses to them, when inhaled (Zhang et al., 2016).

After addition of CeO_2 to diesel fuel, there is release of CeO_2 particles as part of the particulate diesel exhaust. This is currently restricted to a small number of locations across the UK. With the potential for further increases of CeO2 into the environment due to more widespread use of these catalysts, it is of interest to explore how such changes impact pulmonary health. CeO_2NPs are a common form of this type of fuel catalyst and their interaction with biological systems has been examined in some detail within the literature and this thesis.

1.2.2.2 Biological effects of CeO_2 nanomaterials (CeO_2NPs)

CeO_2 is a unique material with special redox characteristics which may impact biological systems. It has the ability to have both pro-oxidative and anti-oxidative effects on cells. Toxicity of CeO_zNPs has been found to be due to the valence state and the percentage of the surface that is Ce^{3+} (Pulido-Reyes et al., 2015a) when compared to Ce^{4+}, which can be reversed with the addition of phosphate ions. Phosphate ions have been found to alter the characteristics of CeO_zNPs, and the redox state. Due to the high abundance of phosphate in biological systems this could be the potential source of the conflicting redox states of CeO_zNPs within the literature (Singh et al., 2011). The fact that CeO_zNPs have this potential to have varying surface chemistry could allow the differences seen in the literature when exposing models to CeO_zNPs to be explained (Dunnick et al., 2015, Xu and Qu, 2014).

CeO_2 nanoparticles can be internalised by some cells and remain within specific vesicles without causing damage to the mitochondria (Xia *et al.*, 2008). There are conflicting opinions on the capability of cerium to be both cytotoxic and cyto-protective of cells. Some studies have found evidence for CeO_2 being protective (Xia *et al.*, 2008), while others have demonstrated the opposite and cytotoxicity (Lin et al., 2006). Some studies have managed to demonstrate both oxidative and antioxidative properties (Horie et al., 2011). This is reflected in the flux in reactive oxygen species (ROS) at high and low concentrations of CeO_2. A higher concentration of the nanoparticles leads to an increase ROS production, while a lower concentration has an anti-oxidative effect, resulting in a lower production of ROS (Horie et al., 2011).

After inhalation of cerium, only around 1% of the particles are translocated throughout the body, but it does appear to have a slow clearance rate from the body (due to low solubility) and accumulation in the lung and liver can cause localised toxic effects at high doses there. CeO_2 can also exist in two different redox states; it has been found that Ce^{3+} is the more toxic of the two and has more biological effects within the body (Yokel et al., 2014).

1.2.2.3 Effects of CeO_2 nanomaterials in models of human disease

There is no current evidence that would suggest that CeO_2 is toxic in humans, there is however evidence that suggests the nano-CeO_2 is potentially more toxic than its microparticle counterparts (Kumari et al., 2014b). For example, potential genotoxic effects of these particles (Franchi et al., 2015, Kumari et al., 2014a)) have been described, as well as potential geno-protective effects (Rubio et al., 2016). Interestingly, nanoparticulate ceria exists in various forms, and within an aquatic environment it has been identified that the oxidative state of the particles and not the shape, concentration or surface charge of the particles influenced their toxicity (Pulido-Reyes et al., 2015b).

1.3 Asthma and allergic airway disease

1.3.1 Background

Asthma is a chronic inflammatory disease of the airways that is characterised by a constriction of the airways associated with, but not limited to; coughing, chest tightness, mucus build up, wheezing and bronchial constriction, that can be triggered by a number of patient specific stimuli (Lambrecht and Hammad, 2012). There are numerous potential triggers of an exacerbation of existing asthma, whilst development of asthma is complex and includes environmental and genetic causes. Not everyone that has an allergic phenotype is asthmatic (Davies et al., 2016).

There is evidence that single nucleotide polymorphisms (SNPs) changes might play a small role in determining the asthmatic risk (Saba et al., 2018, Raeiszadeh Jahromi et al., 2015, Wan et al., 2012) and in the development of this disease, however it is becoming increasingly clear that environmental exposures also play a role. One of the theories for the increase in asthma cases is the "hygiene hypothesis". This states that children are now being brought up in an environment that is too clean and are not exposed to germs and other agents which would normally build up their immune response to these triggers. Consequently, at a later stage of their life, the immune system reacts to a range of biological material to which it should not normally react (Turner, 2017). The hygiene hypothesis is too general a statement for the causes of asthma. It does not explain the increase of allergies found in poorer and less developed areas (van Tilburg Bernardes and Arrieta, 2017). It is thought that there needs to be the perfect storm of genetic and environmental triggers where "genetics loads the gun and the environment pulls the trigger" (Turner, 2017) for asthma to develop.

1.3.2 Cellular physiology

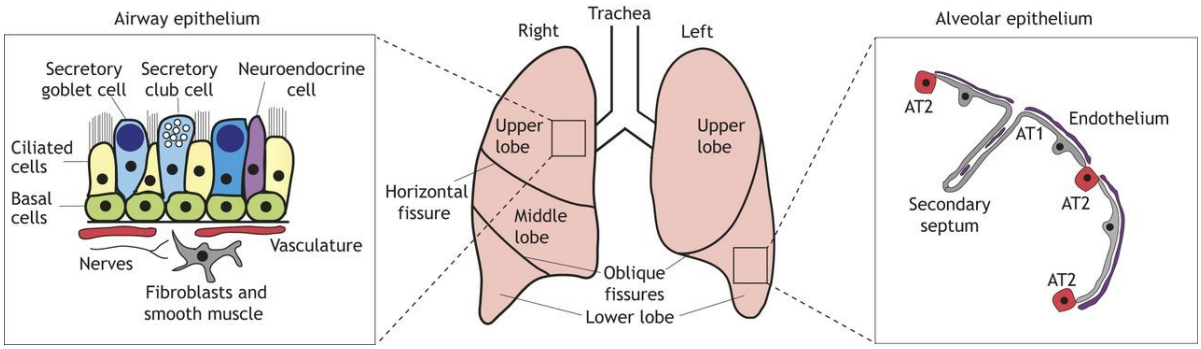


Figure 1-13. Various cells and their location within the lung. Different regions of the lung contain different cells in order for them to fulfil their primary function. The airway epithelium contains cells that allow mucus to be produced and be beaten out of the respiratory system, as well as a layer of basal cells present to differentiate into terminal cells as required. As the alveolar region is for gas exchange, the cell layer reflects that and is composed of a much thinner cell layer, allowing gas exchange across these cells. Immune cells are also present throughout the lungs, but at different concentrations within different regions. Reproduced from Nikolic et al. (2018b).

The cellular physiology of asthma and allergic airways disease depends on the region of interest and the function it has been designed to do (Figure 1-13). For example, in the normal lung, the larger airways have a thicker cell layer with smooth muscle and immune cells, while the alveolar region is made of a single cell layer of specialised cells that secrete surfactant (to stop the lungs from collapsing) and aim gas exchange from the pulmonary system to the cardiovascular. Thus the pathology reflects the site affected.

1.3.2.1 Epithelial barrier

Epithelial cells play an important role in the development of asthma and are the main barrier cells against airborne stress inducing factors, such as oxidative and mechanical stress, allergens, pollutants and viruses (Olin and Wechsler, 2014). Its barrier function is dependent on integrity of the cells and the interactions between these cells (Xiao et al., 2011). The epithelial barrier does this in a number of ways, but the production of type-II cytokines and cross talk and activation of dendritic cells are some of the main ways (Hammad and Lambrecht, 2015), while antimicrobial secretions, mucociliary apparatus and tight junctions physically stop interaction with the subepithelial tissues (Brune et al., 2015).

One of the major features of asthma is epithelial cell activation, and understanding the interactions is important in understanding the disease. The epithelium acts as a sensor of the external and local environment and is a sentinel compartment that maintains homeostasis. Damage to the epithelial layer (including cell shedding, cilia loss and mucus production (Manuyakorn et al., 2013)) plays a role in the airway remodelling that is a key feature of asthma. Altered epithelial behaviour is a major feature of asthma development, caused by increased injury via environmental exposures and a changed injury repair response (Holgate, 2013);

however these changes are not specific to asthma (Manuyakorn et al., 2013) and can be apparent in other airway diseases such as COPD (Tam et al., 2011), and cystic fibrosis (Hiemstra et al., 2015).

The normal epithelial layer in the large airways is composed of goblet cells (secretory cells that produce mucus, which contributes to the construction of a physical barrier to the outside world and a major part of the innate defence system (McCauley and Guasch, 2015)) and ciliated cells (the predominant cell in the airways arising from either basal or secretory cells (Knight and Holgate, 2003)). Each ciliated cell has in the region of 200 cilia per cell allowing sufficient beating to power the mucociliary escalator and clearance of debris out of the airways (Grainge and Davies, 2013). Ciliated cells form a segment of the mucociliary transport system and through their beating they transport foreign bodies trapped in the mucus back out of the respiratory system (Yaghi and Dolovich, 2016). Around 30% of the large airway epithelium is made up of basal cells, these cells anchor the epithelium to the matrix and protect the underlying stroma from the external environment (Rock et al., 2010). They are also important in airway repair as they are stem cells. Around 9% of the small airway epithelium is made up of club cells which produce multifunctional uteroglobin/club cell secretory protein (CC10); antiproteases such as secretory leukoprotease inhibitor; and other molecules important in lung defence and components of lung lining fluid (Rokicki et al., 2016). Club cells are also progenitor cells. In the respiratory units, and not thought to be important in asthma, type II alveolar epithelial cells can be characterised very easily by their distinctive cuboidal shape, numerous microvilli and secretory lamellar bodies which contain and secrete lung surfactant. While type I alveolar epithelial cells which line 95% of the epithelial surface are characterised by their very thin cytoplasm and facilitate gas exchange and passage of small molecules across the membrane (Crapo et al., 1982).

Epithelial cells are capable of interacting with, and activating, cells of the immune system through the release of chemokines, cytokines and by expressing certain receptors on the cell surface (Swindle et al., 2009). Any fault in these mechanisms has the potential to disrupt the airway homeostasis. It was found in a study by Blume et al. (2013) that the epithelial cells released cytokines in response to pollen exposure, but the physical properties of the cells were unchanged (the membrane integrity remained intact and the cellular characteristics did not change with the cytokine release). This allowed the physical barrier (the integrity of which depends on the formation of tight junctions (Wittekindt, 2017)) to remain intact and continue to defend against external factors. This barrier also stops the interaction of various

environmental particles with the surface of the epithelium. Surfactant is produced by type II alveolar epithelial cells. Surfactant consists of 90% lipid and 10% proteins. This allows pathogens etc. to then be cleared via the mucociliary clearance mechanisms (Proud and Leigh, 2011).

Airway epithelial cells express pattern recognition receptors (PRRs) which respond to pathogens via pathogen-associated molecular patterns (PAMPs) that are on their surface and to cell death and stress markers via damage-associated molecular markers (DAMPs) (Lambrecht and Hammad, 2012), such as histamine (Takizawa et al., 1995). This activation causes release of a number of chemokines and cytokines that have multiple downstream effects and have the potential to enhance the asthmatic phenotype. TNF-α, IL-1β, IL-8, IL-6, IL-25, IL-33, TSLP, GM-CSF and MCP-1 (which can be induced by viral and bacterial infections, non-proteolytic allergens, and fungal spores (Wittekindt, 2017)) are released and attract immune cells, including basophils, eosinophils, lymphocytes, dendritic cells and macrophages (Olin and Wechsler, 2014, Lambrecht and Hammad, 2014, Wittekindt, 2017, Proud and Leigh, 2011). IL-4 and IL-13 cause epithelial cells to respond to these chemokines by releasing GM-CSF, IL-8, CCL1, and CCL17 (which further attract neutrophils, eosinophils and T cells), but may also contribute to the further damage to epithelial cells (Lambrecht and Hammad, 2012), due to the interference these chemokines have on the tight junctions in the epithelial barrier (Wittekindt, 2017).

Toll-like receptor (TLR) 4 is a receptor on the surface of epithelial cells which can lead to the triggering of immune responses via allergens found in the air (LPS (found on the wall of gram-negative bacteria) (Alpizar et al., 2017) in low amounts activates a Th2 type response. At higher concentrations Th1 type responses are activated (Na et al., 2016)) and in house dust mites (HDM) for example, both directly and indirectly. TLRs signals result in the activation of NF-κB, which also contributes to the degradation of epithelial tight junctions (Wittekindt, 2017), TLR4 leads to the recruitment of neutrophils, eosinophils and basophils, while TLR2 and TLR5 lead to the activation of dendritic cells (Carlier et al., 2016).

Some allergens can cause damage to the tight junctions by proteolytic cleavage of occludin and claudin, allowing interstitial dendritic cells to access the air-liquid interface to sample more of the environmental material deposited at this site during which they potentially become activated more often. Low IL-13 levels leads to epithelial healing, while high IL-13 levels leans towards allergic sensitisation (Lambrecht and Hammad, 2014).

CCL20 and CCL2 production is activated by various allergens (including but not limited to), HDM inhalation causes the attraction of dendritic cells to the epithelial layer. CCL20 production

is initially simulated by TNF-α, but can also be released after IL-1β and IL-4 and IL-13 (Liu et al., 2018). Production of CCL20 depends on E3 ubiquitin ligase mideline-1, and as well as attracting dendritic cells to the site of secretion, CCL20 also causes activation of the dendritic cells (Lambrecht and Hammad, 2014, Reibman et al., 2003, Liu et al., 2018).

TSLP can induce secretory leukocyte protease inhibitor (SLPI) which can potentially activate the repair of epithelial cells and dampen the airway inflammatory process (Lambrecht and Hammad, 2012). The concentration of TSLP in the airways has also been shown to correlate with the severity of asthma in patients (Ying et al., 2005).

Damage to the epithelial layer, including epithelial shedding, is a significant process in the development of asthma and other inflammatory diseases; it is well established that abnormal epithelial repair mechanisms also contribute to the disease severity (Davies et al., 1999). In asthma, there is an increase in EGFR and loss to columnar epithelial cells, which is a normal repair process that is increased due to the induction of transforming growth factor-β (TGF-β) (Druilhe et al., 2008) and an increase in epithelial repair over time (Grainge and Davies, 2013). There are 40 times more stem cells present in asthmatic epithelium when compared to normal patients, which could be due to a number of different factors, including the increased need for stem cells due to the continuous injury and repair cycles found in this disease (Grainge and Davies, 2013). Basal cells are a form of stem cells and contribute to epithelial repair after injury. Changes to the genome of these cells (via epigenetic alternators due to environmental conditions, and genome mutations) can affect the susceptibility of the patient to airway remodelling (Rock et al., 2010). Changes to the equilibrium of basal injury and repair can lead to basal cell hyperplasia, epithelial hyperplasia, mucous cell hyperplasia, metaplasia and squamous metaplasia (Rock et al., 2010).

Epithelial cells can also internalise particles (as do macrophages); however this uptake varies between different types of epithelial cells. Alveolar type I cells have been found to internalise some nanoparticles at the same rate as macrophages *in vitro* (Ruenraroengsak and Tetley, 2015), while type II cells were slower to internalise the particles *in vitro* (Kuhn et al., 2014). In addition, the size of the particle determines the mechanism of its uptake (due to different endocytotic uptake mechanisms and passive uptake) (Kuhn et al., 2014, Adamson et al., 1990).

Injury to the epithelium by exogenous agents includes induction of cell death and tight junction degradation; in asthmatics, this injury is compounded by incomplete repair processes that mean the epithelial cell layer can never fully recover (Olin and Wechsler, 2014). Asthmatic patients

have a different tight junction profile (including patchy, incomplete, tight junctions and lower transepithelial membrane resistance involving low zonula occludens (ZO)-1 and E-cadherin (adhesion molecules)) when compared to the healthy control tissue (Xiao et al., 2011). Epithelial tight junctions contain claudins (cldn1) 2, 3, 4, 5, 7 and 8, but their intracellular location depends on the region of the airway in which the specific cell is present (Wittekindt, 2017). Loss of E-cadherin in patients with asthma is associated with an increase in TSLP production and causes an increase in the damage to epithelial cell layer (Lambrecht and Hammad, 2012). TSLP, IL-25 and IL-33 are all known as epithelial "alarmins", which are released by epithelial cells if there is perceived danger. Alarmins can activate numerous other cells, including dendritic cells. In addition, over production of these mediators leads to a feedback loop of epithelium damage and airway remodelling even if there is no "danger" present (Mitchell and O'Byrne, 2017). TNF-α and NF-κB have negative effects on the TJs (cldn2, 4, and 5) and inhibit ZO-1 formation; they can also interfere with the localisation of the TJ proteins within the epithelial cells, increasing the cellular permeability and causing the TJs to become leaky. This breakdown of tight junctions can go on to cause lung injury and eventually respiratory failure (Wittekindt, 2017).

1.3.2.2 Immune system activation

It has been well documented that following allergen challenges, the inflammatory profile of the lung changes and therefore the downstream activation of the immune system can also change depending on the challenge.

There are two main pathological components to asthma, the airway remodelling (including mucus production) and the inflammatory response. The disease develops through a combination of the action of different types of immune cells (from both the innate and adaptive immune system) and epithelial cells which cause an increase in bronchial hyper-reactivity (BHR) (Lambrecht and Hammad, 2015). Asthma exhibits a characteristic inflammatory cell profile involving a number of different types of immune cell, including eosinophils, neutrophils and mast cells (Gaffin et al., 2014). Both T cells and B cells play an important role in the development of asthma (Barnes, 2008). Lung biopsies from asthma patients show an increase in the levels of eosinophils, mast cells and T cells.

1.3.2.2.1 T cells

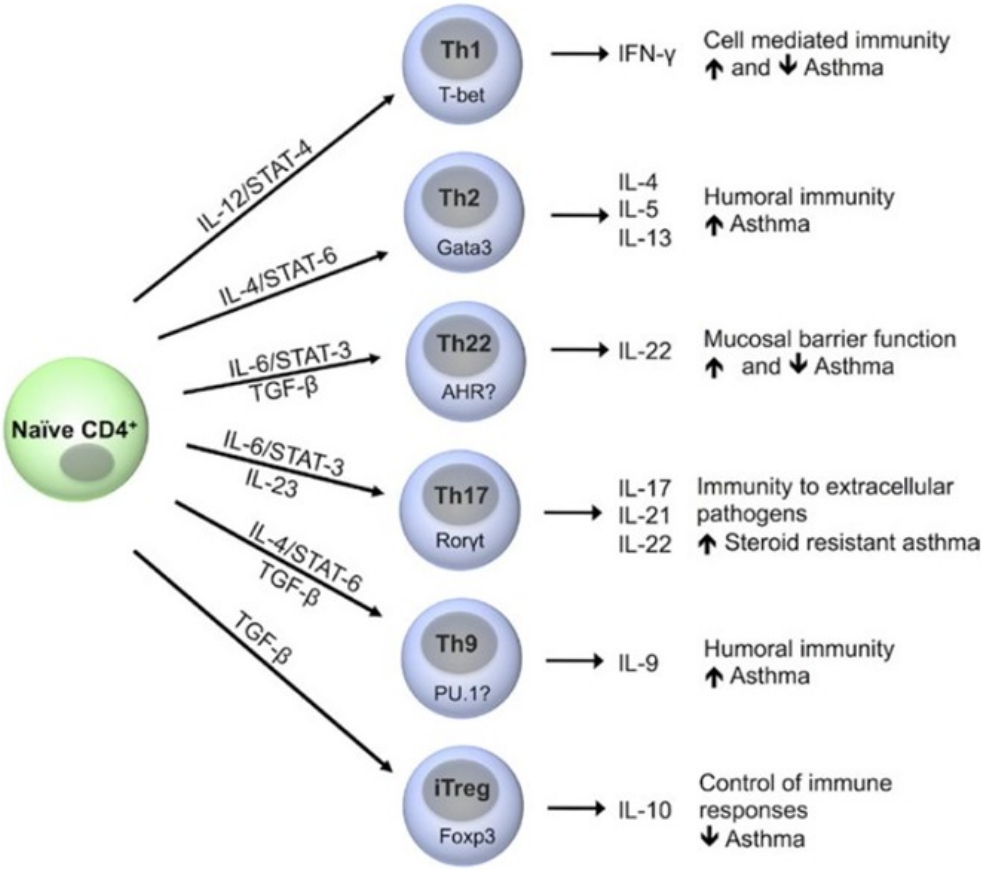


Figure 1-14. Subsets and differentiation of T cells. This figure shows the differentiation of CD4+ T cells after activation and what causes their differentiation. Horizontal arrows indicate cytokines are produced by these subsets and their functions. Reproduced from Tumes et al. (2017).

It is now becoming clear that there are multiple T cell types (Figure 1-14) that are active in asthma. It was previously thought that only Th2 cells were responsible as they produce IL-4, IL-5 and IL-13 cytokines which play an important role in the aetiology of asthma and type II inflammation. IL-4 is required for B cell isotype switching (in order to produce immunoglobulin E (IgE)) (Kato et al., 2013); IL-5 is known to be the main cytokine implemented in the activation of eosinophils (Farne et al., 2017); and IL-13 is an essential cytokine for the development of asthma (including mucus production, airway remodelling and airway hyperresponsiveness) (Corren, 2013, Olin and Wechsler, 2014).

Within atopic asthmatic airways there is a shift in the number of CD4 T cells both in the blood (Huang et al., 2017a) and in forced sputum (Kawayama et al., 2013) when compared to healthy patients. This is not completely true for all asthmatic patients as some have been found to have a neutrophilic phenotype (e.g. severe asthma) that is controlled by the Th17 response rather than the Th2 response (Lambrecht and Hammad, 2015). The Th2 responses require a dual

activation protocol which is composed of a “sensitisation” and a “reactivation” phase (Leomicronn, 2017).

IL-13 is released by Th2 cells, CD4 natural killer T cells, basophils and eosinophils, amongst others. In addition to IgE synthesis, it regulates goblet cell hyperplasia, mucus hypersecretion, airway hyperresponsiveness and fibrosis and induces airway epithelium to produce periostin (contributes to the thickening of the basal membrane (Izuhara et al., 2014) and inducible nitric oxide synthase (iNOS can lead to airway constriction, increased mucus production and downregulation of Th1 cytokines and upregulation of Th2 cytokines (Batra et al., 2007)). Exhaled NOS can be used as a marker for allergic asthma, due to its significant elevation in patients with the condition when compared to the normal control (Roos et al., 2014). IL-13 doesn’t attract eosinophils but induces epithelium to release eosinophil chemoattractants (Arron and Izuhara, 2015). Thus, IL-13 is an important mediator of asthma and remodelling of the airways in asthma.

Th17 cells are another subset of T cells that play a role in asthma development and treatment. Th17 T cells are stimulated by TGF-β with IL-6, IL-21, (Korn et al., 2007) or IL-23 (Aggarwal et al., 2003), differentiating T helper cells into Th17 cells which produce IL-17 and IL-22 (Chen and O'Shea, 2008). They produce IL-17 which interacts with and activates neutrophils causing a neutrophil predominant phenotype (Olin and Wechsler, 2014, Chesne et al., 2014) (Al-Ramli et al., 2009, Bullens et al., 2006) (Newcomb and Peebles, 2013), as well as inducing airway hyperresponsiveness (Kudo et al., 2012). Induction of AHR by IL-17 is due to regulation of secreted phospholipase A2 group X (sPLA2-X), an enzyme that is associated with AHR which increases with asthma severity (Hallstrand et al., 2013).

Regulatory T cells (Tregs) are thought to suppress normal Th2 allergen responses with the induction of Tregs modulating these responses (Robinson et al., 2004) and are allergen specific (Palomares et al., 2017). There are a $CD4^+$ T cell population (Martin-Orozco et al., 2017) that are induced by T cell activation by TGF-β and IL-2 (Chen et al., 2003) and can be split into two main groups; thymus derived (Tregs) and peripherally derived (pTregs) Tregs (Palomares et al., 2017). pTregs are found in the gastrointestinal tract and the lungs during chronic inflammatory episodes (Martin-Orozco et al., 2017), (Palomares et al., 2017). In a normal, healthy population, the Tregs act to suppress the immune system and therefore inhibit an allergic response to allergens that commonly activate the development of asthma (Martin-Orozco et al., 2017).

Th9 cells promote IL-9 production and contribute to mast cell activation and proliferation as well as airway remodelling (Ling and Luster, 2016, Monteyne et al., 1997, Hirahara and Nakayama, 2016). IL-9 has been associated with increases in epithelial mucus production (Soroosh and Doherty, 2009) including the induction of the mucus related gene *muc5ac* (Longphre et al., 1999), and airway remodelling (Soroosh and Doherty, 2009).

1.3.2.2.2 B cells

Antigen presentation by DCs is important in the activation of Th2 cells but is actually not completed without the antigen presenting activity of the B cell (Leomicronn, 2017).

B cells produce IgE, which is released in response to an allergen. IL-5 acts upon B cells and stimulates proliferation so helping maintain them. When exposed to IL-13 and IL-4, B cells use the CD40 ligand to bind to T cells and initiate the secretion of IgE into the environment. IgE then binds to mast cells and basophils to activate them to release their mediators (Olin and Wechsler, 2014).

Isotype switching to IgE production is tightly regulated and requires 2 signals, from either IL-4 or IL-13 and binding to the CD40 ligand found on T cells. The concentration of IgE in the blood is typically very low in healthy individuals and is tightly regulated (Stone, 2010). IgE plays a central role in atopic diseases (including asthma) as it plays a role in activating additional B cells, mast cells and basophils leading to the immune response and the release of histamine and potentially anaphylaxis (Xiong et al., 2012).

1.3.2.2.3 Type 2 Innate Lymphoid Cells (ILC2)

ILC2 cells are a recently identified cell type important in type II inflammatory response (characterised and named within the last 10 years (Spits et al., 2013)). These cells produce IL-4 IL-5, IL-13 and IL-9 and are activated by epithelial cytokines – specifically IL-33, IL-25 and TSLP (Gurram and Zhu, 2019, Kato, 2019, Akdis et al., 2020). They have been identified as being increased at mucosal barriers (the lung, gut and skin), but without antigen receptors that are present on T cell populations (Pasha et al., 2019). One major difference between TH2 and ILC2 cells is the fact that ILC2 activation is not dependant on MHCII (while TH2 activation is), meaning ILC2 cells can respond rapidly (compared to TH2 cells) to an infection and are determined as a first line of defence, but are also capable of having a memory component – ILC2s that have been previously exposed to an allergen respond quicker than naïve ILC2s (Martinez-Gonzalez et al., 2016).

There is evidence that ILC2 cells are responsible for the initial source of TH2 cytokines within allergic asthma and therefore initiate the downstream effects of the type II cytokines as well as activation of TH2 cells (Cosmi and Annunziato, 2017) and the other cells associated with airway inflammation (eosinophils, B cells, mast cell and macrophages) (Kato, 2019).

Therefore, the release of these type II cytokines from either TH2 or ILC2 cells can elicit the same downstream inflammatory response (Gurram and Zhu, 2019).

1.3.2.2.4 Eosinophils

Eosinophils can initiate the adaptive immune response by modulating DC migration, activation, and maturation (Travers and Rothenberg, 2015). They are derived from the bone marrow after stimulation by IL-3, IL-5 and GM-CSF (Her et al., 1991). They exit fully differentiated and enter tissues via the action of CC-chemokine receptor 3 (CCR3) (Rothenberg and Hogan, 2006). Attraction to mucosal tissues is due to eotaxin-1 (CCL11) (the most important chemoattractant (Shamri et al., 2011)) and Th2 cytokines (IL-5 and IL-13) (Travers and Rothenberg, 2015). IL-13 is important for eosinophil recruitment, while IL-5 sustains eosinophil levels through activation and prolonging cell survival. Once activated, eosinophils release cytokines such as IL-5, GM-CSF, and IL-13 (Shamri et al., 2011) that go on to influence the Th2 pathway (Olin and Wechsler, 2014).

1.3.2.2.5 Neutrophils

Neutrophils are one of the first immune defence systems that can kill pathogens that are inhaled due to their production of ROS, and release of granular proteases (Ray and Kolls, 2017). It has been documented that neutrophil influx is associated with an increase in asthma severity (Ray and Kolls, 2017, Moore et al., 2014); they are also associated with COPD (Paplinska-Goryca et al., 2018). Patients with a high sputum neutrophil count do not respond to steroids as a treatment (Green et al., 2002). Within a primary care setting it has been determined that around 8% of asthmatics have a neutrophilic phenotype (Brooks et al., 2017). Smoking (Polosa and Thomson, 2013) and obesity (in women only) (Scott et al., 2011) has been found to increase the neutrophil burden of the lung and worsens asthmatic symptoms. Pathogens have the potential to contribute to neutrophil survival within the airways (Ray and Kolls, 2017).

IL-8 (CXCL8) is a potent neutrophil chemoattractant which is secreted by epithelial cells, T cells ((Th17) (Olin and Wechsler, 2014)), and macrophages as well as neutrophils themselves. This causes a vicious cycle where once the neutrophils have been recruited to the airways it will continue (Gibson et al., 2001), particularly in the absence of other controlling factors.

When steroids are used to suppress asthma symptoms, eosinophils are suppressed (and apoptosis promoted) and neutrophils appear to be activated (Olin and Wechsler, 2014). Increases in neutrophil counts are commonly associated with early lung inflammatory responses, COPD and pulmonary injury (Wittekindt, 2017) as well as severe asthma (Ray and Kolls, 2017). Neutrophils have also been associated with airway remodelling, mucus hyperplasia and a decline in lung function (Ray and Kolls, 2017).

1.3.2.2.6 Macrophages

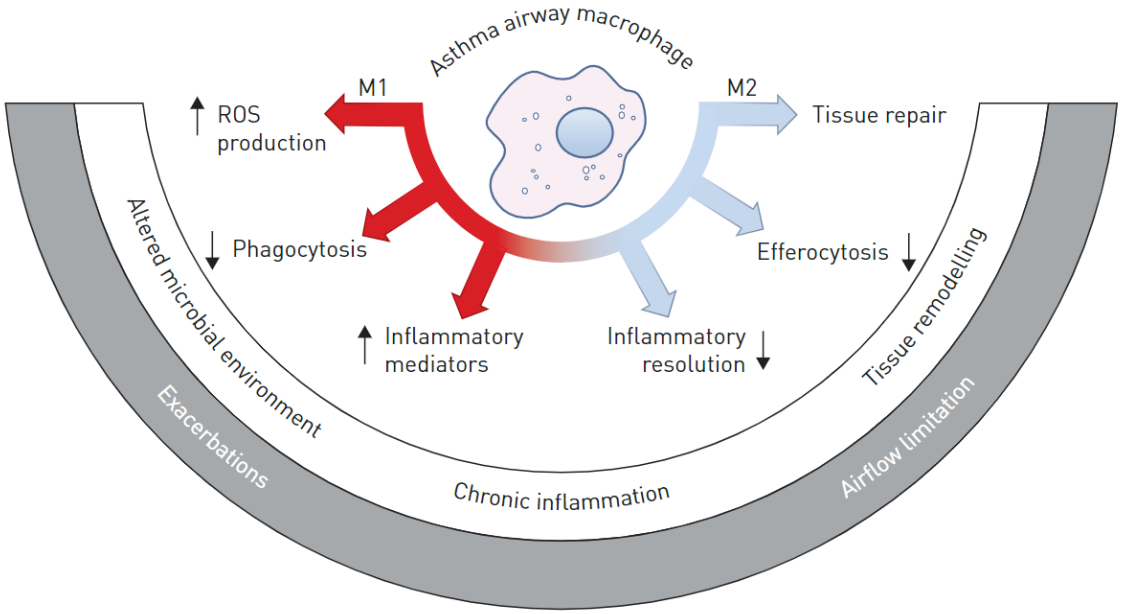


Figure 1-15. Macrophage functions within an allergic asthmatic airway. This figure shows the M1 and M2 subtypes of macrophages and their implications for the airways. Reproduced from Fricker and Gibson (2017).

M1 macrophages are classically activated macrophages and are activated by pro-inflammatory mediators (LPS, TNF-α and INF-γ), while M2 macrophages are alternatively activated macrophages and respond to Th2 cytokines (Fricker and Gibson, 2017, Saradna et al., 2018). It has been identified *in vitro* that macrophages can switch between the 2 states (Tarique et al., 2015) and, in fact, may exhibit properties of both (Figure 1-15).

There are different types of macrophages (which make up the majority of the pulmonary immune cells (Peters, 2014, Lumeng, 2016)) in the lung – bronchial, interstitial and alveolar macrophages. Alveolar macrophages (AMs) are found in the alveolar region, but there is not always a macrophage in every alveolus. AMs are derived from embryonic precursors and are replaced throughout life, they can also be replaced by IMs (Maus et al., 2006, Epelman et al., 2014). Alveolar macrophages can be located in other lung compartments, as they migrate back into the interstium and clear via the lymphatic system, as well as being cleared via the large

airway mucociliary system. These macrophages are a long lived population (Fricker and Gibson, 2017). Interstitial macrophages (IMs) are found in the parenchymal space and bronchial macrophages (BMs) are found in the larger airways (Kopf et al., 2015). It was traditionally thought that macrophages in the lung were derived from circulating monocytes, however, evidence now suggests that these various types of macrophages originate from a "distinct precursor" and cell surface markers allow these differences to be identified (Baharom et al., 2017).

There is a very limited change in the numbers of macrophages in an asthmatic lung, but it is thought that they may differentially contribute to the various phenotypes of asthma (Fricker and Gibson, 2017). The main role of macrophages is to recognise and destroy pathogens (via phagocytosis), and antigen presentation to further the immune response (via production of various mediators that then impact on the inflammatory cascade and the behaviour of epithelial cells).

Phagocytosis is an important mechanism that allows the destruction of pathogens that find their way into the airways. Without this there would potentially be more pathogens present within the airways, however it has been identified that the phagocytic capabilities of macrophages in the lungs of asthmatic patients are diminished (Jiang and Zhu, 2016). This is seen in adults as well as children, and is associated with an increase in asthmatic severity (Fitzpatrick et al., 2008).

Efferocytosis (where the macrophage takes up dead, apoptotic or stressed self-cells) is initiated by macrophages. This process is anti-inflammatory and involves reducing the release of damage-associated molecular patterns (DAMPs) and additional inflammatory mediators (Fricker and Gibson, 2017) by macrophages. It has also been found that this process is reduced in patients with an asthmatic phenotype (Huynh et al., 2005). Macrophages themselves also produce inflammatory mediators and macrophages from asthmatics have been found to produce more TNF-α, IL-1β, IL-6 and IL-8 when compared to healthy individuals (Tang et al., 1999). As previously mentioned, IL-10 is a cytokine that reduces the inflammatory response and has been found to be reduced in both the BAL and the macrophages of asthmatic patients (Fricker and Gibson, 2017).

1.3.2.2.7 Mast cells

Mast cells can be found throughout the vascular system and in particular near surfaces exposed to the external environment (lungs) (Koch et al., 2017). Mast cells are important in producing mediators such as histamine which is important in bronchoconstriction, vasodilation and allergic mediators. They are activated by the cross-linking of IgE which then goes on to induce degranulation and release of histamine, proteases and cytokines (Koch et al., 2017). They are controlled by the release of IL-9 (Olin and Wechsler, 2014), leading to enhanced mast cell survival and expansion when IL-9 is present. Mast cells also produce IL-9 (Koch et al., 2017), leading to a feedback loop. Activation of mast cells is known to play an important role in severe asthma (Hinks et al., 2015) due to their activation after binding IgE, as well as being sources of type II cytokines (Reber and Fahy, 2016). They can be categorised into MC_T and MC_{TC} depending on the protease content of the granules. The majority of mast cells found in the lungs are thought to be MC_T, with MC_{TC} mast cells found in connective tissue (like the skin) (Reber and Fahy, 2016). Mast cells within asthmatic sputum have also been used to identify if a patient would respond to corticosteroids (Wang et al., 2016).

1.3.2.2.8 Dendritic cells

Dendritic cells (DCs) are also elevated during asthma; they are constantly sampling the environment for antigens, which they can then process and present epitopes to the T cells which then become activated and in turn activate the downstream effects, such as T cell activation (Lambrecht and Hammad, 2015).

The lung has its own population of dendritic cells situated in the basolateral site of the lung (van Helden and Lambrecht, 2013) which play an important role in the development of asthma. They are antigen presenting cells that can link between the innate and adaptive immune responses (Qian and Cao, 2018) as well as lead to the activation of the immune response through the presentation to naive T lymphocytes of peptides derived/processed from inhaled antigens (Merad et al., 2013). They are the most potent antigen presenting cells within the airways (Leomicronn, 2017) and are crucial for the activation of T cells. As the epithelial cells are exposed to the external environment, so are DCs. They extend their dendrites between the airway epithelial cells and sample the environment at the air liquid interface, without disturbing the tight junctions of the epithelial cell layer (Lambrecht and Hammad, 2012). They are professional antigen presenting cells, so any material they encounter in the air they process and deliver to the draining mediastinal lymph nodes and present to naïve and immature T cells (van Helden and Lambrecht, 2013). The frequency with which DCs sample the environment depends on their

location in the airways (i.e. which airway generation). Alveolar DCs will sample more often than those in the larger airways (Kopf et al., 2015), this is due to the lower number of DCs found in the alveolar region when compared to the larger airways (Condon et al., 2011). There are various different subsets of DCs, conventional (cDCs), plasmacytoid (pDCs) and monocyte-derived dendritic cells (moDCs) (Lambrecht and Hammad, 2014, Kopf et al., 2015), but all DCs start their lives as undifferentiated cells in the bone marrow, they differentiate to pre-DCs which then enter the lung tissue and differentiate into mature dendritic cells. cDCs development is reliant on Flt3L; the mediators involved in the development of pDCs are not known, and moDCs development is dependent on monocyte-sensitive factors. These subsets have different T cell activation capabilities (Kopf et al., 2015). DCs are also stimulated by the epithelial cytokines that are released (IL-25, IL-33 and TSLP), and attracted to the epithelium (CCL20) and the area of stimulation (Olin and Wechsler, 2014). They produce IL-6, IL-33, IL-1β, and CCL17 after stimulation by various allergens (Lambrecht and Hammad, 2014).

Studies have identified that DCs need to be stimulated by epithelial cell mediators as well as antigens in order for them to activate and initiate the chronic inflammatory cascade (Lambrecht and Hammad, 2015).

1.3.2.3 Airway remodelling and airway hyperresponsiveness

Airway remodelling refers to the structural changes within the airway that occur during asthma (Figure 1-16). It includes injury of the epithelial cell layer, increased basement membrane thickness and smooth muscle tissue, blood vessel development and increased mucus production (Olin and Wechsler, 2014, Manuyakorn et al., 2013). Interestingly, repeated bronchoconstriction causes airway remodelling in asthmatic patients even in the absence of inflammation (Grainge et al., 2011). Originally thought to be due to inflammatory responses, anti-inflammatory drugs only have a limited effect in reducing airway remodelling (Holgate, 2013), and this fits with the knowledge that inflammation alone cannot explain all pathological features of asthma (Manuyakorn et al., 2013). It is not clear why the basement membrane increases in thickness,

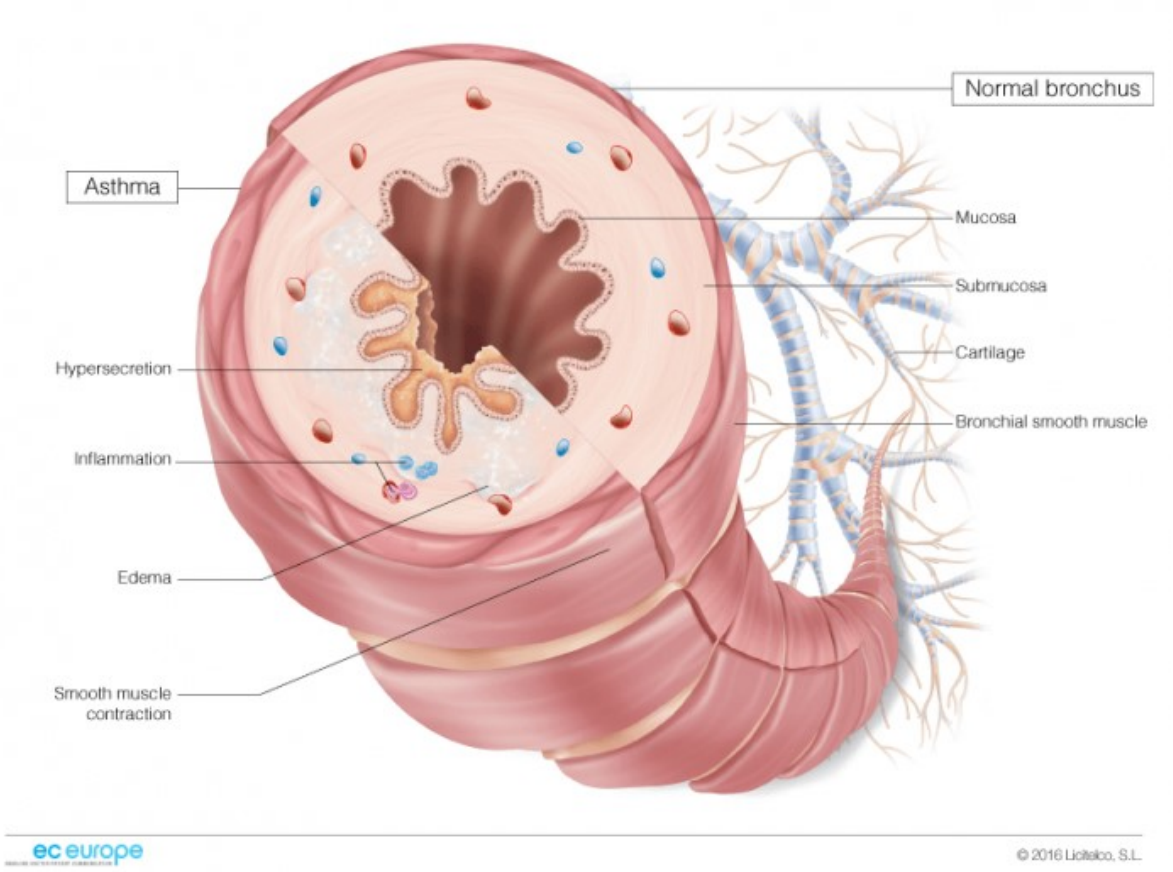


Figure 1-16. Asthmatic airway remodelling. Remodelling is the structural physical change of the airway. It is characterised by an increase in mucus production, an increase in smooth muscle and a decrease in the size of the airway. On the right of the airway depicted is a normal, healthy airway, with the left being an asthmatic airway after remodelling has taken place. Image reproduced from https://www.ec-europe.com/

but it is thought to be due to mediators generated by myofibroblasts (Gizycki et al., 1997). This thickening has been found to begin early in life and in the development of asthma (Manuyakorn et al., 2013). Decreased lung function may, at least in part, be due to thickening of the basement membrane (Lambrecht and Hammad, 2012).

Smooth muscle can also influence the inflammatory response by releasing its own inflammatory mediators that contribute to the inflammatory response. IL-5 release from smooth muscle has been demonstrated; when IL-5 is knocked out in animal models, there is no increase in smooth muscle mass in the airways. IL-13 receptors have also been identified on the surface of smooth muscle and can lead to the production of TGF-β as well as mucin production, fibrosis, airway hyperresponsiveness (Rael and Lockey, 2011) and increased smooth muscle contraction (Chiba et al., 2009). TGF-β is also secreted (chemoattractant of mast cells) by the smooth muscle (Doeing and Solway, 2013) and has the potential to induce smooth muscle cell differentiation (Guo and Chen, 2012). When both chemokines are released, they influence an increase in the proliferation as well as contraction of the smooth muscle, both key factors in the pathology of asthma.

Deep breaths can reverse the effects of bronchoconstriction, however patients with asthma are unable to perform these deep breaths. This mechanism is not fully understood. Increases in smooth muscle and basement membrane thickness are linked to airway hyperresponsiveness (AHR).

AHR is defined as "an exaggerated response of the airways to nonspecific stimuli, which results in airway obstruction" (Postma and Kerstjens, 1998) that would not induce the same effect in healthy lungs (Chapman and Irvin, 2015). In asthmatic patients, this nonspecific stimuli can be methacholine, histamine or even cold air (Postma and Kerstjens, 1998). Methacholine and histamine are known as direct stimuli and act directly on the smooth muscle, while exercise and cold air are indirect and work by mediator release from immune cells (Cockcroft and Davis, 2006, Brannan and Lougheed, 2012). AHR is used to contribute towards making a clinical diagnosis of asthma and bronchial provocation tests are completed within a clinical setting to determine the diagnosis of AHR and asthma (Brannan and Lougheed, 2012).

1.3.3 Aetiology and Pathophysiology

Traditionally there are two forms of asthma: allergic and non-allergic (intrinsic) asthma. The allergic form occurs in the majority of asthmatic children and around half of adult asthmatics. While the intrinsic form is found more often in older women as a complication of other diseases; this form is much harder to treat (Lambrecht and Hammad, 2015).

Due to the variation of these phenotypes, additional markers were then identified to classify patients. Phenotypes are defined as characteristics that result from numerous factors including the environment and genetics, while endotypes define the molecular mechanisms. Due to the

fact patients with identical symptoms may have different underlying mechanisms and respond to a treatment in various ways, this needs to be considered when identifying treatment regimens (Kuruvilla et al., 2019).

1.3.3.1 Asthma types

After much discussion over the categorisation of asthmatic patients, two major groups have been identified: Th2-high and non Th2-high groups, with the majority of patients falling into the Th2-high group (Kuruvilla et al., 2019).

The Th2-high group has the pathophysiology of a Th2 immune response and would be expected to have high concentrations of mediators such as TSLP, IL-25, IL-33, IL-4, IL-5 and IL-13, alongside activation of ILC2 cells to produce IL-5 and IL-13, recruitment of eosinophils, release of IgE and binding to both basophils and mast cells (Kuruvilla et al., 2019). This type of asthma can be classified as early-onset (allergic), late onset eosinophilic (intrinsic), and aspirin-exacerbated respiratory disease (AERD).

Non-Th2 or Th2-low asthma patients are identified by a lack of the Th2 markers that are found in the high Th2 group. Patients in this group can be classified as obesity associated and very late onset asthma (high neutrophil cell count). Measurement of interferon and tumour necrosis factor-alpha as well as inflammasome-associated markers have been used as biomarkers (Kuo et al., 2017), however, as it is a lack of biomarkers that is being used to identify the non-Th2 asthma phenotype, it is difficult to detect with current technologies. One possible marker may be sputum or blood neutrophil cell counts, but the clinical relevance of this count is still unknown (Kuruvilla et al., 2019).

Five phenotypes of asthma have been identified as: allergic, intrinsic, exercise induced (mainly neutrophilic), obesity related and Th17-related. It is important that the right phenotype is diagnosed so that the correct treatment or management plan can be implemented as soon as possible. This can sometimes be difficult as the phenotype of asthma can change as the patient matures or as the triggers change. The use of endotyping may help determine asthma type and thus the most suitable treatments and therapies for that patient (Landgraf-Rauf et al., 2016). The five henotypes of asthma can be categorised as follows (Olin and Wechsler, 2014):

- Allergic (high eosinophil and mast cell counts and IgE levels)
- Intrinsic (high eosinophil count, and IL-4,5 and 13 is in the blood)

- Exercise or aspirin induced (increase in mast cell counts, non-eosinophilic)
- Obesity related (small increase in Th2 responses)
- Th17 signature (high neutrophil count with a reduced Th2 response)

Classification of allergic and non-allergic asthma in school age children is commonly based on blood IgE levels (Landgraf-Rauf et al., 2016). While severity can be determined by a decrease in FEV(1)/FVC (Bacharier et al., 2004). Exacerbations of asthma are most commonly triggered by viral infections in children (Forno and Celedon, 2012), such as upper respiratory tract infection with, for example, rhinovirus (RV) (Barnes, 2008) and respiratory syncytial virus (RSV) (Gaffin et al., 2014, Jartti and Gern, 2017). It has also been found that under certain circumstances viral infections can also protect against the development of asthma (Celedón et al., 2003). House dust mite (HDM), pet dander (cats and dogs etc.), cockroach, rodents, mould, and air pollution exposure in early childhood have also been found to increase the risk in developing asthma (Gaffin et al., 2014). The different triggers of the exacerbations may cause increases in different immune cells and therefore a higher concentration of specific inflammatory mediators (Barnes, 2008, Ishmael, 2011, Holgate, 2011).

There are a number of highly effective treatments for those patients with "mild" asthma, however, those that suffer from severe asthma or asthmatics that smoke have a limited number of treatment options available to them as neutrophils are an important component of the inflammation and are more difficult to treat (Barnes, 2008). There are however overlaps between COPD and asthma and therefore potential therapeutics used for COPD could be applicable (Kim and Rhee, 2010).

1.3.3.2 Genetics of asthma

The difference between the sexes (higher prevalence in males than females) switches after adolescence and there is a higher prevalence of asthma in adult woman than men (Fuseini and Newcomb, 2017). The mechanisms involved are unclear, but it is thought that an increase in testosterone is linked to a decrease in asthma and allergies, while oestrogen has the opposite effect (Cephus et al., 2017, Fuseini and Newcomb, 2017). The impact of menopause and pregnancy (as these both cause changes in the oestrogen concentrations in the body) on allergy and asthma is still to be determined (Fuseini and Newcomb, 2017, Matteis et al., 2014).

In the last two decades there have been multiple studies aiming to identify potential genes that might be involved in the development of asthma. A disintegrin and metalloprotease 33

(ADAM33) is an example of one such gene. ADAM33 was identified after family-based studies were completed in many different populations and ethnicities and was the first asthma gene to be identified (Van Eerdewegh et al., 2002). There are now multiple genes that have been identified as being associated with asthma effecting different pathways but eliciting the same responses (Nieuwenhuis et al., 2016). ADAM33 expression was found in smooth muscle, fibroblasts and myofibroblasts but not in epithelial cells, and polymorphisms were linked to AHR and decline in lung function (Holgate et al., 2006). The soluble form has been identified as a biomarker of asthma, as it was detected in the bronchoalveolar lavage (BAL) fluid of asthma patients, but not normal healthy control subjects (Lee et al., 2006). There is a potential for gene targeting of ADAM33 for therapeutic treatments of asthma (Davies et al., 2016).

IL-13 is an important cytokine in the development of asthma leading to numerous investigations into possible genetic factors relating to the development of asthma. It was discovered that polymorphisms in IL-13 (specifically a single nucleotide polymorphism (SNP) – rs1800925) were significantly related to IgE serum concentration and eosinophil infiltration in certain populations (Hunninghake et al., 2007).

1.3.3.3 Environmental considerations for development of asthma

Asthma cases have increased in the last 40 years, which cannot be put down to the inherent genetic predisposition alone; this implicates environmental factors in the development of asthma (Hansbro et al., 2014).

The hallmarks of asthma, airway hyperresponsiveness (AHR) and allergen responses have genetic links, but the environment also plays an important part. Specifically the environmental exposures *in utero* and in very early life are important (Holgate et al., 2006).

A higher number of boys are affected by asthma between the ages of 8-14 years compared to girls. The boys with asthma are also shorter when compared to age-matched boys without asthma (Protudjer et al., 2015). Again, inner city children with asthma are mostly male, often with damp homes and potentially open gas stoves (Yang et al., 2015), possible environmental triggers.

A number of environmental causes have been studied and have been found to be beneficial, detrimental or have no effect at all in the development of asthma. The potential to develop or aggravate asthma varies greatly, this means the genotype and endotype of the patient is important. It is a complex mixture of many factors which exhibit as asthma.

Early life environmental exposures are mostly contained to indoor environments as that is where children spend the most of their time. Thus, in those with allergic asthma there is a strong connection between early environmental allergen exposures and asthma in childhood and into adulthood when compared to children that have not been sensitised (Gaffin et al., 2014, Balmes, 2009). Studies of numerous birth cohorts support the relationship between allergies and asthma. In addition, children of parents that showed allergic phenotypes were also at a higher risk of developing asthma (Kusel et al., 2007).

Air pollution, as previously noted, is increasing throughout the world, associated with increased respiratory health effects. Air pollution has been associated with a decrease in lung function and an increase in new onsets of asthma (Guarnieri and Balmes, 2014, Balmes, 2009). Various cohorts have shown maternal exposure to air pollution has impacted offspring health (Baiz et al., 2011, Peters et al., 2013). Thus, in addition to classic, well known allergens, evidence suggests that early exposure to air pollution *in utero*, and in young children, may induce allergic asthma. This has yet to be proven unequivocally.

1.3.3.3.1 Pest and pet exposure

House dust mites (HDM) are found throughout the home mostly in soft furnishings, this makes it one of the most important indoor allergens for the development of asthma and allergic rhinitis (Calderón et al., 2015). They have approximately 20 different allergens that induce IgE responses in humans (Lambrecht and Hammad, 2014). Exposure to HDM can promote the development of asthma in a dose dependant manor (Platts-Mills et al., 2001), and it is thought that up to 50% of asthmatic patients are sensitive to HDM (Calderón et al., 2015). It is proteases found in the gut and saliva of the mite that induce the allergy (Gautier and Charpin, 2017). The timespan in children that were at the highest risk for exposure to HDM and potential development of asthma was before the first 5 years of life, and specifically the 1st year of life (Gaffin et al., 2014). Sensitivity to HDM in early life is an indicator of poor lung function in future life even if asthma has not developed (Ulrik and Backer, 1999).

An additional pest that can cause allergic sensitisation is the cockroach, via essentially the same mechanisms as those for HDM. However, the likelihood of exposure is confined to those in areas with a high human population density, in poorer areas and older buildings (Gaffin et al., 2014). Pets, both cats and dogs, are a source of allergens, in their dander and saliva, which, perhaps surprisingly, are found in non-pet households as well as in pet free public places. This may explain, in part, why there is a similar sensitivity rate to pet dander/saliva between children who

have pets and those who do not (Zahradnik and Raulf, 2014). There are many more studies of cat households compared to canine households, but in fact evidence suggests that living with a dog at home reduces the potential for asthma development (Fall et al., 2015), and ergo that cats are responsible for more allergies and allergic asthma than dogs (Gautier and Charpin, 2017).

1.3.3.3.2 Environmental tobacco smoke (ETS) exposure

Passive/bystander exposure to environmental tobacco smoke (ETS), or second-hand smoke, affects those who do not smoke, adults and especially children, and there is increasing evidence that it has significant health effects. A recent review (Strzelak et al., 2018) discusses how ETS stimulates oxidative stress and reactive oxidative species (ROS) and inflammatory cytokines (such as IL-8, IL-6 and TNF-α). Such processes might also affect future generations as a child has a higher risk of asthma or allergy development if their grandmother smoked while pregnant with their mother (Li et al., 2005).

The mechanisms of active smoking and the effects it has on the development and exacerbation of asthma is currently unknown, but it is thought to increase the concentration of IgE in the blood and lead to oxidative stress activating neutrophils and macrophages (Kuruvilla et al., 2019).

1.3.3.3.3 Exercise and outdoor

It is well documented that asthma can be triggered by exercise (exercise-induced bronchoconstriction (EIB)); with atopy the main risk factor for the development of EIB (Caggiano et al., 2017). Swimming is the sport that is deemed to have the highest risk for asthma development compared to other sports. However, this could be due to a number of other reasons, including the use of chemicals within the training area and the additional pressure placed on the respiratory system (Mountjoy et al., 2015). Possible mechanisms of exercise-induced asthma include drying of the airways (due to the changes in temperature causing vasoconstriction while exercising and then rapid warming post exercise (Anderson and Kippelen, 2010)), genetic links (EIB is linked with a water channel – aquaporin 5 (Moreira et al., 2011)), release of mediators (substance P inhibits inflammation and has been identified after exercise (Lind et al., 1996)), and prostaglandins and histamine (Caggiano et al., 2017). Taken together, there are elements of epithelial sensitivity, inflammatory mediator release and genetic links that can be used to identify the potential susceptibility of an asthmatic (Moreira et al., 2011).

Weather and altitude also play a role in triggering, with both extreme hot and cold temperatures triggering exacerbations. Higher altitude reduces the risks of exacerbations, possibly due to a reduction in airborne allergens (Gautier and Charpin, 2017). Where the cold is thought to cool the airways and cause dehydration, this leads to inflammatory mediator release along with airway smooth muscle contraction (Anderson and Daviskas, 2000).

1.3.3.3.4 Infections

Viral infections during infancy have long been linked with the development of asthma and are the largest asthmatic trigger in children (Gautier and Charpin, 2017). Those children that go on to develop asthma have experienced more severe viral infections compared to those that have not, as viral load stimulates the immune system in such a way that eventually leads to the allergic phenotype and asthma (Gaffin et al., 2014).

The two viruses that are commonly associated with bronchiolitis (there is an association between bronchiolitis in the first year of life and the development of asthma) are respiratory syncytial virus (RSV) and human rhinovirus (RV) (Lemanske et al., 2005). RSV bronchiolitis is a strong indicator of those children that will go on to develop asthma (Lemanske et al., 2005). There is evidence that one RSV infection can cause acute and chronic changes in the airway epithelium and the future immune cell attraction (Gaffin et al., 2014). There is not enough evidence to certainly say that this is a causal relationship, as some studies suggest that there are other factors that play into this relationship (Stensballe et al., 2009) such as the severity of the illness, when the virus was caught (the younger the patient catches the virus, the more likely they are to develop asthma) and if the patient has a predisposition to that virus (Saglani, 2013).

1.3.3.3.5 Food and Obesity

Diet is important in several diseases and being overweight or obese has a significant, but weak, correlation with the development of asthma (Wang et al., 2014, Papoutsakis et al., 2013). Although a potential link between lung function, wheeze, asthma and adiposity (BMI) (Wang et al., 2014) has been described, significantly more studies are needed to confirm any correlation between obesity and asthma (Papoutsakis et al., 2013). Additional studies have investigated potential differences between allergic and non-allergic asthma and weight suggesting a potential link between high body weight and non-allergic asthma, but not allergic asthma (Papoutsakis et al., 2013).

Food allergies are also associated with the development of asthma, and it is now well known that having a food allergy increases the risk for development of asthma and increases the severity of the asthma if developed (Foong et al., 2017). Addition of both vitamin D and E to the maternal diet have been shown to reduce wheezing in offspring (Gray et al., 2017). Vitamin D supplementation has been related to reduction in asthma exacerbations and steroid therapies, however the majority of the studies that have identified this are observational (Sutherland et al., 2010, Searing et al., 2010, Majak et al., 2011).

It is becoming more apparent that early life and the mother's early life is potentially important in the development of asthma. As well as environmental exposures in the home, there is also a link between breast milk and either the development of asthma (Lowe et al., 2006, Lim and Kobzik, 2009), protection from asthma (Scholtens et al., 2009, Oddy, 2017), or no effect on asthma (Ek et al., 2018). Analysis of breast milk from breastfeeding mothers who were either allergic or non-allergic indicated that 19 proteins (out of 364) were different in the allergic mother compared to the non-allergic mothers. These proteins have been suggested, but not yet proven, to be linked with the development of allergy and asthma (Hettinga et al., 2015).

1.3.3.3.6 Microbiome

The importance of the microbiome and influence of the environment on this is under intensive investigation. Microbial exposure in early life is very important, but the effect of these exposures can vary depending on the biological background: genetic, environmental, geographical and microbiome populations (van Tilburg Bernardes and Arrieta, 2017). The exposure to farm related microbes at a young age has been found to reduce the risk of asthma development (Fall et al., 2015, Gray et al., 2017). Increased exposure to these microbes at a young age allows the development of a varied microbiota leading to tolerance of these potential asthmatic triggers instead of activation of the immune system when exposed to them or other foreign particles in later life and the development of asthma (Smits et al., 2016). The more diverse the microbiota exposed to, the less likely the pathways to activate asthmatic symptoms are activated (von Mutius, 2016). The gut microbiome has also been identified as influencing the development of allergic diseases including asthma, therefore it also needs to be considered when investigating asthma development risk factors (Smits et al., 2016).

1.4 Air pollution and burden of disease

1.4.1 Susceptible populations

There are some populations of the public that may be more susceptible to the effects of air pollution than a normal healthy person. Increases in air pollutants are linked to an increase in, and exacerbations of, many different disorders in a number of different systems, including the brain, lung, heart, immune and reproductive system (Curtis et al., 2006).

1.4.1.1 Age

The young are a group that have the potential to be greatly affected by air pollution (both after birth and *in utero*) and its various components. There is still a legacy of people developing asthma today which is attributed to the London smog of 1952, as they were in the womb at the time of the event (Bharadwaj et al., 2016). Household air pollution exposure *in utero* has been linked to a reduction of pulmonary function in infants (Lee et al., 2018) as well as outdoor pollution exposure *in utero* (Paulin and Hansel, 2016). Exposure to episodes of high air pollution before 18 years of age can lead to clinically significant decreases in lung function and FEV1 (Gauderman et al., 2004, Schultz et al., 2015).

Children in high traffic or pollution areas are also thought to be at risk of developing exacerbations and asthma like conditions. Living closer to roads has been found to be associated with lower lung function, asthma, and other allergic conditions (hay fever, and eczema for example) in children between the ages of 4 and 6 (Morgenstern et al., 2008) and in children around the ages of 8 that have been followed since birth (Rice et al., 2016). These negative effects are found into adolescence and within a cohort of children aged 16. There appears to be more of a decrease in lung function in males in this age group when compared to the females (Schultz et al., 2016).

1.4.1.2 Cardiovascular patients

There is a relationship between exposure to diesel exhaust and DEP in human studies and cardiovascular endpoints (Ghio et al., 2012). Air pollution has been found to increase the propensity towards blood coagulation and therefore increase in related cardiovascular deaths, particularly in an elderly population (Seaton et al., 1995, Bourdrel et al., 2017, Franklin et al., 2015, Costa et al., 2017, Landrigan, 2017). Increased blood clotting can lead to a number of downstream effects, including heart attacks and strokes (Robertson and Miller, 2018a).

An important early study (Schwartz, 1994) in a population from Philadelphia, USA, showed that high pollution events were related to adverse health effects. There was an increase in both cardiovascular deaths and respiratory deaths. There was also an increase in stroke deaths. This indicated that there was a strong link between respiratory and the cardiovascular deaths. This was the same pattern as was seen in London in 1952 – one difference between the two being the ambient environmental temperature, which indicates that the temperature has no impact on the potential effects of air pollution on vulnerable populations. The other difference between the two was the nature and composition of the pollution, indicating that inhalation of air pollution (regardless of source) has the potential to affect the respiratory system and have knock-on effects for other organs. As previously mentioned, ozone and NO_x are important, but the majority of studies have focused on particulate matter. Further investigation is required to determine the potential effects that gaseous components of air pollution might have on the cardiovascular system (Robertson and Miller, 2018a).

1.4.1.3 Cancer development

Cancer has also been found to be linked to atmospheric particles, and there is a significant increase in cancers after exposure to outdoor air pollution (Curtis et al., 2006), which have previously been linked to smoking (Wong et al., 2014),with respiratory cancer (nasopharyngeal, small cell lung carcinoma and non-small cell lung carcinoma) incidences on the rise in "under developed" countries due to the increased air pollution in these areas when compared to the West (Ding et al., 2015). Lung cancer is one of the most diagnosed cancers, but has one of the lowest survival rates (Hart, 2016) and therefore anything that enhances the potential to cause these cancers (as well as others), needs to be fully assessed.

After exposure to indoor air pollution there has been found to be an association between exposure and cervical, oral, nasopharyngeal and laryngeal cancers (Josyula et al., 2015), breast cancer incidence has been found to have a positive association with an increase in NO_x after assessment of 15 different cohorts (Schmidt, 2018), and various breast cancer subtypes (Reding et al., 2015).

1.4.2 Effects of air pollutants on the respiratory system, including asthma and allergic airway disease

When analysing epidemiology studies of asthma and pollution, it is very difficult to tease out the effects that indoor air pollution may have and which may have been caused by outdoor pollution, as both are equally important (Gaffin et al., 2014). Air pollution causes asthma

exacerbation, with particulates, exhausts and ozone the most important of the previously mentioned air pollution components (D'Amato et al., 2016). It is also difficult to establish links between air pollution and airway effects due to small cohort sizes and lack of consistency between studies (Bowatte et al., 2016, Burte et al., 2016).

There is increasing evidence for an association between increased air pollution exposure and exacerbation of asthma (Gowers et al., 2012, Guarnieri and Balmes, 2014, Tian et al., 2017, Palczynski and Kuna, 2015, Peden, 2018). However, the relative contribution of each component of the air pollution to the development of the condition is less well understood as in epidemiology it is difficult to separate the effects of component parts, such as particles and NO_2; nevertheless, there is the potential for susceptible individuals to become sensitised to any of the components (Bice et al., 2000). The U.K.'s Committee on the Medical Effects of Air Pollutants (COMEAP statements 2008-2010) has established that evidence supports the possibility that air pollution may play a role in the development of asthma in populations living close to heavy traffic (Gowers et al., 2012) and more recent studies have also suggested these links (Kelly and Fussell, 2015a, Gruzieva et al., 2014). Once lung function has decreased due to exposure to episodes of high air pollution, even after that air pollution has been resolved, there is no increase in lung function back to levels of people not exposed to high levels (Santos et al., 2016, Yanagita et al., 2013), indicating that this reduction is irreversible. However, this reduction in lung function has been seen to reverse in children (between 11 and 15), except in the group of children that originally had the lowest lung function at the start of the study (Gauderman et al., 2015).

The majority of studies have focused on children and have linked the increased incidence of respiratory health issues with high air pollution. There have been interactions between GST genes (specifically glutathione S-transferase pi 1 (GSTP1)) and a decrease in lung function and air pollution (Bowatte et al., 2016) within large birth cohorts established (MacIntyre et al., 2014). The elderly are also significantly affected by particulate matter (Curtis et al., 2006). This may reflect an immature immune system in the young, and an ageing/compromised immune system in the elderly. The exact mechanisms by which air pollution has its effects is still unknown and further research is needed into the different components and specific mechanisms as well as potential polymorphisms that may influence the mechanisms (Bice et al., 2000, Moller et al., 2008). Decreases in lung function have been identified after exposures from various air pollutants (particles, nitrogen dioxide and acid vapour) suggesting common pathways/outcomes that do not appear to improve when the pollutants are removed (D'Amato et al., 2016).

1.4.2.1 Particulate matter

There is a known association between exposure to PM2.5 and exacerbation of allergic asthma (Yang et al., 2014), airborne dust is known to influence asthmatic conditions in subjects miles from its source (Curtis et al., 2006) due to relocation on the wind. An asthmatic may not only be reacting to the increased levels of particulate matter in their environment but also to the increased volume of pollutant gas that is produced through the combustion of diesel engines, such as NO_2 (Svartengren et al., 2000). Given that air pollution is far from a uniform exposure type it is important to investigate how individual components within such a complex mixture of particles and chemicals affect exacerbation and potentially the development of this disease; although limits of exposure have been set, PM10 concentrations that are below the American EPA standards still have an impact on childhood asthma (Curtis et al., 2006). Polycyclic aromatic hydrocarbons (PAHs) are found within particulate matter and are known to activate the aryl hydrocarbon receptor (AHR), which has the potential to cause an over production of ROS (via the CYP1A enzyme system (among others)) and therefore oxidative stress within the airways (Vogel et al., 2020). This effect is particularly seen within the lung due to the high abundance of cells that utilise the CYP enzyme pathway. It also regulates MUC5AC and has the potential to cause an increase of mucus production (Wong et al., 2010). Another antioxidant gene (glutathione S-transferase Mu 1 (GSTM1)) has been thoroughly characterised as it has been associated with an increased risk of inflammation within the lung (established from epidemiology studies, human studies, *in vivo* and *in vitro* studies) (Wu et al., 2012).

1.4.2.2 Gases

There are conflicting views that the gaseous components of air pollution can cause adverse health effects independently from particulate matter. The Committee on the Medical Effects of Air Pollution (COMEAP) suggested that evidence from epidemiological studies indicated that NO_2 itself had the potential to cause detrimental impacts to health (COMEAP, 2015). A study was completed in the streets of Edinburgh that determined there was a significant difference in the concentration of NO_2 1.2m from the kerb at adult and child height, indicating that children were at more risk of inhaling a higher concentration of NO_2 compared to the adults with them (Kenagy et al., 2016). Others have identified that these splits are not so clear cut and that it may not be NO_x that is causing adverse health effects. Any studies that try to separate PM and NO_x may have effects on the outcomes of PM alone when compared to exposures to PM+NO_x (Maynard, 2015).

CO, O_3, and SO_2 have effects on childhood asthma at concentrations that are below the American EPA standards (Curtis et al., 2006). Specifically TNF gene expression has been found

to be increased in children after exposure to ozone leading to downstream increases in lung inflammation and asthmatic prevalence (London, 2007).

1.4.2.3 Pollen and Moulds

Higher levels of pollen and mould can increase incidences of asthma exacerbations (Curtis et al., 2006, DellaValle et al., 2012, Osborne et al., 2017), and moulds have been associated with an increased risk of exacerbating both COPD and asthma (D'Amato et al., 2016, Sinclair et al., 2018). As the relationship between air pollution and asthma is difficult to identify, pollen allergy is used as a substitute marker (D'Amato et al., 2015). Pollen exposure has been linked to acute exacerbation events for those already diagnosed with asthma, however, the prevalence of asthma or allergic rhinitis in areas is not increased in areas with a high pollen count (Marchetti et al., 2017).

1.4.3 Diesel exhaust particles (including ultrafines) and effects on asthma

Diesel exhaust particles (DEP) are now considered to be the major source of pollution of major concern in urban environments. It usually makes up 25% of the mass of emissions from the diesel engine. Around 95% of the particles are fine particles ($PM_{2.5}$) (Kittelson, 1998) and the remainder are ultrafine particles (Ghio et al., 2012, Fiebig et al., 2014). The concentrations of DEP in Europe has increased since the use of diesel fuel began in the early 20th century until 2015 as the number of diesel engines in use increased.

Exposure to DEP can not only exacerbate asthmatic symptoms, but has the potential to cause the development of asthma and allergy (Guarnieri and Balmes, 2014). Exposure to particulate matter and specifically diesel exhaust particles is known to have an association with the development of asthma in early years of life, specifically before 3 years of life with an increase in allergies before 4 years (Codispoti et al., 2015). DEP exposure before a child's 1st birthday has been linked to sensitisation to DEP at 3-4 years old (Codispoti et al., 2015). There have been a number of studies that have analysed this relationship (exposure at a young age and DEP) by estimating the exposure to various modes of traffic, health visits and questionnaires (Ryan et al., 2007, Li et al., 2017). Early exposure to DEP alone does not induce asthma. There needs to be a co-stimulation with an allergen (potentially HDM or pet dander) (Pandya et al., 2002). Thus, children with allergic asthma (indicated by a positive skin prick test for aeroallergens (pollens, dander and HDM) or a doctor's diagnosis) that have been exposed to DEP have a higher concentration of IL-17A in their blood when compared to the control (lower concentration DEP exposed) group, possibly reflecting involvement of DEP in previous allergic

exposures (Brandt et al., 2013b). DEP have been found not to induce a specific Th2 response themselves but act as an adjuvant to move the immune response towards a Th2/TH17 response (Finkelman, 2014). When human asthmatic studies have been completed there was a lack of inflammatory responses to DEP alone (Ghio et al., 2012). From these human studies, results taken together suggest that DEP does not induce allergic responses itself but requires an allergen to act as an adjuvant in order to elicit a response.

Studies of human exposure tend to focus on one component of air pollution, which is not representative of a real-life exposure. It is difficult to get ethical approval to investigate the most vulnerable of the population and the studies often tend to employ small subject numbers. Such investigations do have the benefit of employing incredibly clear exposure conditions (concentrations and duration) measuring a wide range of end points (Ghio et al., 2012). In one of the earlier studies, after 1 hour exposure to diesel exhaust, there was an increase in the inflammatory fingerprint 6 hours after the subjects were exposed, including increases in neutrophils, mast cells and T cells in both the BAL and the lung tissue (Salvi et al., 1999); however, there were no changes to lung function in these volunteers (Salvi et al., 2000). After two consecutive 2 hour exposures (100μg/m^3), there was no change in proliferation or apoptosis of the bronchial epithelium in moderate or mild asthmatics or the normal volunteers (Behndig et al., 2015). After a single higher exposure (300μg/m^3) and a recovery period it was determined that DEP stimulated BAL/sputum eosinophils, IL-5 and eosinophil cationic protein (ECP) in the allergic groups and contributed to increases in monocyte chemotactic protein (MCP-1) and macrophage suppression (Carlsten et al., 2016). This was also reflected after a slightly longer recovery period, and with the added effect of exposure during high or low intensity cycling (Giles et al., 2018). When there was a longer period (of 4 weeks) between the two exposures, there was again no significant change in IL-6, TNF-α or neurological markers in healthy volunteers (Cliff et al., 2016). These results taken together suggest that DEP has no immune effect on healthy volunteers either straight after exposures or after a recovery period, but it does influence the effects asthma already has on the airways. Biological effects seen after exposure to either the whole diesel exhaust (gas and particle mixture) or DEPs (the particulate matter alone) is thought to be due to their production of oxidative stress and reactive oxygen species (Ghio et al., 2012, Lawal, 2018, Ovrevik et al., 2017, Kim et al., 2014a, Chio et al., 2007).

1.5 Impact of nanomaterials on Asthma and Allergic airway disease

As well as the impacts air pollutants may have on asthmatics and allergic diseases, the potential impact of nanoparticles alone also needs to be established and studied. This can be done via a

variety of routes (either different inhalation methods or via different models of asthma or allergic airway disease). The majority of these studies have been completed *in vivo* which comes with its own set of problems but is also established as an important tool for determining the potential impacts of these materials.

1.5.1 Impact of nanomaterials on human asthma (human exposure studies)

There have been few studies done on asthmatic patients with nanomaterials, as the majority have been completed on healthy volunteers – this is due to the potential life-threatening effects these particles might have and ethical approval may be difficult to achieve.

When healthy volunteers were exposed to gold nanoparticles there were no effects on the lungs, but there were however cardiovascular effects (Miller et al., 2017) indicating that these particles are able to translocate throughout the body after inhalation. When asthmatic volunteers were exposed to spark generated carbon at rest and while exercising there was no significant changes between the healthy and the asthmatic subjects (Frampton Mark et al., 2006). This was also reflected when the same populations were exposed to collected ultrafine particles from Los Angeles (Gong et al., 2008).

1.5.2 Adjuvant effects of nanomaterials on experimental models of allergic airway disease

Adjuvant models are those models that investigate the potential for a substance or substances to contribute to the development of asthma along with an allergen (such as HDM, animal dander, various nuts and pollens).

Dendritic and T cell interaction have been investigated using both *in vitro* and *in vivo* models of carbon nanoparticle (CNP) exposure and show increased proliferation of both cell types (de Haar et al., 2008). The response was size dependant (as observed with other nanomaterials), where smaller particles (smaller than 25nm) elicited an effect and larger particles did not (larger than 25nm), both *in vivo* and *in vitro* (Koike et al., 2008, Chen et al., 2013a, Hirai et al., 2012). An increase in reactive oxygen species (ROS) and smaller particle nanosize were identified as being related to the increased proliferative response (Nakanishi et al., 2016). The surface chemistry of the particles has also been found to play a role in the differentiation of T cells. TiO_2NPs have been identified as inducing a Th1 profile, while CeO_2NPs have been identified as inducing a Th2 profile (Schanen et al., 2013). This could be due to differences in the particle-specific surface chemistry. The NLRP3 inflammasome which has been demonstrated to be increased in asthma,

is now thought to play a role in the responses of nanoparticles including silver, titanium, silicon and carbon (Mishra et al., 2016, Baron et al., 2015, Sager et al., 2013).

1.5.3 Exacerbation effects of nanomaterials on experimental models of allergic airway disease

Exacerbation models are those models that investigate the potential for a substance or substances to cause an exacerbation of the asthmatic or allergic phenotype once it has already been established after exposure to an allergen. Within these models, the majority exhibit a Th2 type response with IgE production from B cells and FCERIα receptor binding initiating inflammatory responses when in contact with the allergen. With established immune responses, there are already activated cells and airway remodelling that is not present in the adjuvant model or healthy models. TiO_2NPs and AgNPs have been found to induce the release of histamine (Chen et al., 2012, Aldossari et al., 2014, Feltis et al., 2015), without the need for an allergen to stimulate the model. However ZnONPs were found to inhibit the responses of OVA-induced models, including a reduction in mast cell degranulation and histamine production (Feltis et al., 2015).

1.5.4 Impact of nanomaterials on asthma endpoints in non-allergic experimental models

Investigation of the same end points in "healthy" or non-allergic models is also important. This allows us to determine which nanomaterials have the potential to illicit an immune response alone. AHR has been observed without an allergic mediator but after exposure to AgNPs, TiO_2NPs, SWCNTs and MWCNTs (Seiffert et al., 2015, Rydman et al., 2014, Beamer et al., 2012, Hsieh et al., 2012, Scuri et al., 2010). This is thought to be due to interaction of the particles with smooth muscle cells and interacting with the muscarinic receptors, increasing the contractibility of the smooth muscle (Kapilevich et al., 2012b, Kapilevich et al., 2012a). Profibrotic effects after exposure to particles has also been observed (Wang et al., 2015, Ma et al., 2012, Ma et al., 2017, Jacobsen et al., 2015a). There is also evidence to suggest that mucus secretion is also enhanced with the exposure (identified after exposure to both CuONPs and MWCNTs (Park et al., 2016, Rydman et al., 2014)). This increase in mucus production has the potential to inhibit the clearance of these particles.

1.5.5 *In vitro* models for examination of allergic and asthma related endpoints

As research tries to move further from *in vivo* systems in order to use more *in vitro* systems, it is important for them to still represent the systems they are trying to mimic (Blume and Davies,

2013). This can be done using different methods which can either extrapolate from the known responses of *in vivo* models or from patients and healthy volunteers.

Lung on a chip is one of the newer tools within the toxicologist's arsenal that aims to mimic the lung further than traditional cell culture models. These models tend to utilise cell lines instead of primary cells (which come with their own pros and cons), but is able to mimic breathing and implement medium flow (Nikolic et al., 2018a).

Airway diseases are very complex but can potentially be broken down to their cell components (which can mimic the three phases of asthma development) which can then be modelled *in vitro*. The best models are those that contain more than one cell type, and the most commonly used contain epithelial cells, macrophages and dendritic cells (Verstraelen et al., 2008). There are also mechanical components of asthma which rely on smooth muscle cells which need completely different models from those that are previously described (Meurs et al., 2008).

1.5.6 *In vivo* models for examination of allergic and asthma related endpoints

There are numerous animal models available for studying a variety of different disease conditions (Figure 1-17). A brief review of the literature and published protocols was completed, and the HDM model of exposure was chosen for this project. This model required the use of mice, this is a positive thing as there are many more antibodies and cytokines etc that have already been established for mice when compared to other potential animals. As well as deciding which allergen we should use to establish an allergic response, it is also important to determine the exposure schedule in order to focus on the endpoints of interest (Citeq-Biologics).

The major issue with the animal models currently being used to study asthma *in vivo* is that the response does not involve exactly the same triggers and subsequent chronic asthmatic features as those known to be important in human patients. Cats, dogs and horses are able to develop allergic phenotypes, and some strains of rodents are able to produce elements of asthmatic phenotypes (such as eosinophil infiltration and Th2 responses). They also require sensitisation to an allergen, which is most commonly done via an intraperitoneal (IP) injection, which is nowhere near the natural route of respiratory sensitisation (via inhalation or ingestion). Chronic inflammation cannot be developed in these models for unknown reasons, meaning that only the acute effects can be investigated (Bice et al., 2000).

Species	Pros	Cons
Mice	• Many commercially available probes • Easily sensitised to different antigens (Th2 Type response) • Cheap and small • IgE is the primary anaphylactic antibody	• Eosinophils dominate inflammatory response • Mast cells release serotonin (doesn't play a role in asthma) • Unclear if mice are able to exhibit a "late-stage" constriction in the lung • Can develop tolerance instead of a chronic reaction • Has monopodial branching of the lungs (humans have more dichotomous) and lung lobes are different • Lung function measurements are challenging • Proportion s of cell types in the airways varies between species • Don't exhibit spontaneous airway hyperresponsiveness • No histamine response • Little airway smooth muscle • Vasculature is anaphylactic target
Rats	• Cheap and small (but bigger than mice) • Easily sensitised to different antigens (Th2 Type response) • Can generate an early and late stage response • IgE is the primary anaphylactic antibody • Can generate airway hyperresponsiveness	• Tolerance to an allergen instead of a chronic reaction • Lung function measurements are challenging • Requires injection of the allergen for sensitisation • Requires adjuvants for sensitisation • Probes are not common • Poor histamine response • Has monopodial branching of the lungs
Guinea-pigs	• Readily sensitised to OVA • asthmatic phenotypical response • Lung is the primary target of anaphylaxis • Inflammation composed of eosinophils and neutrophils • Response to cholinergic agonists • Sensitisation possible via inhalation route	• Can develop tolerance instead of a chronic reaction • Can have extreme and lethal response to irritants - treated with antihistamines to moderate this • IgG1 is the major anaphylactic antibody • Naturally high eosinophil baseline • Has monopodial branching of the lungs • Few species specific reagents
Rabbit	• Show an early and late stage response • Lung is the primary target of anaphylaxis • IgE is the primary anaphylactic antibody	• Neonatal immunisation required for late phase response
Dogs	• Pre-disposed to develop allergies • Can be sensitised and challenged with *Ascaris suum* • IgE is the primary anaphylactic antibody • Shows airway hyperresponsiveness	• Late stage response not shown • Variability in response to *Ascaris suum* • Larger airway that is less prone to airway constriction
Sheep	• Can be sensitised and challenged with *Ascaris suum* • Can generate an early and late stage response and airway hyperresponsiveness	• Big and can cost a lot • Has slightly less monopodial branching of the lungs
Horse	• Naturally develop respiratory disorders	• Hard to handle and expensive
Monkey	• Develop natural sensitivity to *Ascaris suum* • Allergic response can persist for years • IgE is the primary anaphylactic antibody	• Hard to handle and expensive • Ethical implications

Figure 1-17 Animal models used to investigate asthma. Various models have been implemented in investigating various factors of asthma. Depending on the area of interest different animal models should be used. Adapted from (Zosky and Sly, 2007, Wegmann and Renz, 2005, Shin et al., 2009, Karol, 1994, Chorawala M. R, 2014).

1.6 Overarching hypothesis

We hypothesise that the addition of cerium oxide nanoparticles (CeO_2NPs) will have a moderating effect on the toxicity and bioreactivity of diesel exhaust particles.

1.7 Specific aims of the thesis

- Aim to identify the *in vitro* effects of CeO_2NP alone, DEP alone and CeO_2NPs+DEP on a model of the human large airways with and without allergen stimulation.
- Aim to identify the *in vivo* effects of CeO_2NP alone, DEP alone and CeO_2NPs+DEP on a murine model of asthma (using HDM as a sensitisation agent).
- Aim to combine these models and identify potential human health hazards that may be elicited by these particles either with or without an allergen stimulation.

Chapter 2: Experimental protocols

2.1 Particulates and nanomaterials

Cerium dioxide nanoparticles (CeO_2NPs) were obtained from Sigma Aldrich (cat # 544841) and were characterised before delivery using Brunauer, Emmett and Teller (BET) by the supplier.

Diesel exhaust particles (DEP) were obtained from the National Institute of Standards and Technology (NIST) and are a standard reference material from an industrial forklift (Standard Reference Material 2975). They were characterised before delivery using BET and transmission electron microscopy (TEM).

2.1.1 Preparation of particulate suspension

Both particles were supplied in powder form. Particles were suspended using a method previously defined by Bihari et al. (2008). Particles were weighed and initially suspended in distilled H_2O before being sonicated (QSonica Sonicators, CT, USA) with $4.2x10^5 kJ/m^3$ (the sonicator cylinder size was $7.948x10^{-4} m^3$ so in order to obtain $4.2x10^5 kJ/m^3$, the sample had to be exposed to 333kJ of energy in total). After sonication, samples were both aliquoted and frozen for future use. They were then either stabilised using 0.05% Tween 80 (Sigma Aldrich, Cat# P4780) in phosphate buffered saline (PBS) (Gibco, Life Technologies, Cat# 14190-094) to disperse them more efficiently for *in vivo* exposures or cell culture medium for *in vitro* exposures. After being stabilised the particles were used immediately.

Zhang et al. (2013) determined the percentage of CeO_2NPs contained within the exhaust particles produced after combustion of the diesel and cerium catalyst mixture was 0.08%. Therefore, for all future experimental work, the ratio between the particle types was 1:0.008mg/ml DEP: CeO_2NPs.

2.1.2 Characterisation of cerium dioxide (CeO_2) nanoparticles and diesel exhaust particles (DEP) alone and in combination.

It is important to fully characterise any particulates used. This will allow relevant comparisons to be made between *in vitro* and *in vivo* work. There are numerous ways particles can be characterised, and each method can investigate various features of a particle. It is important to characterise particles, either in suspension or as a dry powder, as these will influence the characteristics of the particles, their interaction with biological systems and ultimately their toxic potential.

Particles were characterised while suspended in both the relevant medium (for cell culture) and PBS with 0.05% Tween 80. They were also characterised alone and as a mixture (in the ratio stated above) with and without the addition of HDM (used *in vivo* only).

2.1.2.1 Transmission Electron Microscopy (TEM)

A transmission electron microscope works in the same way as a conventional light microscope, except instead of light being used to view a sample, an electron beam is used. A light microscope uses photons to view a sample, however if a higher resolution and magnification is required, a shorter wavelength is needed. Electrons have a smaller wavelength than visible light and are therefore used - the smaller the sample, the smaller the wavelength required.

Particles were suspended in distilled H_2O at a concentration of 10µg/ml and 10ul was drop-cast onto a Formvar/Carbon 200 Mesh Copper TEM grid (Agar Scientific, Cat# AGS162), the excess liquid removed and the grid dried overnight at room temperature. An electron beam of 75 kV was applied to the samples and images captured using the transition electron microscope (Hitachi H-7000 TEM (Hitachi, Japan)) at a variety of magnifications (Figure 2-1, A).

2.1.2.2 Zeta potential

The zeta potential is an indicator of the surface charge of the particles and therefore a measurement of the particle suspension stability. It allows a measurement of the electrostatic or charge repulsion/attraction between particles in a solution. Particles with a potential of between -10 to +10mV are neutral and any particles with a value of over (-/+) 30mV are either cationic or anionic. Those solutions with a larger zeta potential are thought to be more stable due to the fact they have an increased repulsion between the particles (Patravale et al., 2012).

The zeta potential of the particles was measured three times over three different days as independent replicates. Zeta potential was measured for all samples separately in distilled H_2O, PBS and differentiation cell culture medium (Figure 2-1, B).

1ml of the solution was injected into a disposable folded capillary cuvette (Malvern, Cat# DTS1070), before being analysed using a Zetasizer Nano (Malvern, Malvern United Kingdom). Zeta potential was measured 3 times with 3 different samples before being averaged for the final measurement. The Zetasizer Nano measures the zeta potential 100 times per sample cycle.

2.1.2.3 Size of particles

Size of the particles was determined using the Nanosight (Nanoparticle analysis system, NS14C, Nanosight Ltd, United Kingdom). Using a laser beam, the Nanosight can track and analyse individual particles in real time. 1ml of the sample is injected into the laser chamber. Particles are tracked by the diffraction of the laser. Individual particles are tracked using Nanosight software, and this allows an indication of the size of particles and the size distribution of the sample (Figure 2-1, B).

2.1.2.4 Endotoxin Assay

It is important to determine the endotoxin content of the particles to confirm that the endotoxin levels are not causing any of the responses and interpreted as due to the particulate action (Figure 2-1, C). The LAL chromogenic endotoxin quantitation kit (Thermo Scientific, Cat# OL186586) was used to detect any gram-negative bacterial endotoxins that may be present in the particle mixtures and medium used. Bacterial endotoxin contributes to the activation of a proenzyme in a modified *Limulus* Amebocyte Lysate (LAL). This leads to the activation of Factor C which goes on to cleave p-nitroalinine producing a colour change that can be measured. This colour production can then be measured and is proportional to the endotoxin level in the sample.

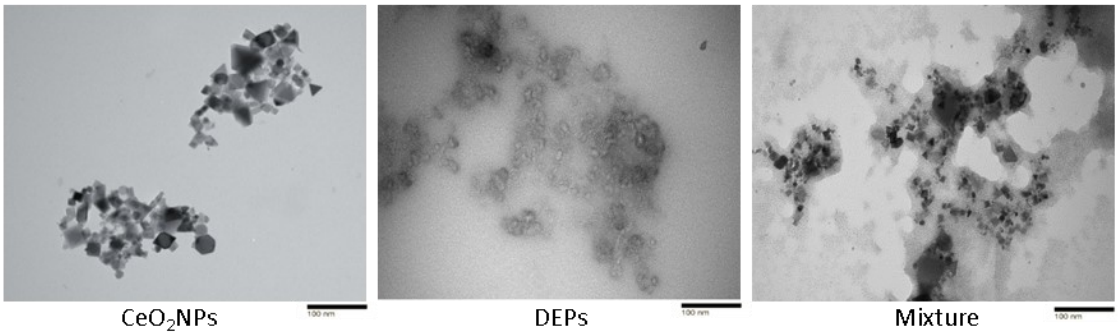
All consumables used need to be endotoxin free to ensure there is no contamination and therefore no false positive results. All samples for analysis were pH adjusted to pH6-8 and all bacteriological activity ceased by storage at -20°C for 24 hours before analysis. The endotoxin standard stock solution was made as directed and mixed vigorously for 15 minutes before use. A serial dilution was made with 1.0EU/ml as the top concentration, with each step being vortexed vigorously before diluting. LAL was reconstituted immediately before use with endotoxin-free H_2O, swirled gently and protected from light. The chromogenic substrate was reconstituted to 2mM with endotoxin-free H_2O before being protected from light.

All reagents and equipment were brought to room temperature before use. Throughout the protocol it was important to ensure reagent addition and pipetting speed remained consistent. A sterile 96 well plate (Thermo Fisher, Cat# 456537) was equilibrated to 37°C for 10 minutes in a heating block before adding 50µl of each standard (including a blank control of endotoxin free H_2O) and unknown samples in replicates and incubated at 37°C for 5 minutes. 50µl of LAL was added to each well and the plate gently shaken for 10 seconds before being heated again at 37°C for 10 minutes. 100µl of chromogenic substrate solution was added to each well, the plate mixed

well and heated again at 37°C for 6 minutes. After this incubation, 50µl of 25% acetic acid was added as a stop solution, and absorbance read at a wavelength of 405-410nm using a plate reader (Bio-Tek Synergy HT).

Control blank absorbance replicates were subtracted from the standards and the test samples and the endotoxin concentration calculated for each sample test from the standard curve using Prism 6 software (Graphpad Prism).

A.



B.

Diluent	H_2O	PBS		Medium	
Parameter	CeO_2NP	CeO_2NP	CeO_2NP + HDM	CeO_2NP	CeO_2NP + HDM
Mean Size (nm)	144.1	166.5	263.8	219.1	229.0
Mode	117.5	122.5	193.4	148.2	213.8
SD	79.3	111.7	130.5	102.7	92.9
ZP (mV)	-13.10±2.07	-8.28±0.37	-10.66±0.57	-11.14±1.23	-9.63±1.36

Diluent	H_2O	PBS		Medium	
Parameter	DEP	DEP	DEP + HDM	DEP	DEP + HDM
Mean Size (nm)	162.9	134.7	141.9	216.7	209.0
Mode	105.9	84.7	92.3	170.3	154.3
SD	73.9	58.9	79.7	100.0	88.0
ZP (mV)	-28.14±0.86	-8.32±1.54	-8.58±1.88	-11.13±1.40	-10.17±1.23

Diluent	H_2O	PBS		Medium	
Parameter	Mixture	Mixture	Mixture + HDM	Mixture	Mixture + HDM
Mean Size (nm)	167.1	179.4	250.9	225.2	236.3
Mode	139.7	173.9	185.5	153.4	164.9
SD	65.2	72.2	91.8	91.8	91.5
ZP (mV)	-39.14±5.14	-7.38±1.84	-10.49±3.23	-12.76±1.41	-8.53±1.05

C.

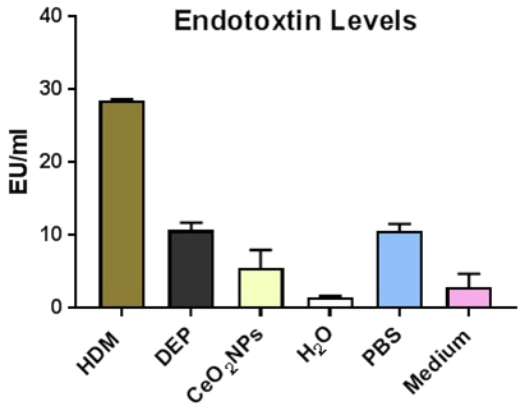


Figure 2-1 Characterisation of Particles. CeO_2NPs, DEPs and the mixture of particles respectively were suspended in water and primary size and structure were visualised (scale bar represents 100nm) using TEM (A). These nanoparticles were also suspended in PBS with and without HDM (indicated by blue columns) and cell medium with and without HDM (indicated by the pink columns) then agglomerate size was determined using nanoparticle tracking analysis (B) with results expressed as mean, mode and standard deviation (SD) of size distribution. Particle charge was also determined as zeta potential (ZP) by dynamic light scattering and expressed in millivolts (mV) mean values ± SEM. Endotoxin contamination was established (C) in each of the particles, and diluents used for exposure. This was determined using a LAL assay kit and expressed as mean EU/ml per sample± SEM.

2.2 *Laser ablation and inductively coupled plasma mass spectrometry (ICP-MS)*

The elemental composition of DEP was measured using inductively coupled plasma mass spectrometry (ICP-MS). The plasma converts the atoms of the sample into ions, which are then separated and detected using mass spectrometry (Thomas, 2004). This is carried out in a complete helium environment (Figure 2-2).

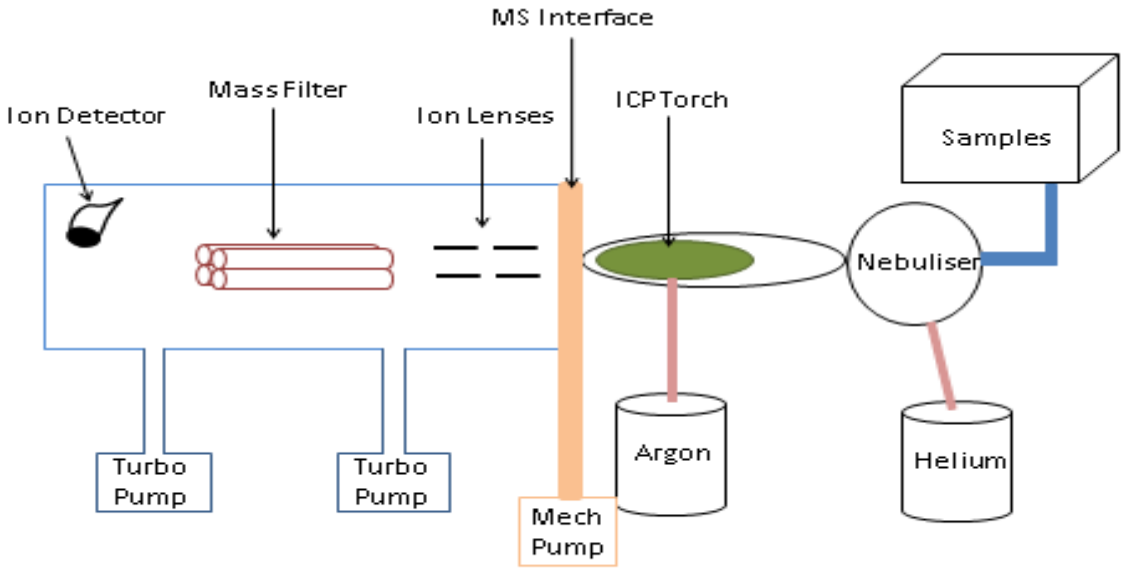


Figure 2-2. Basic components of an ICP-MS. The sample is pumped from the auto sampler into the nebuliser. The sample is then transported into the plasma torch via an injector and positively charged ions are generated. Ions are then directed into the mass spectrometer through the MS interface, and finally the ions are converted to an electronic signal via the ion detector and software is used to analyse these electrical signals and produce an elemental read out (Thomas, 2004, Hartney and Robichaud, 2013, Kaminsky, 2012).

2.2.1 Elemental composition of DEP

DEP samples were suspended at 1mg/ml in 5% nitric acid (Fisher Scientific, Cat#A5509-P500) in triplicate. Samples were then processed using a microwave digester (UltraWAVE Single Reaction Chamber Microwave Digestion System, Milestone S.r.l. Fatebenefratelli, Italy). Quality control Claritas PPT Standard 55 (SPEX CertiPrep, Cat# CL-QC-55) was used to produce a standard curve of 55 different elements allowing the concentration of various elements to be extrapolated. The samples were digested twice before being diluted to 500ppm ($5x10^{-4}$mg/µl) and injected into the iCAP Q ICPMS (Thermo Scientific, Loughborough, UK) for analysis. Elemental composition was then averaged between the triplicates giving the final elemental composition of the samples. This composition was then used to determine the components within the DEP which could be used in the future to locate the DEP within the lung tissue using laser ablation (Figure 2-3). The highest of these elements could not be used due to the potential

for them to be implicated within the biological system (such as Mg, Fe and Na) and therefore give false positive results for DEP within the lung tissue.

Element	Li	Be	Na	Mg	Al	P	K	Ca	Sc	Ge	Re	Ti
Mean Conc (ppb)	0.016	0.006	29.551	139.230	91.863	56.334	37.942	22.757	0.000	0.006	0.000	4825.60
SEM	0.004	0.004	2.922	20.267	8.558	4.308	12.274	2.762	0.000	0.001	0.000	648.719
(N=8)												

V	Cr	Mn	Fe	Co	Ni	Cu	Zn	Ga	Hg	As	Se
0.128	3.433	7.292	817.664	0.515	4.369	7.281	167.068	0.020	0.017	0.370	0.075
0.017	0.440	1.175	159.088	0.046	1.337	1.155	27.100	0.006	0.003	0.058	0.014

Rb	Sr	Y	Mo	Rh	Pd	Ag	Cd	Tl	In	Sn	Te
0.050	0.204	0.012	0.507	0.000	0.001	0.030	0.192	0.006	0.002	301.545	0.000
0.013	0.014	0.007	0.049	0.000	0.000	0.006	0.057	0.003	0.000	79.026	0.000

Cs	Ba	La	Ce	Pr	Nd	Sm	Pb	Eu	Gd	Tb	Dy
0.009	3.257	0.003	1.711	0.001	0.005	0.001	3.773	0.000	0.002	0.000	0.000
0.004	0.531	0.000	0.348	0.000	0.001	0.000	0.527	0.000	0.000	0.000	0.000

Ho	Er	Tm	Yb	Lu	W	Th	U
0.000	0.000	0.000	0.000	0.000	32.239	0.001	0.017
0.000	0.000	0.000	0.000	0.000	5.066	0.000	0.010

Figure 2-3. Elemental Composition of DEPs. ICP-MS was used to identify the metal components that were present within the DEPs with results expressed as mean concentration (ppb ($1x10^{-9}$mg/µl)) and SEM. Highlighted are those elements which are potential candidates for laser ablation ICP-MS as a means to assess pulmonary deposition of DEP after instillation *in vivo*, with dark green having a higher concentration than the light green elements.

2.2.2 Determining the concentration of cerium dioxide nanoparticles in the airways

After cerium alone instillation studies were completed, the right lung lobe was snap frozen ready for further analysis (section 2.6.3). A section of the lobe was cut and weighed (in order for all the samples to be normalised against weight) while ensuring the remainder of the sample was still frozen. 1ml of 20% nitric acid was added to each sample before microwave digesting (section 2.2.1). After digestion has been completed, the sample was filtered and 9.9ml of H_2O (to dilute the samples) and 100µl iridium (10ppb ($1x10^{-8}$mg/µl)) (as an internal standard) was added to each of the samples. Samples were fed through the ICP-MS (section 2.2.1) 3 times per sample and the concentration of the 55 different elements measured within each lung was normalised against its pre-digested weight.

2.2.3 Determining the location of cerium dioxide nanoparticles in the airways

Unstained lung sections were dewaxed and photographed (Leica DFC450C, Leica Microsystems Ltd) (section 2.7.2) before being sealed in the laser ablation chamber. The laser ablates a user pre-determined area of the lung. A vacuum removes the ablated particles and carries them to the ICP-S, where the elemental composition of the sample is processed. From the ICP-MS, a visual representation of the location of various elements can be produced though the use of IGOR Pro software (WaveMetrics), allowing a comparison to be made between various exposure groups, particle types, particulate concentration and location within the whole lung after intranasal instillation.

2.3 RT-PCR (real time – polymerase chain reaction)

All steps were carried out at room temperature, unless stated. Before beginning, all equipment and lab benches used were sprayed with RNAse ZAP (Sigma-Aldrich, Cat# R2020) to ensure none of the mRNA was degraded by residual RNAse (an enzyme that can break down RNA and can be found on most surfaces, including biological surfaces as well in inert surfaces).

2.3.1 mRNA extraction

The mRNA was extracted using a RNeasy mini kit (Qiagen, Cat# 74106) and all buffers and columns used were from this kit unless stated. Cells were lysed by addition of 350µl of RLT buffer, before scraping the cells off the filters (2.5cm handle, 1.8cm blade, Corning Incorporated, Cat# 3010) and adding the cell lysate into a QiAshredder (Qiagen Cat# 79656). The QiAshredder is used to ensure all the cells had lysed and mRNA from all cells can be extracted. The QiAshredders were then centrifuged at 17000xg for 2 minutes. One volume of 70% ethanol was then added to the lysates and mixed well, before being added to RNeasy spin columns, and centrifuged at 8000xg for 15 seconds. The flow through of ethanol is then kept and stored at -80°C before further analysis. 700µl of Buffer RWI was then added to each column and centrifuged at 8000xg for 15 seconds. The flow through was discarded and 500µl of Buffer RPE was added and centrifuged at 8000xg for 15 seconds. This was repeated and centrifuged at 8000xg for 2 minutes. The columns were then placed into new collection tubes and centrifuged at 17000xg for 2 minutes to ensure all the buffer had cleared the filter. The mRNA was then eluded from the column by adding 30µl of RNAse-free water directly onto the filter and centrifuging at 8000xg for 1 minute. Once the mRNA was eluted, it was placed on ice before the concentration was established using a Nanodrop 2000 (Thermo Scientific, Loughborough, UK). Once isolated, the mRNA was then stored at -20°C until required.

2.3.2 cDNA synthesis

All steps were completed on ice to ensure no degradation of the mRNA. 1.5µg of mRNA was made up in a volume of 8µl of RNAse-free water (Qiagen, Cat# 74106) in a PCR reaction tube (VWR tubes and lids, Cat# 732-1517, and 732-1518). The Bioline (London, UK) kit was used as follows. Initially a primary premix was prepared.

1X:

Primary Premix

Solution	Volume
Total mRNA (extracted previously)	nµl (to a max of 8µl)
Random Hexamer (Cat# BIO-38028)	1µl
10mM dNTP Mix (Cat# BIO-39025)	1µl
RNase-free water (Qiagen, Cat# 74106)	To make up to 10µl

The samples were vortexed, centrifuged (VWR Mini Star Silverline) and incubated at 70°C for 5 minutes (Peltier thermal cycler PTC-200, MJ Research) and then chilled on ice for at least 1 minute. While the samples were being incubated, the reaction premix was prepared.

1X:

Reaction Premix

Solution	Volume
5x RT Buffer (Cat# BIO-65028)	4µl
Ribsafe RNase Inhibitor (Cat# BIO-65028)	1µl
BioScript Reverse Transcriptase (Cat# BIO-27036)	1µl
RNase-free water (Qiagen, Cat# 74106)	4 µl

The reaction premix is then added to the primary premix, vortexed and then centrifuged. Samples are then incubated at 25°C for 10 minutes followed by 42°C for 30 minutes. The reaction

is then terminated by incubating the samples at 85°C for 5 mins and then chilling on ice. The samples were then stored at -20°C.

2.3.3 Quantitative RT-PCR analysis

Reverse transcriptase polymerase chain reaction (RT-PCR) is a technique used to investigate gene expression based on the original method developed by Kary Mullis in 1983. It requires the synthesis of cDNA from RNA (using reverse transcriptase as described previously) to implement the "real time" component. PCR can be used to amplify a single copy of DNA into multiple copies of that single strand. It does however require a primer to begin the amplification, but once the amplification has begun, the product quantity increases exponentially.

PCR works by using heating and cooling cycles (thermocycling) to denature and replicate the DNA. Primers (a forward and a reverse primer) are used to select the region of DNA of interest and allow additional nucleotides to bind with DNA polymerase. The more segments of DNA of interest, the quicker the amplification can take place (NCBI). Nucleotide primers were developed after consulting the literature and using the NCBI Nucleotide search to identify the FASTA sequence of the gene of interest. Using Primer 3 (Primer3web version 4.1.10) software, both forward and reverse primers are identified.

Primers are diluted to 2µM; 10µl of the forward and 10µl of the reverse primers are mixed together before adding 480µl of RNAse free water. cDNA samples were defrosted (on ice) and diluted with 1:10 with RNAse-free water (Qiagen, Cat# 74106). 8µl of the diluted cDNA samples were loaded into the 384 well plates (Bioscience, Cat# 4309849) according to the prepared plan, the plates were then sealed and centrifuged for 1 minute at 250xg. A master mix was then prepared allowing for 10% error in the sample pipetting.

1x: **Master Mix**

Solution	Volume
Specific Primer	2.2µl
Power SYBR Green PCR Master Mix (Applied Biosystems, Cat# 4367659)	11µl

12µl of the master mix was then added into each required well (samples were analysed in duplicate), the plates sealed and inverted to mix the contents. The plate was centrifuged for 2

minutes at 250xg, then loaded into the PCR machine (Quant Studio 6 Flex, Applied Biosystems by Life Technologies), and the reporter and quencher set (SYBR and NFQ-MGB respectively)

Expression was normalised to GAPDH (a housekeeping gene) and the ΔΔ CT Method (using the threshold cycle values (CTs) generated from the PCR machine) was used to calculate the fold change of genes after various exposures (Rao et al., 2013). All particle exposures were normalised to the housekeeping gene CT value (ΔCT), before subtracting the CT value of the negative control (an average of the medium alone samples) (ΔΔCT), and the fold change calculated. See Table 2-1 for example data set and calculation. This dataset is related to the gene expression analysis of NQO1 as demonstrated in Figure 3-5.

Table 2-1. Example of PCR data analysis using one concentration of CeO_2NPs and control samples.
HKG = house-keeping gene and is GAPDH

			Sample	HKG		Sample-HKG			
Name	Sample #	**Well No.**	**Ct**	**Ct**		**ΔCT**	**ΔCT-ΔCT**	**Fold Change**	**Average**
Ce0.008	53C	A14	25.358	13.940		11.418	4.739	**0.037**	0.073
Ce0.008	29	I18	25.417	14.341		11.076	4.397	**0.047**	
Ce0.008	53A	I4	23.632	14.058		9.574	2.895	**0.134**	
Medium	73A	B5	20.624	14.086		6.538	-0.141	**1.102**	1.002
Medium	54C	C14	21.330	14.584		6.746	0.067	**0.954**	
Medium	74A	D5	21.495	14.743		6.752	0.073	**0.950**	
Medium Average						6.679			

2.4 Enzyme-Linked Immunosorbent Assay (ELISA)

An enzyme-linked immunosorbent assay (ELISA) is an assay that can be used to measure and detect specific proteins, antibodies, peptides and hormones. The specific component of interest can be detected and measured using a capture antibody that is bound to the plate and ends in a colour or fluorescent change which can be detected and measured. There are two ways this can be detected, through a direct ELISA (a labelled primary antibody) or an indirect ELISA (a labelled secondary antibody). The most common ELISA used is a "sandwich" ELISA – it "sandwiches" the protein of interest between a capture and a detection antibody. Sandwich ELISAs were used throughout this project.

2.4.1 Human ELISAs

IL-33 levels were analysed using DuoSet enzyme-linked immunosorbent assay (ELISA) kits (R&D Systems, United Kingdom), IL-17E (IL-25), CCL20 and TSLP levels were analysed using Quantikine ELISA kits (R&D Systems) following the manufactures' protocol. Medium samples (from cell culture of human cells) from both the basal and the apical side were analysed in triplicate, diluted 1:2 with assay diluent. The kits were reconstituted at room temperature and left for 15 minutes before using. All details of the kits and required concentrations are outlined in Table 2-2.

Table 2-2. Details of and antibody and standard concentrations required for Human ELISAs kits. Working concentrations required for the R&D Systems ELISA kits as outlined by the manufacturer. All components were reconstituted at room temperature and left to stand for 15 minutes before using.

Human ELISAs			Antibody Concentration	
Name	Cat #	Top standard (pg/ml)	Capture (µg/ml)	Detection (ng/ml)
IL-33	D3300	400	1	500
IL-17E (IL-25)	Y1399	4000	2	250
CCL20	DM3A00	500	2	150
TSLP	DTSLP0	2000	0.8	50
IL-6	DY206	600	1	100
IL-8	DY208	600	1	50
SLPI	DY1274	1000	1	100

Plates were coated with 100µl per well of the specific capture antibody (diluted in PBS) and incubated overnight at room temperature. Plates were washed 3 times with wash buffer and blocked with 300µl reagent diluent per well for 1 hour at room temperature. Plates were then washed as previously and 100µl of samples and appropriate standards were added. Plates were then sealed and incubated for 2 hours at room temperature. Plates were then washed again before adding 100µl per well of the specific detection antibody, sealed and incubated for 2 hours before being washed again. 100µl of working concentration Streptavidin-HRP was then added

to each well, sealed and incubated in the dark for 20 minutes. Plates were washed for a final time and 100µl of substrate solution added to each well and incubated in the dark for 20 minutes. After observing a colour change 50µl of the stop solution was then added to each well.

Optical density at 450nm was measured using a plate reader (Bio-Tek Synergy HT). Subtraction of the optical density at 570nm was completed in order to correct for optical imperfections in the plate. A standard curve was derived using the known concentration standards and Prism 6 software (Prism) and used to calculate the cytokine concentration in the basal and apical medium samples. Values were then multiplied in order to account for the original dilution factor.

2.4.2 Mouse ELISAs

ELISAs carried out on the mice samples were either completed using plasma, BAL fluid or homogenised lungs.

2.4.2.1 Plasma IgE by ELISA

IgE levels were analysed using a BD OptEIA enzyme-linked immunosorbent assay (ELISA) kits (BD Bioscience, Cat# 555248) following the manufactures' protocol and BD OptEIA Reagent Set B (BD Bioscience, Cat# 550534). Samples were analysed in duplicate, diluted 1:5 with assay diluent. The top standard was 100ng/ml.

Plates were coated with 100µl per well of capture antibody (1:250 dilution with coating buffer), sealed and incubated overnight at 4°C. Plates were washed 3 times with wash buffer and blocked with 300µl assay diluent per well for 1 hour at room temperature. Plates were then washed and 100µl of samples and appropriate standards were added. Plates were then sealed and incubated for 2 hours at room temperature. Plates were then washed again 5 times before adding 100µl per well of the working detection antibody (detection antibody diluted 1:500 in assay diluent + enzyme reagent (streptavidin-horseradish peroxidase conjugate) diluted 1:250 in detection antibody), sealed and incubated for 1 hour before being washed 7 times with 1 minute soaks between washes. 100µl of substrate solution was then added to each well, the plate sealed and incubated in the dark for 30 minutes. After observing a colour change 50µl of the stop solution was then added to each well.

Optical density at 450nm was measured using a plate reader (Bio-Tek Synergy HT), within 30 minutes of stopping the reaction. Subtraction of the optical density at 570nm was completed in order to correct for optical imperfections in the plate. A standard curve was derived using known concentration standards and Prism 6 software (Prism) and used to calculate the cytokine

concentration in the plasma samples. Values were then multiplied to account for the original dilution factor.

2.4.2.2 Bronchial alveolar lavage (BAL) fluid ELISA analysis

IL-17, TSLP, IL-5, IL-4, IL-13, IL-33, CCL20, IL-1α, CCL8, CCL17 and CCL11 levels were analysed using DuoSet enzyme-linked immunosorbent assay (ELISA) kits (R&D Systems, United Kingdom) following the manufactures' protocol. The kits were reconstituted at room temperature and left for 15 minutes before using. All details of the kits and required concentrations are outlined in Table 2-3. Samples were analysed in triplicate, diluted 1:2 with assay diluent as previously outlined in section 2.4.1.

Table 2-3. Details of antibody and standard concentrations required for Murine ELISAs kits. Working concentrations required for the R&D Systems ELISA kits as outlined by the manufacturer. All components were reconstituted at room temperature and left to stand for 15 minutes before using.

Mouse ELISAs			Antibody Concentration	
Name	Cat #	Top standard (pg/ml)	Capture (µg/ml)	Detection (ng/ml)
IL-17	DY421	1000	2	70
TSLP	DY555	1000	1	200
IL-5	DY405	2000	1	100
IL-4	DY404	1000	4	150
IL-13	DY413	4000	4	200
IL-33	DY3626	1000	0.8	75
CCL20	DY760	2000	2	300
IL-1α	DY400	1000	2	100
CCL8	DY790	1000	1	100
CCL17	DY529	2000	1	100
CCL11	DY420	500	1	100

2.4.2.3 Lung homogenate preparation and ELISA analysis

100mg snap frozen right lung lobes were homogenised using MagNa lyser beads (Roche, Cat# 03358941001) in 1ml lysis buffer (comprised of 10ml Hanks' Balanced Salt Solution (HBSS) (Gibco, Cat#24020-091), 20µl concentrated Triton-x100 and 1 cOmplete ULTRA tablet, mini, EASYpack (Roche, Cat# 05892970001) (this was used to protect the proteins in the tissue from being degraded during the homogenation)). Great care was taken to ensure the snap frozen tissue did not thaw and remained frozen. Once samples were in the MagNa lyser bead containing tubes, to ensure complete homogenisation had occurred they were homogenised twice in a MagNa Lyser (Roche) at 6000xg for 30 seconds. Due to the addition of Triton-x100, there was foam in the MagNa lyser. To compensate for this (and to remove debris), all samples

were centrifuged at 17000xg for 15mins at room temperature (VWR Micro Star 17R). Once completed, the supernatant was removed and frozen at -80°C for future analysis.

Homogenised samples were diluted 1:5 with lysis buffer for ELISA analysis. IL-17, TSLP, IL-5, IL-4, IL-13, IL-33, CCL20, IL-1α, CCL8, CCL17 and CCL11 levels were analysed using DuoSet enzyme-linked immunosorbent assay (ELISA) kits (R&D Systems, United Kingdom) following the manufactures' protocol. The kits were reconstituted at room temperature and left for 15 minutes before using. All details of the kits and required concentrations are outlined in Table 2-3. Samples were analysed in triplicate as previously outlined in section 2.4.1.

2.5 Human Primary Bronchial Airway Epithelial Cell (HPBECs) culture

Bronchial airway epithelial cells were used to investigate the potential effects of these particles due to the fact they are one of the first points of contact when these particulates are inhaled. It is important to understand the specific role bronchial epithelial cells play in the inflammatory responses to these particles. All steps using HPBECs was completed using sterile conditions and under a laminar flow hood.

2.5.1 Air liquid Interface culture media

Human primary bronchial airway epithelial cells (HPBECs) were supplied by Epithelix, and were delivered frozen and stored within liquid nitrogen until required. Various healthy donors were used at various passages (between passage 4 and 10) (Donor identification; AB0372.01, AB0201.02, AB0378091, 2AB050301, AB039401F11, AB0372.01, AB0531.01, AB0510.01, AB0239.01, AB0201.02 and AB0378.01). Various donors were used in order to try and limit the donor variation that is seen between individual donors. In order to develop a model that was similar to that of the lung, the epithelial cells had to be differentiated before being exposed to the various particles and concentrations. In order to optimise the differentiation, various media were compared and assessed for the differentiation capabilities before moving forward with particulate exposures.

2.5.1.1 Thawing and initial seeding of cells

The donor cells were removed from liquid nitrogen storage and placed into a water bath at 37°C for 2 minutes, ensuring the top of the vial did not come into contact with the water. Once thawed, cells were transferred into Dulbecco's Modified Eagle Medium (DMEM) (1x) + GLUTAMAX (Gibco, Life Technologies, Cat# 31966-021) containing 10% low IgG Fetal Bovine Serum (FBS) (Gibco, Life Technologies, Cat# 16250). Cells were centrifuged at 8500xg (Sorvall Legend RT) for 5 minutes at room temperature to obtain the cell pellet. The pellet was then re-

suspended in 1ml of Epithelix growth media (Epithelix, Cat# EP09), before being transferred to a T75cm^2 culture flask (Nunc, Thermo Scientific, Cat# 174952) at a seeding density of 1x10^6 cells/ml containing pre-warmed hAEC culture medium (Epithelix growth medium) (Epithelix, Cat# EP09). The cells were maintained in Epithelix growth medium and medium was changed two days after seeding and then every 2-3 days thereafter. Cells were maintained in a humidified environment, continuously incubated at 37°C and with 5% CO_2.

2.5.1.2 Subculture of cells

Once the flasks were around 70-80% confluent they were then split. Medium was removed from the flask and cells washed with 10ml of pre-warmed PBS (Sigma Aldrich, Cat# RNBD0810) and left for 3 minutes. This was repeated 3 times, or until the cells had started to round. The cells were then trypsinised by incubating with 5ml of 0.05% pre-warmed trypsin (Life Technologies, Cat# 15090046) at 37°C for around 10 minutes while continuously checking to ensure cells had started to detach from the flask. The contents of the flask were then transferred to a 50ml tube before washing the flask with 15ml of neutralising media (DMEM (1x) + GLUTAMAX). The cells were then collected by centrifuge at 8500xg for 10 minutes at 25°C to acquire the cell pellet. The supernatant was removed and the cell pellet re-suspended in 1ml of Epithelix medium. Cells were then counted using a haemocytometer and seeded at a density of 3.5 x10^5 cells/cm^2.

2.5.1.3 Cell cryopreservation

Cell cryopreservation was carried out at the earliest possible passage. Cells were detached from flasks using the previous trypsinisation protocol (section 2.2.1.2), before being harvested and counted. The cells were then centrifuged at 8500xg for 10 mins and re-suspended on ice in FBS with 10% dimethyl sulfoxide (DMSO) (Sigma Aldrich, Cat# D8418) to give a cell concentration of 1 million cells/ml. Aliquots of 1ml were transferred into cryovials (Greiner bio-One, Cat# 122263) and placed in a CoolCell™ (Sigma-Aldrich, Cat# BCS-172) cryopreservation unit (allows accurate cooling of the vials of -1°C/minute for reproducible cryopreservation), and stored overnight at -80°C, before being stored in liquid nitrogen for long term storage.

2.5.1.4 Air-Liquid Interface (ALI) Cultures

Human primary bronchial epithelial cells (HPBEC) from a range of donors were cultured using an ALI culture system (Figure 2-4). This method has been found to produce cells with the highest similarity to cells *in vivo* (Pezzulo et al., 2011).

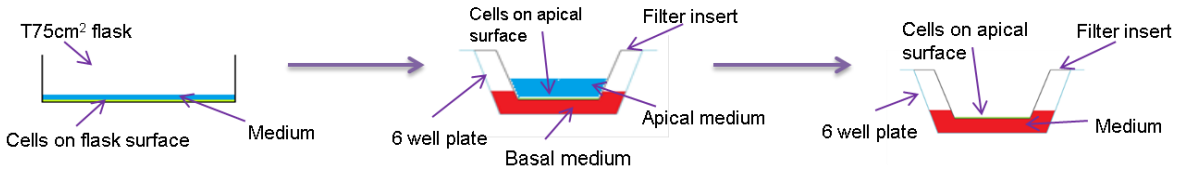


Figure 2-4. Culture Process to Air-Liquid Interface (ALI). Cells are initially seeded in T75² flasks before being split and seeded into Costar Transwell permeable support inserts. Cells were confluent before removing the apical medium from the top of the well and exposing the cells to air.

Before seeding HPBECs onto Costar Transwell Permeable Supports (0.4µm membrane (24mm insert) (Corning, Sigma Aldrich, Cat# 3450)) to initiate the air-liquid interface culture, the filters had to be pre-coated with collagen. Type IV human placenta collagen (Sigma Aldrich, Cat# C5533) was used to coat the filters. A stock concentration of 0.5mg/ml was made up with 10ml sterile distilled water and 25µl of concentrated acetic acid (Fisher Scientific, Cat# A507-P1). 400µl of the working concentration diluted in sterile water (0.05mg/ml) of collagen was added to each filter. The filters were then left to air dry overnight in the laminar flow hood and then exposed to UV for 30 minutes to ensure sterility. Cells were then trypsinised as indicated previously and seeded on the newly coated Transwell membranes at a seeding density of $1x10^5$ cells/cm² in Epithelix medium with 1.5ml medium apically and 2.6ml basally as per the manufactures instructions. Wells were seeded on day 0, and left submerged until confluent (day 4). The apical medium was removed and the cells exposed to air (day 5). On day 7, the basal medium was then changed to the differentiation medium in order for the cells to differentiate.

2.5.1.5 Differentiation protocol

In order to determine the optimal medium composition cellular differentiation, numerous protocols were investigated and four main medium compositions were determined and named after their respective author (Table 2-4). Optimisation was required as there are numerous components that can be added to medium that influence differentiation. Not only was it important to determine what concentration of the component was required, but also if the component was required at all. All differentiation media chosen were selected due to their use with primary cells and their capability to differentiate those cultures.

Table 2-4. Concentrations of the various components added to produce differentiation medium. Various components were diluted to the appropriate concentration (concentrations stated within the figure are final concentrations used) as outlined in the literature (Fulcher et al., 2005, Fulcher and Randell, 2013, Gray et al., 1996, Matsui et al., 1998).

	Fulcher *et al.*, 2012	Gray *et al.*, 1996	Matsui *et al.*, 1998	Fulcher and Randell, 2013
LHC Basal:DMEM-H (50:50)	x	x	x	x
CaCl2	1.0mM		0.08mM	1.0mM
Bovine Serium Albumin	0.5mg/ml	1.5µg/ml	0.5mg/ml	0.05mg/ml
Bovine Pituitary Extract	10µg/ml	180µg/ml	160µg/ml	10µg/ml
Insulin	0.87µM	0.86µM	0.861µM	0.174µM
Transferrin	0.125µM	0.125µM	0.125mM	0.125µM
Hydrocortisone	0.21µM	1.38µM	0.2µM	0.09µM
Triiodothyronine	0.01µM	9.984nM	$x10^{-8}$M	0.01µM
Epinephrine	2.7µM	2.73µM	3.3µM	2.7µM
Epidermal Growth Factor	0.50ng/ml	0.5ng/ml	0.5ng/ml	5ng/ml
Retinoic Acid	$5x10^{-8}$M	$5x10^{-8}$M	-	$5x10^{-8}$M
Phosphorylethanolamine	0.5µM	-	0.5µM	0.5µM
Ethanolamine	0.5µM	-	0.5µM	0.5µM
Zinc Sulfate	3.0µM	-	3.0µM	3.0µM
Ferrous Sulfate	$1.5x10^{-6}$M	-	$1.5x10^{-6}$M	$1.5x10^{-6}$M
Magnesium Chloride	0.6mM	-	0.6mM	0.6mM
Selenium	30nM	-	30nM	30nM
Manganese	1nM	-	1nM	1nM
Silicone	500nM	-	500nM	500nM
Molybdenum	1nM	-	1nM	1nM
Vanadium	5nM	-	5nM	5nM
Nickel Sulfate	1nM	-	1nM	1nM
Tin	0.5nM	-	0.5nM	0.5nM

Using the stock concentration for each supplement (hydrocortisone (Sigma Aldrich, Cat# HO135), triiodothyronine (Sigma Aldrich, Cat# T6397), epinephrine (Sigma Aldrich, Cat# E4250), epidermal growth factor (EGF) (Invitrogen, Cat# PHG0313), retinoic acid (Sigma

Aldrich, Cat# R2625), phosphorylethanolamine (PET) (Sigma Aldrich, Cat#PO503), ethanolamine (Sigma Aldrich, Cat# EO138), penicillin/streptomycin (Sigma Aldrich, Cat# P4333), bovine serium albumin (BSA) (Sigma Aldrich, Cat# A7638), bovine pituitary extract (BPE) (Sigma Aldrich, Cat# P1476), insulin (Sigma Aldrich, Cat# 16634), and transferrin (Sigma Aldrich, Cat# TO665)) the required concentration was added to the base medium. The base medium of the differentiation media was LHC Basal (Life Technologies, Cat# 12677-019) and DMEM-H (Life Technologies, Cat# 41965-039) medium at a ratio of 1:1. Once the media was made up, it was stored at 4°C until required. The basal medium was changed every second day after being switched to the differentiation medium.

2.5.2 Characterisation of ALI cultures

2.5.2.1 Trans Epithelial Electrical Resistance (TEER) measurement

In order to ensure that the cells had completely covered the ALI membrane and produced a monolayer, Trans Epithelial Electrical Resistance (TEER) measurement was completed throughout the growth and differentiation periods. The TEER measurement was carried out using an EVOM² Epithelial Voltohmmeter (World Precision Instruments Ltd, Hertfordshire, United Kingdom) on individual wells throughout their growth period. This comprises of moving the ALI transwell into the Endohm chamber and then measuring the TEER.

Before use, the EVOM² and the Endohm chamber was sterilised using UV light and ethanol. The specific medium the cells were in before being measured was warmed to 37°C before use and the Endohm chamber filled with 2ml of medium (to replicate the basal side of the ALI well), the ALI transwell to be measured was then transferred to the chamber and the apical side filled with 1.5ml of the medium before replacing the Endohm and measuring the TEER. The resistance was measured three times per insert and the mean value established from that. The resistance of an empty insert was subtracted from all the samples and the final value was determined after multiplying the resistance by the surface area of the inserts (1.12cm²).

2.5.2.2 TEM of airway epithelial ALI cultures

TEM was used to characterise the cells and determine the formation of a pseudostratified layer and to determine the uptake of NPs into the cells. Cells were grown to 70% confluence and differentiated as previously described (section 2.2.1.4), and then fixed and processed for transition electron microscopy.

The subsequent processing procedure was carried out by Dr Andy Rogers of the Royal Brompton Hospital. The cells were washed with HEPES buffer and fixed with 2.5% glutaraldehyde for 1 hour. The cells were post-fixed in 1% osmium tetroxide for 30 minutes then dehydrated in ethanol for 15 minutes at room temperature. They were then progressively infiltrated with 25% and 50% araldite resin/ethanol solution and incubated for 15 minutes at room temperature before being embedded in resin. The embedded cells were cut using an ultramicrotome with a 35° diamond knife to a thickness of 50-100nm.

An electron beam of 75 kV was applied to the acquired sections and images were captured with a Hitachi H-7000 TEM (Hitachi, Japan).

2.5.3 *In vitro* particle exposures

All particles were prepared as previously outlined in section 2.1.1 before exposure to the cells. Before using any of the colourmetric assays described within this section, particulate interference was checked. All assays were completed with particles suspended in medium before any of the exposures were completed. There were no interactions from the particles with any of the assays used (the particles did not cause an increase in the colour or fluorescence produced when compared to the medium alone).

2.5.3.1 Initial diesel exhaust particle exposure

The vials for the DEP solution were sterilised under UV light for 2 hours before use, no issues with contamination of the particles were observed. The DEP were re-suspended in sterile PBS at 1mg/ml by sonication at 70Hz as previously described (section 2.1.1) to ensure all the particles have been broken up and suspended within the PBS before being diluted to the required concentrations in the relevant medium. Excess 1mg/ml diesel solution was aliquoted and stored at -80°C for future use. At each dilution step the samples were vortexed and sonicated for 2 minutes before being further diluted to the required treatment concentration.

The diluted DEP samples were votexed and then sonicated for 30 seconds before being warmed to 37°C. Cells were exposed to 200µl of each sample at the apical side of the wells. Samples were allowed to incubate at 37°C for 2 hours on the cellular surface before being removed. Complete coverage of the samples on the apical surface was confirmed before the incubation period. 6 hours, 24 hours and 5 day repeat exposure (exposure every day for 5 days) were investigated. At each of these time points, medium was removed and stored at -80° for further analysis, and the cell cultures had lysis buffer (Qiagen, Cat# 74106) for RNA extraction applied and also placed into -80°C storage after lysis. For the 5 day exposure culture, the culture medium was changed

every second day with the apical surface being washed with 500µl of the specific medium. Samples of the medium before the change were also taken and frozen for future analysis.

2.5.3.2 24 hour exposure of diesel exhaust particles (DEPs), cerium dioxide nanoparticles (CeO_2NPs) and both particles together

ALI cultures were exposed to DEP alone, CeO_2 alone and a DEP/CeO_2 mixture (containing 0.08% CeO_2 for every 1% diesel as previously mentioned) on the apical compartment. ALI cultures were exposed to the particles for 24 hours before being analysed for the chosen allergic markers in both the apical and basal secretions, as outlined in section 2.2.4.1.1.

2.5.3.3 Inflammatory priming and exposure protocols

A cell culture model of inflammation was developed using pre- and co-exposure to type II cytokines (IL-4 (10ng/ml) and IL-13 (10ng/ml) and both IL-4/13 (R&D Systems). In order to replicate the *in vivo* exposures, *in vitro* exposures were completed using the same ratio of particles (DEP, CeO_2NPs, both and HDM (Greer Laboratories)) (as outlined in section 2.3.2). Cells were exposed to IL-4, IL-13 or IL-4/13 either 24 hours before the particles or during the 24 hours of the particulate exposer or exposed to HDM alone, before the particulate exposure or in combination with the particles on the apical side of the ALI. Post analysis was completed as outlined in section 2.2.4.1.1.

2.5.4 Cytotoxicity measurement

The potential dysfunction of the cells and the cytotoxicity due to the various exposures was determined. This allowed cell death to be determined as well as a change in the cellular metabolism (therefore indicating cellular dysfunction).

2.5.4.1 Lactate assay

A lactate assay was performed to determine if there were alterations to the cellular metabolism indicating dysfunction of the cells (Somborac-Bacura et al., 2013). Lactate is produced as a by-product of glycolysis (cytosolic (anaerobic) rather than mitochondrial (aerobic) metabolism via the Kreb's cycle). This assay is based on the conversion of lactate to pyruvate by lactate dehydrogenase (LDH), reducing NAD to NADH (Babson and Phillips, 1965). The concentration of lactate produced by the cells is proportional to an increase in absorbance due to the previously mentioned reduction. The amount of lactate released into the apical and basal medium was measured using 96 well plates (Corning, Sigma Aldrich, Cat# CLS2595).

The reagents were made up as required:

1. TRAM Buffer: 82mM Triethanolamine HCL (Sigma Aldrich, Cat# T1502), 8.2mM Ethylenediaminetetraacetic acid disodium salt dihydrate ($EDTA.Na_2$) (Sigma Aldrich, Cat# 34549), 32mM Magnesium chloride hexahydrate ($MgCl_2.6H_2O$) (Sigma Aldrich, Cat # M2670), pH 7.5 and made up with ddH_2O. Stored at +4°C.

2. Colour Reagent: 0.3mM N-Methylphenazonium methyl sulphate (PMS) (Sigma Aldrich, Cat# P9625), 0.75mM p-iodonitrotetrazolium violet (INT) (Sigma Aldrich, Cat# I8377), 9.5% ethanol, 0.4% Triton X-100 (Sigma Aldrich, Cat# 93426) made up in ddH_2O and heated at 37°C for 5-10 minutes mixing regularly. Stored at +4°C protected from light.

3. Lactate standard: The lactate standard was made up using sodium L-lactate (Sigma Aldrich, Cat# L7022). 0.560g of sodium L-lactate was diluted in 50ml of dH_2O (stock of 100mM) and then diluting to 25mM in the relevant serum free media to produce a serial dilution.

Reagent mix for 1x 96-Well Plate: 4.5mM β-Nicotinamide adenine dinucleotide hydrate (β-NAD) (Sigma Aldrich, Cat# N7004) was dissolved in 15ml of the TRAM Buffer. 4ml of the colour reagent was added and 6.5µl of LDH (Sigma Aldrich, Cat# L2500) was then added.

The samples were thawed and allowed to get to room temperature before being used. They were mixed and centrifuged before the supernatant was sampled. 20µl of each neat unknown sample, the controls (RNase Free Water, and the relevant media) and the serially diluted lactate standard was added in duplicate. 200µl of the reagent mix was then added to each well, mixed and left to incubate for 5-10 minutes at room temperature protected from light. 50µl of the Stop Solution (1N HCL) was added and the plate was read at a wavelength of 490nm within one hour (Bio-Tek Synergy HT).

2.5.4.2 Lactate Dehydrogenase (LDH) assay

This assay is used to measure levels of cell death (specifically necrosis) and cell lysis by measuring levels of lactase dehydrogenase in the cell medium. This assay uses the conversion of iodonitrotetrazolium into a coloured substrate (formazan) after the reduction of NAD^+ to NADH and H^+ through pyruvate oxidation of lactate in the presence of LDH in the culture medium (Chan et al., 2013).

Using a CytoTox 96 Non-Radioactive Cytotoxicity Assay Kit (Promega, Cat# G1780) the percentage of cytotoxicity of the neat samples was measured. The assay buffer was thawed, allowed to reach room temperature and 12ml was added to a bottle of substrate mix. The combination of assay buffer and substrate mix = Cyto Tox96 Reagent. This mixture was inverted gently until dissolved. In order to calculate the cytotoxicity of the samples a number of controls were required to be run with the unknown samples. Controls that were used: background control (medium that has not had any cells grown in it), low control (medium only exposure), high control (maximum LDH release, cells exposed to 2% Triton-X). The cell culture supernatant samples were brought to room temperature before being used. They were mixed and centrifuged before the supernatant was sampled. 50µl of each sample was put into a 96 well plate in duplicate. 50µl of the controls were also added in duplicate to the plate. 50µl of the CytoTox 96 Reagent was added to each well, mixed and the plate incubated at room temperature protected from light for 30 minutes (ensuring that none of the samples became too red before reading). Any large bubbles were popped before reading the absorbance of the plate at 492nm within one hour (Bio-Tek Synergy HT).

The cytotoxicity of each exposure was then calculated using the following equation:

$$\text{Cytotoxicity (\%)} = \frac{\text{unknown sample-low control}}{\text{high control-low control}} \times 100$$

2.6 Murine model exposure and tissue collection

2.6.1 Rodent model of particulate exposure

Female BALB/c mice (6-8 weeks old), obtained from the specific pathogen free breeding unit (Envigo, UK), were used for all experimental work. Food (Special Diets Services Rat and Mouse No.3 Breeding pellets; Special Diets Services, cat# RM3 (P)) and water were available *ab libitum*. Enrichment was added to each cage and a maximum of 6 animals were housed within each cage. Ambient temperature and humidity was maintained (21±2°C and 41±5% respectively) within a 12 hour light/dark cycle. All procedures were approved by the United Kingdom Home Office and completed in compliance with the Animals (Scientific Procedures) Act 1986 under a Home Office granted project licence (30/3021) and personal licences.

2.6.2 Intranasal installation of HDM and particulates

All solutions were prepared just before use using sterile methods. Groups of animals (N=6 or 7) received 25µl intranasally dropwise of CeO_2NPs both with and without DEP (50µg) at various concentrations (50ng, 1.5µg and 15µg) during and after sensitisation with house dust mite

(HDM) (1mg/ml) for 3 weeks. Other studies were conducted exposing groups of animals (N=6 or 7) intranasally to CeO_2NPs both with and without DEP (50µg) at various concentrations (50ng, 1.5µg and 15µg/animal) for 24 hours.

2.6.2.1 HDM induced allergic airway disease

House dust mite (HDM) (Greer Laboratories, Cat# XPB82D3A25 (*Dermatophagoides pteronyssinus*)) was suspended as previously described. All solutions were freshly prepared prior to use from frozen aliquots of stock solution. Groups of mice (n=6 or 7) received 25µl intranasally of 1mg/ml of protein (Brandt et al., 2013b, Canbaz et al., 2015, Farhadi et al., 2014) 3 times a week for 3 weeks (Gregory et al., 2013), either at the same time as particulate exposures or before particulate exposures. Control animals were exposed to PBS at the same time points.

2.6.3 Blood and tissue collection

Animals were anaesthetised using 5% isoflurane in oxygen using a precision vaporiser (V-9 Wall Mount Laboratory Animal Anesthesia System. Item Number: 901810), then euthanized with an overdose of sodium pentobarbital (via intraperitoneal injection) before puncturing the heart with a syringe pre-coated with EDTA (5mM) and removing the blood. The blood was then placed on ice in an EDTA pre-coated Eppendorf with 5µl of EDTA at the bottom of the Eppendorf in order to further prevent coagulation.

After lavaging the whole lung (section 2.6.4.1), it was dissected out and washed with ice cold PBS. The right lung lobe was tied off and snap frozen (in liquid nitrogen), while the left lobe was fixed by perfusion of 10% formalin using 25cm of tubing with a slow perfusion rate for 5 mins. The lung was then stored in formalin for 48 hours before being stored permanently in 70% ethanol. The left kidney and half the liver were also fixed in formalin and processed as above. The right kidney, half the liver, the spleen and thymus were also removed and snap frozen for future analysis.

2.6.3.1 Blood processing for plasma isolation

Blood was centrifuged at 10,000xg for 5 mins at 4°C before removing the plasma and discarding the remaining blood. Plasma was then stored at -80°C before analysis of the IgE levels within the plasma.

2.6.4 Bronchoalveolar lavage (BAL) and inflammatory cell analysis

2.6.4.1 BAL collection

The trachea was viewed upon dissection of the upper throat and a tracheotomy was performed. It is then catheterised using an 18G modified blunt ended needle and sutured into place between the 2nd and 3rd cartilage rings. Bronchoalveolar lavage (BAL) was collected by lavaging the lungs three times with 500µl ice cold sterile PBS via the tracheal cannula, giving a total volume of 1.5ml of BAL. The BAL fluid was then placed on ice before processing and further analysis.

2.6.4.2 BAL processing

BAL fluid was centrifuged at 1500xg for 10mins at 4°C; the supernatant was removed from the first lavage and used for analysis of cytokines via ELISAs. The remaining supernatants were discarded and the cells from all 3 lavages re-suspended in 1ml of ice cold PBS and counted using a haemocytometer. Cells were then re-suspended in ice cold PBS at a concentration of $1x10^6$cells/ml.

2.6.4.3 Cytospin and Inflammatory Cell Counts

200µl of each cell suspension was loaded onto an EZ single cytofunnel (Thermo Scientific, Cat# 97200125) and centrifuged at 480xg for 4mins (Cytospin 4, Thermo Scientific). The remaining cells were then centrifuged at 1500xg for 10mins at 4°C before being suspended in 350µl of lysis buffer (Qiagen) and frozen at -80°C for future analysis. The cytospin slides were then left to dry overnight at room temperature before being stained with Wright-Griemsa stain (Kwik Diff, Thermo Scientific, Cat# 9990700). Slides were then dried overnight again before mounting a

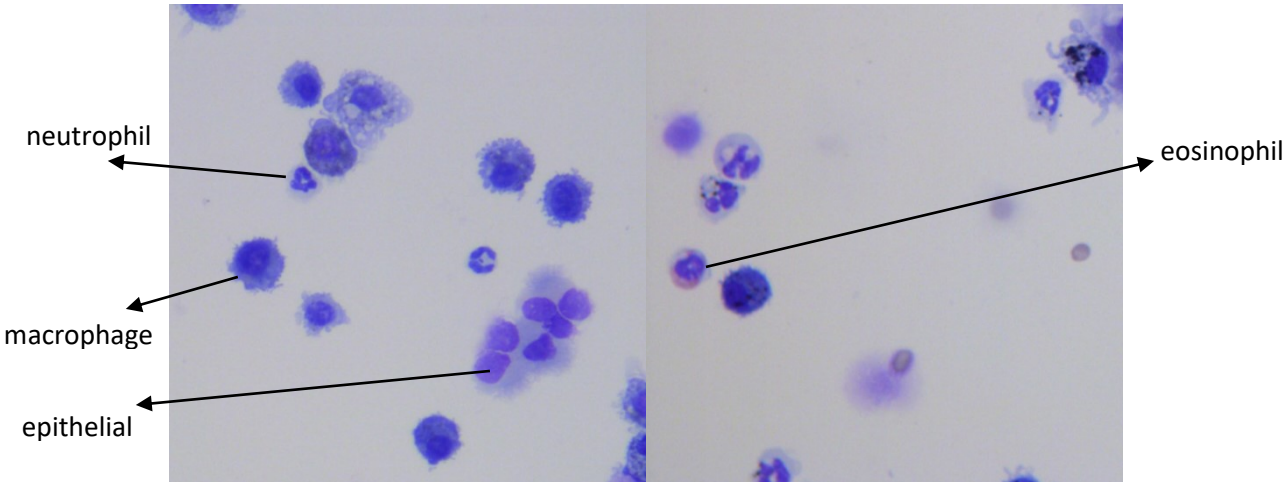


Figure 2-5 Various BAL fluid cells identified. Cells were cytospun and then stained using Kwik Diff stain to identify the various immune cells present.

coverslip and counting 300 cells at 400x magnification. Lymphocytes were identified with a clear blue cytoplasm and red-purple granules; neutrophils were identified with a clear blue cytoplasm and light purple granules in the cytoplasm; eosinophils were identified by bright red/orange granules in the cytoplasm; epithelial cells were identified by light purple nuclei and a light blue cytoplasm and macrophages were identified by a large cytoplasm and dark purple nucleus (Figure 2-5). Cells were counted for each animal over three cytospin slides and an average cell count was obtained for each animal.

2.7 Tissue processing and analysis

It is important to look at both BAL fluid and lung tissue when investigating cytokine release. This is due to the nature of some cytokines and the delayed release of some into the airways, as there may be a difference in the lung tissue (later release) when compared to the BAL fluid (early release).

2.7.1 Bradford assay

The Bradford assay (Bradford, 1976) is a method used to determine the concentration of protein in a sample. It uses an acid solution to bind to the protein, to cause a shift in wavelength and therefore a colour change dependant on protein concentrations.

Using the Bio-Rad Protein Assay Kit II, (Bio-Rad, Cat# 500-0002), a standard was produced using bovine serum albumin and lysis buffer producing a protein concentration standard curve. The dye was prepared by diluting 1:4 with distilled water before filtering with a Whatman #1 filter (GE Healthcare Life Sciences, Cat#10462200). The range of this assay is 0.05 to 0.5mg/ml of protein and therefore a standard was made up to fit within these concentrations. The samples were diluted 1:4 with lysis buffer before 10 µl of each sample and standard was added to a 96 well plate in duplicate. 200µl of the diluted dye was then added to each well, left to incubate at room temperature for at least 5 minutes and the plate absorbance read at 595nm within one hour (Bio-Tek Synergy HT). Any repeats were then carried out if the coefficient variance of the sample concentration was larger than 25%.

2.7.2 Histochemistry and immunohistochemistry

Lungs were fixed in 10% formalin and stored in 70% ethanol before processing as previously described (section 2.6.3). The trachea and heart were removed from the left lung lobe and discarded. The left lobe was then cut bilaterally and both halves processed into paraffin blocks.

2.7.2.1 Dehydration and embedding

Lungs were placed in Tissue Tek Processing Embedding cassettes (Tissue Tek, Cat# 4185TT2), dehydrated and embedded in paraffin wax using the Tissue-Tek (VIP Sakura). Sections were initially placed into formalin for 1 hour, and then moved into fresh formalin for a second hour. After they were then moved into 60%, 70%, 80%, 90%, 100% ethanol for 30mins each time. Sections were then moved into xylene for 45 mins, and then 30 mins before being moved into paraffin wax heated at 60°C for 60 mins and then a further 30 mins. After being embedded, samples where then fixed into moulds and cut to fit the microtome (Leica EG1150H).

2.7.2.2 Cutting and drying

One half of the lung was then cut into 5µm serial sections (Accu-Cut SRM, Sakura) and placed onto frosted microscope slides (Menzeil-Gläser Superfrost Plus, Thermo Scientific, Cat# 10149870), before drying overnight at 37°C.

2.7.2.3 Histochemistry staining

Serial sections were stained for hematoxylin and eosin (H/E) (general histology and inflammation), Periodic acid–Schiff (PAS) (mucin production), Masson's trichrome (extracellular matrix), and toluidine blue (mast cell staining). Sections were automatically stained using a Sakura Tissue Tek Prisma-E2S (Sakura). Before being stained, the sections were dewaxed and hydrated. This involves first removing the paraffin wax by clearing 3 times with xylene (5 minutes each), and then rehydrating through an alcohol series from 100% to distilled water (30 seconds – 1 minute in each concentration). After being stained they were then mounted (a drop of DXP onto the sample) and a cover slip applied before being imaged using Leica DM 2000 and images were captured using the Leica DFC450C (Leica Microsystems Ltd).

2.7.2.4 Haematoxylin and Eosin (H&E) staining

Haematoxylin and Eosin (H&E) staining is a method that has been used to identify various aspects of tissue sections, including the cytoplasm, extracellular matrix and the nucleus. Haematoxylin stains the nucleus blue, while the eosin stains proteins non-specifically pink. This allows various cellular components to be identified and compared between the different exposures. Haematoxylin can also be used without eosin as a nuclear counterstain (Fischer et al., 2008).

Lung sections were dewaxed and rehydrated as previously described in section 2.4.2.3. Sections were then dipped into haematoxylin for 30 seconds, before being rinsed in water for 1 minute,

and then stained with 1% eosin for 30 seconds. Sections were then dehydrated and cleared before being mounted with a coverslip.

2.7.2.5 Periodic acid-Schiff (PAS) staining (Richard-Allan Scientific, Thermo Scientific, Cat# 87007)

Periodic acid-Schiff (PAS) staining is used to stain glycol groups. These compounds are oxidised by the acid and then combined with the Schiff's reagent to produce the distinctive pink colouring. It can be used by pathologists to identify a number of different aliments (PathologyOutlines.com), but in this context, the pink stain is used to identify mucus in the airways.

Lung sections were dewaxed and rehydrated as previously described in section 2.7.2.1. Sections were then placed into periodic acid solution for 5 minutes before being rinsed in deionized water and stained using Schiff reagent for 15 minutes. Slices were then rinsed for 10 minutes in water before staining in haematoxylin for 1 minute and then rinsed again for 30 seconds. Slices were then placed in Bluing reagent for 1 minute and then washed again for 30 seconds. Slices were then dehydrated and cleared before being mounted with a coverslip.

2.7.2.5.1 PAS semi-quantification

Airways of between 100-250µm in diameter (Gregory et al., 2013) were scored for the PAS content. PAS positive cells were shown as a pink colour. The total number of PAS positive cells was divided by the total cell number in order to give a PAS percentage. This percentage was then converted to a PAS score: <10% = 0 11-20% = 1 21-50% = 2 51-75% = 3 and >75% = 4. All airways of correct sizes were included in the count (Empey et al., 2012). All counts were done blinded and per individual animal in order to determine a group average.

2.7.2.6 Masson's trichrome staining (Sigma Aldrich, Cat# HT15-1KT)

Masson's trichrome staining has been developed to stain collagen and can therefore distinguish connective tissue from other tissue. This stain is used to analyse muscular and cardiovascular samples (Munro). This stain is used to determine if any airway remodelling has occurred, identified as an increase in the collagen staining blue.

Lung sections were dewaxed and rehydrated as previously described in section 2.7.2.1. Sections were then placed into pre-heated Bouin's solution at 56°C for 15 minutes and then cooled under running tap water. Sections were then stained in Working Weigert's Iron Hematoxylin Solution for 5 minutes and then washed in running tap water for 5 minutes. Sections were then stained

in Biebrich Scarlet-Acid Fuchsin for 5 minutes, washed and then placed in Working Phosphotungstic/Phosphomolybdic Acid Solution and then Aniline Blue Solution for 5 minutes. Sections were then placed in Acetic Acid for 2 minutes before being dehydrated in alcohol, cleared and then mounted with a coverslip.

2.7.2.7 Toluidine blue staining

Toluidine blue staining is used to identify mast cells, mucins and cartilage. It works by staining any tissues that are rich in both RNA and DNA and are acidic. Mast cells specifically stain darker than surrounding tissue due to their heparin and histamine content. This stain can be used with both wax embedded slides, frozen slides and *in situ* (Sridharan and Shankar, 2012). 0.5% potassium permanganate solution (BDH Chemicals Ltd, Cat# 10217), 1% potassium metabisulphite (Sigma Aldrich, Cat# 60508) and 0.002% toluidine blue solution (Sigma Aldrich, Cat# 198161), distilled water and glacial acetic acid (Sigma Aldrich, Cat# ARK2183) were made up. Lung sections were dewaxed and rehydrated as previously described in section 2.4.2.3. Slides were then placed into the potassium permanganate solution for 2 minutes before being rinsed twice in distilled water and placed into potassium metabisulphite solution for 1 minute. Slides were then rinsed again in running tap water before being submerged in toluidine blue solution for 5 minutes and then rinsed in three changes of distilled water before being dehydrated in alcohol, cleared and then mounted with a coverslip.

2.7.2.8 Immunohistochemistry

Immunohistochemistry utilises the use of antibodies in order to identify specific antigens in tissue sections. Antibody location in the section can be visualised via fluorescence or a peroxidase system which can be linked to either the primary antibody, or a specific secondary antibody (Duraiyan et al., 2012).

All immunohistochemistry stains were carried out using the VECTASTAIN Elite ABC Kit (Vector Laboratories, Cat# PK-6100). An unlabelled primary antibody was applied to the section, then a biotinylated secondary antibody and finally an avidin and biotinylated horseradish peroxidase complex. Sections were dewaxed and rehydrated as previously described in section 2.7.2.1. The antigen unmasking solution was then made up as directed (Vector Labratories, Cat# H-3300) by the manufacturer and sections incubated at 65°C for 30 minutes. All further steps were completed in a humidity chamber and washed with buffer (0.9% saline) between each step. In order to quench endogenous peroxidase activity, the samples are then incubated for 30minutes in 0.3% H_2O_2. Sections were then incubated for 20 minutes with normal blocking serum (150µl

of stock diluted in 10ml of 10mM sodium phosphate, pH 7.5, 0.9% saline (buffer)) and then incubated for 30minutes with the specified primary antibody diluted to the appropriate concentration as outlined (in section 2.7.2.8.1). Sections were then incubated for 30 minutes with the biotinylated secondary antibody (150µl of blocking serum, 50µl of biotinylated antibody stock and 10ml of buffer), before incubating with VECTASTAIN Elite ABC Reagent (2 drops of Reagent A, 5ml of buffer and 2 drops of Reagent B. The bottle is mixed immediately and left to stand for 30 minutes before use. Finally, the sections are incubated with a 3, 3'-diaminobenzidine (DAB) solution (Vector Laboratories, Cat# SK-4100) (84µl of buffer stock solution, 100µl of DAB stock solution and 80µl of hydrogen peroxide solution into 5ml distilled water and mixed well) to obtain a brown colour indicating a positive stain (around 2 minutes of incubation). DAB reaction was stopped by washing the section with distilled water, before being dehydrated in alcohol, cleared and then mounted with a coverslip as previously described (section 2.7.2.3).

2.7.2.8.1 Stains used

Smooth muscle actin antibody (Cat# ab5694, abcam, Cambridge) stains smooth muscle cells in vessel and gut walls. The actin filaments are part of the cytoskeleton and are found in all eukaryotic cells (abcam). The primary antibody was diluted 1:1000 in buffer as indicated by the manufacturer.

Proliferating cell nuclear antigen (PCNA) (Cell Signalling Technology, Cat# 13110) is a marker of proliferation. The primary antibody was diluted 1:8000 in buffer as indicated by the manufacturer.

Chloride channel accessory 1 (CLCA1) (Abcam, Cat# ab180851) is a protein coding gene associated with cystic fibrosis and is thought to play a role in goblet cell metaplasia, mucus hypersecretion and airway hyperresponsiveness (GeneCards). The primary antibody was diluted 1:250 in buffer as indicated by the manufacturer.

2.8 Airway mechanics measurement

Airway mechanics measurements are an established set of tests when investigating, identifying and observing asthma in humans, the clinical assessment and risk of asthma (Walker et al., 2012). Airway hyperresponsiveness is a term that describes airway narrowing in response to a bronchoconstrictor, specifically methacholine and is evaluated by the changes in airway functions (Walker et al., 2012).

The Flexivent (Scireq Scientific Respiratory Equipment Inc) system was run with the Flexiware software (Version 7.6.3). Before an experimental session began, the equipment underwent a full calibration and between each subject the cannula used for measurements was also calibrated.

2.8.1 Anaesthesia and tracheotomy

Animals were anaesthetised with 5% isoflurane in oxygen and maintained intraperitoneally with sodium pentobarbital (90mg/kg), ensuring the subject was at surgical levels of anaesthesia throughout the procedure. The subject was then placed under a heat lamp and the trachea exposed and cannulated (18G ridged cannula). The cannula was inserted between the second and third tracheal ring and mechanical ventilation was initiated immediately (Figure 2-6).

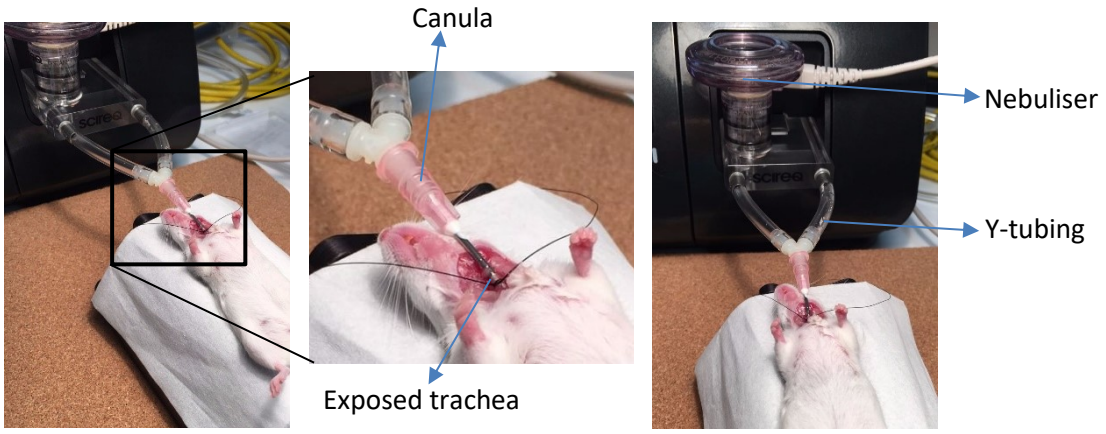


Figure 2-6. Cannulation and airway mechanic measurements. Mice were anesthetised, and the trachea exposed surgically via blunt incisions. The canula was inserted three rings into the trachea and secured with a suture before mechanical ventilation was started immediately and airway hyperresponsiveness measured at various predetermined concentrations.

2.8.2 Airway mechanics protocols

After the subject was connected to the ventilator a deep inflation was initiated. This was to ensure all areas of the airways were opened and lung volume was at its capacity. In order to ensure the subject was fully anesthetised and was not spontaneously respiring, a pressure-

volume curve was measured (PVs-V). Any spontaneous respirations could be seen by any downward inflections within the produced measurements.

The forced oscillation technique (FOT) is a non-spirometric method that is used to measure airway resistance (Kaminsky, 2012). The subject has a normal gentle breathing level (normally under a light sedation), while a mechanical impulse produces a forced perturbation of airflow which can then be measured (Kaminsky, 2012). This technique allows highly detailed measurements to be made while also being reproducible. There are a variety of parameters that can be measured within this method and using the Flexiware software (Version 7.6.3). Within this study we focused on measuring the resistance (R_{RS} and R_N) and the elastance (H and E_{RS}) of the airways (Table 2-5) (Au - McGovern et al., 2013).

Table 2-5. Various measured parameters. Measurement of parameters after the addition of methacholine to the murine airways (Kaminsky, 2012).

PARAMETERS	NAME	DEFINITION
R_{RS}	Respiratory system resistance	Term describing the energy dissipated due to resistive losses
R_N	Newtonian resistance	Term reflecting the opposition of the airways to a flow of air. It is inversely related to the calibre of the large conducting airways.
H	Tissue elastance	Describes the storage of energy in the lung tissue during a forced oscillation manoeuvre.
E_{RS}	Elastance	The stiffness of the respiratory system - including the lung, the chest wall and the airways.

Once it was confirmed there was no spontaneous respiration, the dose response to inhaled methacholine (Acetyl-β-Methylcholine Chloride (Sigma Aldrich, Cat# A2251) aerosol solution could be measured. This was accomplished using a pre-programmed script within the software (mouse inhaled dose response), that allowed an increasing concentration of methacholine to be investigated (0-300mg/ml). Before each set of measurements was completed, 100µl of the specific methacholine dose was placed into the nebuliser. After all the exposures had been completed for the subject, all the y-tubing and cannulas were cleaned and dried before being calibrated again ready for the next subject.

All data was then collected and analysed using the Flexiware software (Version 7.6.3).

2.9 Statistical analysis

The works within this thesis are presented as ± standard error of the mean (SEM).

Before completion of the statistical analysis it was determined that the data sets were independent of each other, there were no significant outliers (identified using Graphpad Prism software), and the samples were normally distributed (also identified using Graphpad Prism software using statistic models).

- For chapter 3, a one-way analysis of variance (ANOVA) analysis (post Fisher's Least Significant Difference (LSD) test) were performed using Prism 6/7/8 software (Graphpad Prism). The p-value was considered significant if p-value <0.05.
- For chapters 4 and 5, a one-way ANOVA analysis (post Fisher's Least Significant Difference (LSD) test) were performed using Prism 6/7/8 software (Graphpad Prism). The p-value was considered significant if p-value <0.05.

Animal numbers for each exposure group were based on previous literature and were randomly assigned groups and consideration for variation implemented (using random blocking (Festing, 2014)), all samples were also scored blinded in order to try and remove any scoring bias.

Materials list

Name	Supplier
10mM dNTP Mix	Bioline
3, 3'-diaminobenzidine (DAB) solution	Vector Laboratories
384 well PCR plates	Bioscience
5x RT Buffer	Bioline
96 well plates	Sigma Aldrich
Acetic acid	Fisher Scientific
Acetic acid	Sigma Aldrich
Acetyl-β-Methylcholine Chloride	Sigma Aldrich
Antigen unmasking solution	Vector Laboratories
BALB/c mice	Envigo, Alconbury, United Kingdom
β-Nicotinamide adenine dinucleotide hydrate (β-NAD)	Sigma Aldrich
Bio-Rad Protein Assay Kit II	Bio-Rad
BioScript Reverse Transcriptase	Bioline
Bovine Pituitary Extract (BPE)	Sigma Aldrich
Bovine Serium Albumin (BSA)	Sigma Aldrich
CCL20 Human ELISA	R&D Systems
CCL20 Mouse ELISA	R&D Systems
Cell scrapper	Corning, Sigma Aldrich
Centifuge	Sorvall Legend RT
Centrifuge	VWR Micro Star 17R
Centrifuge	VWR Mini Star Silverline
Cerium dioxide nanoparticles (CeO_2NPs)	Sigma Aldrich
Chloride channel accessory 1(CLCA1)	Abcam
Claritas PPT Standard 55	SPEX CertiPrep
cOmplete ULTRA tablet, mini, EASYpack	Roche
CoolCell™	Sigma Aldrich
Cryovials	Greiner bio-One
Cytospin 4	Thermo Scientific
CytoTox 96 Non-Radioactive Cytotoxicity Assay Kit	Promega
Diesel exhaust particles (DEP)	National Institute of Standards and Technology (NIST)
Dimethyl sulfoxide	Sigma Aldrich
Disposable folded capillary cuvette	Malvern
DMEM-H	Life Technologies
Dulbecco's Modified Eagle Medium (DMEM) (1x) + GLUTAMAX	Gibco, Life Technologies
DuoSet enzyme-linked immunosorbent assay (ELISA) kits	R&D Systems
ELISA Plates	R&D Systems
Epidermal growth factor (EGF)	Invitrogen
Epinephrine	Sigma Aldrich
Epithelix growth media	Epithelix
Ethanolamine	Sigma Aldrich

Ethylenediaminetetraacetic acid disodium salt dihydrate (EDTA)	Sigma Aldrich
EVOM^2 Epithelial Voltohmmeter	World Precision Instruments Ltd
EZ single cytofunnel	Thermo Scientific
Fetal Bovine Serum	Sigma Aldrich
Flexivent	Scireq Scientific Respiratory Equipment Inc
Formvar/Carbon 200 Mesh Copper TEM grid	Agar Scientific
Hanks' Balanced Salt Solution (HBSS)	Gibco, Life Technologies
House Dust Mite (HDM)	Greer Laboratories, Lenoir
Human primary bronchial airway epithelial cells (hPBECs)	Epithelix
Hydrocortisone	Sigma Aldrich
iCAP Q ICPMS	Thermo Scientific, Loughborough, UK
IgE ELISA	BD Bioscience
IL-13 Mouse ELISA	R&D Systems
IL-17 Mouse ELISA	R&D Systems
IL-17E Human ELISA	R&D Systems
IL-1α Mouse ELISA	R&D Systems
IL-33 Human ELISA	R&D Systems
IL-33 Mouse ELISA	R&D Systems
IL-4 Mouse ELISA	R&D Systems
IL-5 Mouse ELISA	R&D Systems
IL-6 Human ELISA	R&D Systems
IL-8 Human ELISA	R&D Systems
Insulin	Sigma Aldrich
Kartell disposable cuvette	VWR
Kwik Diff Stain	Thermo Scientific
Lactate Dehydrogenase	Sigma Aldrich
Leica (EG1150H)	Leica Microsystems Ltd
Leica DFC450C	Leica Microsystems Ltd
Leica DM 2000	Leica Microsystems Ltd
LHC Basal	Life Technologies
MagNa Lyser	Roche
MagNa lyser beads	Roche
Magnesium chloride hexahydrate (MgCl2.6H2O)	Sigma Aldrich
Masson's trichrome stain	Sigma Aldrich
Menzeil-Gläser Superfrost Plus	Thermo Scientific
Microplate Reader	Bio-Tek Synergy HT
Microtome Accu-Cut SRM	Sakura
Nanodrop 2000	Thermo Scientific, Loughborough, UK
Nanosight (Nanoparticle analysis system, NS14C)	Nanosight Ltd, United Kingdom
Nitric acid	Fisher Scientific
N-Methylphenazonium methyl sulphate (PMS)	Sigma Aldrich
PCR reaction lid	VWR
PCR reaction tube	VWR
Penicillin/Streptomycin	Sigma Aldrich

Periodic acid-Schiff (PAS) stain	Thermo Scientific
Phosphate Buffered Saline (PBS)	Gibco, Life Technologies
Phosphorylethanolamine (PET)	Sigma Aldrich
Pierce LAL chromogenic endotoxin quantitation kit	Thermo Scientific
p-iodonitrotetrazolium violet (INT)	Sigma Aldrich
Potassium metabisulphite	Sigma Aldrich
Potassium permanganate	BDH Chemicals Ltd
Power SYBER Green PCR Master Mix	Applied Biosystems
Proliferating cell nuclear antigen (PCNA)	Cell Signalling Technology
QiAshredder	Qiagen
Quant Studio 6 Flex PCR	Applied Biosystems
Random Hexamer	Bioline
Retinoic acid	Sigma Aldrich
Ribsafe RNase Inhibitor	Bioline
RNase ZAP	Sigma Aldrich
RNeasy mini kit	Qiagen
Sakura Tissue Tek Prisma-E2S	Sakura
SLIP Human ELISA	R&D Systems
Sodium L-lactate	Sigma Aldrich
Sonicator	QSonica Sonicators, CT, USA
Special Diets Services Rat and Mouse No.3 Breeding pellets	Special Diets Services, Essex, United Kingdom
T75cm^2 culture flask	Nunc, Thermo Scientific
Tissue Tek Processing Embedding cassettes	Tissue Tek
Tissue-Tek (VIP Sakura)	Tissue Tek
Toluidine blue	Sigma Aldrich
Transferrin	Sigma Aldrich
Transwell Plates	Corning, Sigma Aldrich
Triethanolamine HCL	Sigma Aldrich
Triiodothyronine	Sigma Aldrich
Triton X-100	Sigma Aldrich
Trypsin	Gibco, Life Technologies
TSLP Human ELISA	R&D Systems
TSLP Mouse ELISA	R&D Systems
Tween80	Sigma Aldrich
Type IV human placenta collagen	Sigma Aldrich
UltraWAVE Single Reaction Chamber Microwave Digestion System	Milestone S.r.l. Fatebenefratelli, Italy
VECTASTAIN Elite ABC Kit	Vector Laboratories
Whatman #1 filter	GE Healthcare Life Sciences
Zetasizer Nano	Malvern, Malvern United Kingdom

Chapter 3: The effect of CeO_2NP / DEP on human primary bronchial cell inflammatory responses *in vitro*.

3.1 Introduction

Envirox™ is a commercially available fuel catalyst comprising of CeO_2NPs that is added to diesel fuel, to reduce fuel consumption and to improve emissions, when used at a recommended concentration of 0.5ml/L of fuel (Zhang et al., 2016). After initial analysis of ambient levels of cerium oxide in the environment following addition of Envirox™ to fuel, it was put forward that chronic exposure to cerium oxide would involve levels less than the no-observed-effect level (NOEL) determined *in vitro* and therefore would be unlikely to cause adverse health effects (Park et al., 2008a). There are a limited number of studies which have examined the potential for adverse health effects of CeO_2NPs from engine emissions particles using fuel catalysts such as Envirox™. Due to the nature of experimental design, it is difficult to establish whether any modifying effects on biological responses can be attributed to CeO_2NPs in fuel emissions or due to modification of emissions characteristics independent of the fuel particles themselves. In addition, the studies that have been performed on emissions from fuel containing Envirox™ focus on characterisation of the chemical and physical attributes of the particles (Dale et al., 2017, Zhang et al., 2013, Zhang et al., 2016), rather than their potential inflammatory and toxic implications. As mentioned above, the Envirox™ particles found within ambient air have varying differences compared to its unburnt form and it is important to establish the health effects of the cerium oxide in the latter format within ambient air.

Envirox™ has been used as a fuel additive in various bus fleets throughout the UK (initially including Newcastle, Birmingham and London before being implemented throughout the UK) via Stagecoach and Abellio buses, as well as North America and Canada (including Quebec and Ontario). As these fuel additives have proven to be cost effective, their popularity is likely to grow, potentially also for domestic use. This is important as release of emissions from these engines will lead to increased ambient levels of cerium oxide as part of diesel exhaust, the potential health impacts of which are yet to be established. Furthermore, people that already have compromised health (including those with respiratory conditions) could be more susceptible to any adverse effects these particles pose.

The most common respiratory disorder worldwide is asthma, but it is not the highest cause of mortality (Burney et al., 2015), which is COPD. The population affected by asthma also contains a high number of young people when compared to other respiratory disorders (Burney et al., 2015). Asthma is a disease that is categorised by its phenotype and cause of exacerbations; its

development is thought to be due to numerous factors, including environmental and genetic (Hekking and Bel, 2014). In terms of environmental exposures previous studies would indicate that asthmatics are susceptible to exacerbations after episodes of high air pollution, including PM2.5, a high proportion by particle number of which is DEP (De Grove et al., 2018, McCreanor et al., 2007, Guarnieri and Balmes, 2014, Bernstein et al., 2004, Pietropaoli et al., 2004, Kurt et al., 2016). It is unclear whether cerium oxide emitted in emissions from diesel fuel containing Envirox™ may modify these effects.

As particles are inhaled, their first interaction within the lung is the bronchial epithelium that comprise the surface of the proximal conducting airways. These cells are the first line of defence against pathogens and particulate matter within the air. They contain ciliated cells as well as producing mucus from secretory and goblet cells to form a physical, mucociliary barrier against environmental insults (Erle and Sheppard, 2014).

In vitro models have been used extensively to investigate the potential effects that particulate matter might have in the lung (Kononenko et al., 2019, Shin et al., 2019, Westphal et al., 2019, Shoeb et al., 2017, Martin et al., 2018, Frohlich, 2017). In order to address the impact particles might have in asthma, epithelial cells from large and small airways would be the best choice, as it is within these regions where the effects of asthma are mostly seen. The large airways are where most of the characteristic inflammatory cells infiltrate (such as eosinophils, neutrophils

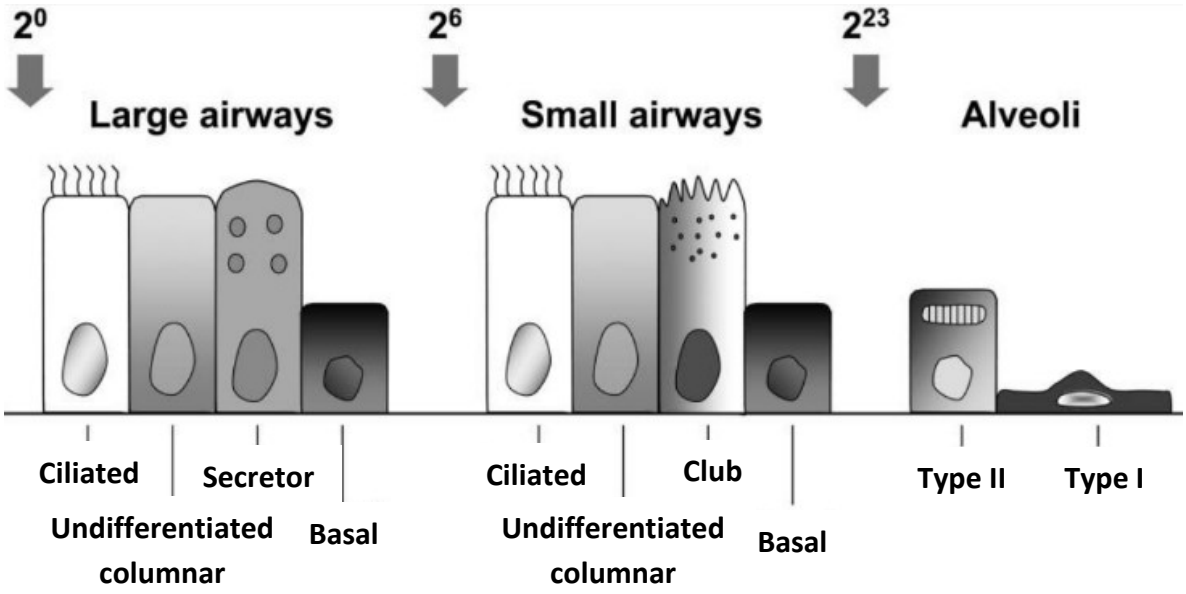


Figure 3-1. Cell types of the epithelial layer within the lung. The large airway spans from 2^0 to 2^5 branches and consists of ciliated, secretory, basal and undifferentiated columnar cells. The small airway spans from 2^6 to 2^{23} branches and contains ciliated, club (Clara), basal and undifferentiated cells. The alveolar unit is present after 2^{23} branches and consists of type I and type II epithelial cells. There are other cells that are not mentioned as they are less common (cartilage cells, mucus glands and neuroendocrine cells). Adapted from Crystal et al., (2008).

and lymphocytes), and also where the effects of mucus hypersecretion, airway remodelling and hyperresponsiveness are identified within an asthmatic airway (Saetta and Turato, 2001). This infiltration and increase in mucus production has also been identified in the smaller airways (Kuyper et al., 2003). Ideally differentiated cells would also be incorporated into models (as previously mentioned) at the specific area of the airway that is under investigation (Figure 3-1) (Crystal et al., 2008). Human primary bronchial epithelial cells (HPBECs) are an invaluable tool when it comes to looking at nanoparticles as they are more representative of what is present in humans *in situ* (rather than, for example, cell lines, although they can be a useful tool). Before application for toxicological assessments, it is important to characterise model composition and to identify appropriate endpoints relevant to tissue pulmonary response in disease (e.g. allergic asthma). In order to achieve organotypic representation of the airway epithelium cultures need to be differentiated before exposure (for example, as described in **Section 2.5**). It is also important to characterise these cells throughout their differentiation to determine culture stability timeframes for treatment. This can be done by measurement of airway cell markers (e.g. Foxj1, SCG1A1, MUC5AC), monolayer integrity (using TEER) and, more specifically, asthmatic markers (such as, TSLP, ADAM33, SLPI, MUC5AC) to establish baselines for treatment. Finally, for many particulate exposure studies, exposure is carried out by suspension in tissue culture medium that overlays the *in vitro* epithelial model (Stoehr et al., 2015, Panas et al., 2014, Herzog et al., 2014, Lenz et al., 2013). A more sophisticated, relevant model would utilise an optimised air-liquid interface (ALI) culture of epithelial cells which are then exposed to environmental particles.

ALI cultures can closely mimic the *in vivo* environment, containing differentiated epithelial cells which form tight junctions, a feature that has been shown to relate to release of additional cytokines when compared to cultures that do not form tight junctions (such as that which are known to be generated *in vivo* (Blume et al., 2013)). This is important as epithelial mediators lead to the activation of both the innate and the adaptive immune system, amongst other processes, depending on the inhaled stimulus. For example, activation of the immune system via DCs (an important mechanism in allergic asthma) can be assisted by epithelial release of cytokines that also attract T cells into the area. As asthma may be classified in part as an immune disorder, changes in the release of mediators from airway epithelial cells upon exposure to airborne material, has the potential to influence the initiation and progression of immune responses underpinning asthmatic disease (Papazian et al., 2015). This may be particularly important in the context of allergen driven asthmatic responses, in which particulate matter may also influence inflammatory responses to common allergens such as HDM and fungal

spores (Papazian et al., 2015). In human studies, asthmatic airways exposed to allergens activate the release of IL-33, IL-25 and TSLP, which in turn leads to the activation of Th2 immunity and other Th2 cytokine release (Wang et al., 2018, Lv et al., 2018). An *in vitro* model of the human conducting airway at ALI offers significant opportunities to investigate such processes.

3.1.1 Hypothesis

We hypothesise that the addition of cerium oxide nanoparticles (CeO_2NPs) will have a moderating effect on the toxicity and bioreactivity of diesel exhaust particles within the human large airway epithelium. We also hypothesise that this effect will manifest in conditions reflective of type II inflammation.

3.1.2 Specific aims

As we have previously stated, there are numerous cell types that make up the airway epithelial layer and it is important that any model used to replicate this layer takes this into consideration. It has also been noted that particulate exposure leads to activation of the epithelial cell layer and the release of various cytokines. These cytokines are an important factor in the activation of the immune response to both particulate matter and inhaled allergens.

The aim of the work in this chapter was to:

- Establish and characterise an *in vitro* conducting airway epithelial cell ALI model for exposure to ambient air pollution nanoparticles.
- Characterise the responses of these cultures to CeO_2NPs alone, DEP alone and CeO_2NPs in combination with DEP.
- Characterise responses to CeO_2NPs alone, DEP alone and CeO_2NPs/DEP in conditions of epithelial type II inflammatory cytokine (IL-4 + IL-13) co-exposure.
- Characterise responses to CeO_2NPs alone, DEP alone and CeO_2NPs/DEP in combination with the common airway allergen HDM.

3.2 Results

3.2.1 Characterisation of HPBECs ALI cultures

Characterisation of the HPBECs cultures was performed to establish that relevant epithelial differentiation had occurred and represented human large airway epithelium as closely as possible – all figures for section 3.2.1 can be found within the appendix. This is an important step, as it also allows baseline levels of relevant endpoints to be established throughout the growth and differentiation periods of culture. Four differentiation media formulations were chosen from the literature. To determine which media and timeframe was most appropriate for exposure studies, HPBECs were differentiated in these media as described (Table 2-4. At the predetermined time points (outlined in Figure 8-1, appendix), light microscopy images were captured (Figure 8-2, appendix), medium was collected (viability and metabolism measurements), transepithelial membrane electrical resistance was measured (Figure 8-3, appendix), and mRNA was processed to determine specific cellular differentiation gene expression markers through PCR analysis (section 2.3.3).

Light microscopy images were captured throughout the growth period (from day 0 to day 43) in both the submerged culture and ALI cultures (Figure 8-12, appendix). This was completed for every donor (n=4) and visualisation of the cells was performed to determine their health and growth patterns before any of the additional analysis was completed. From Figure 8-1 (appendix), cultures that were differentiated in the Matsui media (Figure 8-22, C, appendix) were morphologically different from those in the other media, manifesting as excess mucus production after differentiation.

The TEM image of HPBECs differentiated in Gray medium (Figure 8-2, E, appendix), confirmed that the cells have become pseudostratified (as would be formed within the lungs) with characteristics such as cilia or microvilli present. Although there was formation of microvilli after differentiation of these cells, no ciliated cells were observed. However, there was an upregulation of expression of the cilia-related genes (FOXJ1) (data not shown).

3.2.1.1 Measurement of cellular injury, metabolism and monolayer integrity

Cellular viability (LDH leakage), metabolic status (lactate release) and monolayer integrity (TEER) were measured to assess stability of the model test system. They were also used to inform on which protocol would be taken forward.

Figure 8-3, A (appendix) indicates that at 40 days in culture, there was a significant reduction in the amount of LDH released with the Matsui media after 30 days in culture, which was not

observed with other media. There was an increase in lactate at day 8 (Figure 8-3, B, appendix) in the Gray and Matsui media when compared to the Fulcher and Fulcher+Randell media. Thus, throughout the culture period, differentiation in the Matsui medium resulted in the highest cellular release of lactate from the start through to the end of the times measured. The overall trend in lactate release was an initial increase until the switch to ALI on day 5, a continued increase in the Gray and Fulcher media, which, with the exception of the Matsui medium, decreased. Throughout the culture period, the TEER value was highest in the cells grown in the Gray differentiation medium when compared to the other differentiation media. There was an increase in the TEER values in all the cell cultures from day 0 to day 14 and particularly after the switch to ALI (day 5) (Figure 8-3, C, appendix). Subsequently, TEER fell slowly over the culture period, but was always highest when cells were grown in Gray's medium (Figure 8-3, appendix).

3.2.1.2 Alterations in epithelial mediator gene expression relevant to airway dysfunction.

Gene expression was measured using RT-PCR (data not shown). It is important to note, that mRNA levels may not reflect protein expression of differentiation markers.

Specific marker genes for differentiation of the HPBECs from the literature were investigated to cover the full range of differentiation. This includes markers for mucus (MUC1 and MUC5AC are markers for Membrane-Associated Mucin Genes (Ross et al., 2007)), and are important in the production of mucus and the first line of defence against particulate matter (Ridley and Thornton, 2018); basal cells (KRT14 is a marker for basal cells (Walters et al., 2013)), which are important as they then differentiate into the other cells in the airways; goblet cells, which are present in both the intestines and the airways as a producer of mucus (Birchenough et al., 2015) and club cells (SCGB1A is a club cell marker (Reynolds and Malkinson, 2010)).

KRT14 (cytokeratin 14, CK14) and TP63 (Tumour Protein 63) are both basal cell markers (Dvorak et al., 2011, Wong et al., 2012). The expression of these markers would be expected to initially increase as the cells proliferate. After the differentiation protocol begins, the expression of both KRT14 and TP63 would be expected to decrease as basal cells transition to functional cell types of the airways. It can be observed that KRT14 and TP63 mRNA levels increased with differentiation in the Matsui medium, being significantly higher than all the other media at TP12, TP20, and TP42. This would indicate that the basal cells in this medium were not differentiating. Both KRT14 and TP63 showed an initial increase in expression in all the differentiation media which can be related to cell growth and the formation of a monolayer (up until TP4), followed by a decrease in expression. TP4 was when cells were switched into

differentiation medium and suggests the decrease in expression in these markers was due to changes in cell morphology relating to differentiation.

MUC5AC, TFF3 (Trefoil Factor 3) and MUC1 are representative of either goblet cell/secretory cell differentiation or mucus production, while SCGB1A1 (CC10) is a club cell-specific marker (LeSimple et al., 2007, Dvorak et al., 2011, Ross et al., 2007). Mucus production is an important feature of organotypic conducting airway epithelial models (as mucus is required to remove any foreign bodies that may encounter these cells). mRNA levels of MUC5AC, TFF3 and MUC1 were consistently higher with differentiation in Gray medium compared to other protocols. Fulcher+Randell medium treatment resulted in moderately increased marker expression. This data would suggest that the Gray medium protocol would be the optimum for mucus cell differentiation. SCGB1A1 mRNA expression was increased to a high degree with Fulcher+Randell medium early on during differentiation compared to other media. However, this was not sustained beyond day 28, Gray media resulted in a time dependent and sustained expression of SCGB1A1.

While mucus synthesis is a required feature of a successful conducting airway epithelial cell culture, ciliated cells exist to move the mucus containing foreign bodies via the muco-ciliary apparatus (Mall, 2008). The ideal model would also contain beating cilia, but it is important to be aware that the expression of ciliated cell markers does not indicate beating cilia. TUBB4A (β-Tubulin IV) and FOXJ1 were measured as they are both related to ciliogenesis and differentiation to ciliated cells (Walters et al., 2013, Wong, 2012, LeSimple et al., 2007). FOXJ1 and SCGB1A1 mRNA expression displayed similar expression profiles. At day 20 and day 28, the expression of FOXJ1 in Gray medium was significantly increased when compared to other differentiation protocols. Expression of TUBB4A (beta tubulin) decreased in all the media and expression only started to increase after 40 days of culture. This parallels with observations of a lack of beating cilia within the cultures. However, microvilli were observed by TEM (Figure 8-2, appendix).

Taking the data above into consideration, it was determined that the Gray medium resulted in the optimum differentiation expression when compared to the other medium and would be used in all further *in vitro* studies. This data also suggested that these cultures would remain stable for experimental work until day 35, and that the optimal time to complete particle exposures should be on day 21.

3.2.2 Acute effects of exposure to CeO_2NPs alone, DEP alone and CeO_2NPs+DEP together on HPBECs (24hrs)

To investigate the toxicological and immunological impact of CeO_2NPs and DEP exposure on a model of the conducting airway epithelium, cultures were established using the "Gray medium" differentiation protocol (section 3.2.1). After apical exposure, cells were analysed for adverse effects using biochemical assays and changes in gene and protein expression.

DEP exposure concentrations were determined after an initial dose finding experiment (data not shown within this thesis) and the combined CeO_2NPs+DEP concentrations were calculated based on Park et al. (2008a). Data is summarised in Table 3-1 A and B as well as presented throughout the chapter.

Table 3-1. Summary of PCR and ELISA data from Section 3.2.2. PCR (A) and ELISA (B) data was analysed and summarised in the table below. ↑ indicates an increase in expression; ↑* indicates a significant increase in expression; ↓ indicates a decrease in expression; ↓* indicates a significant decrease in expression; and ↔ indicates no change in the expression of genes of interest.

A.	CeO_2	DEP	CeO_2/DEP
IL-5	↔	↔	↓*
IL-13	↔	↔	↔
TSLP	↔	↑	↔
STAT6	↔	↑*	↑
IL-8	↔	↓*	↑*
IL-6	↓*	↓*	↑
NQ01	↓*	↑	↑
AREG	↔	↔	↓
MUC5AC	↑	↔	↓
CYP1A1	↑	↑	↑*
IL-33	↔	↔	↓*
ADAM33	↓*	↓*	↓*
CCL26	↔	↓*	↓*
CCL20	↔	↔	↓
CCL24	↔	↓*	↓
CCL11	↓*	↓*	↓*
CCL17	↓	↔	↓*
IL-25	↑*	↔	↑*

B.	CeO_2	DEP	CeO_2/DEP
TSLP	↑*	↑*	↑*
IL-33	↑*	↑*	↑*
CCL20	↑	↑	↔
IL-17A	↔	↔	↓
TNF-α	↓*	↓*	↓*
IL-6	↓	↓*	↓
IL-8	↓	↓	↑
SLPI	↔	↔	↔

3.2.2.1 Measurement of cellular viability, metabolism and monolayer integrity

Figure 3-2 indicates that none of the particle combinations had a significant effect on either the viability (LDH release) or metabolic status (lactate production) and monolayer integrity of the cultures 24 hours after particle exposures was also measured using TEER. There was no effect on the TEER value after exposure to CeO_2NPs at any of the concentrations when compared to control media alone. There was, however, a significant increase in the TEER value above unexposed control after exposure to DEP at the lowest three concentrations (1, 10 and 25µg/ml), which was diminished by co-exposure with CeO_2NPs.

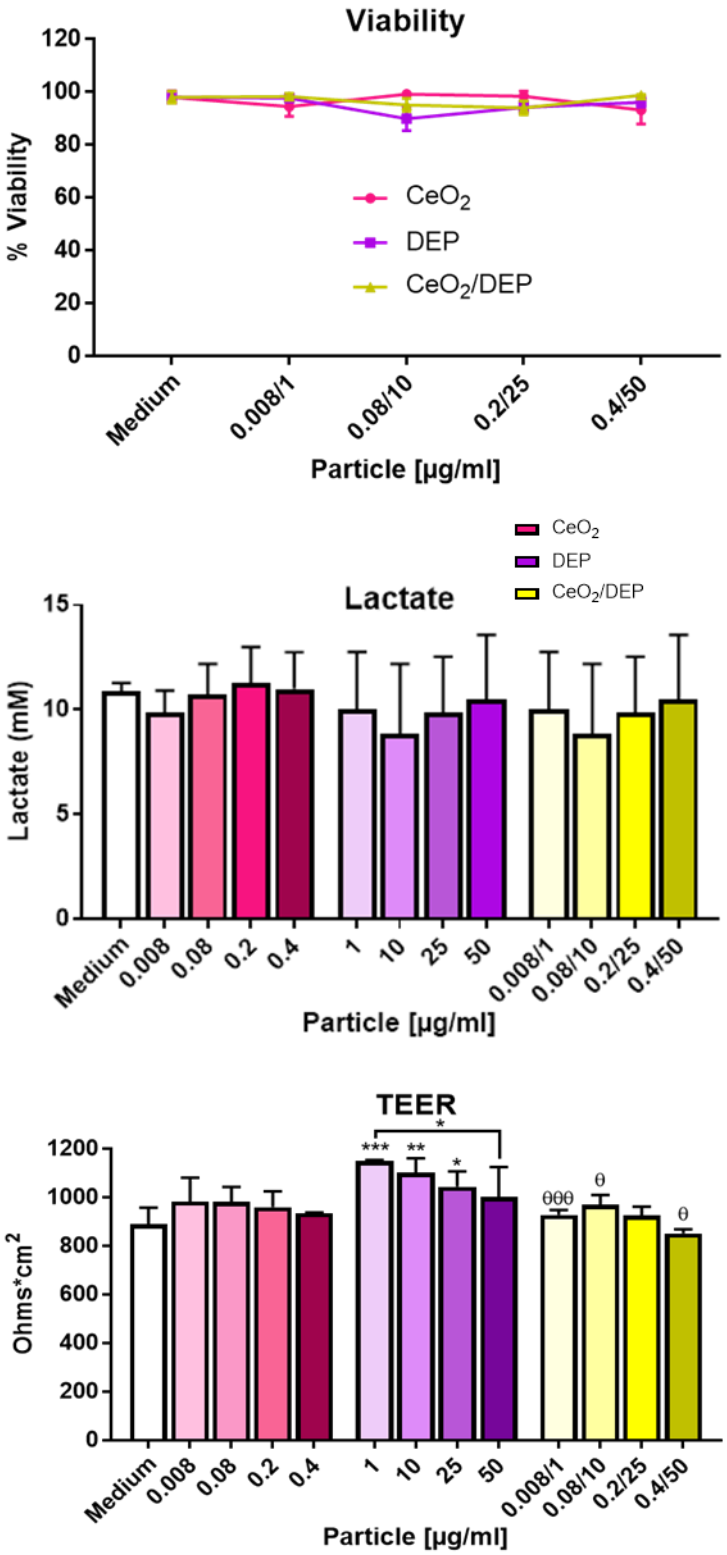


Figure 3-2 Cell viability, cellular metabolism and monolayer integrity after 24 hours exposure to CeO_2NPs alone, DEP alone and CeO_2NPs/DEP combined. Cellular behaviour was measured as LDH release and lactate production in the basolateral compartment, indicating cellular injury and cellular metabolism, and TEER measurements of monolayer integrity were also completed 24 hours after particle exposure, after the particles had been removed from the apical side of the membrane. N=4-8 subjects with all assays performed in triplicate. The data are presented as the mean ±SEM. Significance is denoted as the following: compared to medium control $p<0.05$(*), $p<0.01$(**) and $p<0.001$(***) and compared to DEP alone $p<0.05$(Θ), $p<0.01$(Θ Θ) and $p<0.001$(Θ Θ Θ).

3.2.2.2 *Alterations in epithelial expression of genes that mediate immune responses*

Inflammatory gene expression changes were next examined for any modulating effect of particle exposure using the same differentiated cultures. Figure 3-3 indicates that there was little change in the expression of type II response-related cytokines after exposure to the various particles when compared to the medium control. CeO_2NPs exposure has no effect on TSLP or STAT6 but leads to an inhibition of IL-13 expression at the same degree, regardless of CeO_2NPs concentration and a stimulation of IL-5 expression after exposure to the lower concentrations (but not significantly due to the variation between samples).

There was a trend for the lower concentrations of DEP to stimulate IL-5, and IL-13, while 1µg/ml DEP stimulated STAT6 expression compared to the medium control. TSLP expression was not affected by exposure to DEP when compared to the medium control. Co-exposure to CeO_2NPs/DEP had no effect on the expression of TSLP, IL-13 or STAT6 when compared to the

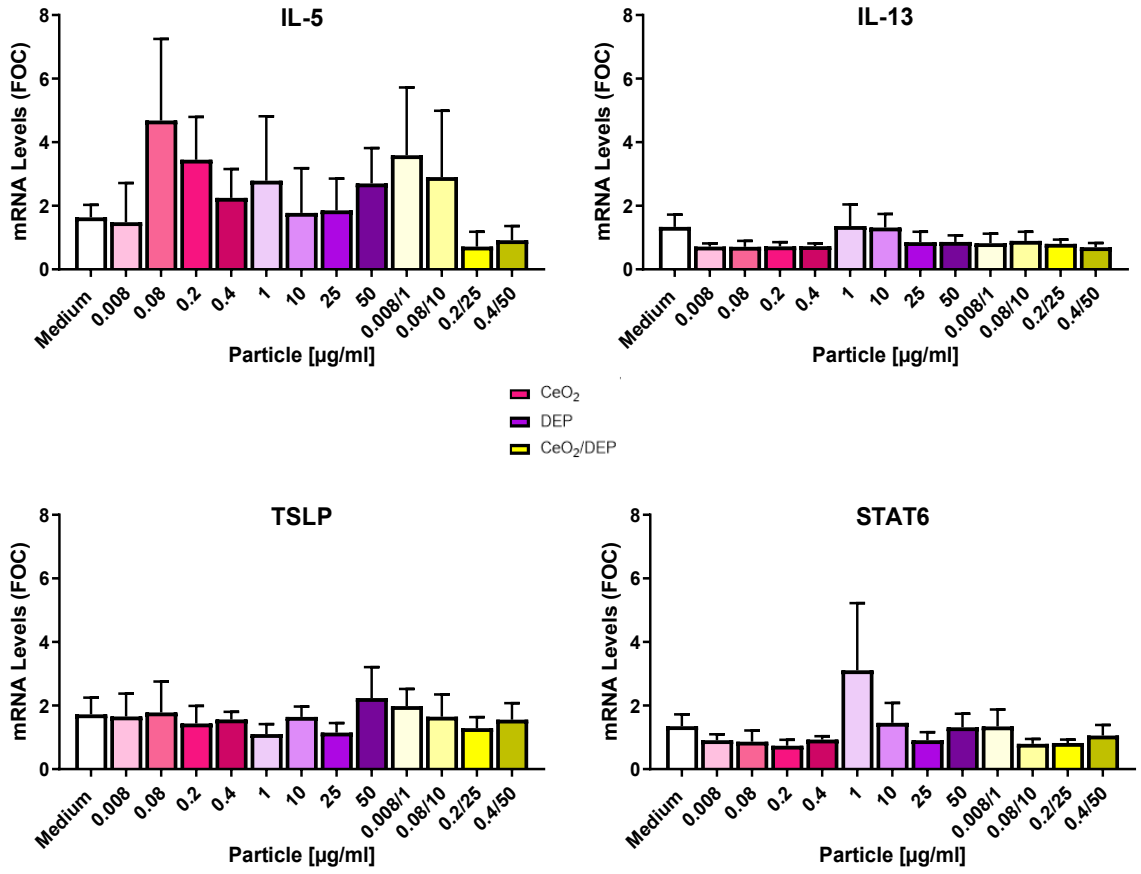


Figure 3-3 Changes in epithelial immune type II response gene expression after 24 hours exposure to CeO_2NPs alone, DEP alone and CeO_2NPs/DEP combined. RT-PCR expression changes in HPBECs after 24 hours of exposure to particles. N =4-8 subjects with all assays performed in triplicate. The data are presented as the mean fold over GAPDH control (FOC) ±SEM. After treatment, mRNA was isolated and examined for transcript levels of the indicated inflammatory markers by RT-PCR analysis identified as type II inflammatory markers. Significance is denoted as the following: compared to medium control $p<0.05$(*).

particles alone and the medium control. There was a suppression in the expression of IL-5 after co-exposure at the highest concentrations when compared to the medium control, but this was not significant when compared to each of the particles individually.

Additional inflammatory endpoints were also assessed (Figure 3-4). CeO_2NPs alone exposure did not influence the mRNA expression of IL-8 but inhibited the expression of IL-6 (except 0.08 and 0.4µg/ml, which had a higher between subject variation in expression compared to the other concentrations) when compared to medium controls. The highest concentration of DEP was observed to increase expression of IL-8 and IL-6 when compared to medium alone. The lower concentrations of DEP also had an inhibitory effect on IL-6; however, this was not significant when compared to the medium alone. Co-exposure to CeO2NP/DEP stimulated IL-8 expression at the lowest concentrations (when compared to the medium control). There was no significant difference in expression of IL-6 with co-exposure, but an increasing trend, which revealed that the reduction in IL-6 expression with the lowest CeO2NP and DEP exposure was also reflected in the co-exposure with CeO_2NPs. Overall, there was a differential response in gene expression when exposed to CeO_2NPs, DEP and CeO_2NPs/DEP with the trend indicating that the addition of CeO_2NPs to DEP increased the effect of DEP alone.

Expression of genes that are activated by oxidative stress and the aryl hydrocabon receptor (ArR), as well as those that are involved in mucus production, airway remodelling and asthma (Figure 3-5) were also measured. CeO_2NPs exposure inhibited expression of NQO1 (after

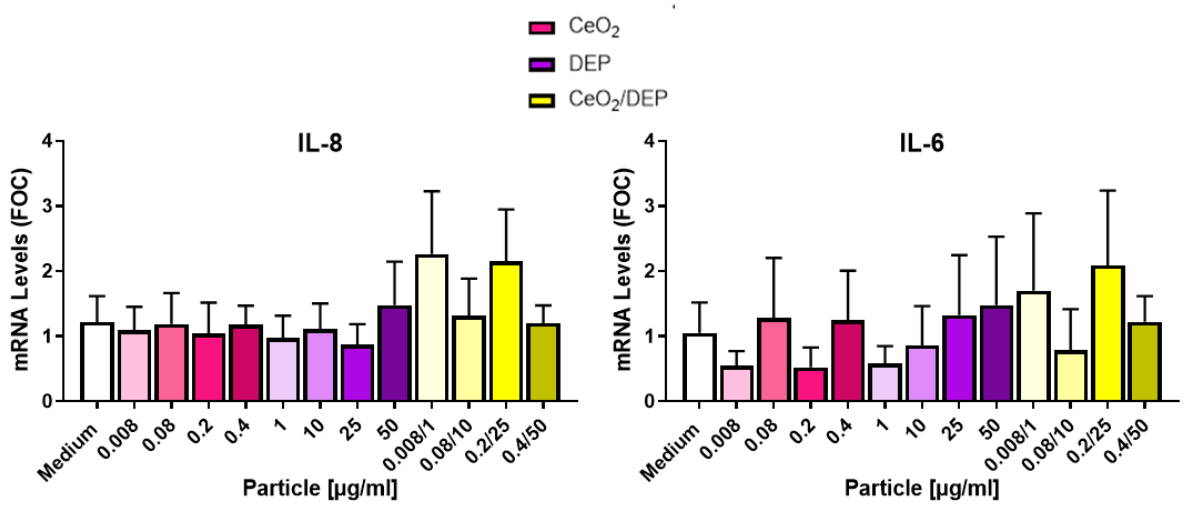


Figure 3-4 Changes in epithelial pro-inflammatory gene expression after 24 hours exposure to CeO_2NPs alone, DEP alone and CeO_2NPs/DEP combined. RT-PCR expression changes in HPBECs after 24 hours of exposure to particles. N =4-8 subjects with all assays performed in triplicate. The data are presented as the mean fold over GAPDH control (FOC) ±SEM. After treatment, mRNA was isolated and examined for transcript levels of the indicated inflammatory markers by RT-PCR analysis identified as transcript levels of indicated pro-inflammatory chemokines. Significance is denoted as the following: compared to medium control $p<0.05$(*) and compared to DEP alone $p<0.05$(Θ).

exposure to the 3 lowest concentrations), and ADAM8 (after exposure to the highest concentration). There was no effect on the expression of AREG or IL-33. DEP exposure inhibited ADAM8 at 10μg/ml. The lower two concentrations stimulated the expression of IL-33 and the higher three concentrations stimulated CYP1A1 expression dose dependently (however not significant). DEP had no effects on the expression of MUS5AC or AREG after exposure to any of the concentrations investigated.

The combined particles had no effect on expression of NQO1 at any of the concentrations, but inhibited expression (not significantly) of AREG and MUC5AC at the highest concentrations when compared to medium alone. The lowest concentration inhibited the expression of ADAM8 when compared to both the medium control and 0.2/25μg/ml combined particles. In addition, the highest concentration of combined particles decreased expression of IL-33 when compared to the medium control and the two lower concentrations. CYP1A1 expression is stimulated at the highest concentration when compared to the medium control and the CeO_2NPs alone. The other concentrations may increase expression, but the variability is too high to determine the significance of this.

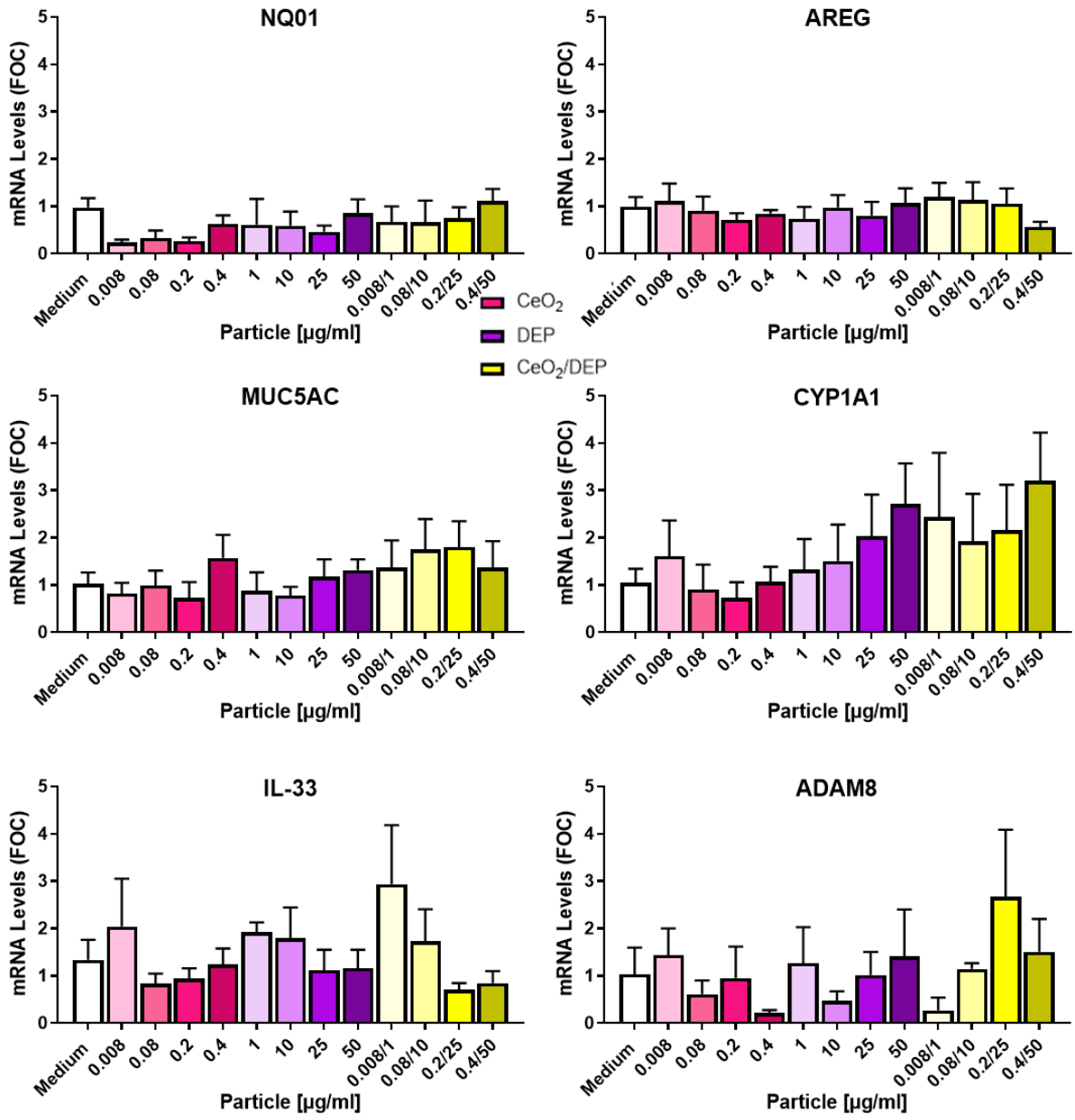


Figure 3-5 Changes in gene expression of molecules that modulate asthma after 24 hours exposure to CeO_2NPs alone, DEP alone and CeO_2NPs/DEP combined exposures. RT-PCR expression changes in HPBECs after 24 hours of exposure to DEP. N=4-8 subjects with all assays performed in triplicate. The data are presented as the mean fold over GAPDH control (FOC) ±SEM. After treatment, mRNA was isolated and examined for transcript levels of the identified markers by RT-PCR analysis. Significance is denoted as the following: compared to medium control $p<0.05$(*), and <0.01(**), compared to CeO_2NPs alone $p<0.05$(▪).

Expression levels of genes involved in chemotactic and immune cell activation were next examined for alterations after particle exposure in differentiated airway cultures (Figure 3-6). Although CeO_2NPs exposure tended to inhibit expression of CCL26, CCL20 and CCL17 to the same degree regardless of concentration, compared to medium control, this was not significant. In contrast, CeO2NPs inhibited expression of CCL11 after exposure to 0.008 and 0.2 µg/ml when compared to the medium control. Exposure may have stimulated the expression of CCL24, however the variability was too high to establish significance. The highest concentration of CeO_2NPs markedly and very significantly stimulated the expression of IL-25. DEP exposure had no effect on the expression of CCL20, CCL17 or IL-25, but caused an inhibition of expression of CCL26 at the highest two concentrations when compared to the lowest concentration of DEP. DEP exposure also inhibited the expression of CCL11 at the lowest concentration when compared to the medium control. The expression of CCL24 was significantly stimulated at the two lowest DEP concentrations when compared to the medium control and the two highest DEP concentrations, but the two highest concentrations had no effects on the expression.

The combined particles had no effect on the expression of CCL20 at any of the concentrations. The lowest combined concentration stimulated an increase in the expression of CCL26 (when compared to the medium control, CeO_2NPs alone and the second lowest and highest combined concentrations), CCL24 (when compared to the medium control), and CCL17 (when compared to CeO_2NPs alone and the second lowest and highest combined concentrations), while the higher concentrations had no effect. CCL11 expression was inhibited by the lowest concentrations of CeO_2NPs/DEP, when compared to the medium control. IL-25 expression was significantly increased at the highest combined particle concentrations when compared to all other combined exposures, the medium control, CeO_2NPs alone and DEP alone.

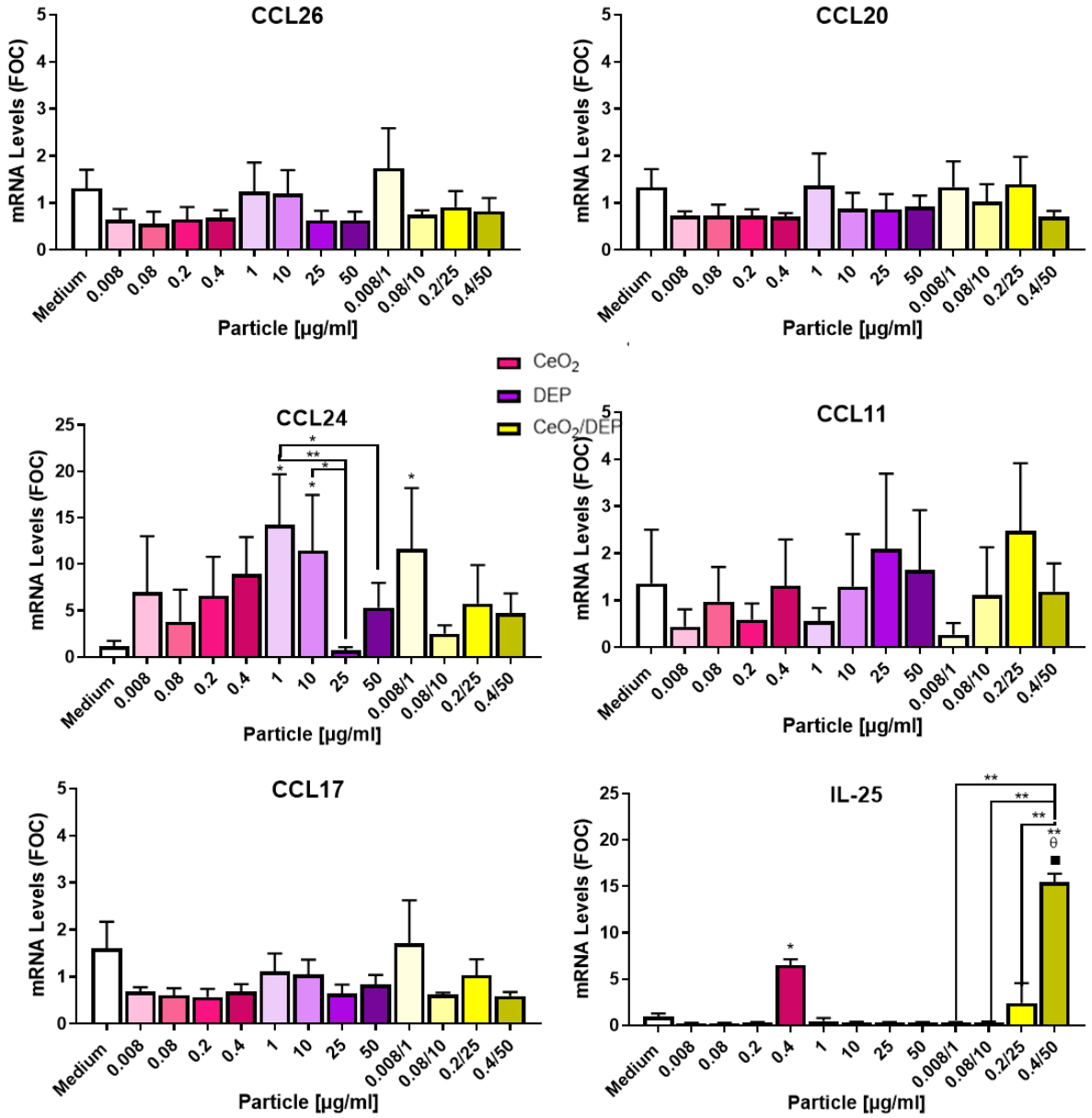


Figure 3-6 Gene expression changes related to induction of immune cell chemotaxis after 24 hours exposure to CeO_2NPs alone, DEP alone and CeO_2NPs/DEP combined. RT-PCR expression changes in HPBECs after 24 hours of exposure to particles. N=4-8 subjects with all assays performed in triplicate. The data are presented as the mean fold over GAPDH control (FOC) ±SEM. After treatment, mRNA was isolated and examined for transcript levels of the indicated inflammatory markers by RT-PCR analysis. Significance is denoted as the following: compared to medium control p<0.05(*), and <0.01(**); CeO_zNPs alone p<0.05(▪); and compared to DEP alone p<0.05(Θ), p<0.01(Θ Θ).

3.2.2.3 *Alteration in levels of epithelial protein mediators of allergic immune responses and inflammation.*

Medium derived protein levels of selected cytokines which mediate inflammation and allergic immune responses were measured in the apical and basal compartments of airway epithelial cultures after 24 hours exposure to particles using the same exposure protocol as described in section 2.4. These levels were derived from the same models used for RNA expression analysis. Levels of these mediators were generally lower in the basal compartment compared to the apical, with either no significant differences observed with particle exposure or the differences were physiologically insignificant compared to the apical levels (Figure 8-4, Figure 8-5 and Figure 8-6 (appendix)).

Considering mediators involved with type II immune responses (Figure 3-7) (TSLP, IL-33 and CCL-20), CeO_2NPs significantly stimulated apical release of TSLP (at all concentrations), and IL-33 (at 0.08µg/ml), but not CCL20. DEP significantly stimulated apical release of TSLP (1 and

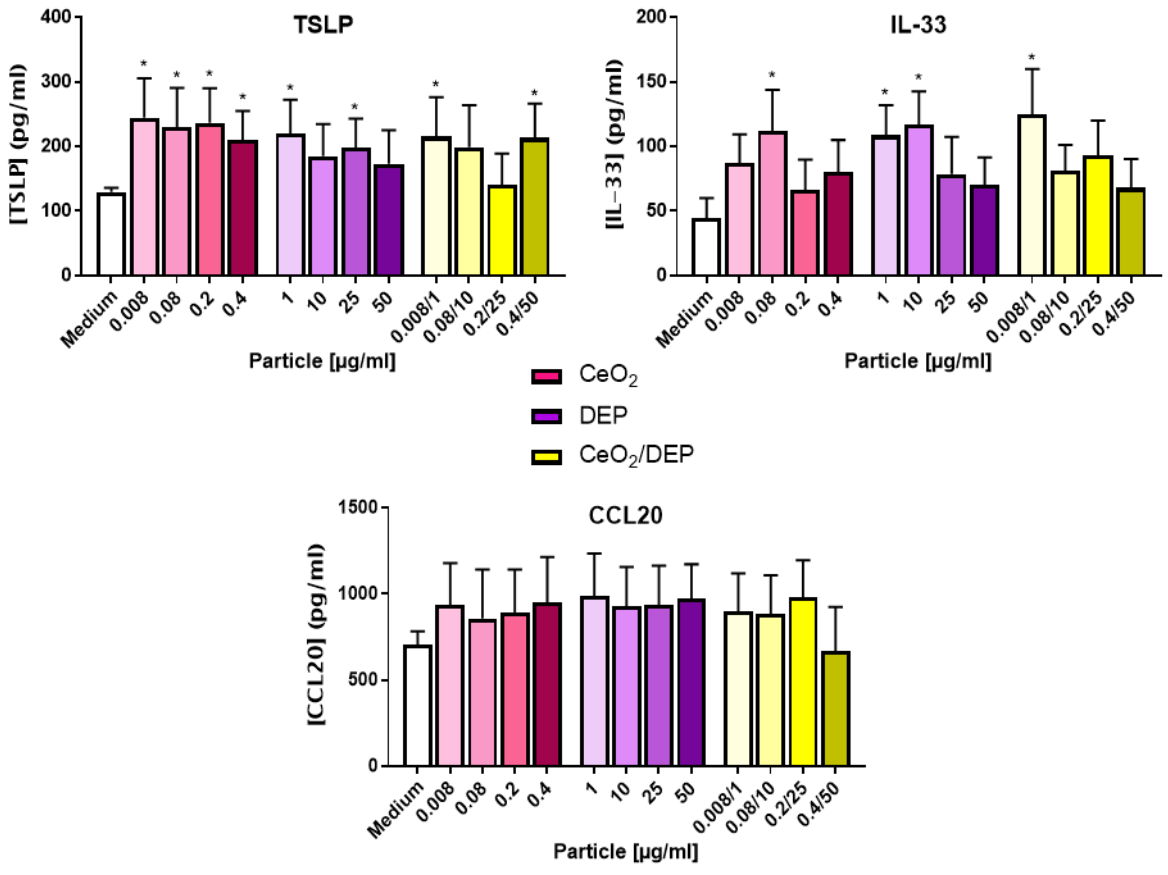


Figure 3-7 Changes in immune type II apical mediator release after exposure for 24 hours to CeO_2NPs alone, DEP alone and CeO_2NPs/DEP combined. Analysis of mediator release in apical medium from HPBECs after 24 hours of exposure to particles. Medium was centrifuged and particles were removed before mediator concentration was analysed via ELISA. The data are presented as the mean ±SEM. N=4-8 subjects with all assays performed in triplicate. Significance is denoted as the following: compared to medium control $p<0.05$(*).

25µg/ml), IL-33 (at the two lowest concentrations) but had no effect on the release of CCL20. The combined particles also significantly stimulated the release of TSLP (at the highest and lowest concentrations), IL-33 (at the lowest concentration), but had no effect on the release of CCL20.

Regarding the pro-inflammatory mediators, IL-17A, TNFα, IL-6 and IL-8 (Figure 3-8). There was a significant 3-fold increase in the apical release of IL-17A after exposure to 0.08µg/ml CeO_2NPs when compared to the medium control and the highest CeO_2NPs exposure. There was a striking significant inhibitory effect of CeO_2NPs on baseline apical TNFα release (>50% reduction at all concentrations, when compared to medium control levels). Neither IL-6 nor IL-8 were significantly affected by CeO_2NPs exposure.

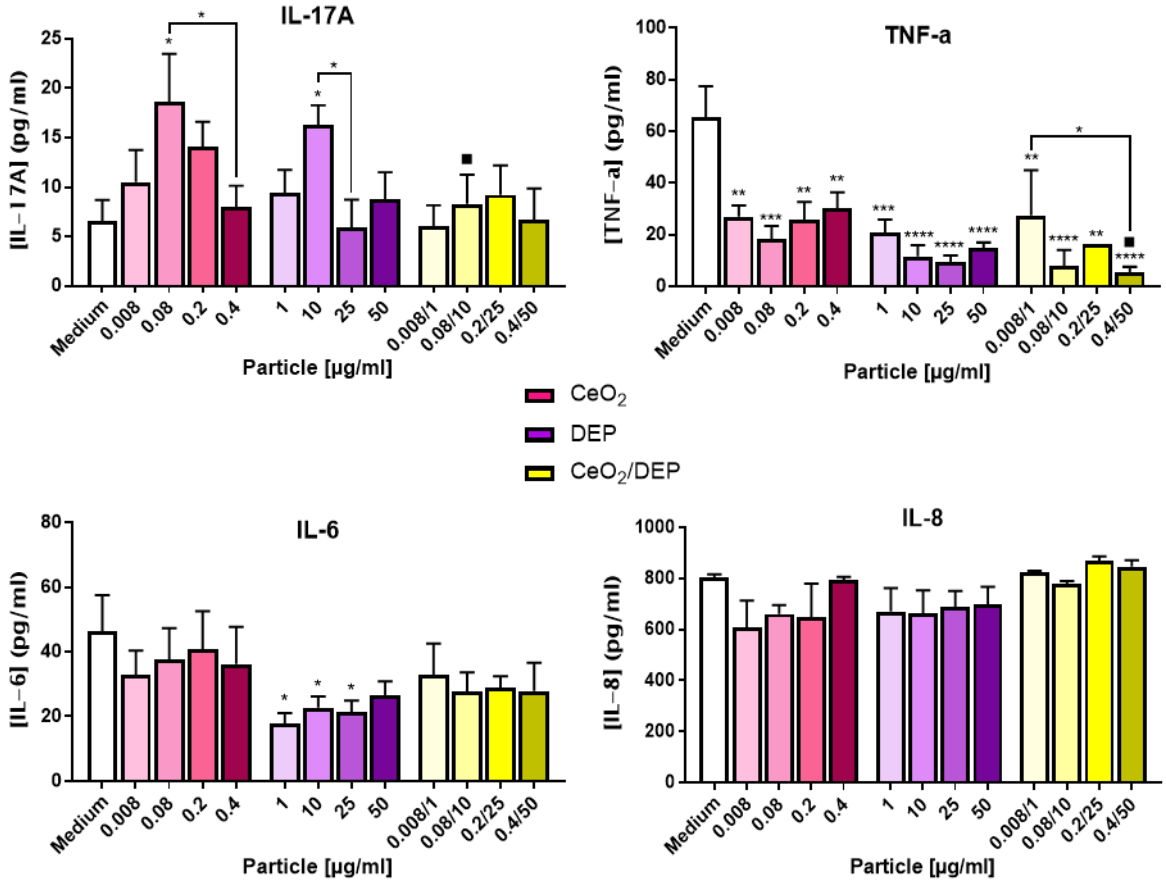


Figure 3-8 Changes in pro-inflammatory apical mediator release after exposure for 24 hours to CeO_2NPs alone, DEP alone and CeO_2NPs/DEP combined. Analysis of mediator release in apical medium from HPBECs after 24 hours of exposure to particles. Medium was centrifuged and particles were removed before mediator concentration was analysed via ELISA. The data are presented as the mean ±SEM. N=4-8 subjects with all assays performed in triplicate. Significance is denoted as the following: compared to medium control $p<0.05$(*), $p<0.01$(**), $p<0.001$(***), $p<0.0001$(****); and CeO_2NPs alone $p<0.05$(▪).

DEP exposure caused a significant increase in IL-17A apical release after exposure to 10µg/ml when compared to the medium control and 25µg/ml exposure. Exposure to DEP at all concentrations significantly decreased apical TNFα when compared to the medium control. It also significantly decreased the apical release of IL-6 after exposure to the three lowest concentrations of DEP when compared to the medium control (~50% of control). There was no change in the release of IL-8 after any of the DEP exposures.

Exposure to the combined particles significantly decreased IL-17A apical release after exposure to 0.08/10µg/ml when compared to the same concentration of CeO_2NPs and DEP alone. The combination of CeO_2NPs/DEP caused lower concentrations of IL-17A when compared to the individual particles alone. TNFα apical release was significantly decreased after exposure to all concentrations of combined particles when compared to the medium control; the highest concentration of CeO_2NPs/DEP caused a significantly greater decrease in TNFα when compared to the lowest concentration and the CeO_2NPs alone exposure. Apical IL-6 levels were significantly lower than the medium control after exposure to the lowest three DEP concentrations. The other exposures also caused a decrease; however, these were not significant. After exposure to CeO_2NPs/DEP the concentration of apical IL-8 was not different from control, as also observed with the particles alone.

Apical SLPI release (Figure 3-9), an antiprotease that is important in lung defence, showed no changes in concentration following CeO_2NPs and/or DEP exposure.

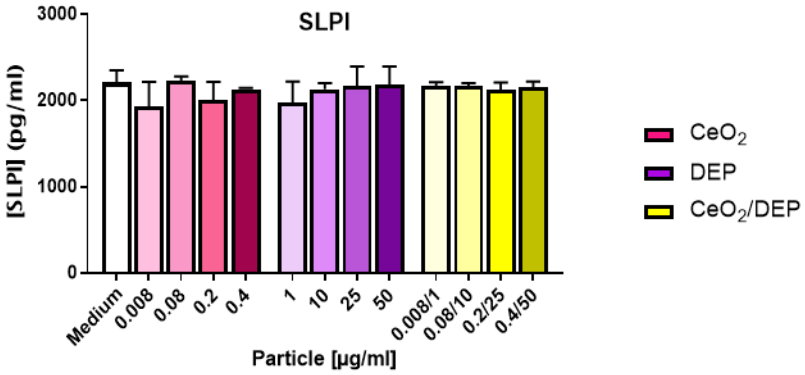


Figure 3-9 Changes in lung defence (SLPI) apical mediator release after exposure for 24 hours to CeO_2NPs alone, DEP alone and CeO_2NPs/DEP combined. Analysis of SLPI release in apical medium from HPBECs after 24 hours of exposure to particles. Medium was centrifuged and particles were removed before SLPI concentration was analysed via ELISA. The data are presented as the mean ±SEM. N=4-8 subjects with all assays performed in triplicate. Significance is denoted as the following: compared to medium control $p<0.05$(*).

3.2.3 Acute effects of exposure to particles in the presence of type II inflammatory signals (IL-4+IL-13) on the phenotype of HPBECs *in vitro*

The impact of co-exposure to type II inflammatory signals on the airway epithelial response to particle exposure was next examined. Data is summarised in Table 3-2 A and B as well as presented throughout the chapter.

Table 3-2 Summary of PCR and ELISA data from Section 3.2.3. PCR (A) and ELISA (B) data was analysed and summarised in the below table. ↑ indicates an increase in expression; ↑* indicates a significant increase in expression; ↓ indicates a decrease in expression; ↓* indicates a significant decrease in expression; and ↔ indicates no change in the expression of genes of interest.

A	CeO_2			DEP			CeO_2/DEP		
	IL-4	IL-13	IL-4+IL-13	IL-4	IL-13	IL-4+IL-13	IL-4	IL-13	IL-4+IL-13
IL-5	↑	↔	↑*	↑	↔	↑*	↔	↔	↑*
IL-13	↑*	↑*	↓	↑*	↑*	↓	↑*	↑*	↓
TSLP	↓*	↑*	↔	↓*	↔	↔	↓*	↑*	↑
STAT6	↔	↔	↓	↑	↔	↔	↔	↑*	↔
IL-8	↑	↔	↓	↑*	↔	↔	↑	↑	↓
IL-6	↑	↑	↑	↑*	↔	↓	↔	↑	↓
NQ01	↓	↓	↔	↑*	↓	↑	↑	↑*	↑
AREG	↑	↑*	↑	↑	↑*	↑	↑	↑*	↑
MUC5AC	↑	↑	↑*	↑	↑	↑*	↑	↑	↑*
CYP1A1	↔	↑	↔	↑*	↑	↔	↑*	↓	↔
IL-33	↔	↔	↑*	↔	↑	↑*	↔	↑	↑*
ADAM33	↓*	↑	↓*	↓*	↑	↓*	↓*	↑	↑
CCL26	↑*	↑	↓	↑*	↑	↓	↑*	↑	↑
CCL20	↔	↔	↔	↔	↔	↔	↔	↑*	↔
CCL24	↑*	↑*	↔	↑*	↑	↑	↑*	↑	↔
CCL11	↑	↔	↔	↑	↔	↔	↑	↔	↔
CCL17	↔	↑	↓	↔	↑	↔	↔	↑*	↔
IL-25	↔	↓	↔	↔	↓	↔	↔	↑	↔

B	CeO_2			DEP			CeO_2/DEP		
	IL-4	IL-13	IL-4+IL-13	IL-4	IL-13	IL-4+IL-13	IL-4	IL-13	IL-4+IL-13
TSLP	↔	↔	↔	↔	↔	↔	↔	↔	↔
IL-33	↑	↑	↔	↑	↔	↔	↔	↔	↑*
CCL20	↔	↔	↓	↓	↔	↓	↓	↔	↓
IL-17A	↔	↑*	↑	↑*	↓	↔	↔	↔	↔

3.2.3.1 Measurement of cellular viability, metabolism and monolayer integrity

Cellular viability, metabolic status and monolayer integrity were assessed as previously outlined in section 3.2.2.1. The differentiated *in vitro* epithelial models were established as outlined in section 2.5.1. IL-4 (10ng/ml), IL-13 (10ng/ml) and IL4+IL-13 (10ng/ml) were applied to the cultures, immediately followed by exposure to CeO_2NPs, DEP and CeO_2NPs/DEP for 24 hours, as described previously (section 2.5.4.4). Cellular viability, as measured by LDH release was, for the most part, relatively unchanged compared to untreated control (Figure 3-10).

Exposures involving IL-4 did not cause greater than 10% decrease in viability with the exception of a decrease (~18%) in the cellular viability after the HPBECs were co-exposed to IL-4 and 0.4µg/ml CeO_2NPs when compared to the medium control (Figure 8-7, appendix). Although most exposures involving IL-13 did not cause more than 10% reduction in viability, treatment with IL-13 alone and co-exposure to IL-13 with 50µg/ml DEP, viability was reduced by ~12%. There was a significant further reduction in the viability, reaching a total of ~ 20% after co-exposure to IL-4/13 and 1µg/ml DEP, which, on exposure to the higher DEP concentrations was only ~8% and remained consistent regardless of the DEP concentration. There were no significant differences from control in viability when cells were exposed to CeO_2NPs/DEP ± cytokines.

In contrast to apparently little effect of the cytokines with and without particles on viability, lactate release was markedly altered by treatment. There was a significant decrease in the lactate released in all the exposures involving IL-4 and IL-13 alone (~30%) and a further significant decrease in the lactate levels in the IL-4/13 exposure (~75%) groups (Figure 3-10). Co-exposure with CeO_2NPs, DEP or CeO_2NPs/DEP had no obvious significant additional effect (Figure 3.22), although there was an apparent particle-dependent non-significant reduction from no particle exposure to CeO_2NPs/DEP co-exposure at 0.4/50 µg/ml. After particle alone exposure the lactate production remained consistent and the same as the non-treated control, regardless of particle type or mixture concentration (Figure 3-10). Similar effects with cytokine + particle exposures were observed at lower doses of particles, albeit non-significant differences between single IL-4 or IL-13 and combined IL-4/13 exposure lactate levels were less pronounced at lower particle co-exposure treatments (Figure 8-7, appendix). This could potentially indicate a change in the metabolic activity of the cells.

Monolayer integrity as assessed by TEER revealed small, non-significant differences on treatment, except for co-exposure to IL-4 and 0.4/50µg/ml CeO_2NPs/DEP, where an increase compared to medium control and other particle exposures was observed. (Figure 3-10, Figure

8-7, appendix). Further examination of the complete TEER data set (Figure 8-7, appendix) shows that co-exposure to IL-4 and the two lower exposures of DEP caused a decrease in TEER.

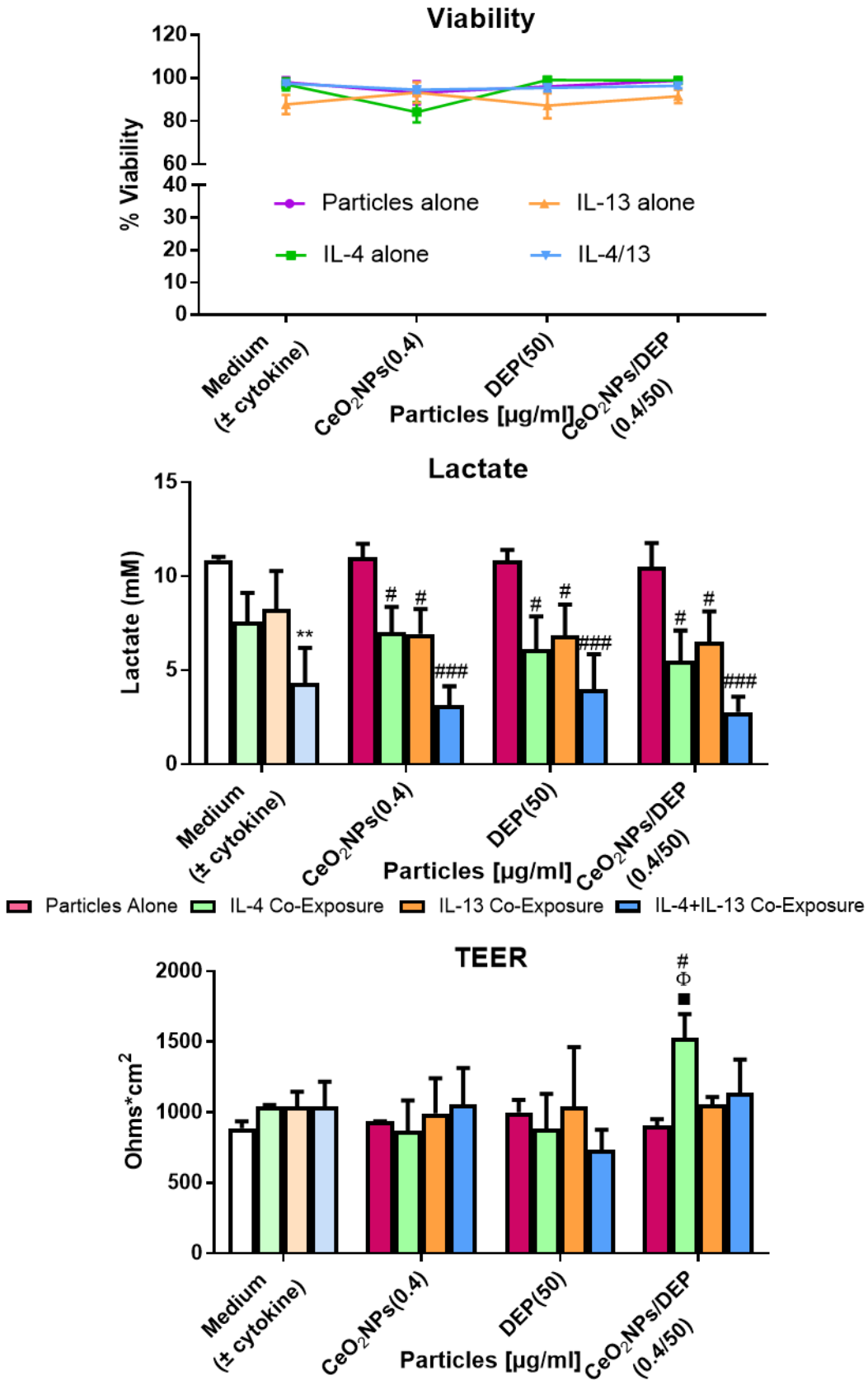


Figure 3-10. Cell viability, cellular metabolism, and monolayer integrity after 24 hours exposure to CeO_2NPs alone, DEP alone and CeO_2NPs/DEP in the presence of type II immune response-related cytokines. Data generated from exposure to the highest particle concentrations are shown. Cellular viability was measured as LDH release, lactate production measured in the basolateral compartment indicating cellular metabolism, and TEER measurements of monolayer integrity completed 24 hours after particle exposure, after the particles had been removed from the apical side of the membrane. N=4-8 subjects with all assays performed in triplicate. The data are presented as the mean ±SEM. Significance is denoted as the following: compared to medium control $p<0.05$(*), $p<0.01$(**); compared to particles alone $p<0.05$(#), $p<0.01$(##) and $p<0.001$(###); compared to CeO_2NPs alone $p<0.05$(▪); and compared to DEP alone $p<0.05$(Φ).

3.2.3.2 Alterations in epithelial gene expression of genes that mediate immune responses

Further examination of airway epithelial responses to particle exposure in a type II inflammatory environment was carried out by assessment of inflammatory gene expression and protein levels. Treatment of differentiated airway cultures were carried out as described (section 2.3).

Initial work focused on examination of type II gene expression (Figure 3-11). When compared to medium control, IL-4 treatment (green bar) resulted in a significant increase in IL-13, which was also significantly increased compared to the particles alone after all the particle co-exposures. No changes in STAT6 expression were observed on co-exposure to particles beyond that induced by IL-4 alone. Interestingly, IL-4-induced TSLP was attenuated with particle co-exposure. IL-5 expression was unaffected by either IL-4 alone, or co-exposure with particles.

IL-13 exposure (orange bar) increased IL-13 mRNA expression in the same pattern as IL-4 exposure. IL-5 expression was unaffected by either IL-13 alone, or co-exposure with particles. TSLP expression was significantly increased after co-exposure to DEP and CeO_2NPs/DEP when compared to the particles alone and the medium control (for CeO_2NPs/DEP only). There were no changes in the expression of STAT6 after any of the co-exposures, except CeO_2NPs/DEP+IL-13, which significantly increased the expression when compared to the medium control, the particles alone, and CeO_2NPs+IL-13 and DEP+IL-13.

Treatment of cells with a combination of IL-4+IL-13 (blue bar) elicited a significant stimulation in IL-5 expression, not observed with the cytokine treatment alone. The exposure to CeO_2NPs/DEP together with IL-4+IL-13 caused a significant increase in the expression of IL-5 when compared to the medium control. Particle treatment either alone or in combination with both IL-4+IL-13 cytokines did not significantly alter mRNA expression of IL-13, TSLP or STAT6 beyond IL-4+IL-13 induced control levels.

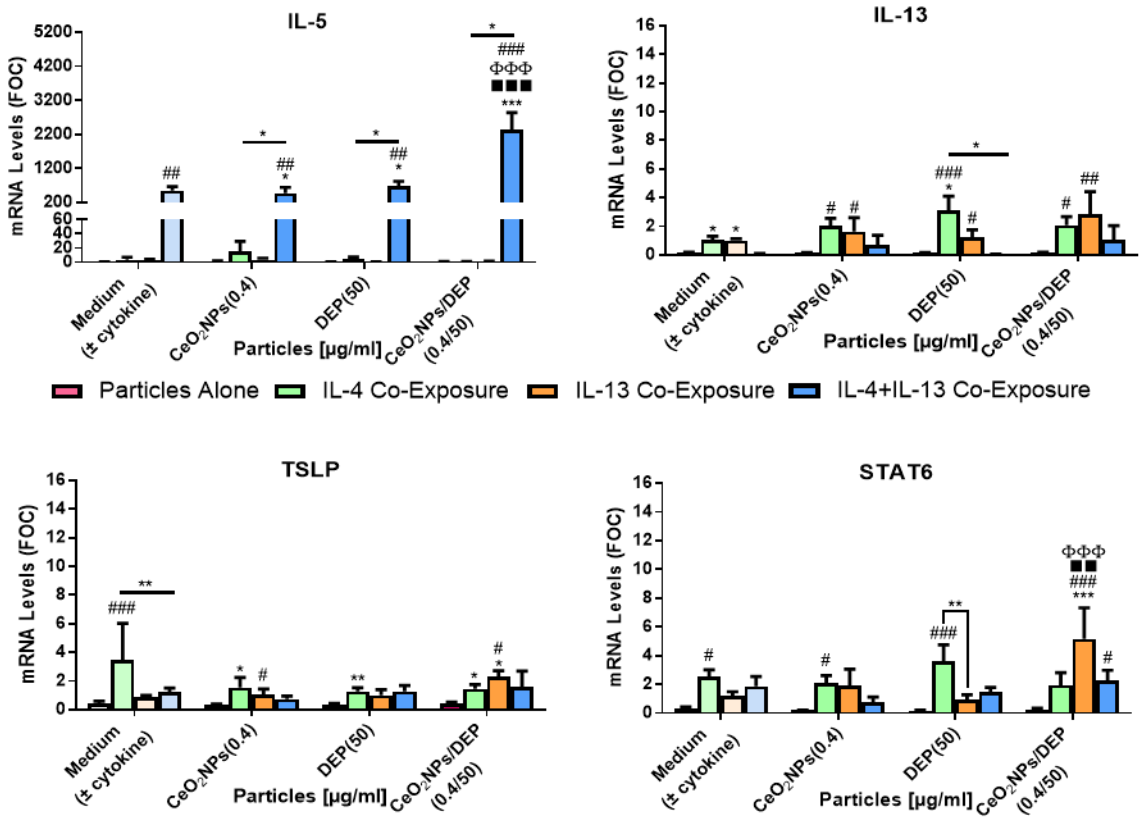


Figure 3-11 Changes in epithelial type II response gene expression after exposure for 24 hours to CeO_2NPs alone, DEP alone and CeO_2NPs/DEP combined in the presence of type II immune response-related cytokines. RT-PCR expression changes in HPBECs after 24 hours of exposure to particles. N=4-8 subjects with all assays performed in triplicate. The data are presented as the mean fold over GAPDH control (FOC) ±SEM. After treatment, mRNA was isolated and examined for transcript levels of the indicated inflammatory markers by RT-PCR analysis identified as type II inflammatory markers. Significance is denoted as the following: compared to medium control p<0.05(*), p<0.01(**) and p<0.001(***); compared to CeO2NP and DEP particles alone p<0.05(#), p<0.01(##) and p<0.001(###); compared to CeO_2NPs alone p<0.05(▪), p<0.01(▪▪) and p<0.001(▪▪▪); and compared to DEP alone p<0.05 (Φ), p<0.01(Φ Φ) and p<0.001(Φ Φ Φ).

Figure 3-12 shows gene expression changes in epithelium pro-inflammatory gene expression and identified that co-exposure with IL-4 seemed to elicit the majority of responses.

When compared to the medium control, there was no change in the gene expression of either IL-8 or IL-6 when co-exposed to IL-4. There was a significant increase in the expression of IL-8 after co-exposure to all the particles when compared to the particles alone. IL-6 expression was significantly increased after co-exposure to DEP (compared to the medium control and the particles alone) and CeO_2NPs/DEP when compared to the particles alone.

When compared to the medium control, there was no change in the gene expression of either IL-8 or IL-6 when co-exposed to IL-13. There were no changes in the expression of IL-8 or IL-6 after any of the co-exposures with the particles, except after co-exposure with DEP which caused an increase in IL-6 expression, and a significant increase in IL-8 expression when compared to the particles alone.

Co-exposure with IL-4+IL-13 causes no significant changes in the expression of IL-8 when compared to the medium control. There is a significant increase in the expression of IL-8 after co-exposure to CeO_2NPs/DEP when compared to the particles alone. IL-6 expression is initially significantly increased in the medium control when compared to medium alone, however the expression of IL-6 decreases when co-exposed to IL-4+IL-13 and the various particles. There is too much variation to determine the significance.

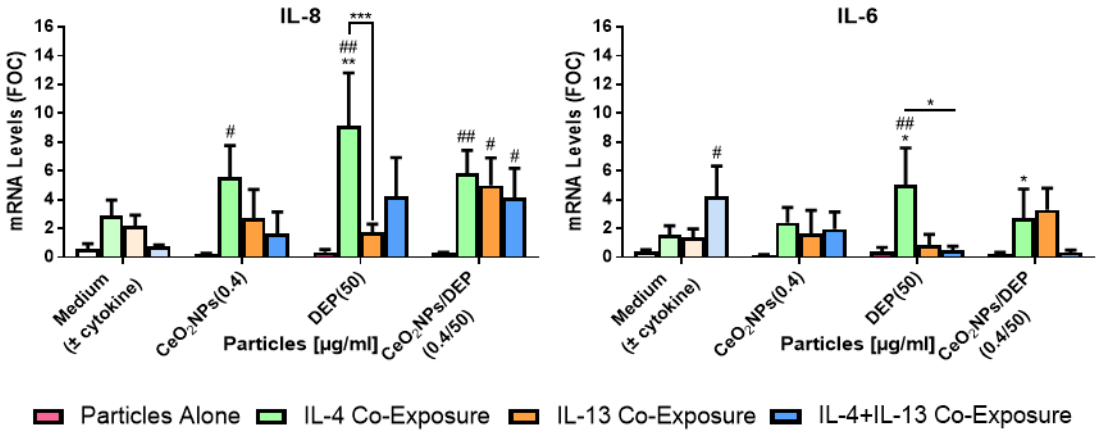


Figure 3-12 Changes in epithelial pro-inflammatory gene expression after exposure for 24 hours to CeO_2NPs alone, DEP alone and CeO_2NPs/DEP combined in the presence of type II immune response-related cytokines. RT-PCR expression changes in HPBECs after 24 hours of exposure to particles. N=4-8 subjects with all assays performed in triplicate. The data are presented as the mean fold over GAPDH control (FOC) ±SEM. After treatment, mRNA was isolated and examined for transcript levels of the indicated inflammatory markers by RT-PCR analysis identified as transcript levels of indicated pro-inflammatory chemokines. Significance is denoted as the following: compared to medium control $p<0.05$(*), $p<0.01$(**) and $p<0.001$(***); and compared to particles alone $p<0.05$(#), $p<0.01$(##) and $p<0.001$(###).

Figure 3-13 analysed the expression of molecules that are implicated in the modulation of asthma. IL-4 co-exposure had no influence on the expression of AREG, MUC5AC or IL-33 after any of the exposures. After co-exposure with DEP, there was a significant stimulation of NQO1 and CYP1A1 when compared to the medium control, and the particles alone. In both genes, the combinations of the particles inhibited the expression of NQO1 and CYP1A1 when compared to DEP alone, but significantly increase expression when compared to CeO_2NPs alone and DEP alone respectively. The expression of ADAM8 was significantly stimulated by the exposure to IL-4 alone when compared to the medium control. This increase in expression was significantly inhibited after exposure to all the particle regimes when compared to IL-4 alone, with expression level decreasing back to medium control levels.

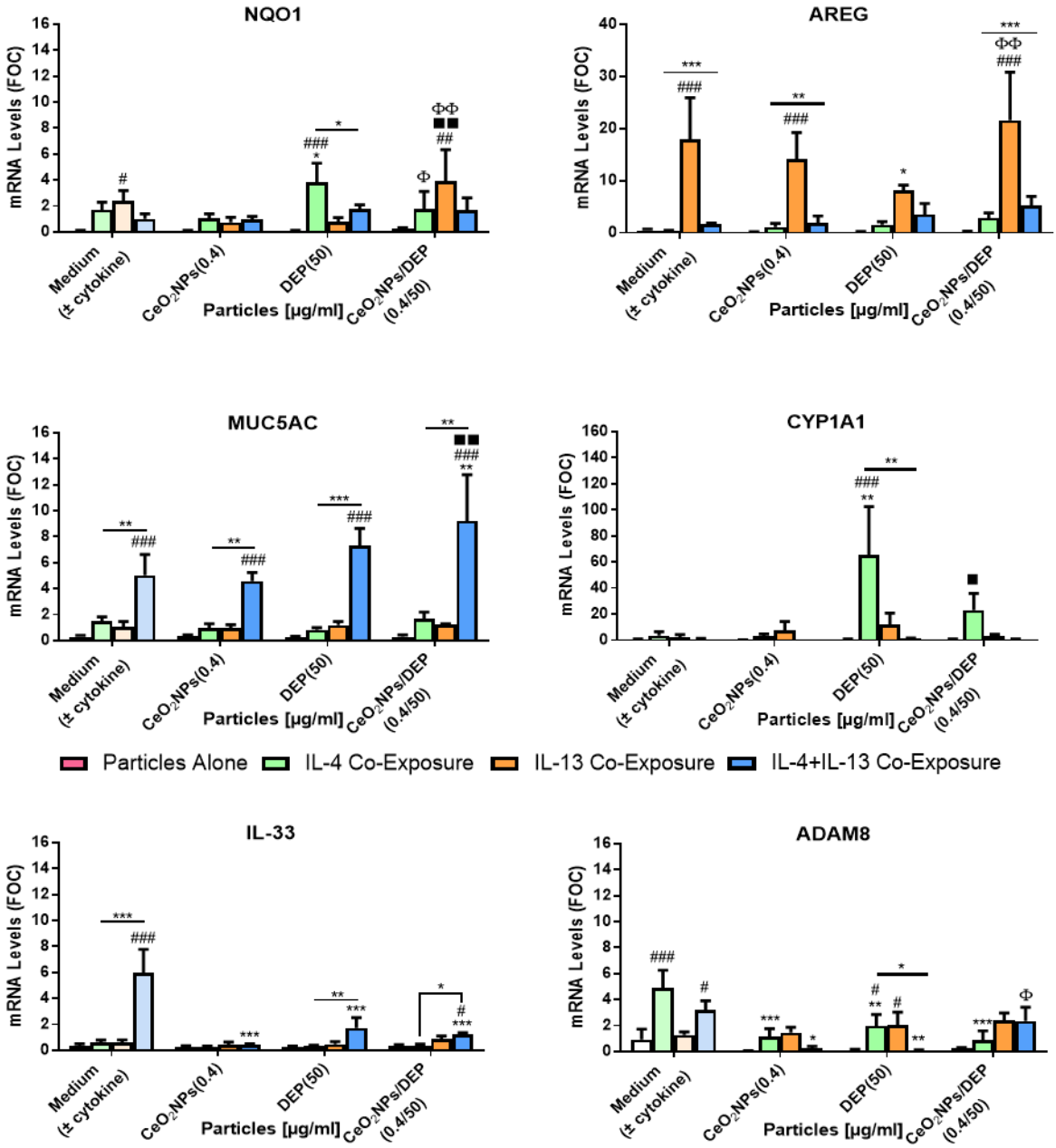


Figure 3-13 Changes in gene expression of molecules that modulate asthma after exposure for 24 hours to CeO_2NPs alone, DEP alone and CeO_2NPs/DEP combined in the presence of type II immune response-related cytokines. RT-PCR expression changes in HPBECs after 24 hours of exposure to DEP. N=4-8 subjects with all assays performed in triplicate. The data are presented as the mean fold over GAPDH control (FOC) ±SEM. After treatment, mRNA was isolated and examined for transcript levels of the identified markers by RT-PCR analysis. Significance is denoted as the following: compared to medium control $p<0.05$(*), $p<0.01$(**) and $p<0.001$(***); compared to particles alone $p<0.05$(#), $p<0.01$(##) and $p<0.001$(###); compared to CeO_2NPs alone $p<0.05$(▪), $p<0.01$(▪▪) and $p<0.001$(▪▪▪); and compared to DEP alone $p<0.05$ (Φ), $p<0.01$(Φ Φ) and $p<0.001$(Φ Φ Φ).

IL-13 co-expression had no influence on the expression of MUC5AC, CYP1A1 or IL-33 after any of the exposures. There was a significant stimulation of NQO1 expression after exposure to IL-13 when compared to the medium control. CeO_2NPs/DEP co-exposure caused a significant stimulation in expression when compared to the particles alone. IL-13 co-exposure caused a significant stimulation of AREG when compared to the medium control and the other cytokine exposures. Addition of particles co-exposed with IL-13 caused no change in the expression, but there was a significant increase of expression after CeO_2NPs+IL-13 and CeO_2NPs+DEP+IL-13 exposure when compared to the particle control, while exposure to DEP+IL-13 significantly decreased the expression of AREG when compared to the medium control but was not significantly different from the other exposure protocols. ADAM8 expression was significantly increased after exposure to DEP+IL-13 when compared to the particles alone.

IL-4+IL-13 co-exposure caused no change in the expression of NQO1, AREG, and CYP1A1. There was a significant increase in the expression of MUC5AC after co-exposure with IL-4+IL-13 alone when compared to the medium control and the particles alone. Expression of IL-33 and ADAM8 was significantly increased after exposure to IL-4+IL-13 alone when compared to the medium control. IL-33 was then significantly inhibited by the co-exposure of any of the particles when compared to the IL-4+IL-13 control. ADAM8 expression was significantly inhibited by the co-exposure to both CeO_2NPs and DEP individually when compared to the medium control.

Gene expression changes related to immune cell chemotaxis was finally analysed (Figure 3-14) in order to determine the influence co-exposure with type II chemokines may have on the attraction of immune cells.

IL-4 caused a significant stimulation in the expression of CCL26, CCL20, CCL24 and CCL11 after all the particulate co-exposures when compared to the particle only exposures. CCL26 was also significantly increased when compared to the medium control and the other co-exposures as was CCL24. IL-25 expression was significantly increased after co-exposure with CeO_2NPs+DEP+IL-4 when compared to the particles alone. There was no change in the expression of CCL17 expression after co-exposure to IL-4.

IL-13 co-exposure caused no changes in the expression of CCL26, and CCL11. Co-exposure with IL-13 caused a significant stimulation in CCL20 expression after exposure with CeO_2NPs+DEP when compared to the medium control, the particle control, CeO_2NPs+IL-4 alone and the other CeO_2NPs+DEP co-exposures. CCL24 expression was increased after exposure to all particles+IL-13, with CeO_2NPs+IL-13 causing a significant increase when compared to the particles alone.

CCL17 expression was also significantly stimulated post co-exposure with all the particle types when compared to the particles alone. IL-25 expression was significantly inhibited after addition to of the particles+IL-13 when compared to the medium control.

There were no changes in expression of CCL26, CCL24, CCL11, CCL17 and IL-25 after co-exposure with the various particles and IL-4+IL-13 compared to the medium controls. The expression of all the majority of these genes analysed after co-exposure with IL-4+IL-13 elicited a decrease in expression when compared to the other cytokine co-exposures.

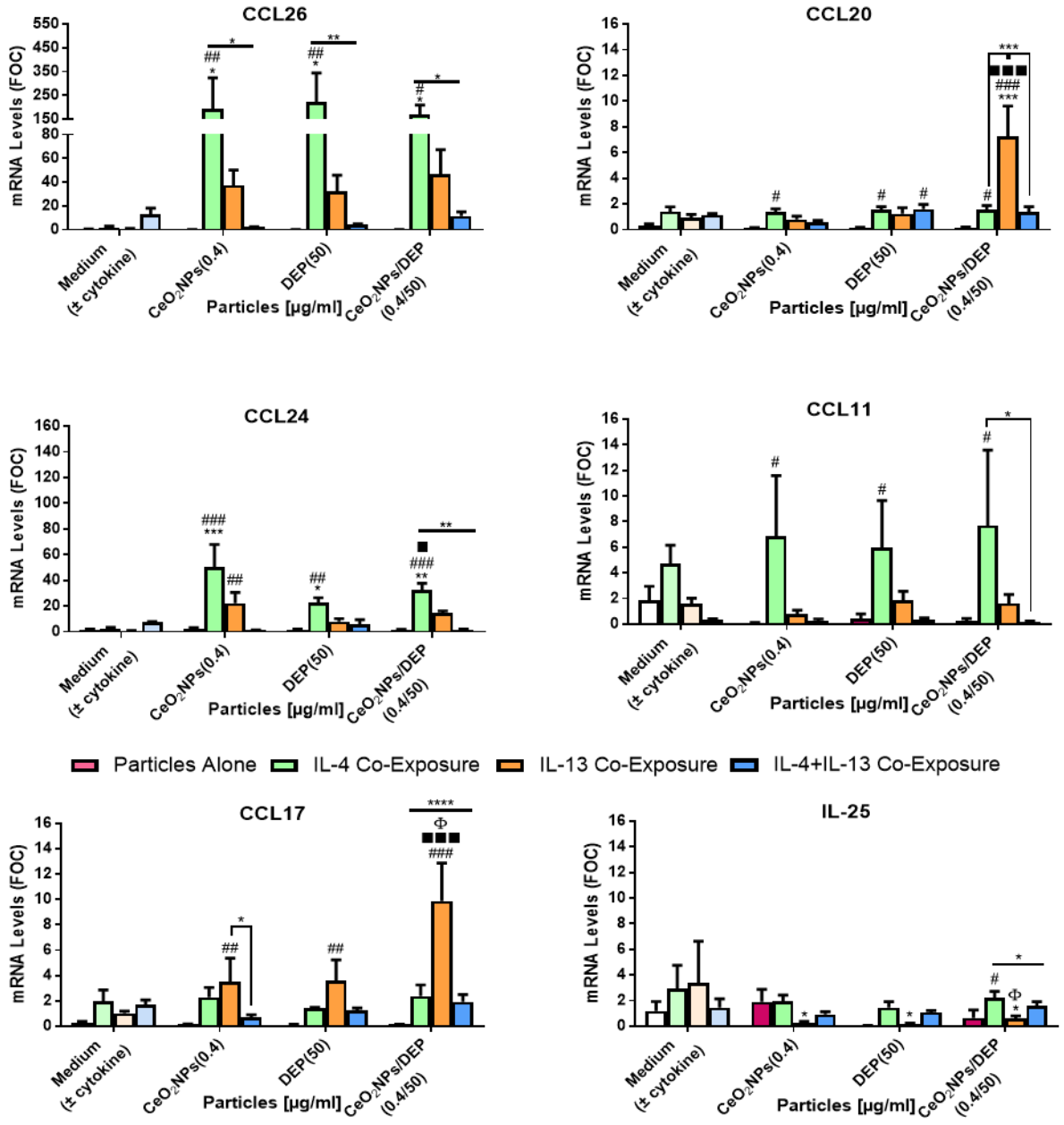


Figure 3-14 Gene expression changes related to induction of immune cell chemotaxis after exposure for 24 hours to CeO_2NPs alone, DEP alone and CeO_2NPs/DEP combined in the presence of type II immune response-related cytokines. RT-PCR expression changes in HPBECs after 24 hours of exposure to particles. N=4-8 subjects with all assays performed in triplicate. The data are presented as the mean fold over GAPDH control (FOC) ±SEM. After treatment, mRNA was isolated and examined for transcript levels of the indicated inflammatory markers by RT-PCR analysis. Significance is denoted as the following: compared to medium control p<0.05(*), p<0.01(**) and p<0.001(***); compared to particles alone p<0.05(#), p<0.01(##) and p<0.001(###); compared to CeO_2NPs alone p<0.05(▪), p<0.01(▪▪) and p<0.001(▪▪▪); and compared to DEP alone p<0.05 (Φ).

3.2.3.3 Alterations in epithelial expression of mediators of immune responses

Having observed changes in cytokines at the mRNA level, alterations in protein levels were next examined after epithelial exposure to particles in combination with IL-4 and IL-13. Analysis was carried out by ELISA as previously outlined in section 3.2.2.3. Mediator release was measured in both the apical and the basal compartments of the ALI; Figure 3-15 and Figure 8-8 and Figure 8-9 (appendix) depict apical and basal levels respectively. As noted above for the particles only study, there was significantly (ANOVA – not shown) less protein released into the basal compartment when compared to the apical compartment for each cytokine (the data are shown using the same scale bars for the apical and the basal side of the membrane). The release of TSLP is only displayed for the apical compartment, as levels in the basal compartment were below the limit of detection.

Within the basal compartment (Figure 8-9, appendix), there was a significant decrease in the release of CCL20 after exposure to CeO_2NPs+IL-4+IL-13 and CeO_2NPs/DEP+IL-4+IL-13 when compared to the medium alone. There were no alterations in basal protein levels for IL-33, IL-17A or CCL20 after particle + cytokine treatment when compared to corresponding cytokine alone. Within the apical compartment, there were no significant changes of either TSLP or CCL20 (Figure 3-15) when treated with cytokines compared to when co-exposed to particles + cytokines. IL-33 apical release was inhibited after exposure to CeO_2NPs+IL-4+IL-13 when compared to the particles alone. Levels of IL-33 increased markedly after co-exposure with CeO_2NPs+DEP+IL-4+IL-13 when compared IL-4+IL-13 alone (Figure 3-15). Addition of particles to the cytokines elicited an increase in the release of IL-17A when compared to the medium alone. IL-17A release was significantly increased after exposure to DEP+IL-13 when compared to the medium control.

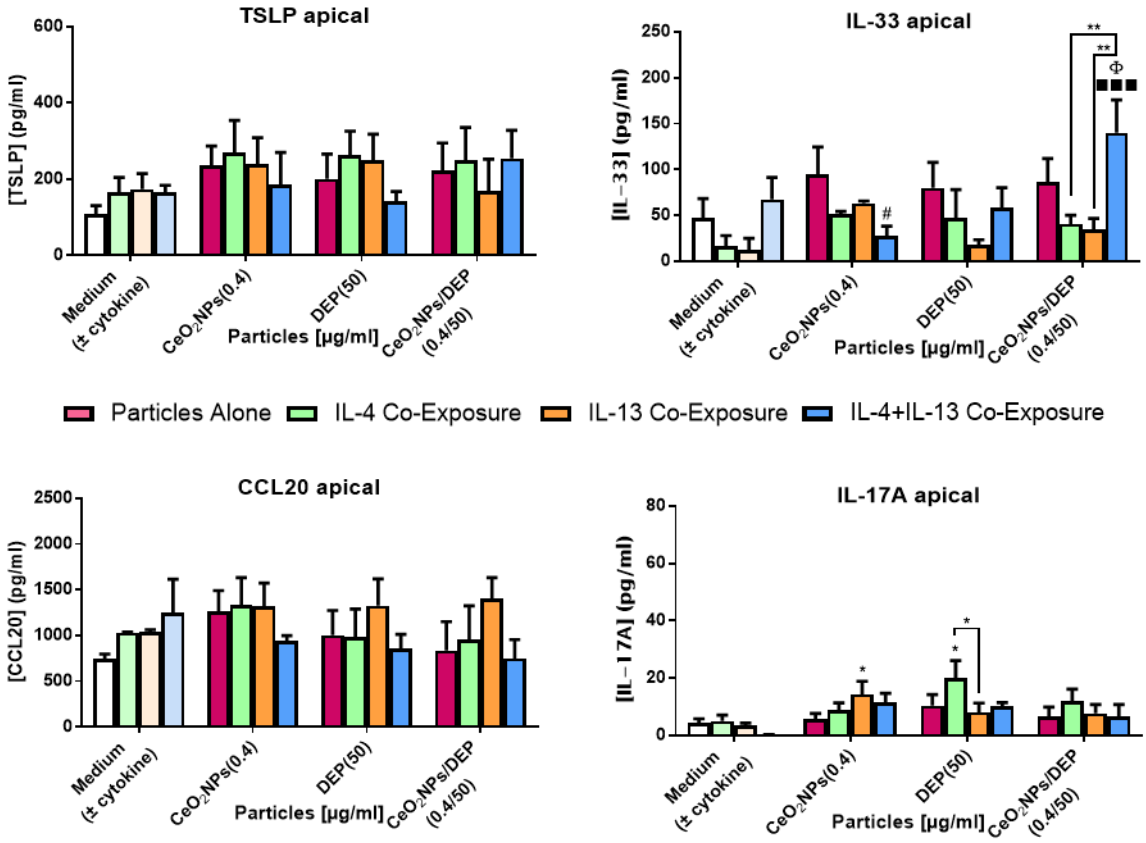


Figure 3-15 Changes in immune type II and pro-inflammatory apical mediator release after exposure for 24 hours to CeO_2NPs alone, DEP alone and CeO_2NPs/DEP combined in the presence of type II immune response-related cytokines. Analysis of mediator release in apical medium from HPBECs after 24 hours of exposure to particles and with and without type II cytokines. Medium was centrifuged and particles were removed before mediator concentration was analysed via ELISA. The data are presented as the mean ±SEM. N=4-8 subjects with all assays performed in triplicate. Significance is denoted as the following: compared to medium control $p<0.05$(*); compared to CeO_2NPs alone $p<0.05$(▪), $p<0.01$(▪▪) and $p<0.001$(▪▪▪); and compared to DEP alone $p<0.05$ (Φ).

3.2.4 Acute effects of CeO_2NPs and DEP and HDM allergen on HPBECs

As an alternative to the cytokines IL-4 and IL-13, which are mediators of the type II inflammation typically observed in allergic airway disease, we used co-exposure of particles with house dust mite (HDM) extracts as a representative environmental co-exposure to which allergic responses are commonly mounted. Cells were exposed to particles and HDM for 24 hours as described in section 2.5.4.5. HDM concentrations mimicked the *in vivo* exposures (1mg/ml of protein (Brandt et al., 2013b, Canbaz et al., 2015, Farhadi et al., 2014)) as outlined in section 2.6.2.1. Only the highest DEP concentration (see section 3.2.2) was investigated along with three CeO_2NPs concentrations, alone and in combination, with and without HDM.

The ratio of CeO_2NPs found in the exhaust particles when analysed after addition of Envirox™ to the fuel (Zhang et al., 2013) was a basis for the concentrations used in these exposures to mimic potential environmental exposures. 0.5, 1.5 and 15µg/ml of CeO_2NPs, 50µg/ml of DEP and 0.5/50, 1.5/50 and 15/50µg/ml CeO2NP/DEP were chosen as appropriate and relevant concentrations.

3.2.4.1 Measurement of cellular viability, metabolism and monolayer integrity

Cellular viability, metabolic status and monolayer integrity were measured as previously outlined in section 3.2.2.1. Data are presented in Figure 3-16. There was no change in lactate production by cells exposed to particles alone. There was however a significant reduction in lactate levels in the media following HDM treatment irrespective of particle co-exposure. Monolayer integrity, assessed as TEER values, fell slightly (~15%), but not significantly compared to medium control after exposure to a combination of CeO_2NPs and DEP. HDM caused an increase (not significant) in TEER values following all the treatment regimens, which was increased, above the particle-alone effect.

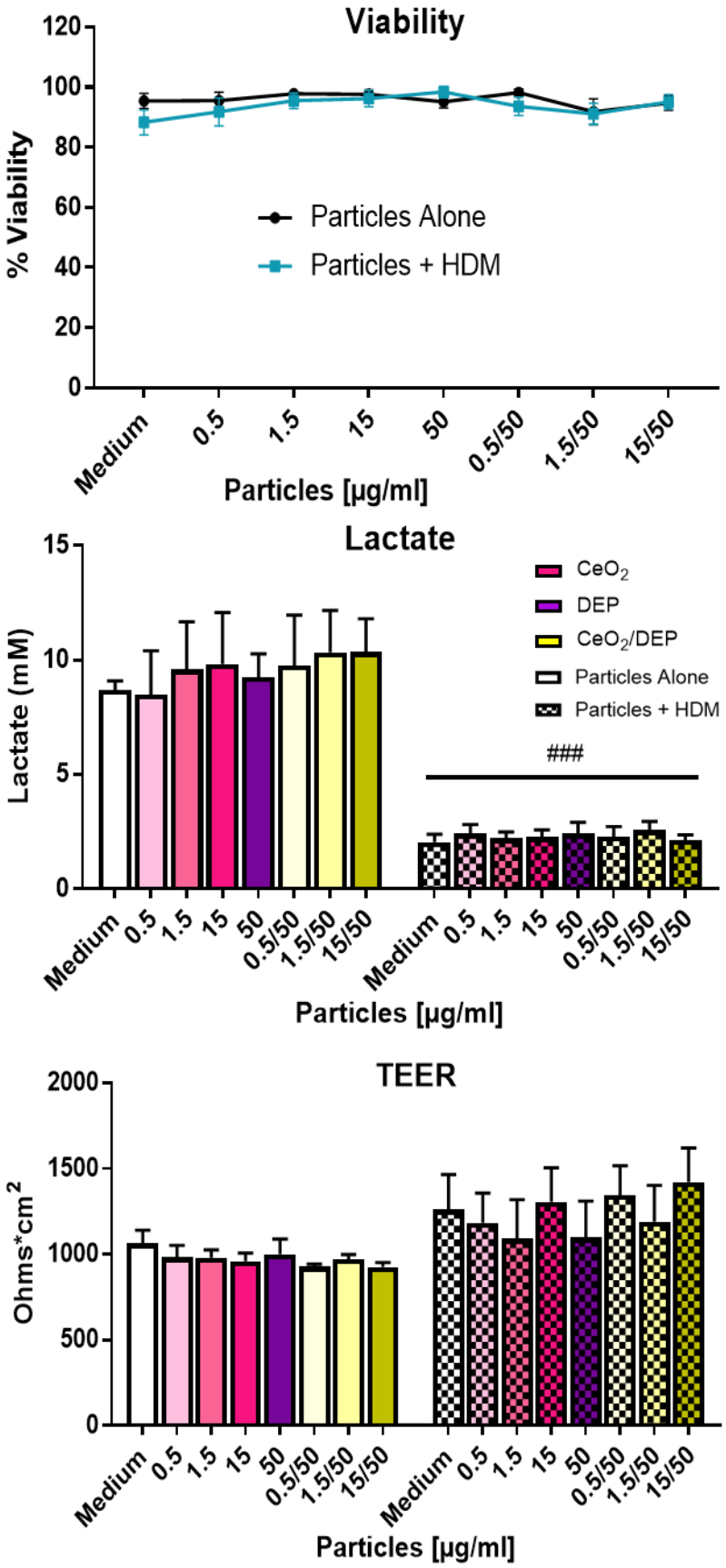


Figure 3-16 Cell viability, cellular metabolism and monolayer integrity after 24 hours exposure to CeO_2NPs alone, DEP alone and CeO_2NPs/DEP in the presence of HDM. Cellular viability was measured as LDH release, lactate production measured in the basolateral compartment indicating cellular metabolism, and TEER measurements of monolayer integrity completed 24 hours after particle exposure, after the particles had been removed from the apical side of the membrane. N=4-8 subjects with all assays performed in triplicate. The data are presented as the mean ±SEM. Significance is denoted as the following: compared to particles alone $p<0.05$(#), $p<0.01$(##) and $p<0.001$(###).

3.2.4.2 Alterations in epithelial expression of mediators of immune responses

Mediator levels were measured after 24 hours of exposure to CeO_2NPs/DEP±HDM using the previously mentioned concentrations. Figure 3-17 shows both the apical concentrations of these cytokines. Only apical, not basal, compartment TSLP levels could be detected. HDM exposure increased apical levels of TSLP, albeit not significantly. This was the same regardless of particle co-exposure.

The apical concentrations of IL-33 after exposure to CeO_2NPs, DEP and CeO_2NPs/DEP co-exposed with HDM was decreased when compared to exposure to the particles alone. Although there were decreases in IL-33 levels in all HDM conditions, the variability meant that the differences were not significant (Figure 3-17). IL-33 concentrations showed no changes in the basal compartment after exposure to particles alone. Basal expression of IL-33 after exposure to CeO_2NPs (15µg/ml) and CeO_2NPs+DEP (1.5/50µg/ml) was increased compared to HDM alone and DEP alone controls respectively, but due to variation these were not significant.

Apical CCL20 release following exposure to particles without HDM was significantly reduced after exposure (by ~45%) regardless of the particle combinations when compared to the medium control (Figure 3-17). When particles were co-exposed with HDM the CCL20 levels fell further, specifically 15µg/ml CeO_2NPs and 50µg/ml DEP (by ~70%) when compared to HDM exposure alone. This added effect of HDM on CeO_2NPs and DEP inhibition of CCL20 was prevented when the CeO_2NPs and DEP were combined at the lowest CeO2NPs concentration, but higher CeO_2NPs+DEP concentrations + HDM again induced a further reduction of CCL20 release when compared to the lowest concentration. The basal compartment concentration of CCL20 did not change regardless of exposure regimen when compared to either medium only control or the HDM alone control (Figure 8-5, appendix).

IL-17A levels in the apical compartment had a similar response profile when exposed to the particles with or without HDM. This suggests no effect of HDM on particle-induced responses.

IL-17A concentration in the basal compartment did not change regardless of particle regimen or co-exposure with HDM when compared to the medium, particle or HDM control.

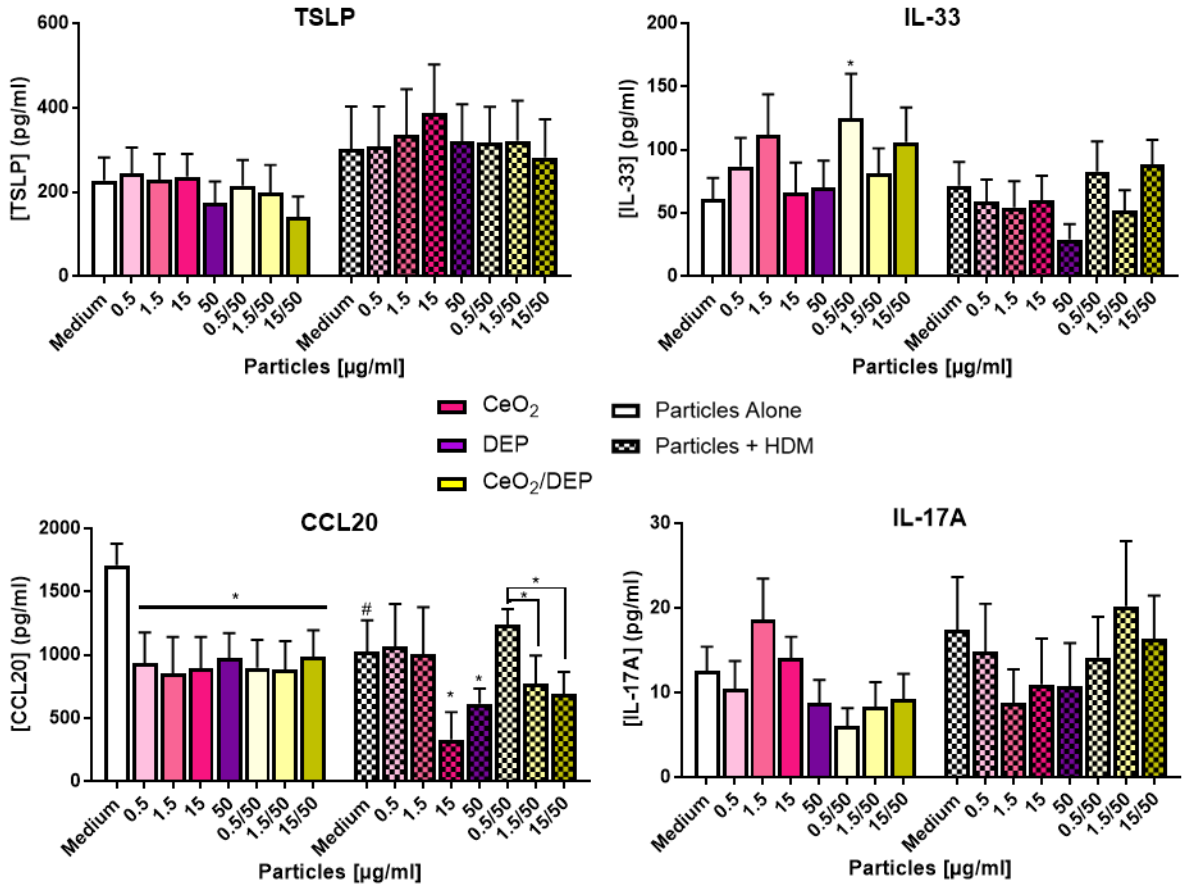


Figure 3-17 Changes in immune type II and pro-inflammatory apical mediator release after exposure for 24 hours to CeO_2NPs alone, DEP alone and CeO_2NPs/DEP combined in the presence of HDM. Analysis of mediator release in apical medium from HPBECs after 24 hours of exposure to particles with and without HDM. Medium was centrifuged and particles were removed before mediator concentration was analysed via ELISA. The data are presented as the mean ±SEM. N=4-8 subjects with all assays performed in triplicate. Significance is denoted as the following: compared to medium control $p<0.05$(*); and compared to particles alone $p<0.05$(#).

3.3 Summary

HPBEC culture at the air-liquid interface and optimisation of culture media conditions (Section 3.2.1):

- Light microscopy images indicated that with all culture media formulations, cells formed monolayers and displayed characteristic epithelial morphology. Cells cultured in the Gray differentiation medium appeared to produce more mucus than in the other media.
- TEM images indicated that a pseudostratified layer is formed.
- There were no changes in the lactate and viability when differentiating in any of the medium. There was a slight increase in the TEER value after differentiation in the Gray medium.
- The basal cell markers were significantly increased (KRT14) after differentiating cells in the Matsui medium.
- Mucus markers were significantly increased (MUC5AC, TFF3 and MUC1) after differentiation in Gray medium.
- There was a significant increase in cilia and club cell markers (FOXJ1, and SCGB1A) when the cells were differentiated in Gray medium.
- Taken together, this indicated that the Gray medium allowed the most physiologically relevant differentiation of the HPBECs at ALI.

Responses of ALI HPBEC cultures to particle treatment (Section 3.2.2):

- There was no change in the viability or lactate production after exposure to any of the particles at any of the concentrations. TEER was significantly increased after exposure to DEP at all concentrations when compared to medium control. These values decreased with co-exposure to CeO_2NPs/DEP.
- For mRNA expression, exposure to DEP caused an increase in the expression of immune type II responses (IL-13 and STAT6) when compared to the CeO_2NPs alone and the co-exposure to CeO_2NPs/DEP. IL-25 expression was significantly increased after exposure to CeO_2NPs alone when compared to the medium control, and after exposure to the highest CeO_2NPs/DEP exposure when compared to the medium control, CeO_2NPs alone and DEP alone.
- IL-6 protein level expression was decreased after exposure to CeO_2NPs alone and DEP alone, but this was ameliorated by the co-exposure, while the IL-8 expression was

significantly increased after the co-exposure to CeO_2NPs/DEP when compared to the medium control and DEP alone.

Co-Exposure with IL-4 and IL-13 (Section 3.2.3):

- There were no changes in the cell viability after any of the co-exposures compared to the particles alone. There was a significant decrease in the lactate production after cytokine exposure (with IL-4+IL-13 causing a lower production than IL-4 and IL-13 alone).
- mRNA expression of IL-5, IL-33 and MUC5AC was significantly increased after CeO_2NPs/DEP co-exposure with IL-4+IL-13 when compared to CeO_2NPs or DEP alone or with cytokines alone. IL-13, TSLP, and STAT6 expression was increased in all cytokine CeO_2NPs/DEP co-exposures when compared to the particles alone. AREG and CCL17 expression was significantly increased after co-exposure with IL-13 compared to the other exposures. CCL26 and CCL11 expression was significantly increased after co-exposure with IL-4 when compared to the other exposures.
- There were no changes in the concentration of TSLP or CCL20 protein levels after any of the co-exposures. There was a significant increase in the concentration of IL-33 after co-exposure to CeO_2NPs/DEP with cytokines when compared to without cytokines.

Co-Exposure with HDM (Section 3.2.4)

- There was no change in the cellular viability after co-exposure with HDM compared to the particles alone. The lactate production was significantly decreased after co-exposure with HDM compared to particles alone after every exposure concentration. The TEER value was also increased, but not significantly.
- There was a slight increase in the concentration of TSLP after co-exposure with HDM and decreases in IL-33 and CCL20. There were no changes in the concentration of IL-17A after any co-exposures.

3.4 Discussion

This study aimed to identify the immunological and gene expression changes caused by a 24-hour exposure to environmentally relevant concentrations of CeO_2NPs reflective of exhaust material after combustion of Envirox™ within a diesel engine. This study specifically focuses on the inflammatory responses and gene expression changes related to the development and exacerbation of asthma and in particular to determine potential adverse effects that CeO2NPs may have on the development and exacerbation of allergic airway disease.

3.4.1 Cellular differentiation

For toxicological assessment of particles within the lung using *in vitro* assays, there are many studies within the literature that use submerged cultures. These involve suspending the particles in the medium, either vortexing or sonicating for a couple of minutes and then applying the particles in suspension onto the cells. This has a number of physiological problems as this is not how airway epithelium would be exposed to such particles on inhalation. A cell line derived from normal human airway bronchial epithelial cells (HBECs) is used within the literature (Boda et al., 2018, Balogh Sivars et al., 2018, Kilin et al., 2017, Gordon et al., 2015), and is more relevant than other cell lines used. There are distinct differences between the primary human large airway bronchial epithelial cells and these cell lines, which potentially affect the responses to these particles. Ideally, any *in vitro* models that are being used to determine the effects of exposure to airborne particles should be differentiated to replicate as closely as possible the region of the human lung of interest. Of the various differentiation media examined Gray medium was chosen as it produced the most representative expression in airway epithelial differentiation markers and stable monolayer integrity compared to other media. The medium was the only thing that differed between the cultures, all the protocols remained the same.

Gray medium has the highest hydrocortisone concentration compared to the other media. Hydrocortisone has been found not to change the cell differentiation but does increase the RNA expression of mucin-related genes (Zaidman et al., 2016). Retinoic acid concentration was the same in multiple differentiation media and is required to trigger mucociliary differentiation (Cozens et al., 2018). Bovine serum albumin in the Gray medium is the highest concentration compared to the other media. This is used to protect against oxidative damage and stabilise the fatty acids in the cell culture medium (Francis, 2010) and also provides a significant proportion of the required nutrients. There were no ciliated cells in this *in vitro* model as determined by TEM, despite increased Foxj1 and Tubba4 expression, but the cells differentiated into a columnar cell type and produced mucus. Epithelix (the commercial supplier of these cells) have

confirmed that the HPBECs can develop cilia and have been proven to do so under other culture conditions (Huang et al., 2017b). The reason we could not establish ciliated cells in our cultures is unknown but it would be the aim of future work in this area to optimise the protocols further. Increased mucus production in our cultures could lead to protection against particle-induced adverse epithelial effects (Loxham et al., 2015) and as such may be considered more representative of the human airway and suitable to address the hypothesis and aims of this study.

3.4.2 CeO_2NPs exposure

3.4.2.1 Acute effects of CeO_2NPs on HPBECs

There is conflicting information in the literature as to whether CeO_2NPs cause cytotoxicity in airway epithelial cells (Lin et al., 2006, Mittal and Pandey, 2014). This may be explained by differences in i) the protocols for exposure and endpoint assessment, ii) model epithelial systems or iii) how particles were prepared and/or sourced. Another explanation is possible differences in valence state of the cerium which could account for contradictory responses to CeO_2NPs (Kroll et al., 2011, Pulido-Reyes et al., 2015a), and the potential for cerium dioxide to have both prooxidative and antioxidative properties (Filippi et al., 2019).

In this study we found that CeO_2NPs (at a maximum concentration of 50µg/ml) did not affect monolayer integrity (measured via TEER) or cellular viability. CeO_2NPs have been found to be non-toxic in cell line models (A549 cells) up to concentrations of 100µg/ml (Demokritou et al., 2013) and as high as 200µg/ml (Zhou et al., 2013) and 1000µg/ml (up to 72hours of exposure) using particle size distributions of between 60-190nm. This is also true for more advanced *in vitro* lung models such as MucilAir (Kooter, 2016). However, other studies have found opposite effects but using a range of cell lines rather than primary cells and have indicated that ROS production and oxidative stress may be a mechanism through which CeO_2NPs cause toxicity in some cells (Eom and Choi, 2009). For example, there was an induction in membrane damage after cerium oxide exposure in A549 cells, but not HeLa-related L-132 cells (originally thought to be derived from embryonic lung tissues but have now been determined to be HeLA cells (i.e. cervix carcinoma)) that were also analysed in parallel. This would suggest that CeO2NPs can cause membrane damage, but only in certain cell types (Kim et al., 2010). CeO_2NPs have also been found to cause apoptotic cell death via ROS-mediated cell damage (both DNA and cell cycle damage) (Mittal and Pandey, 2014, Lin et al., 2006). The fact that A549 cells are a cancerous cell line may play a part in this (Joris et al., 2016) (due to their lack of normal cellular repair mechanisms), while HPBECs are "normal" cells. BEAS-2B is also a cell line that is utilised for the

investigation of nanoparticle toxicology. They have been used to identify mechanistic pathways that CeO_2NPs potentially activate to cause cytotoxicity via induction of heme oxygenase-1 (HO-1) and Nrf-2 pathway signalling (Eom and Choi, 2009). Following exposure to CeO_2NPs in an advanced lung large airway epithelial cell model (MucilAir, Epithelix) there was an increase in HO-1, not Nrf-2, but not to the same levels as observed with A549 or BEAS-2Bs at an ALI (Kooter, 2016). This may reflect the production of protective elements such as mucus in the complex large airway cell models, as exist *in situ*, which do not exist in the simpler models using cell lines. For example, differences between uptake of particles may influence their ability to cause adverse effects on cellular exposure. In a model of the primary bronchial epithelium complete with mucociliary apparatus, CeO_2NPs were not taken up by, and did not translocate into the cells (they also did not cause any adverse effects) (Frieke Kuper et al., 2015). Absence of CeO_2NPs uptake by differentiated airway epithelium could be suggested as one reason for the minimal effect of these particles on our airway epithelial models and may better reflect reality. This however would need to be confirmed through direct assessment.

To establish changes in gene expression after exposure to CeO_2NPs, RT-PCR was used. We identified a range of genes related to type II inflammation in the airway which are likely to be altered within the challenged epithelial environment.

NQO1 expression was significantly decreased at the lowest CeO_2NPs concentrations when compared to the medium control. NQO1 is a gene that is related to oxidative stress and its decrease in expression would suggest a protective effect of the particles within this culture. This protective effect has also been seen in A549 cells after exposure (Guo et al., 2015), however there was no downregulation of NQO1 seen in this study. In BEAS-2B cells, after exposure to 40µg/ml of CeO_2NPs, there was a significant increase in the gene expression of ROS associated genes (Glutathione S transferase, HO-1 and Thioredoxin reductase) after 4 hours of exposure (Park et al., 2008b). In contrast, there was very minimal gene expression change observed in A549, BEAS-2Bs or MucilAir cultures after exposure to 3µg/cm² for an hour (Kooter, 2016). An important consideration is the difference in the concentration of particles used, with the differences in units depending on the size of plate used for exposures and therefore influencing the concentration of particles per cm² the cells were exposed to. This makes it difficult to compare these studies, as it is unclear exactly what the deposition rate and value was for each study, or indeed the surface area exposed to these particles.

CYP1A1 expression was also significantly decreased at the lowest CeO_2NPs concentrations when compared to the medium control, however the expression does increase in a dose dependant

manner from lowest to highest concentration. CYP1A1 is related to NQO1 expression as it is linked to the metabolism of polycyclic aromatic hydrocarbons (PAHs) (Cosma et al., 1993).

ADAM8 is an asthma specific gene (Oreo et al., 2014) and was identified as being significantly decreased after exposure to the highest concentrations of CeO_2NPs when compared to the medium control. This would suggest that at this concentration there is a suppression of the expression of ADAM8 and potentially other asthmatic related genes at this concentration (such as TSLP (Ober and Yao, 2011) and CCL11). CCL11 is related to the chemoattraction of eosinophils and therefore asthma (eosinophil increase in both the sputum and the blood is related to the severity of asthma). The expression of CCL11 was significantly decreased after exposure to any of the concentrations of CeO_2NPs when compared to the medium control. There were also no significant changes between the concentrations.

Overall, this could suggest that the addition of these particles could lead to a reduction in the expression of asthmatic genes identified, as well as an increase in the potential antioxidant and protective effects these particles may have.

TNF-α levels in our model were significantly decreased following exposure to all concentrations of CeO_2NPs. In other studies, at higher concentrations of CeO_2NPs there was no decrease in the concentration of TNF-α after 24 hours of exposure (Kim et al., 2014b).

In our study there was no change in the concentration of IL-8 after any of the CeO_2NPs exposures, but there was a significant decrease in IL-6 concentrations when compared to the medium control. In submerged A549 and BEAS-2B cells (Park et al., 2008a) there were no changes in the production of IL-8, but an increase in the concentration of IL-6 production at a concentration of 100μg/ml after 24 hours (Veranth et al., 2007). At an ALI, there was an increase in IL-8 release by BEAS-2Bs (Kooter, 2016), but this was not observed in a MucilAir model or A549 cells at ALI. This indicates that this increase seen in BEAS-2Bs could be due to the cell type, and not necessarily exposure to particulate matter (Ghio et al., 2013). These changes in IL-6 and IL-8 that are observed following CeO_2NPs exposure has been shown previously in a submerged BEAS-2B cell model but at higher particle exposure concentrations (Veranth et al., 2007). As more than one cell donor was used within our studies this could lend itself to the differences seen between the models. The release of TNF-α and IL-6 are important mediators in pulmonary inflammation and their significant decrease and increase respectively are indicator that CeO2NPs within our model are initiating an inflammatory response. This suggests that

inhalation of CeO_2NPs would stimulate cytokines known to be important in respiratory diseases such as COPD and asthma.

IL-17α levels were also significantly increased after exposure to 0.08μg/ml. This would indicate there is the potential for IL-17α levels to cause a decrease in IL-6 expression (Hekmatimoghaddam et al., 2019). A link between an increase serum IL-17α and asthma severity has been determined, along with an increase in the expression of IL-4, IL-10 (which were not measured in our study) and IL-25 (Hasegawa et al., 2017, Dimitrova et al., 2019), indicating that an increase in measured IL-17α has the potential as a marker of increased asthma severity. IL-25 expression was significantly increased after exposure to the highest concentration of CeO_2NP alone when compared to the medium control and of CeO_2NPs+DEP when compared to CeO_2NPs alone and the various other concentrations of CeO_2NPs+DEP. IL-25 is implicated in the Th2 response and is released in response to various alarmins by the airway epithelial cells (Patel et al., 2019). As both IL-17α and IL-25 expression is significantly increased after exposure to both CeO_2NPs alone and CeO_2NPs+DEP, this could potentially indicate the detrimental effects these particles have on the severity of our model and asthmatic patients exposed to these particles in real-life exposures.

The changes between the higher exposures and lower exposures need to be compared - this could potentially be down to the agglomeration of the particles and therefore a size difference between the high and low exposures (Sukhanova et al., 2018).

The inhalation of CeO_2NPs alone has the ability to cause inflammation within the lung, with a higher concentration potentially limiting the concentration able to be cleared from within the lung (Schwotzer et al., 2017). Their impact on the lung is also determined by the sizes of the particles, with the smaller particles able to penetrate the alveolar region and therefore have longer persistency (Schwotzer et al., 2017). However, there are differences identified in the immunological responses post-exposure which are thought to be down to species variation (rats are more sensitive than mice), deposition within the lung and the size and physical characteristics of the particles inhaled (Dekkers et al., 2018). These effects also have the potential to impair lung function of offspring after maternal exposure (Paul et al., 2017). From these studies and our own, it can be determined than the inhalation of CeO_2NPs alone has the potential to cause inflammation and changes of gene expression that mimic those of a chronic inflammatory response.

3.4.3 DEP exposure

It has previously been shown that the biological relevant concentrations of DEP exposure range between 0.2-20µg/cm² of epithelial surface (calculated from both *in vitro* and *in vivo* studies and various exposure doses (Li et al., 2003)). The concentrations of DEP used in this study were comparable (0.2-10.7µg/cm² epithelial monolayer). Due to the diverse nature of DEPs produced by different vehicles under different conditions, it was decided to use a standard reference material for our experiments (NIST 2975) to address our hypothesis.

3.4.3.1 Acute effects of DEP alone on HPBECs

From our study, DEP caused a significant increase in the TEER values measured when compared to the medium control at the lower doses. Previous work has demonstrated that after exposure to aerosolised DEP for 3 hours there was no change in the TEER value of primary differentiated bronchial cells, but there was a significant decrease in the TEER, one hour after the DEP exposure was completed, which then recovered by 24 hours (Seagrave et al., 2007). In contract, when examining a more advanced, but not the best, co-culture system (containing 16HBE140⁻s, macrophages and dendritic cells), there was a decrease in the TEER value of the epithelial cultures alone (which had a higher starting TEER than the co-culture), but not in the co-culture, after exposure to 125µg/ml of NIST DEP for 24 hours (this is a high exposure dose). This was coupled with no change in mRNA expression of a tight junction molecule, (Lehmann et al., 2009). In contrast, another study found that the TEER value decreased over 24 hours post-exposure to an aerosol of DEP. In this study, the highest DEP exposure (1.87µg/cm²) caused a significant decrease in TEER that did not recover even after another 24 hours post-exposure recovery period. This was accompanied by a decrease in cell viability (though not statistically significant), which was also seen with our DEP exposure studies at the same concentration (10µg/ml) (Zarcone et al., 2016). This response pattern was also found when examining monolayer integrity using dextran blue, with a decrease in integrity after 1 hour, but which returned to control levels 21 hours after exposure (Seagrave et al., 2007). In direct contrast, when A549 cells were exposed to NIST particles there was no decrease in cell viability up to the highest concentration of 3000µg/ml, both in ALI cultures (Turner et al., 2015) and submerged cultures (Don Porto Carero et al., 2001).

In our study there was an increase in expression of MUC5AC and IL-5, and there was no change in IL-33, NQO1, STAT6, IL-13, TSLP and SLC264C gene expression with DEP treatment (Figure 3-3 and Figure 3-5). Previous studies within the group identified that in differentiated epithelial cells 24 hour exposure to DEP (0.1-20µg/ml) caused a significant increase in mRNA levels of CYP1A1 (Meldrum et al., 2017, Longhin et al., 2016), also shown in HBEC3-KTs (Longhin et al.,

2016), and also in HBEC3 cells (immortalised normal bronchial epithelial cells) (Rynning et al., 2018) and after 2 weeks of exposure to DEP (Longhin et al., 2016).

In our study we found a decrease in IL-6 and IL-8 production and significant decrease in TNF-α at the apical side of the membrane. In HBEC3-KT (immortalised human bronchial epithelial cells) cells there was a significant increase in IL-6 and IL-8 mRNA expression after 2 weeks of DEP exposure, but no change after 24 hours of exposure (Longhin et al., 2016) or after 24 hours in HBEC3s (Rynning et al., 2018). 21 hours after an aerosol exposure to DEPs there was no change in the IL-6 concentration from A549 cells or BEAS-2B cells grown in serum free medium (Veranth et al., 2008). There was an increase in both IL-6 and IL-8 in HBEC3-KT cells after 2 weeks of DEP exposure, but not at the earlier time points (Longhin et al., 2016) when compared to the medium control and an increase in IL-6 production from BEAS-2B cells after 24 hours exposure to DEP (Bengalli et al., 2017). After aerosol exposure to DEP, there was only a significant change in IL-4 and IL-6, decreasing the concentration of cytokines produced, but no change in IL-1α, IL-12, GM-CSF, IFNγ and TNF-α (Seagrave et al., 2007). The results for these cytokines indicate that cell type is very important when determining potential responses to DEP. There was no change in the levels of TNF-α in an advanced co-culture model (containing 16HBE140$^-$s, macrophages and dendritic cells) or MucilAIr models after 6 hours of DEP exposure (Bisig et al., 2018). There is a significant volume of research completed with lung epithelial models and IL-6 and IL-8. These responses are not as important in an allergic response as the Type II responses and to our knowledge this is one of the first studies that investigates the effects of DEP on these mediators. We found a significant increase in the concentration of TSLP and IL-33 in the medium after the lower concentration exposures to DEP. These have further downstream effects and are more relevant to an allergic response than the commonly used IL-6/8.

In the present study, we did not investigate oxidative stress or DNA damage directly, but there is evidence in the literature both can occur after exposure to DEP. In our study we identified a significant dose dependent decrease in oxidative stress-related gene expression (NQO1), while primary differentiated epithelial cells were found to have a significant dose dependant increase in oxidative stress-related gene expression (HMOX1 and NQO1) after exposure to aerosolised DEP after both 6 hours and 24 hours after the exposure to DEP (so 6 hours and 24 hours in total) (Zarcone et al., 2016). This could be due to the differences in exposure methods (quasi-ALI exposure (our method) vs aerosol (Zarcone et al., 2016)). In A549 cells there is a significant increase in intracellular ROS production following exposure to greater than 600μg/ml of DEP

(Turner et al., 2015), this is almost to be expected as the concentration of DEP being used is a very high concentration which is not environmentally relevant and is potentially suffocating the cells. In an advance co-culture model (containing 16HBE140$^-$s, macrophages and dendritic cells) and MucilAir models, there was no change in the HMOX1 or NQO1 mRNA expression after 6 hours of exposure with DEP (an undisclosed concentration from various engines and fuel types), this was also found when ELISA analysis was used to confirm for HMOX1 (Bisig et al., 2018).

These results taken together suggest that the more physiologically relevant models – such as, the co-cultures and the MucilAir do not elicit an oxidative stress response post DEP exposure, when compared to our model, however, this could be down to the exposure method, or the concentration of the DEP used.

3.4.4 Effects of CeO_2NPs/DEP exposure

It is important to use a ratio of CeO_2NPs/DEPs that would be environmentally relevant, and the concentration related to the consumer use of Envirox^{TM}. The ratio is 0.008µg/ml of CeO_2NPs in every 1µg/ml of DEP (Park et al., 2008a). When CeO_2NPs are added as Envirox^{TM} into a fuel tank and burnt, the particle size emitted decreased along with the zeta potential. The chemical composition also changed, with the carbon content decreasing, and the cerium content increasing. The higher the concentration of Envirox^{TM} added into the tank the lower the oxidative potential of the emitted particles (Zhang et al., 2016).

3.4.4.1 Acute effects of CeO_2NPs/DEPs alone on HPBECs

After investigating the effects of CeO_2NPs alone and DEP alone, this study aimed to analyse both the secreted cytokines and chemokines and the mRNA expression of genes involved in type II inflammation. There are very few studies within the literature that investigate CeO_2NPs in combination with DEPs on biological responses, either as a mixture, as individual particles added in series or after the particles are combusted together and then added to *in vitro* models.

We identified a significant decrease in the mRNA expression of IL-5 after exposure to the highest concentrations (Figure 3-3) of CeO_2NPs/DEPs when compared to the medium control. There were also significant increases in the expression of CYP1A1 and IL-25 when compared to the medium control and CeO_2NPs alone (Figure 3-5 and Figure 3-6). There was a significant decrease in the expression of IL-5 after exposure to the highest concentrations (Figure 3-3) of CeO_2NPs/DEPs when compared to the medium control. As well as the concentration of TNF-α in the apical medium (Figure 3-8). These results taken together indicate that the combined effect of these particles is having a significant effect (either a positive or a negative) on the

responses of the cells when compared to both the medium control and the particle exposures (CeO_2NPs and DEP) alone.

In one of the only other studies within the literature also investigating these particles, an advanced lung model (containing 16HBE-o$^-$, macrophages and monocytes) at an ALI, there is an increase in mRNA TNF-α and IL-8 expression levels after exposure to CeO_2NPs and then DEP. This study exposes the cells to DEP and then the CeO_2NPs, so they are not mixed as in our study and they are not burnt in the engine together. The addition of CeO2NPs do not increase the toxicity of the DEPs used, but actually lower some of the responses caused by DEP (Steiner et al., 2012). When investigating the immune responses, primary blood monocytes or THP-1 cells were used. They were exposed to particles of CeO_2NPs/DEP that were burnt together in an engine, collected and then added to the cell suspensions. There were significant changes in mRNA of IL-1β, TNF-α, IL-6. INF-γ when compared to the control. It was identified in this study that the physical characterisation changes in the particles post-combustion appear to cause the biological reactivity (Sarkar et al., 2014).

3.4.5 Examination of effects of co-exposure to cytokines on HPBECs

To determine the effects type II cytokines had on the particle responses, we co-exposed with IL-4, IL-13 alone as well as with a combination of both of IL-4/13. We identified significant increases in the mRNA expression of IL-5 after co-exposure with IL-4/13 with every particle exposure (CeO_2NPs alone, DEP alone and CeO_2NPs/DEP), when compared to the medium control, and after CeO_2NPs/DEP exposure when compared to the particles alone (Figure 3-11). This is also reflected in the MUC5AC expression (Figure 3-13). The opposite effect is seen in the expression of IL-33 expression (Figure 3-13). These results taken together suggest that a model that is already in an "inflamed" state and then exposed to these particles significantly increases the expression of mediators related to a type II response and mucus production, but not an "asthmatic" phenotype.

There are very few, if any, studies currently present in the literature that investigate the co-exposure of CeO_2NPs alone, DEP alone and CeO_2NPs/DEP with cytokines and their potential effects of bronchial epithelial cells. It has been identified that as the basal epithelium differentiates, gene expression of IL-4 and IL-13 receptors varies in concentration and location depending on differentiated cell type (White et al., 2010). Previous work within the group has demonstrated that the addition of a TLR cocktail caused a slight decrease in mRNA levels of CYP1A1 when co-exposed to DEP in differentiated epithelial cells. This did not cause a change

in the mRNA levels of CXCL10, but caused a significant decrease in the CXCL10 protein production (Meldrum et al., 2017).

3.4.6 CeO_2NPs, DEPs and HDM exposures

In order to identify the potential effects that HDM exposure might have on the bioreactivity of these particles, we co-exposed the primary human large airway epithelial cells to HDM and particles at concentrations relevant to those used in the *in vivo* studies in Chapters 4 and 5. This study aimed to analyse the viability, TEER and lactate production, and the secreted cytokines and chemokines after exposure to the previously mentioned exposure concentrations. Three CeO_2NPs concentrations were used, with one DEP concentration and a combination of both particles at the same ratio and increasing concentrations. This aimed to replicate concentrations of Envirox^{TM} that were previously investigated (Park et al., 2007).

We identified a significant decrease in the CCL20 concentration after exposure to the highest concentration of CeO_2 and DEP +HDM when compared to -HDM, and a slight decrease in IL-33 concentration with HDM co-exposure (Figure 3-17). There was a slight increase in TSLP concentration after the addition of HDM to the model (Figure 3-17). These results indicate the addition of HDM to the cells has the potential to inhibit the attraction of macrophages but increase the potential of a type II response.

There is again no current literature on the co-exposure of CeO_2NPs/DEP and HDM *in vitro*. One study investigates the potential for co-exposure with pollen (Parietaria officinalis) as an allergen to cause cellular changes in A549 cells. It was found that with co-exposure there are changes in the mitochondria and rough endoplasmic reticulum when compared to the control. This suggests that co-exposure with a potential allergen can cause metabolic changes (Mazzarella et al., 2014).

3.4.7 Limitations and future direction

Cerium oxide nanoparticles have been found to adsorb proteins from the tissue culture medium in which they are suspended; the smaller the particles, the higher their adsorption potential due to their greater surface area. This can theoretically alter the outcome of the toxicological assessments being carried out and thus the bioreactivity attributed to these particles may be irrelevant in situ (Horie et al., 2009). There may also be the potential for these particles to interfere with colourimetric analysis, such as ELISA analysis. It has been found that there can be some interference in the outcome associated with an increase in the BSA concentration in the medium (Veranth et al., 2007). As we did not use any serum in our medium this interference

would not be a consideration in our study. In future, it would be good practise to confirm this is the case for whichever culture medium is used. We did try to mediate any potential interfering effects by centrifuging the medium to remove particulate matter before colourimetric analysis. As the particles would potentially be inhaled, they would not naturally come into contact with some of the proteins found in cell culture medium and therefore may behave differently in life. But the presence of large airway epithelial cell secretions, as observed in our model, would enhance the association of the nanoparticles with natural lung secretions rather than tissue culture medium components. In addition, these models do not cope well with repeat exposures to these particles (they start to break down after 3 days of exposure), additional models need to be built and characterised before applying the particles. Additional exposure systems also need to be set up and use aerosol sprays as the main exposure routes.

As mentioned previously, DEP is a very variable particle that can change depending on numerous factors. We used NIST (2975) particles in this study, and while these are very useful to carry out comparisons between different studies their relevance can be questioned. They were collected from a heavy industrial forklift truck, and engine styles, combustion rates and diesel fuel has changed greatly since the particles were collected bringing into question how comparable they are to modern day exhaust particulates experienced within urban environments. There is also the potential for these particles to have changed during their storage over time. In future experimental work it would be useful to compare these particles to more of a "real-life" particle, either collected from ambient air, or directly from a known engine combusting fuel at set driving cycles. As fuels develop, bio-fuels and various combinations of fuels will also appear on the market. It is also important to compare our standard particles against these new particles.

With new fuels coming onto the market, there is also the impact of driving conditions and if there is a particulate filter operational within the exhaust system, and geographical location, that is being replicated. For future studies using collected particles, it would be important to take these various characteristics into consideration. When the CeO_2NPs are combusted, the particles are changed from pristine particles and their coatings are lost and a new coating is formed on 30% of the particles. These changes suggest that pristine particles commonly used in laboratories (and in this study) may not be the optimal model particle representative of Envirox^{TM} combustion (Dale et al., 2017). More realistic materials need to be used in the future that represents combusted material. Future studies should also consider the ratio of CeO_2NPs

to DEP, something that has been considered in this study even though the particles were not burnt together.

3.4.8 Conclusions

From our research we have identified that the addition of these particles to this specific epithelial lung model has the potential to influence the inflammatory mediator expression, as well as production. This has been identified after CeO_2NPs as genes that are related to the modulation of asthma being significantly decreased (NQO1, CYP1A1 and ADAM8) and those related to a type II response and immune cell chemotaxis (TSLP and IL-25) being significantly increased. This suggests that exposure to CeO_2NPs has the potential to reduce the asthma phenotype and exhibit a type II response. Post-exposure to DEP there were dose dependant increases in genes related to the modulation of asthma (CYP1A1 - CYP1A1 expression is increased by the activation of the AhR which is known to be activated after exposure to DEP due to the polycyclic aromatic hydrocarbons (PAH) content (O'Driscoll et al., 2018)) as well as significant decreases in others (ADAM8), and significant increases in type II apical mediator release (TSLP and IL-33). These results suggest there are mixed messages with DEP exposure that can influence the type II response as well as potentially influencing the severity of the asthmatic phenotype. Exposure of our model to CeO_2NPs/DEP appears to ameliorate the effects seen in the particles alone. Especially the IL-25, CYP1A1 (significant increase) and TNF-α (significant decrease). These results suggest that while the individual particles alone have the potential to enhance the type II response, the combination has the biggest potential and therefore the highest risk to the public if exposed.

Our studies currently only focus on 24hour time points. There is the potential for effects to be seen at earlier time points such as 4, 6, or 12 hours of exposure. IL-33 is an alarmin and released within minutes or hours of appropriate stimuli. Therefore, it may be degraded/processed (Miller, 2011) at time points such as 24hrs. There is the potential to extend the exposures (longer time points) or change to repeated exposures as would more likely occur naturally or occupationally (for example travelling to and from work etc).

The cells used in the *in vitro* model are also important. We only use one cell type in these studies, but others have used more advanced co-culture models but it is fair to say that these "3D" co-culture models also have limitations, often using epithelial cell lines and immune cells derived from blood cells. It is important to further develop these models to better mimic an *in vivo* system. In addition to the primary human lung large airway epithelial cells, additional cells such as immune cells, including dendritic cells, macrophages and immune cells relevant to allergic

responses, as well as other structural cells, including smooth muscle cells, endothelial cells, and fibroblasts, possibly in organoids to achieve a more physiologically relevant system. However, such models are still being developed and the use of primary human cells currently limits the volume of work that could be achieved. Cell lines are freely available and easy to grow, whereas primary cells are harder to obtain, either from a cell supplier or from explants of tissue obtained following clinical procedures.

The model described here, and more complex models could also be used to investigate other asthmatic allergens, such as pollen, animal dander, and cockroach antigens, and comparisons could be made to determine if these various allergens have an effect on the potential effects of airborne pollutant particles.

How the particles are suspended, and the cells exposed to them is also important. Homogeneous suspension of the particles is important, and in this study we sonicated the particles before applying them to the cells. This protocol was used to inhibit aggregation of the particles, but there is every possibility that this still happens and can alter the dosimetry, uptake of the particles and the toxicity (Moore et al., 2015). This potential change in the particle characteristics prior to cell exposure, or after they've been sonicated is important as it may affect the cellular responses. We therefore ensured that the particles used were characterised in water, and in cell culture medium before applying to the cells. Cellular uptake of the particles is also an important consideration. If the particles have been coated with something that makes them no longer biologically relevant, they may not behave in a way that is relevant to the situation *in situ*. Lung lining fluid may also play a role in the coating of particles and the potential protection of the cells from these particles.

As well as ensuring the exposure is as close to a physiological exposure as possible, it would complete the story to investigate the potential impact that lung lining fluid may have in protecting the cells. It is well known that airway secretions contain molecules that contribute to the immune response and can alter particle-cell interactions including uptake of particles into epithelial cells or traditional immune cells. Different particles adsorb different components of the lung lining fluid and alters the corona of the particle that originally enters the lung (Konduru et al., 2017). Additional defence mechanisms that are also in place to protect the lungs from such insults (such as mucus production and beating cilia) would also be required to develop a more advance lung model for *in vitro* exposures to various nanoparticles. Our model is an important starting point for the *in vitro* understanding of how these particles can

potentially affect the lung epithelium, and without this starting point further models cannot be built or developed.

Chapter 4: Investigation of the effects of cerium dioxide nanoparticles in a murine model of allergen exposure.

4.1 Introduction

Animal models are a good way of studying how nanoparticles would behave within a whole lung model. They have also helped greatly in the understanding of the mechanisms and development of asthma (Zosky and Sly, 2007, Shin et al., 2009). Some animals do display allergic tendencies and have elements of asthma (such as either the airway remodelling or the inflammatory response), but not the complete disease. Mice are the most commonly used as an asthmatic model, this is mainly due to the number of species specific probes available, easily sensitised to give a Th2 response, and specific genetic strains (Zosky and Sly, 2007, Karol, 1994, Wegmann and Renz, 2005, Shin et al., 2009) and their general size and small cost.

4.1.1 Cerium dioxide

There have been numerous studies investigating the potential effects inhalation of nanomaterials has on rodents, but fewer focusing specifically on cerium dioxide. Previous inhalation studies have determined that exposure to cerium dioxide has no long term pulmonary or cardiovascular effects after a recovery period of 4 weeks (exposure of 4mg/m^3 for 3hrs/day, 5days/week) (Dekkers et al., 2017), and no genotoxicity after a higher exposure (50mg/m^3 for 6hrs/day, 5days/week) and a longer recovery period of 6 months (Cordelli et al., 2017). As well as considering pulmonary exposure routes, other routes have been investigated (including injection and oral gavage) and indicate that there are various responses associated with the various exposure routes. This may have implications for therapeutic uses of cerium dioxide as mechanism of action varies depending on exposure route (Minarchick et al., 2015). Potential therapeutic uses of cerium dioxide that have been identified *in vivo* include clinical therapy for obesity (nanoceria was found to reduce weight gain and reduce obesity markers in the blood) (Rocca et al., 2015), potential cardioprotective effects (Nassar et al., 2018, El Shaer et al., 2017), and has the potential to be developed as neurodegenerative therapies (Estevez and Erlichman, 2014, Estevez et al., 2011, Naz et al., 2017).

The effects cerium dioxide has on a normal *in vivo* system has been investigated, as well as models that are designed to mimic certain human conditions. For example, mice prone to cardiovascular diseases ($ApoE^{-/-}$), and various neurological diseases (5 x FAD (Dekkers et al., 2017) and $Nrf_2^{-/-}$ (Xu et al., 2016)).

4.1.2 House Dust Mite (HDM) model of allergic airway disease

An *in vivo* model to represent allergic phenotypes has also been developed. In order for any of these animal models to be used, they have to be sensitised to an allergen to give an allergic response. Currently (and historically) ovalbumin (OVA), a protein from egg white, is the sensitisation agent of choice (Rosenberg and Druey, 2018). There are issues with using this protein though. It has been found that a prolonged exposure to OVA can lead to tolerance (Zosky and Sly, 2007). It is also not associated with the natural development of asthma within humans and must be injected into the animal before it is exposed to an allergen. A more clinically relevant allergen is house dust mite (HDM), which is associated with the development of asthma (Reithofer and Jahn-Schmid, 2017, Calderon et al., 2015). This can be administered by inhalation through the nose, again a more clinically relevant exposure. The major drawback of this model is the level of the IgE is much lower than the levels found within an asthmatic patient (Birrell et al., 2010).

This model has various physiological signatures. There is a significant increase in the IgE concentration in the serum after exposure to HDM, as well as an increase in IL-4, IL-13, IL-10, IFN-γ and TGF-β when compared to the control alone. Airway hyperresponsiveness was found to be higher after exposure with methacholine after exposure to HDM, as well as hyperplasia of goblet cells and airway remodelling (seen after staining with M.T.). Th2 cytokines (IL-4, IL-13 and TGF-b) are released and effect the epithelial cells within the airways (Ahn et al., 2007). Expression of TLR4, CD40 and CD86 are also significantly increased after HDM exposure (Hongjia et al., 2010). All the signatures above are relevant for the development of the HDM model and the potential effects CeO_2NPs has alone and with HDM.

MCPT1 is known to promote permeabilization of mucosal membranes and allergic hypersensitivity reactions (Sayed et al., 2008), as well as being a mast cell chemoattractant (Theoharides et al., 2012).

4.2 Hypothesis and aims

Hypothesis:

CeO_2 will potentiate the allergic response of HDM in an animal model of allergic lung disease in relation to dose and acute or chronic exposures.

Aims:

It is important to determine the potential systemic effects the addition of CeO_2NPs have on an allergic model, both the exacerbation and the adjuvant effects of these particles. As the previous chapter has focused on the effects of these particles on the airway epithelial layer, there is no *in vitro* analysis of the whole systems – including the immune cells and consideration of clearance mechanisms. The *in vivo* system is not human, it will not be an exact representative of the human exposure, but it will however allow an indication of the effects these particles have on an allergic phenotype.

The aim of this chapter is to:

- Set up and characterise the animal model of allergic lung disease.
- Determine the effects a single 24-hour (acute) exposure of CeO_2NP±HDM have in a murine model. This will allow us to determine the acute responses to these particles and compare the acute responses to the repeated exposures.
- Determine the effects a single acute exposure of CeO_2NP have on an HDM murine model of allergy (SGL) and repeated chronic exposures of CeO_2NP±HDM (RPT), have on a murine model. This will allow us to establish the potential effects the repeat exposures of CeO_2NP alone have when compared to the HDM exposure protocols.

4.3 Methods

All methods used within this chapter have been previously described in Chapter 2. Individual method sections for reference will be identified throughout this chapter.

The experimental protocol for all the *in vivo* work completed within this thesis varies per chapter. The protocol for this chapter is outlined in Figure 4-1 (A and B) and indicates the various exposure regimes as well as the euthanasia and exposure time points. Figure 4-1, C outlines the end points that are analysed throughout this chapter in order to determine the effects CeO_2NPs have on an animal model of allergic disease and on a healthy animal.

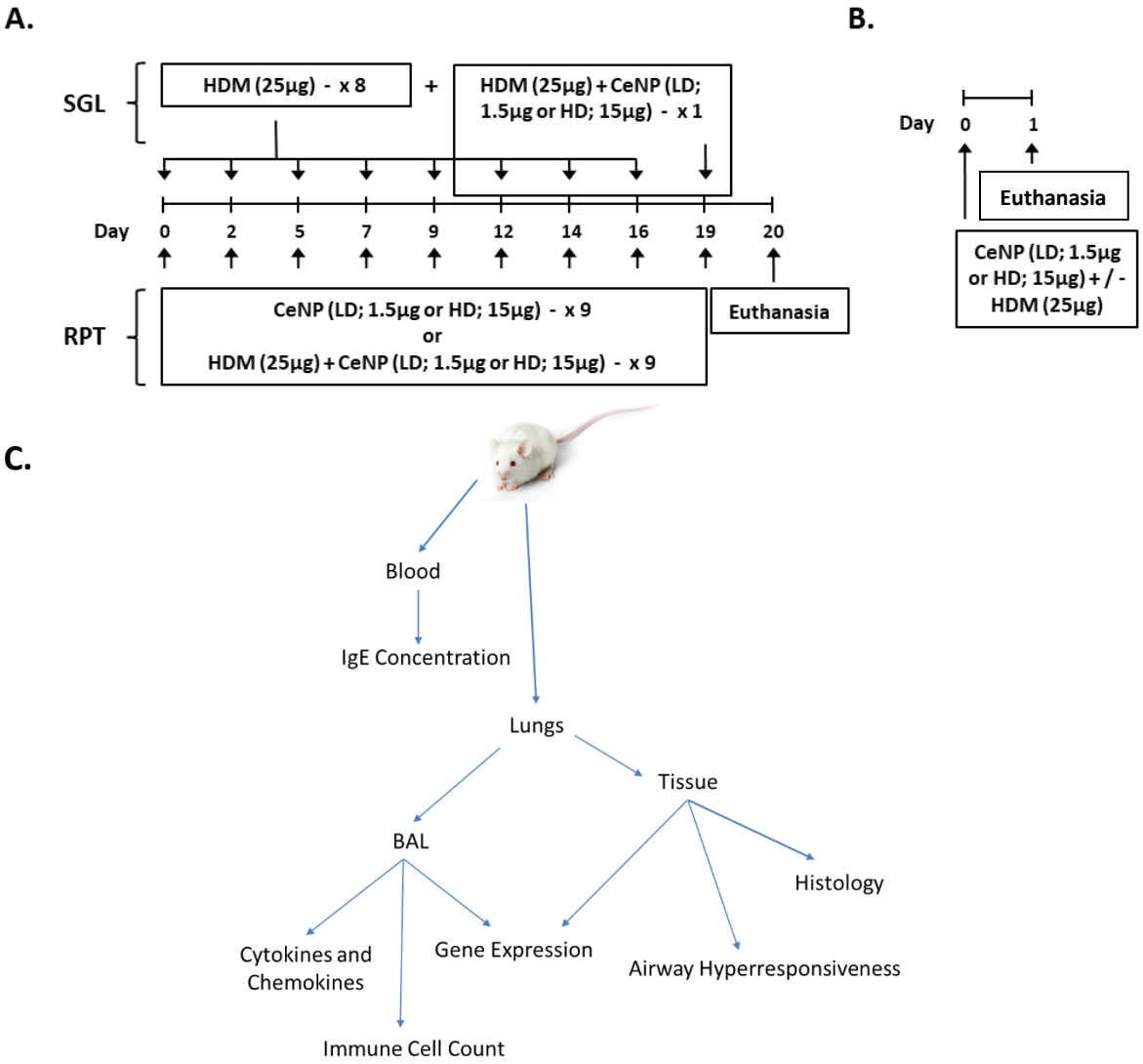


Figure 4-1. Experimental protocol to determine the effect of CeO_2NPs in an animal model of allergic lung disease. A. Chronic exposure protocol. Balb/c mice were repeatedly (RPT) exposed intranasally to CeO_2NPs, low dose (LD) (1.5µg or 75µg/kg) or high dose (HD) (15µg or 750µg/kg), alone or combined with HDM (25µg or 1.25mg protein/kg). This protocol consisted of 9 exposures divided over 3 weeks on the indicated days (lower panel). Single (SGL) exposure protocol involved the pre-exposure to HDM on 8 occasions, with the final 9th exposure consisting of CeO_2NPs (LD and HD) ±HDM (upper panel). B. Acute exposure protocol. Mice were exposed to a single bolus intranasal instillation of CeO_2NPs (LD and HD) ±HDM and euthanised after 24 hours. For all exposures a PBS control was also administered. C. Diagram indicating the various end points that where analysed throughout this chapter in order to determine the potential acute and chronic effects CeO_2NPs±HDM at different concentrations of CeO_2NPs.

4.4 Results

4.4.1 Effect of single acute exposure to CeO_2 NPs ± HDM on airway inflammatory responses after 24 hours

24 hours after acute CeO_2NPs±HDM exposure (Figure 4-1 B), following euthanasia, the lungs were excised and analysed for levels of CeO_2NPs within the lung tissue (as described in section 2.2.2 and section 2.2.3); cell numbers and profile and cytokine levels were analysed in the BAL fluid (section 2.6.4) to determine the effects of this acute exposure.

4.4.1.1 Concentration and location of cerium oxide after acute exposures to CeO_2NPs±HDM and the effects on lung pathology.

Figure 4-2 assesses the concentration (Figure 4-2, A) and location (Figure 4-2, B) of the cerium oxide 24 hours after instillation ±HDM, while Figure 4-3 assess any physiological changes after instillation using H/E, PAS and M.T. staining.

The concentration and location of cerium was identified 24 hours after an acute exposure of CeO_2NPs±HDM. CeO_2µg/g of lung tissue was calculated for each exposure (Figure 4-2, A). This ICP-MS analysis indicates that there was an increase of cerium within the lung after the HD of CeO_2NP alone when compared to the LD as expected. It also indicated that there was a significant increase in the cerium concentration after CeO_2HD+HDM when compared to CeO_2HD alone. This could potentially indicate that the co-exposure with HDM prohibits the clearance of the cerium that is seen in the acute exposures without HDM.

Figure 4-2, B shows the location of the cerium within the lung 24 hours after the acute exposure to CeO_2NPs±HDM. The white spots indicate a higher concentration of particles within that area, and these reflect the cerium concentrations obtained from acid digestion of the lung tissue (Figure 4-2, A). There appears to be a higher concentration of cerium located within the larger airways.

A.

Treatment (24 hours)	Ceμg/g Lung Tissue
PBS	0.00±0.00
HDM	0.00±0.00
CeO_2LD	1.01±0.14
CeO_2HD	1.3±0.00
CeO_2LD+HDM	0.56±0.22
CeO_2HD+HDM	4.38±1.73

B.

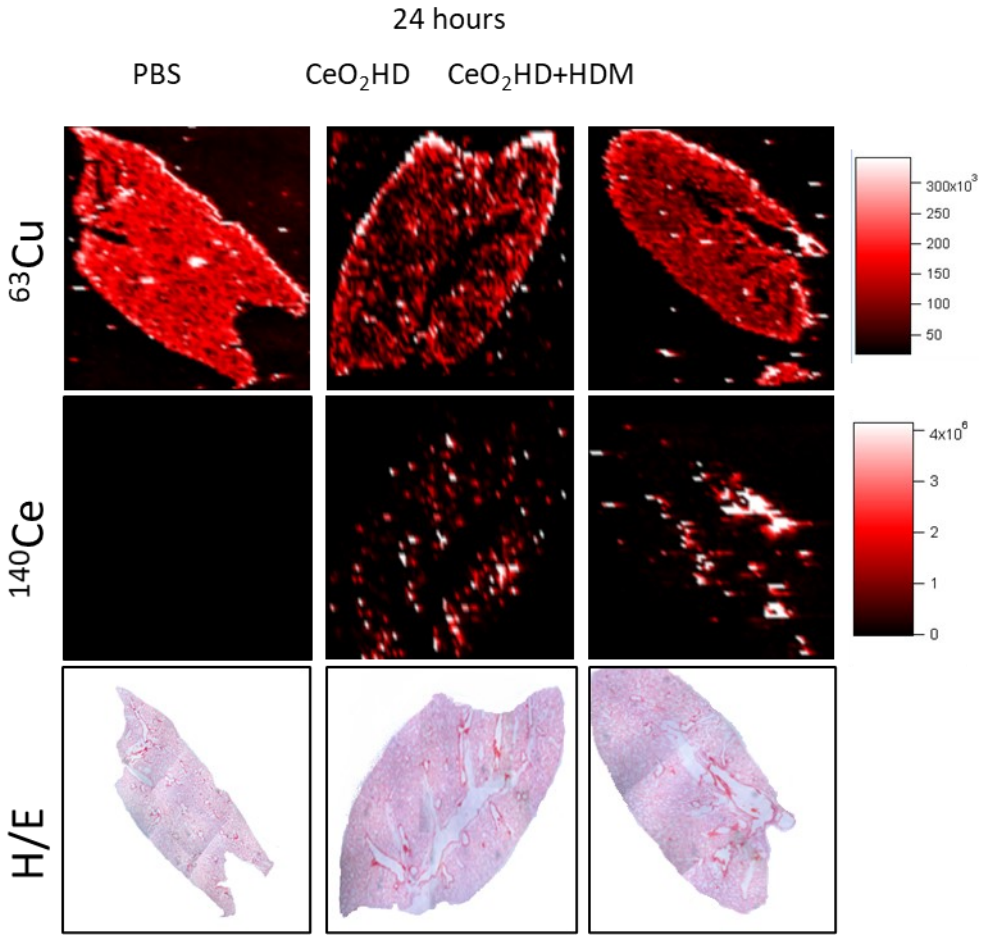


Figure 4-2. Concentration and location of CeO_2NPs after an acute exposure to CeO_2NPs±HDM. A. Concentration (μg/g lung tissue) of CeO_2NPs after an acute, 24 hour exposure to CeO_2NPs±HDM. Lungs were digested as previously described (section 2.2.2) and ICP-MS based quantification of ^{140}Ce content was determined. B. Pulmonary deposition of CeO_2NPs was detected after laser ablation by ICP-MS. Lungs were fixed and sectioned as previously described (section 2.2.3) before being ablated and ^{63}Cu and ^{140}Ce was analysed and compared against serial H/E stained sections (x5 magnification) in order to establish deposition relative to lung structure. 3 lungs were digested per group to determine the concentration of CeO_2μg/g with all assays performed in triplicate. Significance is denoted as the following, as indicated: compared to CeO_2NP alone $p<0.05$.

There does not appear to be any change in the airways after staining for overall structure, mucus and connective tissues (Figure 4-3). This would not be expected 24 hours post exposure, as there is no time for physiological changes to become apparent. It is important to note here that these are serial lung sections, meaning that they are sectioned in serial and then stained in that order. This allows a complete picture to be built up of various airway components using the various stains chosen.

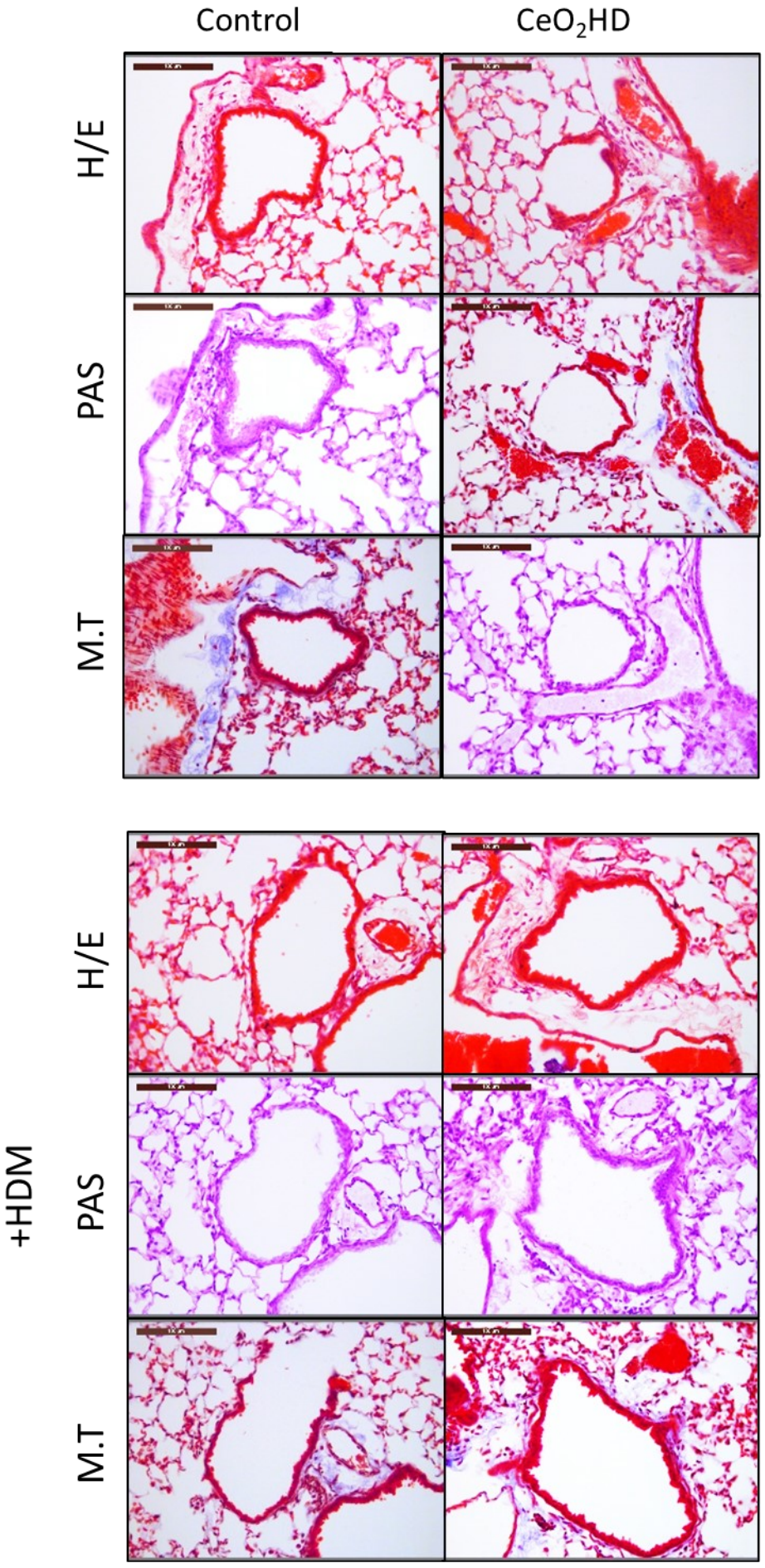


Figure 4-3 Lung sections stained 24 hours after exposure to high dose CeO_2NPs±HDM. Lung tissue was fixed and stained with haematoxylin and eosin stain (H/E) (top panel), Periodic acid-Shiff (PAS) (middle panel) and Masson's Trichrome stain (M.T.) (bottom panel). Representative images of each group are displayed with a scale bar of 100µm (top left of image).

4.4.1.2 *Effect of CeO_2 NPs ± HDM on altered BAL Immune cells*

Macrophages, neutrophils, lymphocytes and eosinophils were counted within the BAL fluid (Figure 4.4) and plotted as cells/ml of BAL fluid. % of total cells counted of each immune cell was also analysed (Figure 8-10, appendix). There was no change in the number of macrophages after exposure to CeO_2NPs alone when compared to the equivalent PBS control. There was a significant decrease in the number of macrophages after co-exposure with CeO_2NPs+HDM for both concentrations of CeO_2NPs when compared to CeO_2NPs alone, and when compared to HDM alone at the higher concentration of CeO_2NPs. Furthermore, there was a decrease in the percentage of macrophages following exposures to CeO_2NPs+HDM, which fell with increasing concentrations of CeO_2 (Figure 4.4).

The number of neutrophils was significantly increased after exposure to HDM when compared to the PBS control, and increased again on co-exposure to CeO_2NPs+HDM exposure when compared to the HDM control (this was only significant after exposure to the higher concentration). There was a significant increase in the neutrophil count after the exposure to the higher CeO_2NPs+HDM when compared to the lower concentration. There were no changes in the number of neutrophils without the addition of HDM to the exposure protocol.

There was no change in the lymphocyte or eosinophil cell counts after any of the exposure protocols.

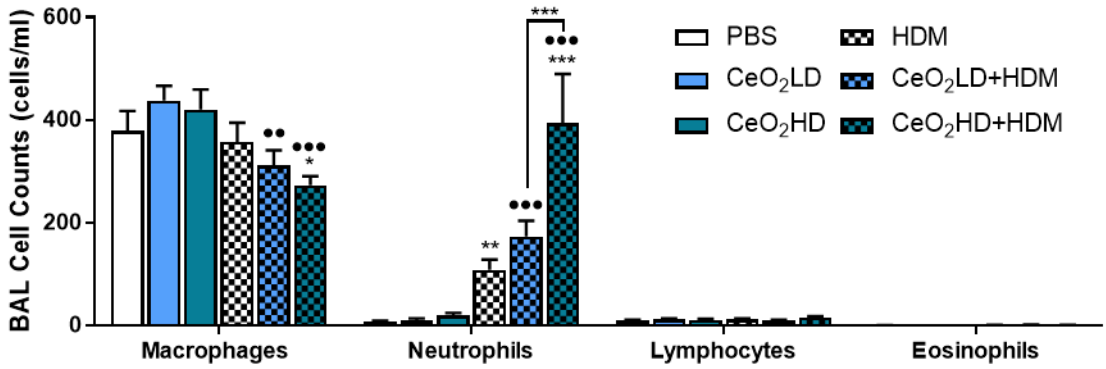


Figure 4-4 Inflammatory cell profile 24-hours after acute exposure to CeO_2NPs±HDM. BAL fluid was analysed for immune cell profile. BAL cells were counted after being fixed and stained as previously outlined (section 2.6.4) and 300-500 cells were counted per animal. The data are presented as the mean ±SEM total cells counted. N=5-9 mice per treatment group, with all assays performed in triplicate. Significance is denoted as the following, as indicated: compared to PBS or HDM control p<0.05(*), <0.01(**), <0.001(***); compared to CeO_2NP alone p<0.05(•), <0.01(••), <0.001(•••).

4.4.1.3 *Effect of CeO_2 NPs ± HDM on inflammatory markers in BAL fluid*

Inflammatory markers were analysed in the BAL fluid 24-hours post-instillation (Figure 4-5). CCL20 was significantly increased (~2-fold) only following exposure to the higher concentration of CeO_2NPs+HDM when compared to the lower. There was a similar response for TSLP release,

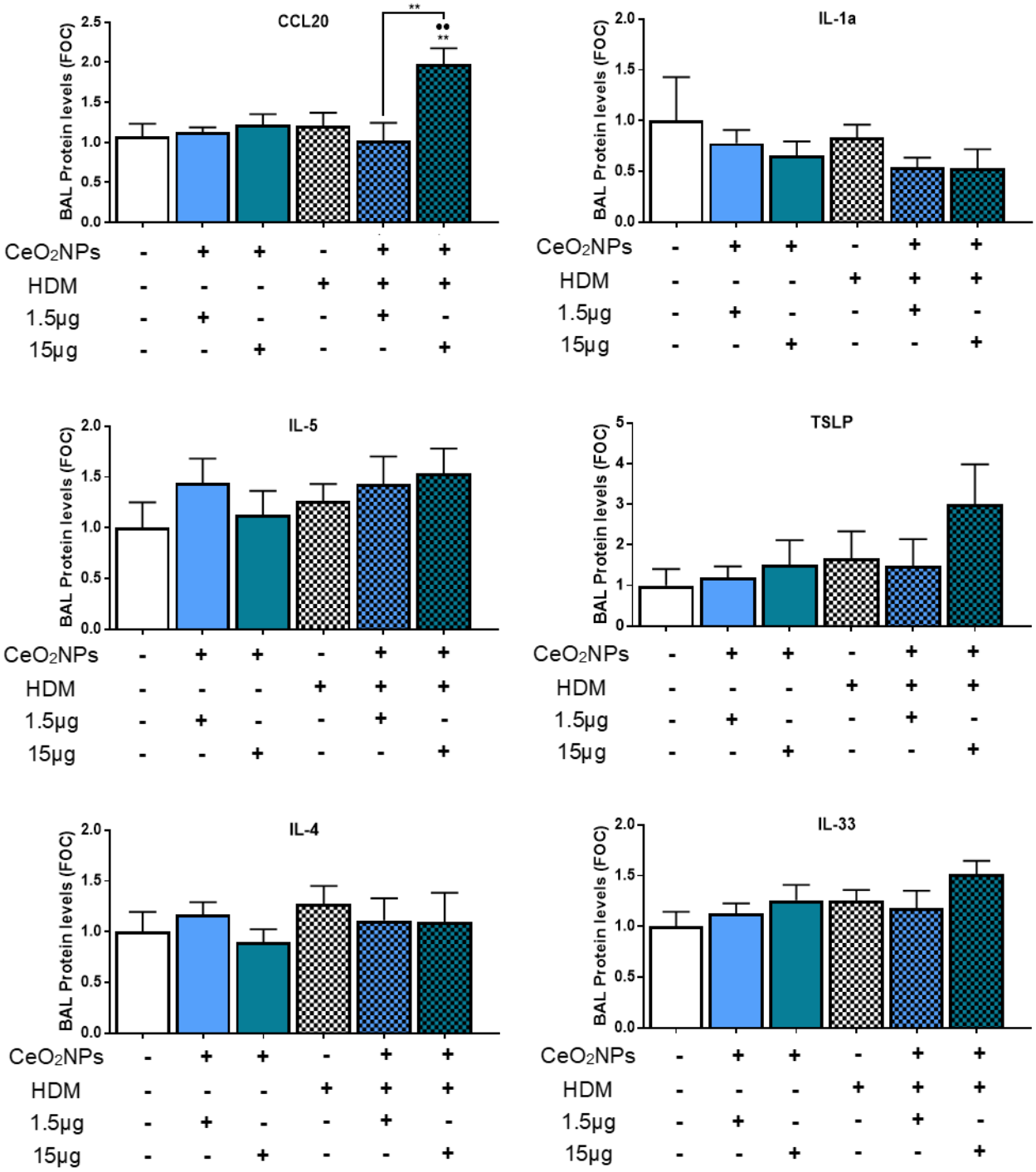


Figure 4-5. Cytokine release 24-hours after acute exposure to CeO_2NPs±HDM. BAL fluid was analysed for immune cell profile and released cytokines. A. BAL cells were counted after being fixed and stained as previously outlined (section 2.6.4) and 300-500 cells were counted per animal. The data are presented as the mean ±SEM total cells counted. B. Cytokines were measured in the BAL fluid and are presented as fold over control levels (FOC±SEM). N=5-9 mice per treatment group, with all assays performed in triplicate. Significance is denoted as the following, as indicated: compared to PBS or HDM control p<0.05(*), <0.01(**); compared to CeO_2NP alone p<0.05(•), <0.01(••).

when compared to the particles alone, the HDM control and the lower concentration of CeO_2NPs+HDM. There was a decrease in the IL-1α concentration after exposure to CeO_2NPs alone in a dose dependant manner when compared to PBS control, there was also a decrease in IL-1α release after exposure to CeO_2NPs+HDM in a dose dependant manner. There was no change in the IL-5, IL-4, and IL-33 concentrations regardless of the exposure protocol.

4.4.2 Effect of single and repeat exposure (9 independent exposures over 3 weeks) to CeO2NPs (±HDM) on pulmonary responses

Three weeks after 3 HDM exposures per week, a number of pulmonary responses were analysed to determine the effect of chronic exposures (repeat dose effects), both investigating adjuvant and exacerbation responses. The exposure protocols are outlined in Figure 4-1, A. These allowed us to identify potential exacerbatory effects of CeO_2NPs (single exposure to CeO_2NPs±HDM after 8 HDM exposures), and adjuvant effects (co-exposure to CeO_2NPs and HDM for 9 consecutive exposures) as well as examining the effects CeO_2NPs alone might have on the airways and the allergic responses.

4.4.2.1 Concentration and location of cerium oxide after acute exposures to CeO_2NPs±HDM and the effects on lung pathology.

Figure 4-6 assesses the concentration (Figure 4-6, A) and location (Figure 4-6, B) of the cerium oxide 3 weeks after instillation ±HDM.

The concentration and location of cerium was identified 24 hours after 3 weeks exposure, either after 8 HDM exposures followed by a single CeO_2 exposure (CeO_2HD+HDM SGL) or 9 co-exposures with CeO_2NPs+HDM (CeO_2NPs+HDM RPT. CeO_2µg/g of lung tissue was calculated for each exposure (Figure 4-6, A). This ICP-MS analysis indicates that there was a significant increase in the concentration of cerium after all of the higher exposure concentrations. There was also a significant increase in the concentration of cerium in the repeated high dose exposure (CeO_2HD+HDM RPT) when compared to the single exposure (CeO_2HD+HDM SGL).

Figure 4-6, B shows the location of the cerium within the lung 3 weeks after the chronic exposures to CeO_2NPs±HDM. The white spots indicate a higher concentration of particles within that area, and these reflect the cerium concentrations obtained from acid digestion of the lung tissue (Figure 4-6, A). There appears to be a higher concentration of cerium located within the larger airways of the lung, as well as in the repeated exposure regime when compared to the single exposure.

A.

	Treatment (3 Weeks)	CeO_2µg/g Lung Tissue	
	PBS	0.00±0.00	
	HDM	0.00±0.00	
	CeO_2LD	2.15±0.91	
	CeO_2HD	24.41±4.85	***
SGL	CeO_2LD+HDM	1.66±0.57	
SGL	CeO_2HD+HDM	2.78±1.52	***
RPT	CeO_2LD+HDM	4.87±2.62	
RPT	CeO_2HD+HDM	24.39±7.31	***

B.

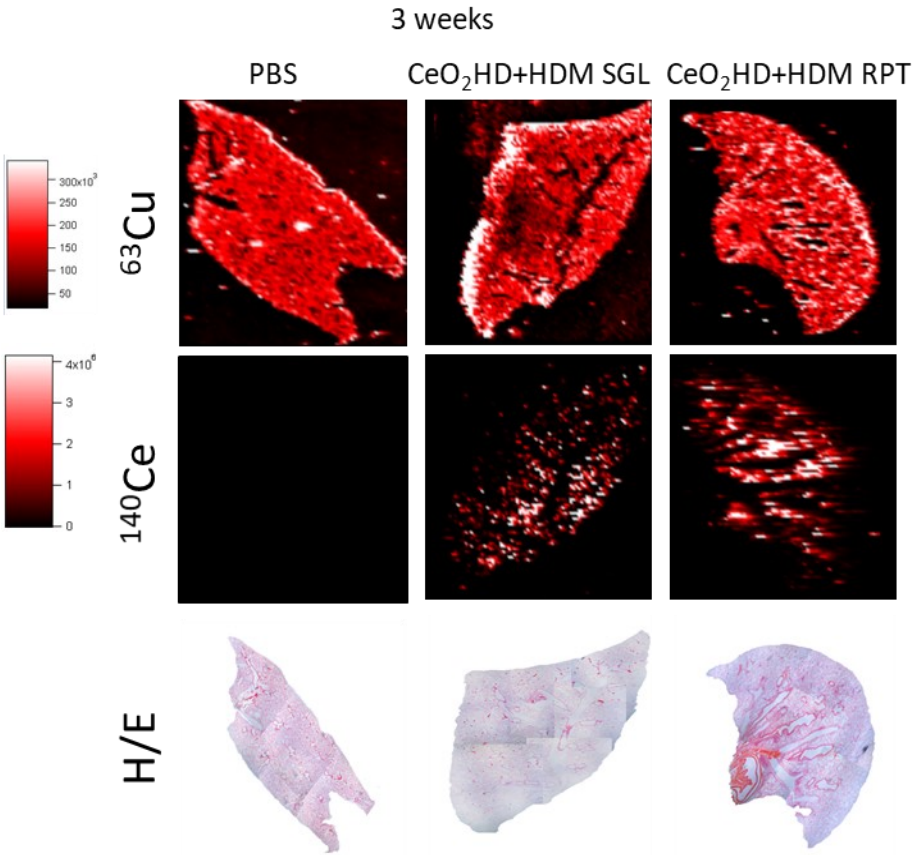


Figure 4-6. Concentration and location of CeO_2NPs after chronic exposures to CeO_2NPs±HDM. A. Concentration (µg/g lung tissue) of CeO_2NPs after chronic, 3 week exposures to CeO_2NPs±HDM, either 8 HDM exposures and a final CeO_2NPs+HDM exposure (SGL) or 9 co-exposures with CeO_2NPs+HDM. Lungs were digested as previously described (**section 2.2.2**) and ICP-MS based quantification of ^{140}Ce content was determined. B. Pulmonary deposition of CeO_2NPs was detected after laser ablation by ICP-MS. Lungs were fixed and sectioned as previously described (section 2.2.3) before being ablated and ^{63}Cu and ^{140}Ce was analysed and compared against serial H/E stained sections (x5 magnification) in order to establish deposition relative to lung structure. 3 lungs were digested per group to determine the concentration of CeO_2µg/g with all assays performed in triplicate. Significance is denoted as the following, as indicated: compared to PBS or HDM control p<0.05(*), <0.01(**), <0.001(***).

4.4.2.2 Effect of single and repeat CeO_2NPs±HDM on altered BAL immune cell profile

It was identified that there were differences between the percentages of the immune cells within the BAL fluid (Figure 8-10, appendix) and the cells/ml counts (Figure 4.7, A). This section will focus on the cells/ml count in order identify potential variation that is too small to be identified by percentages alone.

There was a significant decrease in the number of macrophages after exposure to CeO_2NPs (high or low dose) when compared to the PBS control. HDM caused no changes, when compared to PBS control. However, when mice were treated with HDM for 3 weeks with CeO_2NPs (high or low dose), all exposures caused a significant increase when compared to the CeO_2NPs alone with the high doses significantly increased when compared to HDM alone (Figure 4-7, A).

There was a significant increase in the number of neutrophils (approximately ~3-fold) and lymphocytes (approximately ~5-fold) after exposure to HDM (when compared to the PBS control), which for both was not further affected by the CeO_2 exposures (only the high dose exposures significantly increased the neutrophil count when compared to the particles alone, and both high and low doses significantly increased the lymphocyte count when compared to the particles alone) (Figure 4-7, A).

There was a significant increase in the eosinophil cell count after exposure to a high dose CeO_2 co-administered with HDM (CeO_2HD+HDM RPT; approximately ~20-fold (Figure 4-7, A)) when compared to exposure with the particles alone, CeO_2LD+HDM RPT, and CeO_2HD+HDM SGL. Although HDM also stimulated the proportion of eosinophils, the increase was not significant when compared to the PBS control.

4.4.2.3 Effect of single and repeat CeO_2NPs±HDM on altered mast cell related markers

Mast cells are important in the activation of a Th2 immune response that occurs during the development of asthma (Kubo, 2017, Mukai et al., 2016). Mast Cell Protease-1 (MCPT1) is known to promote permeabilization of mucosal membranes and allergic hypersensitivity reactions (Sayed et al., 2008), as well as being a mast cell chemoattractant (Theoharides et al., 2012). ELISA analysis of MCPT1 was performed on the homogenised lung tissue (Figure 4-7, B) as a marker of mast cell numbers and activation. CeO_2NPs alone stimulated MCPT1 approximately ~3-fold, although there was no difference between the exposure concentrations. There was a marked significant increase in the MCPT1 after exposure to the high dose of CeO_2+HDM repeated co-exposure (CeO_2HD+HDM RPT) when compared to HDM alone, CeO_2HD+HDM SGL and CeO_2LD+HDM RPT exposures (Figure 4-7, B). Tissue mast cells were stained using toluidine blue (TB) in airway sections from exposed animals. A representative section for each group is shown Figure 4-7, D). Mast cells appear as darker blue stained cells around the airways (see increased magnification of HDM exposure group). There does not appear to be any differences between any of the exposure group sections, however no quantification was completed on these sections.

The concentration of IgE in the plasma (Figure 4-7 C), replicated the same pattern of MCPT1 levels in the lung tissue with CeO_2HD+HDM RPT being significantly increased (approximately ~2-fold) when compared with particles alone, HDM control, CeO_2HD+HDM SGL and CeO_2LD+HDM RPT exposures.

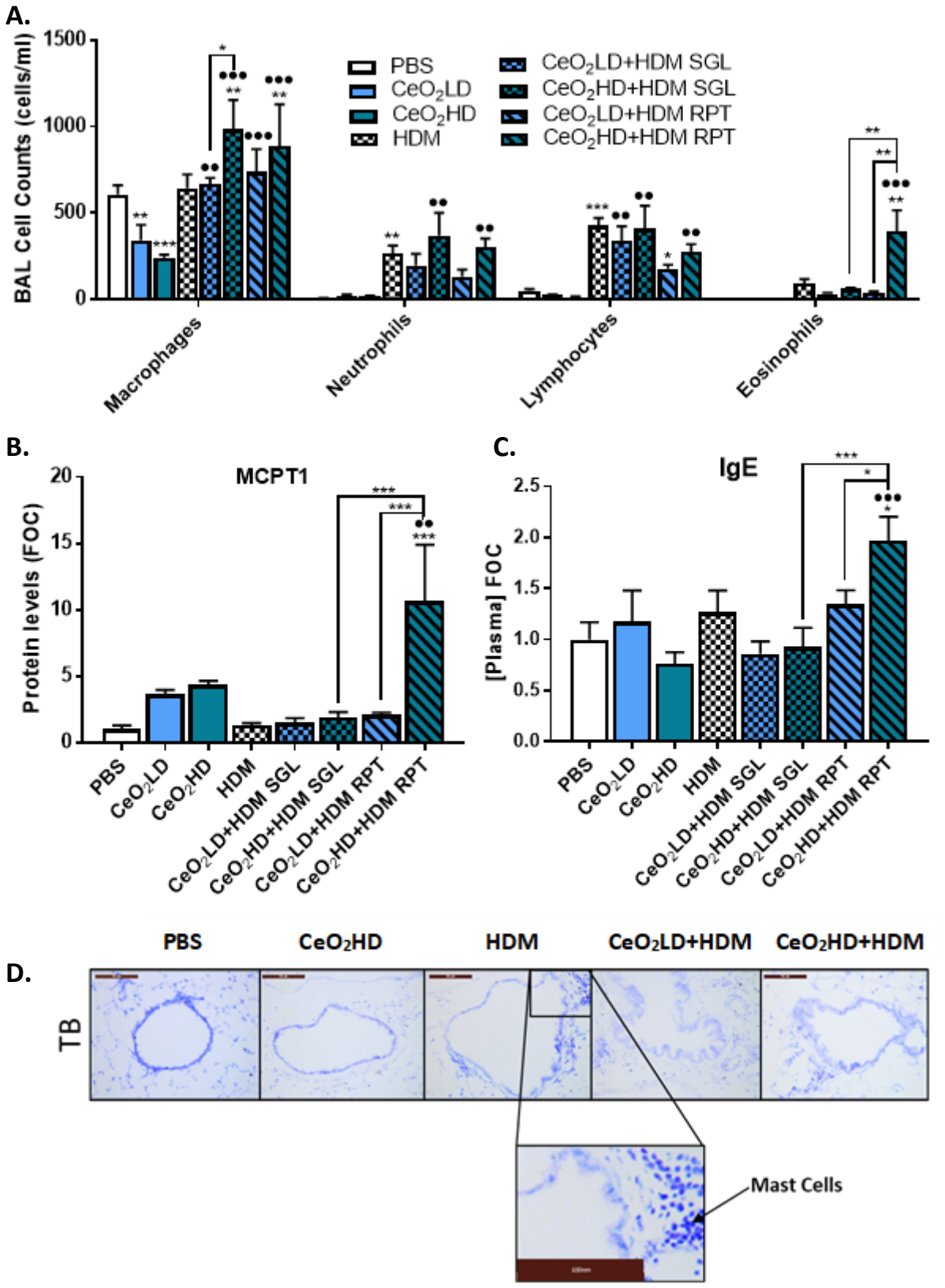


Figure 4-7. Inflammatory cell response and plasma immunoglobulin E after acute and chronic exposure to CeO_2NPs±HDM for 3 weeks. BAL fluid, lung homogenates and blood plasma were analysed for immune cells, tissue mast cell MCPT1 and plasma IgE. A. Cells were counted after being fixed and stained as previously outlined (**section 2.6.4**) and 300-500 cells were counted per animal. The data are presented as the mean ±SEM % total cells counted. B. Lung homogenate MCPT1 (mast cell marker) levels are presented as fold over control levels (FOC±SEM). C. Blood plasma of IgE levels using analysed by ELISA. D. Lung tissue was fixed and stained with toluidine blue (TB), to highlight tissue mast cells (section 2.7.2.7). Representative images of each group are displayed with a scale bar of 100µm (top left of image). N=5-9 mice per treatment group, with all assays performed in triplicate. Significance is denoted as the following, as indicated: compared to PBS or HDM control $p<0.05$(*), <0.01(**), <0.001(***); compared to CeO_2NP alone $p<0.05$(•),<0.01(••), <0.001(•••).

4.4.2.4 *Effect of exposure to single and repeat CeO_2NPs±HDM for 3 weeks on mediator gene expression in lung tissue*

Figure 4-8, Figure 4-9, Figure 4-10, and Figure 4-11 show the changes in gene expression in lung tissue after exposures to CeO_2NPs±HDM as in Figure 4-1, A.

Figure 4-8 investigates gene expression related to the potential type II inflammatory response. There were no significant changes in the expression of IL-13, TSLP, IL-4 or IL-17 after exposure to either concentration of CeO_2NPs, or exposure to HDM alone. IL-13 expression was significantly increased after both high dose exposures when compared to CeO_2NPs alone. The single exposures caused an increase in the TSLP expression when compared to the repeat exposures (significantly in the high dose), and significantly increased when compared to the HDM control. Both IL-4 and IL-17 follow the same pattern of expression. The repeat high dose exposure caused a significant increase in expression when compared to the HDM control and CeO_2NPs alone. IL-4 expression was significantly increased when compared to the single high dose exposure and the repeat low dose exposure. IL-17 expression (activates cells to produce pro-inflammatory cytokines and chemokines) was significantly increased when compared to the repeat low dose exposure.

Figure 4-9 investigates the gene expression related to pro-inflammatory responses after the various exposures. There was no change in the expression of IL-8 after any of the exposures. IL-6 (pleiotropic action during inflammation) expression was significantly increased following exposure to CeO_2LD+HDM SGL, CeO_2HD+HDM SGL and CeO_2HD+HDM RPT when compared to CeO_2NPs alone. CeO_2LD+HDM SGL was also significantly increased when compared to CeO_2LD+HDM RPT (~2-fold). IL-1α expression was significantly increased after exposure to CeO_2LD alone when compared to the PBS control and the CeO_2HD alone exposure. CeO_2LD+HDM RPT exposure caused a significant decrease in expression when compared to CeO_2LD alone. IL-36A expression was significantly increased after a high CeO_2 co-exposure (CeO_2HD+HDM SGL and CeO_2HD+HDM RPT) when compared to HDM alone, the particles alone and CeO_2LD+HDM SGL and CeO_2LD+HDM RPT respectively.

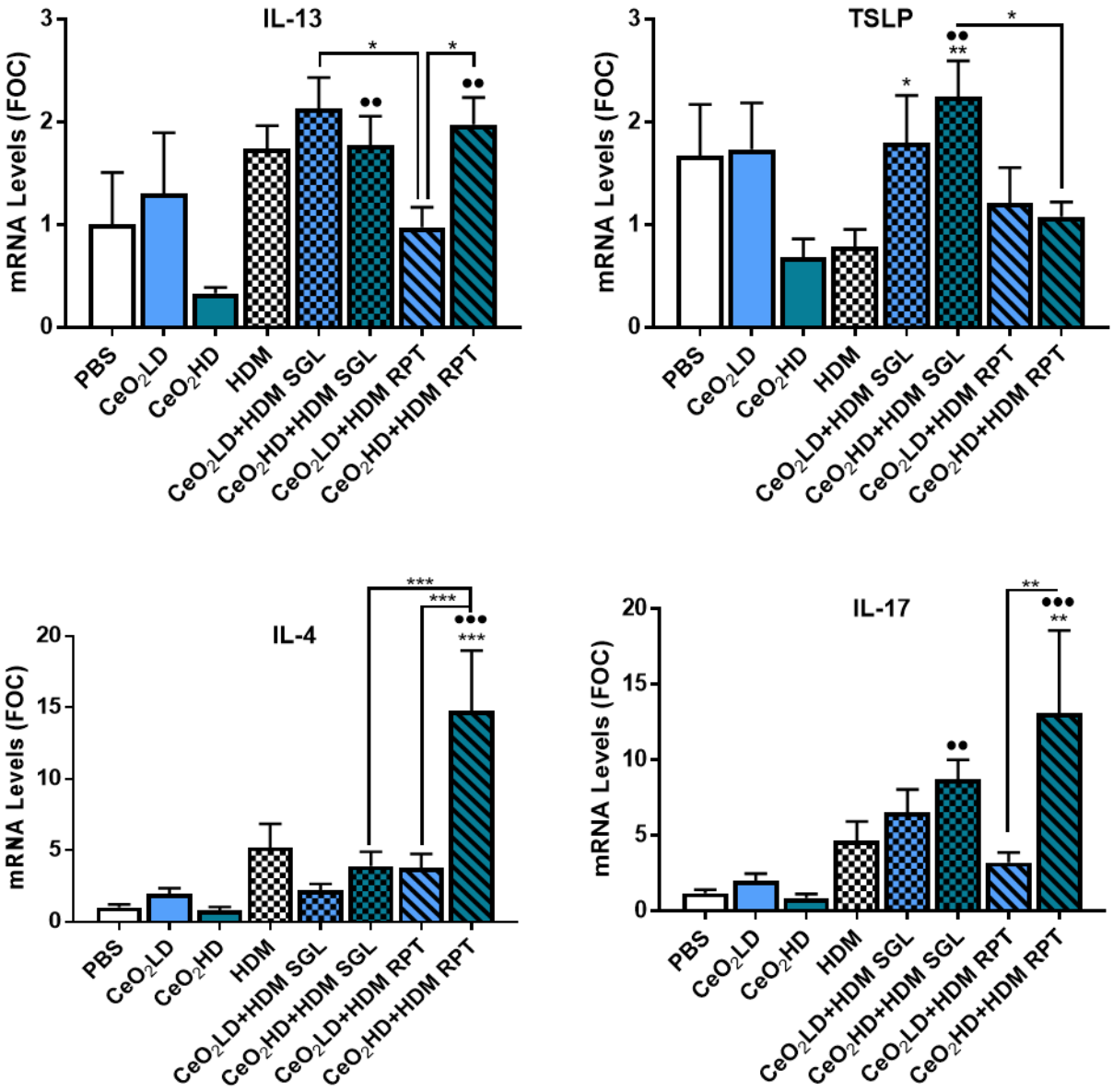


Figure 4-8 Changes in epithelial immune type II response gene expression in lung tissue following acute and chronic exposure to CeO_2NPs±HDM for 3 weeks. Total lung mRNA was isolated for indicated inflammatory markers via RT-PCR. Results are presented as fold over control levels (FOC±SEM). N=5-9 mice per treatment group, with all assays performed in triplicate. Significance is denoted as the following, as indicated: compared to PBS or HDM control p<0.05(*), <0.01(**), <0.001(***); compared to CeO_2NP alone p<0.05(•),<0.01(••), <0.001(•••).

Figure 4-10 investigates the expression of genes related to asthma after the various exposures. There were no changes in the expression of AREG, CYP1A1, IL-33, CD177 and MMP12 after exposure to CeO_2NPs alone. There was a significant increase in expression in NQ01 and MUC1 after exposure to CeO_2LD alone when compared to CeO_2HD and PBS control respectively. after exposure to CeO_2LD alone when compared to CeO_2HD and PBS control respectively. AREG expression is significantly increased after exposure to CeO_2LD+HDM SGL and CeO_2HD+HDM SGL when compared to the HDM control. CeO_2HD+HDM SGL was also significantly increased when compared to the CeO_2NPs alone and CeO_2HD+HDM RPT.

NQO1 expression is significantly decreased after repeated low dose CeO2 (CeO_2LD+HDM RPT) when compared to the particles alone. MUC1 expression was significantly increased after exposure to CeO_2HD+HDM SGL when compared to HDM control, CeO_2NPs alone, CeO_2LD+HDM SGL and CeO_2HD+HDM RPT. CYP1A1 (a cytochrome P450 involved in xenobiotic metabolism) expression was significantly increased after CeO_2HD+HDM SGL and CeO_2HD+HDM RPT when compared to the CeO_2NPs alone. The repeat exposure also caused a significant increase in expression when compared to the CeO_2LD+HDM RPT. IL-33 expression was significantly increased after exposure to CeO_2HD+HDM RPT when compared to CeO_2NPs

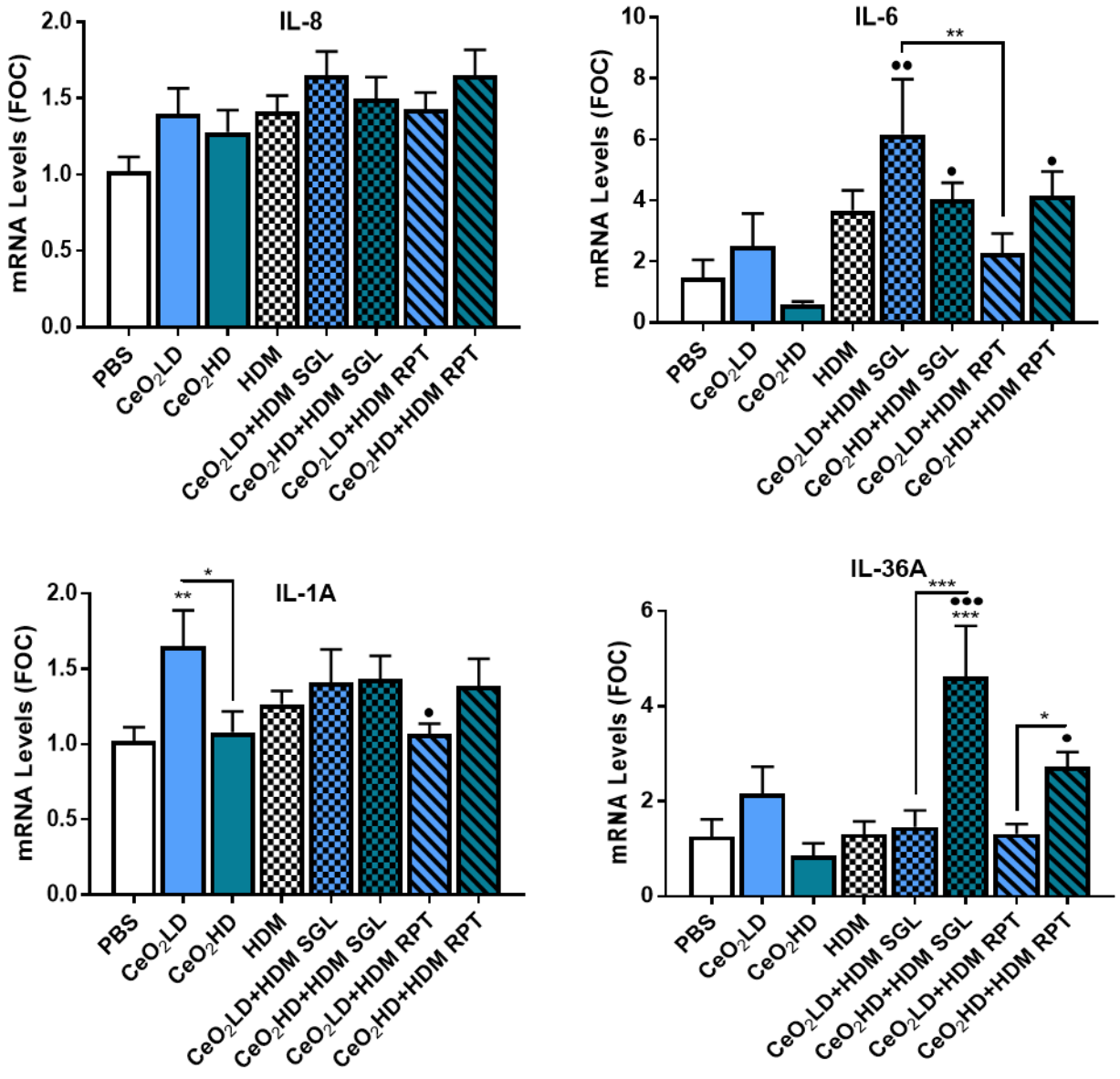


Figure 4-9 Changes in epithelial pro-inflammatory gene expression in lung tissue following acute and chronic exposure to CeO_2NPs±HDM for 3 weeks. Total lung mRNA was isolated for indicated inflammatory markers via RT-PCR. Results are presented as fold over control levels (FOC±SEM). N=5-9 mice per treatment group, with all assays performed in triplicate. Significance is denoted as the following, as indicated: compared to PBS or HDM control p<0.05(*), <0.01(**), <0.001(***); compared to CeO_2NP alone p<0.05(•),<0.01(••), <0.001(•••).

alone. The expression of CD177 (important in leukocyte migration and neutrophil activation) was significantly increased after the high dose CeO_2NPs+HDM regimes regardless of repetition when compared to the HDM control, the CeO_zNPs alone and the comparative single exposure (CeO_2LD+HDM SGL and CeO_2HD+HDM SGL). There was a significant increase in MMP12 (matrix metalloproteinase 12) expression after exposure to repeated high dose CeO2

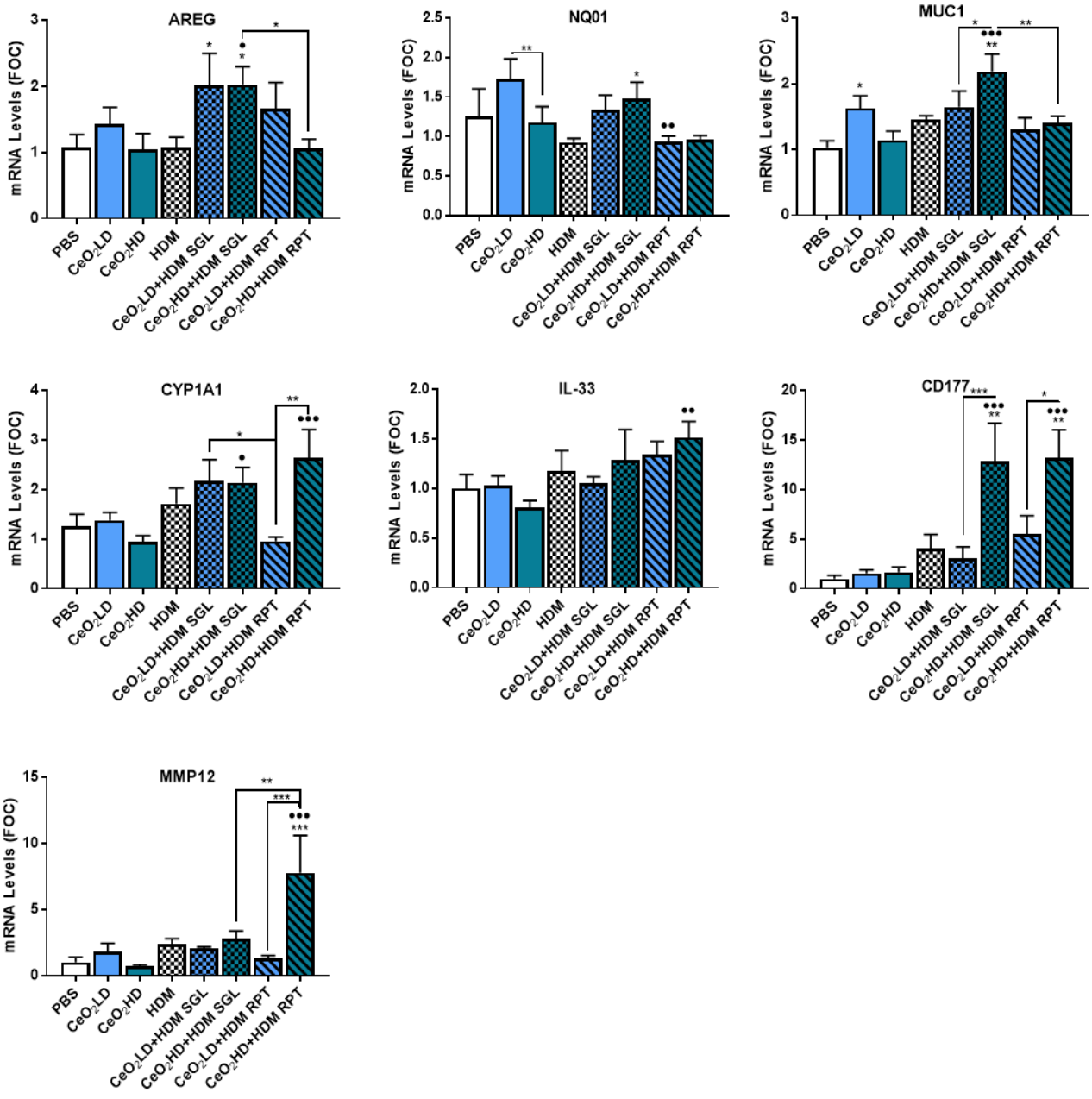


Figure 4-10 Changes in gene expression of molecules that modulate asthma in lung tissue following acute and chronic exposure to CeO_2NPs±HDM for 3 weeks. Total lung mRNA was isolated for indicated inflammatory markers via RT-PCR. Results are presented as fold over control levels (FOC±SEM). N=5-9 mice per treatment group, with all assays performed in triplicate. Significance is denoted as the following, as indicated: compared to PBS or HDM control p<0.05(*), <0.01(**), <0.001(***); compared to CeO_2NP alone p<0.05(•),<0.01(••), <0.001(•••).

(CeO_2HD+HDM RPT) when compared to the particles alone, the HDM control, the repeated low dose (CeO_2LD+HDM RPT) and the single high dose exposure (CeO_2HD+HDM SGL).

Figure 4-11 identifies gene expression changes related to chemotaxis after the various exposure regimes. CCL26, CCl24, CCL17 and IL-25 expression was not changed after exposure to the CeO_2NPs alone at either concentration. CCL26 expression is significantly increased after high dose exposures (both single and repeat - CeO_2HD+HDM SGL and CeO_2HD+HDM RPT) when compared to the low dose equivalent. CeO_2HD+HDM SGL also caused a significant increase in CCL26 expression when compared to HDM control and CeO_2NPS alone. CCL24 expression is also significantly increased after the high dose exposures (CeO_2HD+HDM SGL and CeO_2HD+HDM RPT) when compared to the CeO_2NPs alone. CCL17 expression was significantly increased after exposure to repeated high dose CeO_2 (CeO_2HD+HDM RPT) when compared to the particles alone, the HDM control and the repeated low dose (CeO_2LD+HDM RPT) and the single high dose (CeO_2HD+HDM SGL). IL-25 expression is significantly increased when compared to CeO_2NPs alone after exposure to CeO_2LD+HDM SGL, CeO_2HD+HDM SGL and CeO_2HD+HDM RPT. Expression was also significantly increased after a single low dose (CeO_2LD+HDM SGL) exposure when compared to HDM alone and the repeat exposure (CeO_2HD+HDM RPT). CCL8 (MCP-2 monocyte chemoattractant) expression was significantly increased after exposure to HDM when compared to the PBS control and significantly increased after exposure to any of the CeO_2NPs+HDM regimes when compared to the relevant CeO_2NPs alone. The single dose CeO_2HD+HDM regime significantly subdued the response to HDM alone by approximately 50%, while the CeO_2HD+HDM RPT exposure induced a further significant increase in CCL8 expression over that of HDM alone and when compared to the lower repeated CeO_2+HDM exposure (CeO_2LD+HDM RPT). MCPT1 gene expression increased when exposed to HDM, and was significantly increased (approximately ~4-fold HDM levels) following repeated exposure to high CeO_2+HDM (CeO_2HD+HDM RPT) when compared to particles alone, HDM control, CeO_2HD+HDM SGL and CeO_2LD+HDM RPT. Thus a similar response profile to that seen for CCL8.

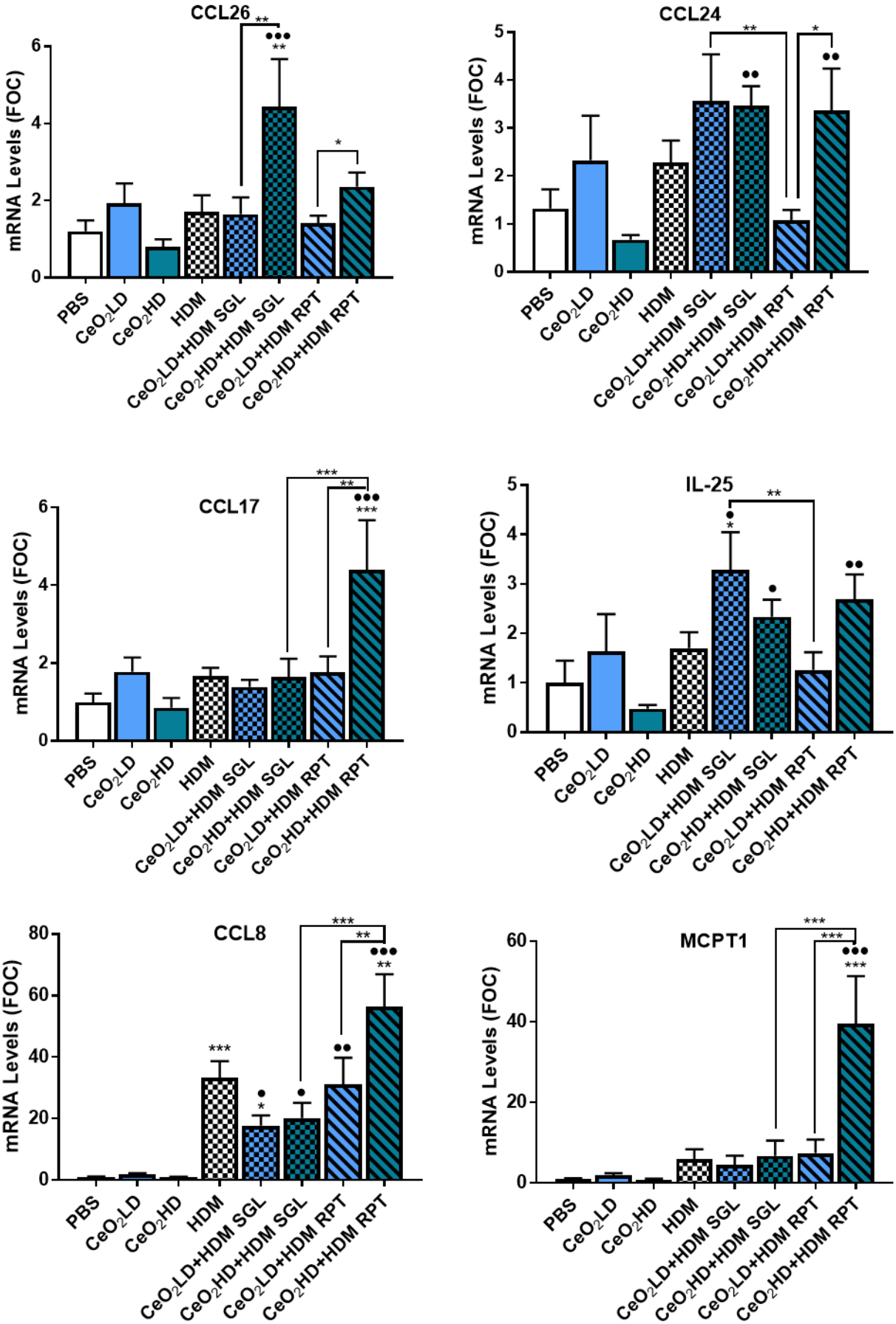


Figure 4-11 Gene expression changes related to induction of immune cell chemotaxis in lung tissue following acute and chronic exposure to CeO_2NPs±HDM for 3 weeks. Total lung mRNA was isolated for indicated inflammatory markers via RT-PCR. Results are presented as fold over control levels (FOC±SEM). N=5-9 mice per treatment group, with all assays performed in triplicate. Significance is denoted as the following, as indicated: compared to PBS or HDM control p<0.05(*), <0.01(**), <0.001(***); compared to CeO_2NP alone p<0.05(•),<0.01(••), <0.001(•••).

4.4.2.5 *Effect of single and repeat exposure to CeO_2NPs±HDM for 3 weeks on inflammatory markers levels in BAL fluid*

Figure 4-12 and Figure 4-13 shows the changes in various inflammatory markers in the BAL fluid after exposures to various CeO_2NPs±HDM regimes for 3 weeks (outlined in Figure 4-1).

Figure 4-12 analyses the concentration of type II markers, pro-inflammatory markers and asthma modulators within the BAL fluid. There was no change in the concentration of TSLP, IL-4, IL-1α and IL-33 after any of the CeO_2NPs exposures. There is however an increase in concentration after co-exposure with HDM when compared to the particles alone. IL-5 concentration was significantly increased after exposure to the high dose particles alone when compared to the low dose. There was also a significant increase in concentration after exposure to CeO_2LD+HDM RPT when compared to the HDM control, particles alone and CeO_2HD+HDM SGL. IL-13 concentration was significantly increased after exposure to HDM alone when compared to the PBS control. Exposure to CeO_2LD+HDM RPT caused a significant decrease to the concentration of IL-13 when compared to the HDM control and the single exposure (CeO_2LD+HDM SGL). The low dose single exposure (CeO_2LD+HDM SGL) concentration was also significantly increased when compared to the particles alone.

Figure 4-13 analyses the concentration of immune cell chemotaxis marker levels in the BAL fluid. There is no change in the concentration of CCL20, CCL11, CCL17 or CCL8 after exposure with the particles alone at either of the concentrations. The low dose exposures +HDM (CeO_2LD+HDM SGL and CeO_2LD+HDM RPT) caused a significant decrease in the concentration of CCL20 when compared to the particles alone, with the CeO_2LD+HDM SGL exposure also significantly decreased compared to the HDM control. CCL11 concentration was significantly decreased after repeat exposure to the high dose (CeO_2HD+HDM RPT) when compared to the repeat low dose (CeO_2LD+HDM RPT). There was a significant increase in CCL17 concentration after repeated exposure to high dose CeO_2+HDM (CeO_2HD+HDM RPT) when compared to HDM and the particles alone. There are also significant decreases in the concentration of CCL11 after exposure to either of the low doses CeO_2+HDM (CeO_2LD+HDM SGL and CeO_2LD+HDM RPT) when compared to particles alone and HDM alone respectively.

HDM alone caused a marked significant increase in BAL CCL8 concentration, which was increased in all the co-exposures +HDM when compared to the particles alone. Interestingly CeO_2LD+HDM SGL, CeO_2HD+HDM SGL and CeO_2LD+HDM RPT significantly subdued CCL8 levels when compared to the HDM control, although CCL8 remained higher than the CeO_2NPs

alone. In contrast repeated exposure to high dose CeO_2+HDM (CeO_2HD+HDM RPT) also stimulated CCL8 and did not subdue the effect of HDM alone.

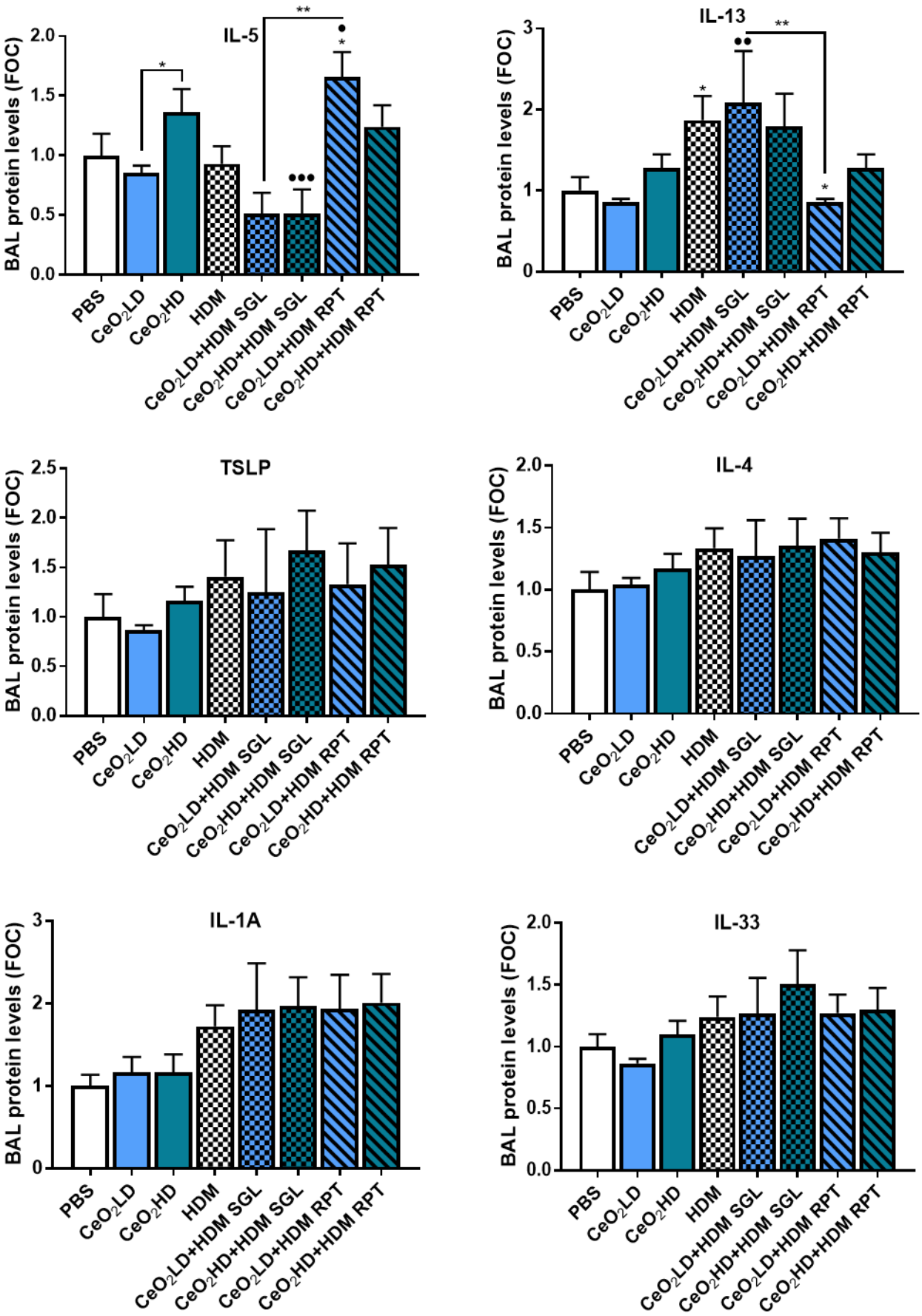


Figure 4-12 Immune type II markers, pro-inflammatory markers and molecules that modulate asthma protein levels in BAL fluid following acute and chronic exposure to CeO_2NPs±HDM for 3 weeks. Lung BAL fluid was analysed for cytokine levels after acute and chronic exposure to CeO_2±HDM for 3 weeks. Results are presented as fold over control levels (FOC±SEM). N=5-9 mice per treatment group, with all assays performed in triplicate. Significance is denoted as the following, as indicated: compared to PBS or HDM control p<0.05(*), <0.01(**); compared to CeO_2NP alone p<0.05(•),<0.01(••), <0.001(•••).

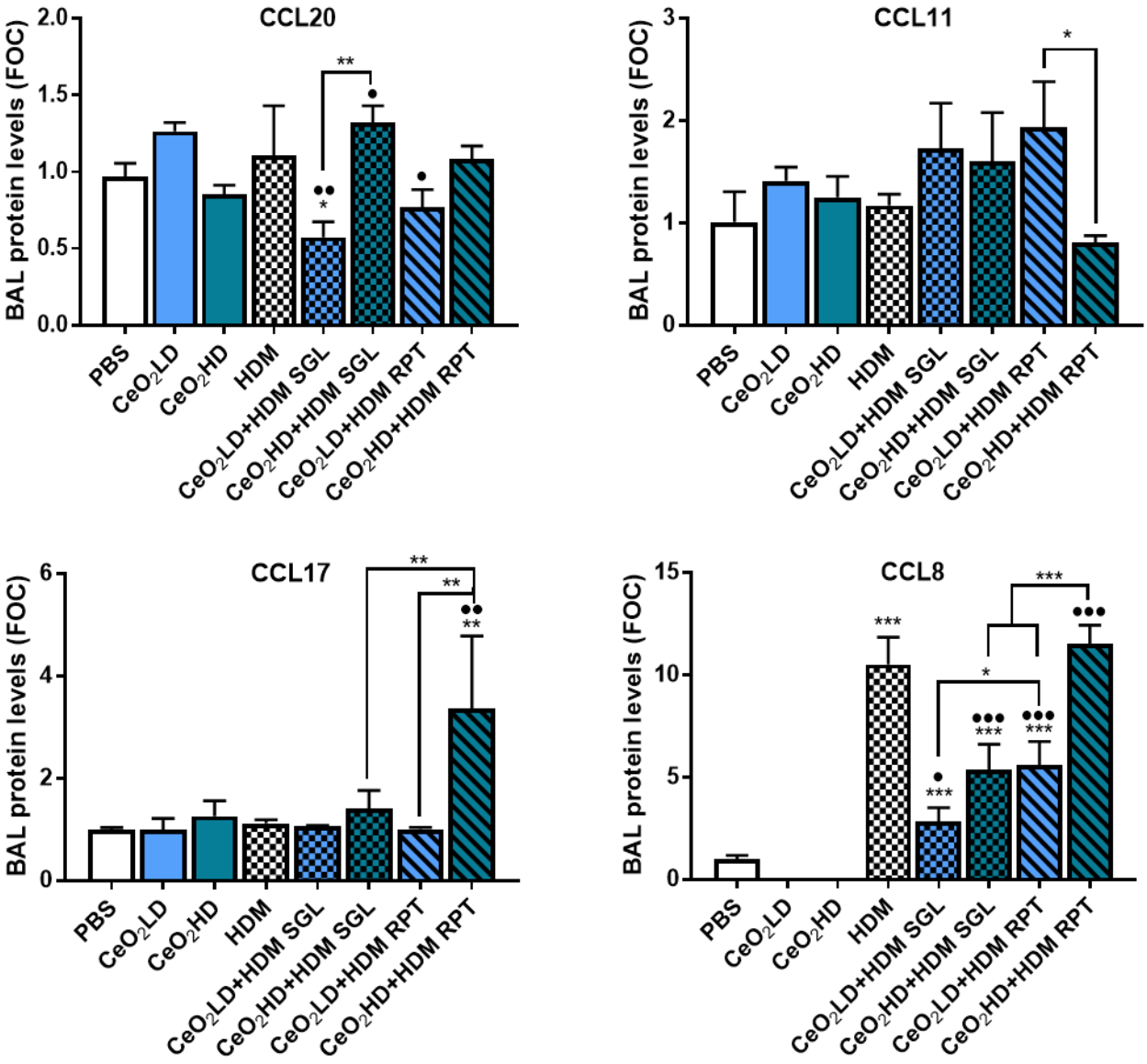


Figure 4-13 Immune cell chemotaxis marker levels in BAL fluid following acute and chronic exposure to CeO_2NPs±HDM for 3 weeks. Lung BAL fluid was analysed for cytokine levels after acute and chronic exposure to CeO_2 ±HDM for 3 weeks. Results are presented as fold over control levels (FOC±SEM). N=5-9 mice per treatment group, with all assays performed in triplicate. Significance is denoted as the following, as indicated: compared to PBS or HDM control p<0.05(*), <0.01(**), <0.001(***); compared to CeO_2NP alone p<0.05(•),<0.01(••), <0.001(•••).

4.4.2.6 Effect of single and repeat CeO_2NPs±HDM for 3 weeks on airway mucin production

Serial sections of lungs were taken and stained with Periodic acid–Schiff (PAS) and CLCA1 (a mucin associated gene) (immunohistochemistry) (Figure 4-14). Sections from animals exposed to the highest CeO_2 doses are represented. Increased PAS stain is indicated by bright pink and CLCA1 is indicated by dark brown staining. It is evident from these sections that there is a heavier staining of both PAS and CLCA1 after exposure to HDM alone, CeO_2HD+HDM SGL and CeO_2HD+HDM RPT when compared to the PBS control. CeO_2NPs alone had little effect. All slides were stained on the same day, using the same kit and protocol, so any difference is not due to differences in the protocol or materials used to stain the sections.

Airway mucin production can be quantified by counting the PAS+ cells within the airways, scored and then graphed (Figure 4-15, A). This indicates CeO_2NPs alone had no effect on the production of mucus. There was a significant increase in the PAS stained cells after to exposure to all the CeO_2NP+HDM regimes (CeO_2LD+HDM SGL (microscopy not shown), CeO_2HD+HDM SGL and CeO_2HD+HDM RPT) when compared to the particles alone and CeO_2HD+HDM RPT when compared to the HDM control.

CLCA1, SLC26A4 and MUC5AC expression was measured as these are genes that are related to mucus production within the airways and their expression in lung tissue after exposures was measured (Figure 4-15, B, C, and D respectively). CeO_2NPs had no effect alone on any of these genes analysed. HDM alone caused a significantly increased expression of all genes over non-HDM treated groups, which was further significantly increased following exposure to CeO_2HD+HDM RPT, although the other CeO_2 exposures had no significant additional effects on that of the HDM alone.

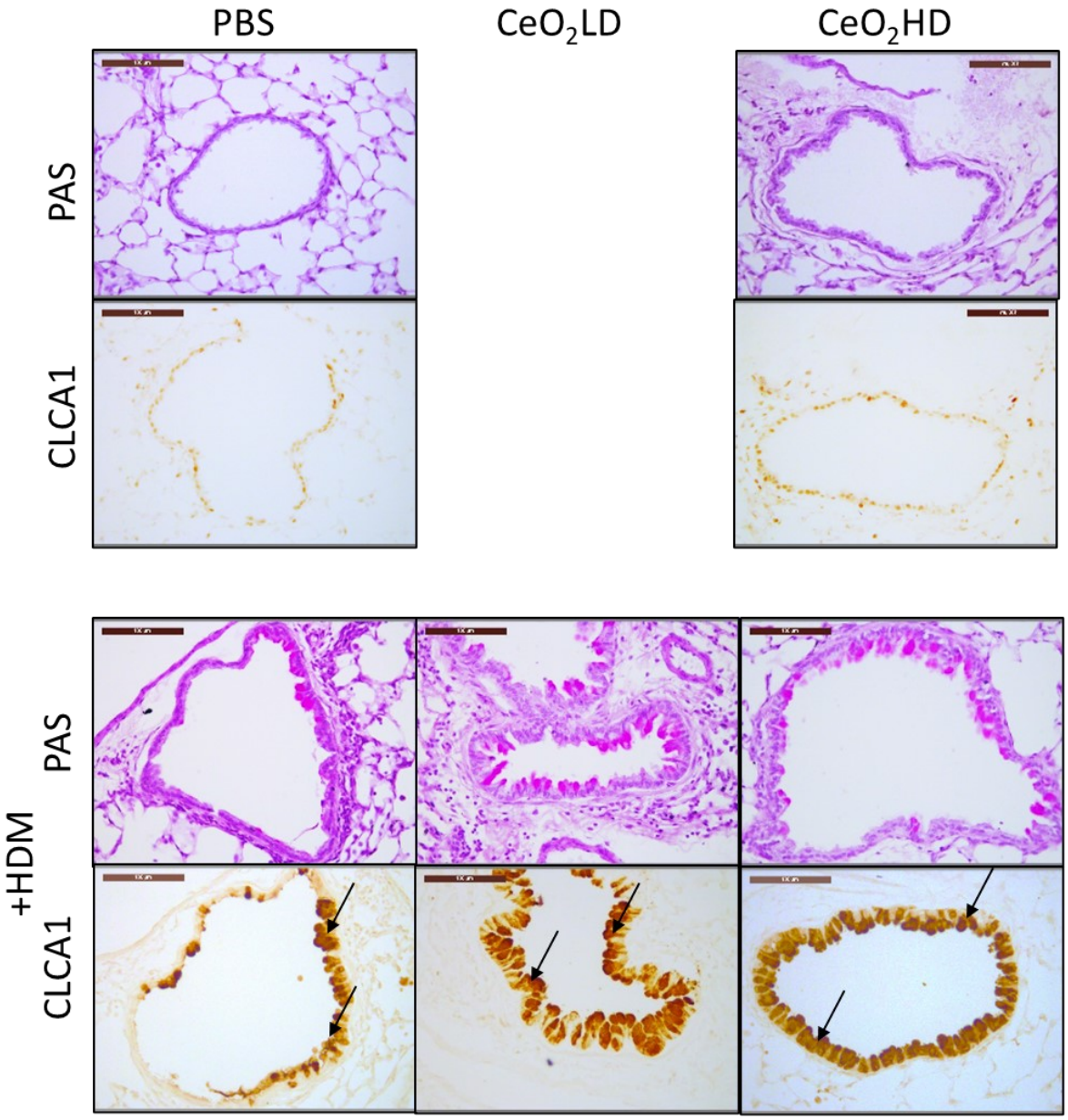


Figure 4-14 Analysis of airway secretion-related molecules following acute and chronic exposure to CeO_2NPs±HDM for 3 weeks. Lung tissue was fixed, and sections processed for PAS staining (top panel) and immunohistochemical staining of CLCA1 (bottom panel). Representative images of each group are displayed with a scale bar of 100µm (top left of image). Quantification of PAS positive cells within the airways was scored and graphed (Figure 4-15 A). Arrows indicate positive stained cells.

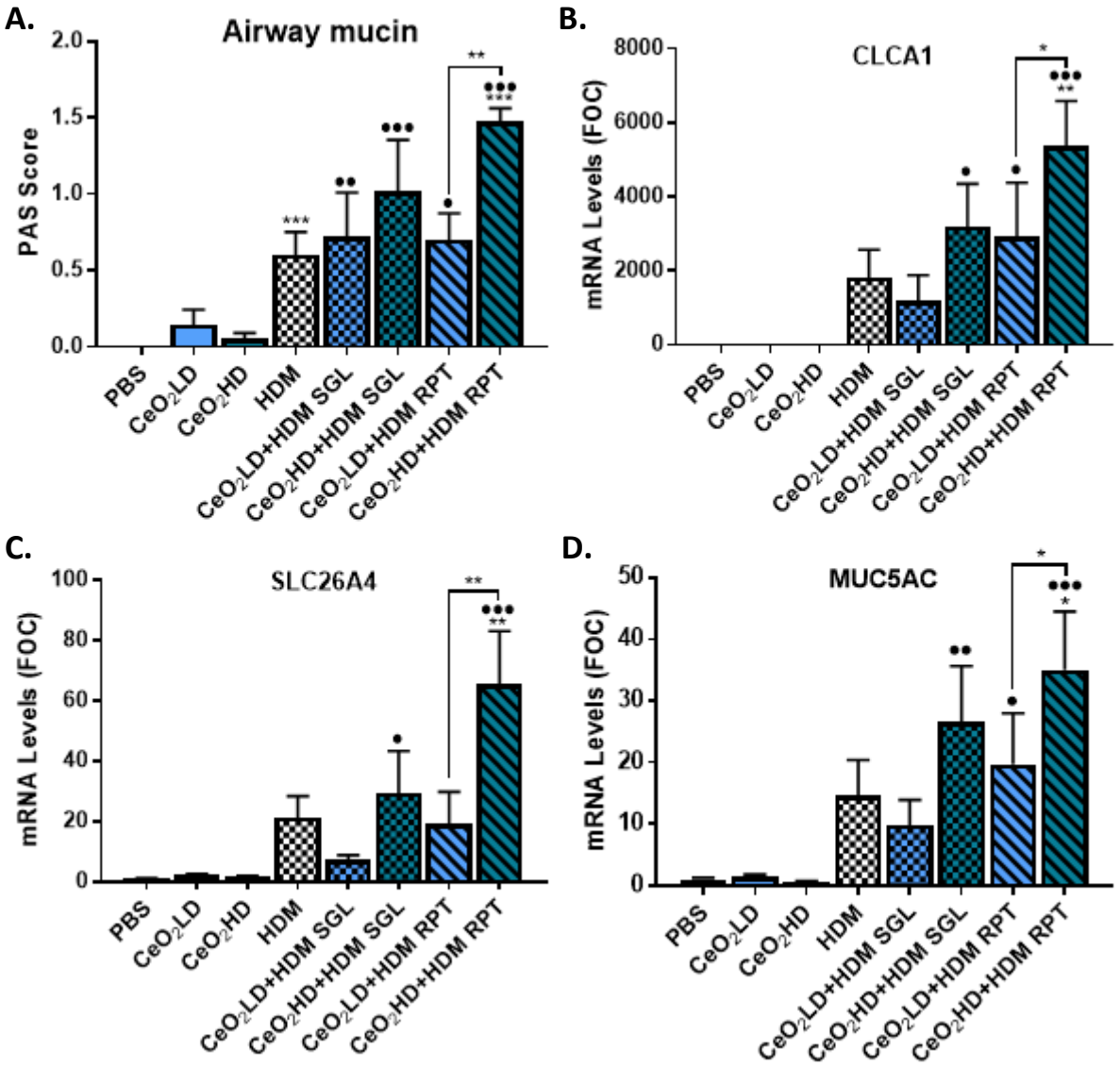


Figure 4-15. Analysis of airway secretion-related molecules following acute and chronic exposure to CeO_2NPs±HDM for 3 weeks. A. Quantification of PAS positive cells within the airways was scored and graphed. B-D. Lung mRNA was isolated and analysed by RT-PCR for expression of mucus related genes. Results are presented as fold over control levels (FOC±SEM). N=5-9 mice per treatment group, with all assays performed in triplicate. Significance is denoted as the following, as indicated: compared to PBS or HDM control $p<0.05$(*), <0.01(**), <0.001(***); compared to CeO_2NP alone $p<0.05$(•),<0.01(••), <0.001(•••).

4.4.2.7 *Effect of acute and chronic exposure to CeO_2NPs±HDM on structure, remodelling and function of the lung*

Serial lung sections were stained with Masson's trichrome (M.T.), for smooth muscle cell actin (-sma) and PCNA (Figure 4-16) after exposures in order to determine if there was any airway remodelling related to the exposure regime. M.T stains collagen blue, -sma immunostains shows brown for smooth muscle cell actin and can indicate increased smooth muscle in the airways, and PCNA stains replicating. If all three stains combined increase, this can indicate potential physiological responses commonly seen in asthma patients. Thus, the images indicate that all three underwent a similar pattern of change after exposure and were seen to increase in the groups that received HDM alone and CeO_2NPs+HDM exposures.

As airway hyperresponsiveness is a feature of allergic airway disease and asthma, airway hyperresponsiveness was also examined. The mice underwent a challenge with methacholine to determine the responsiveness of the airways following HDM and CeO_2 exposures as previously described in section 2.8. The PBS, CeO_2HD alone, HDM and CeO_2HD+HDM RPT groups were analysed. There was a significant increase on challenge with 100mg/ml methacholine in the respiratory system resistance (Rrs) (Figure 4-17, A), and elastance (Ers) (Figure 4-17, D) after exposure to HDM alone (over PBS and CeO_2NP alone groups), which increased further for Rrs and Ers in the CeO_2HD+HDM RPT group. The increase seen in the HDM alone groups is ameliorated by the addition of CeO_2NPs (CeO_2HD+HDM RPT group), but not significantly. There was no change in the tissue elastance (H) (Figure 4-17, C) after any of the exposure regimes.

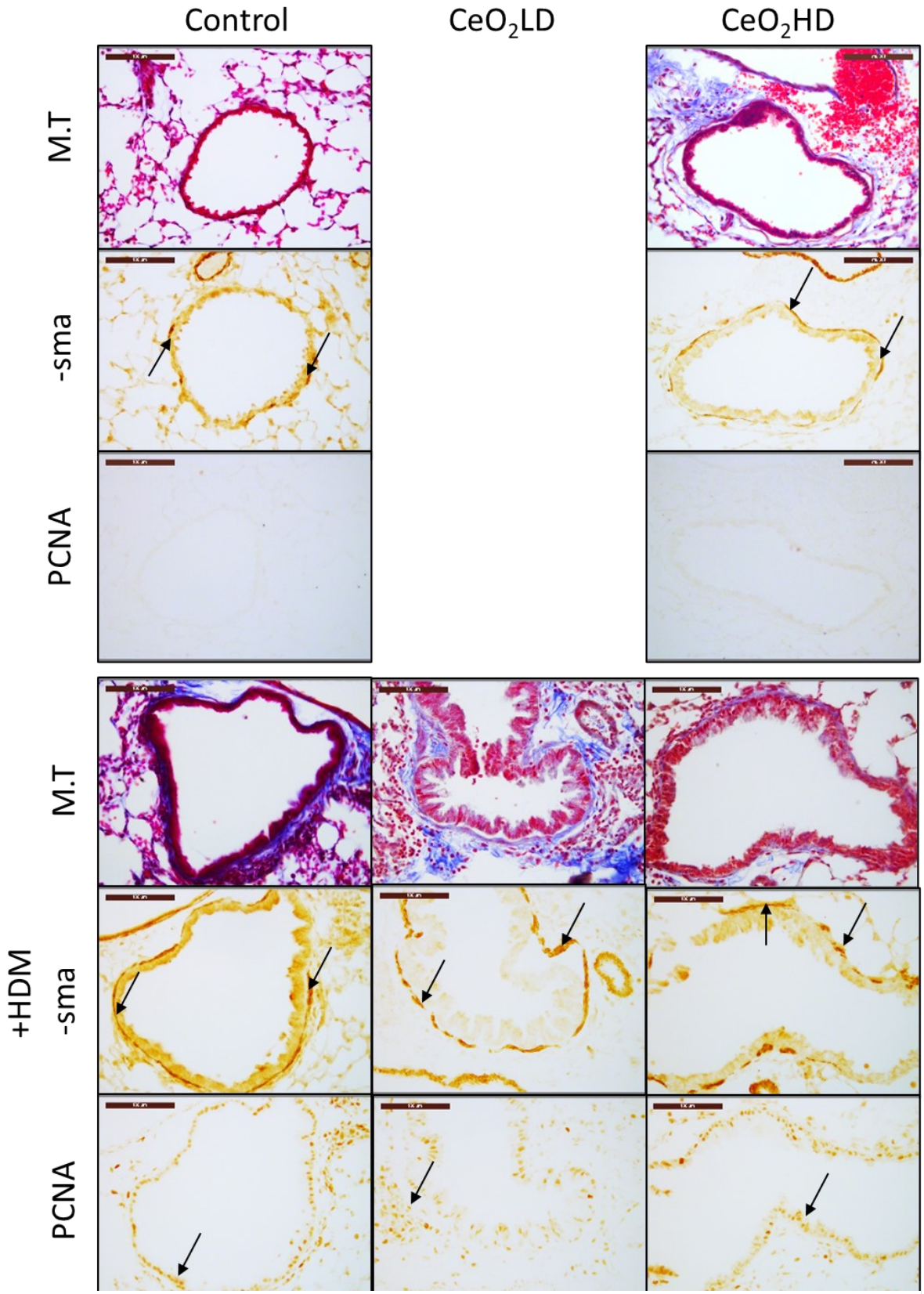


Figure 4-16 Airway structure and remodelling after acute and chronic exposure to CeO_2NPs±HDM for 3 weeks. Lung tissue was fixed, and sections processed for M.T staining (top panel) and immunohistochemical staining of α-smooth muscle cell actin (α-sma) (middle panel) and proliferating cell nuclear antigen (PCNA) (bottom panel). Representative images of each group are displayed with a scale bar of 100µm (top left of image). Arrows indicate positive cell staining.

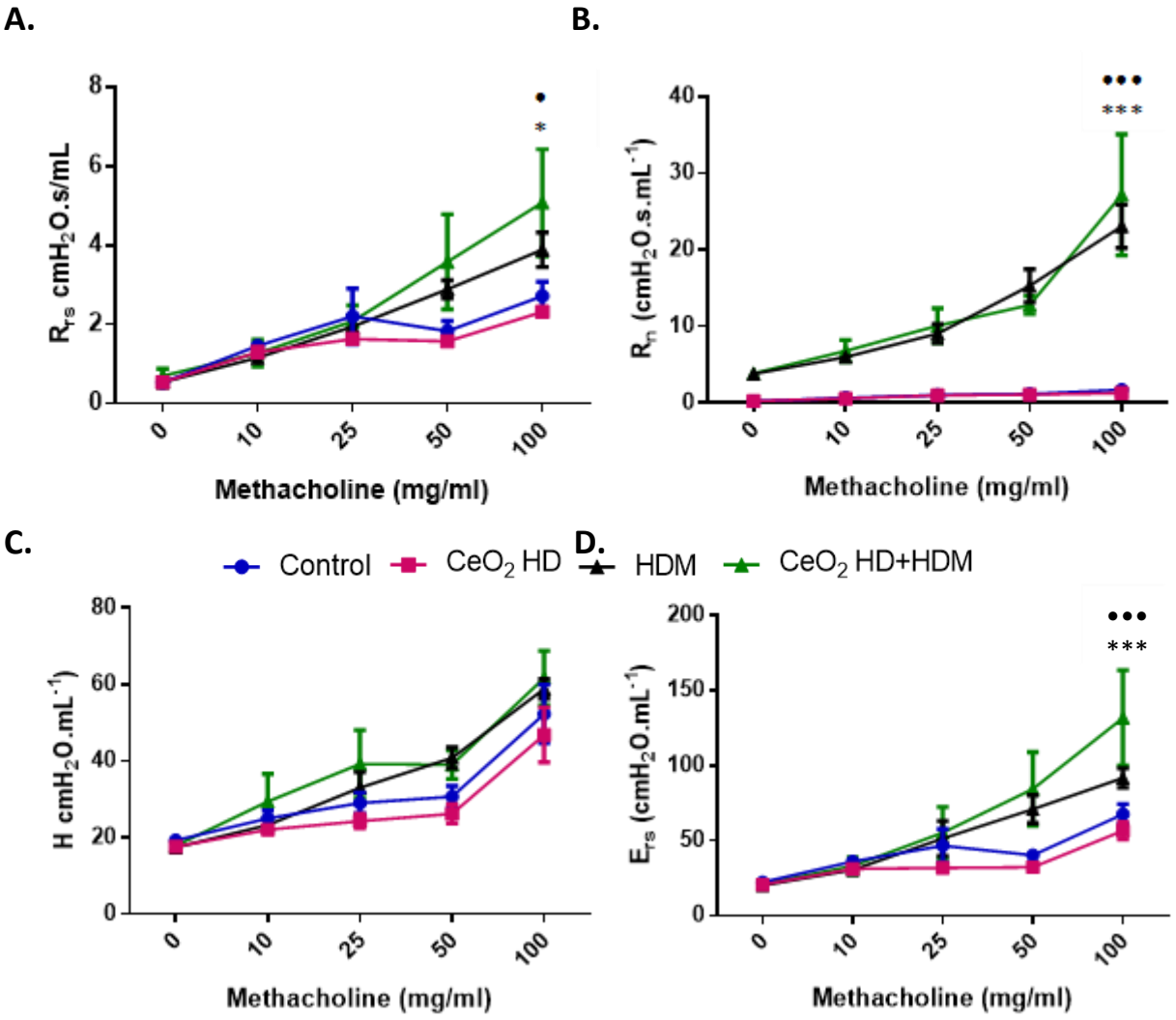


Figure 4-17. Lung function analysis after acute and chronic exposure to CeO_2NPs±HDM for 3 weeks.
Airway hyperresponsiveness to increasing concentrations of inhaled aerosolised methacholine, was assessed using a forced oscillation technique (**section 2.8**). A. Respiratory system resistance (Rrs), B. Newtonian resistance (R_n), C. tissue elastance (H) and D. elastance (E_{rs}) were calculated using flexivent system sotware. Results are presented as mean ±SEM. N=5-9 mice per treatment group, with all assays performed in triplicate. Significance is denoted as the following, as indicated: compared to PBS or HDM control p<0.05(*), <0.01(**), <0.001(***); compared to CeO_2NP alone p<0.05(•),<0.01(••), <0.001(•••).

4.5 Discussion

There is currently no published work on the effects of co-exposures to CeO_2NPs±HDM either acutely or chronically. Thus, to our knowledge, this is the first study of the putative additive and synergistic effects of HDM and CeO_2 in the lung.

The aim of these studies was to establish the potential effects the instillation of CeO_2±HDM had on a murine lung. From the results shown in **Section 4.4**, it is clear that the addition of CeO_2NPs+HDM causes a decrease in the clearance of cerium oxide from the lung when compared to the animals only exposed to CeO_2NPs. 24 hours after exposure there was an increase in the percentage of neutrophils counted in the BAA fluid and an increase in TSLP mRNA after exposure with both CeO_2NPs+HDM when compared to the particles alone. After 3 weeks there was a significant increase in the percentage of eosinophils, lymphocytes and neutrophils in the co-exposed groups compared to the particles alone. In the high dose co-exposure group (CeO_2HD+HDM) there was a significant increase in MCPT1, CCL8, and MMP12 mRNA, plasma IgE, BAL CCL8 and IL-1α. There was also a significant increase in the mucin markers measured after the repeated co-exposure when compared to the other exposure groups. This suggests that the addition of CeO_2NPs to the HDM allergic model enhances the effects that are observed in the HDM model. This includes the enhancement of the Th2 phenotype, as well as asthmatic markers (such as the increase in mucus production and an increase in airway hyperresponsiveness).

4.5.1 Effect of acute, 24 hour exposure to CeO_2NPs in normal and allergic lungs

There is limited literature on the acute (24 hour) effects of CeO_2NPs alone on the lung in either human or rodents. The majority of the literature focuses on the intratracheal instillation of CeO_2NPs, with a few aerosolisation studies, but none use intranasal aspiration. We used intranasal aspiration as it will target the whole airway via aspiration of the material from the back of the throat. The use of 25µl is also important as this volume has been identified in localising material to the conducting airways and not the alveolar region (as identified by the laser ablation and ICP-MS (Figure 4-2 and Figure 4-6), which play a bigger role in the development and exacerbation of asthma).

Our study shows that co-exposure to a single dose of HDM alone and HDM co-exposed with CeO_2NPs for 24 hours caused a significant decrease in the proportion of macrophages and a significant increase in the percentage of neutrophils, which was most marked in the co-exposure

group (Figure 4.4). As this increase was not seen after exposure to high or low dose CeO_2NPs without HDM, this effect appears to be dependent on the presence of HDM.

In a previous study in rats, 24 hour exposure to intratracheal cerium alone (150cm²/rat) caused a significant increase in the total cell number and an increase in the neutrophil count within the BAL, which was mostly due to an increase in PMN numbers (Cho et al., 2010). It is not clear why there is a difference in the inflammatory cell responses after 24 hour CeO_2NPs exposure in the present study compared to that of Cho *et al*. It may reflect different exposure methods (aspiration rather than intratracheal instillation). Supporting the hypothesis of exposure methods being implemented in the differences is a previous study by Nemmar *et al*. In the Nemmar study, Balb/c mice were intratracheally instilled with either 0.1 or 0.5mg/kg (concentrations within the same region of out exposures of 75µg/kg and 750µg/kg CeO_2NPs) of CeO_2NPs alone. 24 hours post-exposure there was a significant increase in the macrophage and neutrophil cell when compared to the PBS control (Nemmar et al., 2017a). Other studies of rats exposed to aerosolised CeO_2NPs alone have, like Cho *et al*., found increases in BAL cell count 24 hours after exposure, including higher BAL lymphocyte and neutrophil cell counts when compared to the control group (Srinivas et al., 2011), even at lower intratracheal CeO_2NPs concentrations of 40µg/kg of ceria (Xue et al., 2013). As this exposure is lower than that used in our study (the lowest concentration investigated in the present study was 75µg/kg) and is still causing increases in cell counts that are not seen 24 hours after our exposure, this would suggest that it is not a difference in species that may cause these changes in cell counts in the BAL fluid, but it may be the exposure method implemented in these various studies. Neither the work of Cho *et al*, nor the present study, led to an increase in the eosinophil cell count in the BAL fluid, even after 4 weeks (Cho et al., 2010).

In the present study, mice were culled 24 hours after exposure to evaluate the effect of an acute exposure to CeO_2NPs; consequently, we do not know any potential longer-term responses of these exposures if the mice had been allowed to recover longer before analysis. In other studies, recovery time does have impact on the responses seen. For example, after exposure to 35mg/kg (a higher concentration than in our study) there was found to be a significant increase in neutrophil cell counts 24 hours after exposure, but also as late as 100 days post-exposure (Toya et al., 2010). With a decrease in concentration to 0.5mg/ml (still higher than our study), there is an initial decrease in macrophage numbers, but there is recovery back to baseline levels after 10 days. This is not true for neutrophils, which are significantly increased 24 hours post exposure and after 10 days of recovery (Ma et al., 2011). 3 days after instillation with rats there was again a

significant increase in lymphocytes and neutrophils (Srinivas et al., 2011). This suggests that any increases in neutrophil cell counts apparent in the exposures of CeO_2NP will have a lasting effect and cause potential responses as late as 100 days post exposure. Regardless of exposure or recovery time or dose concentration, there were no changes in the eosinophil cell counts.

There is currently no published literature that examines the potential effect recovery may have on CeO_2NP+HDM exposures, however, if the effects of CeO_2NP alone is long lived it could be assumed that CeO_2NP+HDM would also have this legacy due to the increased retention of CeO_2NP found in the lung when co-exposed with HDM and therefore continuous activation of these immune cells. Recovery effects of exposure of HDM are also important and would also have to be established.

A number of cytokines were analysed in the BAL fluid after exposure to CeO_2NPs±HDM for 24 hours (Figure 4-5). There were only significant increases in the concentrations of CCL20 and TSLP after exposure to CeO_2HD+HDM when compared to CeO_2LD+HDM and CeO_2LD+HDM, CeO_2LD alone and the HDM control respectively (Figure 4-5). CCL20 and TSLP are both released by epithelial cells and are connections between the innate and adaptive immune response (CCL20 is a dendritic cell chemoattractant, while TSLP regulates dendritic cell tolerance and T cell activation (Liu et al., 2007)). There were no changes in the concentrations of IL-1α, IL-5, IL-4, and IL-33 24 hours after any of the exposures. These cytokines are implemented in the type II immune response and therefore would not be expected to be elevated after 24 hours. This could begin to explain the limited increase in the percentage of eosinophils counted in the BAL fluid. The increase in CCL20 could indicate the activation of the innate immune response within the 24 hour period with the initiation of dendritic cell chemoattractants.

There are a wide variety of cytokines that could have been investigated within our study but were not included for a variety of reasons, these include a focus on the cytokines related to asthma and allergic airways. Other more generic cytokines that were not measured in the current work were found to be significantly increased after an intratracheal instillation of 500μg/kg (an intermediate exposure dose when compared to our study) including TNF-α, IL-6 and IL-1β in the mouse lung tissue (Nemmar et al., 2017b). Similarly, after exposure to a higher intratracheal concentration of CeO_2NPs (1mg/ml), there was no change in BAL fluid concentration of TNF-α, IL-6, and IL-1β 24 hours post exposure (Dunnick et al., 2016). However, in the study by Cho *et al.*, using the same delivery system, but a higher dose concentration, there were no significant changes in TNF-α, IL-13 or IFN-γ in the rat BAL fluid, but a significant

increase in IL-1β and MIP-2 concentrations (Cho et al., 2010). This indicates that it is the dose that can cause the potential differences in the results. As all 3 studies use the same method of installation it can be assumed that the same proportion of particles are being exhaled and deposited in each study. Whereas, in rat aerosol studies of CeO_2NPs (641mg/m^3) after 4 hours there was a significant increase in IL-1β, TNF-α, and IL-6 measured in the BAL fluid (Srinivas et al., 2011) in one study, but no change in CL20, IL-1α, and IL-1β (Schwotzer et al., 2018) in another at a lower concentration (3mg/m^3). These differences could be down to the differences in dose concentration – as the lower exposure dose does not cause the same significant changes the higher exposure does.

In the present study there were no structural changes (analysed via histology staining with H/E, PAS and M.T. (Figure 4-3)) noted in the airways 24 hours after any of the exposures. This was thought to be due to the fact that 24 hours is not enough time for pathological changes to be seen, and has been shown previously (Xue et al., 2013). From laser ablation images (Figure 4-2) it is apparent where in the airways the CeO_2NPs are deposited (in the larger airways, as would be expected with particles of this size) and how much of it remains within the lungs after exposure with and without HDM (the CeO_2HD+HDM has a significantly increased retention of the particles compared to CeO_2NPs alone (~4-fold increase)). It is important to remember lung clearance mechanisms which will also be playing a role in the retention of these particles within the lung. These include macrophage phagocytosis, and mucuciliary clearance. Translocation of the particles from the lungs can also occur and it has been identified that there is the potential for particles to cross the gas-blood barrier and reach other organs via the vascular system (Kreyling and Scheuch, 2000, Kreyling et al., 2014). This and potential translocation of the particles has not been further analysed within this study, but it is important to keep it in mind going forward.

Mast cell infiltration of the airways was not measured in the current study after 24 hours exposure as it was assumed that there would be none and, in fact MCPT1 concentration was not changed in the lung tissue (data not shown). In previous mast cell work using knock-out mice (B6.Cg-*Kit*$^{W\text{-}sh}$ mice) there was no increase in BAL macrophage, lymphocyte or neutrophil cell counts in the WT mice after instillation of CeO_2NP (10μg/ml). These data suggest that mast cells may play an important role in the bioreactivity of CeO_2NP (Wingard et al., 2011). As there was a significant increase in the number of neutrophils counted in the BAL fluid in our study, there is the potential that there is an increase in the mast cells that cannot be established with just the

concentration of MCPT1 being analysed alone and therefore perhaps infiltration should be established in future studies.

4.5.2 Effect of acute and chronic exposure to CeO_2NPs with or without 3 week HDM treatment

After 3 weeks of exposure to CeO_2NP±HDM at both a low and a high dose there was a significant decrease in the macrophage cell counts after the CeO_2NP+HDM, single and repeat exposures (Figure 4-7). Previously, after 2 weeks and 4 weeks of inhalation there was found to be a significant decrease in macrophage proportion, although actual numbers of macrophages increase after exposure to CeO_2NPs alone when compared to the control (Srinivas et al., 2011(Gosens et al., 2014). This is reflected in the significant increase in neutrophil influx (Figure 4-7). For a long term 4 week inhalation exposure (Cho et al., 2010), there was a significant change in the cell count in the BAL fluid after exposure to CeO_2NPs when compared to the control, as well as an increase in the neutrophil count (not significant), but there was no change in the lymphocyte or eosinophil cell counts when compared to the control.

Here, there were no significant changes in the lymphocyte cell counts in the BAL fluid in the absence of HDM treatment, but there was an increase after HDM and co-exposure of CeO_2NPs, although there were no significant differences in the number of elevated lymphocytes between any of the HDM±CeO_2 exposures. Our study looked at effects 24 hours after the last exposure and therefore did not give the animals any time to recover. In the Cho *et al.,* study, four weeks after instillation of a similar concentration of CeO_2NPs alone there was a significant increase in the BAL neutrophil and lymphocyte counts when compared to the control (Cho et al., 2010). However, after inhalation of CeO_2 for two and four weeks (Srinivas et al., 2011), there was no change in lymphocytes when compared to control (as also seen in our study) and a significant increase in neutrophil counts (Srinivas et al., 2011), but only in the males.

In the present study, as mentioned above, there was a significant increase in the number of neutrophils in all the HDM exposed groups, these were significantly increased in the higher CeO_2 exposure groups and HDM alone (Figure 4-7). Neutrophils are involved in the degranulation of goblet cells in asthma patients, and therefore, contribute to airway remodelling (Ahn et al., 2007). The increased BAL neutrophil proportions were accompanied by a significant increase in the lung tissue CD177 mRNA expression (Figure 4-10) (CD177 is expressed by a proportion of neutrophils that plays a role in migration and activation (Bai et al., 2017)) after exposure to CeO_2HD+HDM SGL and CeO_2HD+HDM RPT when compared to HDM and CeO_2

alone, but not at the low cerium oxide dose exposures. CD177 has been implicated in many inflammatory disorders and there is thought to be cross talk between endothelial cells and neutrophils via CD177 (Sachs et al., 2007). It regulates chemotaxis of neutrophils in inflammatory disorders, including asthma, which can develop into a neutrophil phenotype (See introduction, (Wang and Nigrovic, 2013)). CD177 positive neutrophils have also been implicated in the production of IL-17 (Ramirez-Velazquez et al., 2013), which here was found to be significantly increased in CeO_2HD+HDM RPT when compared to the HDM alone (Figure 4-8). HDM exposures significantly increased the IL-17 concentrations. This would suggest that the increase in neutrophil surface markers increased the neutrophil cell count, and also potentially influenced the mRNA expression of IL-17.

Eosinophils are important in the allergic response within the lungs but lung dysfunction can happen without eosinophils, but evidence suggests that they enhance the phenotype, with a worse response than if they were not there (Sivapalan et al., 2014). There are numerous ways of identifying the role of eosinophils during HDM sensitisation, including the use of eosinophil knockout mice (iPHIL mice cannot form mature eosinophils due to the precursors dying before they reach maturity). When these mice were sensitised with HDM, there was a neutrophil led response instead of the eosinophil response seen in our model (Jacobsen et al., 2014).In our study, there was a significant increase in the eosinophil cell count after exposure to CeO_2HD+HDM RPT when compared to particles alone (indicating that the co-exposure to HDM was important to increase the eosinophil count), HDM alone, CeO_2LD+HDM RPT and CeO_2HD+HDM SGL. This suggests that it is the high dose of CeO_2 repeated with HDM that causes the effects seen. However, in a longer term inhalation exposure study (5 days/week for 4 weeks) to 25mg/m^3 CeO_2NPs, there was no change in the eosinophil cell counts in the BAL fluid (Keller et al., 2014), possibly reflecting differences in the amount of CeO_2 deposited within the lungs, or simply due to differences in time scale.

Mast cells and eosinophils form an allergic effector unit and influence chronic (long-term) inflammation stages (Minai-Fleminger and Levi-Schaffer, 2009). It can then be assumed that if an exposure to CeO_2HD+HDM causes increases in both mast cells and eosinophils, there will be an increase in the immune response and the severity of the inflammatory response when compared to either the particles alone or HDM exposures alone. This is due to the releases of histamine from the mast cells and the inflammatory response from the eosinophils is thought to contribute to airway remodelling. This would indicate a severer response to the particle and the allergen when compare to either alone.

CCL8 (or monocyte chemoattractant protein-3 (MCP-3)) is a strong eosinophil chemoattractant and its expression has been found to be increased in asthmatic patients. It is suggested that there is a link between increases in CCL8 mRNA expression and BAL fluid protein concentration and asthma (Humbert et al., 1997). In our study there was a significant increase in the mRNA expression and BAL fluid protein concentration of CCL8 after exposure to HDM, which is significantly further increased after exposure to CeO_2HD+HDM RPT (Figure 4-11 and Figure 4-13). However, after exposure to the low dose CeO2 and the single high dose CeO_2 regimes, there was significantly reduced tissue mRNA expression and BAL fluid protein concentration (when compared to the particles alone, and HDM and CeO_2HD+HDM RPT exposures respectively), though it was never as low as without HDM sensitisation. This would suggest that a single or low dose exposure to CeO_2NPs reduces the potency of the HDM on the expression of CCL8 and that different mechanisms exist in the effects of CeO_2 on CCL8 induction by HDM. The addition of the low concentration particles dampens the initial response seen with HDM exposure alone, and it is only at the highest repeated exposure that causes a significant increase in CCL8 tissue mRNA expression and BAL fluid concentration, but also a significant increase in the proportion of eosinophils in the BAL fluid. The concentrations of CCL8 could be significantly lower after exposure to the lower particle concentrations due to the increase in the proportion of macrophages and therefore increased clearance of the particles. This would reduce the concentration of particles within the lungs and therefore contribute to the reduced CCL8 expression and concentration.

After exposure to HDM alone to develop this asthmatic model there was no change in the IgE concentration in the blood plasma in our study (Figure 4-7), but in other studies (Ahn et al., 2007), there was a signifiant increase when compared to control. Ahn *et al.,* used the same concentration of HDM in their protocol, however the protocol was 1 week longer than the one used in this study. This could potentially indicate that this additional week influences the concentration of IgE produced by HDM alone. Nevertheless, in this study there was a signifiant increase in IgE after exposure to CeO_2HD+HDM RPT when compared to CeO_2LD+HDM RPT, CeO_2HD+HDM SGL and the HDM control. Thus, repeated co-exposure to high concentrations of CeO_2 was likely important to induce an increase in IgE levels, mast cell activation (a significant increase in the expression of MCPT1 mRNA was found in the lung tissue (Figure 4-7)) and translocation to the airways (identified in tissue sections after TB staining (Figure 4-7), but as this has not been quantified, it is difficult to determine any differences between the exposures) when compared to the HDM alone exposures. Increases in IgE also leads to binding by mast cells, eosinophils and basophils enhancing the Th2 response, this is because all three

cell types express FcεRI receptors (but eosinophils only express this after activation) (Medzhitov and Janeway, 1997). Once IgE has started being produced, the immune system is then primed to drive a Th2 immune response, which then causes IgE class switching in BA cells and a further production of IgE (Medzhitov and Janeway, 1997).

In our study there is a significant increase in in IL-4, IL-13, IL-10, IFN-γ and TGF-β when compared to the control alone (Figure 4-8). In our study, we did not see any of these increases in the HDM exposures when compared to the PBS control, or in any of the groups exposed to CeO_2NPs+HDM. There was a slight increase in IL-4 concentration in some of the +HDM groups, but none of them were significantly increased. IL-13 was increased after HDM exposure and the CeO_2LD+HDM SGL exposure and the HDM control but was decreased in the RPT exposures when compared to the control. This would suggest, that even though there is an enhanced IgE and allergic response, this is not quite a Th2 response, as there are also no changes in the concentration of IL-5 in the BAL fluid (Figure 4-12). In a study by Dunnick *et al.*, the mice were left to recover for 4 weeks after an instillation to CeO_2. This led to no changes in the concentration of IL-1β, IL-13, or IFN-γ or of TNF-α, IL-6, and IL-1β after analysis of BAL fluid, but there was a significant increases in the concentration of MIP-2 (Dunnick et al., 2016). After 24 hours of recovery, we saw a significant increase in the expression of MMP12 after exposure to CeO_2HD+HDM when compared to the particle alone exposure.

Aerosol exposure to CeO_2 for 4 hours over 4 weeks enhances the IL-1β, TNF-α, and IL-6 (Srinivas et al., 2011), this exposure did not lead to an increase in CCL17 or CCL22 expression (Schwotzer et al., 2018). In our study we found an increase in CCL17 expression after exposure to CeO_2HD+HDM RPT (not a significant increase) when compared to the other exposure groups. Indicating that it is a potential Th2 response that it is produced when co-exposing with HDM+CeO_2NPs when compared to CeO_2NPs alone.

There was no change in the levels of TSLP in the BAL fluid after any of the exposures (Figure 4-12). This is interesting as TSLP is known to contribute to the remodelling of the airways (Cheng et al., 2018) and reduced lung function in asthmatic patients. It activates dendritic cells (via TSLP-TSLPR and OX40L-OX40) and promotes Th2 signalling processes. Neutralisation of TSLP (via anti-TSLP antibody) has been found to reverse airway inflammation, halted alterations of the airway structure and decreased AHR (Chen et al., 2013b). Allergies to HDM have been found to develop independently to TSLP, so a different inflammatory and allergic pathway could be being implemented after these exposures (Chu et al., 2013). Due to the fact

there is no change in the TSLP concentration would add evidence to the lack of a complete Th2 response after exposure to any of our groups.

IL-33 leads to the induction of T cells, eosinophils, mast cells and basophils and is required to induce antibody production, specifically IgE production, (Canbaz et al., 2015) but there are no changes in the concentration of IL-33 measured in the BAL fluid or the gene expression after any of the exposures in our study (Figure 4-12 and Figure 4-10). This could potentially be down to the fact that it was measured 24 hours after the final exposure and may have already been removed from the BAL fluid. Vaccination against IL-33 inhibited HDM-induced AHR and the increase in eosinophils and total cell count. There was also a reduced IL-17A, IL-25, IL-33 and TSLP concentration in the lung homogenates, this suggests an important role for IL-33 in these models (Lei et al., 2015).

There was no change in the IL-25 mRNA expression after any of the exposures (Figure 4-11). Blocking IL-25 has been found to reduce IL-5 and IL-13 concentration and inhibit the production of IL-33 and TSLP in the lungs (Gregory et al., 2013). IL-13 has the potential to increase SLC26A4 and MUC5AC and therefore the production of IL-13 has the potential to influence mucin production (Lee et al., 2015).

When investigating the potential for the Th2 response to not be fully activated it is important to analyse the activation of cells and if this is working correctly. TLR4 is required for Th2 responses. TLR4 is negatively regulated by Toll-interleukin-1 receptor (TIR)-8 that is expressed by epithelial cells. Without this receptor the Th2 cytokine profile (IL-4, 5, 13 and IL-33), mucus production, eosinophils and AHR was found to be significantly reduced when compared to the control when exposed to allergens (Barry et al., 2013). TLR4 induces the release of IL-1a which then goes on to trigger the release of GM-CSF and IL-33 which in turn attract dendritic cells into the area. There was a significant increase in IL-1α mRNA expression levels after exposure to high dose CeO_2 (both single and repeat exposures) when compared to the particles alone (Figure 4-9). TSLP becomes important at high concentrations of HDM and this suggests that IL-1α is upstream in the cytokine cascade and potentially leads to the activation of both epithelial cells and dendritic cells (Willart et al., 2012).

Airway hyperresponsiveness (AHR) is an important measurement in human asthma diagnosis and prognosis and can be induced by methlycholine in both mice and humans. In our study, investigating AHR there were significant changes in the R_{rs}, E_{rs} and R_n when comparing the CeO_2HD+HDM to the particles alone (Figure 4-17). This was not reflected in the tissue elastance

(H) measurements. AHR has been found to remain the same regardless of the eosinophils, which suggests that the eosinophils are not responsible for the development of AHR (Jacobsen et al., 2014). NF-κB activation may contribute towards airway remodelling, AHR and eventually fibrosis (Tully et al., 2013). This pathway is activated by TNF-α (not measured in this study), IL-1 cytokines (there is an increase in the BAL fluid concentration after exposure to all the groups with HDM), and CD40 ligand (Lawrence, 2009) (as demonstrated by the IgE levels increasing and therefore B cell maturation initiated by binding of the CD40 ligand on the surface of the B cell).

HDM in our study also significantly increased these AHR markers. In another study (Li et al., 2014), HDM significantly increased Rn, but H and G didn't change, this indicates that HDM influences different elements of AHR and some will be enhanced while others will remain unchanged (as seen in our study). The CeO_2HD+HDM augmented the HDM effects and resulted in an increase in the measured parameters of AHR.

Lung sections were also stained and fixed for M.T, -sma and PCNA, no quantification was completed on these stained sections (Figure 4-14). Previous studies quantifying these stains after exposure to HDM indicated that there was a significant increase in a-smastaining (Li et al., 2014), and M.T staining (Ahn et al., 2007). Our study did not quantify the staining, but from visual analysis there is a clear increase in HDM exposed groups and more so in the CeO_2NP+HDM groups when compared to HDM in all the stains when compared to the control.

Chapter 5: Investigation of the effects of cerium dioxide nanoparticles and diesel exhaust particulates in a murine model of allergen exposure.

5.1 Introduction

As well as enabling researchers to identify potential hazards various nanoparticles have, animal models are also incredibly important in allowing us to establish the effects environmental particles may have at environmental relevant concentrations. Diesel exhaust particles are of interest in a model of allergic airway disease, this is due to the high potential of human exposures. With the introduction of Envirox, it is important to also take this into consideration – and the relevant concentration of CeO_2NPs that may now also be burnt with the fuel if this catalyst is added into the tank.

5.1.1 Effects of diesel particulates in experimental models of asthma

Diesel exhaust particles (DEP) have the potential to act as an adjuvant through the release of non-specific airway stimulants (Pandya et al., 2002). There has been a possible link established between the increase in air pollution (specifically diesel) and the prevalence of asthma, but this is a controversial topical and the links are casual. An increase of exposure to diesel in children does lead to an increase in the prevalence of asthma in that population (Munoz et al., 2019, Ghio, 2008). DEP is known to activate oxidative stress pathways and the activation of both Th2 and Th17 responses within the airways (Munoz et al., 2019).

These particles have also been linked to the exacerbation of asthmatics and those with compromised airways. People with more severe asthma have been found to have lower lung function and higher neutrophil infiltration than those with mild asthma when exposed to the same environmental particles (McCreanor et al., 2007) including diesel particles. This is thought to be concentration dependant, as other studies also using asthmatic volunteers did not see these significant effects (Riedl et al., 2012, Rider et al., 2016). These effects have also been identified in HDM murine models of allergic airways (Kim et al., 2011a).

The majority of the studies identifying the mechanisms of diesel particles has been completed on mice and the various allergic models that have been previously described. IL-17A has been identified as a key mediator of this effect, and neutralisation of this cytokine has been found to prevent exacerbation of DEP induced symptoms, including AHR (Brandt et al., 2013b). DEP has also been found to induce the production of mucus, oxidative stress, inflammatory cell

infiltration and increase the concentrations of various CXC chemokines within the BAL fluid (Kim et al., 2011b). DEP can also stimulate the nerves responsible for asthma exacerbations (using a guinea pig model). This activation is related to the polycyclic hydrocarbons that are contained within DEP that activate the aryl hydrocarbon receptor and go on to produce reactive oxygen species (Robinson et al., 2018).

5.1.2 Cerium modification of Diesel particulate effects in experimental models

As far as we are aware, this is the first study completed investigating the potential effects the combination of CeO_2NPs and DEP has on a model of allergic airway disease. This is something that is important to establish as the use of Envirox is increasing, so is the potential for members of the public with allergic airway diseases to come into environmental concentrations of these particles.

There are very few studies that have compared the effects of DEP alone and the combination of both CeO_2NP/DEP, and those that have been done use healthy Sprague-Dawley rats, and these studies identified an increase in pulmonary effects after being exposed to CeO_2NP/DEP when compared to the DEP (including increase in airway thickness, injury biomarkers (Snow et al., 2014a) and inflammation and fibrosis (Ma et al., 2014b)), as well as an increase in the clearance time and systemic translocation (Snow et al., 2014a, Ma et al., 2014b).

For this chapter the concentrations of the particles used was also carefully decided. This was done to try and mimic an environmentally relevant exposure, as well as the correct CeO_2NPs:DEP ratio that was previously determined from engine burning studies. This was previously outlined in **section 2.1.1**, but is summarised below:

CeO_2NPs contained within the exhaust particles produced post-combustion diesel and Envirox catalyst mixture was 0.08%. Therefore, for all future experimental work, the ratio between the particle types was 1:0.008mg/ml DEP:CeO_2NPs (Zhang et al., 2013).

5.2 Hypothesis and aims

Hypothesis:

CeO_2NPs will enhance the allergic response of DEP+HDM in an animal model of allergic lung disease in relation to dose and acute or chronic exposures.

Aims:

It is important to determine the potential systemic effects the addition of DEP alone and CeO_2NPs/DEP have on an allergic model, both the exacerbation and the adjuvant effects of these particles. The previous chapter has focused on the effects of CeO_2NPs on these models, and this chapter aims to further inform with the addition of both DEP and the combination of CeO_2NPs/DEP on an allergic airway disease.

The aim of this chapter is to:

- Determine the effects a single 24-hour (acute) exposure of DEP±HDM has in a murine model. This will allow us to determine the acute responses to these particles and compare the acute responses to the repeated exposures.
- Determine the effects a single acute exposure of DEP have on an HDM murine model of allergy (SGL) and repeated chronic exposures of DEP±HDM (RPT), have on a murine model. This will allow us to establish the potential effects the repeat exposures of DEP alone have when compared to the HDM exposure protocols.
- Determine the effects a single acute exposure of CeO_2NPs/DEP have on an HDM murine model of allergy (SGL) and repeated chronic exposures of CeO_2NPs/DEP±HDM (RPT), have on a murine model. This will allow us to establish the potential effects the repeat exposures of CeO_2NPs/DEP alone have when compared to the HDM exposure protocols.

5.3 Methods

All methods used within this chapter have been previously described in Chapter 2. Individual method sections for reference will be identified throughout this chapter.

The protocol for this chapter is outlined in Figure 5-1 (A, B, C and D) and indicates the various exposure regimes as well as the euthanasia and exposure time points. Figure 5-1, E, outlines the end points that are analysed throughout this chapter in order to determine the effects DEP and CeO_2NP/DEP have on an animal model of allergic disease and on a healthy animal.

The exposures for CeO_2LD+DEP±HDM and CeO_2HD+DEP±HDM will be represented as BothLD±HDM and BothHD±HDM.

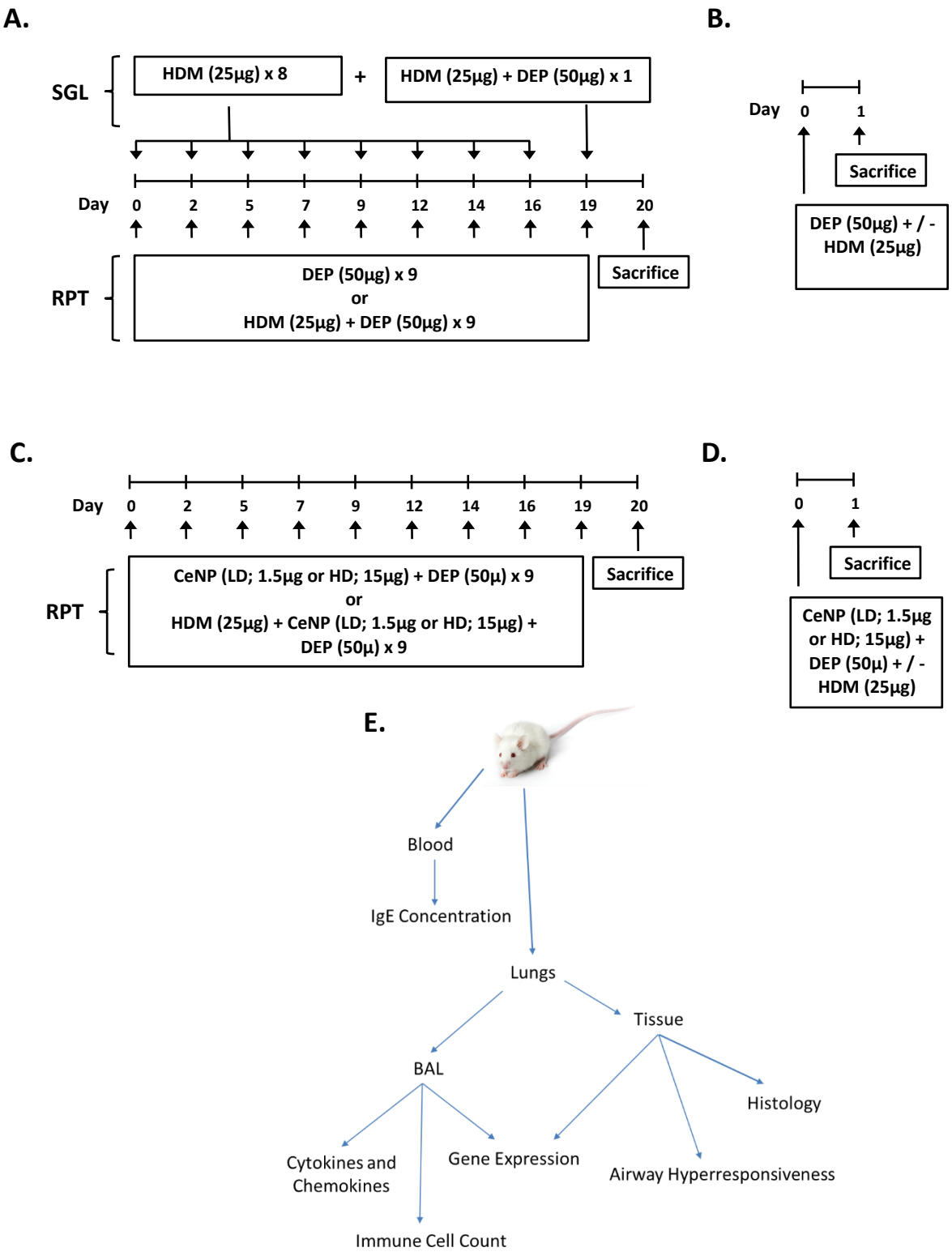


Figure 5-1. Experimental protocol to determine the effect of DEP alone and CeO_2NP/DEP in an animal model of allergic lung disease. A and C. Chronic exposure protocol. Balb/c mice were repeatedly (RPT) exposed intranasally to DEP and CeO_2NP/DEP respectively, (50µg or 3mg protein/kg) low dose (LD) (1.5µg or 75µg/kg) or high dose (HD) (15µg or 750µg/kg), alone or combined with HDM (25µg or 1.25mg protein/kg). This protocol consisted of 9 exposures divided over 3 weeks on the indicated days (lower panel). Single (SGL) exposure protocol involved the pre-exposure to HDM on 8 occasions, with the final 9^{th} exposure ±HDM (upper panel). B and D. Acute exposure protocol. Mice were exposed to a single bolus intranasal instillation of DEP alone and CeO_2NP/DEP respectively (LD and HD) ±HDM and euthanised after 24 hours. For all exposures a PBS control was also administered. E. Diagram indicating the various end points that where analysed throughout this chapter in order to determine the potential acute and chronic effects DEP and CeO_2NP/DEP±HDM at different concentrations of exposures.

5.4 Results

5.4.1 Effect of single acute exposure to DEP ± HDM on airway inflammatory responses after 24 hours

24 hours after acute DEP±HDM exposure (Figure 5-1 B), following euthanasia, the lungs were excised and analysed for cell numbers and profile and cytokine levels in the BAL fluid (section 2.6.4) to determine the effects of this acute exposure.

5.4.1.1 Effects on lung pathology after acute exposure to DEP±HDM

Figure 5-2 assess any potential pathophysiological changes that may have been caused by 24 hours of exposure to DEP and HDM either alone or in combination. Histochemical assessment of lung tissue sections was carried out using H/E, PAS and M.T. staining protocols.

There were no apparent changes in airway structure, tissue inflammation or mucus production after any exposure.

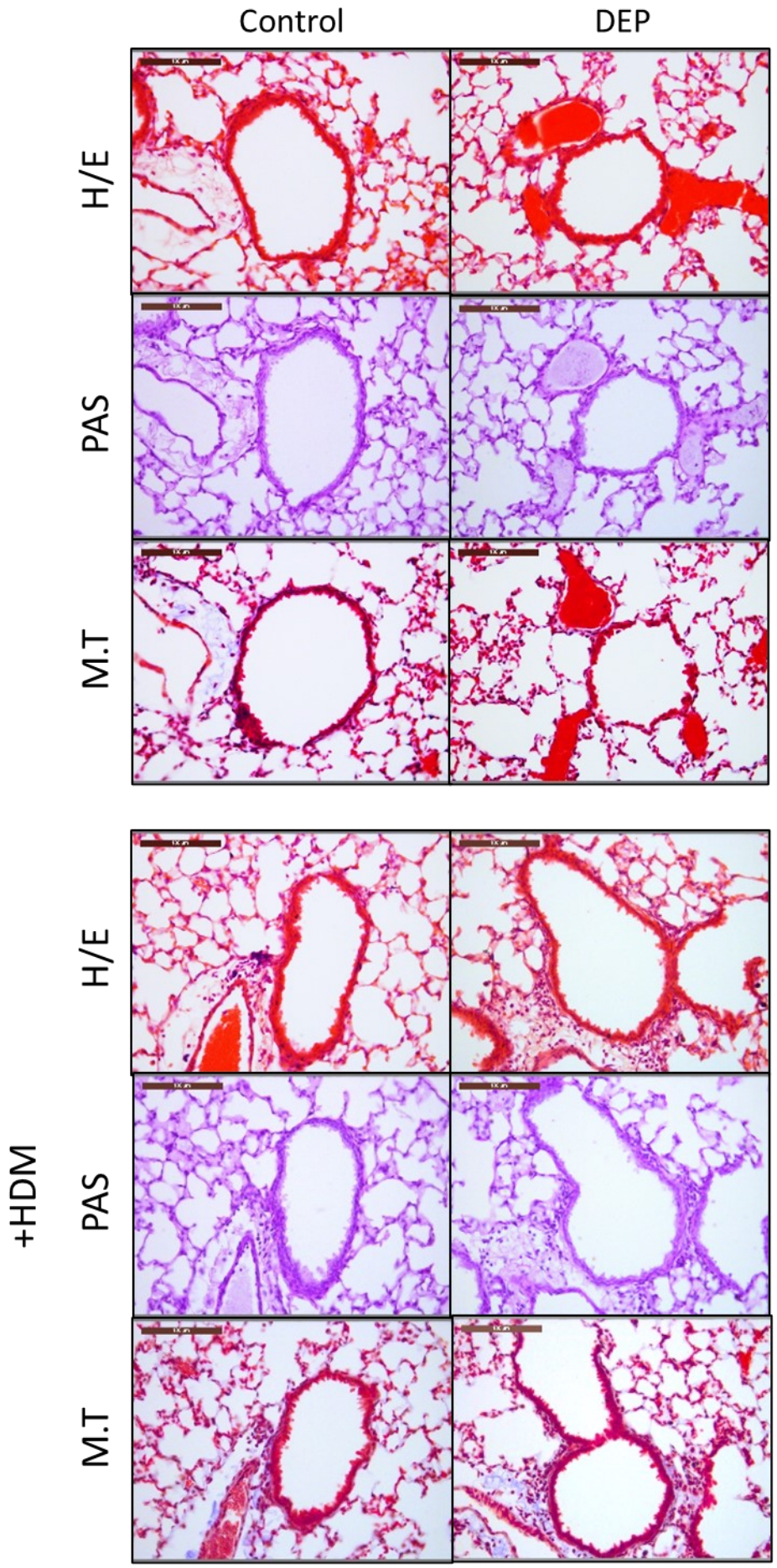


Figure 5-2 Lung sections stained after 24 hours after exposure to DEP±HDM. Lung tissue was fixed and stained with haematoxylin and eosin stain (H/E) (top panel), Periodic acid-Shiff (PAS) (middle panel) and Masson's Trichrome stain (M.T) (bottom panel). Representative images of each group are displayed with a scale bar of 100µm (top left of image).

Differential inflammatory cell counts in BAL fluid were analysed after exposure to DEP and HDM either alone or in combination for 24 hours (Figure 5-3, A) and plotted as cells/ml of BAL fluid % of total cells counted of each immune cell was also analysed (Figure 8-11, appendix). There was a significant increase in the number of macrophages after exposure to DEP alone and HDM when compared to the control and no changes after exposure to DEP+HDM when compared to both HDM and particles alone.

There was a significant increase in neutrophil counts after exposure to HDM when compared to the control and a significant increase after exposure to HDM+DEP when compared to the HDM control and particles alone.

5.4.1.3 Effect of DEP ± HDM on inflammatory markers by ELISA of BAL fluid

Inflammatory markers were analysed in the BAL fluid after 24-hours post-instillation (Figure 5-3, B). There were no changes in the BAL fluid concentrations of CCL20, CCL8, CCL17, and IL-33 regardless of exposure protocol. There was a decrease in CCL11, IL-1α, IL-5 and IL-4 after exposure to DEP when compared to the control, none of these were significant. There was an increase in the concentration of TSLP after exposure to DEP and DEP+HDM when compared to the control and DEP alone. This was also seen in the concentration of IL-5, and significantly increased after DEP+HDM when compared to the HDM control.

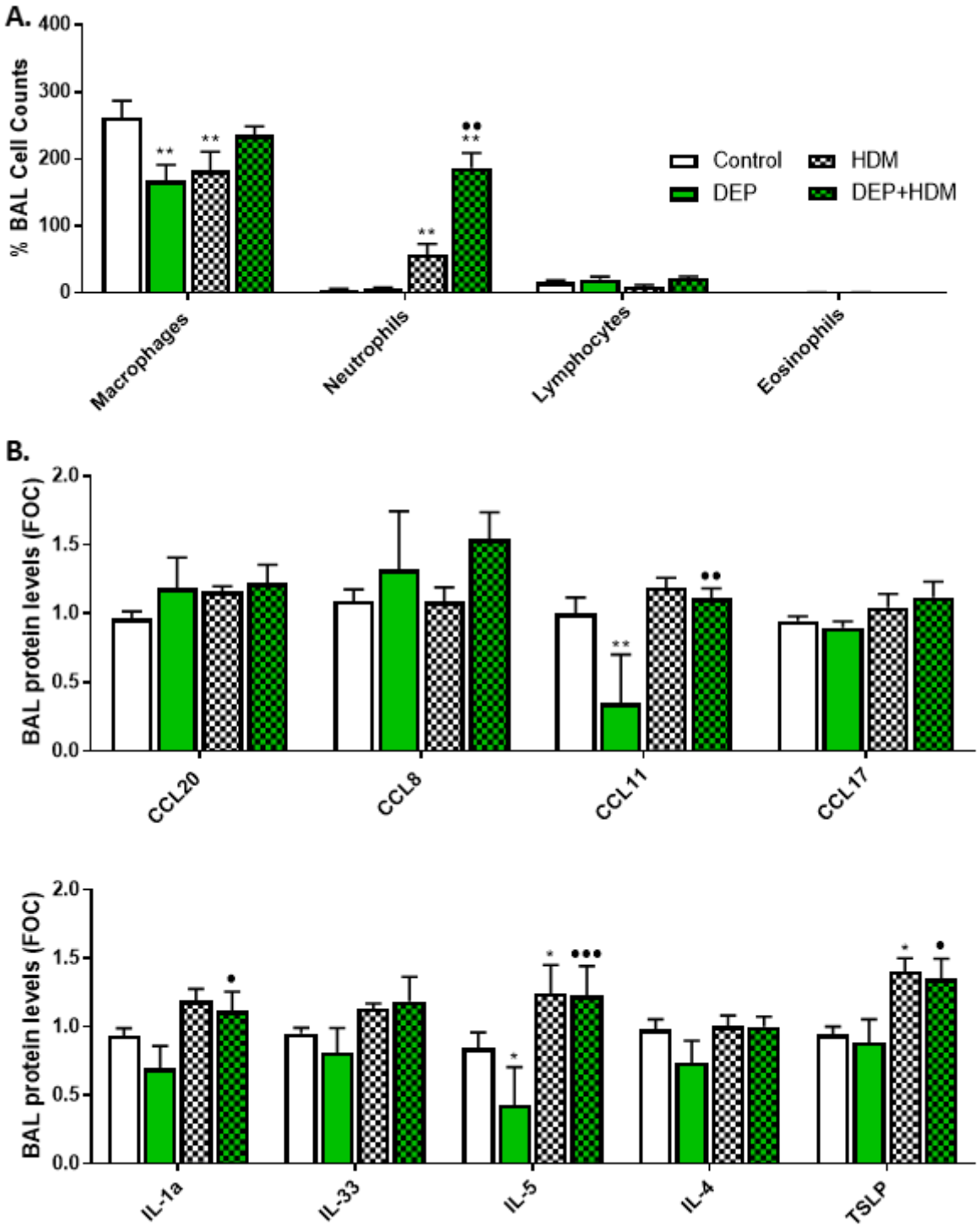


Figure 5-3 Inflammatory cell response and cytokine release after 24-hour exposure to DEP±HDM.
BAL fluid was analysed for different immune cells and released cytokines. A. Cells were counted after being fixed and stained as previously outlined (section 2.6.4) and 300-500 cells were counted per animal. The data is presented as the mean ±SEM % total cells counted/ml. B. Cytokines were measured in the BAL fluid and are presented as ±SEM fold over control levels (FOC). N=5-9 mice per treatment group, with all assays performed in triplicate. Significance is denoted as the following: compared to PBS or HDM control p<0.05(*), <0.01(**), <0.001(***); compared to DEP alone p<0.05(•), <0.01(••), <0.001(•••).

5.4.2 Repeat co-exposure effects of DEP alone and DEP+HDM on pulmonary responses

DEP and HDM either alone or in combination was intranasally instilled 9 times over 3 weeks as described in Figure 5-1. This was in order to determine potential adjuvant (RPT) and exacerbation (SGL) effects of DEP on HDM allergen induced inflammatory events.

5.4.2.1 Effect of single and repeat DEP±HDM on altered BAL Immune cell counts

The cells in the BAL fluid were counted and represented as a percentage (Figure 5-4, A) and plotted as cells/ml of BAL fluid % of total cells counted of each immune cell was also analysed (Figure 8-11, appendix). There was a significant increase in the macrophage number after exposure to HDM compared to the control and DEP+HDM SGL when compared to the HDM control and the particles alone.

There was a significant increase in the neutrophil count after exposure to DEP alone and HDM alone when compared to the control exposure. There was also a significant increase in neutrophils after exposure to DEP+HDM SGL when compared to HDM control and the DEP alone.

There were no changes in the lymphocyte counts. There was a significant increase in the eosinophil cell count following DEP+HDM RPT exposure when compared to the HDM control and DEPs alone.

5.4.2.2 Effect of single and repeat DEP±HDM on altered mast cell related markers

Mast cells are important in the Th2 immune response and form part of the immediate antibody mediated response to allergens. ELISA analysis of Mast Cell Protease-1 (MCPT1), a marker of these cells, was completed on the BAL fluid (Figure 5-4, B). MCPT1 is known to promote permeabilization of mucosal membranes and allergic hypersensitivity reactions, as well as being a mast cell chemoattractant.

There was a significant increase in MCPT1 expression after exposure to DEP+HDM RPT when compared to HDM alone and DEP alone.

Immunoglobulin E (IgE) is an antibody isotype underpinning antigen dependent immune responses in allergy. The concentration of IgE in blood plasma (Figure 5-4, C) replicated the same pattern as MCPT1 with DEP+HDM RPT being significantly increased when compared to HDM, DEP alone and PBS control exposures. Mast cells were stained using toluidine blue (TB) in airway sections from exposed animals and represented as an example section (Figure 5-4, D),

mast cells are identifiable as darker blue stains around the airways. A difference between the exposure groups cannot be observed using these stains, but they allow visual representation of the mast cells in the airways.

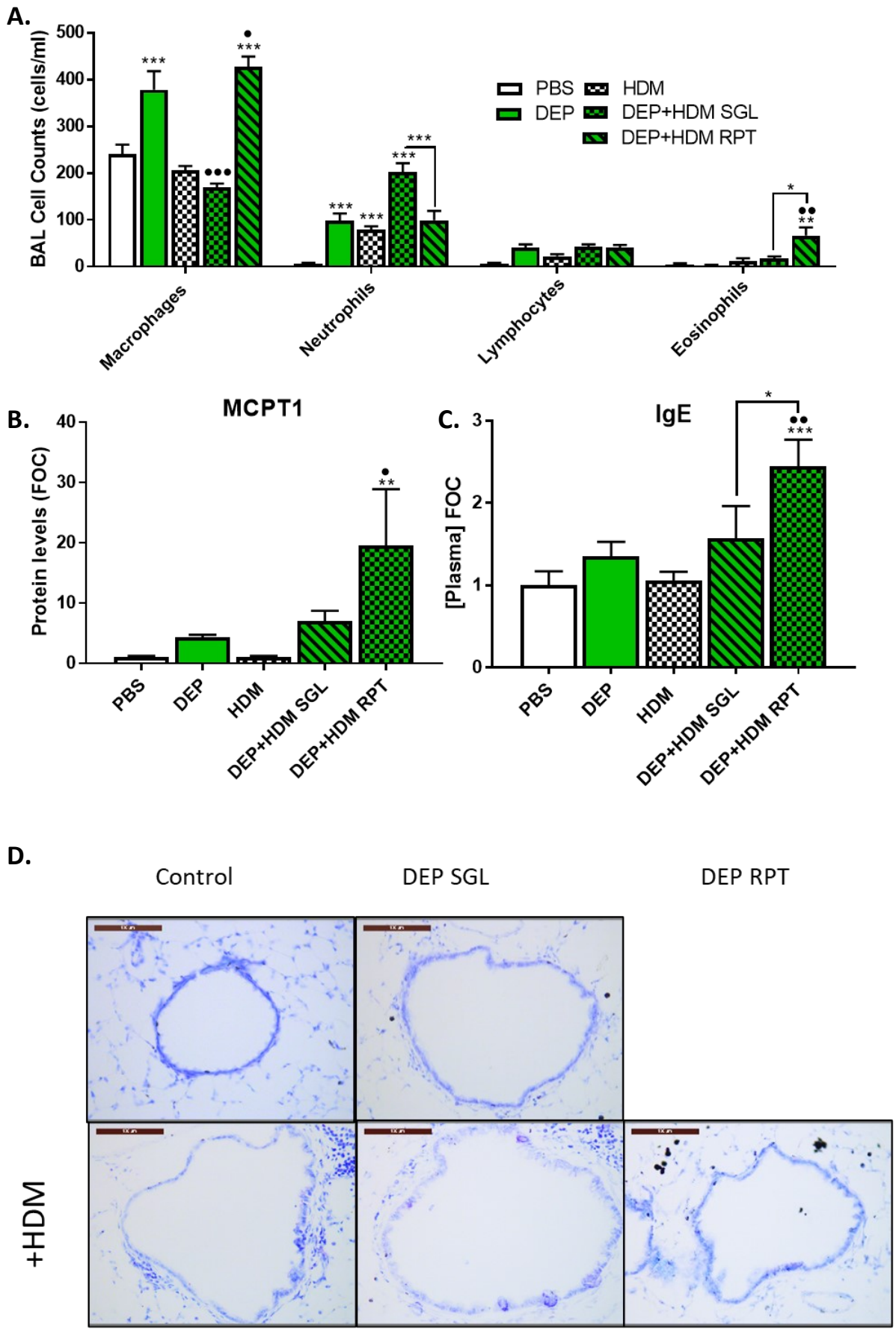


Figure 5-4 Inflammatory cell response and plasma immunoglobulin E after acute and chronic exposure to DEP±HDM for 3 weeks. BAL fluid, lung homogenates and blood plasma were analysed for immune cells, tissue mast cell MCPT1 and plasma IgE. A. Cells were counted after being fixed and stained as previously outlined (section 2.6.4) and 300-500 cells were counted per animal. The data are presented as the mean ±SEM % total cells counted. B. Lung homogenate MCPT1 (mast cell marker) levels are presented as fold over control levels (FOC±SEM). C. Blood plasma of IgE levels using analysed by ELISA. D. Lung tissue was fixed and stained with toluidine blue (TB), to highlight tissue mast cells (**section 2.7.2.7**). Representative images of each group are displayed with a scale bar of 100µm (top left of image). N=5-9 mice per treatment group, with all assays performed in triplicate. Significance is denoted as the following, as indicated: compared to PBS or HDM control p<0.05(*), <0.01(**), <0.001(***); compared to DEP alone p<0.05(•),<0.01(••), <0.001(•••).

5.4.2.3 Effect of single and repeat DEP±HDM on gene expression changes in lung tissue

Figure 5-5 and Figure 5-6 show the changes in gene expression after exposure to DEP±HDM in lung tissue, assessed using real time PCR of mRNA levels.

There were no changes in the expression of IL-4, IL-25, IL-13, CCL17, CCL24, CCL26, AREG, NQO1 and TSLP regardless of the exposure regimen.

IL-8 showed an increase after DEP+HDM RPT when compared to the other exposures, while this increase was significant for CYP1A1 when compared to the DEP alone. IL-6, and IL-36A expression appeared to be increased after exposure to HDM alone when compared to the other groups, but this was not significant.

There was a significant increase in CCL8 expression after exposure to HDM when compared to the control; DEP+HDM SGL and DEP+HDM RPT induced levels were also increased when compared to control and DEP alone. CD177 expression was significantly increased after exposure to DEP alone compared to the control and after DEP+HDM SGL and DEP+HDM RPT when compared to the HDM control. This pattern was also replicated in the expression of MMP12, as there was a significant increase in expression after exposure to DEP when compared to the control. This is also reflective of the pattern of expression observed with protein levels of MCPT1 (Figure 5-5).

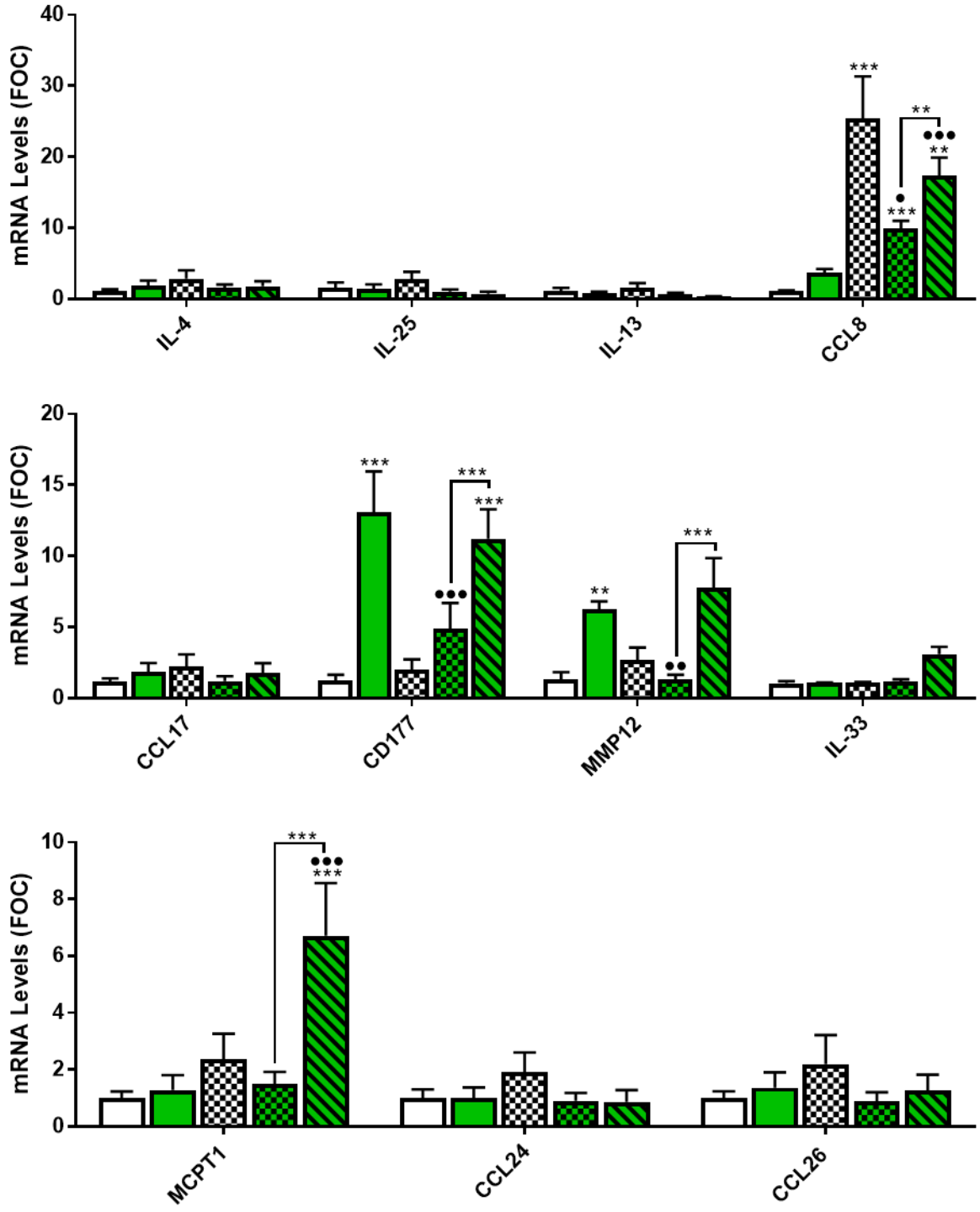


Figure 5-5 Inflammatory marker expression in lung tissue after various DEP±HDM exposures over 3 weeks. Total lung mRNA was isolated for indicated inflammatory markers via RT-PCR. Results are presented as fold over control levels (FOC±SEM). N=5-9 mice per treatment group, with all assays performed in triplicate. Significance is denoted as the following, as indicated: compared to PBS or HDM control p<0.05(*), <0.01(**), <0.001(***); compared to DEP alone p<0.05(•),<0.01(••), <0.001(•••).

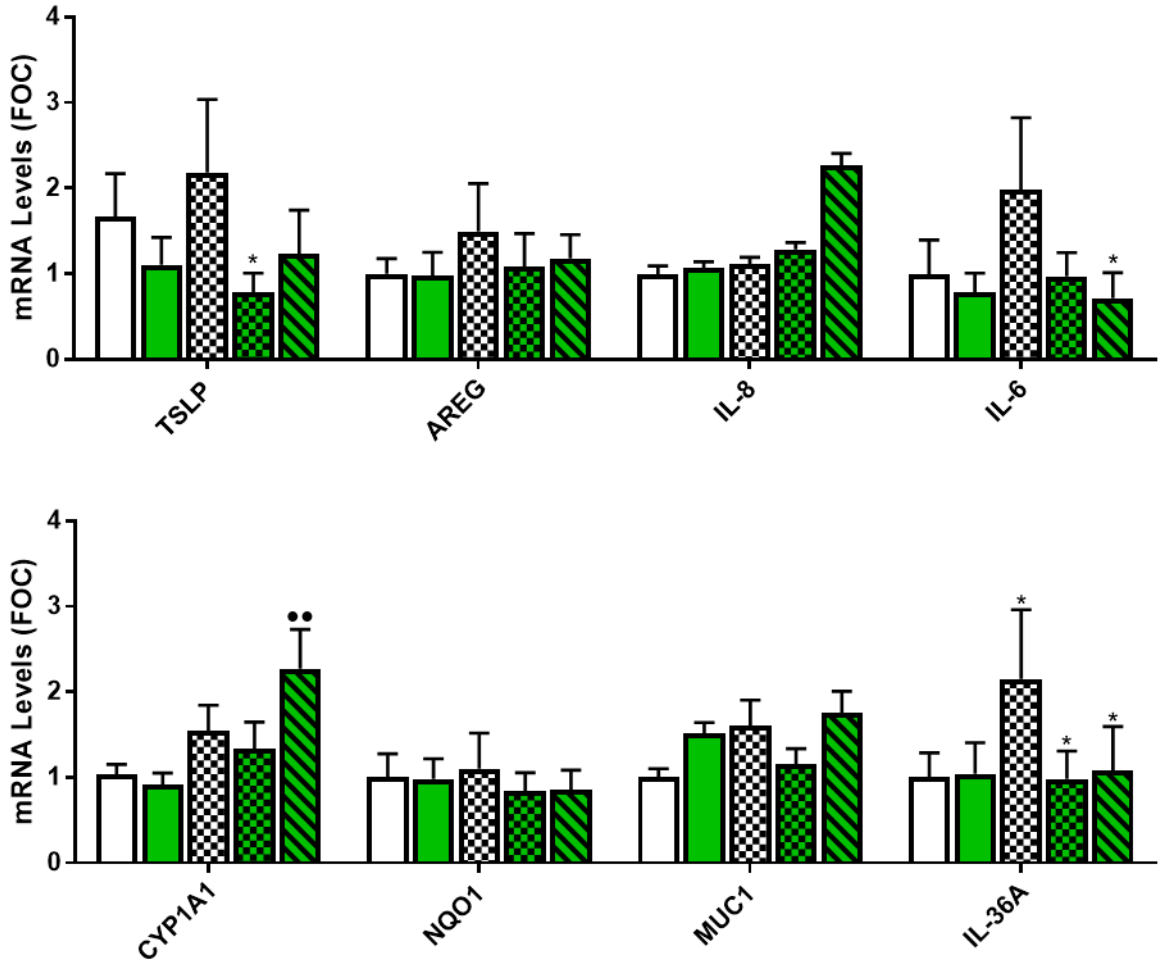


Figure 5-6 Inflammatory marker expression in lung tissue after various DEP±HDM exposures over 3 weeks. Total lung mRNA was isolated for indicated inflammatory markers via RT-PCR. Results are presented as fold over control levels (FOC±SEM). N=5-9 mice per treatment group, with all assays performed in triplicate. Significance is denoted as the following, as indicated: compared to PBS or HDM control p<0.05(*), <0.01(**), <0.001(***); compared to DEP alone p<0.05(•),<0.01(••), <0.001(•••).

5.4.2.4 *Effect of single and repeat DEP±HDM on inflammatory markers assessed by ELISA of BAL fluid*

ELISA analysis of BAL fluid (Figure 5-7) was completed after the exposure regimens (Figure 5-1).

There were no changes in the concentration of CCL11, CCL20, IL-33 or IL-4 measured after exposure to the various particle combinations.

There was a significant increase in the concentration of CCL8 after exposure to DEP+HDM SGL and RPT when compared to the HDM control. IL-5, IL-13 and IL-1α concentrations decreased after exposure to DEP+HDM RPT when compared to the other exposures but not significantly. TSLP concentration was following exposure to HDM, DEP+HDM SGL and DEP+HDM RPT in that order, when compared to the control and the particles alone.

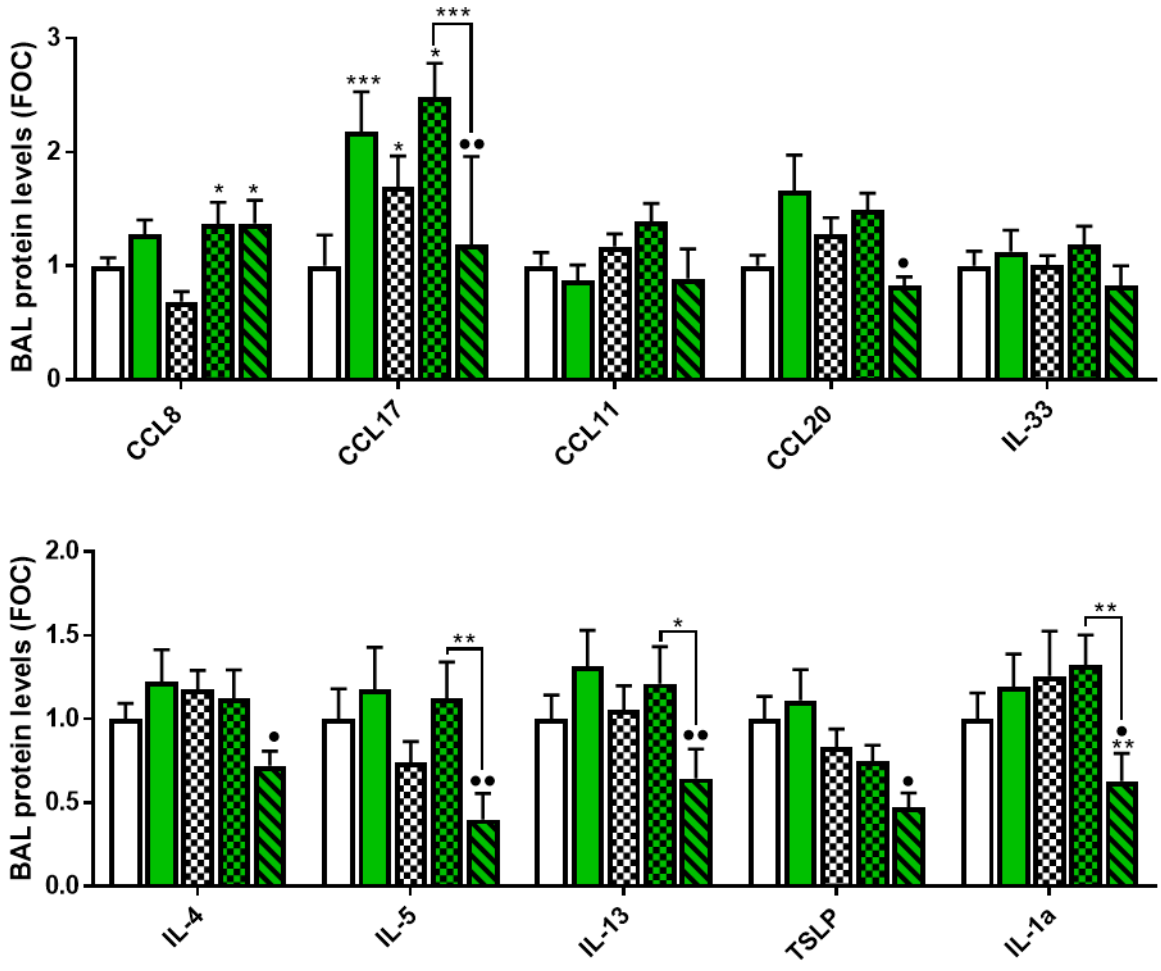


Figure 5-7 Inflammatory protein levels in BAL fluid following acute and chronic exposure to DEP±HDM for 3 weeks. Lung BAL fluid was analysed for cytokine levels after acute and chronic exposure to DEP±HDM for 3 weeks. Results are presented as fold over control levels (FOC±SEM). N=5-9 mice per treatment group, with all assays performed in triplicate. Significance is denoted as the following, as indicated: compared to PBS or HDM control p<0.05(*), <0.01(**); compared to DEP alone p<0.05(•),<0.01(••), <0.001(•••).

5.4.2.5 Effect of single and repeat DEP±HDM on airway mucin production

Serial sections of lungs were taken and stained with Periodic acid–Schiff (PAS) and the mucin regulator CLCA1 (immunohistochemistry) (8). Sections from all exposure groups are represented. It is evident from these sections that there is a heavier staining of both PAS positive cells and CLCA1 after exposure to HDM alone and DEP+HDM RPT when compared to control. Increased PAS stain is indicated by bright pink stains and CLCA1 is indicated by dark brown staining.

Airway mucin production can be quantified by counting the PAS+ cells within the airways, scored and then graphed (Figure 5-9, A) This indicates that there is a significant increase in the PAS stained cells after exposure to DEP+HDM SGL, and DEP+HDM RPT when compared to the particles alone. There was also an increase in the PAS score after exposure to HDM, however this was not significant.

MUC5AC, CLCA1 and SLC26A4 are genes relating to mucus production and their expression after exposure was measured (Figure 5-9, B, C, and D respectively). DEP+HDM RPT tissue was found to significantly increase expression of all three genes when compared to the particles alone, the HDM control and DEP+HDM SGL.

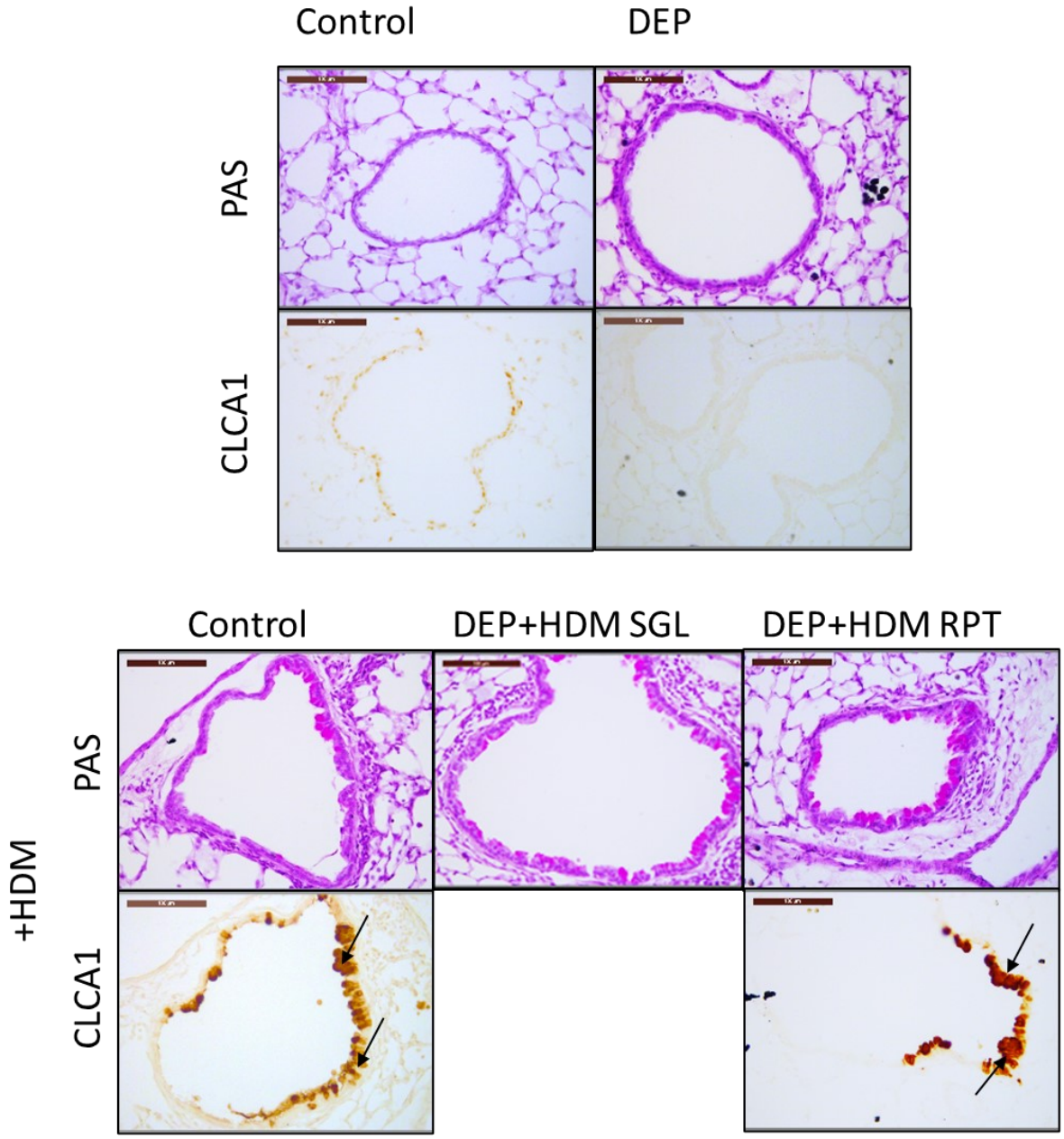


Figure 5-8 Analysis of airway secretion-related molecules following acute and chronic exposure to DEP±HDM for 3 weeks. Lung tissue was fixed, and sections processed for PAS staining (top panel) and immunohistochemical staining of CLCA1 (bottom panel). Representative images of each group are displayed with a scale bar of 100µm (top left of image). Arrows indicate positive stained cells. Quantification of PAS positive cells within the airways was scored and graphed (Figure 5-9, B).

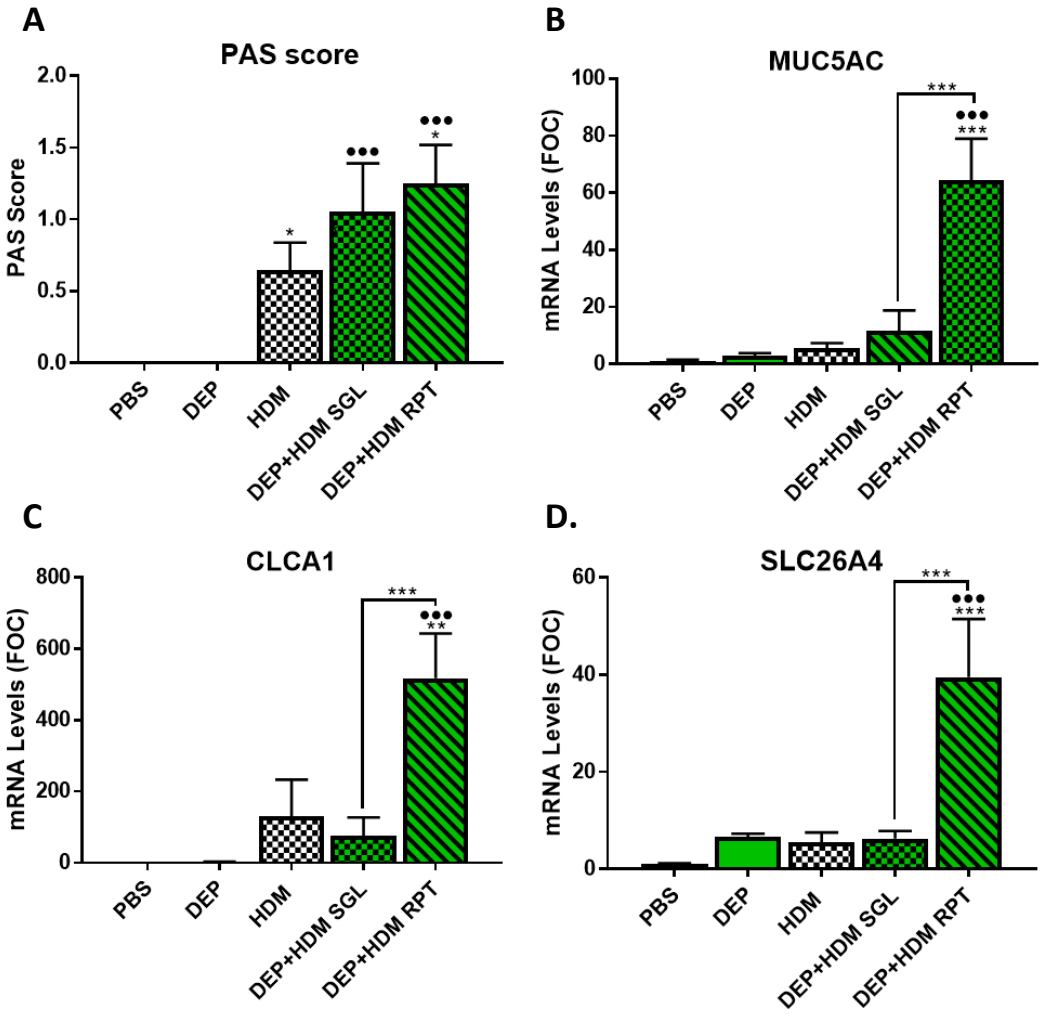


Figure 5-9 Analysis of airway secretion-related molecules following acute and chronic exposure to DEP±HDM for 3 weeks. A. Quantification of PAS positive cells within the airways was scored and graphed. B-D. Lung mRNA was isolated and analysed by RT-PCR for expression of mucus related genes. Results are presented as fold over control levels (FOC±SEM). N=5-9 mice per treatment group, with all assays performed in triplicate. Significance is denoted as the following, as indicated: compared to PBS or HDM control p<0.05(*), <0.01(**), <0.001(***); compared to DEP alone p<0.05(•),<0.01(••), <0.001(•••).

5.4.2.6 *Effect of single and repeat DEP±HDM on structure, remodelling and function of the lung*

Masson's trichrome (M.T.), α-smooth muscle actin (α-sma) and PCNA were stained on serial lung sections (Figure 5-10) after the exposures in order to determine if there was any airway remodelling. M.T. stains blue for collagen, α-sma stains brown for α-smooth muscle actin and can indicate increased muscle in the area, and PCNA stains for cells that are replicating. Increased staining for these parameters is reflective of pathophysiological responses and airway remodelling processes that are commonly seen in asthma patients. All three show a similar pattern after instillation and can be seen to increase in groups that have had both HDM and particle exposures.

Airway hyperresponsiveness (AHR) is a characteristic feature in patients with asthma. Responses to the inhaled muscarinic receptor agonist can be used to assess AHR and were applied in our study. PBS, DEP alone, HDM alone and DEP+HDM RPT were measured. There were no changes in the respiratory system resistance (Rrs) (Figure 5-11, A), the Newtonian resistance (Rn) (Figure 5-11, B), elastance (Ers) (Figure 5-11, D) or tissue elastance (H) (Figure 5-11, C) after exposure to any of the particle combinations.

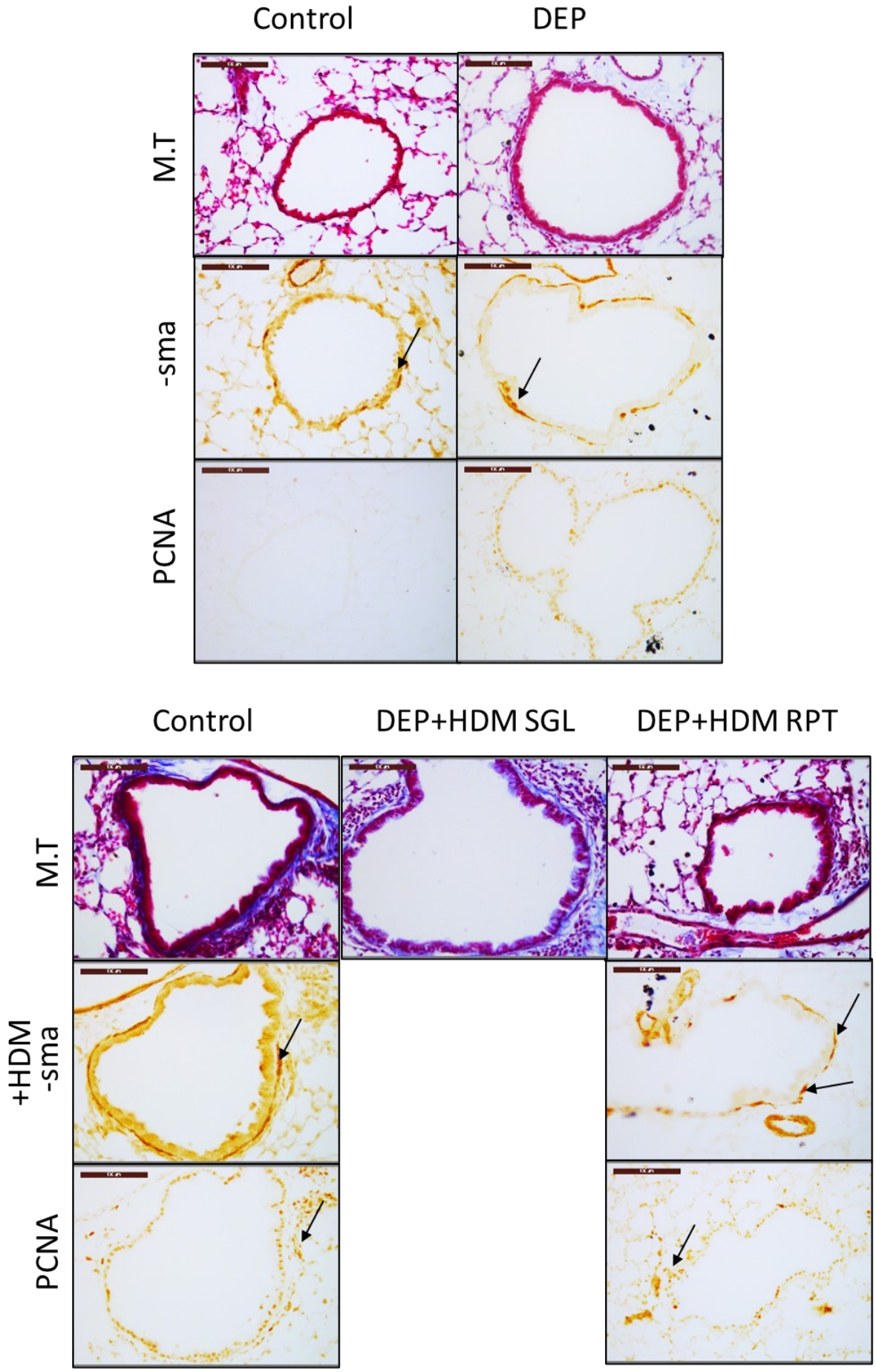


Figure 5-10 Airway structure and remodelling after DEP±HDM exposures over 3 weeks. A. Lung tissue was fixed, and sections processed for M.T staining (top panel) and immunohistochemical staining of α-smooth muscle actin (α-sma) (middle panel) and proliferating cell nuclear antigen (PCNA) (bottom panel). Representative images of each group are displayed with a scale bar of 100μm (top left of image). Arrows indicate positive cell staining.

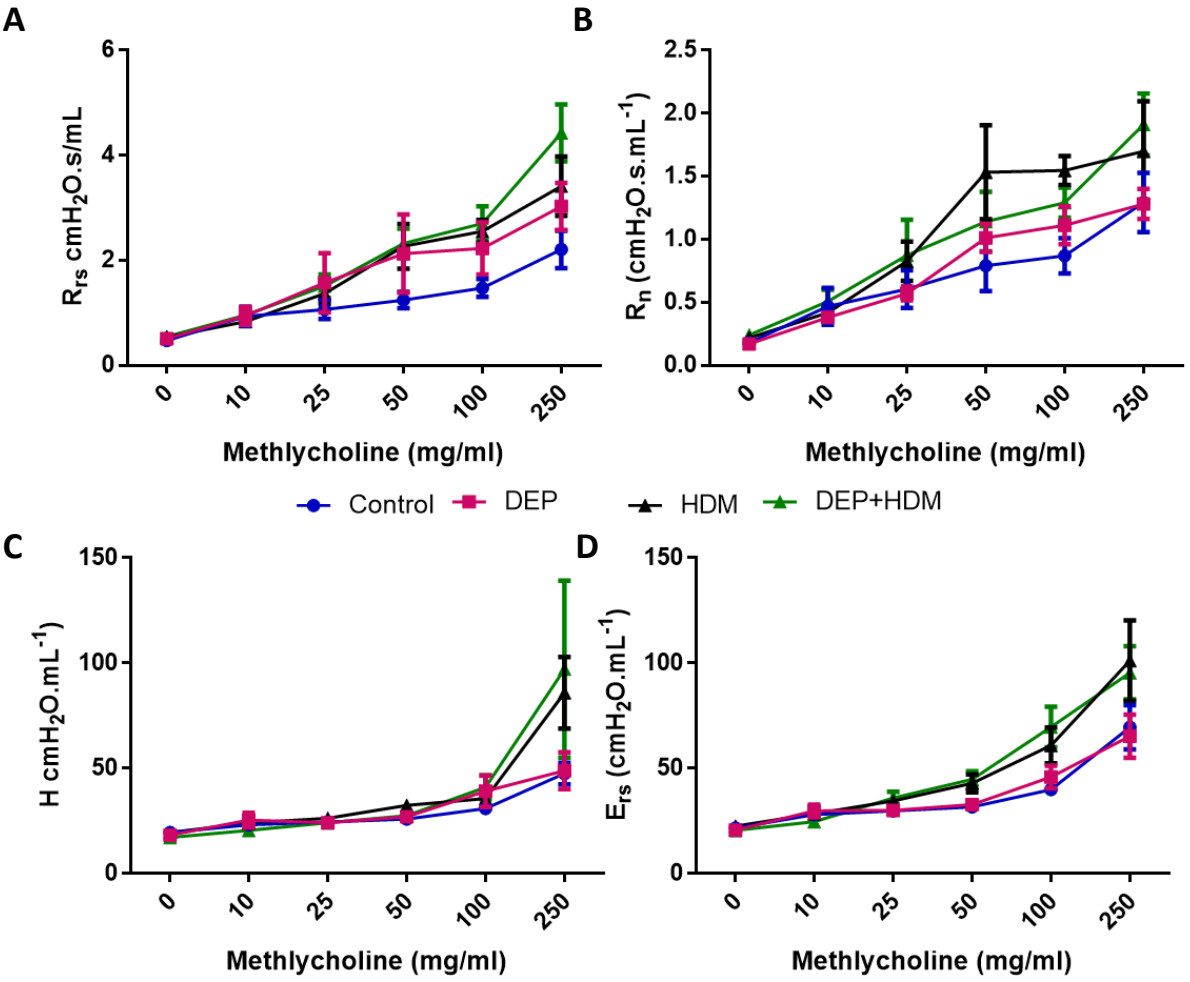


Figure 5-11 Lung function analysis after DEP±HDM exposures over 3 weeks. Airway hyperresponsiveness to increasing concentrations of inhaled aerosolised methacholine, was assessed using a forced oscillation technique. A. Respiratory system resistance (Rrs), B. Newtonian resistance (R_n), C. tissue elastance (H) and D. elastance (E_{rs}) were calculated using flexivent system sotware. Results are presented as ±SEM. N=5-9 mice per treatment group, with all assays performed in triplicate. Significance is denoted as the following, as indicated: compared to PBS or HDM control p<0.05(*), <0.01(**), <0.001(***); compared to DEP alone p<0.05(•),<0.01(••), <0.001(•••).

5.4.3 Acute respiratory effects of both (DEP+CeO_2NPs) and HDM on airway inflammatory responses (24hrs)

24 hours after CeO_2NPs instillation, initial end points were analysed and assessed for acute inflammatory responses. This protocol is outlined in Figure 5-1, D.

5.4.3.1 Effect of DEP, CeO_2NP and HDM on BAL Immune cell counts

Figure 5-12, A shows the cell profiles in the BAL fluid from Balb/c mice after exposure to the various particle combinations and plotted as cells/ml of BAL fluid. % of total cells counted of each immune cell was also analysed (Figure 8-12, appendix). There was a significant decrease in the macrophage counts after exposure to BothLD+HDM and BothHD+HDM when compared to the HDM control.

There was a significant increase in neutrophil cell counts after exposure to BothLD+HDM and BothHD+HDM when compared to the HDM control.

There were no changes in the lymphocyte or the eosinophil cell counts after any of the exposures.

5.4.3.2 Effect of DEP, CeO_2NP and HDM on inflammatory markers within BAL fluid

Figure 5-12, B shows the changes in gene expression after 24 hours of exposure to the various particle combinations. There were no changes in the concentration of IL-33, IL-5, IL-4 in the BAL fluid after any of the Both+HDM exposures.

The levels of CCL20 were significantly increased after exposure to BothHD+HDM when compared to CeO_2HD+HDM, as was the concentration of IL-1α. IL-1α concentration was also significantly increased after BothLD+HDM exposure when compared to CeO_2LD+HDM and DEP+HDM. The concertation of TSLP was significantly increased after BothHD+HDM exposure when compared to CeO_2HD+HDM.

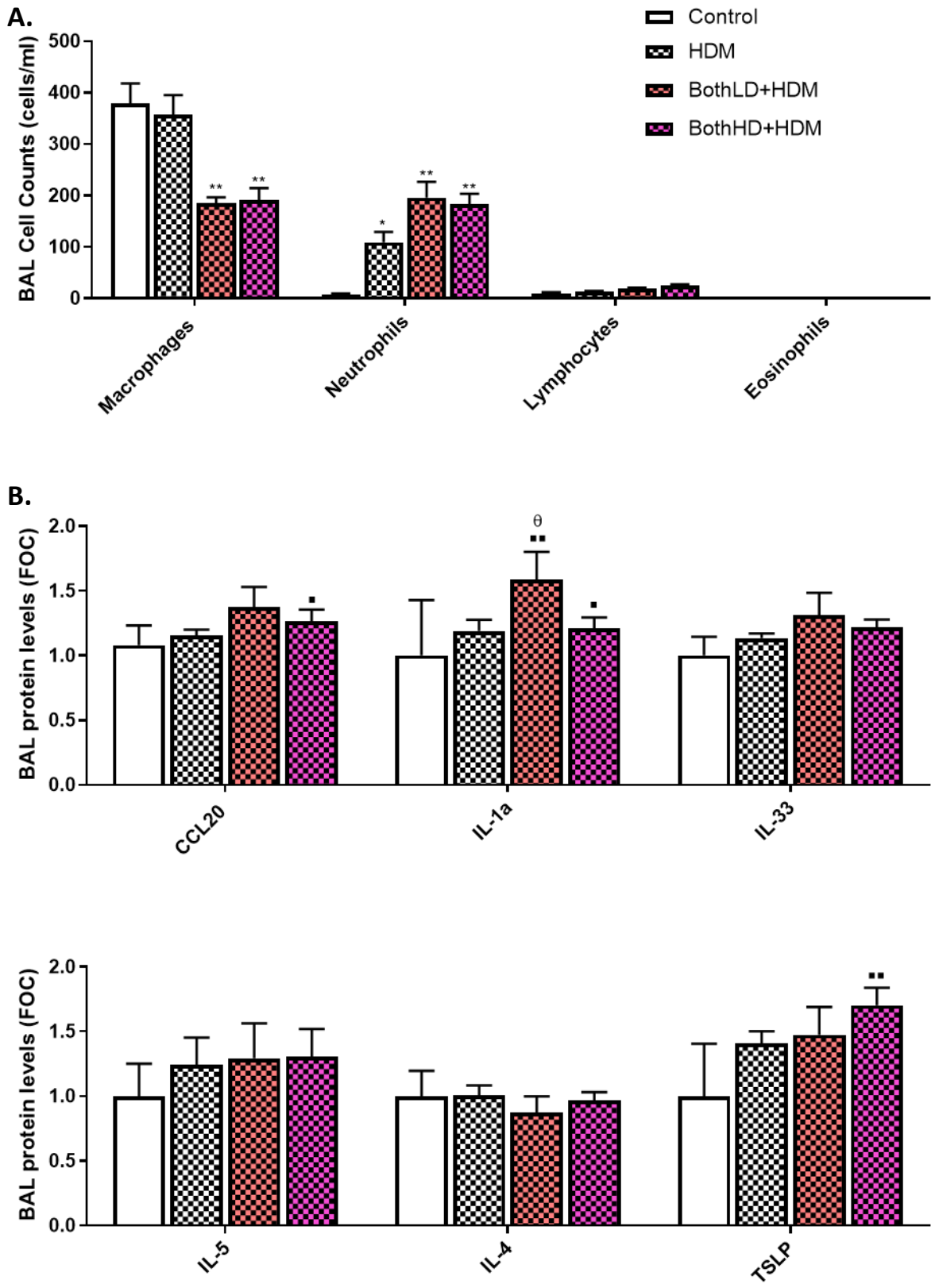


Figure 5-12 Inflammatory marker gene expression in lung tissue after various Both±HDM exposure combinations over 24 hours. Total lung mRNA was isolated for indicated inflammatory markers via RT-PCR. Results are presented as ±SEM fold over control levels (FOC). N=5-9 mice per treatment group, with all assays performed in triplicate. Significance is denoted as the following: compared to PBS or HDM control p<0.05(*), <0.01(**), <0.001(***); compared to particles alone p<0.05(•), <0.01(••), <0.001(•••); compared to CeO_2NPs+HDM p<0.05(▪), <0.01(▪▪), <0.001(▪▪▪); and compared to DEP+HDM p<0.05(Θ), <0.01(Θ Θ), <0.001(Θ Θ Θ).

5.4.3.3 *Effect of DEP, CeO_2NP and HDM on lung cell structure assessed by histochemistry*

When observing the serial sections stained with hematoxylin and eosin (H/E), PAS and M.T (Figure 5-13), there does not appear to be any variation between the different exposure groups. These sections were prepared only 24 hours after exposure and therefore this may not have been long enough to have an impact on the gross cellular and structural appearance of the airways.

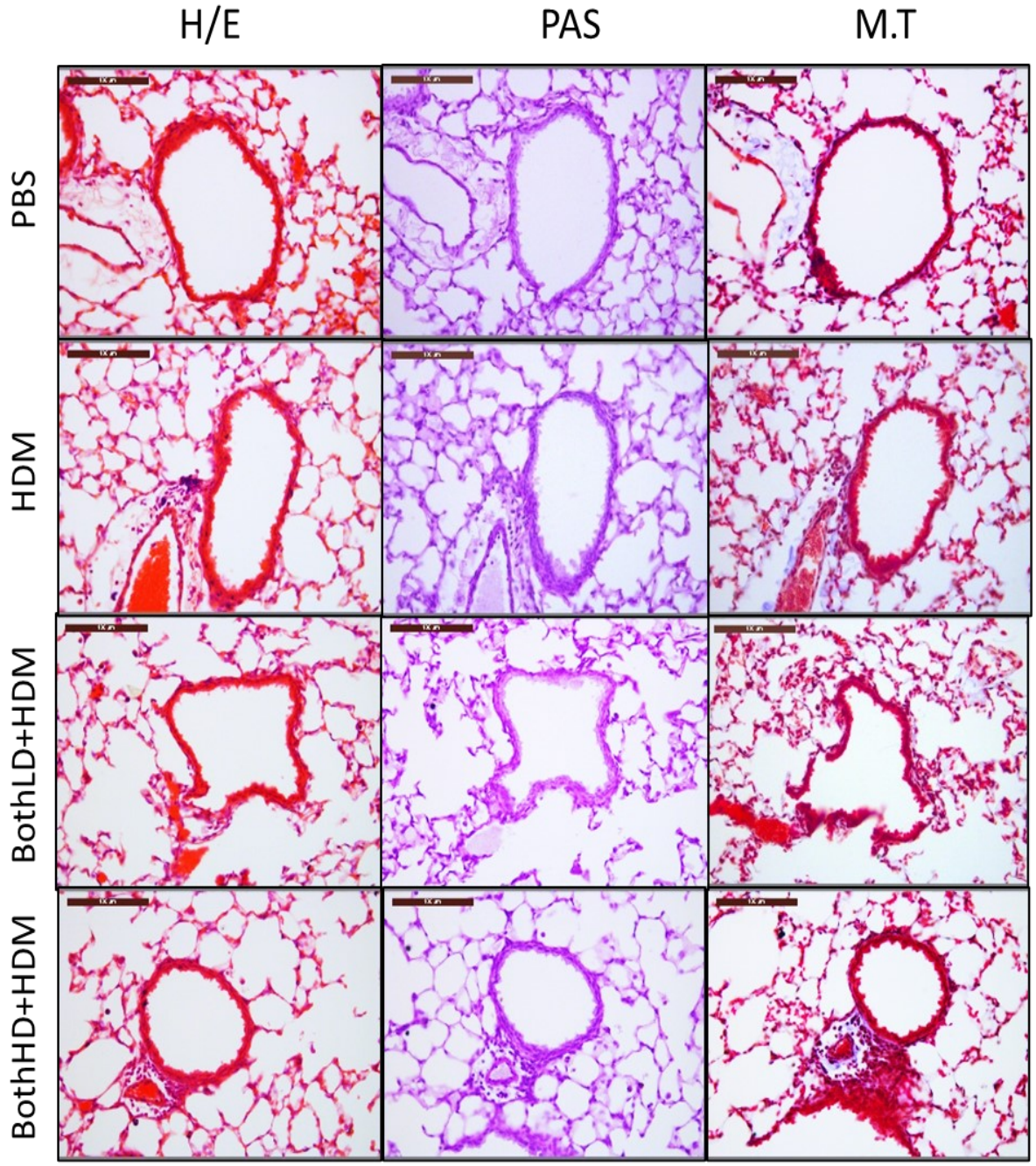


Figure 5-13 Lung sections stained after 24 hours post-exposure to Both±HDM. Lung tissue was fixed and stained with hematoxylin and eosin stain (H/E) (left panels), Periodic acid–Schiff (PAS) (middle panels) and Masson's Trichrome (M.T) stain (right panel). Representative images of each group are displayed with a scale bar of 100µm (top left of image).

5.4.4 Effects of CeO_2NPs+DEP±HDM on pulmonary responses

CeO_2NPs+DEP±HDM was intranasally instilled 9 times over 3 weeks as described in Figure 5-1. This was to determine potential effects of the combination of CeO_2NPs and DEP on the HDM model of asthma during a 3-week exposure protocol.

As the repeated exposure to both DEP+HDM (RPT) has significantly increased effects in the majority of inflammatory parameters when compared to the single exposure of DEP after 3 weeks of HDM (SGL) that was the exposure protocol that was carried on and used in further analysis and co-exposure with CeO_2NPs.

5.4.4.1 Effect of CeO_2NPs+DEP±HDM exposure on altered BAL Immune cell counts

Cell profiles in the BAL fluid from Balb/c mice after exposure to the various particle combinations was plotted as cells/ml of BAL fluid (Figure 5-14, A). % of total cells counted of each immune cell was also analysed (Figure 8-12, appendix). There was a significant decrease in the macrophage count after exposure to BothLD alone and BothHD alone when compared to the control and BothLD+HDM and BothHD+HDM when compared to the appropriate Both alone exposure control groups and HDM alone.

There were no changes in the number of neutrophils counted after exposure to BothLD and BothHD alone, however, there was a significant increase in the number after exposure to BothHD+HDM when compared to BothHD alone.

There was a significant decrease in the lymphocyte count after exposure to BothLD+HDM and BothHD+HDM when compared to HDM alone.

The eosinophil cell count was significantly increased after exposure to BothLD+HDM and BothHD+HDM when compared to BothLD and BothHD alone, indicating the addition of HDM contributed to the significant increase.

5.4.4.2 Effect of single and repeat CeO_2NPs±HDM exposures on altered mast cell related markers

Figure 5-14, B represents mast cell markers that have been analysed via ELISA. There was a significant increase in the concentration of MCPT1 in the lung tissue after exposure to BothLD+HDM and BothHD+HDM when compared to HDM alone, BothLD and BothHD respectively, CeO_2LD and CeO_2HD respectively and DEP+HDM.

IgE concentration in the plasma (Figure 5-14, C) was measured using an ELISA. There was a significant increase after exposure to BothLD+HDM when compared to HDM alone, BothLD

alone and CeO_2LD+HDM and a significant increase after exposure to BothHD+HDM when compared to HDM alone, BothHD alone and CeO_2HD+HDM.

Mast cells were stained using toluidine blue (TB) in airway sections from exposed animals and represented as an example section (Figure 5-14, D). There appears to be more staining in the BothHD+HDM exposed animals when compared to the other exposures; however, as they have not been quantified, this difference cannot be confirmed and is subject to interpretation.

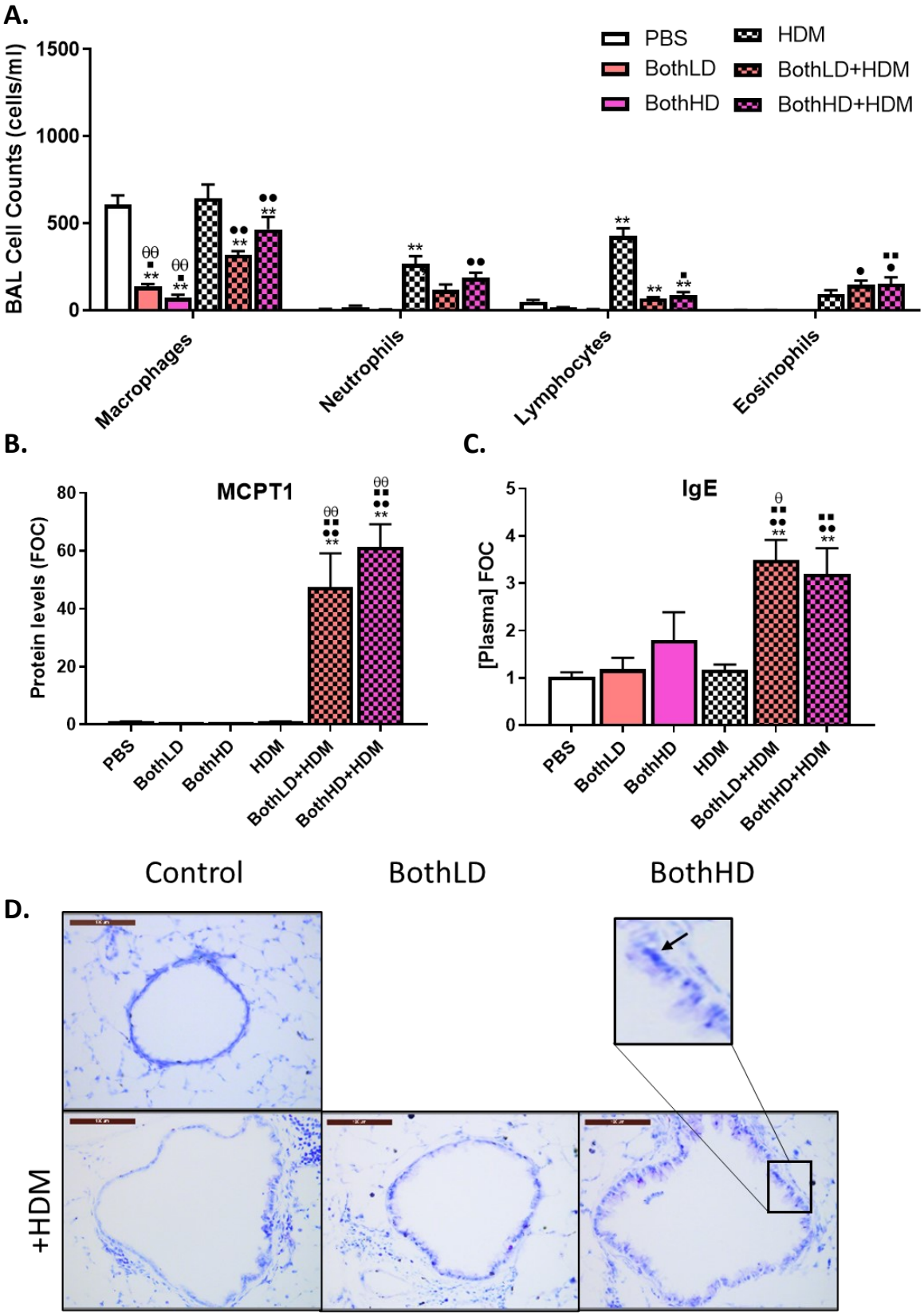


Figure 5-14 Inflammatory cell response and plasma immunoglobulin E after acute and chronic exposure to Both±HDM for 3 weeks. BAL fluid, lung homogenates and blood plasma were analysed for immune cells, tissue mast cell MCPT1 and plasma IgE. A. Cells were counted after being fixed and stained as previously outlined (**section 2.6.4**) and 300-500 cells were counted per animal. The data are presented as the mean ±SEM % total cells counted. B. Lung homogenate MCPT1 (mast cell marker) levels are presented as fold over control levels (FOC±SEM). C. Blood plasma of IgE levels using analysed by ELISA. D. Lung tissue was fixed and stained with toluidine blue (TB), to highlight tissue mast cells (section 2.7.2.7). Representative images of each group are displayed with a scale bar of 100µm (top left of image). N=5-9 mice per treatment group, with all assays performed in triplicate. Significance is denoted as the following, as indicated: compared to PBS or HDM control p<0.05(*), <0.01(**), <0.001(***); compared to DEP alone p<0.05(•),<0.01(••), <0.001(•••).

5.4.4.3 *Effect of single and repeat CeO_2NPs±HDM exposure on gene expression changes in lung tissue*

Gene expression changes were analysed using real time-PCR for a variety of different genes (Figure 5-15). There were no changes in the expression of IL-25, IL-13, CCL24, TSLP and CCL26.

There was a non-significant increase in the expression of CCL17 after exposure to BothLD+HDM and BothHD+HDM when compared to BothLD and BothHD alone and HDM. There were no significant changes in the expression of IL-8, but there was a dose dependant increase when comparing CeO_2LD/HD+HDM to DEP+HDM and BothLD/HD+HDM.

There was only a significant increase of MMP12 in BothHD+HDM when compared to HDM control and CeO_2HD+HDM. This was also seen in the expression of CD177. There was a dose dependent increase in IL-33 expression with a significant increase after exposure to BothLD+HDM when compared to BothLD alone and CeO_2LD+HDM, and after exposure to BothHD+HDM when compared to BothHD alone, CeO_2HD+HDM, and DEP+HDM.

There was a significant decrease in CCL8 expression after exposure with BothHD+HDM when compared to CeO_2HD+HDM, and a significant increase in BothLD+HDM when compared to CeO_2LD+HDM. IL-4 expression was significantly increased after exposure to BothHD+HDM when compared to BothHD alone.

The expression of AREG was significantly increased after exposure to BothLD+HDM and BothHD+HDM when compared to HDM control, BothLD and BothHD alone and CeO_2LD+HDM and CeO_2HD+HDM.

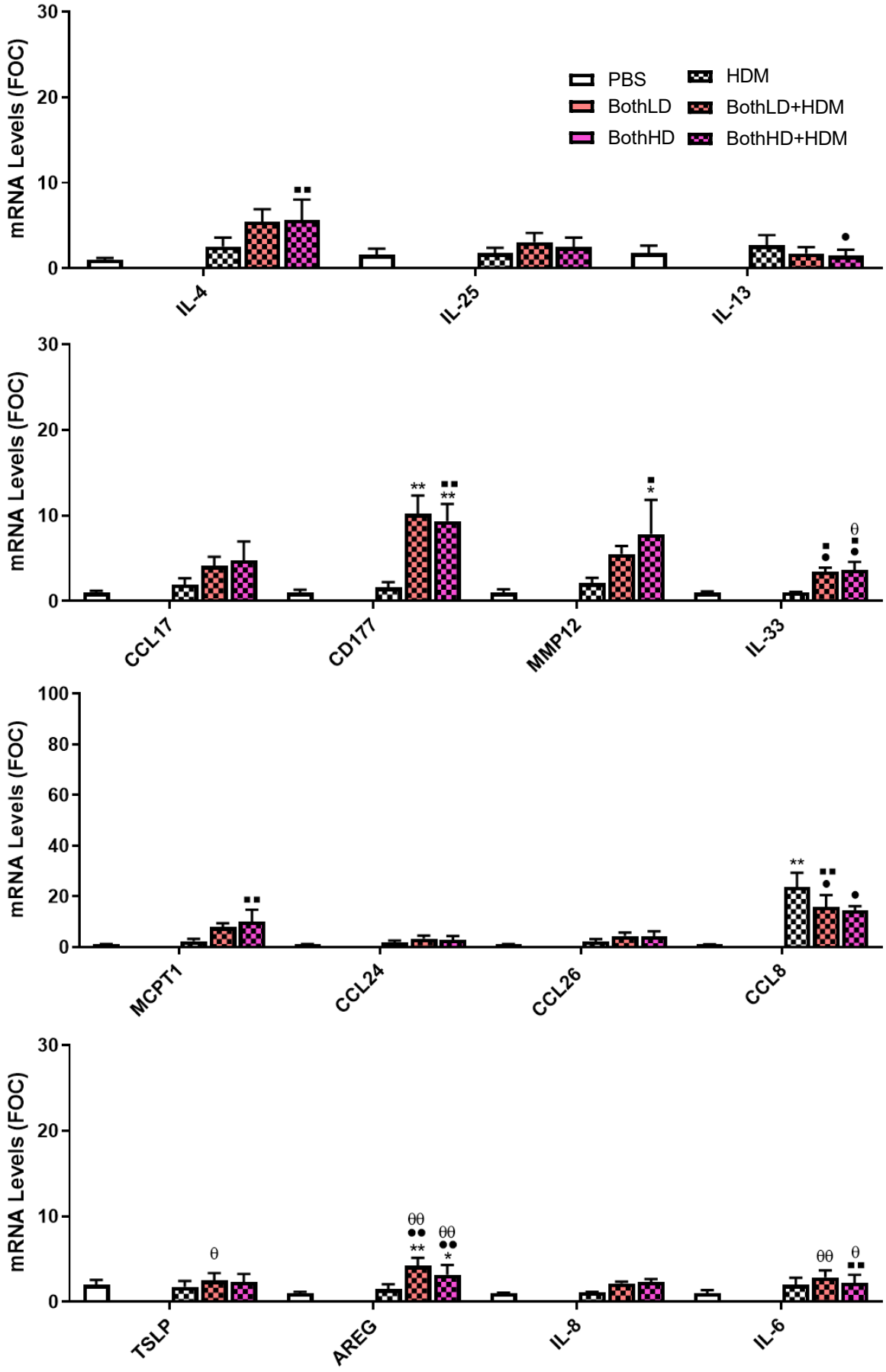


Figure 5-15 Inflammatory marker gene expression in lung tissue after various Both±HDM exposure combinations over 3 weeks. Total lung mRNA was isolated for indicated inflammatory markers via RT-PCR. Results are presented as ±SEM fold over control levels (FOC). N=5-9 mice per treatment group, with all assays performed in triplicate. Significance is denoted as the following: compared to PBS or HDM control p<0.05(*), <0.01(**), <0.001(***); compared to particles alone p<0.05(•), <0.01(••), <0.001(•••); compared to CeO_2NPs+HDM p<0.05(▪), <0.01(▪▪), <0.001(▪▪▪); and compared to DEP+HDM p<0.05(Θ), <0.01(Θ Θ), <0.001(Θ Θ Θ).

5.4.4.4 Effect of CeO_2NPs+DEP±HDM exposure on inflammatory markers assessed by ELISA of BAL fluid

BAL fluid was analysed for a number of cytokines via ELISA (Figure 5-16). There was no change in the BAL fluid concentration of CCL20 or IL-4.

There were no significant differences in the concentration of IL-33 following any of the exposure regimens. There was however a decrease after DEP+HDM exposure when compared to HDM alone which was ameliorated by the addition of cerium and even more so with the higher cerium concentration.

There were significant increases in the CCL17 concentration after exposure to BothLD+HDM and BothHD+HDM when compared to the HDM control, BothLD alone and BothHD alone and DEP+HDM. There was a significant increase in CCL11 concentration in the BAL fluid after exposure to BothLD+HDM when compared to CeO_2LD+HDM, and an increase in IL-5 concentration after exposure to BothHD+HDM when compared to CeO_2HD+HDM.

IL-13 concentration was significantly increased after exposure to BothHD+HDM and BothLD+HDM when compared to BothHD and BothLD, however, it was significantly decreased after these exposures when compared to the HDM control. This was also reflected in the concentration of TSLP when compared to the HDM control.

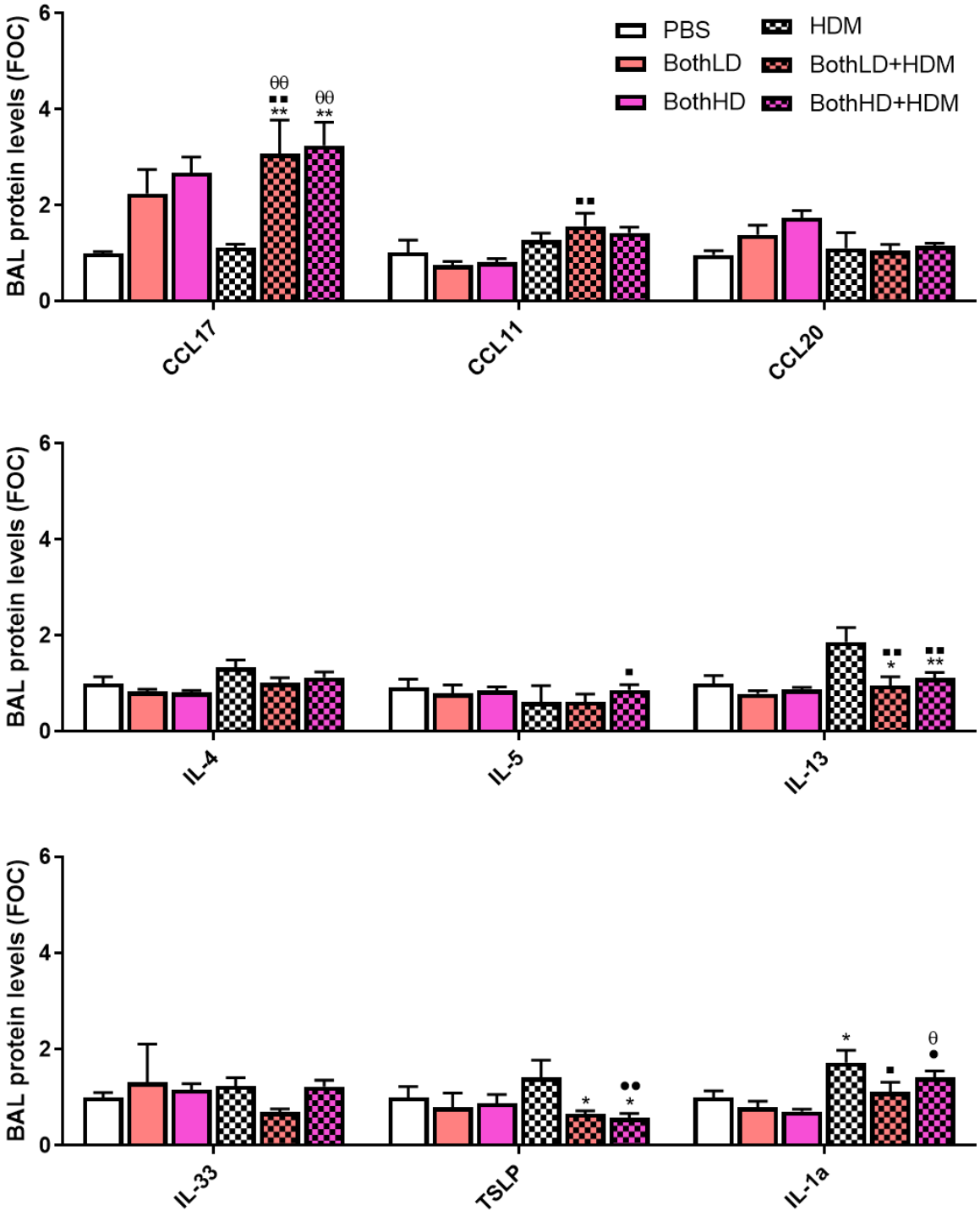


Figure 5-16 Inflammatory cell response and cytokine release after various Both±HDM exposure combinations over 3 weeks. BAL fluid was analysed for different released cytokines. Cytokines were measured in the BAL fluid and are presented as ±SEM fold over control levels (FOC). N=5-9 mice per treatment group, with all assays performed in triplicate. Significance is denoted as the following: compared to PBS or HDM control p<0.05(*), <0.01(**), <0.001(***); compared to DEP alone p<0.05(•), <0.01(••), <0.001(•••).

5.4.4.5 Effect of CeO_2NPs+DEP±HDM exposure on airway mucin production

Mucin production within the airways can be analysed in numerous ways, including PAS, and CLCA1 staining (Figure 5-17), PAS scoring and analysis of gene expression levels of MUC5AC, CLCA1 and SLC26A4 (Figure 5-18).

PAS and CLCA1 stains of serial sections can indicate the levels of the marker within the airways (Figure 5-18, A), and shows that introduction of HDM to the airways does make a difference in the intensity of the PAS and CLCA1 staining when compared to the particle exposures alone.

When the PAS scores were quantified (Figure 5-18, A), a significant increase in the score was observed after exposure to BothLD+HDM and BothHD+HDM when compared to HDM alone, and BothLD and BothHD alone, CeO_2LD+HDM, CeO_2HD+HDM, and DEP+HDM.

There were significant decreases in the MUC5AC, and CLCA1 expression (Figure 5-18, B+C) after exposure to BothLD and BothHD when compared to CeO_2NP+HDM and DEP+HDM. There was a significant increase in the expression of SLC26A4 (Figure 5-18, D) after exposure to BothLD+HDM and BothHD+HDM when compared to the HDM control, and BothHD alone (for BothHD+HDM only).

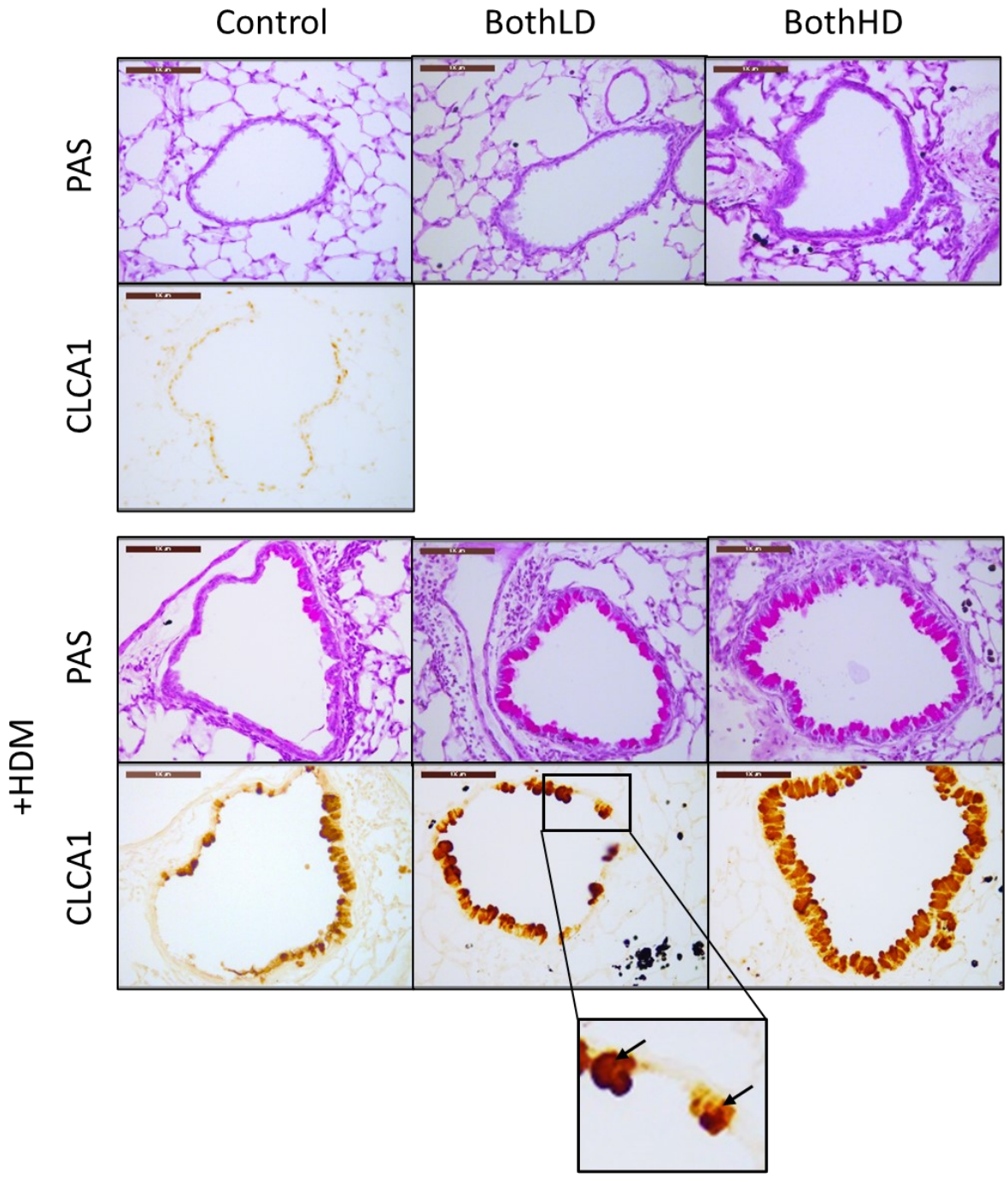


Figure 5-17 Airway mucin analysis after various Both±HDM exposure combinations over 3 weeks.
Lung tissue was fixed, and sections processed for PAS staining (top panel) and immunohistochemical staining of CLCA1 (bottom panel). Representative images of each group are displayed with a scale bar of 100µm (top left of image).

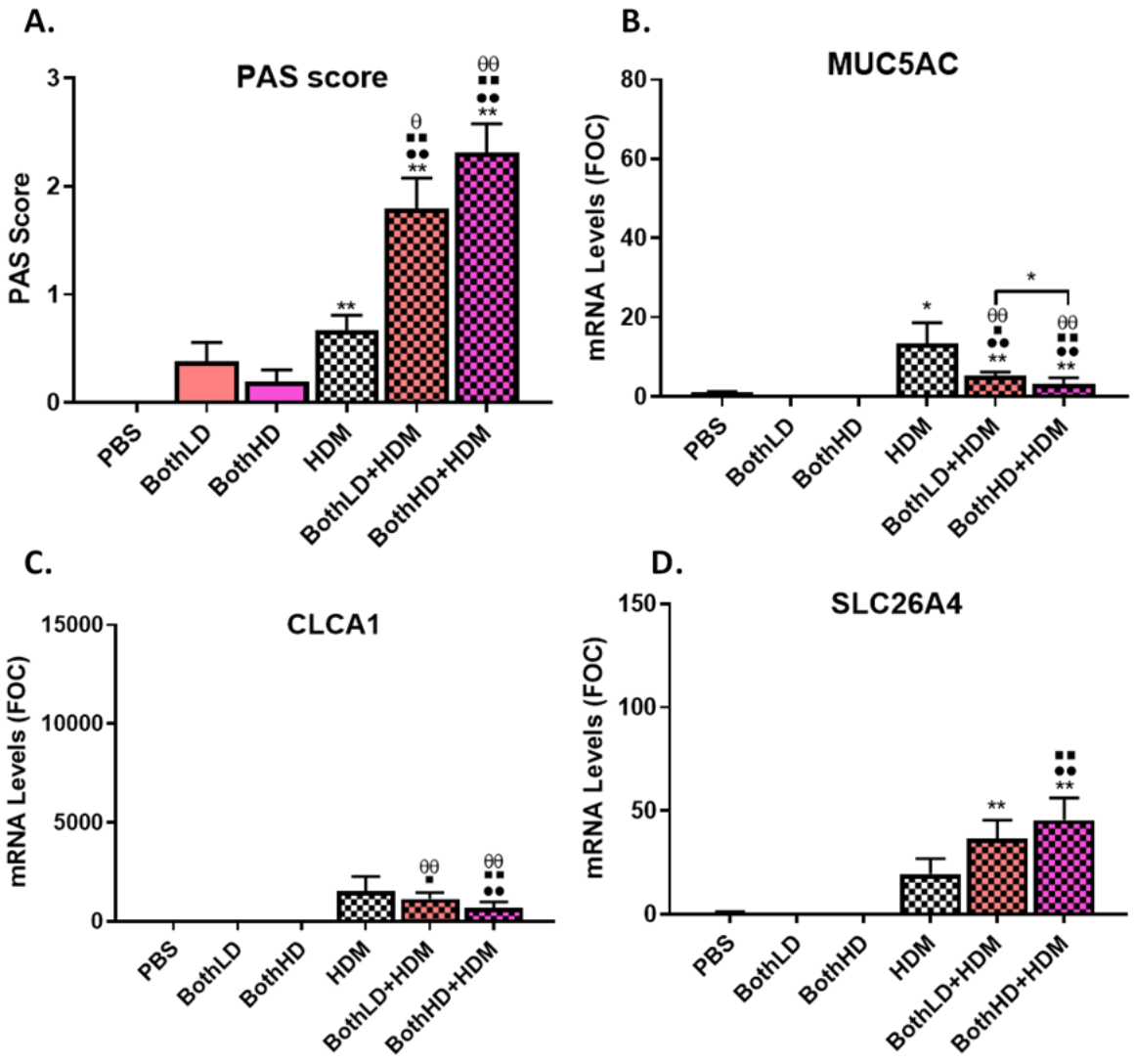


Figure 5-18 Airway mucin analysis after various Both±HDM exposure combinations over 3 weeks.
A. Quantification of PAS positive cells within the airways was scored and graphed. B-D. Lung mRNA was isolated and analysed implementing RT-PCR for expression of mucin related genes. Results are presented as ±SEM fold over control levels (FOC). N=5-9 mice per treatment group, with all assays performed in triplicate. Significance is denoted as the following: compared to PBS or HDM control $p<0.05$(*), <0.01(**), <0.001(***); compared to particles alone $p<0.05$(•), <0.01(••), <0.001(•••); compared to CeO_2NPs+HDM $p<0.05$(▪), <0.01(▪▪), <0.001(▪▪▪); and compared to DEP+HDM $p<0.05$(Θ), <0.01(Θ Θ), <0.001(Θ Θ Θ).

5.4.4.6 Effect of CeO_2NPs+DEP±HDM exposure on structure, remodelling and function of the lung

Masson's trichrome (M.T.), α-smooth muscle actin (α-sma) and PCNA were stained for on serial lung sections (Figure 5-19) after the various exposures in order to determine changes in airway remodelling. All three show a similar pattern of change after instillation and can be seen to increase in groups that have both HDM and particle exposures. It is difficult to determine the differences in the intensity of the colour of the stain further than that and to distinguish if any of the co-HDM exposures have differences between them.

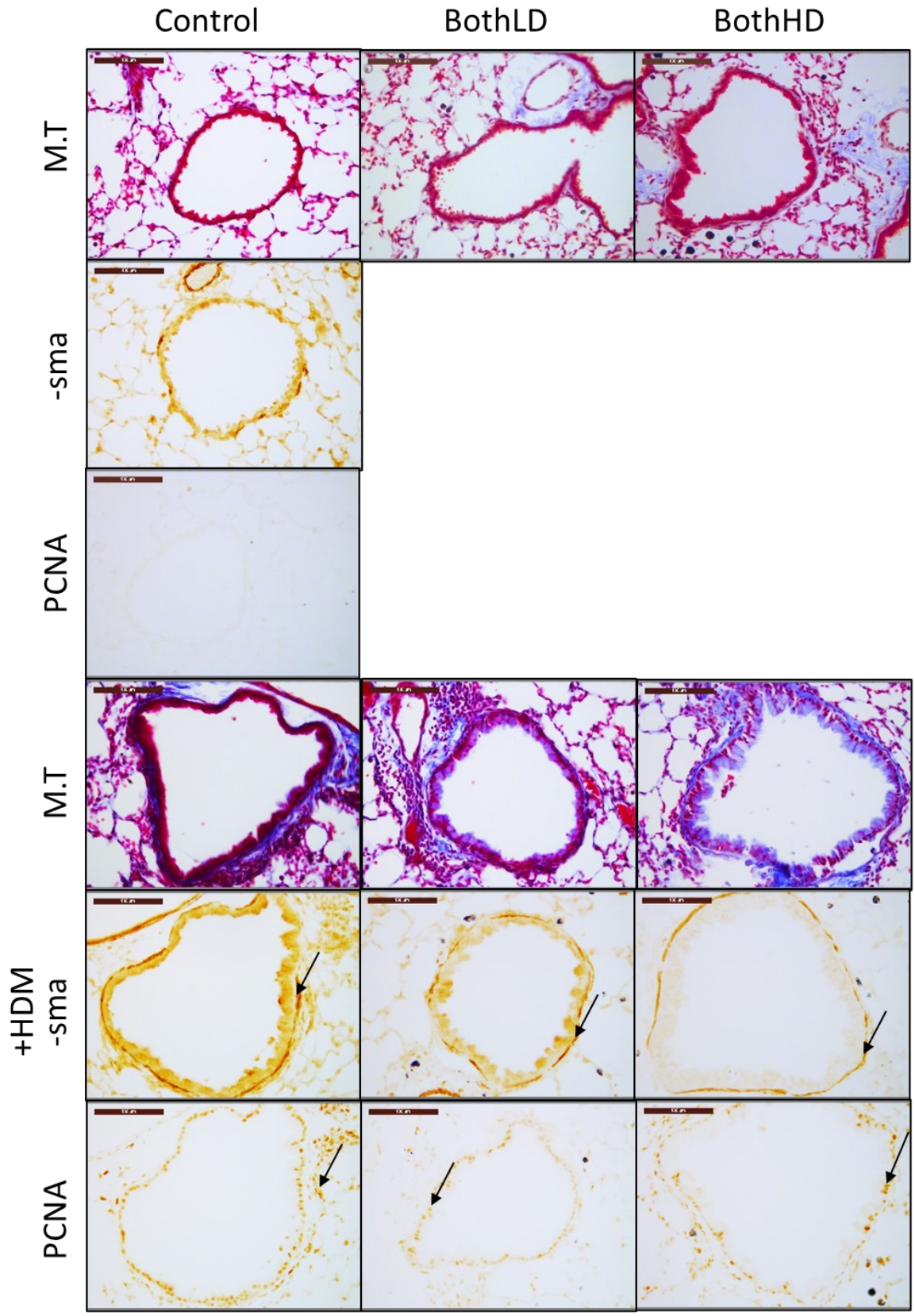


Figure 5-19 Airway structure after Both±HDM exposures over 3 weeks. Lung tissue was fixed, and sections processed for M.T staining (top panel) and immunohistochemical staining of α-smooth muscle actin (α-sma) (middle panel) and proliferating cell nuclear antigen (PCNA) (bottom panel). Representative images of each group are displayed with a scale bar of 100μm (top left of image). Positively stained cells are indicated with arrows.

Using methacholine the responsiveness of the airways can be measured after inhalation. PBS, CeO_2HD alone, DEP alone, HDM alone, CeO_2HD+HDM, DEP+HDM, BothLD and BothHD exposed animals were assessed. There were no changes in the respiratory system resistance (Rrs) (Figure 5-20, A), and tissue elastance (H) (Figure 5-20, C) in any of the groups following inhalation of methacholine. There was a significant increase in the Newtonian resistance (Rn) (Figure 5-20, B), and elastance (Ers) (Figure 5-20, D) after exposure to CeO_2HD+HDM when compared to the other groups.

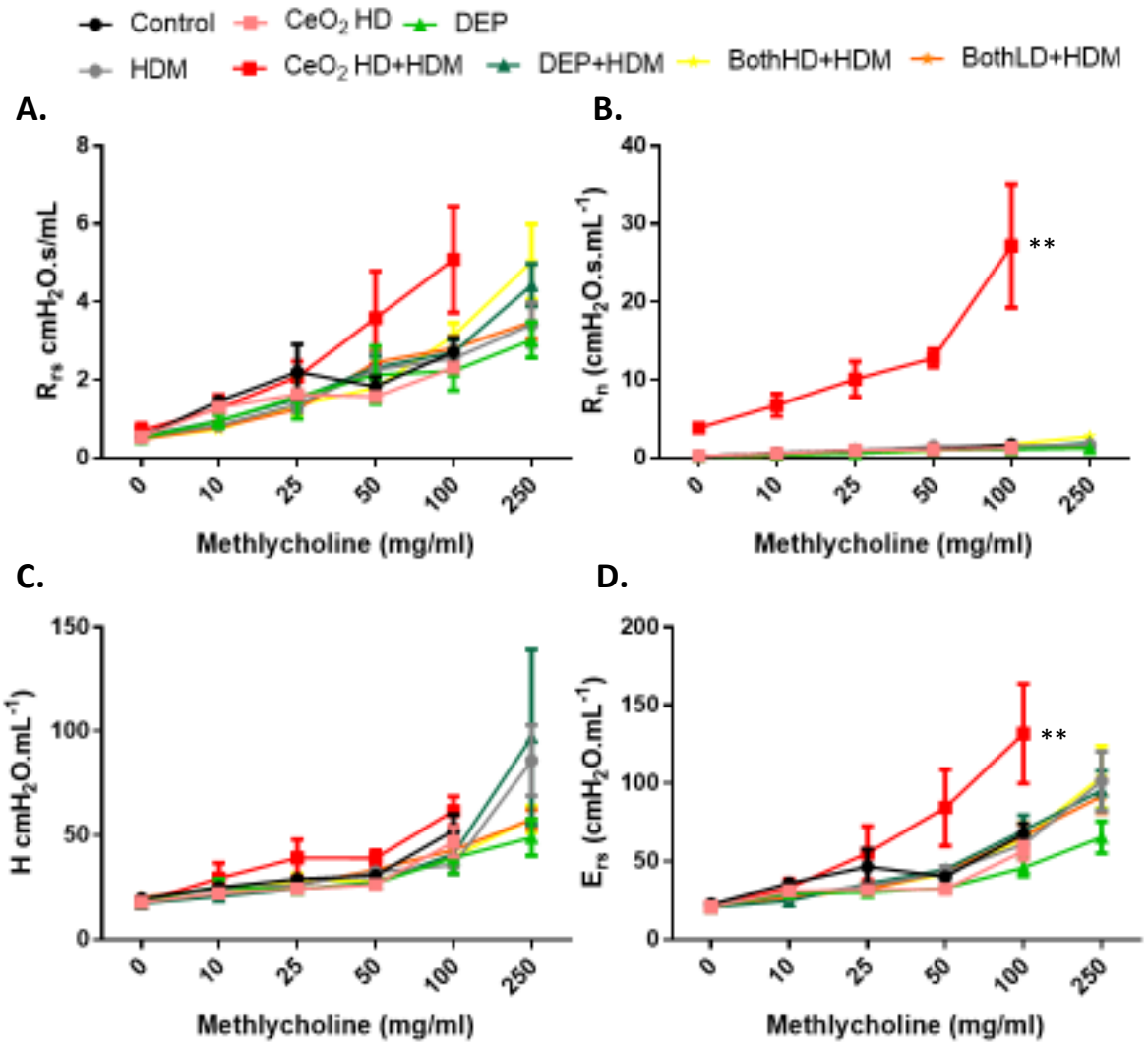


Figure 5-20. Airway lung function analysis after various Both±HDM exposure combinations over 3 weeks. Airway hyperresponsiveness to increasing concentrations of inhaled aerosolised methacholine, was assessed using a forced oscillation technique. A. Respiratory system resistance (Rrs), B. Newtonian resistance (R_n), C. tissue elastance (H) and D. elastance (E_{rs}) were calculated using flexivent system sotware. Results are presented as ±SEM. N=5-9 mice per treatment group, with all assays performed in triplicate. Significance is denoted as the following: compared to PBS or HDM control p<0.05(*), <0.01(**).

5.5 Discussion

In this chapter, we examined how CeO_2NPs as a component of diesel exhaust particulate material may modify the immunological and pathological effects of DEPs and their ability to influence a murine HDM exposure model of allergic airway disease. We first examined the impact of DEP and HDM pulmonary exposure either alone or in combination on markers of airway inflammation including structural and mucin regulation. This was used to determine baseline responses to material exposure and to establish exacerbation and adjuvant interactions of particles and allergens. Pulmonary co-exposure with CeO_2NPs at doses reflective of the ratio present in DEPs from CeO_2NPs fuel catalyst doped diesel fuel exhaust material was designed to reveal any interaction indicative of modifying effects on airway disease.

5.5.1 24 hour exposures

24 hours after exposure to DEP+HDM there was a significant increase in the number of neutrophils when compared to DEP alone and HDM control. Macrophage numbers were significantly decreased after exposure to DEP alone when compared to the control (Figure 5-3, A). An increase in macrophage and neutrophil numbers was also observed 24 hours after a DEP alone inhalation exposure (Dybdahl et al., 2004), indicating that exposure method does not influence changes in cell counts and these changes were independent of exposure methods. These results also resemble the CeO_2NPs cell count results and indicate that the early immune response to both particle types is mainly a macrophage and neutrophil response with no changes in the eosinophils and lymphocyte cell counts and the co-exposure with HDM enhances this response to both particle types. In our study, we saw no changes in eosinophil cell counts after 24 hours of exposure. It has been identified in a different study, if the animals are left to recover for 7 days after a single intratracheal instillation, there was an increase in eosinophil cell counts after DEP+HDM when compared to DEP or HDM alone (Singh et al., 2005), again reinforcing the fact that this response is seen after a longer time scale.

There were no changes in the cytokines measured in the BAL fluid, except for the concentration of IL-5 after exposure to DEP+HDM when compared to DEP alone in our study (Figure 5-3, B). Acute inflammatory response of the airways to DEP consisted of increased expression of IL-8 and IL-13 in the epithelial cells and an increase in NF-kB in humans after inhalation (Pourazar et al., 2005) of DEP in human volunteers. Activation of NF-kB occurs which triggers TNF-α, MIP-2, IL-6, IL-8, COX-II and iNOS (Schins and Donaldson, 2000). Increases in IL-6 concentrations (Nemmar et al., 2011) as well as gene expression (Dybdahl et al., 2004) were identified after exposure to DEP alone when compared to the control. Co-exposure to

DEP+HDM caused an increase in IL-4, 13, and TNF-a after 7 days recovery post instillation in Brown Norway rats (Singh et al., 2005).

There were no changes in any of the histology sections (stained with H/E, PAS or M.T.) at 24 hours after exposure to any of the exposure regimens (Figure 5-2). Any airway remodelling or changes to the histology of the lung might be expected to take longer than 24 hours; pathological changes have been found to develop after months of chronic allergen exposure (McMillan and Lloyd, 2004) and therefore no changes would be expected until a later time point.

The next section will focus on the acute exposure of Both+HDM.

The investigation following exposure to Both+HDM was analysed 24 hours after intranasal instillation. There was a significant decrease in the number of macrophages counted in the BAL fluid after exposure to both BothLD+HDM and BothHD+HDM when compared to HDM alone, however, these exposures lead to a significant increase in the number of neutrophils in the BAL fluid again when compared to the HDM control (Figure 5-12, A).

There was no change in the concentration of IL-33, IL-5 or IL-4 in the BAL fluid after either BothLD+HDM or BothHD+HDM exposures. Concentration of CCL20, IL-1α and TSLP was significantly decreased after exposure to BothHD+HDM when compared to CeO_2HD+HDM (Figure 5-12, B),

There were no identifiable changes in the and in the physiological stained sections (Figure 5-13).

5.5.2 3 week exposures

DEP is a foreign body within the lung and interacts with the lung tissue after inhalation for 4 weeks (Hiramatsu et al., 2003), and therefore causes additional inflammatory responses that are enhanced by the addition of the allergen. When combined, it has been identified that the co-exposure effects of DEP+HDM could be due to Der pII that is found within HDM (Suzuki et al., 1996) and is implicated in the allergic response as well. Der pII protease activity is known to activate the release of IL-6 and IL-8 (Kauffman et al., 2006) and is one of the most clinically relevant allergens in the world (Cao et al., 2016).

After exposure to BothLD and BothHD alone exposures there was a significant decrease in the macrophage count in the BAL fluid when compared to the control (Figure 5-14, A). This was the same after BothLD+HDM and BothHD+HDM exposures when compared to the HDM control.

We saw no changes in the neutrophil cell count after BothLD or BothHD alone when compared to the PBS control, but there was a significant increase after BothHD+HDM exposure when compared to BothHD alone. The expression of CD177 (neutrophil chemoattractant) and CCL8 (monocyte chemoattractant) as well as MMP12 (matrix metalloprotease) all have reduced expression in the mice exposed to BothHD+HDM when compared to the CeO_2HD+HDM, again implying that DEP subdues the pro-inflammatory and possible injurious effects of CeO_2 seen in the presence of HDM (Figure 5-15). In a previous study, an increase in BAL neutrophils was also seen after an IP injection (which is not as relevant as some of the other exposure models) in the eosinophil and neutrophil cell counts when exposed to DEP+HDM when compared to either DEP or HDM alone (Takahashi et al., 2010).

There was also a significant increase in the eosinophil cell count in the BAL after BothLD+HDM and BothHD+HDM when compared to BothLD and BothHD alone. Previous work has shown that DEP alone did not induce traditional asthma-like symptoms of increased eosinophils (Brandt et al., 2013a), as was also seen in our study. Rather, there was an increase in neutrophils after DEP alone (Gavett et al., 2015) when compared with the control, which was equal to the HDM alone count. There were no changes in the expression of CCL24 or CCL26 (eosinophil chemoattractants) following combined particle exposure when compared to any of the other exposure groups. Overall, these data suggest that DEP suppresses the stimulatory effects of CeO_2NPs exposure on immune cell attraction and the immune response, specifically Th2-response mRNA expression.

With regard to the BAL fluid concentrations of cytokines (Figure 5-16) after exposure to both particles with HDM, IL-4, IL-13, TSLP and IL-1α, CeO_2NPs had no effect on the stimulation induced by HDM alone. In contrast, DEP markedly inhibited the effects of HDM. When DEP was instilled with CeO_2+HDM, it also markedly reduced the effects HDM and CeO_2, but not quite to the same extent as for DEP+HDM; this suggests that CeO_2 interfered with the inhibitory effect of DEP alone on the effect of HDM, although it was not significant. The expression of the majority of genes analysed did not change in response to the addition of CeO_2 to the DEP during exposure but there were patterns forming that may have become significant after longer exposure.

There was also a significant increase in mRNA expression of AREG (i.e., pro-fibrotic growth factor) after exposure to BothLD+HDM and BothHD+HDM (Figure 5-15). The upregulation of AREG mRNA indicates the potential for increased lung fibrosis and therefore further damage to the lung after this exposure combination, as suggested previously (Wang et al., 2005). This is supported by an increase in the distinctive blue staining of collagen following M.T staining, observed in the BothHD+HDM group when visually compared to M.T staining following the other exposure regimens (Figure 5-14, D).

The expression of MMP12 (matrix metalloprotease) was only significantly increased after exposure to DEP+HDM RPT when compared to the HDM control (Figure 5-5). With respect to changes in mast cells, there was a significant increase in MCPT1 mRNA expression (mast cell marker) after exposure to BothLD+HDM and BothHD+HDM when compared to the HDM control and BothLD and BothHD alone (Figure 5-14). There were no changes in the in the TB staining, which would highlight mast cells, after any of the exposures, however this was not quantified (Figure 5-14, D).

There were no changes in the eosinophil chemoattractant protein mRNAs (CCL24 and CCL26) after any of the exposures (Figure 5-15) which again agrees with the BAL fluid cell counts (Figure 5-15, A). In other studies, this has been found to not be the case and animals exposed to both DEP+HDM have been found to exhibit a significant increase in neutrophil and eosinophil chemoattractants after intratracheal instillation (Fahy et al., 2000) in the BAL fluid. This could be due to the HDM exposure regime and the method of exposure.

There were also significant increases in the IgE concentration after exposure to BothLD+HDM and BothHD+HDM when compared to the HDM control and BothLD and BothHD alone (Figure 5-14, C).

There were decreases in the Th2 cytokine expression (IL-4 (significant), IL-25, and IL-13) after exposure to BothHD+HDM when compared to CeO_2HD+HDM (Figure 5-15), suggesting that the addition of DEP causes a dampening of the Th2 immune response when compared to the CeO_2NPs alone. This was not found to be the case in the absence of HDM. Ma *et al.,* previously showed that exposure to CeO_2 and DEP combined stimulated further macrophage activation as well as inducing IL-12 and IFN-y secretion and causing an increased fibrotic response when compared to either particle delivered alone (4 weeks post exposure; (Ma et al., 2014a)).

Other studies have found that the repeat instillation of DEP+HDM led to increased inflammation, goblet cell metaplasia, Th2 cytokines/Th17 cytokines, dendritic cells, and T cell activation (IL-17A, IL-17, IL-13, IL-4,5, CCL11, CCL20) (Acciani et al., 2013). Increased IL-13 (Gavett et al., 2015) was linked to an increase in IL-17A, and the neutralising of this IL-17A (using a rat anti-murine antibody) was shown to prevent the increase in asthmatic symptoms in this specific study (Brandt et al., 2013a). This is the opposite to our results where the addition of HDM has actually decreased the TH2 response (both in the BAL fluid concentration (Figure 5-16) and the mRNA expression (Figure 5-15)). This could potentially be due to the differences in DEP used (differences between diesels has been well documented and a simple difference of location of collection and burning engine has the potential to change the immune response to the particles) and the HDM used in the sensitisation process (as previously discussed, the concentration of the HDM does not matter, but the type and supplier does).

It was previously found that, although iNOS and oxidative stress increased after 24 hours, this then decreased after 4 weeks of exposure to DEP (Hiramatsu et al., 2003 and Fahy et al., 2000), suggesting that ROS production is only relevant for a short amount of time, as has been found for other studies (Dickinson and Chang, 2011) and causes its effects during early exposure.

The addition of HDM to the DEP decreased the responses relating to mucin production (increased MUC5C, SLC26A4 and CLCA1 mRNA expression; (Figure 5-9, B, C and D) when compared to the HDM alone, this response was then increased again after addition of CeO_2NPs to the DEP. This would suggest that BothLD or BothHD exposure with HDM is required to change the mucin production response when compared to DEP alone and HDM alone. In contrast, the PAS score (Figure 5-18, A) was enhanced in both BothLD+HDM and BothHD+HDM groups when compared to the DEP alone, HDM alone and BothLD and BothHD alone. Interestingly, HDM alone also caused an increase in PAS positive cells above DEP alone, BothLD and BothHD alone, suggesting that a significant part of the increased PAS response in the combined exposures was due to HDM, which also caused a PAS response. This response was therefore quite independent of the mucin-related change in gene expression which depended on repeat exposures.

Although there was no difference in BAL IL-33 levels (Figure 5-16), there were increases in tissue mRNA expression of IL-33 after exposures to BothLD+HDM and BothHD+HDM when compared to the single particle+HDM exposures (Figure 5-15). As IL-33 is implicated in the development of asthma (Oboki et al., 2011), but also has a short half-life in lung secretions,

upregulation of the tissue mRNA likely better reflects the importance of IL-33 allergic response to combined exposure to Both+HDM.

The combined particle+HDM exposure significantly increases the PAS score (Figure 5-18, A), while all other markers of mucin production are reduced. The exposure of Both+HD matches that of the DEP+HDM exposures and diminishes the stimulatory effects that CeO_2NPs have on the HDM-induced mRNA expression of MUC5AC (Figure 5-18, B), CLCA1 (Figure 5-18, C) and SLC26A4 (Figure 5-18, D). Thus, the BothHD+HDM exposure-response is significantly decreased when compared to the CeO_2HD+HDM exposure. The particles alone (without HDM) caused no changes in any of these parameters measured. This indicates a reduction of mucus production (also seen in the DEP+HDM group) that is then enhanced by the addition of CeO_2NPs to the DEP.

There were no changes in the AHR after any of the exposures (Figure 5-20), nor were there any changes in the collagen deposition, smooth muscle actin and PCNA in the lung sections (Figure 5-19) after any of the exposures. Another study found the opposite of this and the addition of DEP exacerbated increases already seen following HDM exposures, increasing AHR and fibrosis with co-exposure compared to HDM alone (Takahashi et al., 2010). It is worth mentioning that this latter study used a different source of freshly produced DEP, and the HDM was Der f, whilst the study lasted 30 days, all of which could have contributed to this different outcome. The adjuvant effect of both DEP+HDM has been shown previously to cause a significant increase in airway resistance, airway elastance and a decrease in airway compliance after DEP alone (Acciani et al., 2013), which again differs from this study.

Further analysis of location and translocation of these particles within the lungs and other organs are required to be carried out, but it has been identified that there is a time-dependant and concentration dependant accumulation within the lungs and a delayed clearance when mice are exposed to DEP+CeO_2 (Snow et al., 2014b). The increase of AHR and remodelling after exposure to both particles and an allergen when compared to the particles alone have been found to be increased throughout the literature (Inoue et al., 2007).

Taken together, these results indicate that the addition of CeO_2NPs to diesel fuel has the potential to increase the health hazard DEP already poses to both the healthy individual and one with an allergic airway disease. The addition of CeO_2NPs to diesel enhances both the inflammatory and mucin responses within this model in the presence of an allergen (HDM) and

this may lead to the promotion of airway remodelling and a fibrotic phenotype within an allergic airway created with HDM exposures, instead of increasing Th2 responses and AHR.

Chapter 6: General Discussion

6.1 Summary

The aim of this thesis was to determine if pulmonary exposure to cerium dioxide nanoparticles could induce adverse effects with and without diesel particulate exposure in an allergic airway disease murine model. This would then be related back to human health and potential implications for the general population. Health effects of DEP in allergic humans and mice has already been thoroughly established before this study, whereas the addition of CeO_2NPs to the fuel and the potential health effects these particles may have on asthmatics had not previously been investigated and is therefore where the novelty of this thesis lays.

Asthma is a disease that effects many people in the world (Dharmage et al., 2019) and can be caused by numerous different allergens including HDM. The implications of Envirox^{TM} (the CeO_2NP fuel catalyst) on this vulnerable group is important to determine due to the increasing use of this commercially available product and the effects it has on the combustion products of DEP (including reduction of particle size, increase of particulate numbers (Park et al., 2008a)).

From this study it is apparent that DEP and CeO_2 cause different responses within the airways. The concentrations of CeO_2NPs were fifty times less than the DEP concentration used, but this was to replicate a realistic exposure to the concentration of particles found in the environment where these catalysts are being used by commercial vehicles (Park et al., 2008a). CeO_2NPs alone led to the enhancement of an immune response when co-exposed with HDM, but it was unable to induce this response when exposed alone (without HDM). This suggests that CeO_2NPs have the potential to exacerbate asthma symptoms that have already been established but do not have the potential to induce an allergic or asthmatic response by themselves. This could be an important discovery for environmental health and asthmatic patients living in the cities where these catalysts are being used.

DEP enhanced responses were investigated more than the CeO_2NPs, but this could be down to the concentration difference between the two particle types and the receptors that are activated by DEP but not CeO_2NPs such as aryl hydrocarbon receptor due to the polycyclic aromatic hydrocarbons (PAHs) found in the DEPs (Grilli et al., 2018). There was more enhancement of responses to DEP when it was co-exposed with HDM, but there were still responses that are associated with a neutrophilic asthmatic response elicited by DEP exposure alone. This would suggest that DEP can exacerbated asthmatic responses (such as eosinophil attraction, IgE production, and mucus production, but not AHR), but may also potentially led to the

development of a neutrophilic phenotype of asthma after exposure to DEP alone. DEP has previously been implemented in the development of asthma (Pandya et al., 2002) and our results would agree with this potential.

When the particles are mixed (but not burnt) in the same ratio that is found in the environment (and recommended by the manufacturer) there are variations in the responses when compared to the individual particle exposure alone. In some respects, there are protective implications of adding CeO_2NPs to DEP, while in others the addition enhances the DEP response. There is a significant increase in the eosinophils after addition of cerium when compared to the DEP, along with IgE concentrations and mast cell attraction. Th2 cytokines (IL-4, IL-13 and TSLP) are increased as well as CCL17, CCL11 and AREG and the mucus production (PAS score). Responses that are decreased when compared to the cerium exposures include macrophage cell counts MCPT1 expression (but not concentration in the BAL), CCL8, CD177, MUC5AC, CLCA1 and SLC26A4 expression and AHR. This would suggest that there is an increased Th2 response and eosinophil attraction when compared to DEP alone, but a decrease in the neutrophil attraction and gene expression for mucus in the airways as well as AHR when compared to the cerium alone. The combination of both particle types either elicits the same response as DEP, or amplifies the allergic responses seen with co-exposures with HDM. These responses are replicated without HDM, but to a lesser degree. This has implications for public health and there is potential for asthmatic patients in the geographical areas these catalysts are employed to have exacerbation in their symptoms when exposed to these particles, as well as potential effects of these particles on a healthy population.

It is important to compare the *in vivo* to the *in vitro* data to ensure the results are replicable and are consistent between the two models. We initially attempted to expose particles as a dose over area. This was not possible in this study due to incomplete data on cell numbers in murine lungs and concentrations exposed *in vivo* being miniscule when converted to *in vitro* per cm^2. Due to this, the same concentrations were used *in vitro* as *in vivo* for the HDM co-exposure (even thought this will be a much higher exposure per cm^2 when compared to instillation) and smaller concentrations used for the initial particulate exposures without the allergen.

This study has tried to implement as close an environmental exposure as possible with using the correct ratios of particles. As these particles were mixed, they do not represent the physical changes that may have been induced by combustion. The burnt particles would likely be more agglomerated carbon compounds with a cerium core, as it has been identified that after the diesel is burnt with CeO_2NPs there is a decrease in the carbon content (from 91.8% to 79.4%)

and an increase in the cerium content (from 0.3% to 6.5%) after combustion (Zhang et al., 2016). Further work would be to compare the mixture of these particles and the particles that have completed combustion and determine any potential characterisation and cellular response differences between the particles. Consideration also must be made for the fact that these particles are not all that is emitted upon combustion and a variety of different gases would also have to be incorporated into future experimental set ups to establish the full effects of these particles.

As well as the potential changes in characteristics induced by the combustion of the particles, consideration needs to be made for interaction within the airways and after the various exposure methods. This is important if any information wants to be translated between human studies, *in vivo* and *in vitro* studies. This highlights the importance of characterisation of the particles in the exposure medium, to ensure there is consistency between the different exposure methods. These particles will be changed after exposure and will interact with lung lining fluid within the airways which will again change the particulate characterisation. 25µl was used for instillation in this study as it has previously been determined that this volume is sufficient for around 50% deposition of the material within the mouse lung (Southam et al., 2002). To replicate inhalation exposures, higher bolus instillation volumes are required and the nature of exposing a large volume of liquid into the lung potentially causes cytotoxicity itself without considering the particles (Jacobsen et al., 2015b).

6.2 Limitations

Due to the differences in the exposure methods between human studies, *in vivo* and *in vitro*, there is the potential for the protein that coats the particles (the protein corona) to be different between the different exposures. In any biological fluid there are a variety of proteins present which can bind to the surface of the nanoparticles. This creates a protein corona which can then potentially influence how these particles interact in the biological system and the fate of the particle (*in vivo*). This corona can influence the uptake and inflammatory response to these particles. The differences in the protein coronas may induce different cellular responses and therefore cause potential differences between the different exposure methods. This needs to be taken into consideration when thinking about the 3Rs (reduction, refinement and replacement) of scientific animal experimentation. All particles can create a protein corona after being exposed to proteins (from blood, BAL fluid and cell culture medium). The coronas that are formed can be significantly different between particles and exposure fluids (Konduru et al., 2017), and this determines if the particles are taken up by macrophages or not. When DEPs were

incubated with plasma (fibrogen) or BAL fluid (albumin and surfactant protein A and D) DEP+plasma caused no responses from the macrophages, while the DEP+BAL fluid promoted inflammation and significantly increased IL-8 production highlighting the importance of the protein corona on the inflammatory response (Shaw et al., 2016). It is thought that this is a protective mechanism within the respiratory system to stop particulates inhaled having an influence on the epithelial cells (Kendall et al., 2002).

The valence state of CeO_2 is also important in determining the potential toxicity of the particles, and if possible, this state should be measured and recorded. In our study we did not record the valence state of the CeO_2 alone or after it had been mixed with DEP. There are very few studies that focus on the different valence states of CeO_2NPs, and fewer still that measure them. One study analysed the potential differences of CeO_2NPs valences by intratracheally instilling rats and allowing them to recover for 24 hours, 7 days and 84 days before analysis of various end points. This study found that there were no differences in the effects elicited from cerium in either valence state (Dunnick et al., 2016) at any of the recovery time points or any of the inflammatory markers analysed. This suggests that CeO_2 valence state does not matter on inflammatory responses (but this is only one isolated study), but it is still unclear what the addition and sonication may do to the valence state and the influence of inflammatory responses. Due to the fact the particles are being exposed to the cells in culture that have been suspended in medium, the deposition of the particles in this quasi-ALI system (Endes et al., 2014) needs to be considered. The deposition of these particles is important, as the length of time the particles takes to dissipate to the bottom of the liquid (either cell culture medium, or lung lining fluid) is important for how long the cells can interact with the particles and therefore the length of exposure time required with that taken into consideration. Particles diffuse, settle and agglomerate in cell culture medium (Teeguarden et al., 2007) according to their characterisation properties – this means that the characterisation of these particles needs to be completed in the solution they are suspended in and if being aerosolised, the solution they will be entering before the cells. Medium components can be separated into different groups – affect diffusion, agglomeration and gravitational settlings (Teeguarden et al., 2007). The rate and transport of nanoparticles can vary depending on the settling and diffusion rates. An example of nanoparticle settling time is around 1.5 hours in medium 1-2mm deep (100nm gold nanoparticles) (Figure 6-1). For CeO_2NPs specifically, electrostatic interactions may be a major factor in protein absorption and uptake by the cells. A positive zeta potential (Figure 2-1, B)

enhances the absorption of albumin, where a negative zetapotetial enhances A549 cellular uptake (Patil et al., 2007).

Information from the characterisation is also important for determining which *in vitro* model to use (which cell types and culture types). A smaller particle can impact the lung further and

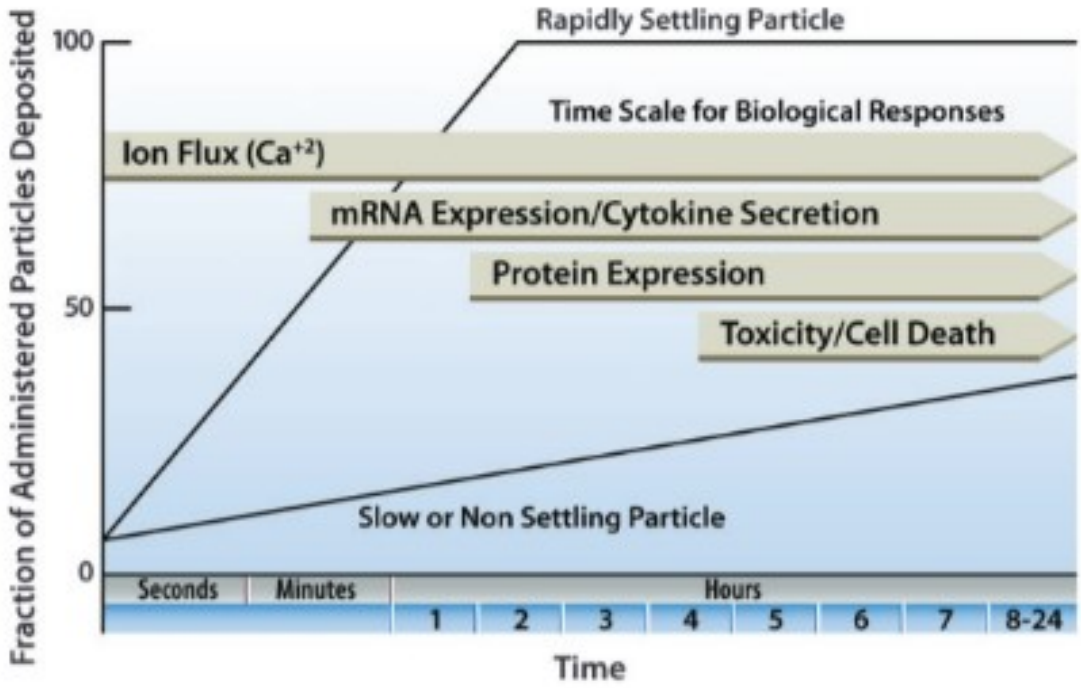


Figure 6-1. Particle transport rate *in vitro*. The influence of the transport rate and time with the biological response. The rate and transport of a particle can vary significantly depending on particulate type due to the differences in settling and diffusion rates (Teeguarden et al., 2007).

be deposited further down the airway into the alveolar areas. Larger particles are more likely to be deposited in the large airways (Heyder, 2004). Deposition can be influenced by both shape, and exposure route (inhalation, instillation (nasal or pharyngeal aspiration), and injections). Obviously, some are more environmentally relevant, but there are numerous reasons why one would be picked over another, including cost and equipment implementations. The deposition from these exposure routes can be modelled *in silico* to determine the potential location. This evidence can also be backed up with laser ablation and ICP-MS on lung sections from our study to determine the deposition within the airways for our specific particles. After analysis of these slices, it allowed us to choose bronchial epithelial cells as our *in vitro* model to represent human cells where these particles are deposited in the *in vivo* models. Another way of determining the particle distribution after various exposures is to radio label them. Radio-labelled CeO_2NPs were intratracheally instilled, inhaled (particles suspended in liquid before being aerosolised and inhaled) and insufflated (this is a dry powder aerosol exposure route). Deposition varies between different exposure methods, instillation and inhalation has similar distribution.

Insufflation has a significant deposition in the trachea and a heterogeneous lung disposition. These techniques change the deposition of the particles and therefore the potential toxicology of the particles (Molina et al., 2016).

To assess various changes between strains of mice, different strains need to be exposed to the same particles in the same way (Ichinose et al., 2004). This study highlighted the variances between mice strains and the potential for the wrong strain to allude to extreme responses that are not present in other strains. It is not feasible to expose various strains of mice/rats to different particles, so care needs to be taken before undergoing such specific inflammatory response studies *in vivo*.

As well as considering the variations in strains, the allergens used to develop this allergic asthma model should also be considered. HDM extracts were used in this study instead of OVA or other allergens due to its implementation in human asthma development. HDM extracts from different sources can also vary massively, this is due to the fact that 17 components have been identified from *Dermatophagoides pteronyssinus* (Der p) (Kim et al., 2015) and Der p 1 and Der p 2 are the major allergens (Van Der Veen et al., 2001). One study (Post et al., 2012) analysed three different HDM extracts and their effects on the epithelial cell layer *in vitro* and *in vivo*. The HDM was acquired from Greer, Citeq Biologics and ALK-Abello (three different companies that are based in three different countries), and it was found that the HDM from Greer had caused the most effects on the epithelial layer compared to the others (Citeq Biologics and ALK-Abello), including reduction of TEER, increases in CCL20 and GM-CSF (*in vitro*) goblet cell hyperplasia, CCL20 and CCL17 IgE and an increase in AHR (*in vivo*). For this reason, HDM from Greer was used throughout our study both *in vitro* and *in vivo*.

In our study we investigated the effects of particles given at specific time points and were only able to analyse these due to time constraints. Further investigation into the behaviour and interaction of the particles and the allergen is required to determine their relationship. One such study would be to switch the exposures and expose the mice to the particles for 3 weeks and then have a single exposure of HDM before analysis or the exposure with DEP throughout and then a change at the end to the burnt DEP+CeO_2NPs to represent a changing environment using these particles. It must also be noted that within our study the *in vivo* work was completed over 3 different sets of experiments. This was due to the number of animals required for these experiments and the time and physical constraints that are expected with this type of work. It was important to ensure the welfare of the animals was at a consistently high standard, something that would not have been possible if all *in vivo* work was completed together.

Our study, as well the majority of the literature, focuses on animals of a certain age (between 6-8 weeks), whereas responses in other age groups (such as the young and the elderly) that are also vulnerable to the development of an asthmatic response and reaction to various particles, including those from vehicles and diesel engines. Mucus hyperplasia, eosinophil and lymphocyte counts and IgG1 were increased in older mice exposed to HDM. AHR was reduced in older mice and a neutrophil profile was increased, enhancing the Th17 response compared to the young mice (Brandenberger et al., 2014). This indicates that there is an age difference and the impact of HDM alone does have an age variation. On the opposite end of the spectrum, the young can also be affected differently to particulate exposure. The youngest and potentially most vulnerable are those still *in utero* (Paul et al., 2017).

There is also a difference in the responses to both HDM and the particles between the sexes. We have used female mice as they are easier to handle and slightly smaller, whereas more males are affected by asthma at a younger age and male mice may be more relevant to study the effects these various particles have in this age group (Postma, 2007). On the opposite side of this, it has been found that female mice were more sensitive to exposures in a COPD model (Tam et al., 2016).

Other groups of people that are more susceptible to the impacts of particulate exposure are these that already have pre-existing conditions or those with an already changed inflammatory profile. For example, there is a strong epidemiological link between obesity and development of asthma. Obese mice had lower eosinophils and higher macrophage counts in BAL when compared to normal mice, increases of M1 and M2 macrophage markers and cytokines (IL-4/5). Obese asthmatics struggle more with treatments options and steroid resistance when compared to normal weight patients (Diaz et al., 2015). There is the potential for the type of inflammatory response to be changed if the baseline response is different from normal.

6.3 Future work

A section that has been omitted from this thesis is the completion of transcriptomics using the samples previously analysed. Samples were sent externally to be analysed, which was not completed during the time frame of this thesis, which is currently being carried out and prepared for publication. It is important to mention that this analysis was completed as it would be a logical next step after both the protein and the RNA analysis of the samples.

With the constant development of diesel fuel trying to improve emissions and economy, the particles used in this study are no longer as relevant as they once were. NIST 2975 particles are

from burning of diesel fuel in a heavy industrial forklift engine and are not representative of what is now being emitted on the roads of the UK. The only way to get representative particles are to physically collect particles from the street and test these on current systems. This approach comes with its own problems, such as the time it takes to collect sufficient material to complete analysis on and exposures with; uncertainty over exactly where the particles have come from (these will be mixed fuel particles as well as general vehicle wear particles (brake and tyre wear for example) and the particles collected will vary massively with seasons, weather, time of day and collection location. Another method is to burn diesel fuel in a specific engine and collect the particles emitted from that engine. This means you know exactly where the particles have come from and the specifications of the engine. The drawback of this method is that each individual engine contributes different metals at different concentrations to the diesel while it is being burnt, therefore every engine is unique in the particle profile produced by burning diesel fuel. This effect may be slight, but also needs to be considered.

Bio-fuels are being developed to replace traditional diesel fuels (Pfister et al., 2017), however these combinations may also have an impact on an allergic asthma model. To assess this, normal DEP, soy-based DEP or an 80/20 mix of the two of them was exposed via inhalation for 4 weeks into healthy and HDM treated mice. DEP caused an inflammatory response that was not seen in the other groups (Gavett et al., 2015) indicating that the potential developments in diesel fuel technology can decrease the inflammatory responses after exposure. The development and addition to traditional diesel fuel has the potential to limit environmental diesel impacts on those that already have compromised pulmonary systems.

The final thing that should be investigated after exposure to these particles is the potential translocation of the particles. After instillation in rats, it was found that around 64% of the cerium remained in the lungs 28 days after exposure and the elimination half-life was 103 days. Cerium penetrated through the alveolar wall and went into the circulation and was then found in various organs (He et al., 2010). In our study, various organs were collected for further analysis. To complete the story, analysis of these organs with ICP-MS to determine the amount of translocation of cerium after a repeated exposure schedule should be completed. It is important to understand where these particles go and the potential systemic effects of these particles.

This thesis has brought together exposure to both an *in vivo* and an *in vitro* exposure model of allergic airway diseases. It has allowed us to identify that the addition of CeO_2NPs to diesel fuels causes enhancement of certain inflammatory endpoints that are implemented in an allergic

response when compared to the diesel burnt alone. There is still the potential for further research that has not been completed and should be in order to determine the whole story and potential implications the addition of this commercially available catalyst may have on a large asthmatic population, both in the UK and across the globe.

Chapter 7: References

References

1905. Smog. *Journal of the American Medical Association,* XLV**,** 637-637.

ABCAM. *Anti-alpha smooth muscle Actin antibody (ab5694)* [Online]. Available: http://www.abcam.com/alpha-smooth-muscle-actin-antibody-ab5694.html [Accessed 23rd November 2017].

ACCIANI, T. H., BRANDT, E. B., KHURANA HERSHEY, G. K. & LE CRAS, T. D. 2013. Diesel exhaust particle exposure increases severity of allergic asthma in young mice. *Clin Exp Allergy,* 43**,** 1406-18.

ADAMSON, I. Y., HEDGECOCK, C. & BOWDEN, D. H. 1990. Epithelial cell-fibroblast interactions in lung injury and repair. *Am J Pathol,* 137**,** 385-92.

AGGARWAL, S., GHILARDI, N., XIE, M. H., DE SAUVAGE, F. J. & GURNEY, A. L. 2003. Interleukin-23 promotes a distinct CD4 T cell activation state characterized by the production of interleukin-17. *J Biol Chem,* 278**,** 1910-4.

AHMED, M. S. 2019. Nanofluid: New Fluids by Nanotechnology. *Thermophysical Properties of Complex Materials.* IntechOpen.

AHN, J. H., KIM, C. H., KIM, Y. H., KIM, S. J., LEE, S. Y., KIM, Y. K., KIM, K. H., MOON, H. S., SONG, J. S., PARK, S. H. & KWON, S. S. 2007. Inflammatory and remodeling events in asthma with chronic exposure to house dust mites: a murine model. *J Korean Med Sci,* 22**,** 1026-33.

AIR-QUALITY.ORG.UK. 2018. *The Key Air Pollutants* [Online]. Available: http://www.air-quality.org.uk/04.php [Accessed 2nd Febuary 2018].

AKDIS, C. A., ARKWRIGHT, P. D., BRÜGGEN, M. C., BUSSE, W., GADINA, M., GUTTMAN-YASSKY, E., KABASHIMA, K., MITAMURA, Y., VIAN, L., WU, J. & PALOMARES, O. 2020. Type 2 immunity in the skin and lungs. *Allergy,* 75**,** 1582-1605.

AKIMOTO, H. 2003. Global Air Quality and Pollution. *Science,* 302**,** 1716.

AL-RAMLI, W., PREFONTAINE, D., CHOUIALI, F., MARTIN, J. G., OLIVENSTEIN, R., LEMIERE, C. & HAMID, Q. 2009. T(H)17-associated cytokines (IL-17A and IL-17F) in severe asthma. *J Allergy Clin Immunol,* 123**,** 1185-7.

ALDOSSARI, A., SHANNAHAN, J., PODILA, R. & BROWN, J. 2014. Influence of Physicochemical Properties of Silver Nanoparticles on Mast Cell Activation and Degranulation. *Toxicology in vitro : an international journal published in association with BIBRA,* 29**,** 195-203.

ALPIZAR, Y. A., BOONEN, B., SANCHEZ, A., JUNG, C., LOPEZ-REQUENA, A., NAERT, R., STEELANT, B., LUYTS, K., PLATA, C., DE VOOGHT, V., VANOIRBEEK, J. A. J., MESEGUER, V. M., VOETS, T., ALVAREZ, J. L., HELLINGS, P. W., HOET, P. H. M., NEMERY, B., VALVERDE, M. A. & TALAVERA, K. 2017. TRPV4 activation triggers protective responses to bacterial lipopolysaccharides in airway epithelial cells. *Nat Commun,* 8**,** 1059.

AMSTER, E. D., HAIM, M., DUBNOV, J. & BRODAY, D. M. 2014. Contribution of nitrogen oxide and sulfur dioxide exposure from power plant emissions on respiratory symptom and disease prevalence. *Environ Pollut,* 186**,** 20-8.

ANDERSON, S. D. & DAVISKAS, E. 2000. The mechanism of exercise-induced asthma is. *J Allergy Clin Immunol,* 106**,** 453-9.

ANDERSON, S. D. & KIPPELEN, P. 2010. Stimulus and mechanisms of exercise-induced bronchoconstriction. 7**,** 25-33.

ARRON, J. R. & IZUHARA, K. 2015. Asthma biomarkers: what constitutes a 'gold standard'? *Thorax,* 70**,** 105-7.
ARUL MOZHI SELVAN, V., ANAND, R. B. & UDAYAKUMAR, M. 2014. Effect of Cerium Oxide Nanoparticles and Carbon Nanotubes as fuel-borne additives in Diesterol blends on the performance, combustion and emission characteristics of a variable compression ratio engine. *Fuel,* 130**,** 160-167.
AU - MCGOVERN, T. K., AU - ROBICHAUD, A., AU - FEREYDOONZAD, L., AU - SCHUESSLER, T. F. & AU - MARTIN, J. G. 2013. Evaluation of Respiratory System Mechanics in Mice using the Forced Oscillation Technique. *JoVE***,** e50172.
BABSON, A. L. & PHILLIPS, G. E. 1965. A rapid colorimetric assay for serum lactic dehydrogenase. *Clin Chim Acta,* 12**,** 210-5.
BACHARIER, L. B., STRUNK, R. C., MAUGER, D., WHITE, D., LEMANSKE, R. F., JR. & SORKNESS, C. A. 2004. Classifying asthma severity in children: mismatch between symptoms, medication use, and lung function. *Am J Respir Crit Care Med,* 170**,** 426-32.
BAHAROM, F., RANKIN, G., BLOMBERG, A. & SMED-SORENSEN, A. 2017. Human Lung Mononuclear Phagocytes in Health and Disease. *Front Immunol,* 8**,** 499.
BAI, M., GRIESHABER-BOUYER, R., WANG, J., SCHMIDER, A. B., WILSON, Z. S., ZENG, L., HALYABAR, O., GODIN, M. D., NGUYEN, H. N., LEVESCOT, A., CUNIN, P., LEFORT, C. T., SOBERMAN, R. J. & NIGROVIC, P. A. 2017. CD177 modulates human neutrophil migration through activation-mediated integrin and chemoreceptor regulation. *Blood,* 130**,** 2092-2100.
BAIZ, N., SLAMA, R., BENE, M. C., CHARLES, M. A., KOLOPP-SARDA, M. N., MAGNAN, A., THIEBAUGEORGES, O., FAURE, G. & ANNESI-MAESANO, I. 2011. Maternal exposure to air pollution before and during pregnancy related to changes in newborn's cord blood lymphocyte subpopulations. The EDEN study cohort. *BMC Pregnancy Childbirth,* 11**,** 87.
BALMES, J. R. 2009. Can traffic-related air pollution cause asthma? *Thorax,* 64**,** 646.
BALOGH SIVARS, K., SIVARS, U., HORNBERG, E., ZHANG, H., BRANDEN, L., BONFANTE, R., HUANG, S., CONSTANT, S., ROBINSON, I., BETTS, C. J. & ABERG, P. M. 2018. A 3D Human Airway Model Enables Prediction of Respiratory Toxicity of Inhaled Drugs In Vitro. *Toxicol Sci,* 162**,** 301-308.
BARNES, P. J. 2008. Immunology of asthma and chronic obstructive pulmonary disease. *Nat Rev Immunol,* 8**,** 183-92.
BARON, L., GOMBAULT, A., FANNY, M., VILLERET, B., SAVIGNY, F., GUILLOU, N., PANEK, C., LE BERT, M., LAGENTE, V., RASSENDREN, F., RITEAU, N. & COUILLIN, I. 2015. The NLRP3 inflammasome is activated by nanoparticles through ATP, ADP and adenosine. *Cell Death & Disease,* 6**,** e1629-e1629.
BARRY, J., LOH, Z., COLLISON, A., MAZZONE, S., LALWANI, A., ZHANG, V., DAVIDSON, S., WYBACZ, E., GARLANDA, C., MANTOVANI, A., MATTES, J., FOSTER, P. S. & PHIPPS, S. 2013. Absence of Toll-IL-1 receptor 8/single immunoglobulin IL-1 receptor-related molecule reduces house dust mite-induced allergic airway inflammation in mice. *Am J Respir Cell Mol Biol,* 49**,** 481-90.
BATRA, J., CHATTERJEE, R. & GHOSH, B. 2007. Inducible nitric oxide synthase (iNOS): role in asthma pathogenesis. *Indian J Biochem Biophys,* 44**,** 303-9.
BEACH, E. 2017. *Do Volcanoes Pollute the Atmosphere?* [Online]. Sciencing. Available: https://sciencing.com/volcanoes-pollute-atmosphere-4707.html [Accessed 04/04/2018 2018].
BEAMER, C., GIRTSMAN, T., SEAVER, B., FINSAAS, K., MIGLIACCIO, C., PERRY, V., ROTTMAN, J., SMITH, D. & HOLIAN, A. 2012. IL-33 mediates multi-walled carbon

nanotube (MWCNT)-induced airway hyper-reactivity via the mobilization of innate helper cells in the lung. *Nanotoxicology,* 7.

BEHNDIG, A. F., SHANMUGANATHAN, K., WHITMARSH, L., STENFORS, N., BROWN, J. L., FREW, A. J., KELLY, F. J., MUDWAY, I. S., SANDSTROM, T. & WILSON, S. J. 2015. Effects of controlled diesel exhaust exposure on apoptosis and proliferation markers in bronchial epithelium - an in vivo bronchoscopy study on asthmatics, rhinitics and healthy subjects. *BMC Pulm Med,* 15**,** 99.

BENGALLI, R., LONGHIN, E., MARCHETTI, S., PROVERBIO, M. C., BATTAGLIA, C. & CAMATINI, M. 2017. The role of IL-6 released from pulmonary epithelial cells in diesel UFP-induced endothelial activation. *Environ Pollut,* 231**,** 1314-1321.

BERNSTEIN, J. A., ALEXIS, N., BARNES, C., BERNSTEIN, I. L., BERNSTEIN, J. A., NEL, A., PEDEN, D., DIAZ-SANCHEZ, D., TARLO, S. M. & WILLIAMS, P. B. 2004. Health effects of air pollution. *J Allergy Clin Immunol,* 114**,** 1116-23.

BHARADWAJ, P., ZIVIN, J. G., MULLINS, J. T. & NEIDELL, M. 2016. Early-Life Exposure to the Great Smog of 1952 and the Development of Asthma. *Am J Respir Crit Care Med,* 194**,** 1475-1482.

BHAWANA, BASNIWAL, R. K., BUTTAR, H. S., JAIN, V. K. & JAIN, N. 2011. Curcumin nanoparticles: preparation, characterization, and antimicrobial study. *J Agric Food Chem,* 59**,** 2056-61.

BICE, D. E., SEAGRAVE, J. & GREEN, F. H. 2000. Animal models of asthma: potential usefulness for studying health effects of inhaled particles. *Inhal Toxicol,* 12**,** 829-62.

BIHARI, P., VIPPOLA, M., SCHULTES, S., PRAETNER, M., KHANDOGA, A. G., REICHEL, C. A., COESTER, C., TUOMI, T., REHBERG, M. & KROMBACH, F. 2008. Optimized dispersion of nanoparticles for biological in vitro and in vivo studies. *Part Fibre Toxicol,* 5**,** 14.

BIRCHENOUGH, G. M., JOHANSSON, M. E., GUSTAFSSON, J. K., BERGSTRÖM, J. H. & HANSSON, G. C. 2015. New developments in goblet cell mucus secretion and function. *Mucosal Immunol,* 8**,** 712-9.

BIRRELL, M. A., VAN OOSTERHOUT, A. J. & BELVISI, M. G. 2010. Do the current house dust mite-driven models really mimic allergic asthma? *Eur Respir J,* 36**,** 1220-1.

BISIG, C., COMTE, P., GÜDEL, M., CZERWINSKI, J., MAYER, A., MÜLLER, L., PETRI-FINK, A. & ROTHEN-RUTISHAUSER, B. 2018. Assessment of lung cell toxicity of various gasoline engine exhausts using a versatile in vitro exposure system. *Environ Pollut,* 235**,** 263-271.

BLUME, C. & DAVIES, D. E. 2013. In vitro and ex vivo models of human asthma. *European Journal of Pharmaceutics and Biopharmaceutics,* 84**,** 394-400.

BLUME, C., SWINDLE, E. J., DENNISON, P., JAYASEKERA, N. P., DUDLEY, S., MONK, P., BEHRENDT, H., SCHMIDT-WEBER, C. B., HOLGATE, S. T., HOWARTH, P. H., TRAIDL-HOFFMANN, C. & DAVIES, D. E. 2013. Barrier responses of human bronchial epithelial cells to grass pollen exposure. *Eur Respir J,* 42**,** 87-97.

BOARD, T. R. & COUNCIL, N. R. 2002. *The Ongoing Challenge of Managing Carbon Monoxide Pollution in Fairbanks, Alaska,* Washington, DC, The National Academies Press.

BODA, B., BENAOUDIA, S., HUANG, S., BONFANTE, R., WISZNIEWSKI, L., TSELIGKA, E. D., TAPPAREL, C. & CONSTANT, S. 2018. Antiviral drug screening by assessing epithelial functions and innate immune responses in human 3D airway epithelium model. *Antiviral Res,* 156**,** 72-79.

BOURDREL, T., BIND, M. A., BEJOT, Y., MOREL, O. & ARGACHA, J. F. 2017. Cardiovascular effects of air pollution. *Arch Cardiovasc Dis,* 110**,** 634-642.

BOWATTE, G., LODGE, C. J., PERRET, J. L., MATHESON, M. C. & DHARMAGE, S. C. 2016. Interactions of GST Polymorphisms in Air Pollution Exposure and Respiratory Diseases and Allergies. *Curr Allergy Asthma Rep,* 16**,** 85.

BRADFORD, M. M. 1976. A rapid and sensitive method for the quantitation of microgram quantities of protein utilizing the principle of protein-dye binding. *Anal Biochem,* 72**,** 248-54.

BRANDENBERGER, C., LI, N., JACKSON-HUMBLES, D. N., ROCKWELL, C. E., WAGNER, J. G. & HARKEMA, J. R. 2014. Enhanced allergic airway disease in old mice is associated with a Th17 response. *Clin Exp Allergy,* 44**,** 1282-92.

BRANDT, E. B., KOVACIC, M. B., LEE, G. B., GIBSON, A. M., ACCIANI, T. H., LE CRAS, T. D., RYAN, P. H., BUDELSKY, A. L. & KHURANA HERSHEY, G. K. 2013a. Diesel exhaust particle induction of IL-17A contributes to severe asthma. *J Allergy Clin Immunol,* 132**,** 1194-1204.e2.

BRANDT, E. B., KOVACIC, M. B., LEE, G. B., GIBSON, A. M., ACCIANI, T. H., LE CRAS, T. D., RYAN, P. H., BUDELSKY, A. L. & KHURANA HERSHEY, G. K. 2013b. Diesel exhaust particle induction of IL-17A contributes to severe asthma. *J Allergy Clin Immunol,* 132**,** 1194-1204 e2.

BRANNAN, J. D. & LOUGHEED, M. D. 2012. Airway hyperresponsiveness in asthma: mechanisms, clinical significance, and treatment. *Front Physiol,* 3**,** 460.

BROOKS, C. R., VAN DALEN, C. J., HARDING, E., HERMANS, I. F. & DOUWES, J. 2017. Effects of treatment changes on asthma phenotype prevalence and airway neutrophil function. *BMC Pulm Med,* 17**,** 169.

BRUNE, K., FRANK, J., SCHWINGSHACKL, A., FINIGAN, J. & SIDHAYE, V. K. 2015. Pulmonary epithelial barrier function: some new players and mechanisms. *Am J Physiol Lung Cell Mol Physiol,* 308**,** L731-45.

BULLENS, D. M., TRUYEN, E., COTEUR, L., DILISSEN, E., HELLINGS, P. W., DUPONT, L. J. & CEUPPENS, J. L. 2006. IL-17 mRNA in sputum of asthmatic patients: linking T cell driven inflammation and granulocytic influx? *Respir Res,* 7**,** 135.

BURNEY, P., JARVIS, D. & PEREZ-PADILLA, R. 2015. The global burden of chronic respiratory disease in adults. *Int J Tuberc Lung Dis,* 19**,** 10-20.

BURTE, E., NADIF, R. & JACQUEMIN, B. 2016. Susceptibility Factors Relevant for the Association Between Long-Term Air Pollution Exposure and Incident Asthma. *Curr Environ Health Rep,* 3**,** 23-39.

CAGGIANO, S., CUTRERA, R., DI MARCO, A. & TURCHETTA, A. 2017. Exercise-Induced Bronchospasm and Allergy. *Front Pediatr,* 5**,** 131.

CALDERON, M. A., LINNEBERG, A., KLEINE-TEBBE, J., DE BLAY, F., HERNANDEZ FERNANDEZ DE ROJAS, D., VIRCHOW, J. C. & DEMOLY, P. 2015. Respiratory allergy caused by house dust mites: What do we really know? *J Allergy Clin Immunol,* 136**,** 38-48.

CALDERÓN, M. A., LINNEBERG, A., KLEINE-TEBBE, J., DE BLAY, F., HERNANDEZ FERNANDEZ DE ROJAS, D., VIRCHOW, J. C. & DEMOLY, P. 2015. Respiratory allergy caused by house dust mites: What do we really know? *Journal of Allergy and Clinical Immunology,* 136**,** 38-48.

CANBAZ, D., UTSCH, L., LOGIANTARA, A., VAN REE, R. & VAN RIJT, L. S. 2015. IL-33 promotes the induction of immunoglobulin production after inhalation of house dust mite extract in mice. *Allergy,* 70**,** 522-32.

CAO, T., ZHANG, Z., LIU, Z.-G., DOU, X., ZHANG, J., ZHANG, W., WU, B., YU, Z.-D., WEI, Z. & YU, B. 2016. High-level expression and purification of the major house dust mite allergen Der p 2 in Escherichia coli. *Protein Expression and Purification,* 121**,** 97-102.

CARLIER, F. M., SIBILLE, Y. & PILETTE, C. 2016. The epithelial barrier and immunoglobulin A system in allergy. *Clin Exp Allergy,* 46**,** 1372-1388.
CARLSTEN, C., BLOMBERG, A., PUI, M., SANDSTROM, T., WONG, S. W., ALEXIS, N. & HIROTA, J. 2016. Diesel exhaust augments allergen-induced lower airway inflammation in allergic individuals: a controlled human exposure study. *Thorax,* 71**,** 35-44.
CARTER, E., NORRIS, C., DIONISIO, K. L., BALAKRISHNAN, K., CHECKLEY, W., CLARK, M. L., GHOSH, S., JACK, D. W., KINNEY, P. L., MARSHALL, J. D., NAEHER, L. P., PEEL, J. L., SAMBANDAM, S., SCHAUER, J. J., SMITH, K. R., WYLIE, B. J. & BAUMGARTNER, J. 2017. Assessing Exposure to Household Air Pollution: A Systematic Review and Pooled Analysis of Carbon Monoxide as a Surrogate Measure of Particulate Matter. *Environ Health Perspect,* 125**,** 076002.
CASSEE, F. R., VAN BALEN, E. C., SINGH, C., GREEN, D., MUIJSER, H., WEINSTEIN, J. & DREHER, K. 2011. Exposure, health and ecological effects review of engineered nanoscale cerium and cerium oxide associated with its use as a fuel additive. *Crit Rev Toxicol,* 41**,** 213-29.
CELEDÓN, J. C., WRIGHT, R. J., LITONJUA, A. A., SREDL, D., RYAN, L., WEISS, S. T. & GOLD, D. R. 2003. Day Care Attendance in Early Life, Maternal History of Asthma, and Asthma at the Age of 6 Years. *American Journal of Respiratory and Critical Care Medicine,* 167**,** 1239-1243.
CEPHUS, J. Y., STIER, M. T., FUSEINI, H., YUNG, J. A., TOKI, S., BLOODWORTH, M. H., ZHOU, W., GOLENIEWSKA, K., ZHANG, J., GARON, S. L., HAMILTON, R. G., POLOSHUKIN, V. V., BOYD, K. L., PEEBLES, R. S., JR. & NEWCOMB, D. C. 2017. Testosterone Attenuates Group 2 Innate Lymphoid Cell-Mediated Airway Inflammation. *Cell Rep,* 21**,** 2487-2499.
CESAR, A. C., CARVALHO, J. A., JR. & NASCIMENTO, L. F. 2015. Association between NOx exposure and deaths caused by respiratory diseases in a medium-sized Brazilian city. *Braz J Med Biol Res,* 48**,** 1130-5.
CHAN, F. K., MORIWAKI, K. & DE ROSA, M. J. 2013. Detection of necrosis by release of lactate dehydrogenase activity. *Methods Mol Biol,* 979**,** 65-70.
CHAPMAN, D. G. & IRVIN, C. G. 2015. Mechanisms of airway hyper-responsiveness in asthma: the past, present and yet to come. *Clin Exp Allergy,* 45**,** 706-19.
CHEN, B. Y., CHEN, C. H., CHUANG, Y. C., WU, Y. H., PAN, S. C. & GUO, Y. L. 2019. Changes in the relationship between ambient fine particle concentrations and childhood lung function over 5 years. *Environ Res,* 179**,** 108809.
CHEN, E. Y., GARNICA, M., WANG, Y.-C., MINTZ, A. J., CHEN, C.-S. & CHIN, W.-C. 2012. A mixture of anatase and rutile TiO2 nanoparticles induces histamine secretion in mast cells. *Particle and Fibre Toxicology,* 9**,** 2.
CHEN, P., ZHANG, Z., GU, N. & JI, M. 2018. Effect of the surface charge density of nanoparticles on their translocation across pulmonary surfactant monolayer: a molecular dynamics simulation. *Molecular Simulation,* 44**,** 85-93.
CHEN, R., HU, B., LIU, Y., XU, J., YANG, G., XU, D. & CHEN, C. 2016. Beyond PM2.5: The role of ultrafine particles on adverse health effects of air pollution. *Biochimica et Biophysica Acta (BBA) - General Subjects,* 1860**,** 2844-2855.
CHEN, T.-M., KUSCHNER, W. G., GOKHALE, J. & SHOFER, S. 2007. Outdoor Air Pollution: Nitrogen Dioxide, Sulfur Dioxide, and Carbon Monoxide Health Effects. *The American Journal of the Medical Sciences,* 333**,** 249-256.
CHEN, W., JIN, W., HARDEGEN, N., LEI, K. J., LI, L., MARINOS, N., MCGRADY, G. & WAHL, S. M. 2003. Conversion of peripheral CD4+CD25- naive T cells to

CD4+CD25+ regulatory T cells by TGF-beta induction of transcription factor Foxp3. *J Exp Med,* 198**,** 1875-86.
CHEN, W., ZHANG, Q., KAPLAN, B., BAKER, G. & KAMINSKI, N. 2013a. Induced T cell cytokine production is enhanced by engineered nanoparticles. *Nanotoxicology,* 8.
CHEN, Z. & O'SHEA, J. J. 2008. Th17 cells: a new fate for differentiating helper T cells. *Immunol Res,* 41**,** 87-102.
CHEN, Z. G., ZHANG, T. T., LI, H. T., CHEN, F. H., ZOU, X. L., JI, J. Z. & CHEN, H. 2013b. Neutralization of TSLP inhibits airway remodeling in a murine model of allergic asthma induced by chronic exposure to house dust mite. *PLoS One,* 8**,** e51268.
CHENG, Z., WANG, X., DAI, L. L., JIA, L. Q., JING, X. G., LIU, Y., WANG, H., LI, P. F., AN, L. & LIU, M. 2018. Thymic Stromal Lymphopoietin Signaling Pathway Inhibition Attenuates Airway Inflammation and Remodeling in Rats with Asthma. *Cell Physiol Biochem,* 47**,** 1482-1496.
CHESNE, J., BRAZA, F., MAHAY, G., BROUARD, S., ARONICA, M. & MAGNAN, A. 2014. IL-17 in severe asthma. Where do we stand? *Am J Respir Crit Care Med,* 190**,** 1094-101.
CHIBA, Y., NAKAZAWA, S., TODOROKI, M., SHINOZAKI, K., SAKAI, H. & MISAWA, M. 2009. Interleukin-13 augments bronchial smooth muscle contractility with an up-regulation of RhoA protein. *Am J Respir Cell Mol Biol,* 40**,** 159-67.
CHIO, C. P., CHEN, S. C., CHIANG, K. C., CHOU, W. C. & LIAO, C. M. 2007. Oxidative stress risk analysis for exposure to diesel exhaust particle-induced reactive oxygen species. *Sci Total Environ,* 387**,** 113-27.
CHO, E. J., HOLBACK, H., LIU, K. C., ABOUELMAGD, S. A., PARK, J. & YEO, Y. 2013. Nanoparticle characterization: state of the art, challenges, and emerging technologies. *Mol Pharm,* 10**,** 2093-110.
CHO, W. S., DUFFIN, R., POLAND, C. A., HOWIE, S. E., MACNEE, W., BRADLEY, M., MEGSON, I. L. & DONALDSON, K. 2010. Metal oxide nanoparticles induce unique inflammatory footprints in the lung: important implications for nanoparticle testing. *Environ Health Perspect,* 118**,** 1699-706.
CHOI, H. S., ASHITATE, Y., LEE, J. H., KIM, S. H., MATSUI, A., INSIN, N., BAWENDI, M. G., SEMMLER-BEHNKE, M., FRANGIONI, J. V. & TSUDA, A. 2010. Rapid translocation of nanoparticles from the lung airspaces to the body. *Nat Biotechnol,* 28**,** 1300-3.
CHORAWALA M. R, P. K. N. 2014. *ANIMAL MODELS OF ASTHMA*.
CHU, D. K., LLOP-GUEVARA, A., WALKER, T. D., FLADER, K., GONCHAROVA, S., BOUDREAU, J. E., MOORE, C. L., SEUNGHYUN IN, T., WASERMAN, S., COYLE, A. J., KOLBECK, R., HUMBLES, A. A. & JORDANA, M. 2013. IL-33, but not thymic stromal lymphopoietin or IL-25, is central to mite and peanut allergic sensitization. *J Allergy Clin Immunol,* 131**,** 187-200.e1-8.
CICHOWICZ, R., WIELGOSIŃSKI, G. & FETTER, W. 2017. Dispersion of atmospheric air pollution in summer and winter season. *Environ Monit Assess,* 189**,** 605.
CITEQ-BIOLOGICS. *HDM induced asthma animal models* [Online]. Available: https://www.citeqbiologics.com/house-dust-mite-induced-asthma-models/ [Accessed].
CLIFF, R., CURRAN, J., HIROTA, J. A., BRAUER, M., FELDMAN, H. & CARLSTEN, C. 2016. Effect of diesel exhaust inhalation on blood markers of inflammation and neurotoxicity: a controlled, blinded crossover study. *Inhal Toxicol,* 28**,** 145-53.
COCKCROFT, D. W. & DAVIS, B. E. 2006. Mechanisms of airway hyperresponsiveness. *Journal of Allergy and Clinical Immunology,* 118**,** 551-559.
CODISPOTI, C. D., LEMASTERS, G. K., LEVIN, L., REPONEN, T., RYAN, P. H., BIAGINI MYERS, J. M., VILLAREAL, M., BURKLE, J., EVANS, S., LOCKEY, J. E.,

KHURANA HERSHEY, G. K. & BERNSTEIN, D. I. 2015. Traffic pollution is associated with early childhood aeroallergen sensitization. *Ann Allergy Asthma Immunol,* 114**,** 126-33.

COMEAP 2015. Statement on the evidence for the effects of nitrogen dioxide on health.

Committee on the Medical Effects of Air Pollutants. https://www.gov.uk/government/publications/nitrogen-dioxide-health-effects-of-exposure.

CONDON, T. V., SAWYER, R. T., FENTON, M. J. & RICHES, D. W. 2011. Lung dendritic cells at the innate-adaptive immune interface. *J Leukoc Biol,* 90**,** 883-95.

CORDELLI, E., KELLER, J., ELEUTERI, P., VILLANI, P., MA-HOCK, L., SCHULZ, M., LANDSIEDEL, R. & PACCHIEROTTI, F. 2017. No genotoxicity in rat blood cells upon 3- or 6-month inhalation exposure to CeO2 or BaSO4 nanomaterials. *Mutagenesis,* 32**,** 13-22.

CORREN, J. 2013. Role of interleukin-13 in asthma. *Curr Allergy Asthma Rep,* 13**,** 415-20.

COSMA, G., CROFTS, F., TAIOLI, E., TONIOLO, P. & GARTE, S. 1993. Relationship between genotype and function of the human CYP1A1 gene. *J Toxicol Environ Health,* 40**,** 309-16.

COSMI, L. & ANNUNZIATO, F. 2017. Group 2 Innate Lymphoid Cells Are the Earliest Recruiters of Eosinophils in Lungs of Patients with Allergic Asthma. *Am J Respir Crit Care Med,* 196**,** 666-668.

COSTA, A. F., HOEK, G., BRUNEKREEF, B. & PONCE DE LEON, A. C. 2017. Air Pollution and Deaths among Elderly Residents of Sao Paulo, Brazil: An Analysis of Mortality Displacement. *Environ Health Perspect,* 125**,** 349-354.

COZENS, D., GRAHAME, E., SUTHERLAND, E., TAYLOR, G., BERRY, C. C. & DAVIES, R. L. 2018. Development and optimization of a differentiated airway epithelial cell model of the bovine respiratory tract. *Sci Rep,* 8**,** 853.

CRAPO, J. D., BARRY, B. E., GEHR, P., BACHOFEN, M. & WEIBEL, E. R. 1982. Cell number and cell characteristics of the normal human lung. *Am Rev Respir Dis,* 126**,** 332-7.

CRYSTAL, R. G., RANDELL, S. H., ENGELHARDT, J. F., VOYNOW, J. & SUNDAY, M. E. 2008. Airway epithelial cells: current concepts and challenges. *Proc Am Thorac Soc,* 5**,** 772-7.

CURTIS, L., REA, W., SMITH-WILLIS, P., FENYVES, E. & PAN, Y. 2006. Adverse health effects of outdoor air pollutants. *Environ Int,* 32**,** 815-30.

D'AMATO, G., PAWANKAR, R., VITALE, C., LANZA, M., MOLINO, A., STANZIOLA, A., SANDUZZI, A., VATRELLA, A. & D'AMATO, M. 2016. Climate Change and Air Pollution: Effects on Respiratory Allergy. *Allergy Asthma Immunol Res,* 8**,** 391-5.

D'AMATO, G., VITALE, C., DE MARTINO, A., VIEGI, G., LANZA, M., MOLINO, A., SANDUZZI, A., VATRELLA, A., ANNESI-MAESANO, I. & D'AMATO, M. J. M. R. M. 2015. Effects on asthma and respiratory allergy of Climate change and air pollution. 10**,** 39.

DALE, J. G., COX, S. S., VANCE, M. E., MARR, L. C. & HOCHELLA, M. F. 2017. Transformation of Cerium Oxide Nanoparticles from a Diesel Fuel Additive during Combustion in a Diesel Engine. *Environ Sci Technol,* 51**,** 1973-1980.

DAVIES, D. E., POLOSA, R., PUDDICOMBE, S. M., RICHTER, A. & HOLGATE, S. T. 1999. The epidermal growth factor receptor and its ligand family: their potential role in repair and remodelling in asthma. *Allergy,* 54**,** 771-83.

DAVIES, E. R., KELLY, J. F., HOWARTH, P. H., WILSON, D. I., HOLGATE, S. T., DAVIES, D. E., WHITSETT, J. A. & HAITCHI, H. M. 2016. Soluble ADAM33

initiates airway remodeling to promote susceptibility for allergic asthma in early life. *JCI Insight,* 1.

DE GROVE, K. C., PROVOOST, S., BRUSSELLE, G. G., JOOS, G. F. & MAES, T. 2018. Insights in particulate matter-induced allergic airway inflammation: Focus on the epithelium. *Clin Exp Allergy,* 48**,** 773-786.

DE HAAR, C., KOOL, M., HASSING, I., BOL, M., LAMBRECHT, B. N. & PIETERS, R. 2008. Lung dendritic cells are stimulated by ultrafine particles and play a key role in particle adjuvant activity. *Journal of Allergy and Clinical Immunology,* 121**,** 1246-1254.

DEKKERS, S., MA-HOCK, L., LYNCH, I., RUSS, M., MILLER, M. R., SCHINS, R. P. F., KELLER, J., ROMER, I., KUTTLER, K., STRAUSS, V., DE JONG, W. H., LANDSIEDEL, R. & CASSEE, F. R. 2018. Differences in the toxicity of cerium dioxide nanomaterials after inhalation can be explained by lung deposition, animal species and nanoforms. *Inhal Toxicol,* 30**,** 273-286.

DEKKERS, S., MILLER, M. R., SCHINS, R. P. F., ROMER, I., RUSS, M., VANDEBRIEL, R. J., LYNCH, I., BELINGA-DESAUNAY, M. F., VALSAMI-JONES, E., CONNELL, S. P., SMITH, I. P., DUFFIN, R., BOERE, J. A. F., HEUSINKVELD, H. J., ALBRECHT, C., DE JONG, W. H. & CASSEE, F. R. 2017. The effect of zirconium doping of cerium dioxide nanoparticles on pulmonary and cardiovascular toxicity and biodistribution in mice after inhalation. *Nanotoxicology,* 11**,** 794-808.

DELLAVALLE, C. T., TRICHE, E. W., LEADERER, B. P. & BELL, M. L. 2012. Effects of ambient pollen concentrations on frequency and severity of asthma symptoms among asthmatic children. *Epidemiology,* 23**,** 55-63.

DEMOKRITOU, P., GASS, S., PYRGIOTAKIS, G., COHEN, J. M., GOLDSMITH, W., MCKINNEY, W., FRAZER, D., MA, J., SCHWEGLER-BERRY, D., BRAIN, J. & CASTRANOVA, V. 2013. An in vivo and in vitro toxicological characterisation of realistic nanoscale CeO_2 inhalation exposures. *Nanotoxicology,* 7**,** 1338-50.

DHARMAGE, S. C., PERRET, J. L. & CUSTOVIC, A. 2019. Epidemiology of Asthma in Children and Adults. *Front Pediatr,* 7**,** 246.

DIAZ, J., WARREN, L., HELFNER, L., XUE, X., CHATTERJEE, P. K., GUPTA, M., SOLANKI, M. H., ESPOSITO, M., BONAGURA, V. & METZ, C. N. 2015. Obesity shifts house dust mite-induced airway cellular infiltration from eosinophils to macrophages: effects of glucocorticoid treatment. *Immunol Res,* 63**,** 197-208.

DICKINSON, B. C. & CHANG, C. J. 2011. Chemistry and biology of reactive oxygen species in signaling or stress responses. *Nat Chem Biol,* 7**,** 504-11.

DIMITROVA, D., YOUROUKOVA, V., IVANOVA-TODOROVA, E., TUMANGELOVA-YUZEIR, K. & VELIKOVA, T. 2019. Serum levels of IL-5, IL-6, IL-8, IL-13 and IL-17A in pre-defined groups of adult patients with moderate and severe bronchial asthma. *Respir Med,* 154**,** 144-154.

DING, N., ZHOU, N., ZHOU, M. & REN, G. M. 2015. Respiratory cancers and pollution. *Eur Rev Med Pharmacol Sci,* 19**,** 31-7.

DOCKERY, D. W. 2009. Health Effects of Particulate Air Pollution. *Annals of Epidemiology,* 19**,** 257-263.

DOEING, D. C. & SOLWAY, J. 2013. Airway smooth muscle in the pathophysiology and treatment of asthma. *J Appl Physiol (1985),* 114**,** 834-43.

DON PORTO CARERO, A., HOET, P. H., VERSCHAEVE, L., SCHOETERS, G. & NEMERY, B. 2001. Genotoxic effects of carbon black particles, diesel exhaust particles, and urban air particulates and their extracts on a human alveolar epithelial cell line (A549) and a human monocytic cell line (THP-1). *Environ Mol Mutagen,* 37**,** 155-63.

DRIVE, R. *Euro 1 to Euro 6 – find out your vehicle's emissions standard* [Online]. Available: https://www.rac.co.uk/drive/advice/emissions/euro-emissions-standards/ [Accessed 5/4/18 2018].

DRUILHE, A., ZAHM, J. M., BENAYOUN, L., EL MEHDI, D., GRANDSAIGNE, M., DOMBRET, M. C., MOSNIER, I., FEGER, B., DEPONDT, J., AUBIER, M. & PRETOLANI, M. 2008. Epithelium expression and function of retinoid receptors in asthma. *Am J Respir Cell Mol Biol,* 38**,** 276-82.

DUNNICK, K. M., MORRIS, A. M., BADDING, M. A., BARGER, M., STEFANIAK, A. B., SABOLSKY, E. M. & LEONARD, S. S. 2016. Evaluation of the effect of valence state on cerium oxide nanoparticle toxicity following intratracheal instillation in rats. *Nanotoxicology,* 10**,** 992-1000.

DUNNICK, K. M., PILLAI, R., PISANE, K. L., STEFANIAK, A. B., SABOLSKY, E. M. & LEONARD, S. S. 2015. The Effect of Cerium Oxide Nanoparticle Valence State on Reactive Oxygen Species and Toxicity. *Biological Trace Element Research,* 166**,** 96-107.

DURAIYAN, J., GOVINDARAJAN, R., KALIYAPPAN, K. & PALANISAMY, M. 2012. Applications of immunohistochemistry. *J Pharm Bioallied Sci,* 4**,** S307-9.

DVORAK, A., TILLEY, A. E., SHAYKHIEV, R., WANG, R. & CRYSTAL, R. G. 2011. Do airway epithelium air-liquid cultures represent the in vivo airway epithelium transcriptome? *Am J Respir Cell Mol Biol,* 44**,** 465-73.

DYBDAHL, M., RISOM, L., BORNHOLDT, J., AUTRUP, H., LOFT, S. & WALLIN, H. 2004. Inflammatory and genotoxic effects of diesel particles in vitro and in vivo. *Mutat Res,* 562**,** 119-31.

EK, W. E., KARLSSON, T., HERNANDES, C. A., RASK-ANDERSEN, M. & JOHANSSON, A. 2018. Breast-feeding and risk of asthma, hay fever, and eczema. *J Allergy Clin Immunol,* 141**,** 1157-1159 e9.

EL SHAER, S. S., SALAHELDIN, T. A., SAIED, N. M. & ABDELAZIM, S. M. 2017. In vivo ameliorative effect of cerium oxide nanoparticles in isoproterenol-induced cardiac toxicity. *Exp Toxicol Pathol,* 69**,** 435-441.

EMPEY, K. M., OREND, J. G., PEEBLES, R. S., JR., EGANA, L., NORRIS, K. A., OURY, T. D. & KOLLS, J. K. 2012. Stimulation of immature lung macrophages with intranasal interferon gamma in a novel neonatal mouse model of respiratory syncytial virus infection. *PLoS One,* 7**,** e40499.

ENDES, C., SCHMID, O., KINNEAR, C., MUELLER, S., CAMARERO-ESPINOSA, S., VANHECKE, D., FOSTER, E. J., PETRI-FINK, A., ROTHEN-RUTISHAUSER, B., WEDER, C. & CLIFT, M. J. 2014. An in vitro testing strategy towards mimicking the inhalation of high aspect ratio nanoparticles. *Part Fibre Toxicol,* 11**,** 40.

EOM, H. J. & CHOI, J. 2009. Oxidative stress of CeO2 nanoparticles via p38-Nrf-2 signaling pathway in human bronchial epithelial cell, Beas-2B. *Toxicol Lett,* 187**,** 77-83.

EPELMAN, S., LAVINE, K. J. & RANDOLPH, G. J. 2014. Origin and functions of tissue macrophages. *Immunity,* 41**,** 21-35.

ERLE, D. J. & SHEPPARD, D. 2014. The cell biology of asthma. *The Journal of Cell Biology,* 205**,** 621-631.

ESTEVEZ, A. Y. & ERLICHMAN, J. S. 2014. The potential of cerium oxide nanoparticles (nanoceria) for neurodegenerative disease therapy. *Nanomedicine (Lond),* 9**,** 1437-40.

ESTEVEZ, A. Y., PRITCHARD, S., HARPER, K., ASTON, J. W., LYNCH, A., LUCKY, J. J., LUDINGTON, J. S., CHATANI, P., MOSENTHAL, W. P., LEITER, J. C., ANDREESCU, S. & ERLICHMAN, J. S. 2011. Neuroprotective mechanisms of cerium oxide nanoparticles in a mouse hippocampal brain slice model of ischemia. *Free Radic Biol Med,* 51**,** 1155-63.

FAHY, O., HAMMAD, H., SÉNÉCHAL, S., PESTEL, J., TONNEL, A. B., WALLAERT, B. & TSICOPOULOS, A. 2000. Synergistic effect of diesel organic extracts and allergen Der p 1 on the release of chemokines by peripheral blood mononuclear cells from allergic subjects: involvement of the map kinase pathway. *Am J Respir Cell Mol Biol,* 23**,** 247-54.

FALL, T., LUNDHOLM, C., ÖRTQVIST, A. K., FALL, K., FANG, F., HEDHAMMAR, Å., KÄMPE, O., INGELSSON, E. & ALMQVIST, C. 2015. Early Exposure to Dogs and Farm Animals and the Risk of Childhood Asthma. *JAMA Pediatr,* 169**,** e153219.

FARHADI, N., LAMBERT, L., TRIULZI, C., OPENSHAW, P. J., GUERRA, N. & CULLEY, F. J. 2014. Natural killer cell NKG2D and granzyme B are critical for allergic pulmonary inflammation. *J Allergy Clin Immunol,* 133**,** 827-35 e3.

FARNE, H. A., WILSON, A., POWELL, C., BAX, L. & MILAN, S. J. 2017. Anti-IL5 therapies for asthma. *Cochrane Database Syst Rev,* 9**,** CD010834.

FELTIS, B. N., ELBAZ, A., WRIGHT, P. F. A., MACKAY, G. A., TURNEY, T. W. & LOPATA, A. L. 2015. Characterizing the inhibitory action of zinc oxide nanoparticles on allergic-type mast cell activation. *Molecular Immunology,* 66**,** 139-146.

FENGER, J. 2009. Air pollution in the last 50 years–From local to global. *Atmospheric environment,* 43**,** 13-22.

FESTING, M. F. 2014. Randomized block experimental designs can increase the power and reproducibility of laboratory animal experiments. *ILAR J,* 55**,** 472-6.

FIEBIG, M., WIARTALLA, A., HOLDERBAUM, B. & KIESOW, S. 2014. Particulate emissions from diesel engines: correlation between engine technology and emissions. *J Occup Med Toxicol,* 9**,** 6.

FILIPPI, A., LIU, F., WILSON, J., LELIEVELD, S., KORSCHELT, K., WANG, T., WANG, Y., REICH, T., PÖSCHL, U., TREMEL, W. & TONG, H. 2019. Antioxidant activity of cerium dioxide nanoparticles and nanorods in scavenging hydroxyl radicals. *RSC Advances,* 9**,** 11077-11081.

FINKELMAN, F. D. 2014. Diesel exhaust particle exposure during pregnancy promotes development of asthma and atopy. *J Allergy Clin Immunol,* 134**,** 73-4.

FINLAYSON-PITTS, B. J. & PITTS, J. N. 1997. Tropospheric Air Pollution: Ozone, Airborne Toxics, Polycyclic Aromatic Hydrocarbons, and Particles. 276**,** 1045-1051.

FISCHER, A. H., JACOBSON, K. A., ROSE, J. & ZELLER, R. 2008. Hematoxylin and eosin staining of tissue and cell sections. *CSH Protoc,* 2008**,** pdb.prot4986.

FITZPATRICK, A. M., HOLGUIN, F., TEAGUE, W. G. & BROWN, L. A. 2008. Alveolar macrophage phagocytosis is impaired in children with poorly controlled asthma. *J Allergy Clin Immunol,* 121**,** 1372-8, 1378 e1-3.

FOONG, R. X., DU TOIT, G. & FOX, A. T. 2017. Asthma, Food Allergy, and How They Relate to Each Other. *Front Pediatr,* 5**,** 89.

FORNO, E. & CELEDON, J. C. 2012. Predicting asthma exacerbations in children. *Curr Opin Pulm Med,* 18**,** 63-9.

FRAMPTON MARK, W., STEWART JUDITH, C., OBERDÖRSTER, G., MORROW PAUL, E., CHALUPA, D., PIETROPAOLI ANTHONY, P., FRASIER LAUREN, M., SPEERS DONNA, M., COX, C., HUANG, L.-S. & UTELL MARK, J. 2006. Inhalation of Ultrafine Particles Alters Blood Leukocyte Expression of Adhesion Molecules in Humans. *Environmental Health Perspectives,* 114**,** 51-58.

FRANCHI, L. P., MANSHIAN, B. B., DE SOUZA, T. A., SOENEN, S. J., MATSUBARA, E. Y., ROSOLEN, J. M. & TAKAHASHI, C. S. 2015. Cyto- and genotoxic effects of metallic nanoparticles in untransformed human fibroblast. *Toxicol In Vitro,* 29**,** 1319-31.

FRANCIS, G. L. 2010. Albumin and mammalian cell culture: implications for biotechnology applications. *Cytotechnology,* 62**,** 1-16.
FRANKLIN, B. A., BROOK, R. & ARDEN POPE, C., 3RD 2015. Air pollution and cardiovascular disease. *Curr Probl Cardiol,* 40**,** 207-38.
FRICKER, M. & GIBSON, P. G. 2017. Macrophage dysfunction in the pathogenesis and treatment of asthma. *Eur Respir J,* 50.
FRIEDERIKE FACHINGER , F. D. K., RETO GIERÉ , STEPHAN BORRMANN 2017. How the user can influence particulate emissions from residential wood and pellet stoves: Emission factors for different fuels and burning conditions. *Atmospheric Environment,* 158**,** 216 - 226.
FRIEKE KUPER, C., GROLLERS-MULDERIJ, M., MAARSCHALKERWEERD, T., MEULENDIJKS, N. M., REUS, A., VAN ACKER, F., ZONDERVAN-VAN DEN BEUKEN, E. K., WOUTERS, M. E., BIJLSMA, S. & KOOTER, I. M. 2015. Toxicity assessment of aggregated/agglomerated cerium oxide nanoparticles in an in vitro 3D airway model: the influence of mucociliary clearance. *Toxicol In Vitro,* 29**,** 389-97.
FROHLICH, E. 2017. Hemocompatibility of inhaled environmental nanoparticles: Potential use of in vitro testing. *J Hazard Mater,* 336**,** 158-167.
FULCHER, M. L., GABRIEL, S., BURNS, K. A., YANKASKAS, J. R. & RANDELL, S. H. 2005. Well-differentiated human airway epithelial cell cultures. *Methods Mol Med,* 107**,** 183-206.
FULCHER, M. L. & RANDELL, S. H. 2013. Human nasal and tracheo-bronchial respiratory epithelial cell culture. *Methods Mol Biol,* 945**,** 109-21.
FUSEINI, H. & NEWCOMB, D. C. 2017. Mechanisms Driving Gender Differences in Asthma. *Curr Allergy Asthma Rep,* 17**,** 19.
GAFFIN, J. M., KANCHONGKITTIPHON, W. & PHIPATANAKUL, W. 2014. Reprint of: Perinatal and early childhood environmental factors influencing allergic asthma immunopathogenesis. *Int Immunopharmacol,* 23**,** 337-46.
GAUDERMAN, W. J., AVOL, E., GILLILAND, F., VORA, H., THOMAS, D., BERHANE, K., MCCONNELL, R., KUENZLI, N., LURMANN, F., RAPPAPORT, E., MARGOLIS, H., BATES, D. & PETERS, J. 2004. The effect of air pollution on lung development from 10 to 18 years of age. *N Engl J Med,* 351**,** 1057-67.
GAUDERMAN, W. J., URMAN, R., AVOL, E., BERHANE, K., MCCONNELL, R., RAPPAPORT, E., CHANG, R., LURMANN, F. & GILLILAND, F. 2015. Association of Improved Air Quality with Lung Development in Children. *New England Journal of Medicine,* 372**,** 905-913.
GAUTIER, C. & CHARPIN, D. 2017. Environmental triggers and avoidance in the management of asthma. *J Asthma Allergy,* 10**,** 47-56.
GAVETT, S. H., WOOD, C. E., WILLIAMS, M. A., CYPHERT, J. M., BOYKIN, E. H., DANIELS, M. J., COPELAND, L. B., KING, C., KRANTZ, T. Q., RICHARDS, J. H., ANDREWS, D. L., JASKOT, R. H. & GILMOUR, M. I. 2015. Soy biodiesel emissions have reduced inflammatory effects compared to diesel emissions in healthy and allergic mice. *Inhal Toxicol,* 27**,** 533-44.
GEISER, M. 2010. Update on macrophage clearance of inhaled micro- and nanoparticles. *J Aerosol Med Pulm Drug Deliv,* 23**,** 207-17.
GENECARDS. *CLCA1 Gene(Protein Coding)* [Online]. Available: http://www.genecards.org/cgi-bin/carddisp.pl?gene=CLCA1 [Accessed 23rd November 2017].
GHIO, A. J. 2008. Mechanism of asthmatic exacerbation by ambient air pollution particles. *Expert Rev Respir Med,* 2**,** 109-18.

GHIO, A. J., DAILEY, L. A., SOUKUP, J. M., STONEHUERNER, J., RICHARDS, J. H. & DEVLIN, R. B. 2013. Growth of human bronchial epithelial cells at an air-liquid interface alters the response to particle exposure. *Part Fibre Toxicol,* 10**,** 25.

GHIO, A. J., SOBUS, J. R., PLEIL, J. D. & MADDEN, M. C. 2012. Controlled human exposures to diesel exhaust. *Swiss Med Wkly,* 142**,** w13597.

GIBSON, P. G., SIMPSON, J. L. & SALTOS, N. 2001. Heterogeneity of airway inflammation in persistent asthma : evidence of neutrophilic inflammation and increased sputum interleukin-8. *Chest,* 119**,** 1329-36.

GILES, L. V., CARLSTEN, C. & KOEHLE, M. S. 2018. The pulmonary and autonomic effects of high-intensity and low-intensity exercise in diesel exhaust. *Environ Health,* 17**,** 87.

GIZYCKI, M. J., ADELROTH, E., ROGERS, A. V., O'BYRNE, P. M. & JEFFERY, P. K. 1997. Myofibroblast involvement in the allergen-induced late response in mild atopic asthma. *Am J Respir Cell Mol Biol,* 16**,** 664-73.

GONG, H., LINN, W. S., CLARK, K. W., ANDERSON, K. R., SIOUTAS, C., ALEXIS, N. E., CASCIO, W. E. & DEVLIN, R. B. 2008. Exposures of Healthy and Asthmatic Volunteers to Concentrated Ambient Ultrafine Particles in Los Angeles. *Inhalation Toxicology,* 20**,** 533-545.

GORDON, S., DANESHIAN, M., BOUWSTRA, J., CALONI, F., CONSTANT, S., DAVIES, D. E., DANDEKAR, G., GUZMAN, C. A., FABIAN, E., HALTNER, E., HARTUNG, T., HASIWA, N., HAYDEN, P., KANDAROVA, H., KHARE, S., KRUG, H. F., KNEUER, C., LEIST, M., LIAN, G., MARX, U., METZGER, M., OTT, K., PRIETO, P., ROBERTS, M. S., ROGGEN, E. L., TRALAU, T., VAN DEN BRAAK, C., WALLES, H. & LEHR, C. M. 2015. Non-animal models of epithelial barriers (skin, intestine and lung) in research, industrial applications and regulatory toxicology. *ALTEX,* 32**,** 327-78.

GOSENS, I., MATHIJSSEN, L. E., BOKKERS, B. G., MUIJSER, H. & CASSEE, F. R. 2014. Comparative hazard identification of nano- and micro-sized cerium oxide particles based on 28-day inhalation studies in rats. *Nanotoxicology,* 8**,** 643-53.

GOWERS, A. M., CULLINAN, P., AYRES, J. G., ANDERSON, H. R., STRACHAN, D. P., HOLGATE, S. T., MILLS, I. C. & MAYNARD, R. L. 2012. Does outdoor air pollution induce new cases of asthma? Biological plausibility and evidence; a review. *Respirology,* 17**,** 887-98.

GRAINGE, C. L. & DAVIES, D. E. 2013. Epithelial injury and repair in airways diseases. *Chest,* 144**,** 1906-1912.

GRAINGE, C. L., LAU, L. C., WARD, J. A., DULAY, V., LAHIFF, G., WILSON, S., HOLGATE, S., DAVIES, D. E. & HOWARTH, P. H. 2011. Effect of bronchoconstriction on airway remodeling in asthma. *N Engl J Med,* 364**,** 2006-15.

GRAY, L. E., O'HELY, M., RANGANATHAN, S., SLY, P. D. & VUILLERMIN, P. 2017. The Maternal Diet, Gut Bacteria, and Bacterial Metabolites during Pregnancy Influence Offspring Asthma. *Front Immunol,* 8**,** 365.

GRAY, T. E., GUZMAN, K., DAVIS, C. W., ABDULLAH, L. H. & NETTESHEIM, P. 1996. Mucociliary differentiation of serially passaged normal human tracheobronchial epithelial cells. *Am J Respir Cell Mol Biol,* 14**,** 104-12.

GREEN, R. H., BRIGHTLING, C. E., WOLTMANN, G., PARKER, D., WARDLAW, A. J. & PAVORD, I. D. 2002. Analysis of induced sputum in adults with asthma: identification of subgroup with isolated sputum neutrophilia and poor response to inhaled corticosteroids. *Thorax,* 57**,** 875-9.

GREGORY, L. G., JONES, C. P., WALKER, S. A., SAWANT, D., GOWERS, K. H., CAMPBELL, G. A., MCKENZIE, A. N. & LLOYD, C. M. 2013. IL-25 drives remodelling in allergic airways disease induced by house dust mite. *Thorax,* 68**,** 82-90.

GRILLI, A., BENGALLI, R., LONGHIN, E., CAPASSO, L., PROVERBIO, M. C., FORCATO, M., BICCIATO, S., GUALTIERI, M., BATTAGLIA, C. & CAMATINI, M. 2018. Transcriptional profiling of human bronchial epithelial cell BEAS-2B exposed to diesel and biomass ultrafine particles. *BMC Genomics,* 19**,** 302.

GRUZIEVA, O., GEHRING, U., AALBERSE, R., AGIUS, R., BEELEN, R., BEHRENDT, H., BELLANDER, T., BIRK, M., DE JONGSTE, J. C., FUERTES, E., HEINRICH, J., HOEK, G., KLUMPER, C., KOPPELMAN, G., KOREK, M., KRAMER, U., LINDLEY, S., MOLTER, A., SIMPSON, A., STANDL, M., VAN HAGE, M., VON BERG, A., WIJGA, A., BRUNEKREEF, B. & PERSHAGEN, G. 2014. Meta-analysis of air pollution exposure association with allergic sensitization in European birth cohorts. *J Allergy Clin Immunol,* 133**,** 767-76 e7.

GUARNIERI, M. & BALMES, J. R. 2014. Outdoor air pollution and asthma. *Lancet,* 383**,** 1581-92.

GUO, C., SMITH, R., GANT, T. W. & LEONARD, M. O. 2015. Cerium dioxide nanoparticles protect against oxidative stress induced injury through modulation of TGF-β signalling. *Toxicology Research,* 4**,** 464-475.

GUO, X. & CHEN, S. Y. 2012. Transforming growth factor-beta and smooth muscle differentiation. *World J Biol Chem,* 3**,** 41-52.

GURRAM, R. K. & ZHU, J. 2019. Orchestration between ILC2s and Th2 cells in shaping type 2 immune responses. *Cell Mol Immunol,* 16**,** 225-235.

HACKENBERG, S., SCHERZED, A., TECHNAU, A., KESSLER, M., FROELICH, K., GINZKEY, C., KOEHLER, C., BURGHARTZ, M., HAGEN, R. & KLEINSASSER, N. 2011. Cytotoxic, genotoxic and pro-inflammatory effects of zinc oxide nanoparticles in human nasal mucosa cells in vitro. *Toxicol In Vitro,* 25**,** 657-63.

HALLSTRAND, T. S., LAI, Y., ALTEMEIER, W. A., APPEL, C. L., JOHNSON, B., FREVERT, C. W., HUDKINS, K. L., BOLLINGER, J. G., WOODRUFF, P. G., HYDE, D. M., HENDERSON, W. R., JR. & GELB, M. H. 2013. Regulation and function of epithelial secreted phospholipase A2 group X in asthma. *Am J Respir Crit Care Med,* 188**,** 42-50.

HANSBRO, P. M., STARKEY, M. R., MATTES, J. & HORVAT, J. C. 2014. Pulmonary immunity during respiratory infections in early life and the development of severe asthma. *Ann Am Thorac Soc,* 11 Suppl 5**,** S297-302.

HART, J. E. 2016. Air pollution affects lung cancer survival. *Thorax,* 71**,** 875-6.

HARTNEY, J. M. & ROBICHAUD, A. 2013. Assessment of airway hyperresponsiveness in mouse models of allergic lung disease using detailed measurements of respiratory mechanics. *Methods Mol Biol,* 1032**,** 205-17.

HASEGAWA, T., UGA, H., MORI, A. & KURATA, H. 2017. Increased serum IL-17A and Th2 cytokine levels in patients with severe uncontrolled asthma. *Eur Cytokine Netw,* 28**,** 8-18.

HAWKES, N. 2015. Air pollution in UK: the public health problem that won't go away. 350.

HE, X., ZHANG, H., MA, Y., BAI, W., ZHANG, Z., LU, K., DING, Y., ZHAO, Y. & CHAI, Z. 2010. Lung deposition and extrapulmonary translocation of nano-ceria after intratracheal instillation. *Nanotechnology,* 21**,** 285103.

HEKKING, P. P. & BEL, E. H. 2014. Developing and emerging clinical asthma phenotypes. *J Allergy Clin Immunol Pract,* 2**,** 671-80; quiz 681.

HEKMATIMOGHADDAM, S., IMAN, M., SHAHDADI SARDO, H. & JEBALI, A. 2019. Gelatin hydrogel containing cerium oxide nanoparticles covered by interleukin-17 aptamar as an anti- inflammatory agent for brain inflammation. *J Neuroimmunol,* 326**,** 79-83.

HER, E., FRAZER, J., AUSTEN, K. F. & OWEN, W. F. 1991. Eosinophil hematopoietins antagonize the programmed cell death of eosinophils. Cytokine and glucocorticoid effects on eosinophils maintained by endothelial cell-conditioned medium. *J Clin Invest,* 88**,** 1982-7.

HERZOG, F., LOZA, K., BALOG, S., CLIFT, M. J., EPPLE, M., GEHR, P., PETRI-FINK, A. & ROTHEN-RUTISHAUSER, B. 2014. Mimicking exposures to acute and lifetime concentrations of inhaled silver nanoparticles by two different in vitro approaches. *Beilstein J Nanotechnol,* 5**,** 1357-70.

HETTINGA, K. A., REINA, F. M., BOEREN, S., ZHANG, L., KOPPELMAN, G. H., POSTMA, D. S., VERVOORT, J. J. & WIJGA, A. H. 2015. Difference in the breast milk proteome between allergic and non-allergic mothers. *PLoS One,* 10**,** e0122234.

HEYDER, J. 2004. Deposition of inhaled particles in the human respiratory tract and consequences for regional targeting in respiratory drug delivery. *Proc Am Thorac Soc,* 1**,** 315-20.

HIEMSTRA, P. S., MCCRAY, P. B., JR. & BALS, R. 2015. The innate immune function of airway epithelial cells in inflammatory lung disease. *Eur Respir J,* 45**,** 1150-62.

HINKS, T. S., ZHOU, X., STAPLES, K. J., DIMITROV, B. D., MANTA, A., PETROSSIAN, T., LUM, P. Y., SMITH, C. G., WARD, J. A., HOWARTH, P. H., WALLS, A. F., GADOLA, S. D. & DJUKANOVIC, R. 2015. Innate and adaptive T cells in asthmatic patients: Relationship to severity and disease mechanisms. *J Allergy Clin Immunol,* 136**,** 323-33.

HIRAHARA, K. & NAKAYAMA, T. 2016. CD4+ T-cell subsets in inflammatory diseases: beyond the Th1/Th2 paradigm. *Int Immunol,* 28**,** 163-71.

HIRAI, T., YOSHIOKA, Y., TAKAHASHI, H., ICHIHASHI, K.-I., YOSHIDA, T., TOCHIGI, S., NAGANO, K., ABE, Y., KAMADA, H., TSUNODA, S.-I., NABESHI, H., YOSHIKAWA, T. & TSUTSUMI, Y. 2012. Amorphous silica nanoparticles enhance cross-presentation in murine dendritic cells. *Biochemical and biophysical research communications,* 427**,** 553-6.

HIRAMATSU, K., AZUMA, A., KUDOH, S., DESAKI, M., TAKIZAWA, H. & SUGAWARA, I. 2003. Inhalation of diesel exhaust for three months affects major cytokine expression and induces bronchus-associated lymphoid tissue formation in murine lungs. *Exp Lung Res,* 29**,** 607-22.

HOEK, G., BRUNEKREEF, B., GOLDBOHM, S., FISCHER, P. & VAN DEN BRANDT, P. A. 2002. Association between mortality and indicators of traffic-related air pollution in the Netherlands: a cohort study. *The Lancet,* 360**,** 1203-1209.

HOEK, G., KRISHNAN, R. M., BEELEN, R., PETERS, A., OSTRO, B., BRUNEKREEF, B. & KAUFMAN, J. D. 2013. Long-term air pollution exposure and cardio- respiratory mortality: a review. *Environ Health,* 12**,** 43.

HOLGATE, S. T. 2011. Asthma: a simple concept but in reality a complex disease. *Eur J Clin Invest,* 41**,** 1339-52.

HOLGATE, S. T. 2013. Mechanisms of asthma and implications for its prevention and treatment: a personal journey. *Allergy Asthma Immunol Res,* 5**,** 343-7.

HOLGATE, S. T., YANG, Y., HAITCHI, H. M., POWELL, R. M., HOLLOWAY, J. W., YOSHISUE, H., PANG, Y. Y., CAKEBREAD, J. & DAVIES, D. E. 2006. The genetics of asthma: ADAM33 as an example of a susceptibility gene. *Proc Am Thorac Soc,* 3**,** 440-3.

HONGJIA, L., QINGLING, G., MEIYING, L., WEIXUAN, W., LIHONG, Z., YONGSHENG, G., YANLI, L., JINXIANG, W. & LIANG, D. 2010. House dust mite regulate the lung inflammation of asthmatic mice through TLR4 pathway in airway epithelial cells. *Cell Biochem Funct,* 28**,** 597-603.

HORIE, M., NISHIO, K., FUJITA, K., ENDOH, S., MIYAUCHI, A., SAITO, Y., IWAHASHI, H., YAMAMOTO, K., MURAYAMA, H., NAKANO, H., NANASHIMA, N., NIKI, E. & YOSHIDA, Y. 2009. Protein adsorption of ultrafine metal oxide and its influence on cytotoxicity toward cultured cells. *Chem Res Toxicol,* 22**,** 543-53.

HORIE, M., NISHIO, K., KATO, H., FUJITA, K., ENDOH, S., NAKAMURA, A., MIYAUCHI, A., KINUGASA, S., YAMAMOTO, K., NIKI, E., YOSHIDA, Y., HAGIHARA, Y. & IWAHASHI, H. 2011. Cellular responses induced by cerium oxide nanoparticles: induction of intracellular calcium level and oxidative stress on culture cells. *J Biochem,* 150**,** 461-71.

HOSEINNEJAD, M., JAFARI, S. M. & KATOUZIAN, I. 2018. Inorganic and metal nanoparticles and their antimicrobial activity in food packaging applications. *Crit Rev Microbiol,* 44**,** 161-181.

HSIEH, W.-Y., CHOU, C.-C., HO, C.-C., YU, S.-L., CHEN, H.-Y., CHOU, H.-Y. E., CHEN, J. J. W., CHEN, H.-W. & YANG, P.-C. 2012. Single-Walled Carbon Nanotubes Induce Airway Hyperreactivity and Parenchymal Injury in Mice. *American Journal of Respiratory Cell and Molecular Biology,* 46**,** 257-267.

HUANG, F., YIN, J. N., WANG, H. B., LIU, S. Y. & LI, Y. N. 2017a. Association of imbalance of effector T cells and regulatory cells with the severity of asthma and allergic rhinitis in children. *Allergy Asthma Proc,* 38**,** 70-77.

HUANG, S., BODA, B., VERNAZ, J., FERREIRA, E., WISZNIEWSKI, L. & CONSTANT, S. 2017b. Establishment and characterization of an in vitro human small airway model (SmallAir™). *Eur J Pharm Biopharm,* 118**,** 68-72.

HUMBERT, M., YING, S., CORRIGAN, C., MENZ, G., BARKANS, J., PFISTER, R., MENG, Q., VAN DAMME, J., OPDENAKKER, G., DURHAM, S. R. & KAY, A. B. 1997. Bronchial mucosal expression of the genes encoding chemokines RANTES and MCP-3 in symptomatic atopic and nonatopic asthmatics: relationship to the eosinophil-active cytokines interleukin (IL)-5, granulocyte macrophage-colony-stimulating factor, and IL-3. *Am J Respir Cell Mol Biol,* 16**,** 1-8.

HUNNINGHAKE, G. M., SOTO-QUIRÓS, M. E., AVILA, L., SU, J., MURPHY, A., DEMEO, D. L., LY, N. P., LIANG, C., SYLVIA, J. S., KLANDERMAN, B. J., LANGE, C., RABY, B. A., SILVERMAN, E. K. & CELEDÓN, J. C. 2007. Polymorphisms in IL13, total IgE, eosinophilia, and asthma exacerbations in childhood. *J Allergy Clin Immunol,* 120**,** 84-90.

HUYNH, M. L., MALCOLM, K. C., KOTARU, C., TILSTRA, J. A., WESTCOTT, J. Y., FADOK, V. A. & WENZEL, S. E. 2005. Defective apoptotic cell phagocytosis attenuates prostaglandin E2 and 15-hydroxyeicosatetraenoic acid in severe asthma alveolar macrophages. *Am J Respir Crit Care Med,* 172**,** 972-9.

HVIDTFELDT, U. A., GEELS, C., SORENSEN, M., KETZEL, M., KHAN, J., TJONNELAND, A., CHRISTENSEN, J. H., BRANDT, J. & RAASCHOU-NIELSEN, O. 2019. Long-term residential exposure to PM2.5 constituents and mortality in a Danish cohort. *Environ Int,* 133**,** 105268.

ICHINOSE, T., TAKANO, H., SADAKANE, K., YANAGISAWA, R., YOSHIKAWA, T., SAGAI, M. & SHIBAMOTO, T. 2004. Mouse strain differences in eosinophilic airway inflammation caused by intratracheal instillation of mite allergen and diesel exhaust particles. *J Appl Toxicol,* 24**,** 69-76.

ICRP 1994. Human respiratory tract model for radiological protection. A report of a Task Group of the International Commission on Radiological Protection. *Ann ICRP,* 24**,** 1-482.

INOUE, K., TAKANO, H., YANAGISAWA, R., SAKURAI, M., ABE, S., YOSHINO, S., YAMAKI, K. & YOSHIKAWA, T. 2007. Effects of nanoparticles on lung physiology in the presence or absence of antigen. *Int J Immunopathol Pharmacol,* 20**,** 737-44.

ISHMAEL, F. T. 2011. The inflammatory response in the pathogenesis of asthma. *J Am Osteopath Assoc,* 111**,** S11-7.

IZUHARA, K., ARIMA, K., OHTA, S., SUZUKI, S., INAMITSU, M. & YAMAMOTO, K. 2014. Periostin in allergic inflammation. *Allergol Int,* 63**,** 143-51.

JACOBSEN, E. A., LESUER, W. E., WILLETTS, L., ZELLNER, K. R., MAZZOLINI, K., ANTONIOS, N., BECK, B., PROTHEROE, C., OCHKUR, S. I., COLBERT, D., LACY, P., MOQBEL, R., APPLETON, J., LEE, N. A. & LEE, J. J. 2014. Eosinophil activities modulate the immune/inflammatory character of allergic respiratory responses in mice. *Allergy,* 69**,** 315-27.

JACOBSEN, N. R., STOEGER, T., VAN DEN BRULE, S., SABER, A. T., BEYERLE, A., VIETTI, G., MORTENSEN, A., SZAREK, J., BUDTZ, H. C., KERMANIZADEH, A., BANERJEE, A., ERCAL, N., VOGEL, U., WALLIN, H. & MØLLER, P. 2015a. Acute and subacute pulmonary toxicity and mortality in mice after intratracheal instillation of ZnO nanoparticles in three laboratories. *Food and Chemical Toxicology,* 85**,** 84-95.

JACOBSEN, N. R., STOEGER, T., VAN DEN BRULE, S., SABER, A. T., BEYERLE, A., VIETTI, G., MORTENSEN, A., SZAREK, J., BUDTZ, H. C., KERMANIZADEH, A., BANERJEE, A., ERCAL, N., VOGEL, U., WALLIN, H. & MØLLER, P. 2015b. Acute and subacute pulmonary toxicity and mortality in mice after intratracheal instillation of ZnO nanoparticles in three laboratories. *Food Chem Toxicol,* 85**,** 84-95.

JARTTI, T. & GERN, J. E. 2017. Role of viral infections in the development and exacerbation of asthma in children. *J Allergy Clin Immunol,* 140**,** 895-906.

JIANG, Z. & ZHU, L. 2016. Update on the role of alternatively activated macrophages in asthma. *J Asthma Allergy,* 9**,** 101-7.

JORIS, F., VALDEPEREZ, D., PELAZ, B., SOENEN, S. J., MANSHIAN, B. B., PARAK, W. J., DE SMEDT, S. C. & RAEMDONCK, K. 2016. The impact of species and cell type on the nanosafety profile of iron oxide nanoparticles in neural cells. *J Nanobiotechnology,* 14**,** 69.

JOSYULA, S., LIN, J., XUE, X., ROTHMAN, N., LAN, Q., ROHAN, T. E. & HOSGOOD, H. D., 3RD 2015. Household air pollution and cancers other than lung: a meta-analysis. *Environ Health,* 14**,** 24.

JUNG, H. J., KITTELSON, D. B. & ZACHARIAH, M. R. 2005. The influence of a cerium additive on ultrafine diesel particle emissions and kinetics of oxidation. *Combustion and Flame,* 142**,** 276-288.

KAMINSKY, D. A. 2012. What Does Airway Resistance Tell Us About Lung Function? *Respiratory Care,* 57**,** 85.

KAPILEVICH, L., ZAĬTSEVA, T., NOSAREV, A., D'IAKOVA, E., PETLINA, Z., OGORODOVA, L., AGEEV, B., MAGAEVA, A., ITIN, V., TEREKHOVA, O. & MEDVEDEV, M. 2012a. [Influence of nanosize particles of cobalt ferrite on contractile responses of smooth muscle segment of airways]. *Rossiĭskii fiziologicheskiĭ zhurnal imeni I.M. Sechenova / Rossiĭskaia akademiia nauk,* 98**,** 228-35.

KAPILEVICH, L. V., ZAYTSEVA, T. N., NOSAREV, A. V., AGEV, B. G., DYAKOVA, E. Y., OGORODOVA, L. M., MAGAEVA, A. A., TERECOVA, O. G. & ITIN, V. I. 2012b. Contractile Reactions of Guinea Pig Airway Smooth Muscles in the Presence of Stannum Oxide Nanosized Particles. *Bulletin of Experimental Biology and Medicine,* 153**,** 98-100.

KAROL, M. H. 1994. Animal models of occupational asthma. *Eur Respir J,* 7**,** 555-68.

KATO, A. 2019. Group 2 Innate Lymphoid Cells in Airway Diseases. *Chest,* 156**,** 141-149.

KATO, A., HULSE, K. E., TAN, B. K. & SCHLEIMER, R. P. 2013. B-lymphocyte lineage cells and the respiratory system. *Journal of Allergy and Clinical Immunology,* 131**,** 933-957.

KAUFFMAN, H. F., TAMM, M., TIMMERMAN, J. A. B. & BORGER, P. 2006. House dust mite major allergens Der p 1 and Der p 5 activate human airway-derived epithelial cells by protease-dependent and protease-independent mechanisms. *Clinical and Molecular Allergy,* 4**,** 5.

KAWAYAMA, T., MATSUNAGA, K., KAKU, Y., YAMAGUCHI, K., KINOSHITA, T., O'BYRNE, P. M. & HOSHINO, T. 2013. Decreased CTLA4(+) and Foxp3(+) CD25(high)CD4(+) cells in induced sputum from patients with mild atopic asthma. *Allergol Int,* 62**,** 203-13.

KELLER, J., WOHLLEBEN, W., MA-HOCK, L., STRAUSS, V., GRÖTERS, S., KÜTTLER, K., WIENCH, K., HERDEN, C., OBERDÖRSTER, G., VAN RAVENZWAAY, B. & LANDSIEDEL, R. 2014. Time course of lung retention and toxicity of inhaled particles: short-term exposure to nano-Ceria. *Arch Toxicol,* 88**,** 2033-59.

KELLY, F., ARMSTRONG, B., ATKINSON, R., ANDERSON, H. R., BARRATT, B., BEEVERS, S., COOK, D., GREEN, D., DERWENT, D., MUDWAY, I., WILKINSON, P. & COMMITTEE, H. E. I. H. R. 2011. The London low emission zone baseline study. *Res Rep Health Eff Inst***,** 3-79.

KELLY, F. J. & FUSSELL, J. C. 2015a. Air pollution and public health: emerging hazards and improved understanding of risk. *Environ Geochem Health,* 37**,** 631-49.

KELLY, F. J. & FUSSELL, J. C. 2015b. Linking ambient particulate matter pollution effects with oxidative biology and immune responses. *Ann N Y Acad Sci,* 1340**,** 84-94.

KENAGY, H. S., LIN, C., WU, H., HEAL, M. R. J. A. Q., ATMOSPHERE & HEALTH 2016. Greater nitrogen dioxide concentrations at child versus adult breathing heights close to urban main road kerbside. 9**,** 589-595.

KENDALL, M., HODGES, N. J., WHITWELL, H., TYRRELL, J. & CANGUL, H. 2015. Nanoparticle growth and surface chemistry changes in cell-conditioned culture medium. *Philos Trans R Soc Lond B Biol Sci,* 370**,** 20140100.

KENDALL, M., TETLEY, T. D., WIGZELL, E., HUTTON, B., NIEUWENHUIJSEN, M. & LUCKHAM, P. 2002. Lung lining liquid modifies PM(2.5) in favor of particle aggregation: a protective mechanism. *Am J Physiol Lung Cell Mol Physiol,* 282**,** L109-14.

KESSLER, R. 2011. Engineered nanoparticles in consumer products: understanding a new ingredient. *Environ Health Perspect,* 119**,** a120-5.

KHAN, I., SAEED, K. & KHAN, I. 2017. Nanoparticles: Properties, applications and toxicities. *Arabian Journal of Chemistry*.

KILIN, V., MAS, C., CONSTANT, S., WOLF, J. P. & BONACINA, L. 2017. Health state dependent multiphoton induced autofluorescence in human 3D in vitro lung cancer model. *Sci Rep,* 7**,** 16233.

KIM, D., CHEN, Z., ZHOU, L. F. & HUANG, S. X. 2018. Air pollutants and early origins of respiratory diseases. *Chronic Dis Transl Med,* 4**,** 75-94.

KIM, H. S., KANG, S. H., WON, S., LEE, E. K., CHUN, Y. H., YOON, J. S., KIM, H. H. & KIM, J. T. 2015. Immunoglobulin E to allergen components of house dust mite in Korean children with allergic disease. *Asia Pac Allergy,* 5**,** 156-62.

KIM, I. S., BAEK, M. & CHOI, S. J. 2010. Comparative cytotoxicity of Al2O3, CeO2, TiO2 and ZnO nanoparticles to human lung cells. *J Nanosci Nanotechnol,* 10**,** 3453-8.

KIM, J., NATARAJAN, S., VAICKUS, L. J., BOUCHARD, J. C., BEAL, D., CRUIKSHANK, W. W. & REMICK, D. G. 2011a. Diesel exhaust particulates

exacerbate asthma-like inflammation by increasing CXC chemokines. *Am J Pathol,* 179**,** 2730-9.

KIM, J., NATARAJAN, S., VAICKUS, L. J., BOUCHARD, J. C., BEAL, D., CRUIKSHANK, W. W. & REMICK, D. G. 2011b. Diesel Exhaust Particulates Exacerbate Asthma-Like Inflammation by Increasing CXC Chemokines. *The American Journal of Pathology,* 179**,** 2730-2739.

KIM, S. R. & RHEE, Y. K. 2010. Overlap Between Asthma and COPD: Where the Two Diseases Converge. *Allergy Asthma Immunol Res,* 2**,** 209-14.

KIM, Y. D., LANTZ-MCPEAK, S. M., ALI, S. F., KLEINMAN, M. T., CHOI, Y. S. & KIM, H. 2014a. Effects of ultrafine diesel exhaust particles on oxidative stress generation and dopamine metabolism in PC-12 cells. *Environ Toxicol Pharmacol,* 37**,** 954-9.

KIM, Y. H., BOYKIN, E., STEVENS, T., LAVRICH, K. & GILMOUR, M. I. 2014b. Comparative lung toxicity of engineered nanomaterials utilizing in vitro, ex vivo and in vivo approaches. *J Nanobiotechnology,* 12**,** 47.

KITTELSON, D. B. 1998. Engines and nanoparticles: a review. *Journal of Aerosol Science,* 29**,** 575-588.

KLUMPP, J. & BERTELLI, L. 2017. KDEP: A Resource for Calculating Particle Deposition in the Respiratory Tract. *Health Phys,* 113**,** 110-121.

KNIGHT, D. A. & HOLGATE, S. T. 2003. The airway epithelium: structural and functional properties in health and disease. *Respirology,* 8**,** 432-46.

KOCH, S., SOPEL, N. & FINOTTO, S. 2017. Th9 and other IL-9-producing cells in allergic asthma. *Semin Immunopathol,* 39**,** 55-68.

KOIKE, E., TAKANO, H., INOUE, K.-I., YANAGISAWA, R. & KOBAYASHI, T. 2008. Carbon black nanoparticles promote the maturation and function of mouse bone marrow-derived dendritic cells. *Chemosphere,* 73**,** 371-376.

KONDURU, N. V., MOLINA, R. M., SWAMI, A., DAMIANI, F., PYRGIOTAKIS, G., LIN, P., ANDREOZZI, P., DONAGHEY, T. C., DEMOKRITOU, P., KROL, S., KREYLING, W. & BRAIN, J. D. 2017. Protein corona: implications for nanoparticle interactions with pulmonary cells. *Part Fibre Toxicol,* 14**,** 42.

KONONENKO, V., WARHEIT, D. B. & DROBNE, D. 2019. Grouping of Poorly Soluble Low (Cyto)Toxic Particles: Example with 15 Selected Nanoparticles and A549 Human Lung Cells. *Nanomaterials (Basel),* 9.

KOOTER, I. A. G.-M. M. A. S. M. A. D. E. A. A. F. A. S. Y. A. T. P. A. S. E. A. K. C. A. V. S. E. 2016. Cellular Effects in an In Vitro Human 3D Cellular Airway Model and A549/BEAS-2B In Vitro Cell Cultures Following Air Exposure to Cerium Oxide Particles at an Air–Liquid Interface. 2**,** 56-66.

KOPF, M., SCHNEIDER, C. & NOBS, S. P. 2015. The development and function of lung-resident macrophages and dendritic cells. *Nat Immunol,* 16**,** 36-44.

KORN, T., BETTELLI, E., GAO, W., AWASTHI, A., JAGER, A., STROM, T. B., OUKKA, M. & KUCHROO, V. K. 2007. IL-21 initiates an alternative pathway to induce proinflammatory T(H)17 cells. *Nature,* 448**,** 484-487.

KORTEN, I., RAMSEY, K. & LATZIN, P. 2017. Air pollution during pregnancy and lung development in the child. *Paediatr Respir Rev,* 21**,** 38-46.

KREYLING, W. & SCHEUCH, G. 2000. Clearance of Particles Deposited in the Lungs. *Particle-Lung Interactions***,** 323-376.

KREYLING, W. G., HIRN, S., MOLLER, W., SCHLEH, C., WENK, A., CELIK, G., LIPKA, J., SCHAFFLER, M., HABERL, N., JOHNSTON, B. D., SPERLING, R., SCHMID, G., SIMON, U., PARAK, W. J. & SEMMLER-BEHNKE, M. 2014. Air-blood barrier translocation of tracheally instilled gold nanoparticles inversely depends on particle size. *ACS Nano,* 8**,** 222-33.

KREYLING, W. G., HIRN, S. & SCHLEH, C. 2010. Nanoparticles in the lung. *Nat Biotechnol,* 28**,** 1275-6.

KROLL, A., DIERKER, C., ROMMEL, C., HAHN, D., WOHLLEBEN, W., SCHULZE-ISFORT, C., GÖBBERT, C., VOETZ, M., HARDINGHAUS, F. & SCHNEKENBURGER, J. 2011. Cytotoxicity screening of 23 engineered nanomaterials using a test matrix of ten cell lines and three different assays. *Part Fibre Toxicol,* 8**,** 9.

KRUG, H. F. 2014. Nanosafety research--are we on the right track? *Angew Chem Int Ed Engl,* 53**,** 12304-19.

KUBO, M. 2017. Innate and adaptive type 2 immunity in lung allergic inflammation. *Immunol Rev,* 278**,** 162-172.

KUDO, M., MELTON, A. C., CHEN, C., ENGLER, M. B., HUANG, K. E., REN, X., WANG, Y., BERNSTEIN, X., LI, J. T., ATABAI, K., HUANG, X. & SHEPPARD, D. 2012. IL-17A produced by alphabeta T cells drives airway hyper-responsiveness in mice and enhances mouse and human airway smooth muscle contraction. *Nat Med,* 18**,** 547-54.

KUHN, D. A., VANHECKE, D., MICHEN, B., BLANK, F., GEHR, P., PETRI-FINK, A. & ROTHEN-RUTISHAUSER, B. 2014. Different endocytotic uptake mechanisms for nanoparticles in epithelial cells and macrophages. *Beilstein J Nanotechnol,* 5**,** 1625-36.

KUMARI, M., KUMARI, S. I., KAMAL, S. S. & GROVER, P. 2014a. Genotoxicity assessment of cerium oxide nanoparticles in female Wistar rats after acute oral exposure. *Mutat Res Genet Toxicol Environ Mutagen,* 775-776**,** 7-19.

KUMARI, M., SINGH, S. P., CHINDE, S., RAHMAN, M. F., MAHBOOB, M. & GROVER, P. 2014b. Toxicity study of cerium oxide nanoparticles in human neuroblastoma cells. *Int J Toxicol,* 33**,** 86-97.

KUO, C.-H. S., PAVLIDIS, S., LOZA, M., BARIBAUD, F., ROWE, A., PANDIS, I., SOUSA, A., CORFIELD, J., DJUKANOVIC, R., LUTTER, R., STERK, P. J., AUFFRAY, C., GUO, Y., ADCOCK, I. M. & CHUNG, K. F. 2017. T-helper cell type 2 (Th2) and non-Th2 molecular phenotypes of asthma using sputum transcriptomics in U-BIOPRED. *European Respiratory Journal,* 49**,** 1602135.

KURT, O. K., ZHANG, J. & PINKERTON, K. E. 2016. Pulmonary health effects of air pollution. *Curr Opin Pulm Med,* 22**,** 138-43.

KURUVILLA, M. E., LEE, F. E. & LEE, G. B. 2019. Understanding Asthma Phenotypes, Endotypes, and Mechanisms of Disease. *Clin Rev Allergy Immunol,* 56**,** 219-233.

KUSEL, M. M., DE KLERK, N. H., KEBADZE, T., VOHMA, V., HOLT, P. G., JOHNSTON, S. L. & SLY, P. D. 2007. Early-life respiratory viral infections, atopic sensitization, and risk of subsequent development of persistent asthma. *J Allergy Clin Immunol,* 119**,** 1105-10.

KUYPER, L. M., PARE, P. D., HOGG, J. C., LAMBERT, R. K., IONESCU, D., WOODS, R. & BAI, T. R. 2003. Characterization of airway plugging in fatal asthma. *Am J Med,* 115**,** 6-11.

LAMBRECHT, B. N. & HAMMAD, H. 2012. The airway epithelium in asthma. *Nat Med,* 18**,** 684-92.

LAMBRECHT, B. N. & HAMMAD, H. 2014. Allergens and the airway epithelium response: gateway to allergic sensitization. *J Allergy Clin Immunol,* 134**,** 499-507.

LAMBRECHT, B. N. & HAMMAD, H. 2015. The immunology of asthma. *Nat Immunol,* 16**,** 45-56.

LANDGRAF-RAUF, K., ANSELM, B. & SCHAUB, B. 2016. The puzzle of immune phenotypes of childhood asthma. *Mol Cell Pediatr,* 3**,** 27.

LANDRIGAN, P. J. 2017. Air pollution and health. *Lancet Public Health,* 2**,** e4-e5.

LAWAL, A. O. 2018. Diesel Exhaust Particles and the Induction of Macrophage Activation and Dysfunction. *Inflammation,* 41**,** 356-363.

LAWRENCE, T. 2009. The nuclear factor NF-kappaB pathway in inflammation. *Cold Spring Harb Perspect Biol,* 1**,** a001651.

LEE, A., KAALI, S., KINNEY, P. L., DELMINI, R., QUINN, A., OPOKU-MENSAH, J., BURKART, K., ASAYAH, K., YAWSON, A., CHILLRUD, S., KAALI, E. B., JACK, D. & ASANTE, K. P. 2018. In Utero Household Air Pollution Exposure Is Associated with Reduced Pulmonary Function in Infants. *A16. AIR POLLUTION AND PEDIATRIC ASTHMA.* American Thoracic Society.

LEE, H. J., YOO, J. E., NAMKUNG, W., CHO, H. J., KIM, K., KANG, J. W., YOON, J. H. & CHOI, J. Y. 2015. Thick airway surface liquid volume and weak mucin expression in pendrin-deficient human airway epithelia. *Physiol Rep,* 3.

LEE, J. Y., PARK, S. W., CHANG, H. K., KIM, H. Y., RHIM, T., LEE, J. H., JANG, A. S., KOH, E. S. & PARK, C. S. 2006. A disintegrin and metalloproteinase 33 protein in patients with asthma: Relevance to airflow limitation. *Am J Respir Crit Care Med,* 173**,** 729-35.

LEHMANN, A. D., BLANK, F., BAUM, O., GEHR, P. & ROTHEN-RUTISHAUSER, B. M. 2009. Diesel exhaust particles modulate the tight junction protein occludin in lung cells in vitro. *Part Fibre Toxicol,* 6**,** 26.

LEI, Y., BOINAPALLY, V., ZOLTOWSKA, A., ADNER, M., HELLMAN, L. & NILSSON, G. 2015. Vaccination against IL-33 Inhibits Airway Hyperresponsiveness and Inflammation in a House Dust Mite Model of Asthma. *PLoS One,* 10**,** e0133774.

LEMANSKE, R. F., JACKSON, D. J., GANGNON, R. E., EVANS, M. D., LI, Z., SHULT, P. A., KIRK, C. J., REISDORF, E., ROBERG, K. A., ANDERSON, E. L., CARLSON-DAKES, K. T., ADLER, K. J., GILBERTSON-WHITE, S., PAPPAS, T. E., DASILVA, D. F., TISLER, C. J. & GERN, J. E. 2005. Rhinovirus illnesses during infancy predict subsequent childhood wheezing. *J Allergy Clin Immunol,* 116**,** 571-7.

LENZ, A. G., KARG, E., BRENDEL, E., HINZE-HEYN, H., MAIER, K. L., EICKELBERG, O., STOEGER, T. & SCHMID, O. 2013. Inflammatory and oxidative stress responses of an alveolar epithelial cell line to airborne zinc oxide nanoparticles at the air-liquid interface: a comparison with conventional, submerged cell-culture conditions. *Biomed Res Int,* 2013**,** 652632.

LEOMICRONN, B. 2017. T Cells in Allergic Asthma: Key Players Beyond the Th2 Pathway. *Curr Allergy Asthma Rep,* 17**,** 43.

LESIMPLE, P., VAN SEUNINGEN, I., BUISINE, M. P., COPIN, M. C., HINZ, M., HOFFMANN, W., HAJJ, R., BRODY, S. L., CORAUX, C. & PUCHELLE, E. 2007. Trefoil factor family 3 peptide promotes human airway epithelial ciliated cell differentiation. *Am J Respir Cell Mol Biol,* 36**,** 296-303.

LI, M., HU, M., DU, B., GUO, Q., TAN, T., ZHENG, J., HUANG, X., HE, L., WU, Z. & GUO, S. 2017. Temporal and spatial distribution of PM. *Sci Total Environ,* 605-606**,** 337-346.

LI, N., HAO, M., PHALEN, R. F., HINDS, W. C. & NEL, A. E. 2003. Particulate air pollutants and asthma. A paradigm for the role of oxidative stress in PM-induced adverse health effects. *Clin Immunol,* 109**,** 250-65.

LI, S., ALIYEVA, M., DAPHTARY, N., MARTIN, R. A., POYNTER, M. E., KOSTIN, S. F., VAN DER VELDEN, J. L., HYMAN, A. M., STEVENSON, C. S., PHILLIPS, J. E. & LUNDBLAD, L. K. 2014. Antigen-induced mast cell expansion and bronchoconstriction in a mouse model of asthma. *Am J Physiol Lung Cell Mol Physiol,* 306**,** L196-206.

LI, Y. F., LANGHOLZ, B., SALAM, M. T. & GILLILAND, F. D. 2005. Maternal and grandmaternal smoking patterns are associated with early childhood asthma. *Chest,* 127**,** 1232-41.

LIM, R. H. & KOBZIK, L. 2009. REVIEW ARTICLE: Maternal Transmission of Asthma Risk. *American Journal of Reproductive Immunology,* 61**,** 1-10.

LIN, W., HUANG, Y. W., ZHOU, X. D. & MA, Y. 2006. Toxicity of cerium oxide nanoparticles in human lung cancer cells. *Int J Toxicol,* 25**,** 451-7.

LIND, H., BRUDIN, L., LINDHOLM, L. & EDVINSSON, L. 1996. Different levels of sensory neuropeptides (calcitonin gene-related peptide and substance P) during and after exercise in man. *Clin Physiol,* 16**,** 73-82.

LING, M. F. & LUSTER, A. D. 2016. Allergen-Specific CD4(+) T Cells in Human Asthma. *Ann Am Thorac Soc,* 13 Suppl 1**,** S25-30.

LIU, C., ZHANG, X., XIANG, Y., QU, X., LIU, H., LIU, C., TAN, M., JIANG, J. & QIN, X. 2018. Role of epithelial chemokines in the pathogenesis of airway inflammation in asthma (Review). *Mol Med Rep,* 17**,** 6935-6941.

LIU, Y. J., SOUMELIS, V., WATANABE, N., ITO, T., WANG, Y. H., MALEFYT RDE, W., OMORI, M., ZHOU, B. & ZIEGLER, S. F. 2007. TSLP: an epithelial cell cytokine that regulates T cell differentiation by conditioning dendritic cell maturation. *Annu Rev Immunol,* 25**,** 193-219.

LONDON, S. J. 2007. Gene-air pollution interactions in asthma. *Proc Am Thorac Soc,* 4**,** 217-20.

LONGHIN, E., GUALTIERI, M., CAPASSO, L., BENGALLI, R., MOLLERUP, S., HOLME, J. A., ØVREVIK, J., CASADEI, S., DI BENEDETTO, C., PARENTI, P. & CAMATINI, M. 2016. Physico-chemical properties and biological effects of diesel and biomass particles. *Environ Pollut,* 215**,** 366-375.

LONGPHRE, M., LI, D., GALLUP, M., DRORI, E., ORDONEZ, C. L., REDMAN, T., WENZEL, S., BICE, D. E., FAHY, J. V. & BASBAUM, C. 1999. Allergen-induced IL-9 directly stimulates mucin transcription in respiratory epithelial cells. *J Clin Invest,* 104**,** 1375-82.

LOWE, A. J., CARLIN, J. B., BENNETT, C. M., ABRAMSON, M. J., HOSKING, C. S., HILL, D. J. & DHARMAGE, S. C. 2006. Atopic disease and breast-feeding—cause or consequence? *Journal of Allergy and Clinical Immunology,* 117**,** 682-687.

LOXHAM, M., MORGAN-WALSH, R. J., COOPER, M. J., BLUME, C., SWINDLE, E. J., DENNISON, P. W., HOWARTH, P. H., CASSEE, F. R., TEAGLE, D. A., PALMER, M. R. & DAVIES, D. E. 2015. The effects on bronchial epithelial mucociliary cultures of coarse, fine, and ultrafine particulate matter from an underground railway station. *Toxicol Sci,* 145**,** 98-107.

LUMENG, C. N. 2016. Lung Macrophage Diversity and Asthma. *Ann Am Thorac Soc,* 13 Suppl 1**,** S31-4.

LV, J., YU, Q., DI, C., LIN, X., SU, W., WU, M. & XIA, Z. 2018. Airway epithelial TSLP production of TLR2 drives type 2 immunity in allergic airway inflammation. *Eur J Immunol*.

MA, J., BISHOFF, B., MERCER, R. R., BARGER, M., SCHWEGLER-BERRY, D. & CASTRANOVA, V. 2017. Role of epithelial-mesenchymal transition (EMT) and fibroblast function in cerium oxide nanoparticles-induced lung fibrosis. *Toxicology and Applied Pharmacology,* 323.

MA, J., MERCER, R., BARGER, M., SCHWEGLER-BERRY, D., SCABILLONI, J., MA, J. & CASTRANOVA, V. 2012. Induction of pulmonary fibrosis by cerium oxide nanoparticles. *Toxicology and applied pharmacology,* 262**,** 255-64.

MA, J. Y., YOUNG, S. H., MERCER, R. R., BARGER, M., SCHWEGLER-BERRY, D., MA, J. K. & CASTRANOVA, V. 2014a. Interactive effects of cerium oxide and diesel exhaust nanoparticles on inducing pulmonary fibrosis. *Toxicol Appl Pharmacol,* 278**,** 135-47.

MA, J. Y., ZHAO, H., MERCER, R. R., BARGER, M., RAO, M., MEIGHAN, T., SCHWEGLER-BERRY, D., CASTRANOVA, V. & MA, J. K. 2011. Cerium oxide nanoparticle-induced pulmonary inflammation and alveolar macrophage functional change in rats. *Nanotoxicology,* 5**,** 312-25.

MA, J. Y. C., YOUNG, S.-H., MERCER, R. R., BARGER, M., SCHWEGLER-BERRY, D., MA, J. K. & CASTRANOVA, V. 2014b. Interactive effects of cerium oxide and diesel exhaust nanoparticles on inducing pulmonary fibrosis. *Toxicology and Applied Pharmacology,* 278**,** 135-147.

MACINTYRE, E. A., BRAUER, M., MELEN, E., BAUER, C. P., BAUER, M., BERDEL, D., BERGSTROM, A., BRUNEKREEF, B., CHAN-YEUNG, M., KLUMPER, C., FUERTES, E., GEHRING, U., GREF, A., HEINRICH, J., HERBARTH, O., KERKHOF, M., KOPPELMAN, G. H., KOZYRSKYJ, A. L., PERSHAGEN, G., POSTMA, D. S., THIERING, E., TIESLER, C. M., CARLSTEN, C. & GROUP, T. A. G. S. 2014. GSTP1 and TNF Gene variants and associations between air pollution and incident childhood asthma: the traffic, asthma and genetics (TAG) study. *Environ Health Perspect,* 122**,** 418-24.

MAJAK, P., OLSZOWIEC-CHLEBNA, M., SMEJDA, K. & STELMACH, I. 2011. Vitamin D supplementation in children may prevent asthma exacerbation triggered by acute respiratory infection. *J Allergy Clin Immunol,* 127**,** 1294-6.

MALEKKHAIAT HAFFNER, S. & MALMSTEN, M. 2017. Membrane interactions and antimicrobial effects of inorganic nanoparticles. *Adv Colloid Interface Sci,* 248**,** 105-128.

MALL, M. A. 2008. Role of cilia, mucus, and airway surface liquid in mucociliary dysfunction: lessons from mouse models. *J Aerosol Med Pulm Drug Deliv,* 21**,** 13-24.

MANUYAKORN, W., HOWARTH, P. H. & HOLGATE, S. T. 2013. Airway remodelling in asthma and novel therapy. *Asian Pac J Allergy Immunol,* 31**,** 3-10.

MARCAZZAN, G. M., VACCARO, S., VALLI, G. & VECCHI, R. 2001. Characterisation of PM10 and PM2.5 particulate matter in the ambient air of Milan (Italy). *Atmospheric Environment,* 35**,** 4639-4650.

MARCHETTI, P., PESCE, G., VILLANI, S., ANTONICELLI, L., ARIANO, R., ATTENA, F., BONO, R., BELLISARIO, V., FOIS, A., GIBELLI, N., NICOLIS, M., OLIVIERI, M., PIRINA, P., SCOPANO, E., SINISCALCO, C., VERLATO, G. & MARCON, A. 2017. Pollen concentrations and prevalence of asthma and allergic rhinitis in Italy: Evidence from the GEIRD study. *Sci Total Environ,* 584-585**,** 1093-1099.

MARTIN-OROZCO, E., NORTE-MUNOZ, M. & MARTINEZ-GARCIA, J. 2017. Regulatory T Cells in Allergy and Asthma. *Front Pediatr,* 5**,** 117.

MARTIN, R., DOWLING, K., NANKERVIS, S., PEARCE, D., FLORENTINE, S. & MCKNIGHT, S. 2018. In vitro assessment of arsenic mobility in historical mine waste dust using simulated lung fluid. *Environ Geochem Health,* 40**,** 1037-1049.

MARTINEZ-GONZALEZ, I., MATHA, L., STEER, C. A., GHAEDI, M., POON, G. F. & TAKEI, F. 2016. Allergen-Experienced Group 2 Innate Lymphoid Cells Acquire Memory-like Properties and Enhance Allergic Lung Inflammation. *Immunity,* 45**,** 198-208.

MATSUI, H., RANDELL, S. H., PERETTI, S. W., DAVIS, C. W. & BOUCHER, R. C. 1998. Coordinated clearance of periciliary liquid and mucus from airway surfaces. *J Clin Invest,* 102**,** 1125-31.

MATTEIS, M., POLVERINO, F., SPAZIANO, G., ROVIEZZO, F., SANTORIELLO, C., SULLO, N., BUCCI, M. R., ROSSI, F., POLVERINO, M., OWEN, C. A. & D'AGOSTINO, B. 2014. Effects of sex hormones on bronchial reactivity during the menstrual cycle. *BMC Pulm Med,* 14**,** 108.

MAUS, U. A., JANZEN, S., WALL, G., SRIVASTAVA, M., BLACKWELL, T. S., CHRISTMAN, J. W., SEEGER, W., WELTE, T. & LOHMEYER, J. 2006. Resident alveolar macrophages are replaced by recruited monocytes in response to endotoxin-induced lung inflammation. *Am J Respir Cell Mol Biol,* 35**,** 227-35.

MAYNARD, R. L. 2015. The effects on health of ambient particles: time for an agonizing reappraisal? *Cell Biol Toxicol,* 31**,** 131-47.

MAYNARD, R. L., DONALDSON, K. & TETLEY, T. D. 2013. Type 1 pulmonary epithelial cells: a new compartment involved in the slow phase of particle clearance from alveoli. *Nanotoxicology,* 7**,** 350-1.

MAZZARELLA, G., LUCARIELLO, A., BIANCO, A., CALABRESE, C., THANASSOULAS, T., SAVARESE, L., FIUMARELLA, A., ESPOSITO, V. & DE LUCA, A. 2014. Exposure to submicron particles (PM1.0) from diesel exhaust and pollen allergens of human lung epithelial cells induces morphological changes of mitochondria tonifilaments and rough endoplasmic reticulum. *In Vivo,* 28**,** 557-61.

MCCAULEY, H. A. & GUASCH, G. 2015. Three cheers for the goblet cell: maintaining homeostasis in mucosal epithelia. *Trends Mol Med,* 21**,** 492-503.

MCCREANOR, J., CULLINAN, P., NIEUWENHUIJSEN, M. J., STEWART-EVANS, J., MALLIAROU, E., JARUP, L., HARRINGTON, R., SVARTENGREN, M., HAN, I. K., OHMAN-STRICKLAND, P., CHUNG, K. F. & ZHANG, J. 2007. Respiratory effects of exposure to diesel traffic in persons with asthma. *N Engl J Med,* 357**,** 2348-58.

MCMILLAN, S. J. & LLOYD, C. M. 2004. Prolonged allergen challenge in mice leads to persistent airway remodelling. *Clin Exp Allergy,* 34**,** 497-507.

MEDZHITOV, R. & JANEWAY, C. A. 1997. Innate immunity: impact on the adaptive immune response. *Curr Opin Immunol,* 9**,** 4-9.

MELDRUM, K., GANT, T. W. & LEONARD, M. O. 2017. Diesel exhaust particulate associated chemicals attenuate expression of CXCL10 in human primary bronchial epithelial cells. *Toxicol In Vitro,* 45**,** 409-416.

MERAD, M., SATHE, P., HELFT, J., MILLER, J. & MORTHA, A. 2013. The dendritic cell lineage: ontogeny and function of dendritic cells and their subsets in the steady state and the inflamed setting. *Annu Rev Immunol,* 31**,** 563-604.

MEURS, H., GOSENS, R. & ZAAGSMA, J. 2008. Airway hyperresponsiveness in asthma: lessons from in vitro model systems and animal models. *European Respiratory Journal,* 32**,** 487.

MILLER, A. M. 2011. Role of IL-33 in inflammation and disease. *J Inflamm (Lond),* 8**,** 22.

MILLER, M. R., RAFTIS, J. B., LANGRISH, J. P., MCLEAN, S. G., SAMUTRTAI, P., CONNELL, S. P., WILSON, S., VESEY, A. T., FOKKENS, P. H. B., BOERE, A. J. F., KRYSTEK, P., CAMPBELL, C. J., HADOKE, P. W. F., DONALDSON, K., CASSEE, F. R., NEWBY, D. E., DUFFIN, R. & MILLS, N. L. 2017. Inhaled Nanoparticles Accumulate at Sites of Vascular Disease. *ACS Nano,* 11**,** 4542-4552.

MILLER, M. R., SHAW, C. A. & LANGRISH, J. P. 2012. From particles to patients: oxidative stress and the cardiovascular effects of air pollution. *Future Cardiol,* 8**,** 577-602.

MILLS, N. L., AMIN, N., ROBINSON, S. D., ANAND, A., DAVIES, J., PATEL, D., DE LA FUENTE, J. M., CASSEE, F. R., BOON, N. A., MACNEE, W., MILLAR, A. M., DONALDSON, K. & NEWBY, D. E. 2006. Do inhaled carbon nanoparticles

translocate directly into the circulation in humans? *Am J Respir Crit Care Med,* 173**,** 426-31.
MINAI-FLEMINGER, Y. & LEVI-SCHAFFER, F. 2009. Mast cells and eosinophils: the two key effector cells in allergic inflammation. *Inflamm Res,* 58**,** 631-8.
MINARCHICK, V. C., STAPLETON, P. A., FIX, N. R., LEONARD, S. S., SABOLSKY, E. M. & NURKIEWICZ, T. R. 2015. Intravenous and gastric cerium dioxide nanoparticle exposure disrupts microvascular smooth muscle signaling. *Toxicol Sci,* 144**,** 77-89.
MISHRA, A., ZHENG, J., TANG, X. & GOERING, P. 2016. Silver Nanoparticle-Induced Autophagic-Lysosomal Disruption and NLRP3-Inflammasome Activation in HepG2 Cells Is Size-Dependent. *Toxicological Sciences,* 150**,** kfw011.
MITCHELL, P. D. & O'BYRNE, P. M. 2017. Biologics and the lung: TSLP and other epithelial cell-derived cytokines in asthma. *Pharmacol Ther,* 169**,** 104-112.
MITTAL, S. & PANDEY, A. K. 2014. Cerium oxide nanoparticles induced toxicity in human lung cells: role of ROS mediated DNA damage and apoptosis. *Biomed Res Int,* 2014**,** 891934.
MOLINA, R. M., KONDURU, N. V., HIRANO, H., DONAGHEY, T. C., ADAMO, B., LAURENZI, B., PYRGIOTAKIS, G. & BRAIN, J. D. 2016. Pulmonary distribution of nanoceria: comparison of intratracheal, microspray instillation and dry powder insufflation. *Inhal Toxicol,* 28**,** 550-560.
MOLLER, P., FOLKMANN, J. K., FORCHHAMMER, L., BRAUNER, E. V., DANIELSEN, P. H., RISOM, L. & LOFT, S. 2008. Air pollution, oxidative damage to DNA, and carcinogenesis. *Cancer Lett,* 266**,** 84-97.
MONTEYNE, P., RENAULD, J. C., VAN BROECK, J., DUNNE, D. W., BROMBACHER, F. & COUTELIER, J. P. 1997. IL-4-independent regulation of in vivo IL-9 expression. *J Immunol,* 159**,** 2616-23.
MOORE, T. L., RODRIGUEZ-LORENZO, L., HIRSCH, V., BALOG, S., URBAN, D., JUD, C., ROTHEN-RUTISHAUSER, B., LATTUADA, M. & PETRI-FINK, A. 2015. Nanoparticle colloidal stability in cell culture media and impact on cellular interactions. *Chem Soc Rev,* 44**,** 6287-305.
MOORE, W. C., HASTIE, A. T., LI, X., LI, H., BUSSE, W. W., JARJOUR, N. N., WENZEL, S. E., PETERS, S. P., MEYERS, D. A., BLEECKER, E. R., NATIONAL HEART, L. & BLOOD INSTITUTE'S SEVERE ASTHMA RESEARCH, P. 2014. Sputum neutrophil counts are associated with more severe asthma phenotypes using cluster analysis. *J Allergy Clin Immunol,* 133**,** 1557-63 e5.
MOREIRA, A., DELGADO, L. & CARLSEN, K. H. 2011. Exercise-induced asthma: why is it so frequent in Olympic athletes? *Expert Rev Respir Med,* 5**,** 1-3.
MORGENSTERN, V., ZUTAVERN, A., CYRYS, J., BROCKOW, I., KOLETZKO, S., KRAMER, U., BEHRENDT, H., HERBARTH, O., VON BERG, A., BAUER, C. P., WICHMANN, H. E., HEINRICH, J., GROUP, G. S. & GROUP, L. S. 2008. Atopic diseases, allergic sensitization, and exposure to traffic-related air pollution in children. *Am J Respir Crit Care Med,* 177**,** 1331-7.
MOSLEY, S. 2014. Environmental History of Air Pollution and Protection. *In:* AGNOLETTI, M. & NERI SERNERI, S. (eds.) *The Basic Environmental History.* Cham: Springer International Publishing.
MOSTOVENKO, E., YOUNG, T., MULDOON, P. P., BISHOP, L., CANAL, C. G., VUCETIC, A., ZEIDLER-ERDELY, P. C., ERDELY, A., CAMPEN, M. J. & OTTENS, A. K. 2019. Nanoparticle exposure driven circulating bioactive peptidome causes systemic inflammation and vascular dysfunction. *Particle and Fibre Toxicology,* 16**,** 20.

MOUNTJOY, M., FITCH, K., BOULET, L. P., BOUGAULT, V., VAN MECHELEN, W. & VERHAGEN, E. 2015. Prevalence and characteristics of asthma in the aquatic disciplines. *J Allergy Clin Immunol*.
MUKAI, K., TSAI, M., STARKL, P., MARICHAL, T. & GALLI, S. J. 2016. IgE and mast cells in host defense against parasites and venoms. *Semin Immunopathol,* 38**,** 581-603.
MUNOZ, X., BARREIRO, E., BUSTAMANTE, V., LOPEZ-CAMPOS, J. L., GONZALEZ-BARCALA, F. J. & CRUZ, M. J. 2019. Diesel exhausts particles: Their role in increasing the incidence of asthma. Reviewing the evidence of a causal link. *Sci Total Environ,* 652**,** 1129-1138.
MUNRO, B. H. Manual of Histologic Staining Methods of the Armed Forces Institute of Pathology. *Pathology,* 3**,** 249.
NA, H., CHO, M. & CHUNG, Y. 2016. Regulation of Th2 Cell Immunity by Dendritic Cells. *Immune Netw,* 16**,** 1-12.
NAKANE, H. 2012. Translocation of particles deposited in the respiratory system: a systematic review and statistical analysis. *Environ Health Prev Med,* 17**,** 263-74.
NAKANISHI, K., TSUKIMOTO, M., TANUMA, S.-I., TAKEDA, K. & KOJIMA, S. 2016. Silica nanoparticles activate purinergic signaling via P2X7 receptor in dendritic cells, leading to production of pro-inflammatory cytokines. *Toxicology in Vitro,* 35**,** 202-211.
NASSAR, S. Z., HASSAAN, P. S., ABDELMONSIF, D. A. & ELACHY, S. N. 2018. Cardioprotective effect of cerium oxide nanoparticles in monocrotaline rat model of pulmonary hypertension: A possible implication of endothelin-1. *Life Sci,* 201**,** 89-101.
NAZ, S., BEACH, J., HECKERT, B., TUMMALA, T., PASHCHENKO, O., BANERJEE, T. & SANTRA, S. 2017. Cerium oxide nanoparticles: a 'radical' approach to neurodegenerative disease treatment. *Nanomedicine (Lond),* 12**,** 545-553.
NCBI. *PCR* [Online]. Available: https://www.ncbi.nlm.nih.gov/genome/probe/doc/TechPCR.shtml [Accessed 27/11/2017].
NEMMAR, A., AL-SALAM, S., BEEGAM, S., YUVARAJU, P. & ALI, B. H. 2017a. The acute pulmonary and thrombotic effects of cerium oxide nanoparticles after intratracheal instillation in mice. *Int J Nanomedicine,* 12**,** 2913-2922.
NEMMAR, A., YUVARAJU, P., BEEGAM, S., FAHIM, M. A. & ALI, B. H. 2017b. Cerium Oxide Nanoparticles in Lung Acutely Induce Oxidative Stress, Inflammation, and DNA Damage in Various Organs of Mice. *Oxid Med Cell Longev,* 2017**,** 9639035.
NEWCOMB, D. C. & PEEBLES, R. S., JR. 2013. Th17-mediated inflammation in asthma. *Curr Opin Immunol,* 25**,** 755-60.
NIEUWENHUIS, M. A., SIEDLINSKI, M., VAN DEN BERGE, M., GRANELL, R., LI, X., NIENS, M., VAN DER VLIES, P., ALTMULLER, J., NURNBERG, P., KERKHOF, M., VAN SCHAYCK, O. C., RIEMERSMA, R. A., VAN DER MOLEN, T., DE MONCHY, J. G., BOSSE, Y., SANDFORD, A., BRUIJNZEEL-KOOMEN, C. A., GERTH VAN WIJK, R., TEN HACKEN, N. H., TIMENS, W., BOEZEN, H. M., HENDERSON, J., KABESCH, M., VONK, J. M., POSTMA, D. S. & KOPPELMAN, G. H. 2016. Combining genomewide association study and lung eQTL analysis provides evidence for novel genes associated with asthma. *Allergy,* 71**,** 1712-1720.
NIKOLIC, M., SUSTERSIC, T. & FILIPOVIC, N. 2018a. In vitro Models and On-Chip Systems: Biomaterial Interaction Studies With Tissues Generated Using Lung Epithelial and Liver Metabolic Cell Lines. *Front Bioeng Biotechnol,* 6**,** 120.
NIKOLIC, M. Z., SUN, D. & RAWLINS, E. L. 2018b. Human lung development: recent progress and new challenges. *Development,* 145.
NORDLING, E., BERGLIND, N., MELEN, E., EMENIUS, G., HALLBERG, J., NYBERG, F., PERSHAGEN, G., SVARTENGREN, M., WICKMAN, M. & BELLANDER, T.

2008. Traffic-related air pollution and childhood respiratory symptoms, function and allergies. *Epidemiology,* 19**,** 401-8.
NOVAK, P., SHEVCHUK, A., RUENRAROENGSAK, P., MIRAGOLI, M., THORLEY, A. J., KLENERMAN, D., LAB, M. J., TETLEY, T. D., GORELIK, J. & KORCHEV, Y. E. 2014. Imaging single nanoparticle interactions with human lung cells using fast ion conductance microscopy. *Nano Lett,* 14**,** 1202-7.
O'DRISCOLL, C. A., OWENS, L. A., GALLO, M. E., HOFFMANN, E. J., AFRAZI, A., HAN, M., FECHNER, J. H., SCHAUER, J. J., BRADFIELD, C. A. & MEZRICH, J. D. 2018. Differential effects of diesel exhaust particles on T cell differentiation and autoimmune disease. *Part Fibre Toxicol,* 15**,** 35.
OBER, C. & YAO, T. C. 2011. The genetics of asthma and allergic disease: a 21st century perspective. *Immunol Rev,* 242**,** 10-30.
OBOKI, K., NAKAE, S., MATSUMOTO, K. & SAITO, H. 2011. IL-33 and Airway Inflammation. *Allergy, asthma & immunology research,* 3**,** 81-88.
ODDY, W. H. 2017. Breastfeeding, Childhood Asthma, and Allergic Disease. *Ann Nutr Metab,* 70 Suppl 2**,** 26-36.
OLIN, J. T. & WECHSLER, M. E. 2014. Asthma: pathogenesis and novel drugs for treatment. *BMJ,* 349**,** g5517.
OREO, K. M., GIBSON, P. G., SIMPSON, J. L., WOOD, L. G., MCDONALD, V. M. & BAINES, K. J. 2014. Sputum ADAM8 expression is increased in severe asthma and COPD. *Clin Exp Allergy,* 44**,** 342-52.
OSBORNE, N. J., ALCOCK, I., WHEELER, B. W., HAJAT, S., SARRAN, C., CLEWLOW, Y., MCINNES, R. N., HEMMING, D., WHITE, M., VARDOULAKIS, S. & FLEMING, L. E. 2017. Pollen exposure and hospitalization due to asthma exacerbations: daily time series in a European city. *Int J Biometeorol,* 61**,** 1837-1848.
OVREVIK, J., REFSNES, M., LAG, M., BRINCHMANN, B. C., SCHWARZE, P. E. & HOLME, J. A. 2017. Triggering Mechanisms and Inflammatory Effects of Combustion Exhaust Particles with Implication for Carcinogenesis. *Basic Clin Pharmacol Toxicol,* 121 Suppl 3**,** 55-62.
PALCZYNSKI, C. & KUNA, P. 2015. Air pollution and childhood asthma. *Pneumonol Alergol Pol,* 83**,** 247-9.
PALLAVI PANT, R. M. H. 2013. Estimation of the contribution of road traffic emissions to particulate matter concentrations from field measurements: A review. *Atmospheric Environment,* 77**,** 78 - 97.
PALOMARES, O., AKDIS, M., MARTIN-FONTECHA, M. & AKDIS, C. A. 2017. Mechanisms of immune regulation in allergic diseases: the role of regulatory T and B cells. *Immunol Rev,* 278**,** 219-236.
PANAS, A., COMOUTH, A., SAATHOFF, H., LEISNER, T., AL-RAWI, M., SIMON, M., SEEMANN, G., DOSSEL, O., MULHOPT, S., PAUR, H. R., FRITSCH-DECKER, S., WEISS, C. & DIABATE, S. 2014. Silica nanoparticles are less toxic to human lung cells when deposited at the air-liquid interface compared to conventional submerged exposure. *Beilstein J Nanotechnol,* 5**,** 1590-1602.
PANDYA, R. J., SOLOMON, G., KINNER, A. & BALMES, J. R. 2002. Diesel exhaust and asthma: hypotheses and molecular mechanisms of action. *Environ Health Perspect,* 110 Suppl 1**,** 103-12.
PAPAZIAN, D., WAGTMANN, V. R., HANSEN, S. & WÜRTZEN, P. A. 2015. Direct contact between dendritic cells and bronchial epithelial cells inhibits T cell recall responses towards mite and pollen allergen extracts in vitro. *Clin Exp Immunol,* 181**,** 207-18.

PAPLINSKA-GORYCA, M., NEJMAN-GRYZ, P., GORSKA, K., BIALEK-GOSK, K., HERMANOWICZ-SALAMON, J. & KRENKE, R. 2018. Expression of Inflammatory Mediators in Induced Sputum: Comparative Study in Asthma and COPD. *Adv Exp Med Biol,* 1040**,** 101-112.

PAPOUTSAKIS, C., PRIFTIS, K. N., DRAKOULI, M., PRIFTI, S., KONSTANTAKI, E., CHONDRONIKOLA, M., ANTONOGEORGOS, G. & MATZIOU, V. 2013. Childhood overweight/obesity and asthma: is there a link? A systematic review of recent epidemiologic evidence. *J Acad Nutr Diet,* 113**,** 77-105.

PARK, B., DONALDSON, K., DUFFIN, R., TRAN, L., KELLY, F., MUDWAY, I., MORIN, J. P., GUEST, R., JENKINSON, P., SAMARAS, Z., GIANNOULI, M., KOURIDIS, H. & MARTIN, P. 2008a. Hazard and risk assessment of a nanoparticulate cerium oxide-based diesel fuel additive - a case study. *Inhal Toxicol,* 20**,** 547-66.

PARK, B., MARTIN, P., HARRIS, C., GUEST, R., WHITTINGHAM, A., JENKINSON, P. & HANDLEY, J. 2007. Initial in vitro screening approach to investigate the potential health and environmental hazards of Enviroxtrade mark - a nanoparticulate cerium oxide diesel fuel additive. *Part Fibre Toxicol,* 4**,** 12.

PARK, E. J., CHOI, J., PARK, Y. K. & PARK, K. 2008b. Oxidative stress induced by cerium oxide nanoparticles in cultured BEAS-2B cells. *Toxicology,* 245**,** 90-100.

PARK, J.-W., LEE, I.-C., SHIN, N.-R., JEON, C.-M., KWON, O.-K., KO, J.-W., KIM, J.-C., OH, S.-R., SHIN, I.-S. & AHN, K.-S. 2016. Copper oxide nanoparticles aggravate airway inflammation and mucus production in asthmatic mice via MAPK signaling. *Nanotoxicology,* 10**,** 445-452.

PASHA, M. A., PATEL, G., HOPP, R. & YANG, Q. 2019. Role of innate lymphoid cells in allergic diseases. *Allergy Asthma Proc,* 40**,** 138-145.

PATEL, N. N., KOHANSKI, M. A., MAINA, I. W., WORKMAN, A. D., HERBERT, D. R. & COHEN, N. A. 2019. Sentinels at the wall: epithelial-derived cytokines serve as triggers of upper airway type 2 inflammation. *Int Forum Allergy Rhinol,* 9**,** 93-99.

PATHOLOGYOUTLINES.COM. *PAS (Periodic Acid-Schiff)* [Online]. Available: http://www.pathologyoutlines.com/topic/stainspas.html [Accessed 21st Novemember 2017].

PATIL, S., SANDBERG, A., HECKERT, E., SELF, W. & SEAL, S. 2007. Protein adsorption and cellular uptake of cerium oxide nanoparticles as a function of zeta potential. *Biomaterials,* 28**,** 4600-7.

PATRAVALE, V., DANDEKAR, P. & JAIN, R. 2012. 3 - Characterization techniques for nanoparticulate carriers. *Nanoparticulate Drug Delivery.* Woodhead Publishing.

PATTERSON, C. C. 1965. Contaminated and Natural Lead Environments of Man. *Archives of Environmental Health: An International Journal,* 11**,** 344-360.

PAUL, E., FRANCO-MONTOYA, M. L., PAINEAU, E., ANGELETTI, B., VIBHUSHAN, S., RIDOUX, A., TIENDREBEOGO, A., SALOME, M., HESSE, B., VANTELON, D., ROSE, J., CANOUI-POITRINE, F., BOCZKOWSKI, J., LANONE, S., DELACOURT, C. & PAIRON, J. C. 2017. Pulmonary exposure to metallic nanomaterials during pregnancy irreversibly impairs lung development of the offspring. *Nanotoxicology,* 11**,** 484-495.

PAULIN, L. & HANSEL, N. 2016. Particulate air pollution and impaired lung function. *F1000Res,* 5.

PEDEN, D. B. 2018. The Unexpected Health Effects of Air Pollution. *N C Med J,* 79**,** 309-311.

PETERS, J. L., BOYNTON-JARRETT, R. & SANDEL, M. 2013. Prenatal environmental factors influencing IgE levels, atopy and early asthma. *Curr Opin Allergy Clin Immunol,* 13**,** 187-92.

PETERS, S. P. 2014. Asthma phenotypes: nonallergic (intrinsic) asthma. *J Allergy Clin Immunol Pract,* 2**,** 650-2.
PEZZULO, A. A., STARNER, T. D., SCHEETZ, T. E., TRAVER, G. L., TILLEY, A. E., HARVEY, B. G., CRYSTAL, R. G., MCCRAY, P. B., JR. & ZABNER, J. 2011. The air-liquid interface and use of primary cell cultures are important to recapitulate the transcriptional profile of in vivo airway epithelia. *Am J Physiol Lung Cell Mol Physiol,* 300**,** L25-31.
PFISTER, K. F., BAADER, S., BAADER, M., BERNDT, S. & GOOSSEN, L. J. 2017. Biofuel by isomerizing metathesis of rapeseed oil esters with (bio)ethylene for use in contemporary diesel engines. *Sci Adv,* 3**,** e1602624.
PIETROPAOLI, A. P., FRAMPTON, M. W., HYDE, R. W., MORROW, P. E., OBERDORSTER, G., COX, C., SPEERS, D. M., FRASIER, L. M., CHALUPA, D. C., HUANG, L. S. & UTELL, M. J. 2004. Pulmonary function, diffusing capacity, and inflammation in healthy and asthmatic subjects exposed to ultrafine particles. *Inhal Toxicol,* 16 Suppl 1**,** 59-72.
PLATTS-MILLS, T., VAUGHAN, J., SQUILLACE, S., WOODFOLK, J. & SPORIK, R. 2001. Sensitisation, asthma, and a modified Th2 response in children exposed to cat allergen: a population-based cross-sectional study. *Lancet,* 357**,** 752-6.
POLOSA, R. & THOMSON, N. C. 2013. Smoking and asthma: dangerous liaisons. *Eur Respir J,* 41**,** 716-26.
POPE, C. A. 2000. Epidemiology of fine particulate air pollution and human health: biologic mechanisms and who's at risk? *Environ Health Perspect,* 108**,** 713-23.
POST, S., NAWIJN, M. C., HACKETT, T. L., BARANOWSKA, M., GRAS, R., VAN OOSTERHOUT, A. J. & HEIJINK, I. H. 2012. The composition of house dust mite is critical for mucosal barrier dysfunction and allergic sensitisation. *Thorax,* 67**,** 488-95.
POSTMA, D. S. 2007. Gender differences in asthma development and progression. *Gend Med,* 4 Suppl B**,** S133-46.
POSTMA, D. S. & KERSTJENS, H. A. 1998. Characteristics of airway hyperresponsiveness in asthma and chronic obstructive pulmonary disease. *Am J Respir Crit Care Med,* 158**,** S187-92.
POURAZAR, J., MUDWAY, I. S., SAMET, J. M., HELLEDAY, R., BLOMBERG, A., WILSON, S. J., FREW, A. J., KELLY, F. J. & SANDSTRÖM, T. 2005. Diesel exhaust activates redox-sensitive transcription factors and kinases in human airways. *Am J Physiol Lung Cell Mol Physiol,* 289**,** L724-30.
PROTUDJER, J. L., LUNDHOLM, C. & ALMQVIST, C. 2015. Asthma and height in twins: a cohort and within-pair analyses study. *Twin Res Hum Genet,* 18**,** 142-50.
PROUD, D. & LEIGH, R. 2011. Epithelial cells and airway diseases. *Immunol Rev,* 242**,** 186-204.
PULIDO-REYES, G., RODEA-PALOMARES, I., DAS, S., SAKTHIVEL, T. S., LEGANES, F., ROSAL, R., SEAL, S. & FERNANDEZ-PINAS, F. 2015a. Untangling the biological effects of cerium oxide nanoparticles: the role of surface valence states. *Sci Rep,* 5**,** 15613.
PULIDO-REYES, G., RODEA-PALOMARES, I., DAS, S., SAKTHIVEL, T. S., LEGANES, F., ROSAL, R., SEAL, S. & FERNÁNDEZ-PIÑAS, F. 2015b. Untangling the biological effects of cerium oxide nanoparticles: the role of surface valence states. *Scientific Reports,* 5**,** 15613.
QIAN, C. & CAO, X. 2018. Dendritic cells in the regulation of immunity and inflammation. *Seminars in Immunology,* 35**,** 3-11.
RAEISZADEH JAHROMI, S., MAHESH, P. A., JAYARAJ, B. S., HOLLA, A. D., VISHWESWARAIAH, S. & NALLUR, R. B. 2015. Single nucleotide polymorphism

and asthma: A study on the genetic basis of asthma. *European Respiratory Journal,* 46**,** PA1231.
RAEL, E. L. & LOCKEY, R. F. 2011. Interleukin-13 signaling and its role in asthma. *World Allergy Organ J,* 4**,** 54-64.
RAFTIS, J. B. & MILLER, M. R. 2019. Nanoparticle translocation and multi-organ toxicity: A particularly small problem. *Nano Today,* 26**,** 8-12.
RAMIREZ-VELAZQUEZ, C., CASTILLO, E. C., GUIDO-BAYARDO, L. & ORTIZ-NAVARRETE, V. 2013. IL-17-producing peripheral blood CD177+ neutrophils increase in allergic asthmatic subjects. *Allergy Asthma Clin Immunol,* 9**,** 23.
RAO, X., HUANG, X., ZHOU, Z. & LIN, X. 2013. An improvement of the 2^(-delta delta CT) method for quantitative real-time polymerase chain reaction data analysis. *Biostat Bioinforma Biomath,* 3**,** 71-85.
RAY, A. & KOLLS, J. K. 2017. Neutrophilic Inflammation in Asthma and Association with Disease Severity. *Trends Immunol,* 38**,** 942-954.
REBER, L. L. & FAHY, J. V. 2016. Mast cells in asthma: biomarker and therapeutic target. *European Respiratory Journal,* 47**,** 1040-1042.
REDING, K. W., YOUNG, M. T., SZPIRO, A. A., HAN, C. J., DEROO, L. A., WEINBERG, C., KAUFMAN, J. D. & SANDLER, D. P. 2015. Breast Cancer Risk in Relation to Ambient Air Pollution Exposure at Residences in the Sister Study Cohort. *Cancer Epidemiol Biomarkers Prev,* 24**,** 1907-9.
REIBMAN, J., HSU, Y., CHEN, L. C., BLECK, B. & GORDON, T. 2003. Airway epithelial cells release MIP-3alpha/CCL20 in response to cytokines and ambient particulate matter. *Am J Respir Cell Mol Biol,* 28**,** 648-54.
REITHOFER, M. & JAHN-SCHMID, B. 2017. Allergens with Protease Activity from House Dust Mites. *Int J Mol Sci,* 18.
REYNOLDS, S. D. & MALKINSON, A. M. 2010. Clara cell: progenitor for the bronchiolar epithelium. *Int J Biochem Cell Biol,* 42**,** 1-4.
RICE, M. B., RIFAS-SHIMAN, S. L., LITONJUA, A. A., OKEN, E., GILLMAN, M. W., KLOOG, I., LUTTMANN-GIBSON, H., ZANOBETTI, A., COULL, B. A., SCHWARTZ, J., KOUTRAKIS, P., MITTLEMAN, M. A. & GOLD, D. R. 2016. Lifetime Exposure to Ambient Pollution and Lung Function in Children. *Am J Respir Crit Care Med,* 193**,** 881-8.
RIDER, C. F., YAMAMOTO, M., GUNTHER, O. P., HIROTA, J. A., SINGH, A., TEBBUTT, S. J. & CARLSTEN, C. 2016. Controlled diesel exhaust and allergen coexposure modulates microRNA and gene expression in humans: Effects on inflammatory lung markers. *J Allergy Clin Immunol,* 138**,** 1690-1700.
RIDLEY, C. & THORNTON, D. J. 2018. Mucins: the frontline defence of the lung. *Biochem Soc Trans*.
RIEDL, M. A., DIAZ-SANCHEZ, D., LINN, W. S., GONG, H., JR., CLARK, K. W., EFFROS, R. M., MILLER, J. W., COCKER, D. R., BERHANE, K. T. & COMMITTEE, H. E. I. H. R. 2012. Allergic inflammation in the human lower respiratory tract affected by exposure to diesel exhaust. *Res Rep Health Eff Inst***,** 5-43; discussion 45-64.
ROBERTSON, S. & MILLER, M. R. 2018a. Ambient air pollution and thrombosis. *Part Fibre Toxicol,* 15**,** 1.
ROBERTSON, S. & MILLER, M. R. 2018b. Ambient air pollution and thrombosis. *Particle and Fibre Toxicology,* 15**,** 1.
ROBINSON, D. S., LARCHE, M. & DURHAM, S. R. 2004. Tregs and allergic disease. *J Clin Invest,* 114**,** 1389-97.

ROBINSON, R. K., BIRRELL, M. A., ADCOCK, J. J., WORTLEY, M. A., DUBUIS, E. D., CHEN, S., MCGILVERY, C. M., HU, S., SHAFFER, M. S. P., BONVINI, S. J., MAHER, S. A., MUDWAY, I. S., PORTER, A. E., CARLSTEN, C., TETLEY, T. D. & BELVISI, M. G. 2018. Mechanistic link between diesel exhaust particles and respiratory reflexes. *Journal of Allergy and Clinical Immunology,* 141**,** 1074-1084.e9.

ROCCA, A., MOSCATO, S., RONCA, F., NITTI, S., MATTOLI, V., GIORGI, M. & CIOFANI, G. 2015. Pilot in vivo investigation of cerium oxide nanoparticles as a novel anti-obesity pharmaceutical formulation. *Nanomedicine,* 11**,** 1725-34.

ROCK, J. R., RANDELL, S. H. & HOGAN, B. L. 2010. Airway basal stem cells: a perspective on their roles in epithelial homeostasis and remodeling. *Dis Model Mech,* 3**,** 545-56.

ROKICKI, W., ROKICKI, M., WOJTACHA, J. & DŻELJIJLI, A. 2016. The role and importance of club cells (Clara cells) in the pathogenesis of some respiratory diseases. *Kardiochir Torakochirurgia Pol,* 13**,** 26-30.

ROOS, A. B., MORI, M., GRONNEBERG, R., OSTERLUND, C., CLAESSON, H. E., WAHLSTROM, J., GRUNEWALD, J., EKLUND, A., ERJEFALT, J. S., LUNDBERG, J. O. & NORD, M. 2014. Elevated exhaled nitric oxide in allergen-provoked asthma is associated with airway epithelial iNOS. *PLoS One,* 9**,** e90018.

ROSENBERG, H. F. & DRUEY, K. M. 2018. Modeling asthma: Pitfalls, promises, and the road ahead. *J Leukoc Biol,* 104**,** 41-48.

ROSENFELD, D., LAHAV, R., KHAIN, A. & PINSKY, M. 2002. The Role of Sea Spray in Cleansing Air Pollution over Ocean via Cloud Processes. 297**,** 1667-1670.

ROSS, A. J., DAILEY, L. A., BRIGHTON, L. E. & DEVLIN, R. B. 2007. Transcriptional profiling of mucociliary differentiation in human airway epithelial cells. *Am J Respir Cell Mol Biol,* 37**,** 169-85.

ROTHENBERG, M. E. & HOGAN, S. P. 2006. The eosinophil. *Annu Rev Immunol,* 24**,** 147-74.

RUBIO, L., ANNANGI, B., VILA, L., HERNANDEZ, A. & MARCOS, R. 2016. Antioxidant and anti-genotoxic properties of cerium oxide nanoparticles in a pulmonary-like cell system. *Arch Toxicol,* 90**,** 269-78.

RUENRAROENGSAK, P. & TETLEY, T. D. 2015. Differential bioreactivity of neutral, cationic and anionic polystyrene nanoparticles with cells from the human alveolar compartment: robust response of alveolar type 1 epithelial cells. *Part Fibre Toxicol,* 12**,** 19.

RYAN, P. H., LEMASTERS, G. K., BISWAS, P., LEVIN, L., HU, S., LINDSEY, M., BERNSTEIN, D. I., LOCKEY, J., VILLAREAL, M., KHURANA HERSHEY, G. K. & GRINSHPUN, S. A. 2007. A comparison of proximity and land use regression traffic exposure models and wheezing in infants. *Environ Health Perspect,* 115**,** 278-84.

RYDMAN, E. M., ILVES, M., KOIVISTO, A. J., KINARET, P. A. S., FORTINO, V., SAVINKO, T. S., LEHTO, M. T., PULKKINEN, V., VIPPOLA, M., HÄMERI, K. J., MATIKAINEN, S., WOLFF, H., SAVOLAINEN, K. M., GRECO, D. & ALENIUS, H. 2014. Inhalation of rod-like carbon nanotubes causes unconventional allergic airway inflammation. *Particle and Fibre Toxicology,* 11**,** 48.

RYNNING, I., NECA, J., VRBOVA, K., LIBALOVA, H., ROSSNER, P., HOLME, J. A., GÜTZKOW, K. B., AFANOU, A. K. J., ARNOLDUSSEN, Y. J., HRUBA, E., SKARE, Ø., HAUGEN, A., TOPINKA, J., MACHALA, M. & MOLLERUP, S. 2018. In vitro transformation of human bronchial epithelial cells by diesel exhaust particles: gene expression profiling and early toxic responses. *Toxicol Sci*.

SABA, N., YUSUF, O., REHMAN, S., MUNIR, S., NOOR, A., SAQLAIN, M., MANSOOR, A. & RAJA, G. K. 2018. Single nucleotide polymorphisms in asthma candidate genes

TBXA2R, ADAM33 FCER1B and ORMDL3 in Pakistani asthmatics a case control study. *Asthma Research and Practice,* 4**,** 4.
SACHS, U. J., ANDREI-SELMER, C. L., MANIAR, A., WEISS, T., PADDOCK, C., ORLOVA, V. V., CHOI, E. Y., NEWMAN, P. J., PREISSNER, K. T., CHAVAKIS, T. & SANTOSO, S. 2007. The neutrophil-specific antigen CD177 is a counter-receptor for platelet endothelial cell adhesion molecule-1 (CD31). *J Biol Chem,* 282**,** 23603-12.
SAETTA, M. & TURATO, G. 2001. Airway pathology in asthma. *European Respiratory Journal,* 18**,** 18s.
SAGER, T., WOLFARTH, M., FRIEND, S., HUBBS, A., HAMILTON, R., WU, N., YANG, F., PORTER, D. & HOLIAN, A. 2013. Effect of multi-walled carbon nanotube surface modification on bioactivity in the C57BL/6 mouse model. *Nanotoxicology,* 8.
SAGLANI, S. 2013. Viral infections and the development of asthma in children. *Ther Adv Infect Dis,* 1**,** 139-50.
SALVI, S., BLOMBERG, A., RUDELL, B., KELLY, F., SANDSTRÖM, T., HOLGATE, S. T. & FREW, A. 1999. Acute inflammatory responses in the airways and peripheral blood after short-term exposure to diesel exhaust in healthy human volunteers. *Am J Respir Crit Care Med,* 159**,** 702-9.
SALVI, S. S., NORDENHALL, C., BLOMBERG, A., RUDELL, B., POURAZAR, J., KELLY, F. J., WILSON, S., SANDSTRÖM, T., HOLGATE, S. T. & FREW, A. J. 2000. Acute exposure to diesel exhaust increases IL-8 and GRO-alpha production in healthy human airways. *Am J Respir Crit Care Med,* 161**,** 550-7.
SAMBANDAM, B., PALANISAMI, E., ABBUGOUNDER, R., PRAKHYA, B. & THIYAGARAJAN, D. 2014. Characterizations of coal fly ash nanoparticles and induced in vitro toxicity in cell lines. *Journal of Nanoparticle Research,* 16**,** 1-9.
SANTOS, U. P., GARCIA, M. L., BRAGA, A. L., PEREIRA, L. A., LIN, C. A., DE ANDRE, P. A., DE ANDRE, C. D., SINGER, J. D. & SALDIVA, P. H. 2016. Association between Traffic Air Pollution and Reduced Forced Vital Capacity: A Study Using Personal Monitors for Outdoor Workers. *PLoS One,* 11**,** e0163225.
SARADNA, A., DO, D. C., KUMAR, S., FU, Q. L. & GAO, P. 2018. Macrophage polarization and allergic asthma. *Transl Res,* 191**,** 1-14.
SARKAR, S., ZHANG, L., SUBRAMANIAM, P., LEE, K. B., GARFUNKEL, E., STRICKLAND, P. A., MAINELIS, G., LIOY, P. J., TETLEY, T. D., CHUNG, K. F., ZHANG, J., RYAN, M., PORTER, A. & SCHWANDER, S. 2014. Variability in bioreactivity linked to changes in size and zeta potential of diesel exhaust particles in human immune cells. *PLoS One,* 9**,** e97304.
SAYED, B. A., CHRISTY, A., QUIRION, M. R. & BROWN, M. A. 2008. The master switch: the role of mast cells in autoimmunity and tolerance. *Annu Rev Immunol,* 26**,** 705-39.
SCHÄFER, K., EMEIS, S., HOFFMANN, H. & JAHN, C. 2006. Influence of mixing layer height upon air pollution in urban and sub-urban areas. *Meteorologische Zeitschrift,* 15**,** 647-658.
SCHANEN, B. C., DAS, S., REILLY, C. M., WARREN, W. L., SELF, W. T., SEAL, S. & DRAKE, D. R., III 2013. Immunomodulation and T Helper TH1/TH2 Response Polarization by CeO2 and TiO2 Nanoparticles. *PLOS ONE,* 8**,** e62816.
SCHINS, R. P. & DONALDSON, K. 2000. Nuclear Factor Kappa-B Activation by Particles and Fibers. *Inhal Toxicol,* 12 Suppl 3**,** 317-26.
SCHMIDT, C. W. 2018. Air Pollution and Breast Cancer in Postmenopausal Women: Evidence across Cohorts. *Environ Health Perspect,* 126**,** 034001.
SCHMITZ, R. 2005. Modelling of air pollution dispersion in Santiago de Chile. *Atmospheric Environment,* 39**,** 2035-2047.

SCHOLTENS, S., WIJGA, A. H., BRUNEKREEF, B., KERKHOF, M., HOEKSTRA, M. O., GERRITSEN, J., AALBERSE, R., DE JONGSTE, J. C. & SMIT, H. A. 2009. Breast feeding, parental allergy and asthma in children followed for 8 years. The PIAMA birth cohort study. *Thorax,* 64**,** 604-9.

SCHULTZ, E. S., HALLBERG, J., BELLANDER, T., BERGSTROM, A., BOTTAI, M., CHIESA, F., GUSTAFSSON, P. M., GRUZIEVA, O., THUNQVIST, P., PERSHAGEN, G. & MELEN, E. 2016. Early-Life Exposure to Traffic-related Air Pollution and Lung Function in Adolescence. *Am J Respir Crit Care Med,* 193**,** 171-7.

SCHULTZ, E. S., HALLBERG, J., BELLANDER, T., BERGSTRÖM, A., BOTTAI, M., CHIESA, F., GUSTAFSSON, P. M., GRUZIEVA, O., THUNQVIST, P., PERSHAGEN, G. & MELÉN, E. 2015. Early-Life Exposure to Traffic-related Air Pollution and Lung Function in Adolescence. *American Journal of Respiratory and Critical Care Medicine,* 193**,** 171-177.

SCHWARTZ, J. 1994. What are people dying of on high air pollution days? *Environ Res,* 64**,** 26-35.

SCHWOTZER, D., ERNST, H., SCHAUDIEN, D., KOCK, H., POHLMANN, G., DASENBROCK, C. & CREUTZENBERG, O. 2017. Effects from a 90-day inhalation toxicity study with cerium oxide and barium sulfate nanoparticles in rats. *Part Fibre Toxicol,* 14**,** 23.

SCHWOTZER, D., NIEHOF, M., SCHAUDIEN, D., KOCK, H., HANSEN, T., DASENBROCK, C. & CREUTZENBERG, O. 2018. Cerium oxide and barium sulfate nanoparticle inhalation affects gene expression in alveolar epithelial cells type II. *J Nanobiotechnology,* 16**,** 16.

SCOTT, H. A., GIBSON, P. G., GARG, M. L. & WOOD, L. G. 2011. Airway inflammation is augmented by obesity and fatty acids in asthma. *Eur Respir J,* 38**,** 594-602.

SCURI, M., CHEN, B. T., CASTRANOVA, V., REYNOLDS, J. S., JOHNSON, V. J., SAMSELL, L., WALTON, C. & PIEDIMONTE, G. 2010. Effects of titanium dioxide nanoparticle exposure on neuroimmune responses in rat airways. *J Toxicol Environ Health A,* 73**,** 1353-69.

SEAGRAVE, J., DUNAWAY, S., MCDONALD, J. D., MAUDERLY, J. L., HAYDEN, P. & STIDLEY, C. 2007. Responses of differentiated primary human lung epithelial cells to exposure to diesel exhaust at an air-liquid interface. *Exp Lung Res,* 33**,** 27-51.

SEARING, D. A., ZHANG, Y., MURPHY, J. R., HAUK, P. J., GOLEVA, E. & LEUNG, D. Y. 2010. Decreased serum vitamin D levels in children with asthma are associated with increased corticosteroid use. *J Allergy Clin Immunol,* 125**,** 995-1000.

SEATON, A., MACNEE, W., DONALDSON, K. & GODDEN, D. 1995. Particulate air pollution and acute health effects. *Lancet,* 345**,** 176-8.

SEIFFERT, J., HUSSAIN, F., WIEGMAN, C., LI, F., BEY, L., BAKER, W., PORTER, A., RYAN, M. P., CHANG, Y., GOW, A., ZHANG, J., ZHU, J., TETLEY, T. D. & CHUNG, K. F. 2015. Pulmonary Toxicity of Instilled Silver Nanoparticles: Influence of Size, Coating and Rat Strain. *PLOS ONE,* 10**,** e0119726.

SHAMRI, R., XENAKIS, J. J. & SPENCER, L. A. 2011. Eosinophils in innate immunity: an evolving story. *Cell Tissue Res,* 343**,** 57-83.

SHAW, C. A., MORTIMER, G. M., DENG, Z. J., CARTER, E. S., CONNELL, S. P., MILLER, M. R., DUFFIN, R., NEWBY, D. E., HADOKE, P. W. & MINCHIN, R. F. 2016. Protein corona formation in bronchoalveolar fluid enhances diesel exhaust nanoparticle uptake and pro-inflammatory responses in macrophages. *Nanotoxicology,* 10**,** 981-91.

SHIN, N., VELMURUGAN, K., SU, C., BAUER, A. K. & TSAI, C. S. J. 2019. Assessment of fine particles released during paper printing and shredding processes. *Environ Sci Process Impacts*.

SHIN, Y. S., TAKEDA, K. & GELFAND, E. W. 2009. Understanding asthma using animal models. *Allergy Asthma Immunol Res,* 1**,** 10-8.

SHOEB, M., KODALI, V., FARRIS, B., BISHOP, L. M., MEIGHAN, T., SALMEN, R., EYE, T., ROBERTS, J. R., ZEIDLER-ERDELY, P., ERDELY, A. & ANTONINI, J. M. 2017. Evaluation of the molecular mechanisms associated with cytotoxicity and inflammation after pulmonary exposure to different metal-rich welding particles. *Nanotoxicology,* 11**,** 725-736.

SINCLAIR, R., RUSSELL, C., KRAY, G. & VESPER, S. 2018. Asthma Risk Associated with Indoor Mold Contamination in Hispanic Communities in Eastern Coachella Valley, California. *J Environ Public Health,* 2018**,** 9350370.

SINGH, P., MADDEN, M. & GILMOUR, M. I. 2005. Effects of diesel exhaust particles and carbon black on induction of dust mite allergy in brown norway rats. *J Immunotoxicol,* 2**,** 41-9.

SINGH, S., DOSANI, T., KARAKOTI, A. S., KUMAR, A., SEAL, S. & SELF, W. T. 2011. A phosphate-dependent shift in redox state of cerium oxide nanoparticles and its effects on catalytic properties. *Biomaterials,* 32**,** 6745-53.

SIVAPALAN, N., WATTIE, J., INMAN, M. D. & SEHMI, R. 2014. Lung-homing of endothelial progenitor cells and airway vascularization is only partially dependant on eosinophils in a house dust mite-exposed mouse model of allergic asthma. *PLoS One,* 9**,** e109991.

SMITS, H. H., HIEMSTRA, P. S., PRAZERES DA COSTA, C., EGE, M., EDWARDS, M., GARN, H., HOWARTH, P. H., JARTTI, T., DE JONG, E. C., MAIZELS, R. M., MARSLAND, B. J., MCSORLEY, H. J., MULLER, A., PFEFFERLE, P. I., SAVELKOUL, H., SCHWARZE, J., UNGER, W. W., VON MUTIUS, E., YAZDANBAKHSH, M. & TAUBE, C. 2016. Microbes and asthma: Opportunities for intervention. *J Allergy Clin Immunol,* 137**,** 690-7.

SNOW, S. J., MCGEE, J., MILLER, D. B., BASS, V., SCHLADWEILER, M. C., THOMAS, R. F., KRANTZ, T., KING, C., LEDBETTER, A. D., RICHARDS, J., WEINSTEIN, J. P., CONNER, T., WILLIS, R., LINAK, W. P., NASH, D., WOOD, C. E., ELMORE, S. A., MORRISON, J. P., JOHNSON, C. L., GILMOUR, M. I. & KODAVANTI, U. P. 2014a. Inhaled diesel emissions generated with cerium oxide nanoparticle fuel additive induce adverse pulmonary and systemic effects. *Toxicological sciences : an official journal of the Society of Toxicology,* 142**,** 403-417.

SNOW, S. J., MCGEE, J., MILLER, D. B., BASS, V., SCHLADWEILER, M. C., THOMAS, R. F., KRANTZ, T., KING, C., LEDBETTER, A. D., RICHARDS, J., WEINSTEIN, J. P., CONNER, T., WILLIS, R., LINAK, W. P., NASH, D., WOOD, C. E., ELMORE, S. A., MORRISON, J. P., JOHNSON, C. L., GILMOUR, M. I. & KODAVANTI, U. P. 2014b. Inhaled diesel emissions generated with cerium oxide nanoparticle fuel additive induce adverse pulmonary and systemic effects. *Toxicol Sci,* 142**,** 403-17.

SOMBORAC-BACURA, A., VAN DER TOORN, M., FRANCIOSI, L., SLEBOS, D. J., ZANIC-GRUBISIC, T., BISCHOFF, R. & VAN OOSTERHOUT, A. J. 2013. Cigarette smoke induces endoplasmic reticulum stress response and proteasomal dysfunction in human alveolar epithelial cells. *Exp Physiol,* 98**,** 316-25.

SOMMAR, J. N., EK, A., MIDDELVELD, R., BJERG, A., DAHLEN, S. E., JANSON, C. & FORSBERG, B. 2014. Quality of life in relation to the traffic pollution indicators NO2 and NOx: results from the Swedish GA(2)LEN survey. *BMJ Open Respir Res,* 1**,** e000039.

SOROOSH, P. & DOHERTY, T. A. 2009. Th9 and allergic disease. *Immunology,* 127**,** 450-8.
SOUTHAM, D. S., DOLOVICH, M., O'BYRNE, P. M. & INMAN, M. D. 2002. Distribution of intranasal instillations in mice: effects of volume, time, body position, and anesthesia. *Am J Physiol Lung Cell Mol Physiol,* 282**,** L833-9.
SPITS, H., ARTIS, D., COLONNA, M., DIEFENBACH, A., DI SANTO, J. P., EBERL, G., KOYASU, S., LOCKSLEY, R. M., MCKENZIE, A. N., MEBIUS, R. E., POWRIE, F. & VIVIER, E. 2013. Innate lymphoid cells--a proposal for uniform nomenclature. *Nat Rev Immunol,* 13**,** 145-9.
SRIDHARAN, G. & SHANKAR, A. A. 2012. Toluidine blue: A review of its chemistry and clinical utility. *J Oral Maxillofac Pathol,* 16**,** 251-5.
SRINIVAS, A., RAO, P. J., SELVAM, G., MURTHY, P. B. & REDDY, P. N. 2011. Acute inhalation toxicity of cerium oxide nanoparticles in rats. *Toxicol Lett,* 205**,** 105-15.
STATISTICS, O. F. N. 2018 *Number of deaths from accidental carbon monoxide poisoning* [Online]. Available: https://www.ons.gov.uk/peoplepopulationandcommunity/healthandsocialcare/causesofdeath/adhocs/006135numberofdeathsfromaccidentalcarbonmonoxidepoisoning [Accessed 2nd Febuary 2018].
STEINER, S., MUELLER, L., POPOVICHEVA, O. B., RAEMY, D. O., CZERWINSKI, J., COMTE, P., MAYER, A., GEHR, P., ROTHEN-RUTISHAUSER, B. & CLIFT, M. J. 2012. Cerium dioxide nanoparticles can interfere with the associated cellular mechanistic response to diesel exhaust exposure. *Toxicol Lett,* 214**,** 218-25.
STENSBALLE, L. G., SIMONSEN, J. B., THOMSEN, S. F., LARSEN, A. M., LYSDAL, S. H., AABY, P., KYVIK, K. O., SKYTTHE, A., BACKER, V. & BISGAARD, H. 2009. The causal direction in the association between respiratory syncytial virus hospitalization and asthma. *J Allergy Clin Immunol,* 123**,** 131-137.e1.
STOEHR, L. C., ENDES, C., RADAUER-PREIML, I., BOYLES, M. S., CASALS, E., BALOG, S., PESCH, M., PETRI-FINK, A., ROTHEN-RUTISHAUSER, B., HIMLY, M., CLIFT, M. J. & DUSCHL, A. 2015. Assessment of a panel of interleukin-8 reporter lung epithelial cell lines to monitor the pro-inflammatory response following zinc oxide nanoparticle exposure under different cell culture conditions. *Part Fibre Toxicol,* 12**,** 29.
STONE, D. D. M. C. P. K. D. 2010. IgE, mast cells, basophils, and eosinophils. *Journal of Allergy and Clinical Immunology,* 125**,** S73 - S80.
STRZELAK, A., RATAJCZAK, A., ADAMIEC, A. & FELESZKO, W. 2018. Tobacco Smoke Induces and Alters Immune Responses in the Lung Triggering Inflammation, Allergy, Asthma and Other Lung Diseases: A Mechanistic Review. *Int J Environ Res Public Health,* 15.
SUKHANOVA, A., BOZROVA, S., SOKOLOV, P., BERESTOVOY, M., KARAULOV, A. & NABIEV, I. 2018. Dependence of Nanoparticle Toxicity on Their Physical and Chemical Properties. *Nanoscale Res Lett,* 13**,** 44.
SUTHERLAND, E. R., GOLEVA, E., JACKSON, L. P., STEVENS, A. D. & LEUNG, D. Y. 2010. Vitamin D levels, lung function, and steroid response in adult asthma. *Am J Respir Crit Care Med,* 181**,** 699-704.
SUZUKI, T., KANOH, T., ISHIMORI, M., IKEDA, S. & OHKUNI, H. 1996. Adjuvant activity of diesel exhaust particulates (DEP) in production of anti-IgE and anti-IgG1 antibodies to mite allergen in mice. *J Clin Lab Immunol,* 48**,** 187-99.
SVARTENGREN, M., STRAND, V., BYLIN, G., JARUP, L. & PERSHAGEN, G. 2000. Short-term exposure to air pollution in a road tunnel enhances the asthmatic response to allergen. *Eur Respir J,* 15**,** 716-24.

SWINDLE, E. J., COLLINS, J. E. & DAVIES, D. E. 2009. Breakdown in epithelial barrier function in patients with asthma: identification of novel therapeutic approaches. *J Allergy Clin Immunol,* 124**,** 23-34; quiz 35-6.

SWINNERTON, J. W., LINNENBOM, V. J. & LAMONTAGNE, R. A. 1970. The ocean: a natural source of carbon monoxide. *Science,* 167**,** 984-6.

TAKAHASHI, G., TANAKA, H., WAKAHARA, K., NASU, R., HASHIMOTO, M., MIYOSHI, K., TAKANO, H., YAMASHITA, H., INAGAKI, N. & NAGAI, H. 2010. Effect of diesel exhaust particles on house dust mite-induced airway eosinophilic inflammation and remodeling in mice. *J Pharmacol Sci,* 112**,** 192-202.

TAKIZAWA, H., OHTOSHI, T., KIKUTANI, T., OKAZAKI, H., AKIYAMA, N., SATO, M., SHOJI, S. & ITO, K. 1995. Histamine activates bronchial epithelial cells to release inflammatory cytokines in vitro. *Int Arch Allergy Immunol,* 108**,** 260-7.

TAM, A., CHURG, A., WRIGHT, J. L., ZHOU, S., KIRBY, M., COXSON, H. O., LAM, S., MAN, S. F. & SIN, D. D. 2016. Sex Differences in Airway Remodeling in a Mouse Model of Chronic Obstructive Pulmonary Disease. *Am J Respir Crit Care Med,* 193**,** 825-34.

TAM, A., WADSWORTH, S., DORSCHEID, D., MAN, S. F. & SIN, D. D. 2011. The airway epithelium: more than just a structural barrier. *Ther Adv Respir Dis,* 5**,** 255-73.

TANG, C., ROLLAND, J. M., WARD, C., LI, X., BISH, R., THIEN, F. & WALTERS, E. H. 1999. Modulatory effects of alveolar macrophages on CD4+ T-cell IL-5 responses correlate with IL-1beta, IL-6, and IL-12 production. *Eur Respir J,* 14**,** 106-12.

TANG, M., LI, D., LIEW, Z., WEI, F., WANG, J., JIN, M., CHEN, K. & RITZ, B. 2019. The association of short-term effects of air pollution and sleep disorders among elderly residents in China. *Sci Total Environ***,** 134846.

TARIQUE, A. A., LOGAN, J., THOMAS, E., HOLT, P. G., SLY, P. D. & FANTINO, E. 2015. Phenotypic, functional, and plasticity features of classical and alternatively activated human macrophages. *Am J Respir Cell Mol Biol,* 53**,** 676-88.

TEEGUARDEN, J. G., HINDERLITER, P. M., ORR, G., THRALL, B. D. & POUNDS, J. G. 2007. Particokinetics in vitro: dosimetry considerations for in vitro nanoparticle toxicity assessments. *Toxicol Sci,* 95**,** 300-12.

THEOHARIDES, T. C., ALYSANDRATOS, K. D., ANGELIDOU, A., DELIVANIS, D. A., SISMANOPOULOS, N., ZHANG, B., ASADI, S., VASIADI, M., WENG, Z., MINIATI, A. & KALOGEROMITROS, D. 2012. Mast cells and inflammation. *Biochim Biophys Acta,* 1822**,** 21-33.

THOMAS, R. 2004. *Practical Guide to ICP-MS* **New York**, Marcel Dekker, Inc.

THORLEY, A. J., RUENRAROENGSAK, P., POTTER, T. E. & TETLEY, T. D. 2014. Critical determinants of uptake and translocation of nanoparticles by the human pulmonary alveolar epithelium. *ACS Nano,* 8**,** 11778-89.

TIAN, Y., XIANG, X., JUAN, J., SUN, K., SONG, J., CAO, Y. & HU, Y. 2017. Fine particulate air pollution and hospital visits for asthma in Beijing, China. *Environ Pollut,* 230**,** 227-233.

TOLSTIK, E., OSMINKINA, L. A., AKIMOV, D., GONGALSKY, M. B., KUDRYAVTSEV, A. A., TIMOSHENKO, V. Y., HEINTZMANN, R., SIVAKOV, V. & POPP, J. 2016. Linear and Non-Linear Optical Imaging of Cancer Cells with Silicon Nanoparticles. *Int J Mol Sci,* 17.

TOYA, T., TAKATA, A., OTAKI, N., TAKAYA, M., SERITA, F., YOSHIDA, K. & KOHYAMA, N. 2010. Pulmonary toxicity induced by intratracheal instillation of coarse and fine particles of cerium dioxide in male rats. *Ind Health,* 48**,** 3-11.

TRAVERS, J. & ROTHENBERG, M. E. 2015. Eosinophils in mucosal immune responses. *Mucosal Immunol,* 8**,** 464-75.

TULLY, J. E., HOFFMAN, S. M., LAHUE, K. G., NOLIN, J. D., ANATHY, V., LUNDBLAD, L. K., DAPHTARY, N., ALIYEVA, M., BLACK, K. E., DIXON, A. E., POYNTER, M. E., IRVIN, C. G. & JANSSEN-HEININGER, Y. M. 2013. Epithelial NF-κB orchestrates house dust mite-induced airway inflammation, hyperresponsiveness, and fibrotic remodeling. *J Immunol,* 191**,** 5811-21.

TUMES, D. J., PAPADOPOULOS, M., ENDO, Y., ONODERA, A., HIRAHARA, K. & NAKAYAMA, T. 2017. Epigenetic regulation of T-helper cell differentiation, memory, and plasticity in allergic asthma. *Immunol Rev,* 278**,** 8-19.

TURNER, J., HERNANDEZ, M., SNAWDER, J. E., HANDOREAN, A. & MCCABE, K. M. 2015. A toxicology suite adapted for comparing parallel toxicity responses of model human lung cells to diesel exhaust particles and their extracts. *Aerosol Sci Technol,* 49**,** 599-610.

TURNER, S. 2017. Gene-Environment Interactions-What Can These Tell Us about the Relationship between Asthma and Allergy? *Front Pediatr,* 5**,** 118.

ULRIK, C. S. & BACKER, V. 1999. Markers of impaired growth of pulmonary function in children and adolescents. *Am J Respir Crit Care Med,* 160**,** 40-4.

VAN DER VEEN, M. J., JANSEN, H. M., AALBERSE, R. C. & VAN DER ZEE, J. S. 2001. Der p 1 and Der p 2 induce less severe late asthmatic responses than native Dermatophagoides pteronyssinus extract after a similar early asthmatic response. *Clin Exp Allergy,* 31**,** 705-14.

VAN EERDEWEGH, P., LITTLE, R. D., DUPUIS, J., DEL MASTRO, R. G., FALLS, K., SIMON, J., TORREY, D., PANDIT, S., MCKENNY, J., BRAUNSCHWEIGER, K., WALSH, A., LIU, Z., HAYWARD, B., FOLZ, C., MANNING, S. P., BAWA, A., SARACINO, L., THACKSTON, M., BENCHEKROUN, Y., CAPPARELL, N., WANG, M., ADAIR, R., FENG, Y., DUBOIS, J., FITZGERALD, M. G., HUANG, H., GIBSON, R., ALLEN, K. M., PEDAN, A., DANZIG, M. R., UMLAND, S. P., EGAN, R. W., CUSS, F. M., RORKE, S., CLOUGH, J. B., HOLLOWAY, J. W., HOLGATE, S. T. & KEITH, T. P. 2002. Association of the ADAM33 gene with asthma and bronchial hyperresponsiveness. *Nature,* 418**,** 426-30.

VAN HELDEN, M. J. & LAMBRECHT, B. N. 2013. Dendritic cells in asthma. *Current Opinion in Immunology,* 25**,** 745-754.

VAN TILBURG BERNARDES, E. & ARRIETA, M. C. 2017. Hygiene Hypothesis in Asthma Development: Is Hygiene to Blame? *Arch Med Res,* 48**,** 717-726.

VERANTH, J. M., CUTLER, N. S., KASER, E. G., REILLY, C. A. & YOST, G. S. 2008. Effects of cell type and culture media on Interleukin-6 secretion in response to environmental particles. *Toxicol In Vitro,* 22**,** 498-509.

VERANTH, J. M., KASER, E. G., VERANTH, M. M., KOCH, M. & YOST, G. S. 2007. Cytokine responses of human lung cells (BEAS-2B) treated with micron-sized and nanoparticles of metal oxides compared to soil dusts. *Part Fibre Toxicol,* 4**,** 2.

VERSTRAELEN, S., BLOEMEN, K., NELISSEN, I., WITTERS, H., SCHOETERS, G. & VAN DEN HEUVEL, R. 2008. Cell types involved in allergic asthma and their use in in vitro models to assess respiratory sensitization. *Toxicol In Vitro,* 22**,** 1419-31.

VIVIER, L. & DUPREZ, D. 2010. Ceria-based solid catalysts for organic chemistry. *ChemSusChem,* 3**,** 654-78.

VOGEL, C. F. A., VAN WINKLE, L. S., ESSER, C. & HAARMANN-STEMMANN, T. 2020. The aryl hydrocarbon receptor as a target of environmental stressors - Implications for pollution mediated stress and inflammatory responses. *Redox Biol,* 34**,** 101530.

VON MUTIUS, E. 2016. The microbial environment and its influence on asthma prevention in early life. *J Allergy Clin Immunol,* 137**,** 680-9.

WALKER, J. K., KRAFT, M. & FISHER, J. T. 2012. Assessment of murine lung mechanics outcome measures: alignment with those made in asthmatics. *Front Physiol,* 3**,** 491.

WALTERS, M. S., GOMI, K., ASHBRIDGE, B., MOORE, M. A., ARBELAEZ, V., HELDRICH, J., DING, B. S., RAFII, S., STAUDT, M. R. & CRYSTAL, R. G. 2013. Generation of a human airway epithelium derived basal cell line with multipotent differentiation capacity. *Respir Res,* 14**,** 135.

WAN, Y. I., SHRINE, N. R. G., SOLER ARTIGAS, M., WAIN, L. V., BLAKEY, J. D., MOFFATT, M. F., BUSH, A., CHUNG, K. F., COOKSON, W. O. C. M., STRACHAN, D. P., HEANEY, L., AL-MOMANI, B. A. H., MANSUR, A. H., MANNEY, S., THOMSON, N. C., CHAUDHURI, R., BRIGHTLING, C. E., BAFADHEL, M., SINGAPURI, A., NIVEN, R., SIMPSON, A., HOLLOWAY, J. W., HOWARTH, P. H., HUI, J., MUSK, A. W., JAMES, A. L., BROWN, M. A., BALTIC, S., FERREIRA, M. A. R., THOMPSON, P. J., TOBIN, M. D., SAYERS, I. & HALL, I. P. 2012. Genome-wide association study to identify genetic determinants of severe asthma. *Thorax,* 67**,** 762-768.

WANG, G., BAINES, K. J., FU, J. J., WOOD, L. G., SIMPSON, J. L., MCDONALD, V. M., COWAN, D. C., TAYLOR, D. R., COWAN, J. O. & GIBSON, P. G. 2016. Sputum mast cell subtypes relate to eosinophilia and corticosteroid response in asthma. *Eur Respir J,* 47**,** 1123-33.

WANG, J.-X. & NIGROVIC, P. 2013. CD177 participates in a novel mechanism for regulating neutrophil recruitment (P3093). *The Journal of Immunology,* 190**,** 43.9-43.9.

WANG, R., CUSTOVIC, A., SIMPSON, A., BELGRAVE, D. C., LOWE, L. A. & MURRAY, C. S. 2014. Differing associations of BMI and body fat with asthma and lung function in children. *Pediatr Pulmonol,* 49**,** 1049-57.

WANG, S. W., OH, C. K., CHO, S. H., HU, G., MARTIN, R., DEMISSIE-SANDERS, S., LI, K., MOYLE, M. & YAO, Z. 2005. Amphiregulin expression in human mast cells and its effect on the primary human lung fibroblasts. *J Allergy Clin Immunol,* 115**,** 287-94.

WANG, W., LI, Y., LV, Z., CHEN, Y., HUANG, K., CORRIGAN, C. J. & YING, S. 2018. Bronchial Allergen Challenge of Patients with Atopic Asthma Triggers an Alarmin (IL-33, TSLP, and IL-25) Response in the Airways Epithelium and Submucosa. *J Immunol*.

WANG, X., DUCH, M. C., MANSUKHANI, N., JI, Z., LIAO, Y.-P., WANG, M., ZHANG, H., SUN, B., CHANG, C. H., LI, R., LIN, S., MENG, H., XIA, T., HERSAM, M. C. & NEL, A. E. 2015. Use of a Pro-Fibrogenic Mechanism-Based Predictive Toxicological Approach for Tiered Testing and Decision Analysis of Carbonaceous Nanomaterials. *ACS Nano,* 9**,** 3032-3043.

WEGMANN, M. & RENZ, H. 2005. Animal models of experimental asthma. *Ernst Schering Res Found Workshop***,** 69-87.

WESTPHAL, G. A., ROSENKRANZ, N., BRIK, A., WEBER, D., FOHRING, I., MONSE, C., KAISER, N., HELLACK, B., MATTENKLOTT, M., BRUNING, T., JOHNEN, G. & BUNGER, J. 2019. Multi-walled carbon nanotubes induce stronger migration of inflammatory cells in vitro than asbestos or granular particles but a similar pattern of inflammatory mediators. *Toxicol In Vitro,* 58**,** 215-223.

WHITE, S. B., SHIH, A. J. & PIPE, K. P. 2011. Investigation of the electrical conductivity of propylene glycol-based ZnO nanofluids. *Nanoscale Res Lett,* 6**,** 346.

WHITE, S. R., MARTIN, L. D., STERN, R., LAXMAN, B. & MARROQUIN, B. A. 2010. Expression of IL-4/IL-13 receptors in differentiating human airway epithelial cells. *Am J Physiol Lung Cell Mol Physiol,* 299**,** L681-93.

WICHMANN, H. E. 2007. Diesel exhaust particles. *Inhal Toxicol,* 19 Suppl 1**,** 241-4.

WILKENING, K. E., BARRIE, L. A. & ENGLE, M. 2000. Trans-Pacific Air Pollution. 290**,** 65-67.

WILKINS, E. T. 1954. Air Pollution and the London Fog of December, 1952. *Journal of the Royal Sanitary Institute,* 74**,** 1-21.

WILLART, M. A., DESWARTE, K., POULIOT, P., BRAUN, H., BEYAERT, R., LAMBRECHT, B. N. & HAMMAD, H. 2012. Interleukin-1α controls allergic sensitization to inhaled house dust mite via the epithelial release of GM-CSF and IL-33. *J Exp Med,* 209**,** 1505-17.

WINGARD, C. J., WALTERS, D. M., CATHEY, B. L., HILDERBRAND, S. C., KATWA, P., LIN, S., KE, P. C., PODILA, R., RAO, A., LUST, R. M. & BROWN, J. M. 2011. Mast cells contribute to altered vascular reactivity and ischemia-reperfusion injury following cerium oxide nanoparticle instillation. *Nanotoxicology,* 5**,** 531-45.

WITTEKINDT, O. H. 2017. Tight junctions in pulmonary epithelia during lung inflammation. *Pflugers Arch,* 469**,** 135-147.

WONG, A. A. B. C. A. C. S. A. P. P. A. O. T. T. A. H. L.-J. A. R. F. A. E. J. A. R. J. 2012. Directed differentiation of human pluripotent stem cells into mature airway epithelia expressing functional CFTR protein. 30.

WONG, A. P., BEAR, C. E., CHIN, S., PASCERI, P., THOMPSON, T. O., HUAN, L. J., RATJEN, F., ELLIS, J. & ROSSANT, J. 2012. Directed differentiation of human pluripotent stem cells into mature airway epithelia expressing functional CFTR protein. *Nat Biotechnol,* 30**,** 876-82.

WONG, I. C., NG, Y. K. & LUI, V. W. 2014. Cancers of the lung, head and neck on the rise: perspectives on the genotoxicity of air pollution. *Chin J Cancer,* 33**,** 476-80.

WONG, P. S., VOGEL, C. F., KOKOSINSKI, K. & MATSUMURA, F. 2010. Arylhydrocarbon receptor activation in NCI-H441 cells and C57BL/6 mice: possible mechanisms for lung dysfunction. *Am J Respir Cell Mol Biol,* 42**,** 210-7.

WU, W., PEDEN, D. & DIAZ-SANCHEZ, D. 2012. Role of GSTM1 in resistance to lung inflammation. *Free Radic Biol Med,* 53**,** 721-9.

XIAO, C., PUDDICOMBE, S. M., FIELD, S., HAYWOOD, J., BROUGHTON-HEAD, V., PUXEDDU, I., HAITCHI, H. M., VERNON-WILSON, E., SAMMUT, D., BEDKE, N., CREMIN, C., SONES, J., DJUKANOVIC, R., HOWARTH, P. H., COLLINS, J. E., HOLGATE, S. T., MONK, P. & DAVIES, D. E. 2011. Defective epithelial barrier function in asthma. *J Allergy Clin Immunol,* 128**,** 549-56 e1-12.

XIONG, H., CUROTTO DE LAFAILLE, M. A. & LAFAILLE, J. J. 2012. Chapter Four - What is Unique About the IgE Response? *In:* ALT, F. W. (ed.) *Advances in Immunology.* Academic Press.

XU, C. & QU, X. 2014. Cerium oxide nanoparticle: a remarkably versatile rare earth nanomaterial for biological applications. *Npg Asia Materials,* 6**,** e90.

XU, M. X., ZHU, Y. F., CHANG, H. F. & LIANG, Y. 2016. Nanoceria restrains PM2.5-induced metabolic disorder and hypothalamus inflammation by inhibition of astrocytes activation related NF-kappaB pathway in Nrf2 deficient mice. *Free Radic Biol Med,* 99**,** 259-272.

XUE, L., HE, X., LI, Y., QU, M. & ZHANG, Z. 2013. Pulmonary toxicity of ceria nanoparticles in mice after intratracheal instillation. *J Nanosci Nanotechnol,* 13**,** 6575-80.

YAGHI, A. & DOLOVICH, M. B. 2016. Airway Epithelial Cell Cilia and Obstructive Lung Disease. *Cells,* 5.

YANAGITA, Y., SENJYU, H., ASAI, M., TANAKA, T., YANO, Y., MIYAMOTO, N., NISHINAKAGAWA, T., KOTAKI, K., KOZU, R., TABUSADANI, M. & HONDA, S. 2013. Air pollution irreversibly impairs lung function: a twenty-year follow-up of officially acknowledged victims in Japan. *Tohoku J Exp Med,* 230**,** 177-84.

YANG, I. V., PEDERSEN, B. S., LIU, A., O'CONNOR, G. T., TEACH, S. J., KATTAN, M., MISIAK, R. T., GRUCHALLA, R., STEINBACH, S. F., SZEFLER, S. J., GILL, M. A., CALATRONI, A., DAVID, G., HENNESSY, C. E., DAVIDSON, E. J., ZHANG, W., GERGEN, P., TOGIAS, A., BUSSE, W. W. & SCHWARTZ, D. A. 2015. DNA methylation and childhood asthma in the inner city. *J Allergy Clin Immunol,* 136**,** 69-80.

YANG, S. N., HSIEH, C. C., KUO, H. F., LEE, M. S., HUANG, M. Y., KUO, C. H. & HUNG, C. H. 2014. The effects of environmental toxins on allergic inflammation. *Allergy Asthma Immunol Res,* 6**,** 478-84.

YANG, Y., QIN, Z., ZENG, W., YANG, T., CAO, Y., MEI, C. & KUANG, Y. 2017. Toxicity assessment of nanoparticles in various systems and organs. *Nanotechnology Reviews.*

YING, S., O'CONNOR, B., RATOFF, J., MENG, Q., MALLETT, K., COUSINS, D., ROBINSON, D., ZHANG, G., ZHAO, J., LEE, T. H. & CORRIGAN, C. 2005. Thymic stromal lymphopoietin expression is increased in asthmatic airways and correlates with expression of Th2-attracting chemokines and disease severity. *J Immunol,* 174**,** 8183-90.

YOKEL, R. A., HUSSAIN, S., GARANTZIOTIS, S., DEMOKRITOU, P., CASTRANOVA, V. & CASSEE, F. R. 2014. The Yin: An adverse health perspective of nanoceria: uptake, distribution, accumulation, and mechanisms of its toxicity. *Environ Sci Nano,* 1**,** 406-428.

ZAHRADNIK, E. & RAULF, M. 2014. Animal allergens and their presence in the environment. *Front Immunol,* 5**,** 76.

ZAIDMAN, N. A., PANOSKALTSIS-MORTARI, A. & O'GRADY, S. M. 2016. Differentiation of human bronchial epithelial cells: role of hydrocortisone in development of ion transport pathways involved in mucociliary clearance. *Am J Physiol Cell Physiol,* 311**,** C225-36.

ZARCONE, M. C., DUISTERMAAT, E., VAN SCHADEWIJK, A., JEDYNSKA, A., HIEMSTRA, P. S. & KOOTER, I. M. 2016. Cellular response of mucociliary differentiated primary bronchial epithelial cells to diesel exhaust. *Am J Physiol Lung Cell Mol Physiol,* 311**,** L111-23.

ZHANG, J., NAZARENKO, Y., ZHANG, L., CALDERON, L., LEE, K. B., GARFUNKEL, E., SCHWANDER, S., TETLEY, T. D., CHUNG, K. F., PORTER, A. E., RYAN, M., KIPEN, H., LIOY, P. J. & MAINELIS, G. 2013. Impacts of a nanosized ceria additive on diesel engine emissions of particulate and gaseous pollutants. *Environ Sci Technol,* 47**,** 13077-85.

ZHANG, J. J., LEE, K. B., HE, L., SEIFFERT, J., SUBRAMANIAM, P., YANG, L., CHEN, S., MAGUIRE, P., MAINELIS, G., SCHWANDER, S., TETLEY, T., PORTER, A., RYAN, M., SHAFFER, M., HU, S., GONG, J. & CHUNG, K. F. 2016. Effects of a nanoceria fuel additive on the physicochemical properties of diesel exhaust particles. *Environ Sci Process Impacts,* 18**,** 1333-1342.

ZHOU, X., WANG, B., CHEN, Y., MAO, Z. & GAO, C. 2013. Uptake of cerium oxide nanoparticles and their influences on functions of A549 cells. *J Nanosci Nanotechnol,* 13**,** 204-15.

ZOSKY, G. R. & SLY, P. D. 2007. Animal models of asthma. *Clin Exp Allergy,* 37**,** 973-88.

Appendix

8.1 Additional figures

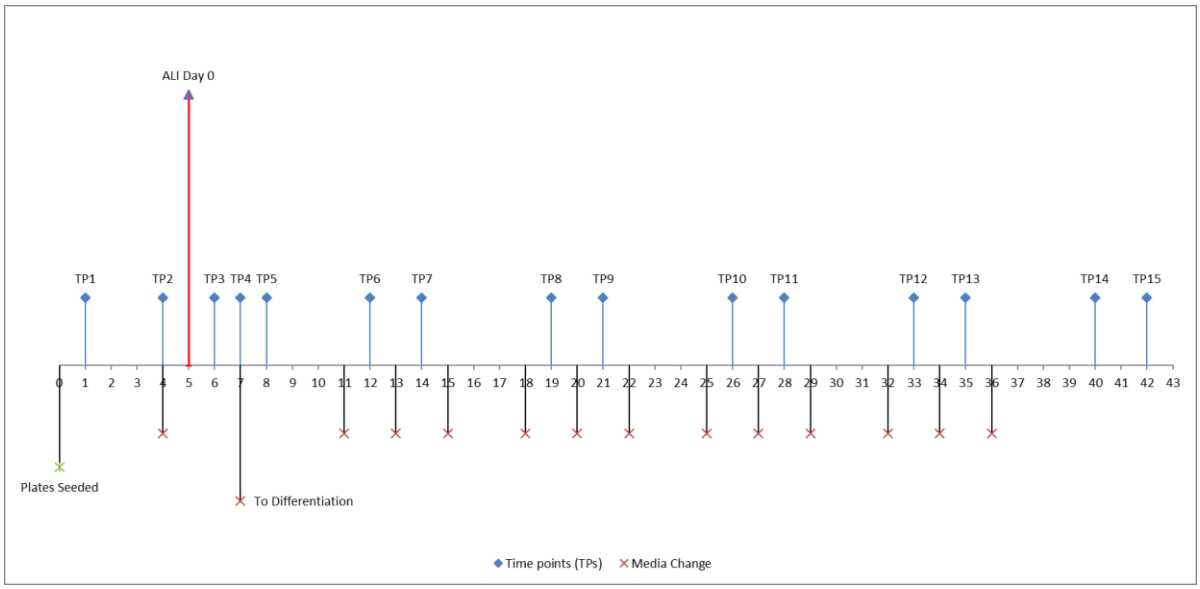


Figure 8-1. Time points for analysis of various characterisations. At these time points various samples were taken and analysed for predetermined end points. The wells were seeded on day 0 at a concentration of $1x10^5$cells/cm^2. ALI day 0 is when medium is removed from the apical side of the membrane exposing the cells to air. Red crosses indicate medium changes, with the specifically indicated change on day 7 to the various differentiation media which was then continued throughout the culture life.

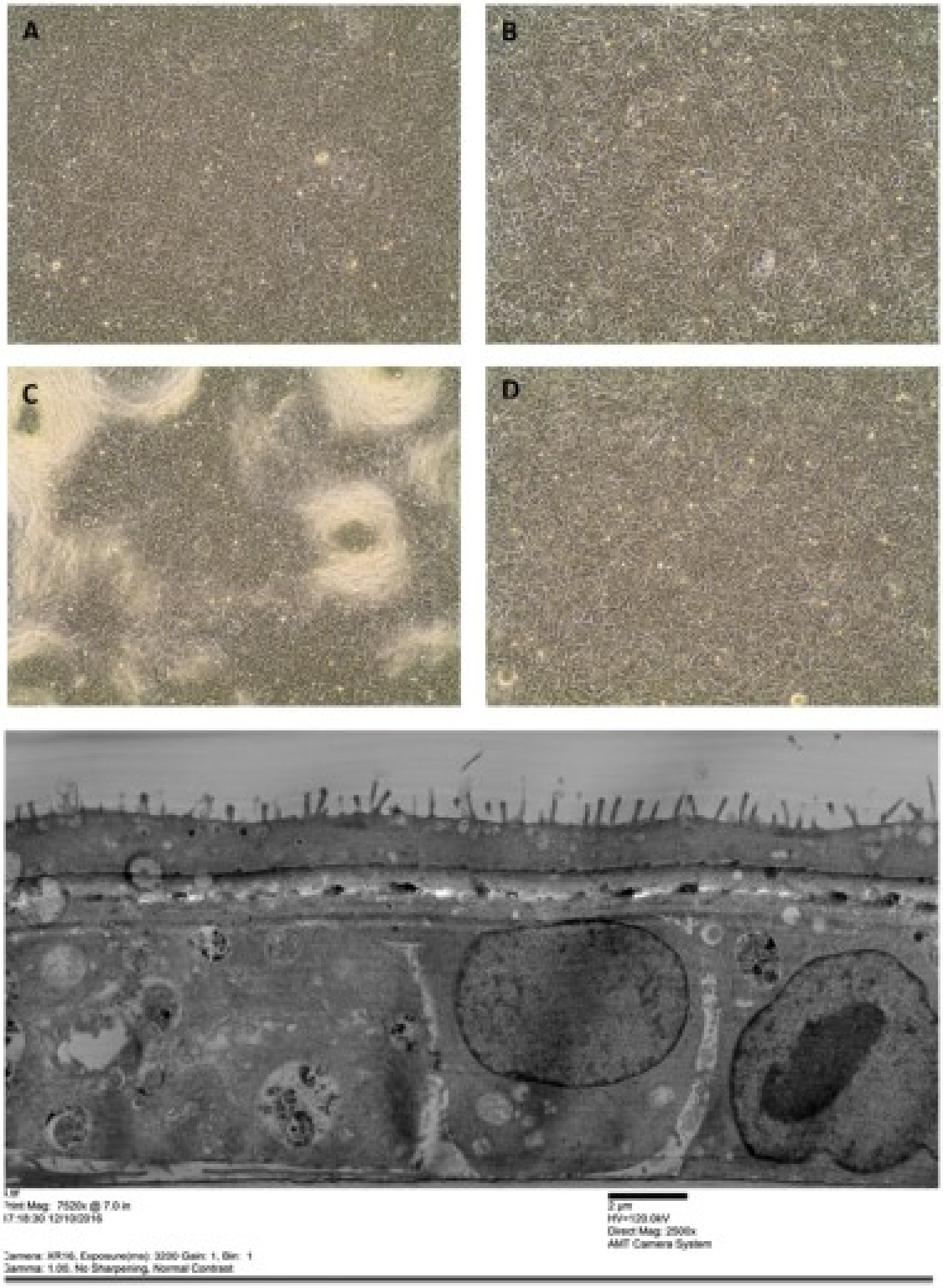


Figure 8-2. Confocal microscopy images showing HPBECs growing in the various differentiation media and TEM microscopy image of HPBECs grown in Gray medium. A. represents HPBECs grown in Fulcher medium; B. represents HPBECs grown in Gray medium; C. represents HPBECs grown in Matsui medium; and D.. represents HPBECs grown in Fulcher and Randell medium. All HPBECs are from the same donor, initially seeded at $1x10^5$cells/cm^2 on day 0 and pictured 12 days after seeding (7 days at ALI). Magnification x20 and the scale bar represents 100µm. E. TEM image on day 21 after the cells have been differentiated in Gray medium. Scale bar represents 2µm.

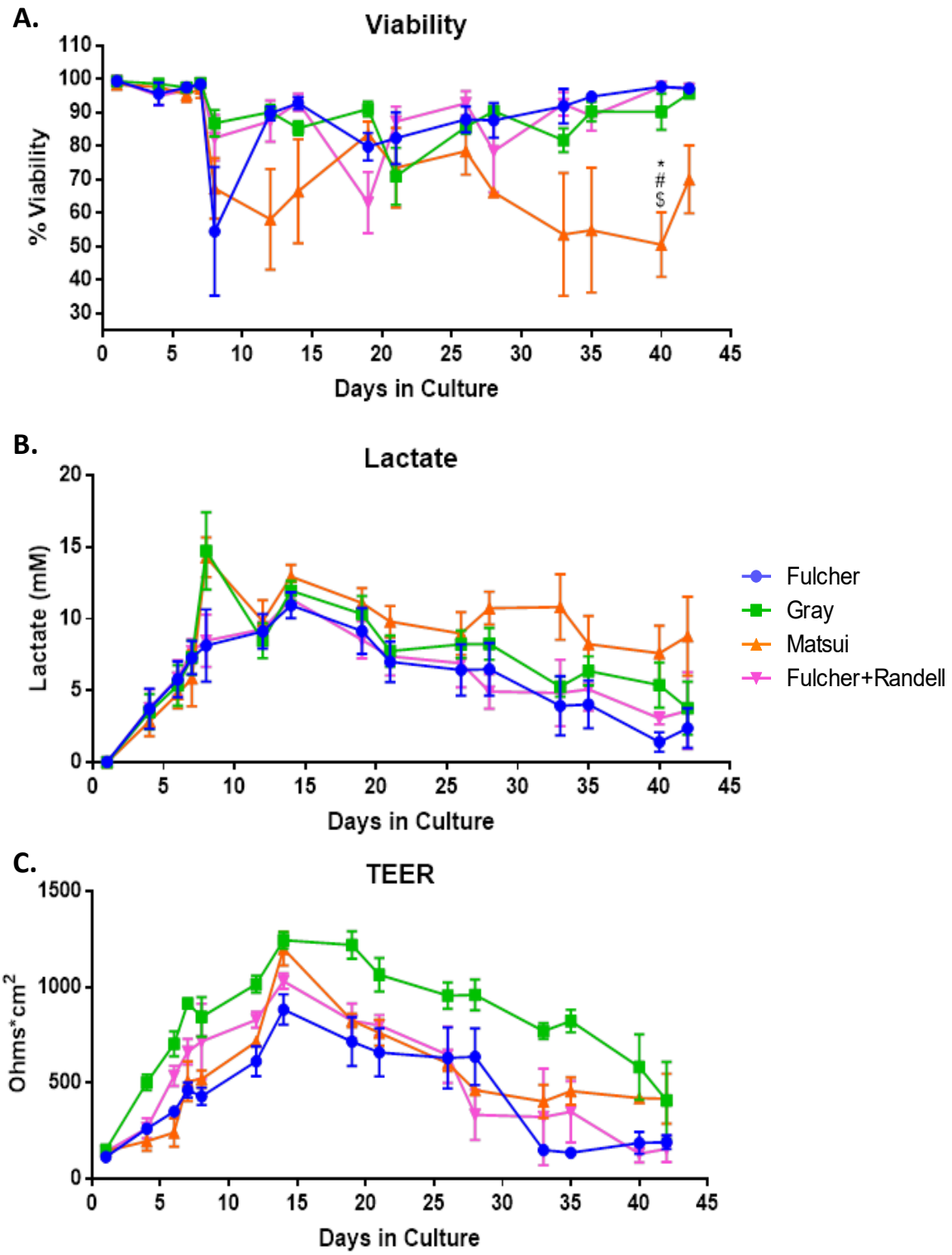


Figure 8-3. Cellular injury and dysfunction measurements for the four differentiation medium types. **A.** Cellular viability measured with LDH production; **B.** Lactate levels in the basal compartment and **C.** TEER measurements at the pre-defined TPs. N=4 subjects with all assays performed in triplicate. The data is presented as the mean ±SEM. Significance is denoted as the following: compared to Fulcher medium P<0.05(*); compared to Gray medium P<0.05(#); and compared to Fulcher+Randell medium P<0.05($).

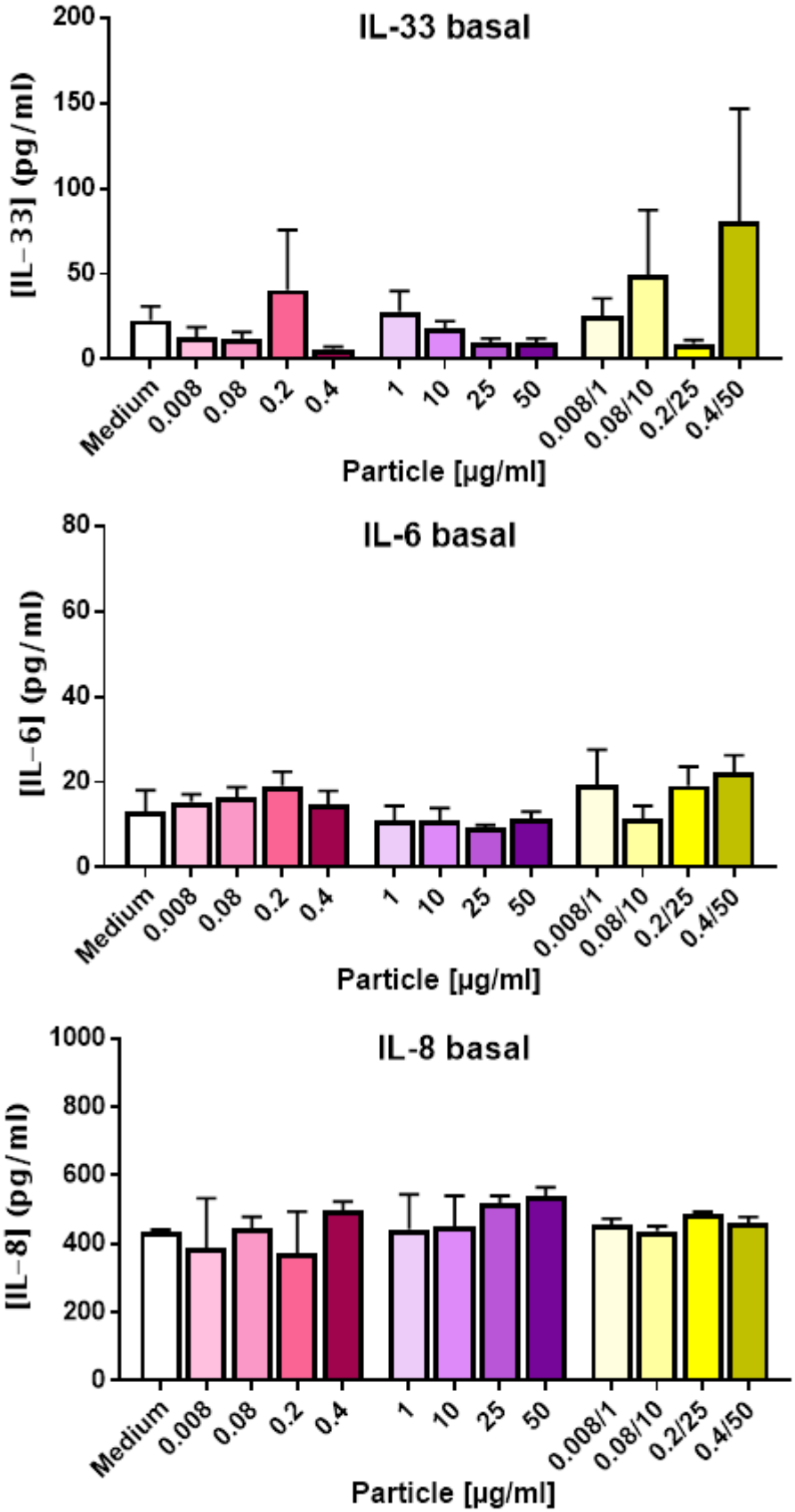


Figure 8-4. Basal protein expression changes after 24 hours of CeO_2NPs alone, DEP alone and CeO_2/DEP combined exposures. ELISA expression changes in SAECs after 24 hours of exposure to CeO_2/DEP. Analysed 24 hours after particulate exposure, after the particles had been removed from the apical side of the membrane. Cytokine and chemokine release was measured in both the apical and basal compartments. The data is presented as the mean ±SEM. N=4-8 subjects with all assays performed in triplicate. Significance is denoted as the following: compared to medium control $p<0.05$(*).

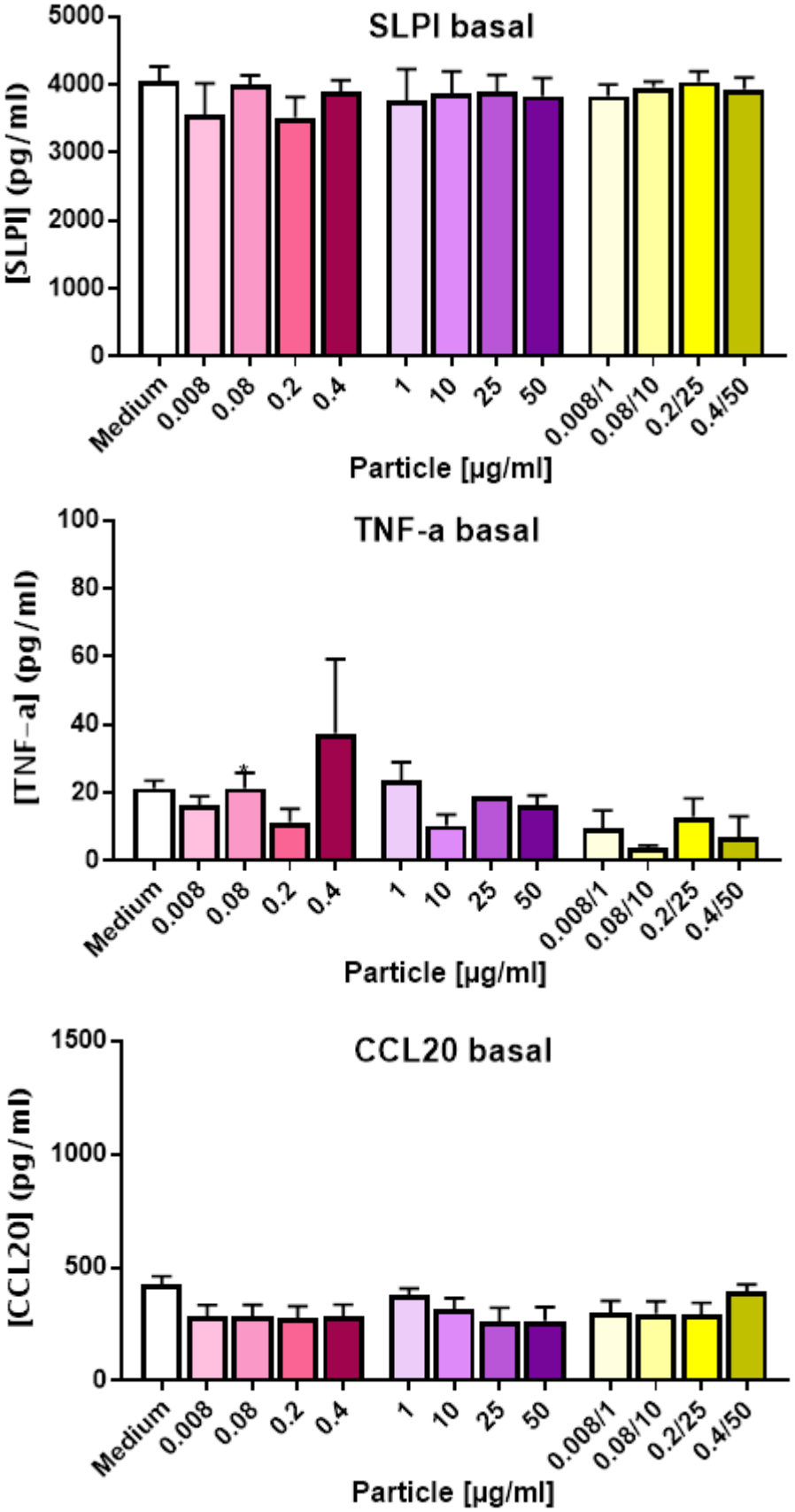


Figure 8-5. Basal protein expression changes after 24 hours of CeO_2NPs alone, DEP alone and CeO_2/DEP combined exposures. ELISA expression changes in SAECs after 24 hours of exposure to CeO_2/DEP. Analysed 24 hours after particulate exposure, after the particles had been removed from the apical side of the membrane. Cytokine and chemokine release was measured in both the apical and basal compartments. The data is presented as the mean ±SEM. N=4-8 subjects with all assays performed in triplicate. Significance is denoted as the following: compared to medium control $p<0.05$(*).

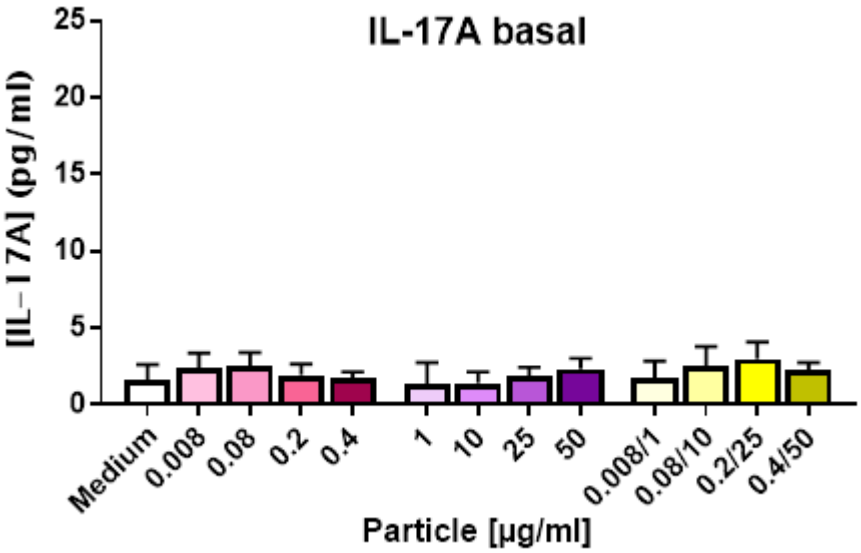


Figure 8-6. Basal protein expression changes after 24 hours of CeO_2NPs alone, DEP alone and CeO_2/DEP combined exposures. ELISA expression changes in SAECs after 24 hours of exposure to CeO_2/DEP. Analysed 24 hours after particulate exposure, after the particles had been removed from the apical side of the membrane. Cytokine and chemokine release was measured in both the apical and basal compartments. The data is presented as the mean ±SEM. N=4-8 subjects with all assays performed in triplicate. Significance is denoted as the following: compared to medium control $p<0.05$(*).

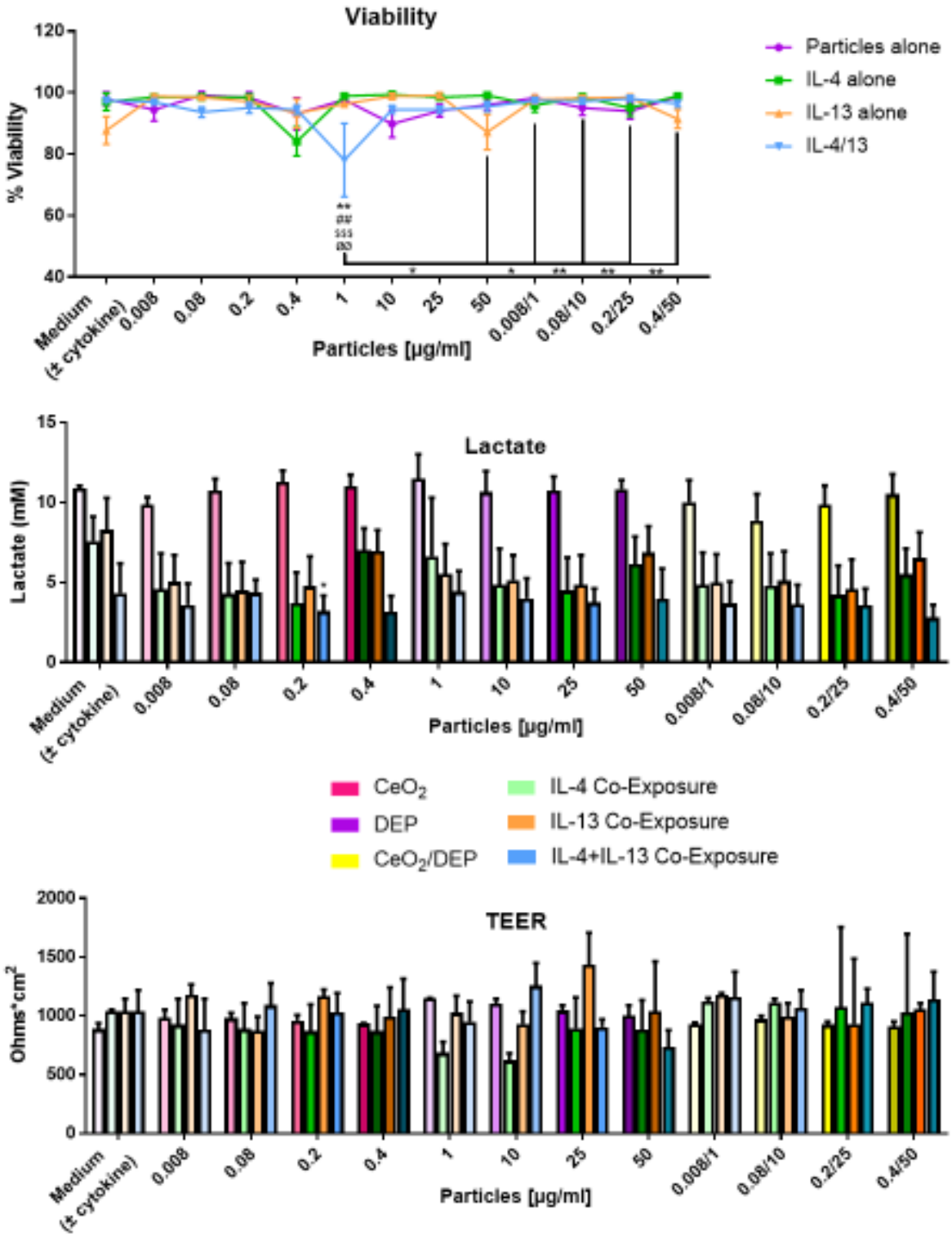


Figure 8-7. Cell viability, cellular injury and membrane integrity after 24 hours of both CeO_2/DEP and cytokine co-exposure. Cellular viability measured with LDH production, lactate production measured in the basolateral compartment indicating cellular injury and cellular metabolism, and TEER measurements completed 24 hours after particulate exposure, after the particles had been removed from the apical side of the membrane. N=4-8 subjects with all assays performed in triplicate. The data is presented as the mean ±SEM. Significance is denoted as the following: compared to medium control p<0.05(*), <0.01(**), <0.001(***), compared to particle control p<0.05(#), <0.01(##), <0.001(###), compared to IL-4 co-exposure p<0.05($), <0.01($$), <0.001($$$), and compared to IL-13 co-exposure p<0.05(ø), <0.01(øø), <0.001(øøø).

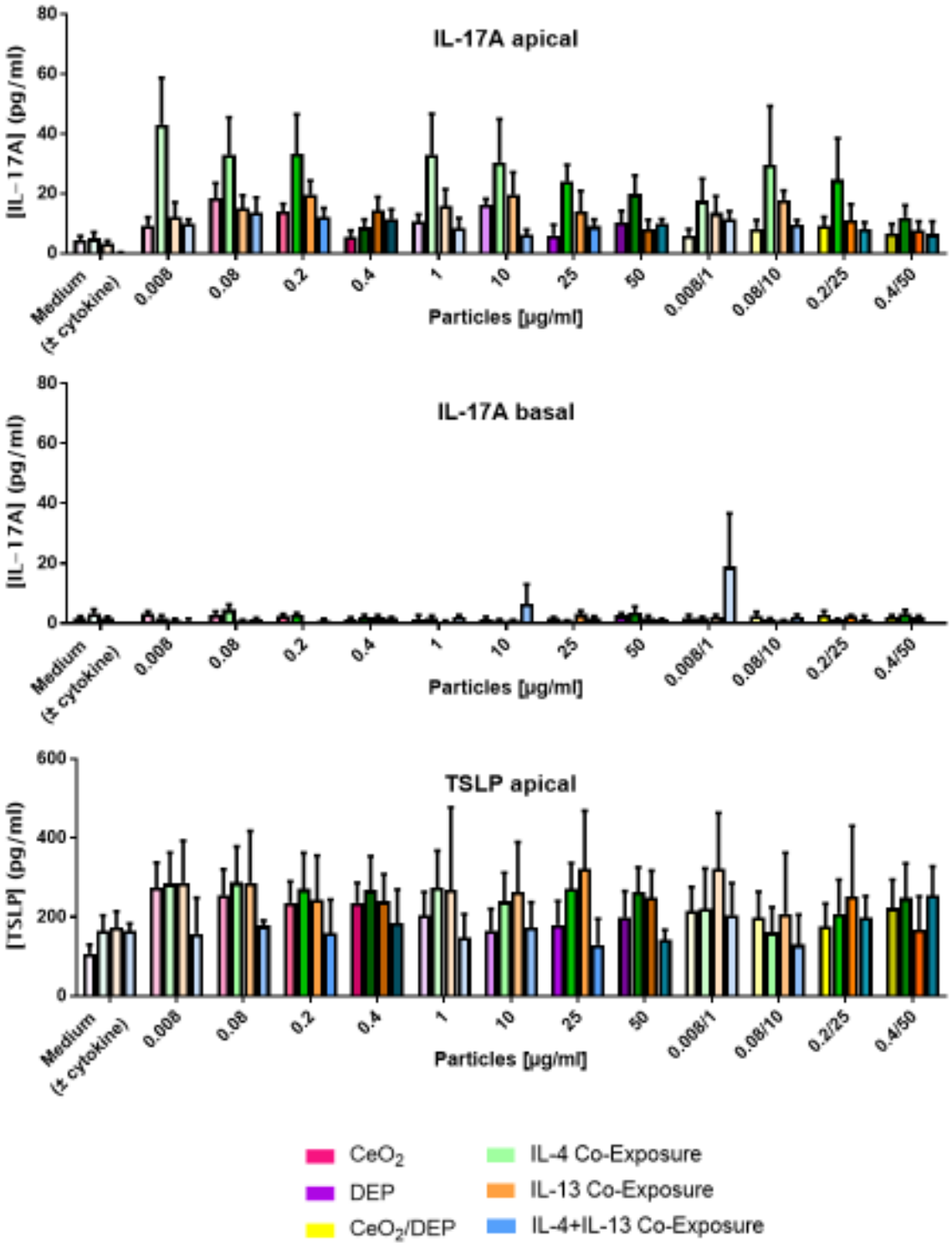


Figure 8-8. Protein expression changes after 24 hour co-exposure of both CeO_2/DEP and cytokines.
ELISA expression changes in SAECs after 24 hours of exposure to CeO_2/DEP. Analysed 24 hours after particulate exposure, after the particles had been removed from the apical side of the membrane. Cytokine and chemokine release was measured in both the apical and basal compartments. The data is presented as the mean ±SEM. N=4-8 subjects with all assays performed in triplicate. Significance is denoted as the following: compared to medium control $p<0.05$(*), <0.01(**), <0.001(***), <0.0001(****).

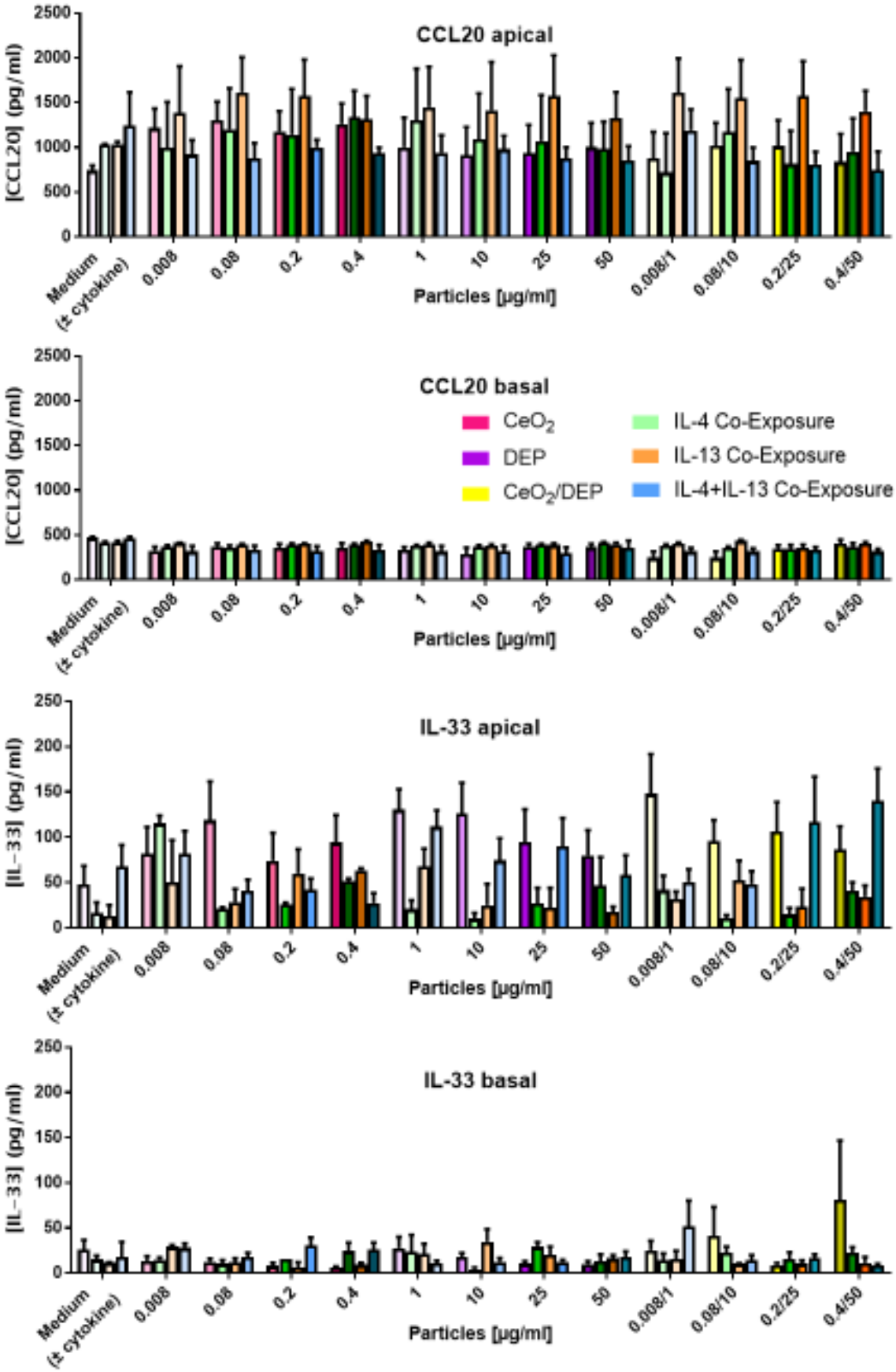


Figure 8-9 Protein expression changes after 24 hour co-exposure of both CeO_2/DEP and cytokines.
ELISA expression changes in SAECs after 24 hours of exposure to CeO_2/DEP. Analysed 24 hours after particulate exposure, after the particles had been removed from the apical side of the membrane. Cytokine and chemokine release was measured in both the apical and basal compartments. The data is presented as the mean ±SEM. N=4-8 subjects with all assays performed in triplicate. Significance is denoted as the following: compared to medium control p<0.05(*), <0.01(**), <0.001(***), <0.0001(****).

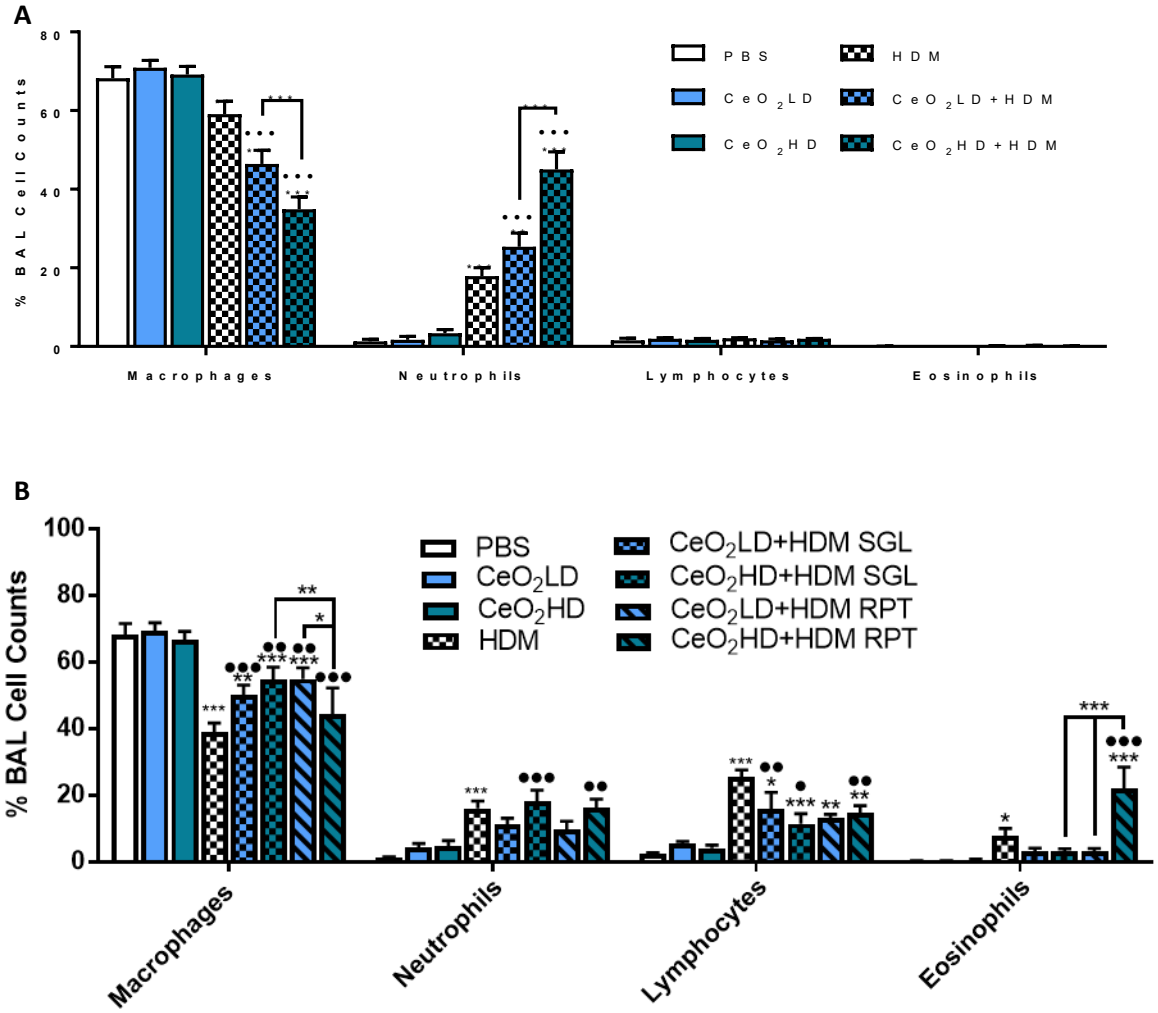


Figure 8-10 Inflammatory cell profile after exposure to CeO_2NPs±HDM. BAL fluid was analysed for immune cell profile. A. Cell profile 24 hours after exposure. B. Cell profile 3 weeks after exposure (acute and chronic exposures). BAL cells were counted after being fixed and stained as previously outlined (**section 2.6.4**) and 300-500 cells were counted per animal. The data are presented as the mean ±SEM % total cells counted. N=5-9 mice per treatment group, with all assays performed in triplicate. Significance is denoted as the following, as indicated: compared to PBS or HDM control p<0.05(*), <0.01(**), <0.001(***); compared to CeO_2NP alone p<0.05(•), <0.01(••), <0.001(•••).

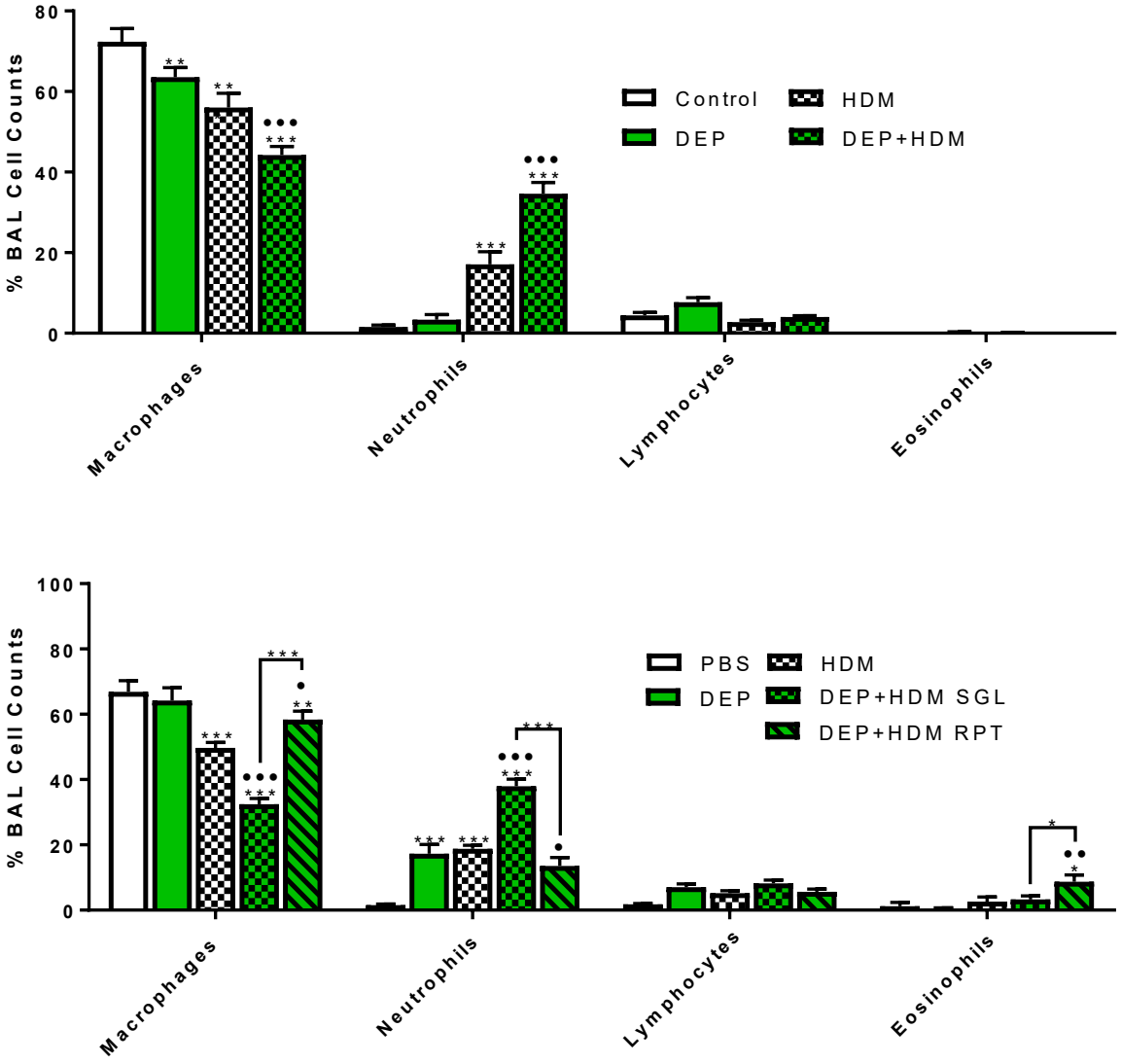


Figure 8-11 Inflammatory cell profile after exposure to DEP±HDM. BAL fluid was analysed for immune cell profile. A. Cell profile 24 hours after exposure. B. Cell profile 3 weeks after exposure (acute and chronic exposures). BAL cells were counted after being fixed and stained as previously outlined (**section 2.6.4**) and 300-500 cells were counted per animal. The data are presented as the mean ±SEM % total cells counted. N=5-9 mice per treatment group, with all assays performed in triplicate. Significance is denoted as the following, as indicated: compared to PBS or HDM control p<0.05(*), <0.01(**), <0.001(***); compared to DEP alone p<0.05(•), <0.01(••), <0.001(•••).

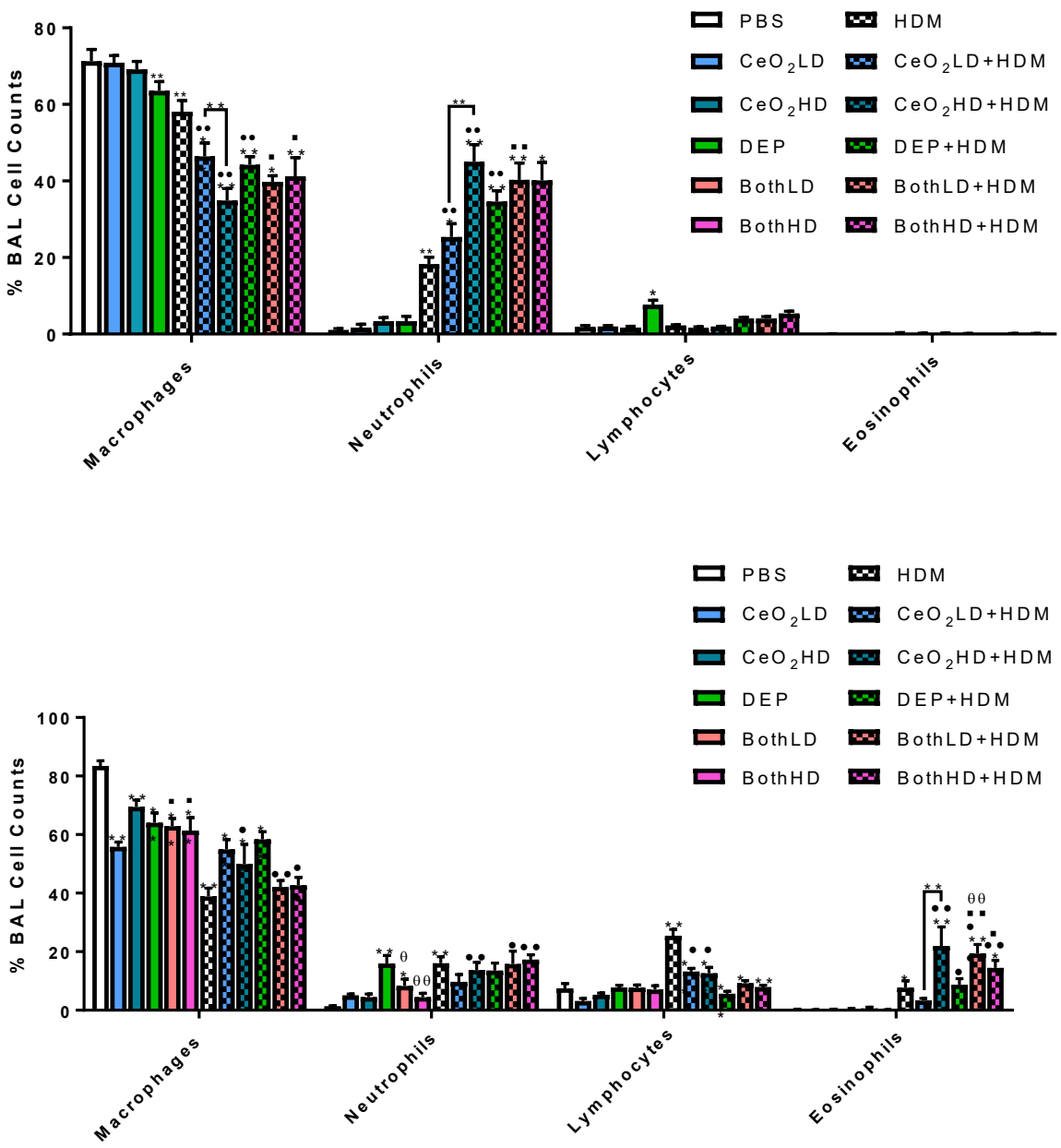


Figure 8-12. Inflammatory cell profile after exposure to Both±HDM. BAL fluid was analysed for immune cell profile. A. Cell profile 24 hours after exposure. B. Cell profile 3 weeks after exposure (acute and chronic exposures). BAL cells were counted after being fixed and stained as previously outlined (**section 2.6.4**) and 300-500 cells were counted per animal. The data are presented as the mean ±SEM % total cells counted. N=5-9 mice per treatment group, with all assays performed in triplicate. Significance is denoted as the following: compared to PBS or HDM control p<0.05(*), <0.01(**), <0.001(***); compared to particles alone p<0.05(•), <0.01(••), <0.001(•••); compared to CeO_2NPs+HDM p<0.05(▪), <0.01(▪▪), <0.001(▪▪▪); and compared to DEP+HDM p<0.05(Θ), <0.01(Θ Θ), <0.001(Θ Θ Θ).

Meldrum *et al. Particle and Fibre Toxicology* (2017) 14:45
DOI 10.1186/s12989-017-0228-y

Particle and Fibre Toxicology

REVIEW Open Access

Mechanistic insight into the impact of nanomaterials on asthma and allergic airway disease

Kirsty Meldrum, Chang Guo, Emma L. Marczylo, Timothy W. Gant, Rachel Smith and Martin O. Leonard*

Abstract: Asthma is a chronic respiratory disease known for its high susceptibility to environmental exposure. Inadvertent inhalation of engineered or incidental nanomaterials is a concern for human health, particularly for those with underlying disease susceptibility. In this review we provide a comprehensive analysis of those studies focussed on safety assessment of different nanomaterials and their unique characteristics on asthma and allergic airway disease. These include *in vivo* and *in vitro* approaches as well as human and population studies. The weight of evidence presented supports a modifying role for nanomaterial exposure on established asthma as well as the development of the condition. Due to the variability in modelling approaches, nanomaterial characterisation and endpoints used for assessment in these studies, there is insufficient information for how one may assign relative hazard potential to individual nanoscale properties. New developments including the adoption of standardised models and focussed *in vitro* and *in silico* approaches have the potential to more reliably identify properties of concern through comparative analysis across robust and select testing systems. Importantly, key to refinement and choice of the most appropriate testing systems is a more complete understanding of how these materials may influence disease at the cellular and molecular level. Detailed mechanistic insight also brings with it opportunities to build important population and exposure susceptibilities into models. Ultimately, such approaches have the potential to more clearly extrapolate relevant toxicological information, which can be used to improve nanomaterial safety assessment for human disease susceptibility.

Keywords: Asthma, Allergy, Nanomaterials, Nanoparticles, Ultrafine Pollutant, Inhalation, Lung

Background

Asthma affects over 330 million individuals worldwide and is associated with significant avoidable mortality, morbidity and economic burden [1]. In pathophysiological terms, asthma is a chronic inflammatory condition of the airway and is increasingly considered a term to cover a broad spectrum disease category with multiple causes and phenotypes [2]. Clinical symptoms include airway obstruction, bronchospasm, wheezing, coughing, shortness of breath and airway hyper-responsiveness (AHR) [3]. The most common underlying disease process is chronic inflammation, which encompasses a wide array of resident and immune cell types. As a consequence of this inflammation, airway remodelling occurs with specific changes manifesting as sub-epithelial fibrosis, smooth muscle thickening, neo-vascularisation and epithelial barrier modification. This restructuring together with increased smooth muscle contractility and enhanced mucus secretion cause obstructive events and the clinical symptoms of disease [4–7].

There are a number of environmental factors with strong links to the development of asthma, including early *in utero* and childhood exposure to microbes, infection, diet, obesity, vitamin D levels, allergens, chemicals and tobacco smoke [8–17]. Exposures, particularly to allergens, particulates and chemicals, and respiratory infections also account for the majority of known triggers for obstructive events in asthma [9, 18–20]. It has been recognised for some time that certain chemicals can cause asthma and allergic airway disease (AAD) [21, 22]. Properties intrinsic to these chemicals and more recently for particulate exposure, have been suggested to govern their ability to produce adverse effects. Nanomaterials (NMs), including ultrafine particulates, defined as having at least one

* Correspondence: Martin.Leonard@phe.gov.uk
Toxicology Department, Centre for Radiation, Chemical and Environmental Hazards, Public Health England, Chilton, Harwell Campus OX11 0RQ, UK

© The Author(s). 2017 **Open Access** This article is distributed under the terms of the Creative Commons Attribution 4.0 International License (http://creativecommons.org/licenses/by/4.0/), which permits unrestricted use, distribution, and reproduction in any medium, provided you give appropriate credit to the original author(s) and the source, provide a link to the Creative Commons license, and indicate if changes were made. The Creative Commons Public Domain Dedication waiver (http://creativecommons.org/publicdomain/zero/1.0/) applies to the data made available in this article, unless otherwise stated.

dimension less than 100nm [23, 24], are recognised as possessing not simply chemical but also physical characteristics, with the potential to modify disease risk and outcome.

Concerns have been raised regarding the safety of both engineered NMs and incidental ultrafine particulates upon inadvertent exposure in humans [25]. Epidemiological approaches to understanding how nanoscale materials affect asthma and AAD have been restricted to a handful of studies with limited power to attribute causal effect. The study of pollutant mixtures has suggested that nanoscale components of fossil fuel combustion products such as diesel exhaust particulates may contribute to asthma and allergic airway disease [20, 26, 27]. As chemicals including polycyclic aromatic hydrocarbons and quinones adhered to ultrafine particles are increasingly suggested as the primary factor responsible for adverse effects [26, 28–30], it is important to properly define the nanoscale characteristic contribution. Such information also has the potential to increase our understanding of how engineered nanoscale materials may impact asthma. As a focus for this review, we will describe current knowledge from human and experimental observations, on how respiratory exposure to nanomaterials with different compositions and characteristics modify asthma and AAD. We will also describe current understanding of the mechanisms through which such modification can occur, and explore important knowledge gaps to allow prioritisation of research focus into the future.

There are different ways in which nanomaterial (NM) effects on asthma can be considered. In terms of experimental modelling, there are those approaches that have examined either naïve or genetically susceptible animals in the absence of allergen initiated disease. There are other approaches that have used allergen induced inflammation as a conditioning step for disease initiation and used different protocols to examine effects on the development (adjuvancy) or exacerbation of established allergic airway disease. Using the search criteria detailed in Additional file 1 to encompass all aspects of disease susceptibility, we have performed a comprehensive analysis of those studies, which examine the effect of pulmonary exposure to nanoparticles (NPs), including nano-sized ultrafine pollutants, on humans and experimental models of asthma and AAD. Those studies focussed on medical applications of NMs were excluded from the main analysis and discussed separately.

Experimental models and evidence for modifying effect of nanomaterials

Experimental modelling as a means to identify hazards and develop risk assessment and management approaches is fundamental to how materials are assessed for potential safety concerns. The majority of such testing is carried out using *in vivo* exposure systems and occasionally incorporates models of disease susceptibility. A number of experimental *in vivo* approaches have been used to assess the impact of NMs on asthma and AAD. In order to interpret these findings as translational information that can be applied to human exposure, we must first describe the pathological features of asthma and its endotype subcategories as measurable endpoints that can be experimentally modelled and assessed.

Current approaches to the categorisation of asthma involve subdivision based on immunological characteristics as well as clinical symptoms and severity of disease [2]. The most common form of asthma found in children and half of adults is atopic in nature and correlates with increased IgE antibody levels and/or a positive skin prick test for allergens such as house dust mite (HDM). Increased IgE levels in atopic conditions are a functional consequence of CD4+ T-cell patterning towards a Th2 phenotype, which switches B-cell antibody production to IgE. In AAD, IgE coated eosinophils, mast cells and basophils are activated upon re-exposure to allergen and an inflammatory response is initiated. Allergen specific activation of Th2 CD4+ T-cells in lung tissue increases the production of IL-4, IL-5 and IL-13 cytokines. This results in an increase in IgE production from B-cells, eosinophil recruitment and goblet cell metaplasia as well as increased mucus production (MUC5AC), all of which contribute to airway restriction [31]. Within the category of a high Th2 asthma endotype, there is a subdivision of disease, which displays eosinophilia and a Th2 cytokine environment in the absence of an adaptive immune response and is often referred to as intrinsic asthma [32]. It has been proposed that the newly discovered innate lymphoid ILC2 cells drive this type of disease in response to chronic stimulation from infection, pollution and irritants. Injury to and activation of the epithelial cell layer in the airway is a key feature of Th2 mediated responses with epithelial derived factors including IL-33, TSLP, IL-25 and GM-CSF all suggested to play a role [31].

Another important endotype typically associated with late onset and more severe forms of asthma is one where there is a predominant neutrophilic inflammation and the presence of a mixed Th1 and Th17 immune response, producing IL-17A, IL-22, IFNγ and TNFα among other mediators [33]. It is also important to consider overlapping endotypes, where individuals will have varying degrees of inflammation and disease severity, for example combined eosinophilic and neutrophilic disease with a Th2 and Th17 profile [34]. Airway obstruction, hyperresponsiveness, remodelling (cellular proliferation & extracellular matrix deposition) and excessive mucus production with goblet cell hyperplasia are common features across all endotypes of asthma and are directly

measureable in model systems [35, 36]. Together with endotype specific endpoints as described above, they can all be used to model the impact of material exposure on disease outcome.

Nanomaterial exposure and the development of allergic airway disease

Models of atopic asthma typically involve sensitisation to allergens such as ovalbumin (OVA) in rodents and testing of materials for their ability to modify allergic inflammation and airway function, and have allowed a greater understanding of key events in asthmatic disease progression. NM testing for their impact on the sensitisation steps in these models aims to examine how such materials may influence the development and severity of new cases of the disease, which includes adjuvant activity and have been summarized in Table 1. One of the earliest studies investigating adjuvant activity of NPs demonstrated that carbon nanoparticles (CNPs) with a smaller size (14nm) and greater surface area aggravated OVA induced allergic inflammation and mucus hypersecretion, while larger sized particles (56nm) of the same material did not [37]. Similar adjuvant effects were observed in other studies from this group using the same particles [38] [39] but there was not always a size dependent distinction for example when examining AHR [40]. The adjuvant effects of CNPs have also been observed in studies from other groups [41] and display dose dependent effects [42] as well as material composition dependent differences when compared to titanium dioxide NPs (TiO_2NPs) for example [43].

Comparison to non-nano sized particles has also been carried out within these adjuvant studies and further supports the hypothesis that smaller size and greater surface area have a larger impact on biological reactivity and AAD. This was observed for example, when comparing nano-sized carbon and TiO_2 to sub-micron sized particles of the same material [43]. It has also been observed with polystyrene particles (PSP), where nano-sized PSP produced stronger allergic inflammatory responses to OVA than sub-micron or micron sized PSPs [44]. Interestingly this study addressed potential gender response differences and observed that while PSPs had adjuvant effects in both male and female mice, there were significantly higher IgE and eosinophilic responses in females when compared to males. Examination of silicon dioxide NPs (SiO_2NPs) also demonstrated size and dose dependent effects, where 30nm sized SiO_2NPs increased OVA specific IgE and Th2 type cytokine production while larger sized SiO_2NPs (70nm) or sub-micron and micron sized silica did not [45]. The adjuvant effects of SiO_2NPs have been well documented with additional studies revealing dose dependent increases in AHR, allergic as well as innate airway inflammation (both Th2 and Th17 related) and mucus hypersecretion [46, 47]. A more detailed exploration of how SiO_2NPs have adjuvant effects was recently carried out using three different types of SiO_2NPs (unmodified, mesoporous and polyethylene glycol (PEG) conjugated). The strongest adjuvant activity, measured as increased AHR, inflammatory responses and mucus hypersecretion, was found for the mesoporous form of SiO_2NPs. This form has a similar size to the unmodified SiO_2NPs but has a much larger surface area. It was argued that surface area is the key component for adjuvant activity. This was further supported by the observation that the PEG-SiO_2NPs, which had agglomerates four times larger, and thus a lower surface area per mass dose, failed to produce any adjuvant activity [48].

Multi-walled carbon nanotubes (MWCNTs) are a particular concern for human health and have been observed to worsen the development of AAI with increased IgE, eosinophils, lymphocytes, IL-4 and mucus hypersecretion in a mouse model of AAD [49]. This was also accompanied by innate immune responses including increased neutrophils, IL-1β and IL-33 [49]. Similar effects for MWCNTs [50, 51] and single walled carbon nanotubes (SWCNTs) [52, 53] were observed in subsequent studies. Intriguingly, an analysis of different carbon NMs revealed that both SWCNTs and MWCNTs produced significantly higher levels of IgE and pulmonary eosinophils than either carbon nanofibres (CNFs) or CNPs. CNFs in general had a lesser impact on inflammatory responses and were correlated to a lower specific surface area. Different surface areas however were not sufficient to fully explain allergic airway responses, and nanoparticle (NP) characteristics such as thin tubular structure and biopersistance were suggested as more likely factors contributing to adverse effects [54].

In addition to size, material type and structure, solubility of NPs has also been proposed as an important factor for the ability to modulate the development of AAD. Comparison of different NPs for their potential to modify IgE responses to OVA in mice, revealed that zinc oxide nanoparticles (ZnONPs) but not SiO_2NPs or TiO_2NPs produced an adjuvant effect [55]. It was suggested that the higher solubility of ZnONPs as a contributing factor. Similar to effects independent of allergen, worsening of OVA induced allergic airway inflammation has also been demonstrated in response to ZnONPs but not $ZnCl_2$ ion treatment [56]. Given the suggestion that the nanoparticle intracellular release of Zn ions over a sustained period of time is the key factor for biological effect [57], the use of an ionic metal bolus may not be entirely appropriate to replicate all effects.

Table 1 Effect of nanomaterials on development of allergic airway disease *in vivo*

Nanomaterial Properties				Model Characteristics				Disease Related Endpoints								
Material (coating)	*Size (nm)*	*Surface area (m^2/g)*	*Agg Size: nm*	*Species (Strain - Gender)*	*Allergen (Route)*	*Particle (Route)*	*Dose*	*AHR (LF test)*	*IgE*	*Eos*	*Neu*	*Lym*	*MΦ*	*Total Cells*	*Pathophysiological Indicators*	*GCH-MS*	*Reference*
C	14	300	-	Mice (ICR –m)	OVA (Int T)	Int T	1.61 mg/kg x6	-	↑	↑	↑	-	↑	↑	↑ (IL5, IL13, MCP1, IL6); nc (IL4)	↑ Goblet cells	[37]
C	56	45	-	Mice (ICR –m)	OVA (Int T)	Int T	1.61 mg/kg x6	-	nc	nc	nc	-	nc	↑	↑ (IL5, IL4, IL6, MCP1); nc (IL13)	nc Goblet cells	[37]
C	14	300	-	Mice (ICR –m)	OVA (Int T)	Int T	1.61 mg/kg x6	-	-	-	-	-	-	-	↑ (MIP1α, IL2, IL10, TARC)	-	[38]
C	56	45	-	Mice (ICR –m)	OVA (Int T)	Int T	1.61 mg/kg x6	-	-	-	-	-	-	-	↑ (MIP1α, TARC), nc (IL2, IL10)	-	[38]
C	14	300	-	Mice (ICR –m)	OVA (Int T)	Int T	1.61 mg/kg x6	↑ (Resist)	-	-	-	-	-	-	-	nc MUC5AC	[40]
C	56	45	-	Mice (ICR –m)	OVA (Int T)	Int T	1.61 mg/kg x6	↑ (Resist)	-	-	-	-	-	-	-	↑ MUC5AC	[40]
C	14	-	887	Mice (BALB/c –f)	OVA (PA)	PA	2.5 mg/kg x4	-	↑	↑	↑	-	nc	↑	↑ (CXCL1, IL13), nc (IL4)	-	[41]
C	30-50	-	-	Mice (BALB/c –f)	OVA (IP)	Int N	11 mg/kg	-	↑	↑	nc	nc	nc	↑	↑ TNFα, IL4, IL5, IL10, INFγ	↑ PAS	[42]
C	14.3	253.9	-	Mice (BALB/c –f)	OVA (Int N)	Int N	3.6 mg/kg x3	-	nc	↑	↑	nc	nc	↑	↑ (IL4, IL5, IL10, IL13, INFγ, TNFα)	-	[43]
C	30-50	-	-	Mice (BALB/c –f)	OVA (Int N)	Int N	3.6 mg/kg x3	-	-	-	-	-	nc	-	↑ (IL-4, IL-5, IL-10, IL-13, IFN-γ, TNFα)	-	[72]
C	14	300	-	Mice (ICR –m)	OVA (Int T)	Int T	1.61 mg/kg x6	-	-	-	-	-	↑	↑	↑ (CD86, CD80, MHC II, DEC205, CD19)	-	[39]
C	56	45	-	Mice (ICR –m)	OVA (Int T)	Int T	1.61 mg/kg x6	-	-	-	-	-	nc	nc	nc (CD86, CD80, MHC II, DEC205, CD19)	-	[39]
C	13	-	<10 μm	Rat (BN –m)	OVA (IP)	Int T	0.5 mg/kg x3	nc (Resist)	nc	↓	nc	↑	nc	nc	nc (INFγ, IL1β, TNFα, IL4, IL5, IL13)	-	[238]
TiO_2	29	49.8	-	Mice (BALB/c –f)	OVA (Int N)	Int N	11 mg/kg	-	↑	nc	nc	nc	nc	↑	↑ (TNFα, IL4, IL5, IL10, IL13) nc(INF-γ)	-	[43]
C_{70} Fullerene	-	-	-	Mice (BALB/c)	OVA (IP)	Int N	1.1 mg/kg	↓ (Resist)	↓	↓	nc	-	nc	↓	↓ (IL4, IL5), ↑ (CYP1B1)	-	[106]
Fe_2O_3	35	39	-	Mice (BALB/c –f)	OVA (IP)	Int T	27.7 mg/kg x4	-	↓	↓	nc	↓	-	-	↓ IL4, INFγ	-	[80]
GO	D 0.6 L 0.02-2μm	-	-	Mice (BALB/c –f)	OVA (IP)	PA	2.2 mg/kg	↑ (Penh)	↓	↓	nc	nc	↑	-	↓ (IL4, IL13) nc (IL5)	↑ GCH/PAS	[65]
Latex	25	-	-	Mice (ICR –m)	OVA (Int T)	Int T	13.8 mg/kg	-	nc	nc	↑	↑	↑	↑	↑ (IL18, MIP1α, MCP1); nc (IL5, IL13)	-	[272]
Latex	50	-	-	Mice (ICR –m)	OVA (Int T)	Int T	13.8 mg/kg	-	nc	nc	↑	↑	↑	↑	↑ (IL18, MIP1α, MCP1); nc (IL5, IL13)	-	[272]
Latex	100	-	-	Mice (ICR –m)	OVA (Int T)	Int T	13.8 mg/kg	-	nc	nc	nc	nc	nc	nc	↑ (IL18, MIP1α, MCP1); nc (IL5, IL13)	-	[272]
PS (Glycine)	50	-	-	Mice (BALB/c –f)	OVA (IP)	Int T	11 mg/kg	-	-	↓	nc	↓	nc	↓	↓ (IL5, IL13)	-	[79]
PS	59	-	-	Mice (BALB/c –f)	OVA (Int N)	Int N	16 mg/kg x3	-	↑	↑	↑	↑	↑	↑	-	-	[44]
PS	59	-	-	Mice (BALB/c –m)	OVA (Int N)	Int N	16 mg/kg x3	-	↑	↑	↑	↑	↑	↑	-	-	[44]

Table 1 Effect of nanomaterials on development of allergic airway disease *in vivo (Continued)*

Nanomaterial Properties				Model Characteristics				Disease Related Endpoints									
Material (coating)	*Size (nm)*	*Surface area (m^2/g)*	*Agg Size: nm*	*Species (Strain - Gender)*	*Allergen (Route)*	*Particle (Route)*	*Dose*	*AHR (LF test)*	*IgE*	*Eos*	*Neu*	*Lym*	*MΦ*	*Total Cells*	*Pathophysiological Indicators*	*GCH-MS*	*Reference*
PS (Glycine)	45-49	-	-	Mice (BALB/c)	OVA (Int T)	Int T	11 mg/kg x2	nc	↓	↓	nc	nc	nc	↓	↓ (IL-4, IL-5, IL-13), nc (IFN-γ)	↓ PAS	[78]
SiO_2	7	300	-	Mice (C57BL/6-f)	OVA (Inh)	PA	2.7 mg/kg	-	nc	-	-	-	-	-	↑(HO1); nc(TNFα,,IL1β, Cxcl2, Ccl2)	-	[55]
SiO_2	34	80	-	Mice (C57BL/6-f)	OVA (Inh)	PA	2.7 mg/kg	-	nc	-	-	-	-	-	↑(HO1); nc(TNFα,,IL1β, Cxcl2, Ccl2)	-	[55]
TiO_2 ($Al(OH)_3$)	30-50	37.1	-	Mice (C57BL/6-f)	OVA (Inh)	PA	2.7 mg/kg	-	nc	-	-	-	-	-	nc (HO1, TNFα, IL1β, Cxcl2, Ccl2)	-	[55]
ZnO	21	49.6	-	Mice (C57BL/6-f)	OVA (Inh)	PA	2.7 mg/kg	-	↑	-	-	-	-	-	nc (HO1, TNFα, IL1β, Cxcl2, Ccl2)	-	[55]
ZnO (SiO_2)	25	-	-	Mice (C57BL/6-f)	OVA (Inh)	PA	2.7 mg/kg	-	↑	-	-	-	-	-	-	-	[55]
SiO_2	10-20	140-180	-	Rat (Wistar –m)	OVA (IP)	Int T	1.6 mg/kg x30	↑ (Resist)	-	↓	-	-	-	-	↑ (IL-4), nc (INF-γ)	-	[46]
SiO_2 (PEG)	90	-	-	Mice (BALB/c –f)	OVA (Int N)	Int N	22.2 mg/Kg x4	-	↑	↑	↑	↑	nc	↑	↑ (IL-6, IL-5, IL-1β, IL-4, TNF-α, INF-γ	↑ PAS, MUC5AC	[47]
SiO_2	100	12.7	119.6	Mice (BALB/c –f)	OVA (Int N)	Int N	10 mg/kg x6	↑ (Resist)	-	↑	↑	↑	nc	↑	↑ (IL-5, IL-13, IL-1β, INF-γ	nc PAS	[48]
SiO_2 (Meso)	100	70.6	100.5	Mice (BALB/c –f)	OVA (Int N)	Int N	10 mg/kg x6	↑ (Resist)	-	↑	↑	↑	↑	↑	↑ (IL-1β, INF-γ) nc (IL-5, IL-13)	↑ PAS	[48]
SiO_2 (PEG)	100	12.7	439.1	Mice (BALB/c –f)	OVA (Int N)	Int N	10 mg/kg x6	nc (Resist)	-	nc	nc	nc	nc	nc	↑ (INF-γ) nc (IL-1β, IL-5, IL-13)	nc PAS	[48]
TiO_2	21	-	1.5 μm	Mice (BALB/c –f)	OVA (IP)	A (Nose only)	193μg, deposited	nc (resist)	↓	↓	nc	↓	nc	↓	↓ (IL-5, IL-6, INF-γ, IL-13, IL-4)	-	[120]
TiO_2 (SiO_2)	10x40	132	100	Mice (BALB/c –f)	OVA (IP)	A	10mg/m^3 2h/d x12d	↓ (Penh)	nc	↓	nc	↓	↓	-	↓ (IL-1β, TNF-α, IL-4, IL-13, IL-10)	↓ PAS	[81]
TiO_2	4-8	130	244	Mice (BALB/c)	OVA (IP)	Int N	11 mg/kg	↑ (Resist)	↑	-	-	-	-	-	nc (IL-5) ↑ (IL-4, IL-13,JL-6, TNFa)	-	[273]
ZnO	50	10.8	-	Mice (Balb/c –f)	OVA (OA)	OA	0.5 mg/kg x2	-	nc	↑	-	-	-	↑	↑ (IL-4, IL-5, IL-6, IL-13)	-	[56]
CNF	D-35, L-10μm	103	-	Mice (BALB/c –f)	OVA (IP)	Int N	7.4mg/kg x3	-	↑	nc	nc	nc	nc	nc	nc (MCP-1, TNF-α)	-	[54]
CNF	D- 36, L-5μm	124	-	Mice (BALB/c –f)	OVA (IP)	Int N	7.4mg/kg x3	-	↑	nc	↑	nc	↑	↑	nc (MCP-1, TNF-α)	-	[54]
CNF	D-70, L-5μm	56	-	Mice (BALB/c –f)	OVA (IP)	Int N	7.4mg/kg x3	-	↑	nc	nc	nc	nc	nc	nc (MCP-1, TNF-α)	-	[54]
CNF	D- 83, L-10μm	61	-	Mice (BALB/c –f)	OVA (IP)	Int N	7.4mg/kg x3	-	↑	nc	↑	nc	nc	↑	nc (MCP-1, TNF-α)	-	[54]
SWCNT	D- 1.1, L-100μm	543	-	Mice (BALB/c –f)	OVA (IP)	Int N	7.4mg/kg x3	-	↑	↑	↑	↑	↑	↑	nc (MCP-1, TNF-α)	-	[54]
MWCNT	D20-30, L-200μm	140	-	Mice (BALB/c –f)	OVA (IP)	Int N	7.4mg/kg x3	-	↑	↑	↑	nc	↑	↑	nc (MCP-1, TNF-α)	-	[54]
C (PrinteX 90)	14	300		Mice (BALB/c –f)	OVA (IP)	Int N	7.4mg/kg x3	-	↑	↑	↑	↑	↑	↑	↑(MCP-1), nc (TNF-α)	-	[54]
SWCNT	D 1.2-2, L 1-15μm	-	-	Mice (ICR –m)	OVA (Int T)	Int T	1.3 mg/kg x7	-	↑	↑	↑	↑	↑	↑	↑ (IL4, IL33, IL5, IL13, INFγ, IL17)	↑ MUC5AC	[52]
SWCNT	D 0.8-1.2, L 0.1-1μm	-	-	Mice (ICR –m)	OVA (Int T)	Int T	1.3 mg/kg x7	-	↑	↑	↑	↑	nc	↑	↑ (IL5, IL13)	↑ MUC5AC	[52]

Table 1 Effect of nanomaterials on development of allergic airway disease *in vivo (Continued)*

Nanomaterial Properties				Model Characteristics				Disease Related Endpoints									
Material (coating)	*Size (nm)*	*Surface area (m^2/g)*	*Agg Size: nm*	*Species (Strain - Gender)*	*Allergen (Route)*	*Particle (Route)*	*Dose*	*AHR (LF test)*	*IgE*	*Eos*	*Neu*	*Lym*	*MΦ*	*Total Cells*	*Pathophysiological Indicators*	*GCH-MS*	*Reference*
MWCNT	D ~15 nm, L 1-10μm	-	-	Mice (BALB/c –m)	OVA (Int N)	Int N	1mg/kg	↑ (sRaw)	↑	↑	↑	↑	↑	↑	↑ (IL-4, IL-5, IL-13, IL-17)	-	[50]
SWCNT	D 0.93-1.63	-	-	Rat (Wistar –m)	OVA (Int T)	Int T	2 mg/kg x13	↑ (Resist)	↑	↑	↑	↑	-	↑	↑ (IL4, ROS) ↓(INFγ)	↑ PAS	[53]
MWCNT	D ~15 nm, L 1-10μm	-	~350 μm	Mice (BALB/c –m)	HDM (Int N)	Int N	12.5mg/kg x10	-	-	↑	↑	↑	↑	↑	↑ IL-13, TGF-β1, IL-33, TSLP, IL-25	↑ mucin	[51]
MWCNT	D 67, L 0.1-10μm	26	-	Mice (ICR –m)	OVA (Int I)	Int T	4.6 mg/kg x6	-	↑	↑	↑	↑	nc	↑	↑ (IL-4, INF-γ, IL-33, IL-1β, TARC, MCP-1)	↑ PAS	[49]
MWCNT	D 2–20, L 0.1-10μm	-	-	Mice (ICR –m)	OVA (Int I)	Int T	4.6 mg/kg x6	-	↑	↑	↑	↑	nc	↑	↑ (IL-4, INF-γ, IL-33, MCP-1, IL-1β);	-	[49]
SiO_2	33	-	-	Mice (BALB/c –f)	OVA (Int N)	Int N	13.8 mg/kg x3	-	↑	-	-	-	-	-	↑ (IL-4, IL-5)	-	[45]
SiO_2	79	-	-	Mice (BALB/c –f)	OVA (Int N)	Int N	13.8 mg/kg x3	-	nc	-	-	-	-	-	nc (IL-4, IL-5)	-	[45]

Abbreviations: *Agg* agglomerate, *AHR* airway hyperresponsiveness, *LF* lung function, *Resist* Resistance, *Penh* Enhanced pause, *Eos* eosinophils, *Neu* neutrophils, *Lym* lymphocytes, MΦ macrophages, *GCH-MS* goblet cell hyperplasia-mucus secretion, *–m* –male, *OVA* ovalbumin, *Int T* intratracheal instillation, ↑ increase, *nc* no change, – not determined, *–f* –female, *PA* pharyngeal aspiration, *Int N* intranasal instillation, *PAS* Periodic acid–Schiff staining, *BN* Brown Norway, *IP* intraperitoneal injection, ↓ decrease, *PS* polystyrene, *Inh* inhalation, *PEG* Polyethylene glycol, *Meso* mesoporous, *OA* oropharyngeal aspiration, *A* aerosol, *D* diameter; *L* length; *CNF* carbon nanofiber, *SWCNT* single-walled carbon nanotubes, *MWCNT* multi-walled carbon nanotubes, *HDM* house dust mite

Nanomaterial effects on established allergic airway disease

Modification of pre-existing asthma involves alterations to airway function and inflammatory status. In this section we will summarise current information on how nanomaterials can modify established allergic airway disease *in vivo* (Table 2).

Early investigations into CNPs and their ability to modify pre-existing ragweed pollen induced AAI in the beagle dog, apart from a mild neutrophilic response, did not show any major effects on airway reactivity or immune activation [58]. More recent studies demonstrated a neutrophilic response when CNPs were administered in mouse models of OVA induced inflammatory disease [59, 60]. In addition, earlier studies from these same authors revealed exacerbation effects of CNPs on AHR, eosinophils, lymphocytes, IL-13 and mucus hypersecretion, which was more severe when CNPs were administered just before, rather than after allergen challenge [61, 62]. Gold NPs (AuNPs) and TiO_2NPs have been examined using a model of occupational asthma, where exposure of toluene diisocyanate sensitised mice to either NP resulted in an increase in AAD with AuNPs showing greater effects [63]. The doses used in this study were comparably lower than the majority of other similar *in vivo* studies and aimed to reproduce occupational exposure levels.

Copper oxide NPs (CuONPs) displayed noted potency for their ability to exacerbate AHR, mucus hypersecretion and allergic inflammatory markers including IgE, IL-5 and IL-13 in murine OVA induced AAD, with dose dependent effects observed from 25 to 100μg/kg [64]. Graphene oxide (GO) is another NP examined for exacerbation effects in an allergic airway model of exposure. Repeat administration at the challenge phase of the protocol did not significantly modulate allergic endpoints but did cause significant neutrophilia [65]. Dose dependent increases in inflammatory cell infiltrates including macrophages and eosinophils were induced by SiO_2NPs and accompanied by increased Th2 type inflammation and mucin hypersecretion [66].

Interestingly, the effects of MWCNTs in their ability to aggravate pre-existing AAD appear modest. Ryman-Rasmussen and colleagues demonstrated no effect on inflammatory cell infiltration at either 1 or 14 days post challenge exposure. There was however a modest increase in IL-5 which was suggested as a potential contributor to fibrotic events observed only with MWCNTs and OVA treatment at day 14 [67]. This lack of modifying effect was also observed in a rat model of trimellitic anhydride induced allergy [68] and a murine OVA allergy model [69] while inhibitory effects were observed for eosinophil and macrophage infiltration in another study [70]. Moderate exacerbation responses were also observed in a HDM model of AAI [71].

Mechanistic insight into how nanomaterials may influence asthma

An understanding of how NMs with defined characteristics influence models of asthma and AAD has the potential to identify characteristics or material types that can be linked to molecular and cellular events critical for disease initiation and exacerbation in humans. This information can be used to identify NM "properties of concern" but importantly can also be used to improve choices surrounding relevant endpoints of disease, model selection, testing approaches and prediction strategies towards a more complete assessment of NM hazard. In this part of the review we will document those studies, which have explored key mechanistic events in models of asthma and AAD suggested as underpinning NM adverse effects. This will include discussion of not just *in vivo* approaches but those attempts at modelling key events *in vitro* (Additional file 1: Table S3).

Direct effects on sensitisation in allergic airway disease

The development of an adaptive immune response to an allergen is central to those with AAD. This process typically involves dendritic cells, which take up antigen, become activated, mature and travel to lymph nodes where they present these antigens to T and B cells to direct their differentiation to specific functional phenotypes.

The influence of NMs on this process has been examined *in vivo* and *in vitro*, with initial studies focussing on the role of the dendritic cell and T-cell interaction. Using adoptively transferred DO11.10 CD4+ T-cells in mice, which respond specifically to OVA peptides presented from antigen presenting cells, CNPs when administered to the lung in combination with OVA induced a proliferative response [72]. This T-cell response indicates increased dendritic cell (DC) antigen presentation. The number of myeloid dendritic cells (DCs) as well as the expression of DC maturation markers CD80 and CD86 in the peribronchial lymph nodes of these mice were also increased. Knockout (KO) mice deficient for these dendritic cell costimulatory molecules failed to produce the adjuvant effects of CNPs on AAI. A direct maturation effect of CNPs on dendritic cells *in vitro* was also demonstrated, altogether providing strong evidence that the sensitising effects of CNPs in AAD in this KO model arise from direct effects on dendritic cell maturation [72]. A size dependent accumulation of antigen presenting cells induced by CNPs in the mouse lung has also been observed, where 14nm but not 56nm sized particles increased the number of cells positive for CD80, CD86 and MHC class II [39]. Moreover, this size dependency was observed *in vitro* through the ability of 14nm but not 56nm CNPs to

Table 2 Effect of nanomaterials on experimental *in vivo* models of established allergic airway disease

Nanomaterial Properties				Model Characteristics				Disease Related Endpoints									
Material (coating)	*Size (nm)*	*Surface area (m^2/g)*	*Agg size (nm)*	*Species (Strain - Gender)*	*Allergen (Route)*	*Particle (Route)*	*Dose*	*AHR (LF test)*	*IgE*	*Eos*	*Neu*	*Lym*	*MΦ*	*Total Cells*	*Pathophysiological Indicators*	*GCH-MS*	*Reference*
Ag	6	0.11	-	Mice (BALBc –f)	OVA (IP)	A	40mg/kg x5d	↓ (Penh)	-	↓	nc	-	nc	↓	↓ (IL-4 IL-5, IL-13, VEGF)	↓ MUC5AC	[112]
Ag	6	-	-	Mice (C57BL/6 –f)	OVA (IP)	A	40mg/kg x5d	↓ (Penh)	-	↓	nc	↓	nc	↓	↓ (IL-4 IL-5, IL-13, NFkB)	-	[111]
Ag	33	-	-	Mice (BALB/c –f)	OVA (IP)	A	3.3mg/m^3 x6h/d x7d	-	↑	-	-	-	-	-	-	-	[274]
Ag	33	0.016	-	Mice (BALB/c –f)	OVA (Int N)	A	3.3mg/m^3 x6h x7d	nc (Penh)	nc	nc	nc	nc	nc	nc	nc (IL-13) -	-	[116]
Au	40	-	-	Mice (BALB/c –m)	TDI (dermal)	OA	0.8 mg/kg	↑ (Resist)	nc	nc	↑	-	↑	↑	↓ (TNF-α, IL-6) nc (MIP-2, MCP-1)	-	[63]
Au	6.3	-	-	Mice (A/J –m)	OVA (IP)	Int N	60μg/Kg x2	↓ (Resist)	-	↓	-	-	-	-	↓ (IL-4, IL-13, CCL11, CCL24)	↓ PAS	[117]
Au	6.3	-	-	Mice (Swiss Webster –m)	OVA (IP)	Int N	60μg/Kg x2	-	-	↓	↓	-	↓	↓	↓ (Il-5, Il-1β, IL-6, ROS)	-	[117]
TiO_2	22	-	272	Mice (BALB/c –m)	TDI (dermal)	OA	0.8 mg/kg	nc (Resist)	nc	nc	↑	-	↑	↑	nc (TNF-α, IL-6, MIP-2, MCP-1)	-	[63]
CuO	46.67	-	375.8	Mice 0(BALB/c –f)	OVA (IP)	Int N	100μg/kg x3	↑ (Penh)	↑	↑	↑	↑	↑	↑	↑ (ROS, IL-5, IL-6, TNF-α, IL-13, IL-4	↑ MUC5AC	[64]
C	20	442	344-5720	Mice (C57BL/6 –f)	OVA (IP)	PA	10mg/kg	-	-	-	↑	-	nc	↑	-	-	[60]
C	34.8	-	-	Mice (BALB/c)	OVA (A)	A	526μg/m^3 x24h	↑ (Penh)	-	↑	-	↑	↑	-	↑(IL-13), ↓(IL-5), nc (IL-4)	↑ PAS	[61]
C	53.2	-	-	Mice (BALB/c –f)	OVA (IP)	A	504μg/m3 (24h)	↑ (Penh)	-	↑	-	↑	nc	↑	↑ (IL-5, IL-13)	-	[110]
C	35.2	-	-	Dog (Beagle)	Ragweed (IP)	A	232.3μg/m^3	nc (Resist)	nc	nc	↑	nc	nc	nc	-	-	[58]
C	7	-	-	Mice (BALB/c –f)	OVA (IP)	A	507μg/m^3 x24h	-	-	nc	↑*	-	nc	-	↑ (LTB_4, PGE_2), nc (8-isoprostane)	-	[59]
C	7	-	-	Mice (BALB/c)	OVA (IP)	A	507μg/m^3 x24h	-	-	-	-	-	-	-	↑ (TNF-α), nc (CC16)	↑ PAS	[62]
α-Fe_2O_3	30	28.98	950-2000	Mice (BALB/c –f)	OVA (IP)	Int T	5mg/kg	-	nc	↓	nc	↓	↓	↓	nc (TNF-α, Il-1β, IL6)	-	[275]
FeO_2	43	41.95	200	Mice (BALB/c –m)	OVA (IP)	Int T	1.1mg/kg x3	-	-	-	-	↑	-	↑	↑ (IFN-γ), nc (IL-4)	-	[93]
GO	D 0.61, L 0.02-2μm	-	-	Mice (BALB/c –f)	OVA (IP)	PA	2.2mg/kg x4	nc (Penh)	nc	nc	↑	↓	nc	-	nc (IL-4, IL-5, IL-13)	-	[65]
SiO_2	14	-	-	Mice (BALB/c –f)	OVA (IP)	Int T	2.7mg/kg	nc (Resist)	-	↑	↑	↑	↓	-	↑ (IL-13, MCP-1, MIP-1, Tarc); nc (IL-4, INF-γ, TNF-α, KC)	↑ MUC5AC PAS	[66]
SiO_2 (PEG)	14	-	-	Mice (BALB/c –f)	OVA (IP)	Int T	2.7mg/kg	↑ (Resist)	-	↑	↑	↑	↓	-	↑ (IL-4, IL-13, MCP-1, MIP-1, Tarc, KC), nc (INF-γ, TNF-α)	↑ MUC5AC PAS	[66]
SiO_2 (PO_4)	14	-	-	Mice (BALB/c –f)	OVA (IP)	Int T	2.7mg/kg	nc (Resist)	-	nc	nc	nc	nc	-	↑ (MIP-1); nc (IL-13, IL-4, INF-γ, TNF-α, MCP-1, Tarc, KC)	nc MUC5AC PAS	[66]

Table 2 Effect of nanomaterials on experimental *in vivo* models of established allergic airway disease *(Continued)*

Nanomaterial Properties				Model Characteristics				Disease Related Endpoints									
Material (coating)	*Size (nm)*	*Surface area (m^2/g)*	*Agg size (nm)*	*Species (Strain - Gender)*	*Allergen (Route)*	*Particle (Route)*	*Dose*	*AHR (LF test)*	*IgE*	*Eos*	*Neu*	*Lym*	*MΦ*	*Total Cells*	*Pathophysiological Indicators*	*GCH-MS*	*Reference*
SiO_2 (Amino)	15	-	-	Mice (BALB/c –f)	OVA (IP)	Int T	2.7mg/kg	nc (Resist)	-	nc	nc	nc	↑	-	↑ (IL-13, IL-4); ↓ (Tarc); nc (INF-γ, TNFα, MCP1, KC)	nc MUC5AC PAS	[66]
SiO_2	100	12.7	-	Mice (BALB/c –f)	OVA (IP)	Int N	11 mg/kg x3	nc (Resist)	nc	nc	nc	nc	↑	↑	nc (IL-5, IL-13, IL-1β, INF-γ)	nc PAS	[276]
SiO_2 (Meso)	100	70.6		Mice (BALB/c –f)	OVA (IP)	Int N	11 mg/kg x3	nc (Resist)	nc	nc	nc	nc	↑	nc	nc (IL-5, IL-13, IL-1β, INF-γ)	nc PAS	[276]
SiO_2 (PEG)	100	12.7	-	Mice (BALB/c –f)	OVA (IP)	Int N	11 mg/kg x3	nc (Resist)	nc	nc	nc	nc	nc	nc	nc (IL-5, IL-13, IL-1β, INF-γ)	nc PAS	[276]
TiO_2	5	-	168	Rat (BN –m)	OVA (IP)	A	9.4mg/m^3 x6h	-	-	↓	nc	↓	↓	↓	↓ (MCP-1, IL-4, IL-6, INF-γ)	↓ PAS	[118]
TiO_2	21	-	4200	Rat (BN –m)	OVA (In)	A	159 μg, deposited	nc (Resist)	nc	↓	nc	nc	nc	↓	-	-	[119]
TiO_2	21	-	4200	Rat (DA-m)	OVA (In)	A	168 μg, deposited	nc (Resist)	nc	↓	↑	↑	nc	nc	-	-	[119]
TiO_2	21	-	1.5 μm	Mice (BALB/c –f)	OVA (IP)	A	193 μg, deposited	↓ (Resist)	nc	↓	↑	↓	nc	↓	↓ (IL-4, IL-13, IL-5,IL-6, INF-γ)	-	[120]
TiO_2	21	-	1.5 μm	Mice (BALB/c –f)	OVA (IP)	A	32 μg, deposited	↑ (Resist)	-	↑	↑	↑	↑	↑	nc (IL-4, IL-13, IL-5,IL-6, INF-γ)	-	[120]
TiO_2	4-8	130	244	Mice (BALB/c)	OVA (IP)	Int N	5.5 mg/kg x4	nc (Resist)	-	-	-	-	-	-	-	-	[273]
MWCNT	D – 9.5, L–1.5μm	250-300	-	Rats (BN –f)	TMA (dermal)	A	22mg/m3 x5h x7d	-	nc	nc	nc	↓	nc	nc	-	-	[68]
MWCNT	D - 20–30, L-5-10μm	-	324	Mice (C57BL/6)	HDM (Int N)	O	2 mg/kg	-	nc	nc	↑	nc	↓	↑	nc (IL-1β, IL-13, IL-4, IL-5 CCL20) ↑(CCL2, CXCL1/2)	-	[71]
MWCNT	D 30–50 L 0.3-50μm	109.29	>2 μm	Mice (C57BL/6J)	OVA (IP)	OA	4mg/kg	-	nc	↓*	nc	nc	↓	-	nc (IL-13, IL-5,, IL-17α) ↓(TGF-β1)	nc PAS	[70]
MWCNT	D 30–50 L 0.3-50μm	109.29	-	Mice (C57BL/6 –)	OVA (IP)	A	100mg/m^3	-	-	nc	nc	nc	nc	-	nc (IL-13) ↑ (IL-5, TGF-β1)	-	[67]
MWCNT	D 10–30 L 0.3-56μm	-	-	Mice (WT –m)	OVA (IP)	OA	4mg/kg	-	-	nc	nc	nc	nc	nc	nc (IL-13, IL-1β, TGF-β1, TNF –α, IL-10)	nc PAS	[69]

Abbreviations: *Agg* agglomerate, *AHR* airway hyperresponsiveness, *LF* lung function, *Resist* Resistance, *Penh* Enhanced pause, *Eos* eosinophils, *Neu* neutrophils, *Lym* lymphocytes, MΦ macrophages, *GCH-MS* goblet cell hyperplasia-mucus secretion, *–f* –female, *OVA* ovalbumin, *IP* intraperitoneal injection, *A* aerosol, ↓ decrease, *nc* no change, ↑ increase, – not determined, *–m* –male, *Int N* intranasal instillation, *PA* pharyngeal aspiration, *PAS* Periodic acid–Schiff staining, *TDI* toluene diisocyanate, *OA* oropharyngeal aspiration, *Int T* intratracheal instillation, *PEG* Polyethylene glycol, *Meso* mesoporous, *BN* Brown Norway, *DA* Dark Agouti, *MWCNT* multi-walled carbon nanotubes, *D* diameter; *L* length, *TMA* trimellitic anhydride, *HDM* house dust mite

enhance T-cell proliferation in an allogeneic mixed lymphocyte reaction assay [73]. Direct effects of CNPs on T-cell differentiation have also been documented. Splenic leukocytes from DO11.10 transgenic mice were incubated with ovalbumin and two different sizes of CNPs (22nm and 39nm) were examined and shown to have little effect on OVA induced T-cell proliferation. However, the smaller CNPs induced the expression of Th2 cytokines including IL-4 and IL-13 to a greater extent than the larger [74]. Interestingly, cell free BAL from CNPs instilled mice can induce the maturation of bone marrow derived dendritic cells (CCR7 expression) pointing towards soluble factors released within the lung as also having a role in directing the sensitisation process [41].

In addition to CNPs other types of nanomaterials have been investigated for their ability to modify dendritic and T-cell responses. Chen and colleagues demonstrated that PEGylated SiO_2NPs have direct effects on T-cell differentiation signals (IL-2 and IFNγ), but this was only observed for CD8+, not CD4+ T-cells [75]. The ability of SiO_2NPs to enhance cross-presentation of dendritic cell antigens to CD8+ T-cells has also been observed [76]. Both these studies demonstrate size dependent effects and while no direct effects on allergy related CD4+ T cell differentiation were observed, it is further evidence that NPs can influence the adaptive immune response.

Studies on the mechanisms through which adjuvant activity of NPs may occur have focussed not only on how cellular behaviour and differentiation can be altered but also on what molecular interactions drive such responses. Early insight stemmed from initial observations that CNPs enhanced AAD, and that this correlated with the level of cellular oxidative damage in lung tissue [37]. This oxidative injury has also been observed with SWCNTs as increased lipid peroxidation and 8-hydroxy-2′-deoxyguanosine staining within the lung [52]. These changes were paralleled by an increase in the maturation of bone marrow derived dendritic cells and antigen-specific syngeneic T-cell-stimulating capacity *in vitro*. However, it was not determined which cell type accounted for oxidative injury or what characteristic of the SWCNTs may be responsible for these changes [52]. A role for oxidative injury in SWCNTs mediated worsening of AAD development and adjuvant activity was also suggested from the observations that vitamin E co-administration attenuated oxidation biomarkers and the detrimental effects of the NP [53]. Again however, there was no suggestion as to the precise cellular and molecular events underlying these observations.

Oxidative surface chemistry and increases in reactive oxidant species (ROS) within living systems are not necessarily directly related but have been put forward to explain differential dendritic cell maturation and T-cell responses. Human primary monocyte derived dendritic cells were exposed to either TiO_2NPs or cerium dioxide NPs (CeO_2NPs) identified as having oxidative and reductive surface chemistry respectively. TiO_2NPs induced cellular injury was accompanied by DC maturation and increased expression of CD83, CD80, CD86 and CCR7 together with the induction of IL-12 and TNF-α. CeO_2NPs on the other hand did not result in any significant changes in cellular viability or maturation markers, but did produce IL-10 and IL-6. T-cell responses to these NP treated dendritic cells (DCs) were also examined, with TiO_2NPs inducing a profile of Th1 cytokine production (IL-2, IFN-y) and CeO_2NPs inducing a Th2 response (IL-4, IL-5, IL-10). The authors suggest that the oxidative capacity of TiO_2NPs was responsible for increased ROS mediated inflammasome activation (IL-1β), DC maturation and differentiation of T-cells towards a Th1 profile. They also suggest, in contrast that the CeO_2NPs, which induced anti-inflammatory IL-10 and Th2 biased responses, could be attributed to the anti-oxidant surface chemistry of this NP [77]. While this is an interesting set of observations, it cannot be ruled out that surface chemistry independent effects played a role.

The effects of PSNPs on AAD have also been attributed to alterations in DC function. These NPs (PS50G; glycine coated 50nm size) when administered 12 days before sensitisation to OVA resulted in an inhibition of AAI, mucus hypersecretion, allergen specific IgE levels and Th2 cytokines in the lung draining lymph nodes [78], effects not observed with larger sub-micron sized particles of the same material [79]. This inhibition was not attributed to effects on sensitisation but rather DC function at the challenge phase, explained by a reduction in the numbers of allergen-containing $CD11b^{hi}MHCII^{hi}$ DCs in the lung and $CD11c^{+}MHCII^{hi}$ DCs in the lung and draining lymph nodes. An additional mechanism was suggested as PS50G abolished the ability of $CD11b^{+}$ DCs to induce OVA specific CD4+ T-cell proliferation [78]. Further investigation into these effects demonstrated that PS50G induced DC recruitment and maturation through cytokine induction in the lung but with a reduced number of stimulatory DCs translocating to the lymph node [79]. Interestingly the authors have suggested that given the timescale of NP administration 12 days before the start of sensitisation, DC refractoriness as a consequence of activation in the absence of OVA may account for the inability to mount an adaptive immune response at the challenge phase [78]. Furthermore, it was speculated that evolutionary conserved responses to viral sized particles, which would aim to limit inflammatory reactions not focussed on anti-viral immunity (e.g. Th1 T-cell activation) such as Th2 type adaptive immune responses, may be activated by the nanoscale properties of NPs and contribute to the inhibitory effects. This can be supported by observations that PS50G did not result in inhibition of allergen specific

lymph node production of IFNγ or have any effect on Th1 anti-viral immunity in an acute lung influenza virus infection model [78].

The inhibitory effects of PS50G on AAI also did not extend to inhibition of AHR [78]. This disparity between NP effects on allergic inflammation and AHR has been observed for other types of NPs. Graphene oxide (GO) augments AHR, goblet cell hyperplasia and smooth muscle hypertrophy in OVA induced allergic airway disease while at the same time inhibiting Th2 cytokine production, eosinophilia and IgE levels [65]. The mechanism put forward to explain this suggested that increased macrophages within the lung and their production of chitinases such as CHI3L1 contributes to airway remodelling/hyperresponsiveness and favours the development of Th1 over Th2 type responses. These observations were supported by increased levels of OVA specific IgG2a [65]. Inhibition of adjuvant activity and AAI has been observed for other nanomaterials, including Fe_2O_3 [80] and SiO_2 coated TiO_2 [81] where they were found to have size and dose dependent effects. While the authors speculate that the mechanism through which this inhibition occurred involved dendritic cell modification, modulation of the balance of Th1/Th2 T-cell responses and direct effects on regulatory T-cells, no supporting evidence was offered.

Aluminium salts, the most commonly used adjuvant in humans, have been well characterised for their ability to promote the development of adaptive immunity to co-administered allergens, such as OVA, producing a predominant Th2 type immune response [82]. The classic understanding of how these adjuvants have their effects has been described in terms of their ability to aggregate antigens, stabilise protein structure, prevent degradation and to provide a pool of material for continuous release to antigen presenting cells [83]. However, recent work has suggested that other mechanisms are involved as a likely consequence of direct cellular injury, including the activation of innate immune responses and the recruitment of inflammatory cells. Activation of the NLRP3 inflammasome as a consequence of particulate lysosomal overload in resident phagocytes (including macrophages and dendritic cells), uric acid release and subsequent caspase-1 activation and release of inflammatory cytokines, such as IL-1β, IL-18 and IL-33, have also been suggested as important events underlying adjuvant activity [84, 85].

Given the particulate nature of NPs it is perhaps unsurprising that these same mechanisms have been suggested to underlie NP modifying effects on adjuvancy [86]. Particular attention has been given to the potential role of the NLRP3 inflammasome, with nanomaterials including AgNPs, TiO_2NPs, SiO_2NPs and CNTs all inducing markers of this pathway's activation [87–89]. Using gene KO approaches, a direct role for the NLRP3 inflammasome in mediating the IL-1β response to TiO_2NPs in macrophages and dendritic cells has been demonstrated. IL-1α but not NLRP3 however, was identified as a major control point for neutrophilic responses after instillation in murine lung [90]. Nano sized particulate forms of TiO_2 and SiO_2 were observed to have a greater impact than submicron sized particles of the same material on the maturation of bone marrow derived dendritic cells. Using KO mice, IL-1β responses to these NPs in dendritic cells were found to be NLRP3 and caspase-1 dependent [91]. Mechanistic insight into how NPs may preferentially activate the inflammasome to induce release of IL-1β and IL-18 in dendritic cells stemmed from observations that production of these mediators was greater with 30nm SiO_2NPs than larger nano or sub-micron sized particles. The authors went on to demonstrate size dependent effects on cellular uptake, ATP release and ROS production and through interventional studies suggest a sequential mechanism involving NP uptake, lysosomal injury, ATP mediated activation of purinergic receptors and NADPH oxidase dependent production of ROS as a terminal signalling event for inflammasome activation [92].

Other mechanisms of NP effects on the adaptive immune system include examples where exosomes were induced in the alveolar region after inhalation of magnetic iron NPs. These exosomes incorporate antigen for systemic delivery to antigen presenting cells such as dendritic cells and modulate T-cell differentiation towards a Th1 T-cell phenotype [93]. While Th2 and Th17 immune responses are more commonly associated with asthma it is still of considerable interest that modulation of the immune system in this way by NPs can occur. Furthermore, it is interesting to speculate as to whether other types of material can induce exosome formation to direct other types of hypersensitivity reactions.

Th17 inflammation and the neutrophilic response are a significant component within the asthma phenotype particularly in those with severe asthma [94, 95]. Through the use of genetic KO and cell depletion models, evidence points towards a direct role for neutrophils in controlling AHR [96]. Whether NP induced neutrophilic responses contribute to AHR and modify Th17 responses is relatively unexplored. One study using the chemical compound ectoine, which preferentially reduced BAL neutrophils (with no changes in other BAL cells), suggested that the protective effects of this compound on CNPs adjuvancy (IgE, Th2 profile) may be attributed to the reduction in neutrophils [41].

Lastly, the airway epithelium has been observed to play a central role in the development of sensitisation in asthma, mainly through the ability to detect allergens and associated injury and respond by producing signals

such as TSLP, GMCSF, IL-25 and IL-33, which target dendritic cells to initiate sensitisation mechanisms [97]. Examples of how NPs can impact on this process include an *in vivo* HDM induced allergy model where the airway epithelium was proposed as the primary source for signals governing airway sensitisation in response to MWCNTs [51]. Similar suggestions have been made for IL-33 production in the murine lung by MWCNTs in an OVA induced AAD model [49]. 16HBE14o- airway epithelial cell exposure to CNPs and TiO_2 NPs resulted in an increase in GMCSF, which was suggested as a consequence of either NP intrinsic capability or cellular induction of oxidative stress depending on the material type, and that this effect was size, surface area and cellular internalisation dependent [98]. SiO_2NPs have also been observed to induce GMCSF from BEAS2B airway epithelial cells [99].

Insight into the impact of nanomaterials on established allergic airway disease

With the shift to Th2 type adaptive immunity in allergy, B-cell class switching to IgE production and its subsequent release occurs. This is followed by FCERIα receptor binding in cells and tissues resulting in inflammatory responses when allergen is reencountered. In atopic individuals, allergen binding to IgE present on mast cells and basophils induces the release of pre-existing pro-inflammatory mediators such as histamine, proteases, proteoglycans and cytokines [100, 101]. This process is a central mechanism for how allergen induced asthma exacerbations manifest at a cellular level.

A number of studies have examined how NPs can impact mast cell function. TiO_2NPs have been demonstrated to induce the degranulation of RBL-2H3 mast cells with the release of histamine, in an oxidative stress and calcium flux signalling dependent manner [102]. This effect was observed without any IgE mast cell priming and suggests that these NPs may directly activate mast cells *in vivo* independent of allergen. Similar findings were observed with AgNPs where degranulation of murine bone marrow derived mast cells was also examined for effects independent of IgE. The smaller sized 20nm but not 110nm sized particles resulted in degranulation, which was found to be dependent on scavenger receptor signalling, indicating cellular uptake as important. Extracellular Ag^+ ions did not have any effect [103]. Interestingly, pulmonary instillation of CeO_2NPs induced inflammatory cell and mediator production, which was not observed in mice deficient in mast cells. This study also examined bone marrow derived mast cells and found that CeO_2NPs induced inflammatory mediator production from IgE/allergen primed cells but did not induce degranulation [104]. As observations of the effects of nano-sized materials on asthma exacerbation also include inhibitory or protective effects, it is interesting to note examples where attempts have been made to interrogate how this may occur. Fullerene derivatives have been observed to stabilise mast cells, prevent IgE dependent activation and to attenuate disease parameters in both exacerbation and sensitisation models of asthma [105, 106]. These fullerene derivatives possess inherent anti-oxidant capabilities derived from their ability to catalytically scavenge large numbers of oxygen free radicals [107] and this has been suggested as a mechanism through which they elicit their biological effects. This material has also been reported to increase production of P-450 derived cis-epoxyeicosatrienoic acids, eicosanoid metabolites in the lung, which stabilise and prevent IgE mediated mast cell degranulation [106]. SWCNTs were also observed to inhibit IgE mediated RBL2H3 degranulation. In this study the authors pointed to structural similarities to fullerene derivatives but in the absence of a demonstrated ROS scavenging capability of SWCNTs the mechanism underlying this attenuating effect is yet to be determined [108]. ZnONPs were found to inhibit OVA induced degranulation of OVA specific IgE primed RBL2H3 cells, which was not observed with larger sized ZnO particles. These effects were correlated with levels of intracellular Zn^{2+} ions, and administration of $ZnSO_4$ also produced an inhibitory effect on mast cell degranulation. ZnONPs have also been observed to inhibit both basal and IgE mediated degranulation of RBL2H3 and bone marrow derived mast cells, which was observed to a much greater extent for the 30nm rather than the 200nm sized particles. In contrast, TiO_2NPs examined in the same study, produced a modest increase in mast cell degranulation. Observations that smaller particles produced a greater increase in intracellular Zn^{2+} ions and a decrease in Ca^{2+} concentrations than larger particles was suggested as a mechanism through which degranulation was inhibited [109].

Similar to investigations of sensitisation and AAD development, oxidative and electrophilic stress has also been put forward as a molecular control point for exacerbation of pre-existing AAD. Inhalation of CNPs, for example just prior to allergen challenge *in vivo* resulted in exacerbation of allergic inflammation and AHR, which was attenuated by systemic administration of the anti-oxidant compound N-acetyl cysteine [110]. CuONPs have also been reported to increase disease associated ROS levels in a murine model of OVA induced AAI, which correlated with the degree of exacerbation [64]. NPs can have pro-oxidant functional groups, can possess redox cycling ability and may generate ROS from perturbation of cellular processes such as the mitochondria. Determining whether a NP has any or all of these characteristics will be important for attempts at classification of materials likely to contribute to asthma exacerbations in humans.

In addition to fullerene derivatives [105, 106], anti-oxidant capabilities have also been suggested as a mechanism of inhibition of OVA induced AAD by AgNPs [111]. The authors in this study did not identify cellular targets for the attenuating effects on ROS levels and disease parameters, or whether inherent anti-oxidant properties of AgNPs or the prevention of cellular events leading to ROS generation were responsible for the observed inhibitory effects. Using the same model in a follow on study the authors suggest signalling molecules including HIF-1α and RTK signalling as possible contributors [112]. In contrast, AgNPs have been observed to induce ROS in cell free [113] as well as upon interaction with cellular [114, 115] systems, and have been demonstrated to induce oxidative stress in other investigations of OVA induced murine AAD [116]. The reasons for these differential effects with AgNPs could be attributed to particle differences such as size, as well as model specific parameters including dose effects. The inhibitory effects of AuNPs on AAD have been reported in a study by Barreto and colleagues, using two different mouse strains, an effect that was associated with a decrease in ROS generation in BAL cells [117]. One similarity between these studies on AuNPs and AgNPs was that the smaller primary-sized particles (6nm) of both materials were associated with inhibitory effects, while the larger-sized was associated with exacerbation effects.

TiO_2NPs have been observed to reduce AAI in rats with pre-existing disease. Here it was argued that a direct effect on Th2 type inflammation was the mechanism through which this effect manifested. It was also suggested that the lack of inhibitory effects in other studies, could be attributable to different routes of administration (aerosol versus instillation) causing different agglomeration, deposition patterns and biological responses within the lung [118]. Inhibitory effects of TiO_2NPs on AAI were also observed in different rat strains [119]. This was paralleled by TiO_2NPs induced increases in neutrophil and lymphocyte pulmonary responses in dark agouti rats, which are predisposed to chronic inflammatory disorders, but not in Brown Norway rats, which are pre-disposed to allergic responses. [119]. In addition to these effects, another study demonstrated that a single dose of TiO_2NPs given at the challenge phase resulted in an exacerbation of AAI and AHR. Repeat dose exposure in the same model, while resulting in reduced allergic inflammatory markers and AHR, resulted in a marked neutrophilic response and body weight loss pointing towards effects associated with general health decline rather than any protective response attributable to the particles [120]. The authors also suggest that activation of the inflammasome via ROS generation may contribute to the responses observed in this study.

Surface chemistry has been proposed as an important determinant of NM effects on biological systems. Uncoated SiO_2NPs were observed to exacerbate AAD in an OVA-induced mouse model. When the NPs were coated with either amino or phosphate groups this exacerbation effect was attenuated. Macrophage activation markers were not induced by the modified particles and it was suggested that recognition and uptake of the NPs by macrophages were attenuated potentially as a result of protein corona differences in the NPs. Other mechanisms suggested for the lack of effect with coated materials include a modified ability to affect the thermodynamic characteristics of lipid monolayers, including lung surfactant and cell membranes [66].

Additional mechanisms for how NM may affect those with pre-existing AAD include the ability to enhance the presentation of allergens. The HDM allergen DERP1 when coated onto AuNPs produced stronger basophil activation from allergic patients compared to exposure to the same amount of free allergen and was correlated with protease activity of the allergen [121]. In addition to activation and degranulation of mast cells and basophils as part of exacerbation events, direct effects of NPs on neutrophil and eosinophil responses have also been investigated. Primary human peripheral blood derived neutrophil degranulation was significantly induced by TiO_2NPs and CeO_2NPs with ZnONPs producing a more modest effect. Interestingly these effects were more potent than the classical bacterial FMLP agonist [122]. A number of other studies have demonstrated activation of neutrophils by NPs, with intracellular events such as calcium signalling proposed as key in the induction of a respiratory burst and inflammatory mediator transcription and release. One such study investigated the sub-lethal impact of different NPs on HL-60 neutrophil like cells and found that AgNPs but not TiO_2NPs, ZnONPs, CNPs or MWCNTs induced increases in intracellular Ca^{2+} levels [123]. Direct activation of eosinophils was observed for ZnONPs and 20nm AgNPs but not CeO_2NPs, TiO_2NPs and 70nm AgNPs [124]. ZnONPs were also observed to have similar effects in primary human eosinophils in another study from the same group [125]. Whether such effects are relevant for modulation of exacerbation in AAD has yet to be determined.

Regulation, recruitment and control of immune and inflammatory signalling is becoming more of a focus for how NMs elicit biological responses and contribute to exacerbation of airway disease. Interventional strategies including gene KO approaches have been used to interrogate how particular inflammatory signalling events and pathways contribute to NM exacerbation effects. Using such knockout approaches, MWCNTs were shown to exacerbate OVA induced AAI through a mechanism involving cyclooxygenase 2 (PTGS2) activity, an enzyme that controls levels of prostaglandins, key regulators of immune system responses [70]. In addition, the ability of MWCNTs to cause exacerbation of AAI *in vivo* was

further enhanced through KO of the STAT1 gene [69], a transcription factor important for mediating interferon and Th1 signals, immune cell signals suggested as having protective effects in allergic asthma. Similar to effects on sensitisation, exosome formation in the alveolar region after inhalation of magnetic iron oxide (Fe_2O_3) NPs, has also been suggested as a mechanism through which regulation of Th1 T-cell responses are guided in exacerbation of AAI [93]. Lastly, MWCNTs administered to mice were found to produce a strong neutrophilic response, which was diminished in animals with pre-existing HDM induced AAI [71]. MWCNTs did not alter the level of eosinophils or other Th2 inflammatory markers but did result in a more severe airway fibrosis. Decreased IL-1β levels together with *in vitro* investigations in this study suggest that an allergic inflammatory environment inhibits inflammasome activation through a STAT6 mechanism and that this may be responsible for the exacerbated fibrotic response observed with MWCNTs exposure [71].

Mechanisms of asthma development and exacerbation independent of allergic sensitisation

Modelling of asthma using rodent allergic airway disease models as the prototypical testing paradigm does not reflect all types of asthmatic disease in humans. Mechanistic insight into how environmental exposures may influence disease is therefore, potentially overshadowed by predominant discussion of how materials affect allergic responses and Th2 type inflammation. A summary of those studies with observations independent of allergy driven disease identified within our search parameters are documented in Additional file 1: Tables S1 and S2. Those studies primarily focussed on allergen independent models are summarized in Additional file 1: Table S1, while those observations independent of allergen effects but documented as part of larger allergen driven model studies are summarized in Additional file 1: Table S2.

Some of the earliest studies to investigate the pulmonary effects of nanomaterial exposure did not specifically set out to model the potential impact on disease conditions such as asthma. However observations including neutrophil and inflammatory mediator alterations can be viewed not just in terms of broad pulmonary toxicity effects but as having the potential to influence disease initiation and progression in conditions such as asthma and AAD. One of these early studies set out to compare similar sized metallic NPs after pulmonary instillation in rats. It was demonstrated that the level of toxicity and neutrophil response was material specific with nickel (Ni) and cobalt (Co) having the greatest effects. It was suggested that the surface chemistry of these materials as expressed in terms of their ability to generate reactive oxygen species, governed specific potency [126, 127]. Other factors including NP solubility and surface area have been put forward as the most significant characteristics influencing NP toxicity after pulmonary exposure and have been reviewed extensively elsewhere [128, 129].

In a clinical setting, treatment strategies targeting Th2 type inflammation reduce allergic exacerbation rates but have little effect on baseline measures of asthma activity such as AHR [130]. These and other observations support the suggestion that asthma should be considered as a condition with a fundamental abnormality in smooth muscle function that underlies diminished lung function and AHR [130, 131]. The concept that AHR and allergic inflammation are not exclusively linked is consistent with observations in this review and has been discussed previously. Indeed, direct effects on AHR have been observed in the absence of allergic airway modelling for AgNPs, TiO_2NPs, SWCNTs and MWCNTs exposures [132–136]. While an understanding of how such effects on AHR manifest is unknown at this time, it is clear that smooth muscle cells are likely to have a central role [137]. The direct impact of nanomaterials on smooth muscle has been explored to a limited extent. TiO_2NPs instillation in mice resulted in changes in lung gene expression consistent with effects on ion homeostasis and smooth muscle contractibility [138]. *Ex vivo* examination of AgNP applied directly to rat tracheal rings found that the nanoparticles caused a non-reversible contractile response to acetylcholine [139]. It was suggested that these NPs may interact with and modify muscarinic receptors on smooth muscle and induce nitric oxide as a mechanism to directly influence contractility. Additional observations using *ex vivo* smooth muscle preparations have also revealed increased contractility on exposure to SnO_2NPs and $CoFe_2O_4$NPs [140, 141]. *In vitro* modelling of smooth muscle cells and exposure to NPs has also been attempted to a limited extent. AuNPs were observed to directly alter plasma membrane potential and intracellular calcium signalling in human airway smooth muscle cells in a charge dependent manner [142]. Intracellular calcium signalling is intimately involved in muscle contraction and suggests such direct modifications by AuNPs could impact contractility and ultimately AHR. An examination of different NP effects on human airway smooth muscle cell mechanical function after direct exposure, using optical magnetic twisting cytometry revealed material specific, dose and size dependent effects [143]. These included CuONPs, which inhibited smooth muscle cell stiffness, histamine contractility and isoproterenol relaxation, while larger micron sized CuO particles did not.

In addition to smooth muscle cells, airway remodelling and AHR in asthma are associated with peribronchial fibrosis and fibroblast expansion [144]. Nanomaterial influence on this aspect of airway disease has revealed direct

effects, including the ability of graphene oxide, NiNPs and MWCNTs to increase extracellular matrix deposition after pulmonary instillation [145–148]. This profibrotic effect within the lung has also been observed for CeO_2NPs, ZnONPs and SWCNTs [148–151]. The involvement of the innate immune system may also play a role here. An investigation into MWCNTs effects suggests that airway epithelial signals initiated by inflammasome activation induce fibroblast proliferation and pro-fibrotic gene expression [152]. IL-33 is an epithelial cell derived innate immune signal, which can influence type 2 inflammatory events. Knockout (KO) of IL-33 in mice causes an inhibition of the inflammation, peribronchial fibrosis and AHR induced by MWCNTs [153]. The STAT1 transcription factor, which is involved in intracellular inflammatory signalling, also contributes to MWCNTs induced airway profibrotic exacerbation in mice [69]. Further examination of NP effects in pre-existing allergic airway disease revealed that SWCNTs and MWCNTs also induce airway fibrosis [53, 67]. Whether allergic inflammation was necessary for these later effects was not fully investigated. Airway epithelial cells have been argued as central players not only in directing inflammation but also in the control of fibrotic signalling in response to inhaled material. In addition to fibroblast to myofibroblast transition, epithelial to mesenchymal transition (EMT) in response to MWCNTs exposure has been proposed to contribute to pulmonary fibrosis. [154]. Instillation of MWCNTs in the mouse lung also resulted in peribronchial as well as alveolar fibrosis in another study and a role for epithelial mesenchymal transition was also suggested [155]. While a significant body of work has focussed on MWCNTs, there is a distinct lack of interrogation of other types of particles for their effects on airway remodelling and fibrosis.

Airway hyper-responsiveness and excessive mucin production are the principal mechanisms contributing to airway obstruction in asthma. The airway epithelium is the primary site for mucin release and is therefore an essential focus for the examination of nanomaterial effects. A recent study investigating the effects of NPs on mucin rheology found that positively charged polystyrene nanoparticles impaired mucin gel swelling causing mucin aggregation [156]. It was suggested that NPs with these properties would impinge mucociliary clearance and contribute to adverse disease outcomes in conditions such as asthma. Studies to date have shown induction of mucus secretion accompanied by AHR independent of allergic sensitisation for CuONPs [64] and MWCNTs [134]. It is unclear how nanomaterials cause these effects. Whether it is a result of direct action on epithelial cells, secondary signalling events from inflammatory and other resident cells or a combination of all is still unknown. Some insight however has emerged from observations that cytokines including IL-13, Il-17A and IL-1β can induce mucin production from airway epithelial cells. For example, in a rat pulmonary exposure study, it could be argued that TiO_2NPs induced goblet cell hyperplasia and MUC5AC expression may be attributable to IL-13 produced from mast cells [157]. Direct effects on airway epithelial cells through ROS and calcium signalling was also suggested to control TiO_2NPs induced mucin secretion [158]. Additional signalling events that may be important in the control of mucin production include airway epithelial MAPK signalling, an observation documented for CuONPs induced MUC5AC in H292 epithelial cells [159].

Airway epithelial cells are a primary target for inhaled material deposition and a control point for the recruitment of inflammatory cells. Chemokines such as IL-8, MCP1 and CCL28 act to recruit cells including neutrophils, monocytes, lymphocytes, eosinophils and dendritic cells. Production of these mediators from airway epithelial cells has been demonstrated in response to NPs including CNPs, TiO_2NPs, MWCNTs, CeO_2NPs, SiO_2NPs, CoNPs and ZnONPs [160–167]. A greater understanding of these primary events in nanomaterial exposure and airway response is likely to lead to a more complete mechanistic understanding of the potential to contribute to asthma and airway disease.

Mast cells are an important part not only for atopic but also non-atopic asthma [168]. Exposure of mice to MWCNTs resulted in inflammatory responses and pulmonary functional changes similar to those observed in asthma, which were dependent on the presence of mast cells and their ability to respond to IL-33 [169]. Additional investigations demonstrated a role for the IL-33/ST2 axis together with IL-13 signalling in MWCNTs induced AHR and inflammatory events, which were independent of T and B cell involvement [135]. The authors suggest type 2 innate lymphoid cells (ILC2) recruited to the airways as a consequence of epithelial injury and IL-33 release as the primary events governing adverse effects. As these cells have the ability to produce type 2 cytokines such as IL-4, IL-5 and IL-13 in the absence of any adaptive immune response, they also represent an important target for how nanomaterials may impact asthma and obstructive airway disease [170]. Other innate lymphoid cells such as ILC3 cells, which produce IL-22 and IL-17, through inflammasome activation, may also be important as they have been directly implicated in the mechanisms of AHR induction in the absence of adaptive immunity [171].

It is recognised that respiratory tract viral infection, mainly from rhinovirus (RV), is associated with the majority of asthma exacerbations in children and more than half of adults [172]. The presence of Th2 type inflammation and asthma has also been associated with reduced antiviral defence in plasmacytoid dendritic cells and the

airway epithelium, indicating increased susceptibility to viral mediated exacerbations in those with allergic inflammation [173, 174]. Despite this being a primary mechanism for asthma exacerbation, only a handful of investigations have been directed towards understanding how nanomaterial exposure, including ultrafine components of air pollution, may impact respiratory viral infections relevant for asthma. This is also true for the development of asthma. One of the earliest studies that did investigate such interactions focussed on mice exposed to CNPs prior to respiratory syncytial virus (RSV) infection [175]. This virus causes lower respiratory tract infection and bronchiolitis and the severity of infection has been associated with the development of asthma. Despite alterations in the inflammatory response, including induction of Th2 markers such as IL-13, there were no significant effects of CNPs on RSV replication or viral clearance [175]. In a similar study from the same group, CNPs were administered to mice after RSV infection and despite there being no difference in viral titre and clearance, there was an increase in pulmonary inflammation with CNPs, which was correlated to an increase in AHR [176]. Similar to CNPs, TiO_2NPs when administered prior to RSV infection in mice did not alter viral titres but did exacerbate inflammation and pneumonia [177]. Gold nanorods interestingly have been observed to inhibit RSV infection levels in mice and airway epithelial cells, which correlated with the induction of antiviral gene expression and modulation of pattern recognition receptors [178]. Other nanomaterials including SWCNTs, AgNPs and polystyrene NPs have all demonstrated modifying effects on viral infectivity or inflammatory consequences of respiratory viral infection [179–181]. These later studies however did not focus on viruses typically associated with asthma.

Insight from nanomedicine approaches to vaccines and allergy

NPs intended for medical use have also been investigated for modulation of sensitisation. PVA coated superparamagnetic iron oxide nanoparticles (PVA-SPIONs) caused an inhibition of monocyte derived dendritic cells' ability to process antigen and stimulate CD4+ T cells, without affecting antigen uptake or markers of maturation. It was suggested that PVA-SPIONs induced reversion to a more immature dendritic cell phenotype involving the regulation of lysosomal function as a potential mechanism of action. PVA-SPIONs have a slightly positive charge and therefore bind proteins with an isoelectric point (pI) of > 5.5. While not tested, it was suggested that NPs may bind proteins with a higher pI involved in antigen processing, such as Cathepsin B, H, L1 and DMB, and subsequently sequester their function, as a mechanism for how they attenuate dendritic cell function [182]. The use of NMs in the development of novel vaccines has contributed significantly to our understanding of how NMs direct dendritic cell function and sensitisation to antigen. Supporting a role for particle charge in this process, a number of studies have observed that cationic NPs produce superior adjuvant responses following pulmonary delivery, when compared to anionic particles of the same material. Pulmonary immunization using OVA conjugated cationic rod shaped hydrogel NPs led to increased antibody titres, B-cell expansion and increased activation of CD4+ T-cell populations in the draining lymph nodes. These effects were not observed using anionic particles of the same material. *Ex vivo* treatment of dendritic cells with these cationic conjugated particles induced dendritic cell maturation markers and robust antigen specific T-cell proliferation, effects not observed with anionic particles or with OVA alone [183]. In a follow on study from the same group, it was demonstrated that these positively charged NPs are preferentially taken up by dendritic cells (DCs) in contrast to negatively charged NPs, and were associated with an increased expression of the chemokines Ccl2 and Cxcl10, which possibly contribute to recruitment of Th2 promoting CD11b DCs to the lung [184]. Using the same approach as the previous hydrogel studies to modify NP surface by the addition of chemical species for negative carboxyl (–COOH) and positive amino (–NH2) charge, a study examining the effect of PVA coated AuNPs found that after instillation into the lung, cationic particles were preferentially taken up by all antigen presenting cells including macrophages and DCs. This was accompanied by an increase in CD4+ T-cell OVA proliferative responses in lung draining lymph nodes, an effect not observed with the anionic NPs [185].

Interestingly, rapid translocation of NPs to the lymph nodes after pulmonary instillation, suggested as independent of cell mediated transport, in addition to being influenced by charge is highly size dependent [186]. Size dependent preferential uptake of NPs by dendritic cells and translocation to lymph nodes was accompanied by enhanced T-cell responses when compared to larger sized particles [187]. These studies have suggested an optimal NP uptake size of between 20 and 50nm for lymph node homing migratory DCs and other antigen presenting cells after pulmonary administration. In contrast, other studies have suggested roles for larger particles in adaptive immunity modulation. As part of strategic approaches to improve vaccine development, one study examined how antigen conjugated to particles in the viral size range influenced induction of adaptive immune responses. Intranasal administration of larger 200nm pluronic-stabilized poly(propylene sulphide) NPs (PSPNPs) were observed to deliver OVA antigen more efficiently into both MHC I and II presentation pathways and increase the number of poly

functional CD+ T-cells when compared to the smaller 30nm size [188]. Moreover, immunisation approaches using different size OVA conjugated PS beads administered intradermally found that larger sized beads (93nm, 101nm & 123nm) induced IL-4 release from spleen derived CD4+ T-cells *ex vivo*, while smaller sized (40nm, 49nm) induced the release of IFN-γ from CD8+ T-cells. This size dependent effect on adaptive immunity patterning was suggested to be a direct result of modification of dendritic cells [189].

Immunotherapy is an established treatment for allergies. New approaches using viral like particles (VLPs) loaded with TLR ligands such as unmethylated CpG, targeting antiviral innate immune responses have the potential for more effective treatment in the absence of side effects associated with other strategies [190]. It is proposed that the advantages of this approach stem from the nanosized structure of VLPs, allowing transport to lymph nodes where they can be taken up by resident DCs. Processing then allows endosomal TLR9 activation by unmethylated CpG and the subsequent patterning of T-cells towards a Th1 phenotype, which in turn competes and/or inhibits Th2 type allergic responses [190]. It has been suggested that improvements to the nanocarrier approach to delivering unmethylated CpG within the lung may further enhance the ability of this TLR ligand to modulate and inhibit allergy and to overcome aspects of efficacy of VLPs observed in preclinical and clinical trials. One approach involved conjugation of unmethylated CpG to the surface of PSPNPs, where intranasal administration prior to sensitisation significantly reduced AAI and IgE levels in a murine model of HDM induced disease [191]. It was suggested that surface associated, rather than encapsulated CpG (observed with VLP approaches) may allow a more robust approach to modifying adaptive immunity towards Th1 responses. This mechanism of delivery for these nanomaterial associated pathogen associated molecular patterns (PAMPs), towards antigen processing, presentation and adaptive immune response influence, is one which should be considered carefully as a significant component to allergy development and exacerbation events. Indeed, the bacterial cell component and TLR4 agonist lipopolysaccharide (LPS) is necessary for the induction of metal allergy to Ag when administered as AgNPs [192]. Ag^+ ions and metal NPs of low solubility failed to induce allergy under similar conditions. These observations again highlight the importance of nanostructure and co-exposure to pattern recognition receptor (PRR) ligands in allergy development. Interestingly, in addition to being suggested as a central mechanism for how adjuvants can enhance and direct adaptive immune responses [83, 85], PRR activation has been observed directly by NPs. TLR4 binding and activation by TiO_2NPs for example has been observed in pulmonary epithelial cells [193] and using a TLR4 KO murine inhalation model system was also demonstrated to mediate ZnONPs pulmonary inflammatory effects [194].

Ultrafine pollutant nanomaterial exposure and asthma

Air pollution is one of the greatest non communicable disease related public health concerns. An estimated 3.3 million premature deaths worldwide per year have been attributed to outdoor air pollution with the particulate fraction playing a major role [195]. Respiratory health effects are among the primary concerns, with asthma accounting for a large proportion [196]. Evidence for an association between air pollution and in particular traffic derived material, and asthma has accumulated over the last decades, with systematic reviews continuing to build a weight of evidence for direct causal effects [20, 196–199]. The precise nature of the exposure material(s) and the mechanisms underlying these associations is not complete and further understanding may allow more targeted and efficient strategies to reduce adverse health effects. The ultrafine particulate (UFP) component of pollutant exposure has been highlighted as a particular focus for investigation due to unique physicochemical properties and interactions with biological systems. It is the aim of the discussion in this section, to document evidence for the role ultrafine particulates (UFPs) may play in asthmatic disease and the potential mechanisms involved.

Human ultrafine and nanomaterial exposure effects

Most of the information on human exposure to nanoscale materials and their influence on asthma has originated from the study of pollutant ultrafine material. The majority of particles in terms of numbers within urban pollutant particulate matter (PM) are found within the UFP fraction (typically described as <100nm diameter), while most of the mass is found in particles >100nm in size [200]. One of the earliest epidemiological studies in asthmatic adults found that associations between the UFP fraction and asthma outcome, assessed using lung function parameters (Peak Expiratory Flow (PEF)), were greater than those of the fraction between 0.1-10μm (PM10) [200]. A follow on study from the same research group in an independent adult asthmatic population, found associations between cumulative (up to 14 days) exposure to both fine (<2.5μm (PM2.5)) and UFP fractions and asthma steroid medication use. It was however, difficult to separate out the effect of UFP material on asthma symptoms from other pollutant components, including NO_2 and larger particulates [201]. An association between UFP levels and asthma incidence has also been observed in an urban environment

but again confounding factors including other pollutants cannot be ruled out [202]. A separate series of studies examining air pollutant exposure in a Finnish adult asthmatic population found an association between a larger particle number and decreased lung function (PEF), which they suggested could be attributed to the level of UFPs. Yet, they did stress that the associations could not be entirely separated from the potential effects of other pollutants such as SO_2, NO_2 and CO [203, 204]. Separation of the UFP effects of air pollutant material on asthma has been observed to some extent, however, in a study examining lung function (forced expiratory volume-one second (FEV_1) and forced volume capacity (FVC)) in adult asthma sufferers after a 2hr walk in either high or low air pollutant environments. In this study significant associations between higher levels of atmospheric pollutants and reduced lung function were observed for UFP and carbon content, which were not observed to the same extent for PM2.5 or NO_2 levels. These effects were more pronounced in those volunteers with moderate versus mild asthma [205]. Severe asthma sufferers were not recruited in this study. A similar 2hr walking adult volunteer study found associations between lung function decline and higher levels of pollutant material, the effects being greater in those with severe asthma. In this study however it was not possible to separate out the effect of UFPs from other pollutants [206].

Studies in paediatric asthmatic populations have also been carried out. One early examination failed to distinguish any association of UFPs with diminished lung function as distinct from other pollutant material [207]. Indeed, more recent observations have found that nitrogen oxide pollutants, coarse and fine particles but not UFPs in urban air correlated with hospital admissions for asthma in children [208]. There are however other studies that do suggest associations between UFPs and reduced lung function/respiratory problems/asthma in children. Paediatric visits to health care facilities for acute asthmatic events requiring prednisolone were significantly associated with UFP levels in the previous 7 days. This association was also found for CO levels but not for larger particles, carbon black, ozone or SO_2 [209]. Similarly, a separate study demonstrated paediatric asthma hospital admissions were associated with ambient urban background levels of total particle numbers, UFPs (mass) and NO_2 but not PM10 (mass) [210]. When examining wheezing in infants, researchers found a positive correlation with increased UFPs in those below 1 year. Caution was expressed, however, over this observation due to a protective effect observed in over 3 year olds [211]. A more recent analysis of asthmatic children, referred to a clinic for respiratory symptoms found that levels of UFPs in breath condensate correlated with wheezing, eosinophilia and breath symptom score [212]. Other studies in children have also indicated some correlation with increased levels of UFPs and functional asthma outcomes but again additional confounding factors cannot be ruled out [213–216].

Additional investigations to identify the effects of NMs on asthma have centred mainly on experimentally controlled exposure studies in human volunteers. These include a study examining the effect of isolated UFPs collected from a motor vehicle polluted area in the US, which found decreases in lung function (FEV_1). There was, however, no difference between asthmatic and control volunteers [217]. Other studies have investigated the effects of inhaled CNPs as model UFPs. Allergic asthmatic subjects exposed to CNPs 28 days before allergen challenge demonstrated increased markers of disease including eosinophilia. There was however no alteration in lung function (FEV_1) [218]. Another study found that inhalation of CNPs caused mild small airway dysfunction together with impaired alveolar gas exchange in normal subjects. When examined in asthmatic subjects there were no differences in responses to those observed for normal volunteers [219]. An additional study from the same group found that there were some small changes in vasculature function after CNPs exposure but there were no changes in asthmatic symptoms, pulmonary function, or markers of airway inflammation in both asthmatic and control volunteers [220]. This study did, however, identify that asthmatic subjects have an increased deposition of NMs after inhalation as compared to control volunteers, an observation also found in other studies [221, 222]. This effect raises the possibility of increased potentially hazardous effects of these materials in asthmatic populations due to higher exposures over the long term.

Despite there being a weight of evidence for adverse effects of UFPs on conditions such as cardiovascular disease in humans [223–225], the picture is less clear for asthmatic disease. Much of the epidemiology suffers from a lack of ability to separate the effects of UFPs from other pollutant material, while human volunteer exposure studies are limited and do not offer clear cut evidence for a direct impact. The studies described in this section focus almost completely on the potential for acute exacerbation effects of these nanosized materials. Apart from a study indicating long term and repeated exposure to NP abrasion products from diamond polishing [226] and a case report on long term exposure to Nickel NPs [227], there are virtually no long term epidemiological analysis of the effects of NPs and their potential to influence the development of asthma.

Experimental models of ultrafine air pollutant exposure effects in asthma

Concern for how particulate pollutants and the nanoscale constituents therein, contribute to adverse health effects

were raised by early *in vivo* observations that pulmonary exposure of rats to urban PM10 produces an inflammatory response. In one such study the authors demonstrated a greater inflammatory response with CNPs and proposed that the UFP component of PM10 was the main contributor to the effects seen [228]. In this section we will summarise those studies that have attempted to examine the effect of the UFP fraction of air pollution on models of asthma exacerbation and development (Table 3).

The UFP fraction of urban PM produced a greater lung inflammatory response than the larger sub-micron-sized fraction, when administered during the sensitisation phase of a HDM murine model of AAD. The effects were correlated with an oxidative stress cellular response [229]. Labile chemicals were suggested as responsible for the increases in antigen presentation marker expression on monocytes induced by coarse, fine and ultrafine fractions of freshly collected urban PM [230]. Indeed, in a murine OVA model of AAD, the higher level of redox cycling organic chemicals, PAHs and intrinsic oxidative potential within the ultrafine fraction (<150nm) of ambient PM, was put forward as the mechanism for increased adjuvancy observed with these particulates when compared to the larger PM2.5 sized fraction [231]. The idea that oxidative potential of ultrafine material is a determining factor for adjuvant behaviour was also supported by another study from the same group, which demonstrated an increase in Th2 inflammation and augmentation of UFP directed adjuvant activity in KO mice lacking the antioxidant transcription factor Nrf2 in dendritic cells [232]. Moreover, maternal exposure of mice to free radical chemical containing UFPs (engineered flame combustion particulates) resulted in enhanced OVA induced AAD in offspring, including increased AHR, eosinophils and Th2 responses, which was attributable to an imbalance in T-cell development and inhibition of Th1 maturation [233]. Using similar particles also containing free radical chemicals, the same group demonstrated increased oxidative injury and AHR in mice. These effects were not observed however when UFPs had the pro-oxidant chemicals removed [234].

In another study, these oxidant chemical containing UFPs were observed to induce EMT in infant mouse lungs. The authors suggest that these changes could represent a mechanism through which pollutant material affects airway development and predisposition to conditions such as asthma [235]. In a similar study, UFPs high in PAH chemicals were observed to have increased toxicity in neonatal as compared to adult mice. The authors suggest that neonates have an impaired response to environmental exposures that make them susceptible to pollutant oxidant toxicity and that this may impact airway development and predispose to pulmonary disease development [236]. The effect of nanoscale properties as opposed to adhered chemicals effects in these studies were not investigated, but given that these materials have carbonaceous properties which also have the potential to induce oxidative stress [237] it is possible that the NPs themselves also contribute. Indeed, CNPs as well as OVA and NO_2 have all been observed to reduce the rate of end expiratory lung volume increase in maturing rats, indicating a direct impact on lung development [238]. As reduced lung function has been put forward as a contributor for the development of asthma [239] and given the observations that air pollution exposure is associated with compromised lung development [240, 241], the potential for both nanoscale effects and chemical components within pollutant materials to adversely affect lung development, and thus ultimately to influence the development asthma is an important consideration that warrants further investigation.

In vitro models investigating the effects of ultrafine pollutant material on aspects of asthma pathophysiology have focussed mainly on airway epithelial responses. An early study demonstrated that UFPs (<0.18μm), but not the larger-sized fractions of ambient urban PM, induced GMCSF production from primary human bronchial epithelial cells. This effect on GMCSF, which is a cytokine involved in activation of dendritic cells and Th2 type allergic inflammatory responses was not replicated by exposure of cells to similar sized CNPs, with the suggestion that chemicals adhered to the UFPs were responsible for the observed effects [242]. Fine and UFP fractions from urban Paris were also found to induce GMCSF from the human bronchial 16HBE14o- epithelial cell line [243]. A subsequent study from the same group correlated GMCSF production from airway epithelium with the organic fraction, also suggesting that chemical composition in PM is a major determinant of this response [244]. In a separate study also examining Paris urban as well as rural PM, induction of GMCSF was only induced by the smaller UFP and fine fractions and was correlated to the induction of CYP1A1, NQO1 and HO-1, pointing towards chemical induced aryl hydrocarbon receptor activation (indicative of PAH content) and oxidative stress inducing activity as contributory agents [245]. A more recent study of Lebanese fine and UFPs also indicated the chemical organic fraction as inducing significant effects *in vitro* [246].

Diesel exhaust particulates (DEPs) are estimated to account for a significant proportion of the UFP fraction found in ambient and traffic related air pollution. There is evidence that DEPs levels are associated with exacerbation of pre-existing asthma and more recently evidence also points towards a direct impact on sensitisation and respiratory effects in early life [247, 248]. Indeed, DEPs have been observed to produce adjuvant effects in humans [249]. Experimental modelling in mice further supports the hypothesis that respiratory exposure to DEPs can act

Table 3 Ultrafine pollutant particular matter effects in experimental *in vivo* models of asthma.

Nanomaterial Properties			Model Characteristics				Disease Related Endpoints									Ref
Material	*1° Size (nm)*	*Location*	*Species (strain)*	*Allergen (route)*	*Exposure Route*	*Dose*	*AHR (test)*	*IgE*	*Eos*	*Neu*	*Lym*	*MΦ*	*Total cell*	*Gene Expression Markers*	*GCH-MS*	
Ultrafine Particles	<150	Los Angeles	Mice (BALB/c -f)	OVA (Int N)	Int N	0.95 μg/kg	-	↑	nc	nc	nc	-	nc	↑ (TNF-α, IL-5, IL-13, IL-6, MCP-1, MIPI-α) nc (IL-4, INF-γ)	-	[231]
DCB-230	200	-	Rats (BN–neonates)	n/a	A	200 μg/m^3 (20min x7d)	↑ (Resist)	-	nc	↑	↑	-	-	↓ (IL-18, VEGF, TNF-α, MCP-1, IL-6, IL-1β)	-	[234]
Ultrafine Particles	<180	Downtown Los Angeles	Mice (BALB/c –f)	OVA (Int N)	Int N	0.01 μg/kg	-	nc	↑	nc	↑	-	↑	↑ (IL-12, IL-6, IL-1β) nc (IL-13)	-	[232]
Ultrafine Particles	<150	Downtown Los Angeles	Mice (BALB/c –f)	OVA (Int N)	Int N	297 – 394 μg/m3	-	nc	nc	nc	-	-	-	↑ (IL-5) nc (IL-13)	-	[256]
Ultrafine Particles	<170	Fresno, CA, USA (Summer Night)	Mice (BALB/c –m)	HDM (Int N)	Int N	45 μg/m3	-	-	nc	nc	nc	nc	nc	nc (HO-1)	-	[229]
Ultrafine Particles	<170	Fresno, CA, USA (Winter Day)	Mice (BALB/c –m)	HDM (Int N)	Int N	45 μg/m3	-	-	↑	nc	↑	nc	↑	↑ (HO-1)	-	[229]
Ultrafine Particles	<170	Fresno, CA, USA (Winter Night)	Mice (BALB/c –m)	HDM (Int N)	Int N	45 μg/m3	-	-	nc	nc	nc	nc	nc	nc (HO-1)	-	[229]
Ultrafine Particles	<170	Fresno, CA, USA (Summer Day)	Mice (BALB/c –m)	HDM (Int N)	Int N	45 μg/m3	-	-	nc	nc	↑	nc	nc	↑ (HO-1)	-	[229]
Ultrafine Particles	<180	Los Angeles	Mice (BALB/c –f)	OVA (Int N)	Int N	0.04 μg/kg	-	↑	↑	↑	-	-	-	↑ (IL-5, IL-13, IL-17a)	↑ sig MUC5AC	[258]
Ultrafine Particles	<180	Los Angeles	Mice (Il4raR576)	OVA (IP)	Int N	0.18 μg/kg	↑ (Resist)	↑	↑	-	-	-	↑	↑ (IL-4, IL-13, IL-17, IFN-γ, IL-5)	-	[259]
Ultrafine Particles	<180	Detroit (upwind/downwind)	Mice (BALB/c –f)	OVA (IP)	OA	0.28, 1.4 μg/kg	-	nc	nc	nc	-	-	-	↑ (IL-5 (1.4 only))	-	[257]

Abbreviations: 1 primary, *AHR* airway hyperresponsiveness, *LF* lung function, *Resist* Resistance, *Eos* eosinophils, *Neu* neutrophils, *Lym* lymphocytes, MΦ macrophages, *GCH-MS* goblet cell hyperplasia-mucus secretion, *–f* –female, *OVA* ovalbumin, *Int N* intranasal instillation, ↑ increase, *nc* no change; – not determined, *DCB* combustion-generated ultrafine particles containing environmental persistent free radicals using 1,2-dichlorobenzene, *BN* Brown Norway, *A* aerosol, ↓ decrease, – not determined, *–m* –male, *HDM* house dust mite, *IP* intraperitoneal injection, *OA* oropharyngeal aspiration

as an adjuvant [250]. Similar to studies of ambient PM in mice, it has been proposed that the chemical content, in particular the PAH content of DEPs, are the major contributor to adjuvant activity [251]. In contrast, work carried out by Tanaka and colleagues revealed that exposure of mice to NP rich DEPs, optimised to maintain relevant organic chemical content, resulted in an adjuvant effect on OVA induced AAD. Interestingly, this adjuvant effect remained when particulates were filtered from the exhaust material, implicating gaseous pollutants as the main effector of adjuvancy [252]. The examination of gaseous pollutants, such as NO_2 and ozone, for adjuvant effects in experimental AAD has revealed mixed responses [253, 254]. Clarity is still needed regarding the relative contribution of individual pollutant components including the UFP fraction, in complex mixtures.

Exacerbation of AAD, including effects on AHR has been documented in experimental models of ambient PM exposure [255]. The extent to which individual size fractions within such material contribute to exacerbation outcomes has also been examined. Exposure of OVA sensitised mice to the PM2.5 fraction collected close to a motorway resulted in an increase in inflammatory responses, which were not observed to the same extent with UFP fraction exposures [256]. Another study examining near road collected PM and exacerbation of inflammatory events in OVA sensitised mice found that the PM10 and PM2.5 fractions resulted in a greater inflammatory cell response than the UFP fraction, with responses more pronounced in samples with a higher level of traffic related material [257]. The UFP fraction of near motorway PM has been observed to exacerbate OVA induced AAD in mice but this study did not examine other fractions of PM to allow size comparisons to be made [258]. Both the fine (PM2.5) and UFP fractions of traffic associated PM were found to exacerbate AAD in OVA sensitised mice through a mechanisms involving JAG1 and the NOTCH signalling pathway, events which were not observed with carbon black fine particle exposure [259]. This study also examined antigen presentation aspects and T-cell responses *in vitro* and *in vivo* and through interventional and knockout strategies demonstrated that UFP induced exacerbation of AAD, including IgE responses was mediated through the aryl hydrocarbon receptor. The authors proposed that since UFPs have chemicals associated with them including PAHs, which are potent ligands for the aryl hydrocarbon receptor, that such receptor activation drives JAG1 expression in dendritic cells and consequently allows enhancement of T-cell responses to aggravate AAD [259].

Additional aspects of exacerbation impacts have been discussed as a consequence of PM and UFP exposure, including inhibition of macrophage phagocytosis and clearance of microorganisms [260]. Interestingly, a recent study demonstrated that neonates exposed to model ultrafine particulates with high oxidant potential enhanced the severity of influenza virus infection [261]. Whether similar effects occur for other respiratory viral infections, including asthma associated rhinovirus and RSV exacerbations, is currently unknown.

Knowledge gaps and future directions

Broadly speaking from the studies summarised in this review, there appears to be evidence for an impact of NMs on asthma and AAD. There are however many significant knowledge gaps that need to be addressed in order to build any weight of evidence towards a confident assignment of hazard potential relevant for human exposure. Specifically there is an urgent need for much more detailed and mechanistic information surrounding the vast collection of different types of NM and their properties and how they may each affect the range of different manifestations of asthma and AAD observed in humans. There is also a need for study designs to be tailored towards more human relevant exposure scenarios, in order to increase confidence in testing being relevant for human disease. Only a handful of nanomaterial inhalation studies have been carried out to date. These studies capture relevant particle dynamics, properties and deposition patterns, not properly accounted for when the nanomaterial is administered in solution. Future efforts should encourage inhalation exposures coupled with real world dose equivalents to minimise translational uncertainties. Furthermore, there is a lack of information on long term exposures to NMs. New studies together with the development of new approaches, including *in vitro* and mechanistic insight to address these knowledge gaps are to be encouraged.

Nanomaterial characteristics as a predictor for adverse effects

The application of appropriate NM characterisation approaches is at the forefront of addressing knowledge gaps. This is fundamental to accurately attribute nanoscale properties to biological interaction and toxicological outcome. The extent to which NM characterisation was carried out across the studies in this review can be considered substantially inadequate in the vast majority of cases. Adoption of guidance proposals for minimum sets of NM characterisation requirements previously proposed in regulatory and other broader contexts [262, 263] would greatly enhance the power to assign hazard potential in future work.

How one may confidently assign particular characteristics of NMs to specific adverse outcome endpoints, is a substantial challenge and has only been attempted on a limited scale. Initial attempts were made to compare nanoparticle composition and characteristics across

studies in this review. However, it was ultimately judged unworkable as the variabilities in models used; including, exposure protocol, material dose and route, time points and endpoints of disease, among many other parameters, including the extent of NM characterisation, made it impossible to reliably compare. Therefore the only realistic comparisons that can be made to assign NM characteristics to adverse effects with any degree of confidence are from those studies, which focussed on addressing NM characteristics within a specific study. These studies are summarised in Table 4.

Size dependent effects have been observed for sensitisation, inflammation and airway disease parameters. This cannot however be said to be a universal effect for all materials and disease situations (due to lack of ability to compare across studies). Interestingly, smaller-sized NMs such as AgNPs and ZnONPs were observed to have more of an impact on mast cells and eosinophils *in vitro* when compared to larger sized particles of the same material. In addition, smaller primary-sized particles of both AuNPs and AgNPs materials were associated with inhibitory effects on AAD, while larger-sized particles were associated with exacerbation effects. While it is interesting to speculate as to whether there is a common size dependent mechanism involved here, the observations are too few and the models used too variable to reliably say. Importantly, no *in vivo* studies have reported the role of nanomaterial size on exacerbation effects in AAD. This is a significant knowledge gap in our understanding.

Agglomeration size whether in aerosol or instillation fluid was not documented to the same extent as primary NP size. Agglomeration size and its potential to influence disease is an often overlooked and little discussed characteristic that may influence tissue distribution and cellular interaction. In addition, how the transition to and from agglomerate state(s) affects biological interaction and localisation (including subcellular) and whether this behaviour is material and/or nano property dependent is unknown.

Solubility, surface charge and surface coating of NPs have been a focus for a number of studies and have demonstrated potential mechanisms and concerns. However these too would be considered of insufficient weight to attribute hazard with any great confidence to any specific property or material. The nature of the biological corona surrounding NPs as they interact with living tissue has been put forward as an important factor determining toxicological impact [264, 265]. To what degree this is true and to what extent material type and associated properties influences this, remains to be determined.

In terms of NP composition, attempts can be made at some general observations, albeit with obvious caveats. CNTs would appear to have a strong adjuvant activity and a detrimental impact on AAD when exposure occurs during sensitisation. In contrast, the effect of CNTs on exacerbation is absent or present to a lesser extent. In some studies, CNTs have been associated with an increase in Th2 type inflammation in the absence of adaptive immune responses, indicating a possible concern for exacerbation of intrinsic type asthma. Whether such categorisation based on asthma endotype can be made confidently, is possibly premature but is something that should be considered in the future. In addition, whether these observations can be linked to the high aspect ratio of CNTs is unknown but also worth further investigation. Some materials like titanium and fullerenes are associated more with inhibitory effects on AAD than others. In addition, there are a number of materials that have not been tested in different types of exposure settings. For example AuNPs, AgNPs and CuONPs have all been tested for their ability to affect pre-existing AAD but not for any effect on sensitisation and the development of AAD. SWCNTs on the other hand have been examined for adjuvant effects but not investigated for any impact on pre-existing disease.

Surface area is a critical factor for pulmonary toxicity of NMs, particularly soluble metal NPs [266]. Much more work is needed to investigate this NM characteristic as a determinant of adverse effects of NMs in asthma and AAD. Concerted efforts to categorise NMs according to their adverse effects by reference to their characteristics such as size, solubility, surface reactivity, shape (e.g. high aspect ratio, spherical, fibres, platelet-like) and metal content among other characteristics is a particular focus for nanotoxicology. While the lack of NM characterisation data, together with model variability, in the studies in this review currently limits attempts to link adverse effects to these groupings, it is imperative to prioritise such approaches for future work.

Model selection, comparability across studies and protocol standardisation

There is a large variability in the types of protocol and disease-associated endpoints used to assess adverse effects relevant for asthma and AAD, which make it extremely difficult to directly compare results across studies. Adoption of a standardised set of protocols, addressing these concerns would allow more confident comparisons to be made across studies. We have summarised those approaches used to date in terms of model set-up and characteristics, target cells and tissues, key events in disease manifestation as well as molecular endpoints of adverse effects (Fig. 1) in order to highlight the immense set of challenges, which need to be addressed if one is to bring forward NM testing approaches to become more informative and relevant for human disease.

Table 4 Summary studies of *in vivo* exposures and focussed investigation of engineered nanomaterial characteristics

Material Type	Models of Asthma and Allergic Airway Disease				Nanomaterial Characteristics Specifically Investigated for Effects in Models of Asthma and Allergic Airway Disease							
	Allergen Exposure Models of AAD			Pulmonary Exposure	Primary Size	Solubility	Shape/ Structure	Agg size	Charge	Composition	Surface Area	Surface Chemistry/ Coating
	ALLERGEN INDEP	SENSITISATION	EXACERBATION									
CNPs	[41] [40] [60] [37] [38] [59] [58] [62] [238]	[37] [38] [39] [40] [41] [42] [43] [54] [72] [238]	[58] [59, 60] [61, 62] [110]	[127] [277]	[37] [38] [39] [40] [42] [54] [40] [37] [38]		[54]			[43] [127]	[54]	
MWCNT	[169] [134] [135] [50] [278] [67] [69] [70] [51] [49]	[49] [50, 51] [54]	[67] [68] [69] [70] [71]	[147]	[49] [54]		[49] [54] [134]				[54]	
SWCNT	[136] [52]	[52, 53] [54]			[54] [52]		[54] [52]				[54]	
CNF		[54]			[54]		[54]				[54]	
AgNP	[132] [111] [116]		[111] [112] [116] [274]		[132]				[132]			[132]
AuNP			[63] [117]							[63]		
Co_3O_4NP				[126] [127] [279]						[126] [127] [279]		
CuONP	[64] [64]		[64]	[279] [280]		[280]				[279] [280]		
NiONP				[126] [127] [279] [280] [281] [282] [146]		[280] [281]				[126] [127] [279] [280]		
TiO_2NP	[119] [133] [81] [119]	[43] [55] [120] [81] [273]	[63] [120] [118] [119] [273]	[126] [127] [283]		[55]				[43] [55] [63] [126] [127]		
CeO_2NP				[104]								
ZnONP	[56] [56]	[55] [56]		[280] [194]		[55] [56] [280] [194]				[55] [280]		[55]
Fullerene		[106]										
FeNP	[275] [80]	[80]	[275] [93]									
GONP	[65]	[65]	[65]									
Latex NP	[272]	[272]			[272] [272]							
PSPNP	[79]	[44] [79]			[44]							
SiO_2NP	[48] [46] [47] [276] [48]	[45] [46, 47] [48] [55]	[66] [276]		[45] [55]	[55]		[48]	[66]	[55]	[48] [55] [276]	[48] [66] [276]
TOTALS	42	30	27	12	17	5	4	1	2	7	4	5

Abbreviations: *Agg* agglomerate, *GO* Graphene Oxide, *MWCNT* multi-walled carbon nanotubes, *SWCNT* Single-walled carbon nanotubes, *CNF* Carbon Nanofibres

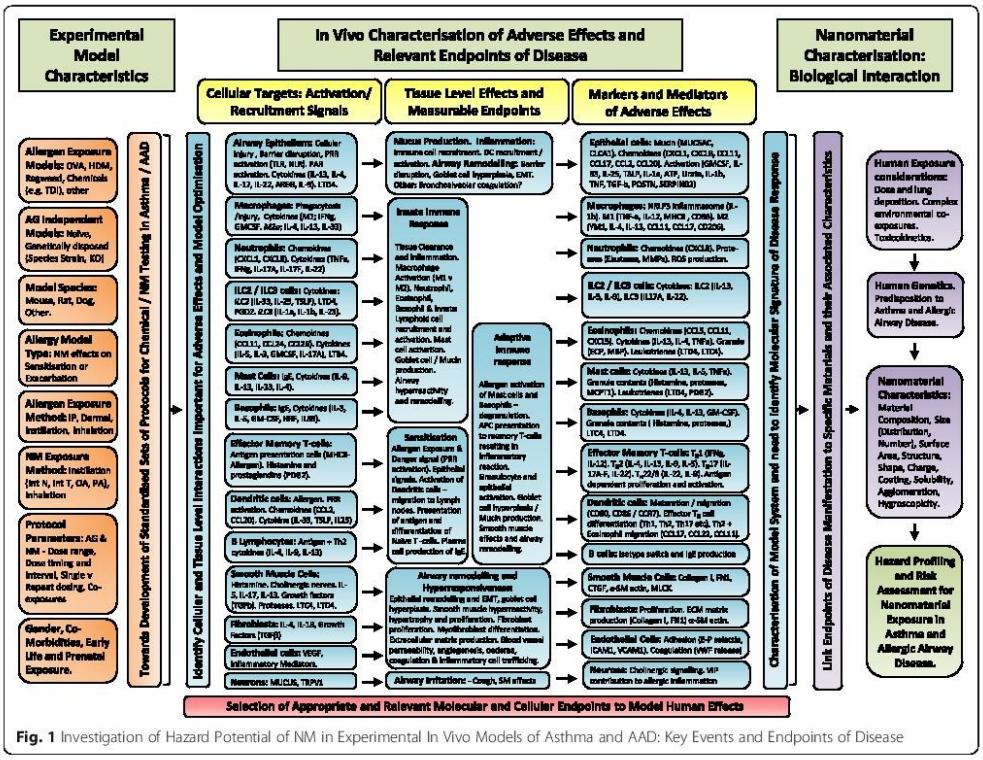


Fig. 1 Investigation of Hazard Potential of NM in Experimental In Vivo Models of Asthma and AAD: Key Events and Endpoints of Disease

Given the diversity of asthma in terms of atopic, non-atopic and mixed forms of the disease together with the different stages of susceptibility (e.g. sensitisation and exacerbation), the ability to compare a defined set of disease indicators specific for the type of disease stage, across studies would aid greatly in further clarifying NM effects within a standardised protocol framework. Importantly, reversible airway obstruction is the primary observation used to diagnose those with asthma, and AHR assessment is used to model this *in vivo*. There is a significant knowledge gap surrounding the effects of NMs on AHR as well as a lack of examination of smooth muscle effects and airway remodelling as underlying causes and targets. This can also be said for mucin production and goblet cell hyperplasia modelling as another overlooked and underreported aspect to airway disease in asthma and NM exposure. Both of these features should be included as a basic requirement for any NM studies examining the potential impact on asthma and AAD.

There is also an overrepresentation of *in vivo* modelling using ovalbumin sensitisation protocols. The inclusion of more human relevant antigen exposures such as house dust mite may allow for broader capture of effects that may otherwise be protocol type specific. Aerosolised delivery of nanomaterials in test systems is also significantly lacking in studies to date. This is particularly important given that this is the route by which humans are exposed to NM. The consequences that instillation of NM dispersions have on deposition patterns, nanomaterial characteristics and biological response is rarely discussed. Moreover, the range of doses applied across all studies is highly variable and how it relates to human exposure levels is not often referred to.

Translational relevance for human nanomaterial and pollutant exposure

Information on direct effects of engineered nanomaterials on asthma and AAD in humans is limited and evidence for the potential for adverse effects comes mainly from *in vivo* and *in vitro* experimental modelling. However, inadvertent exposure to airborne PM mainly from traffic related pollution brings with it the concern that nanosized particles contained within this

inhaled mixture have particular detrimental health effects including an influence on asthma. Epidemiological studies have suggested a role for the UFP fraction of pollutant material in asthma exacerbation, although the role for confounding factors including other pollutants cannot be entirely excluded. Evidence from experimental modelling also suggests that the UFP fraction from ambient and traffic related pollutant material may play a role in the sensitisation and development of AAD. However, experimental models *in vivo* suggest that the UFP fraction may be less important for exacerbation effects than the larger fractions, particularly the fine (typically PM1 and PM2.5) fractions. This apparent discordance with epidemiological observations necessitates clarification.

Such discussion of ultrafine effects in Asthma and AAD must also be considered in the context of other constituents of air pollutant materials. Across all experimental studies including *in vitro* work, there is strong evidence that the particle associated chemical component, containing PAHs among other organics, rather than the particles themselves are the critical determinant responsible for pollutant particulate mediated biological impact in asthma and AAD. However, given that nanomaterials including carbon nanoparticles can directly impact these same model systems, further investigation is needed to address direct versus indirect particulate effects within a pollutant mixture. It should not be overlooked that more labile and gaseous components of airborne pollution also are likely to have a significant role [252].

Population studies have pointed towards genetic susceptibility for air pollutant exposures and asthma outcome. These include exposures such as PM10, PM2.5, ozone and NO_2 and effects associated with altered asthma outcomes in those with particular single nucleotide polymorphisms in genes such as GSTP1, NQO1 and GSTT1 [267–269]. These genes are part of the antioxidant defence pathway within the cell, altered function of which may impact susceptible individuals through an inability to mount an appropriate anti-oxidant response. However, gene-environment interactions have not been investigated for associations with the smaller UFP fraction of airborne pollution and represent a significant knowledge gap. This is also true to a degree for engineered NP exposure, although some initial studies comparing different animal strains suggest genetic background is a strong determinant of pulmonary response to inhaled or instilled NMs [117, 119, 132]. Indeed, a wider analysis of up to 20 different strains of mice for responses to inhaled ZnONPs found that there were up to 10 fold differences in PMN accumulation in the lung [270]. Similarly, in a study of 8 different mouse strains, lung inflammation and injury in response to inhaled AgNPs was also found to be strain dependent [271]. These later studies did not focus on models of asthma or AAD but do highlight pulmonary response susceptible populations. Interestingly, no studies to date have been reported examining how genetic background affects NM impact on sensitisation and development of AAD. Other types of susceptibilities that exist and may play a role in how pollutant UFPs and engineered NMs impact asthma include *in utero* exposure, age, gender, diet and co-morbidities, including obesity, and have not been examined to any great extent.

Mechanistic understanding and focus for future testing

The development of new and more refined approaches to NM testing for effects on asthma and AAD have begun to incorporate concepts of how mechanistic information can lead to more detailed understanding of the most important molecular targets responsible for pathophysiological change. Identification of molecular initiating events that are coupled to detailed mechanistic understanding and NM characterisation, furthers the potential to more clearly define NM properties of concern. A more complete understanding of events that are responsible for NM effects at a tissue, cellular and molecular level through the use of standardised *in vivo* protocols can also lead to the development of more targeted testing approaches such as those using *in vitro* modelling. While *in vitro* modelling to date has been used to identify adverse effects as they may affect sensitisation and other approaches, these remain abstracted from other cellular and tissue compartments that may have important contribution to the overall NM effect at an organism level. Through greater understanding of *in vivo* targets we can begin to prioritise and standardise *in vitro* tests, which may ultimately replace animal testing. The adoption of *in vitro* systems has many advantages including the ability to greatly increase the number of different NMs that can be tested. Given the many combinations of different material types and characteristics, this is crucial. *In vitro* testing will also allow for testing to be carried in a human rather than an animal system, removing particular concerns regarding species specific effects (Fig. 2). In addition, technologies including the use of induced pluripotent stem cells (iPSC) to develop *in vitro* testing models will allow for the integration of population diverse as well as human disease specific genetic backgrounds, further optimising towards human relevant testing. Of particular note is the recently funded Marie Curie - Innovative Training Network "in3", which aims to incorporate iPSC models into an overall strategy to develop better models for chemical and NM safety assessment.

The recent momentum behind understanding modes of toxicity and development of adverse outcome pathways for xenobiotic effects has the potential to help

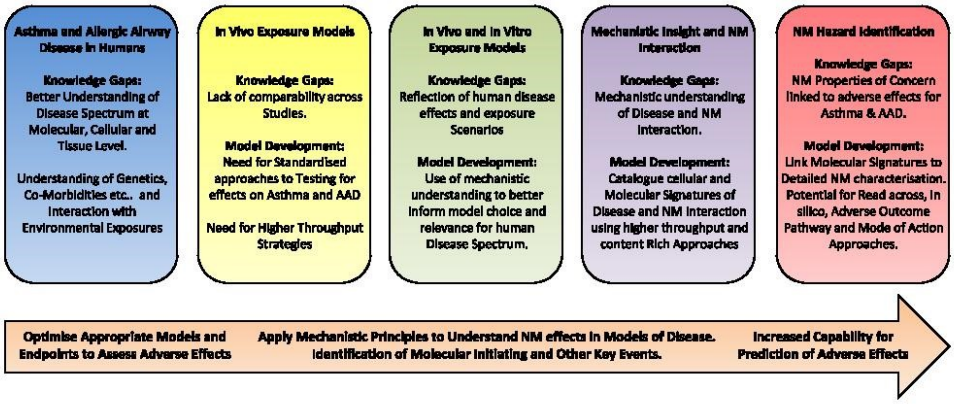


Fig. 2 Approaches for the Development of a Better Understanding and Prediction of Adverse Effects of NM on Asthma and AAD

translate *in vitro* findings to a whole organism level. Additionally, it is the hope that through accrual of data from standardised and higher throughput systems, that *in silico* modelling and read across strategies may develop to a point where experimental testing for new materials can be minimised (Fig. 2). Through a greater and more detailed understanding of how NMs may impact respiratory disease outcome and the identification of adverse effect linked molecular signatures, including epigenetic marks, it is hoped that more informative biomarkers of NM exposure and effect may be developed. These may also be useful for refining epidemiological studies of asthma and NM or air pollutant exposure.

Microbial exposure

Lastly, it is becoming ever clearer that microbial exposure is a critical factor influencing both the development and exacerbation of asthma and AAD. Exposure to bacterial and fungal diversity within the microbiome has been strongly associated with a reduced development of atopy and asthma [8]. Viral infection is also considered a major factor for both the development and exacerbation of disease. These interactions and their biological effects should not be examined in isolation from other environmental exposures such as air pollution. Whether NMs can influence these microbial interactions remains to be fully explored.

Conclusions

Within this review we have produced a detailed analysis of studies directed to investigate how nanomaterials including nano-sized pollutant particulates may impact asthma and allergic airway disease. We have identified significant knowledge gaps including a lack of investigations targeted towards understanding how different nanomaterial properties influence disease outcome *in vivo*. Attempts at standardisation for testing may overcome the diverse nature of different disease models and allow meaningful comparison of different nanomaterials and their effects across studies. The development of *in vitro* models as representative of *in vivo* exposure and disease progression is immature, particularly in terms of how nanomaterial effects on airway remodelling may be captured. This is also true for how multiple cell types may interact to produce adverse effects. In terms of human exposure, epidemiological studies are rare for engineered materials and represent another important knowledge gap. Investigations into how pollutant nanomaterials affect asthma and AAD in human populations are far from clear due to the inability to separate co-pollutant effects.

In order to address these knowledge gaps, mechanistic understanding at a cellular and molecular level, of disease pathology as well as NM specific outcomes is required. Some attempts have been made in studies covered in this review. Apart from some direct effects on the process of sensitisation involving dendritic cells and studies examing specific gene function through KO approaches, mechanistic insight is generally lacking. As knowledge progresses in our understanding of human asthma development and exacerbation events, it is important that cellular and molecular discoveries underlying adverse effects and outcomes are incorporated into model development. This allows for a more targeted and translational approach to testing. With the inclusion of more detailed NM characterisation, this approach also allows for increased power to identify properties of concern that can be linked more readily to relevant endpoints of disease. Specifically, in terms

of adjuvant activity and the development of sensitisation to antigen, there is a need to determine how the innate immune response, including airway epithelial, macrophage, mast and dendritic cells handle and respond to different NMs as they are first encountered within the lung. How NM properties including size and surface area impact how antigens attached to their surface are handled by these cells is something to consider as a priority research area. For established AAD, there is also a need to tie down how NMs propagate an allergic response. There is also a need for models to be able to capture information relevant for other asthma endotypes such as intrinsic asthma or severe asthma, where allergy does not play a role. Mechanistic insight should be prominent in our attempts to achieve this. Finally, an understanding of airway remodelling and hyperreactivity is urgently needed; given these events underlie airway obstruction, arguably the pathological feature with the greatest impact on patient morbidity and mortality. Mechanistic understanding of physical airway responses and in particular how smooth muscle cells, fibroblasts and other airway resident cells react to NM exposure is lacking and should also be encouraged as a priority research area.

Additional file

Additional file 1: Table S1. Effects of nanomaterials in non-allergic *in vivo* models of experimental pulmonary exposure. Table S2. Allergen independent effects of nanomaterials in *in vivo* models of experimental pulmonary exposure documented as part of larger allergy driven models of asthma and allergic airway disease. Table S3. *In vitro* models and nanomaterial exposure. (DOCX 295 kb)

Acknowledgements
Not Applicable

Funding
This work was part funded through the Public Health England PhD Studentship Project Scheme. This work was also part funded by the National Institute for Health Research Health Protection Research Unit (NIHR HPRU) in Health Impact of Environmental Hazards at King's College London in partnership with Public Health England (PHE). The views expressed are those of the authors and not necessarily those of the NHS, the NIHR, the Department of Health or Public Health England.

Availability of data and materials
Not Applicable.

Authors' contributions
All authors have made a significant contribution to the review of published material and writing of this manuscript. All authors read and approved the final manuscript.

Ethics approval and consent to participate
Not Applicable.

Consent for publication
All authors consent to publication of this review on acceptance by the journal.

Competing interests
The authors declare that they have no competing interests.

Publisher's Note

Springer Nature remains neutral with regard to jurisdictional claims in published maps and institutional affiliations.

Received: 10 May 2017 Accepted: 10 November 2017
Published online: 21 November 2017

References

1. Network GA. The global asthma report 2014. Auckland: Global Asthma Network; 2014. p. 769. http://www.globalasthmareport.org.
2. Lockey RF. Asthma phenotypes: an approach to the diagnosis and treatment of asthma. J Allergy Clin Immunol Pract. 2014;2(6):682–5. doi:10.1016/j.jaip.2014.09.008. http://www.ncbi.nlm.nih.gov/pubmed/25439357
3. Murphy DM, O'Byrne PM. Recent advances in the pathophysiology of asthma. Chest. 2010;137(6):1417–26. doi:10.1378/chest.09-1895. http://www.ncbi.nlm.nih.gov/pubmed/20525652
4. Bergeron C, Tulic MK, Hamid Q. Airway remodelling in asthma: from benchside to clinical practice. Can Respir J. 2010;17(4):e85–93. http://www.ncbi.nlm.nih.gov/pubmed/20808979
5. Folli C, Descalzi D, Scordamaglia F, Riccio AM, Gamalero C, Canonica GW. New insights into airway remodelling in asthma and its possible modulation. Curr Opin Allergy Clin Immunol. 2008;8(5):367–75. doi:10.1097/ACI.0b013e32830a7086. http://www.ncbi.nlm.nih.gov/pubmed/18769186
6. Walters EH, Soltani A, Reid DW, Ward C. Vascular remodelling in asthma. Curr Opin Allergy Clin Immunol. 2008;8(1):39–43. doi:10.1097/ACI.0b013e3282f42696. http://www.ncbi.nlm.nih.gov/pubmed/18188016
7. Bara I, Ozier A, Tunon de Lara JM, Marthan R, Berger P. Pathophysiology of bronchial smooth muscle remodelling in asthma. Eur Respir J. 2010;36(5):1174–84. doi:10.1183/09031936.00019810. http://www.ncbi.nlm.nih.gov/pubmed/21037369
8. Ege MJ, Mayer M, Normand AC, Genuneit J, Cookson WO, Braun-Fahrlander C, et al. Exposure to environmental microorganisms and childhood asthma. N Engl J Med. 2011;364(8):701–9. doi:10.1056/NEJMoa1007302. http://www.ncbi.nlm.nih.gov/pubmed/21345099
9. Edwards MR, Bartlett NW, Hussell T, Openshaw P, Johnston SL. The microbiology of asthma. Nat Rev Microbiol. 2012;10(7):459–71. doi:10.1038/nrmicro2801. http://www.ncbi.nlm.nih.gov/pubmed/22669219
10. Holguin F, Bleecker ER, Busse WW, Calhoun WJ, Castro M, Erzurum SC, et al. Obesity and asthma: an association modified by age of asthma onset. J Allergy Clin Immunol. 2011;127(6):1486–93 e2. doi:10.1016/j.jaci.2011.03.036. http://www.ncbi.nlm.nih.gov/pubmed/21624618
11. Paul G, Brehm JM, Alcorn JF, Holguin F, Aujla SJ, Celedon JC. Vitamin D and asthma. Am J Respir Crit Care Med. 2012;185(2):124–32. doi:10.1164/rccm.201108-1502CI. http://www.ncbi.nlm.nih.gov/pubmed/22016447
12. McGwin G, Lienert J, Kennedy JI. Formaldehyde exposure and asthma in children: a systematic review. Environ Health Perspect. 2010;118(3):313–7. doi:10.1289/ehp.0901143. http://www.ncbi.nlm.nih.gov/pubmed/20064771
13. Jaakkola JJ, Knight TL. The role of exposure to phthalates from polyvinyl chloride products in the development of asthma and allergies: a systematic review and meta-analysis. Environ Health Perspect. 2008;116(7):845–53. doi:10.1289/ehp.10846. http://www.ncbi.nlm.nih.gov/pubmed/18629304
14. Bornehag CG, Nanberg E. Phthalate exposure and asthma in children. Int J Androl. 2010;33(2):333–45. doi:10.1111/j.1365-2605.2009.01023.x. http://www.ncbi.nlm.nih.gov/pubmed/20059582
15. Liu AH. Something old, something new: indoor endotoxin, allergens and asthma. Paediatr Respir Rev. 2004;5 Suppl A:S65-S71. http://www.ncbi.nlm.nih.gov/pubmed/14980246.
16. Ahluwalia SK, Matsui EC. The indoor environment and its effects on childhood asthma. Curr Opin Allergy Clin Immunol. 2011;11(2):137–43. doi:10.1097/ACI.0b013e3283445921. http://www.ncbi.nlm.nih.gov/pubmed/21301330
17. Baena-Cagnani CE, Gomez RM, Baena-Cagnani R, Canonica GW. Impact of environmental tobacco smoke and active tobacco smoking on the development and outcomes of asthma and rhinitis. Curr Opin Allergy Clin Immunol. 2009;9(2):136–40. doi:10.1097/ACI.0b013e3283294038. http://www.ncbi.nlm.nih.gov/pubmed/19307883
18. Arruda LK, Sole D, Baena-Cagnani CE, Naspitz CK. Risk factors for asthma and atopy. Curr Opin Allergy Clin Immunol. 2005;5(2):153–9. http://www.ncbi.nlm.nih.gov/pubmed/15764906

19. Donaldson K, Gilmour MI, MacNee W. Asthma and PM10. Respir Res. 2000; 1(1):12–5. doi:10.1186/rr5. http://www.ncbi.nlm.nih.gov/pubmed/11667958
20. Gowers AM, Cullinan P, Ayres JG, Anderson HR, Strachan DP, Holgate ST, et al. Does outdoor air pollution induce new cases of asthma? Biological plausibility and evidence; a review. Respirology. 2012;17(6):887–98. doi:10.1111/j.1440-1843.2012.02195.x. https://www.ncbi.nlm.nih.gov/pubmed/22672711
21. Zammit-Tabona M, Sherkin M, Kijek K, Chan H, Chan-Yeung M. Asthma caused by diphenylmethane diisocyanate in foundry workers. Clinical, bronchial provocation, and immunologic studies. Am Rev Respir Dis. 1983; 128(2):226–30. http://www.ncbi.nlm.nih.gov/pubmed/6881681
22. Zeiss CR. Advances in acid anhydride induced occupational asthma. Curr Opin Allergy Clin Immunol. 2002;2(2):89–92. http://www.ncbi.nlm.nih.gov/pubmed/11964754
23. Nowack B, Bucheli TD. Occurrence, behavior and effects of nanoparticles in the environment. Environ Pollut. 2007;150(1):5–22. doi:10.1016/j.envpol.2007.06.006. http://www.ncbi.nlm.nih.gov/pubmed/17658673
24. Stone V, Nowack B, Baun A, van den Brink N, Kammer F, Dusinska M, et al. Nanomaterials for environmental studies: classification, reference material issues, and strategies for physico-chemical characterisation. Sci Total Environ. 2010;408(7):1745–54. doi:10.1016/j.scitotenv.2009.10.035. http://www.ncbi.nlm.nih.gov/pubmed/19903569
25. Sajid M, Ilyas M, Basheer C, Tariq M, Daud M, Baig N, et al. Impact of nanoparticles on human and environment: review of toxicity factors, exposures, control strategies, and future prospects. Environ Sci Pollut Res Int. 2015;22(6):4122–43. doi:10.1007/s11356-014-3994-1. http://www.ncbi.nlm.nih.gov/pubmed/25548015
26. Li N, Georas S, Alexis N, Fritz P, Xia T, Williams MA, et al. A work group report on ultrafine particles (American Academy of Allergy, Asthma & Immunology): Why ambient ultrafine and engineered nanoparticles should receive special attention for possible adverse health outcomes in human subjects. J Allergy Clin Immunol. 2016;138(2):386–96. doi:10.1016/j.jaci.2016.02.023. https://www.ncbi.nlm.nih.gov/pubmed/27130856
27. Hosseini A, Hirota JA, Hackett TL, McNagny KM, Wilson SJ, Carlsten C. Morphometric analysis of inflammation in bronchial biopsies following exposure to inhaled diesel exhaust and allergen challenge in atopic subjects. Part Fibre Toxicol. 2016;13:2. doi:10.1186/s12989-016-0114-z. https://www.ncbi.nlm.nih.gov/pubmed/26758251
28. Kumagai Y, Abiko Y, Cong NL. Chemical toxicology of reactive species in the atmosphere: two decades of progress in an electron acceptor and an electrophile. J Toxicol Sci. 2016;41 Special:SP37-SP47; doi:10.2131/jts.41.SP37. https://www.ncbi.nlm.nih.gov/pubmed/28003638.
29. Meldrum K, Gant TW, Leonard MO. Diesel exhaust particulate associated chemicals attenuate expression of CXCL10 in human primary bronchial epithelial cells. Toxicol In Vitro. 2017; doi:10.1016/j.tiv.2017.06.023. https://www.ncbi.nlm.nih.gov/pubmed/28655636
30. Robinson RK, Birrell MA, Adcock JJ, Wortley MA, Dubuis ED, Chen S, et al. Mechanistic link between diesel exhaust particles and respiratory reflexes. J Allergy Clin Immunol. 2017; doi:10.1016/j.jaci.2017.04.038. https://www.ncbi.nlm.nih.gov/pubmed/28532657
31. Lambrecht BN, Hammad H. The immunology of asthma. Nature immunology. 2015;16(1):45–56. doi:10.1038/ni.3049. http://www.ncbi.nlm.nih.gov/pubmed/25521684
32. Porter PC, Lim DJ, Maskatia ZK, Mak G, Tsai CL, Citardi MJ, et al. Airway surface mycosis in chronic TH2-associated airway disease. J Allergy Clin Immunol. 2014;134(2):325–31. doi:10.1016/j.jaci.2014.04.028. http://www.ncbi.nlm.nih.gov/pubmed/24928648
33. Manni ML, Trudeau JB, Scheller EV, Mandalapu S, Elloso MM, Kolls JK, et al. The complex relationship between inflammation and lung function in severe asthma. Mucosal immunology. 2014;7(5):1186–98. doi:10.1038/mi.2014.8. http://www.ncbi.nlm.nih.gov/pubmed/24549277
34. Irvin C, Zafar I, Good J, Rollins D, Christianson C, Gorska MM, et al. Increased frequency of dual-positive TH2/TH17 cells in bronchoalveolar lavage fluid characterizes a population of patients with severe asthma. J Allergy Clin Immunol. 2014;134(5):1175–86 e7. doi:10.1016/j.jaci.2014.05.038. http://www.ncbi.nlm.nih.gov/pubmed/25042748
35. Saglani S, Lloyd CM. Novel concepts in airway inflammation and remodelling in asthma. Eur Respir J. 2015;46(6):1796–804. doi:10.1183/13993003.01196-2014. http://www.ncbi.nlm.nih.gov/pubmed/26541520
36. Sagar S, Akbarshahi H, Uller L. Translational value of animal models of asthma: Challenges and promises. Eur J Pharmacol. 2015;759:272–7. doi:10.1016/j.ejphar.2015.03.037. http://www.ncbi.nlm.nih.gov/pubmed/25823808
37. Inoue K, Takano H, Yanagisawa R, Sakurai M, Ichinose T, Sadakane K, et al. Effects of nano particles on antigen-related airway inflammation in mice. Respir Res. 2005;6:106. doi:10.1186/1465-9921-6-106. http://www.ncbi.nlm.nih.gov/pubmed/16164761
38. Inoue K, Takano H, Yanagisawa R, Ichinose T, Sakurai M, Yoshikawa T. Effects of nano particles on cytokine expression in murine lung in the absence or presence of allergen. Arch Toxicol. 2006;80(9):614–9. doi:10.1007/s00204-006-0075-3. http://www.ncbi.nlm.nih.gov/pubmed/16482471
39. Koike E, Takano H, Inoue KI, Yanagisawa R, Sakurai M, Aoyagi H, et al. Pulmonary exposure to carbon black nanoparticles increases the number of antigen-presenting cells in murine lung. Int J Immunopathol Pharmacol. 2008;21(1):35–42. http://www.ncbi.nlm.nih.gov/pubmed/18336729
40. Inoue K, Takano H, Yanagisawa R, Sakurai M, Abe S, Yoshino S, et al. Effects of nanoparticles on lung physiology in the presence or absence of antigen. Int J Immunopathol Pharmacol. 2007;20(4):737–44. http://www.ncbi.nlm.nih.gov/pubmed/18179746
41. Kroker M, Sydlik U, Autengruber A, Cavelius C, Weighardt H, Kraegeloh A, et al. Preventing carbon nanoparticle-induced lung inflammation reduces antigen-specific sensitization and subsequent allergic reactions in a mouse model. Part Fibre Toxicol. 2015;12:20. doi:10.1186/s12989-015-0093-5. http://www.ncbi.nlm.nih.gov/pubmed/26141115
42. de Haar C, Hassing I, Bol M, Bleumink R, Pieters R. Ultrafine carbon black particles cause early airway inflammation and have adjuvant activity in a mouse allergic airway disease model. Toxicol Sci. 2005;87(2):409–18. doi:10.1093/toxsci/kfi255. http://www.ncbi.nlm.nih.gov/pubmed/16014737
43. de Haar C, Hassing I, Bol M, Bleumink R, Pieters R. Ultrafine but not fine particulate matter causes airway inflammation and allergic airway sensitization to co-administered antigen in mice. Clin Exp Allergy. 2006;36(11):1469–79. doi:10.1111/j.1365-2222.2006.02586.x. http://www.ncbi.nlm.nih.gov/pubmed/17083358
44. Alberg T, Hansen JS, Lovik M, Nygaard UC. Particles influence allergic responses in mice--role of gender and particle size. J Toxicol Environ Health Part A. 2014;77(5):281–92. doi:10.1080/15287394.2013.863746. http://www.ncbi.nlm.nih.gov/pubmed/24588227
45. Yoshida T, Yoshioka Y, Fujimura M, Yamashita K, Higashisaka K, Morishita Y, et al. Promotion of allergic immune responses by intranasally-administrated nanosilica particles in mice. Nanoscale research letters. 2011;6(1):195. doi:10.1186/1556-276X-6-195. http://www.ncbi.nlm.nih.gov/pubmed/21711705
46. Han B, Guo J, Abrahaley T, Qin L, Wang L, Zheng Y, et al. Adverse effect of nano-silicon dioxide on lung function of rats with or without ovalbumin immunization. PloS one. 2011;6(2):e17236. doi:10.1371/journal.pone.0017236. http://www.ncbi.nlm.nih.gov/pubmed/21359146
47. Brandenberger C, Rowley NL, Jackson-Humbles DN, Zhang Q, Bramble LA, Lewandowski RP, et al. Engineered silica nanoparticles act as adjuvants to enhance allergic airway disease in mice. Part Fibre Toxicol. 2013;10:26. doi:10.1186/1743-8977-10-26. http://www.ncbi.nlm.nih.gov/pubmed/23815813
48. Han H, Park YH, Park HJ, Lee K, Um K, Park JW, et al. Toxic and adjuvant effects of silica nanoparticles on ovalbumin-induced allergic airway inflammation in mice. Respir Res. 2016;17(1):60. doi:10.1186/s12931-016-0376-x. http://www.ncbi.nlm.nih.gov/pubmed/27194244
49. Inoue K, Koike E, Yanagisawa R, Hirano S, Nishikawa M, Takano H. Effects of multi-walled carbon nanotubes on a murine allergic airway inflammation model. Toxicol Appl Pharmacol. 2009;237(3):306–16. doi:10.1016/j.taap.2009.04.003. http://www.ncbi.nlm.nih.gov/pubmed/19371758
50. Mizutani N, Nabe T, Yoshino S. Exposure to multiwalled carbon nanotubes and allergen promotes early- and late-phase increases in airway resistance in mice. Biol Pharm Bull. 2012;35(12):2133–40. http://www.ncbi.nlm.nih.gov/pubmed/23207765
51. Ronzani C, Casset A, Pons F. Exposure to multi-walled carbon nanotubes results in aggravation of airway inflammation and remodeling and in increased production of epithelium-derived innate cytokines in a mouse model of asthma. Arch Toxicol. 2014;88(2):489–99. doi:10.1007/s00204-013-1116-3. http://www.ncbi.nlm.nih.gov/pubmed/23948970
52. Inoue K, Yanagisawa R, Koike E, Nishikawa M, Takano H. Repeated pulmonary exposure to single-walled carbon nanotubes exacerbates allergic inflammation of the airway: Possible role of oxidative stress. Free Radic Biol Med. 2010;48(7):924–34. doi:10.1016/j.freeradbiomed.2010.01.013. http://www.ncbi.nlm.nih.gov/pubmed/20093178
53. Li J, Li L, Chen H, Chang Q, Liu X, Wu Y, et al. Application of vitamin E to antagonize SWCNTs-induced exacerbation of allergic asthma. Sci Rep. 2014;4:4275. doi:10.1038/srep04275. http://www.ncbi.nlm.nih.gov/pubmed/24589727

54. Nygaard UC, Samuelsen M, Marioara CD, Lovik M. Carbon nanofibers have IgE adjuvant capacity but are less potent than nanotubes in promoting allergic airway responses. BioMed Res Int. 2013;2013:476010. doi:10.1155/2013/476010. http://www.ncbi.nlm.nih.gov/pubmed/24024193
55. Horie M, Stowe M, Tabei M, Kuroda E. Pharyngeal aspiration of metal oxide nanoparticles showed potential of allergy aggravation effect to inhaled ovalbumin. Inhal Toxicol. 2015;27(3):181–90. doi:10.3109/08958378.2015.1026618. http://www.ncbi.nlm.nih.gov/pubmed/25864991
56. Huang KL, Lee YH, Chen HI, Liao HS, Chiang BL, Cheng TJ. Zinc oxide nanoparticles induce eosinophilic airway inflammation in mice. J Hazard Mater. 2015;297:304–12. doi:10.1016/j.jhazmat.2015.05.023. http://www.ncbi.nlm.nih.gov/pubmed/26010476
57. Fukui H, Horie M, Endoh S, Kato H, Fujita K, Nishio K, et al. Association of zinc ion release and oxidative stress induced by intratracheal instillation of ZnO nanoparticles to rat lung. Chem Biol Interact. 2012;198(1–3):29–37. doi:10.1016/j.cbi.2012.04.007. http://www.ncbi.nlm.nih.gov/pubmed/22640810
58. Barrett EG, Rudolph K, Bowen LE, Muggenburg BA, Bice DE. Effect of inhaled ultrafine carbon particles on the allergic airway response in ragweed-sensitized dogs. Inhal Toxicol. 2003;15(2):151–65. doi:10.1080/08958370304474. http://www.ncbi.nlm.nih.gov/pubmed/12528044
59. Beck-Speier I, Karg E, Behrendt H, Stoeger T, Alessandrini F. Ultrafine particles affect the balance of endogenous pro- and anti-inflammatory lipid mediators in the lung: in-vitro and in-vivo studies. Part Fibre Toxicol. 2012;9:27. doi:10.1186/1743-8977-9-27. http://www.ncbi.nlm.nih.gov/pubmed/22809365
60. Unfried K, Kroker M, Autengruber A, Gotic M, Sydlik U. The compatible solute ectoine reduces the exacerbating effect of environmental model particles on the immune response of the airways. J Allergy. 2014;2014:708458. doi:10.1155/2014/708458. http://www.ncbi.nlm.nih.gov/pubmed/24822073
61. Alessandrini F, Schulz H, Takenaka S, Lentner B, Karg E, Behrendt H, et al. Effects of ultrafine carbon particle inhalation on allergic inflammation of the lung. J Allergy Clin Immunol. 2006;117(4):824–30. doi:10.1016/j.jaci.2005.11.046. http://www.ncbi.nlm.nih.gov/pubmed/16630940
62. Alessandrini F, Weichenmeier I, van Miert E, Takenaka S, Karg E, Blume C, et al. Effects of ultrafine particles-induced oxidative stress on Clara cells in allergic lung inflammation. Part Fibre Toxicol. 2010;7:11. doi:10.1186/1743-8977-7-11. http://www.ncbi.nlm.nih.gov/pubmed/20420656
63. Hussain S, Vanoirbeek JA, Luyts K, De Vooght V, Verbeken E, Thomassen LC, et al. Lung exposure to nanoparticles modulates an asthmatic response in a mouse model. Eur Respir J. 2011;37(2):299–309. doi:10.1183/09031936.00168509. http://www.ncbi.nlm.nih.gov/pubmed/20530043
64. Park JW, Lee IC, Shin NR, Jeon CM, Kwon OK, Ko JW, et al. Copper oxide nanoparticles aggravate airway inflammation and mucus production in asthmatic mice via MAPK signaling. Nanotoxicology. 2016;10(4):445–52. doi:10.3109/17435390.2015.1078851. http://www.ncbi.nlm.nih.gov/pubmed/26472121
65. Shurin MR, Yanamala N, Kisin ER, Tkach AV, Shurin GV, Murray AR, et al. Graphene oxide attenuates Th2-type immune responses, but augments airway remodeling and hyperresponsiveness in a murine model of asthma. ACS nano. 2014;8(6):5585–99. doi:10.1021/nn406454u. http://www.ncbi.nlm.nih.gov/pubmed/24847914
66. Marzaioli V, Aguilar-Pimentel JA, Weichenmeier I, Luxenhofer G, Wiemann M, Landsiedel R, et al. Surface modifications of silica nanoparticles are crucial for their inert versus proinflammatory and immunomodulatory properties. Int J Nanomedicine. 2014;9:2815–32. doi:10.2147/IJN.S57396. http://www.ncbi.nlm.nih.gov/pubmed/24940059
67. Ryman-Rasmussen JP, Tewksbury EW, Moss OR, Cesta MF, Wong BA, Bonner JC. Inhaled multiwalled carbon nanotubes potentiate airway fibrosis in murine allergic asthma. Am J Respir Cell Mol Biol. 2009;40(3):349–58. doi:10.1165/rcmb.2008-0276OC. http://www.ncbi.nlm.nih.gov/pubmed/18787175
68. Staal YC, van Triel JJ, Maarschalkerweerd TV, Arts JH, Duistermaat E, Muijser H, et al. Inhaled multiwalled carbon nanotubes modulate the immune response of trimellitic anhydride-induced chemical respiratory allergy in brown Norway rats. Toxicol Pathol. 2014;42(7):1130–42. doi:10.1177/0192623313519874. http://www.ncbi.nlm.nih.gov/pubmed/24705883
69. Thompson EA, Sayers BC, Glista-Baker EE, Shipkowski KA, Ihrie MD, Duke KS, et al. Role of signal transducer and activator of transcription 1 in murine allergen-induced airway remodeling and exacerbation by carbon nanotubes. Am J Respir Cell Mol Biol. 2015;53(5):625–36. doi:10.1165/rcmb.2014-0221OC. http://www.ncbi.nlm.nih.gov/pubmed/25807359
70. Sayers BC, Taylor AJ, Glista-Baker EE, Shipley-Phillips JK, Dackor RT, Edin ML, et al. Role of cyclooxygenase-2 in exacerbation of allergen-induced airway remodeling by multiwalled carbon nanotubes. Am J Respir Cell Mol Biol. 2013;49(4):525–35. doi:10.1165/rcmb.2013-0019OC. http://www.ncbi.nlm.nih.gov/pubmed/23642096
71. Shipkowski KA, Taylor AJ, Thompson EA, Glista-Baker EE, Sayers BC, Messenger ZJ, et al. An allergic lung microenvironment suppresses carbon nanotube-induced inflammasome activation via STAT6-dependent inhibition of caspase-1. PloS one. 2015;10(6):e0128888. doi:10.1371/journal.pone.0128888. http://www.ncbi.nlm.nih.gov/pubmed/26091108
72. de Haar C, Kool M, Hassing I, Bol M, Lambrecht BN, Pieters R. Lung dendritic cells are stimulated by ultrafine particles and play a key role in particle adjuvant activity. J Allergy Clin Immunol. 2008;121(5):1246–54. doi:10.1016/j.jaci.2008.01.010. http://www.ncbi.nlm.nih.gov/pubmed/18313130
73. Koike E, Takano H, Inoue K, Yanagisawa R, Kobayashi T. Carbon black nanoparticles promote the maturation and function of mouse bone marrow-derived dendritic cells. Chemosphere. 2008;73(3):371–6. doi:10.1016/j.chemosphere.2008.05.054. http://www.ncbi.nlm.nih.gov/pubmed/18602660
74. Lefebvre DE, Pearce B, Fine JH, Chomyshyn E, Ross N, Halappanavar S, et al. In vitro enhancement of mouse T helper 2 cell sensitization to ovalbumin allergen by carbon black nanoparticles. Toxicol Sci. 2014;138(2):322–32. doi:10.1093/toxsci/kfu010. http://www.ncbi.nlm.nih.gov/pubmed/24449417
75. Chen W, Zhang Q, Kaplan BL, Baker GL, Kaminski NE. Induced T cell cytokine production is enhanced by engineered nanoparticles. Nanotoxicology. 2014;8(Suppl 1):11–23. doi:10.3109/17435390.2013.848302. http://www.ncbi.nlm.nih.gov/pubmed/24256152
76. Hirai T, Yoshioka Y, Takahashi H, Ichihashi K, Yoshida T, Tochigi S, et al. Amorphous silica nanoparticles enhance cross-presentation in murine dendritic cells. Biochem Biophys Res Commun. 2012;427(3):553–6. doi:10.1016/j.bbrc.2012.09.095. http://www.ncbi.nlm.nih.gov/pubmed/23022188
77. Schanen BC, Das S, Reilly CM, Warren WL, Self WT, Seal S, et al. Immunomodulation and T helper TH(1)/TH(2) response polarization by CeO(2) and TiO(2) nanoparticles. PloS one. 2013;8(5):e62816. doi:10.1371/journal.pone.0062816. http://www.ncbi.nlm.nih.gov/pubmed/23667525
78. Hardy CL, LeMasurier JS, Belz GT, Scalzo-Inguanti K, Yao J, Xiang SD, et al. Inert 50-nm polystyrene nanoparticles that modify pulmonary dendritic cell function and inhibit allergic airway inflammation. J Immunol. 2012;188(3):1431–41. doi:10.4049/jimmunol.1100156. http://www.ncbi.nlm.nih.gov/pubmed/22190179
79. Hardy CL, Lemasurier JS, Mohamud R, Yao J, Xiang SD, Rolland JM, et al. Differential uptake of nanoparticles and microparticles by pulmonary APC subsets induces discrete immunological imprints. J Immunol. 2013;191(10):5278–90. doi:10.4049/jimmunol.1203131. http://www.ncbi.nlm.nih.gov/pubmed/24123688
80. Ban M, Langonne I, Huguet N, Guichard Y, Goutet M. Iron oxide particles modulate the ovalbumin-induced Th2 immune response in mice. Toxicol Lett. 2013;216(1):31–9. doi:10.1016/j.toxlet.2012.11.003. http://www.ncbi.nlm.nih.gov/pubmed/23147377
81. Rossi EM, Pylkkanen L, Koivisto AJ, Nykasenoja H, Wolff H, Savolainen K, et al. Inhalation exposure to nanosized and fine TiO2 particles inhibits features of allergic asthma in a murine model. Part Fibre Toxicol. 2010;7:35. doi:10.1186/1743-8977-7-35. http://www.ncbi.nlm.nih.gov/pubmed/21108815
82. Grun JL, Maurer PH. Different T helper cell subsets elicited in mice utilizing two different adjuvant vehicles: the role of endogenous interleukin 1 in proliferative responses. Cellular Immunol. 1989;121(1):134–45. http://www.ncbi.nlm.nih.gov/pubmed/2524278
83. Bergmann-Leitner ES, Leitner WW. Adjuvants in the Driver's Seat: How Magnitude, Type, Fine Specificity and Longevity of Immune Responses Are Driven by Distinct Classes of Immune Potentiators. Vaccines (Basel). 2014;2(2):252–96. doi:10.3390/vaccines2020252. http://www.ncbi.nlm.nih.gov/pubmed/26344620
84. Marrack P, McKee AS, Munks MW. Towards an understanding of the adjuvant action of aluminium. Nat Rev Immunol. 2009;9(4):287–93. doi:10.1038/nri2510. http://www.ncbi.nlm.nih.gov/pubmed/19247370
85. Oleszycka E, Lavelle EC. Immunomodulatory properties of the vaccine adjuvant alum. Curr Opin Immunol. 2014;28:1–5. doi:10.1016/j.coi.2013.12.007. http://www.ncbi.nlm.nih.gov/pubmed/24463269
86. Sayan M, Mossman BT. The NLRP3 inflammasome in pathogenic particle and fibre-associated lung inflammation and diseases. Part Fibre Toxicol. 2016;13(1):51. doi:10.1186/s12989-016-0162-4. http://www.ncbi.nlm.nih.gov/pubmed/27650313
87. Mishra A, Zheng J, Tang X, Goering PL. Silver Nanoparticle-Induced Autophagic-Lysosomal Disruption and NLRP3-Inflammasome Activation in

HepG2 Cells is Size-Dependent. Toxicol Sci. 2016; doi:10.1093/toxsci/kfw011. http://www.ncbi.nlm.nih.gov/pubmed/26801583
88. Baron L, Gombault A, Fanny M, Villeret B, Savigny F, Guillou N, et al. The NLRP3 inflammasome is activated by nanoparticles through ATP, ADP and adenosine. Cell Death Dis. 2015;6:e1629. doi:10.1038/cddis.2014.576. http://www.ncbi.nlm.nih.gov/pubmed/25654762
89. Sager TM, Wolfarth MW, Andrew M, Hubbs A, Friend S, Chen TH, et al. Effect of multi-walled carbon nanotube surface modification on bioactivity in the C57BL/6 mouse model. Nanotoxicology. 2014;8(3):317–27. doi:10.3109/17435390.2013.779757. http://www.ncbi.nlm.nih.gov/pubmed/23432020
90. Yazdi AS, Guarda G, Riteau N, Drexler SK, Tardivel A, Couillin I, et al. Nanoparticles activate the NLR pyrin domain containing 3 (Nlrp3) inflammasome and cause pulmonary inflammation through release of IL-1alpha and IL-1beta. Proc Natl Acad Sci U S A. 2010;107(45):19449–54. doi:10.1073/pnas.1008155107. http://www.ncbi.nlm.nih.gov/pubmed/20974980
91. Winter M, Beer HD, Hornung V, Kramer U, Schins RP, Forster I. Activation of the inflammasome by amorphous silica and TiO2 nanoparticles in murine dendritic cells. Nanotoxicology. 2011;5(3):326–40. doi:10.3109/17435390.2010.506957. http://www.ncbi.nlm.nih.gov/pubmed/20846021
92. Nakanishi K, Tsukimoto M, Tanuma S, Takeda K, Kojima S. Silica nanoparticles activate purinergic signaling via P2X7 receptor in dendritic cells, leading to production of pro-inflammatory cytokines. Toxicol In Vitro. 2016;35:202–11. doi:10.1016/j.tiv.2016.06.003. http://www.ncbi.nlm.nih.gov/pubmed/27311643
93. Zhu M, Tian X, Song X, Li Y, Tian Y, Zhao Y, et al. Nanoparticle-induced exosomes target antigen-presenting cells to initiate Th1-type immune activation. Small. 2012;8(18):2841–8. doi:10.1002/smll.201200381. http://www.ncbi.nlm.nih.gov/pubmed/22674628
94. Ricciardolo FL, Sorbello V, Folino A, Gallo F, Massaglia GM, Favata G, et al. Identification of IL-17F/frequent exacerbator endotype in asthma. J Allergy Clin Immunol. 2016; doi:10.1016/j.jaci.2016.10.034. http://www.ncbi.nlm.nih.gov/pubmed/27931975
95. Chesne J, Braza F, Mahay G, Brouard S, Aronica M, Magnan A. IL-17 in severe asthma. Where do we stand? Am J Respir Crit Care Med. 2014;190(10):1094–101. doi:10.1164/rccm.201405-0859PP. http://www.ncbi.nlm.nih.gov/pubmed/25162311
96. Wilson RH, Whitehead GS, Nakano H, Free ME, Kolls JK, Cook DN. Allergic sensitization through the airway primes Th17-dependent neutrophilia and airway hyperresponsiveness. Am J Respir Crit Care Med. 2009;180(8):720–30. doi:10.1164/rccm.200904-0573OC. http://www.ncbi.nlm.nih.gov/pubmed/19661246
97. Lambrecht BN, Hammad H. Allergens and the airway epithelium response: gateway to allergic sensitization. J Allergy Clin Immunol. 2014;134(3):499–507. doi:10.1016/j.jaci.2014.06.036. http://www.ncbi.nlm.nih.gov/pubmed/25171864
98. Hussain S, Boland S, Baeza-Squiban A, Hamel R, Thomassen LC, Martens JA, et al. Oxidative stress and proinflammatory effects of carbon black and titanium dioxide nanoparticles: role of particle surface area and internalized amount. Toxicology. 2009;260(1–3):142–9. doi:10.1016/j.tox.2009.04.001. http://www.ncbi.nlm.nih.gov/pubmed/19464580
99. Gualtieri M, Skuland T, Iversen TG, Lag M, Schwarze P, Bilanicova D, et al. Importance of agglomeration state and exposure conditions for uptake and pro-inflammatory responses to amorphous silica nanoparticles in bronchial epithelial cells. Nanotoxicology. 2012;6(7):700–12. doi:10.3109/17435390.2011.604441. http://www.ncbi.nlm.nih.gov/pubmed/21793771
100. Presta L, Shields R, O'Connell L, Lahr S, Porter J, Gorman C, et al. The binding site on human immunoglobulin E for its high affinity receptor. J Biol Chem. 1994;269(42):26368–73. http://www.ncbi.nlm.nih.gov/pubmed/7929356
101. Turner H, Kinet JP. Signalling through the high-affinity IgE receptor Fc epsilonRI. Nature. 1999;402(6760 Suppl):B24–30. http://www.ncbi.nlm.nih.gov/pubmed/10586892
102. Chen EY, Garnica M, Wang YC, Mintz AJ, Chen CS, Chin WC. A mixture of anatase and rutile TiO(2) nanoparticles induces histamine secretion in mast cells. Part Fibre Toxicol. 2012;9:2. doi:10.1186/1743-8977-9-2. http://www.ncbi.nlm.nih.gov/pubmed/22260553
103. Aldossari AA, Shannahan JH, Podila R, Brown JM. Influence of physicochemical properties of silver nanoparticles on mast cell activation and degranulation. Toxicol In Vitro. 2015;29(1):195–203. doi:10.1016/j.tiv.2014.10.008. http://www.ncbi.nlm.nih.gov/pubmed/25458489
104. Wingard CJ, Walters DM, Cathey BL, Hilderbrand SC, Katwa P, Lin S, et al. Mast cells contribute to altered vascular reactivity and ischemia-reperfusion injury following cerium oxide nanoparticle instillation. Nanotoxicology. 2011;5(4):531–45. doi:10.3109/17435390.2010.530004. http://www.ncbi.nlm.nih.gov/pubmed/21043986
105. Ryan JJ, Bateman HR, Stover A, Gomez G, Norton SK, Zhao W, et al. Fullerene nanomaterials inhibit the allergic response. J Immunol. 2007;179(1):665–72. http://www.ncbi.nlm.nih.gov/pubmed/17579089
106. Norton SK, Wijesinghe DS, Dellinger A, Sturgill J, Zhou Z, Barbour S, et al. Epoxyeicosatrienoic acids are involved in the C(70) fullerene derivative-induced control of allergic asthma. J Allergy Clin Immunol. 2012;130 3:761–769 e2; doi:10.1016/j.jaci.2012.04.023. http://www.ncbi.nlm.nih.gov/pubmed/22664166.
107. Djordjevic A, Bogdanovic G, Dobric S. Fullerenes in biomedicine. J BUON. 2006;11(4):391–404. http://www.ncbi.nlm.nih.gov/pubmed/17309168
108. Umemoto EY, Speck M, Shimoda LM, Kahue K, Sung C, Stokes AJ, et al. Single-walled carbon nanotube exposure induces membrane rearrangement and suppression of receptor-mediated signalling pathways in model mast cells. Toxicol Lett. 2014;229(1):198–209. doi:10.1016/j.toxlet.2014.06.009. http://www.ncbi.nlm.nih.gov/pubmed/24910985
109. Feltis BN, Elbaz A, Wright PF, Mackay GA, Turney TW, Lopata AL. Characterizing the inhibitory action of zinc oxide nanoparticles on allergic-type mast cell activation. Mol Immunol. 2015;66(2):139–46. doi:10.1016/j.molimm.2015.02.021. http://www.ncbi.nlm.nih.gov/pubmed/25771180
110. Alessandrini F, Beck-Speier I, Krappmann D, Weichenmeier I, Takenaka S, Karg E, et al. Role of oxidative stress in ultrafine particle-induced exacerbation of allergic lung inflammation. Am J Respir Crit Care Med. 2009;179(11):984–91. doi:10.1164/rccm.200807-1061OC. http://www.ncbi.nlm.nih.gov/pubmed/19264975
111. Park HS, Kim KH, Jang S, Park JW, Cha HR, Lee JE, et al. Attenuation of allergic airway inflammation and hyperresponsiveness in a murine model of asthma by silver nanoparticles. Int J Nanomedicine. 2010;5:505–15. http://www.ncbi.nlm.nih.gov/pubmed/20957173
112. Jang S, Park JW, Cha HR, Jung SY, Lee JE, Jung SS, et al. Silver nanoparticles modify VEGF signaling pathway and mucus hypersecretion in allergic airway inflammation. Int J Nanomedicine. 2012;7:1329–43. doi:10.2147/IJN.S27159. http://www.ncbi.nlm.nih.gov/pubmed/22457593
113. He D, Garg S, Waite TD. H2O2-mediated oxidation of zero-valent silver and resultant interactions among silver nanoparticles, silver ions, and reactive oxygen species. Langmuir. 2012;28(27):10266–75. doi:10.1021/la300929g. http://www.ncbi.nlm.nih.gov/pubmed/22616806
114. Hsin YH, Chen CF, Huang S, Shih TS, Lai PS, Chueh PJ. The apoptotic effect of nanosilver is mediated by a ROS- and JNK-dependent mechanism involving the mitochondrial pathway in NIH3T3 cells. Toxicol lett. 2008;179(3):130–9. doi:10.1016/j.toxlet.2008.04.015. http://www.ncbi.nlm.nih.gov/pubmed/18547751
115. Piao MJ, Kang KA, Lee IK, Kim HS, Kim S, Choi JY, et al. Silver nanoparticles induce oxidative cell damage in human liver cells through inhibition of reduced glutathione and induction of mitochondria-involved apoptosis. Toxicology lett. 2011;201(1):92–100. doi:10.1016/j.toxlet.2010.12.010. http://www.ncbi.nlm.nih.gov/pubmed/21182908
116. Chuang HC, Hsiao TC, Wu CK, Chang HH, Lee CH, Chang CC, et al. Allergenicity and toxicology of inhaled silver nanoparticles in allergen-provocation mice models. Int J Nanomedicine. 2013;8:4495–506. doi:10.2147/IJN.S52239. http://www.ncbi.nlm.nih.gov/pubmed/24285922
117. Barreto E, Serra MF, Dos Santos RV, Dos Santos CE, Hickmann J, Cotias AC, et al. Local Administration of Gold Nanoparticles Prevents Pivotal Pathological Changes in Murine Models of Atopic Asthma. J Biomed Nanotechnol. 2015;11(6):1038–50. http://www.ncbi.nlm.nih.gov/pubmed/26353593
118. Scarino A, Noel A, Renzi PM, Cloutier Y, Vincent R, Truchon G, et al. Impact of emerging pollutants on pulmonary inflammation in asthmatic rats: ethanol vapors and agglomerated TiO2 nanoparticles. Inhal Toxicol. 2012;24(8):528–38. doi:10.3109/08958378.2012.696741. http://www.ncbi.nlm.nih.gov/pubmed/22746402
119. Gustafsson A, Jonasson S, Sandstrom T, Lorentzen JC, Bucht A. Genetic variation influences immune responses in sensitive rats following exposure to TiO2 nanoparticles. Toxicology. 2014;326:74–85. doi:10.1016/j.tox.2014.10.004. http://www.ncbi.nlm.nih.gov/pubmed/25456268
120. Jonasson S, Gustafsson A, Koch B, Bucht A. Inhalation exposure of nano-scaled titanium dioxide (TiO2) particles alters the inflammatory responses in asthmatic mice. Inhal Toxicol. 2013;25(4):179–91. doi:10.3109/08958378.2013.770939. http://www.ncbi.nlm.nih.gov/pubmed/23480194
121. Radauer-Preiml I, Andosch A, Hawranek T, Luetz-Meindl U, Wiederstein M, Horejs-Hoeck J, et al. Nanoparticle-allergen interactions mediate human

allergic responses: protein corona characterization and cellular responses. Part Fibre Toxicol. 2016;13:3. doi:10.1186/s12989-016-0113-0. http://www.ncbi.nlm.nih.gov/pubmed/26772182
122. Babin K, Antoine F, Goncalves DM, Girard D. TiO2, CeO2 and ZnO nanoparticles and modulation of the degranulation process in human neutrophils. Toxicol Lett. 2013;221(1):57–63. doi:10.1016/j.toxlet.2013.05.010. http://www.ncbi.nlm.nih.gov/pubmed/23726862
123. Johnston H, Brown DM, Kanase N, Euston M, Gaiser BK, Robb CT, et al. Mechanism of neutrophil activation and toxicity elicited by engineered nanomaterials. Toxicol In Vitro. 2015;29(5):1172–84. doi:10.1016/j.tiv.2015.04.021. http://www.ncbi.nlm.nih.gov/pubmed/25962642
124. Vallieres F, Simard JC, Noel C, Murphy-Marion M, Lavastre V, Girard D. Activation of human AML14.3D10 eosinophils by nanoparticles: Modulatory activity on apoptosis and cytokine production. J Immunotoxicol. 2016:1–10. doi:10.1080/1547691X.2016.1203379. http://www.ncbi.nlm.nih.gov/pubmed/27404512
125. Silva LR, Girard D. Human eosinophils are direct targets to nanoparticles: Zinc oxide nanoparticles (ZnO) delay apoptosis and increase the production of the pro-inflammatory cytokines IL-1beta and IL-8. Toxicol Lett. 2016;259:11–20. doi:10.1016/j.toxlet.2016.07.020. http://www.ncbi.nlm.nih.gov/pubmed/27452280
126. Zhang Q, Kusaka Y, Sato K, Nakakuki K, Kohyama N, Donaldson K. Differences in the extent of inflammation caused by intratracheal exposure to three ultrafine metals: role of free radicals. J Toxicol Environ Health A. 1998;53(6):423–38. http://www.ncbi.nlm.nih.gov/pubmed/9537280
127. Dick CA, Brown DM, Donaldson K, Stone V. The role of free radicals in the toxic and inflammatory effects of four different ultrafine particle types. Inhal Toxicol. 2003;15(1):39–52. doi:10.1080/08958370304454. http://www.ncbi.nlm.nih.gov/pubmed/12476359
128. Stone V, Miller MR, Clift MJD, Elder A, Mills NL, Moller P, et al. Nanomaterials Versus Ambient Ultrafine Particles: An Opportunity to Exchange Toxicology Knowledge. Environ Health Perspect. 2017;125(10):106002. doi:10.1289/EHP424. https://www.ncbi.nlm.nih.gov/pubmed/29017987
129. Braakhuis HM, Oomen AG, Cassee FR. Grouping nanomaterials to predict their potential to induce pulmonary inflammation. Toxicol Appl Pharmacol. 2016;299:3–7. doi:10.1016/j.taap.2015.11.009. https://www.ncbi.nlm.nih.gov/pubmed/26603513
130. Dunican EM, Fahy JV. The Role of Type 2 Inflammation in the Pathogenesis of Asthma Exacerbations. Annals Am Thoracic Soc. 2015;12(Suppl 2):S144–9. doi:10.1513/AnnalsATS.201506-377AW. http://www.ncbi.nlm.nih.gov/pubmed/26595730
131. An SS, Mitzner W, Tang WY, Ahn K, Yoon AR, Huang J, et al. An inflammation-independent contraction mechanophenotype of airway smooth muscle in asthma. J Allergy Clin Immunol. 2016;138 1:294–297 e4; doi:10.1016/j.jaci.2015.12.1315. http://www.ncbi.nlm.nih.gov/pubmed/26936804.
132. Seiffert J, Hussain F, Wiegman C, Li F, Bey L, Baker W, et al. Pulmonary toxicity of instilled silver nanoparticles: influence of size, coating and rat strain. PloS one. 2015;10(3):e0119726. doi:10.1371/journal.pone.0119726. http://www.ncbi.nlm.nih.gov/pubmed/25747867
133. Scuri M, Chen BT, Castranova V, Reynolds JS, Johnson VJ, Samsell L, et al. Effects of titanium dioxide nanoparticle exposure on neuroimmune responses in rat airways. J Toxicol Environ Health A. 2010;73(20):1353–69. doi:10.1080/15287394.2010.497436. http://www.ncbi.nlm.nih.gov/pubmed/20818535
134. Rydman EM, Ilves M, Koivisto AJ, Kinaret PA, Fortino V, Savinko TS, et al. Inhalation of rod-like carbon nanotubes causes unconventional allergic airway inflammation. Part Fibre Toxicol. 2014;11:48. doi:10.1186/s12989-014-0048-2. http://www.ncbi.nlm.nih.gov/pubmed/25318534
135. Beamer CA, Girtsman TA, Seaver BP, Finsaas KJ, Migliaccio CT, Perry VK, et al. IL-33 mediates multi-walled carbon nanotube (MWCNT)-induced airway hyper-reactivity via the mobilization of innate helper cells in the lung. Nanotoxicology. 2013;7(6):1070–81. doi:10.3109/17435390.2012.702230. http://www.ncbi.nlm.nih.gov/pubmed/22686327
136. Hsieh WY, Chou CC, Ho CC, Yu SL, Chen HY, Chou HY, et al. Single-walled carbon nanotubes induce airway hyperreactivity and parenchymal injury in mice. Am J Respir Cell Mol Biol. 2012;46(2):257–67. doi:10.1165/rcmb.2011-0010OC. http://www.ncbi.nlm.nih.gov/pubmed/21960547
137. Lauzon AM, Martin JG. Airway hyperresponsiveness; smooth muscle as the principal actor. F1000Research. 2016;5; doi:10.12688/f1000research.7422.1. http://www.ncbi.nlm.nih.gov/pubmed/26998246.
138. Husain M, Saber AT, Guo C, Jacobsen NR, Jensen KA, Yauk CL, et al. Pulmonary instillation of low doses of titanium dioxide nanoparticles in mice leads to particle retention and gene expression changes in the absence of inflammation. Toxicol Appl Pharmacol. 2013;269(3):250–62. doi:10.1016/j.taap.2013.03.018. http://www.ncbi.nlm.nih.gov/pubmed/23557971
139. Gonzalez C, Salazar-Garcia S, Palestino G, Martinez-Cuevas PP, Ramirez-Lee MA, Jurado-Manzano BB, et al. Effect of 45 nm silver nanoparticles (AgNPs) upon the smooth muscle of rat trachea: role of nitric oxide. Toxicol Lett. 2011;207(3):306–13. doi:10.1016/j.toxlet.2011.09.024. http://www.ncbi.nlm.nih.gov/pubmed/21983655
140. Kapilevich LV, Zaytseva TN, Nosarev AV, Agev BG, Dyakova EY, Ogorodova LM, et al. Contractile reactions of guinea pig airway smooth muscles in the presence of stannum oxide nanosized particles. Bull Exp Biol Med. 2012;153(1):98–100. http://www.ncbi.nlm.nih.gov/pubmed/22808504
141. Kapilevich LV, Zaitseva TN, Nosarev AV, D'iakova E, Petlina ZR, Ogorodova LM, et al. Influence of nanosize particles of cobalt ferrite on contractile responses of smooth muscle segment of airways. Rossiiskii fiziologicheskii zhurnal imeni IM Sechenova. 2012;98 2:228–35. http://www.ncbi.nlm.nih.gov/pubmed/22650066.
142. Arvizo RR, Miranda OR, Thompson MA, Pabelick CM, Bhattacharya R, Robertson JD, et al. Effect of nanoparticle surface charge at the plasma membrane and beyond. Nano lett. 2010;10(7):2543–8. doi:10.1021/nl101140t. http://www.ncbi.nlm.nih.gov/pubmed/20533851
143. Berntsen P, Park CY, Rothen-Rutishauser B, Tsuda A, Sager TM, Molina RM, et al. Biomechanical effects of environmental and engineered particles on human airway smooth muscle cells. J R Soc Interface. 2010;7(Suppl 3):S331–40. doi:10.1098/rsif.2010.0068.focus. http://www.ncbi.nlm.nih.gov/pubmed/20356875
144. Benayoun L, Druilhe A, Dombret MC, Aubier M, Pretolani M. Airway structural alterations selectively associated with severe asthma. Am J Respir Crit Care Med. 2003;167(10):1360–8. doi:10.1164/rccm.200209-1030OC. http://www.ncbi.nlm.nih.gov/pubmed/12531777
145. Li B, Yang J, Huang Q, Zhang Y, Peng C, Zhang Y, et al. Biodistribution and pulmonary toxicity of intratracheally instilled graphene oxide in mice. NPG Asia Materials. 2013;5(4):e44.
146. Glista-Baker EE, Taylor AJ, Sayers BC, Thompson EA, Bonner JC. Nickel nanoparticles cause exaggerated lung and airway remodeling in mice lacking the T-box transcription factor, TBX21 (T-bet). Part Fibre Toxicol. 2014;11:7. doi:10.1186/1743-8977-11-7. http://www.ncbi.nlm.nih.gov/pubmed/24499286
147. Hussain S, Ji Z, Taylor AJ, DeGraff LM, George M, Tucker CJ, et al. Multiwalled Carbon Nanotube Functionalization with High Molecular Weight Hyaluronan Significantly Reduces Pulmonary Injury. ACS nano. 2016;10(8):7675–88. doi:10.1021/acsnano.6b03013. http://www.ncbi.nlm.nih.gov/pubmed/27459049
148. Wang X, Duch MC, Mansukhani N, Ji Z, Liao YP, Wang M, et al. Use of a pro-fibrogenic mechanism-based predictive toxicological approach for tiered testing and decision analysis of carbonaceous nanomaterials. ACS Nano. 2015;9(3):3032–43. https://www.ncbi.nlm.nih.gov/pubmed/25646681. doi:10.1021/nn507243w.
149. Ma JY, Mercer RR, Barger M, Schwegler-Berry D, Scabilloni J, Ma JK, et al. Induction of pulmonary fibrosis by cerium oxide nanoparticles. Toxicol Appl Pharmacol. 2012;262(3):255–64. doi:10.1016/j.taap.2012.05.005. https://www.ncbi.nlm.nih.gov/pubmed/22613087
150. Ma J, Bishoff B, Mercer RR, Barger M, Schwegler-Berry D, Castranova V. Role of epithelial-mesenchymal transition (EMT) and fibroblast function in cerium oxide nanoparticles-induced lung fibrosis. Toxicol Appl Pharmacol. 2017;323:16–25. doi:10.1016/j.taap.2017.03.015. https://www.ncbi.nlm.nih.gov/pubmed/28315692
151. Jacobsen NR, Stoeger T, van den Brule S, Saber AT, Beyerle A, Vietti G, et al. Acute and subacute pulmonary toxicity and mortality in mice after intratracheal instillation of ZnO nanoparticles in three laboratories. Food Chem Toxicol. 2015;85:84–95. doi:10.1016/j.fct.2015.08.008. https://www.ncbi.nlm.nih.gov/pubmed/26260750
152. Hussain S, Sangtian S, Anderson SM, Snyder RJ, Marshburn JD, Rice AB, et al. Inflammasome activation in airway epithelial cells after multi-walled carbon nanotube exposure mediates a profibrotic response in lung fibroblasts. Part Fibre Toxicol. 2014;11:28. doi:10.1186/1743-8977-11-28. http://www.ncbi.nlm.nih.gov/pubmed/24915862
153. Wang X, Shannahan JH, Brown JM. IL-33 modulates chronic airway resistance changes induced by multi-walled carbon nanotubes. Inhal Toxicol. 2014;26(4):240–9. doi:10.3109/08958378.2014.880202. http://www.ncbi.nlm.nih.gov/pubmed/24502429

154. Wang P, Wang Y, Nie X, Braini C, Bai R, Chen C. Multiwall carbon nanotubes directly promote fibroblast-myofibroblast and epithelial-mesenchymal transitions through the activation of the TGF-beta/Smad signaling pathway. Small. 2015;11(4):446–55. doi:10.1002/smll.201303588. http://www.ncbi.nlm.nih.gov/pubmed/25255886
155. Chen T, Nie H, Gao X, Yang J, Pu J, Chen Z, et al. Epithelial-mesenchymal transition involved in pulmonary fibrosis induced by multi-walled carbon nanotubes via TGF-beta/Smad signaling pathway. Toxicol Lett. 2014;226(2):150–62. doi:10.1016/j.toxlet.2014.02.004. http://www.ncbi.nlm.nih.gov/pubmed/24530353
156. Chen EY, Wang YC, Chen CS, Chin WC. Functionalized positive nanoparticles reduce mucin swelling and dispersion. PLoS One. 2010;5(11):e15434. doi:10.1371/journal.pone.0015434. http://www.ncbi.nlm.nih.gov/pubmed/21085670
157. Ahn MH, Kang CM, Park CS, Park SJ, Rhim T, Yoon PO, et al. Titanium dioxide particle-induced goblet cell hyperplasia: association with mast cells and IL-13. Respir Res. 2005;6:34. doi:10.1186/1465-9921-6-34. http://www.ncbi.nlm.nih.gov/pubmed/15829015
158. Chen EY, Garnica M, Wang YC, Chen CS, Chin WC. Mucin secretion induced by titanium dioxide nanoparticles. PloS one. 2011;6(1):e16198. doi:10.1371/journal.pone.0016198. http://www.ncbi.nlm.nih.gov/pubmed/21283816
159. Ko JW, Park JW, Shin NR, Kim JH, Cho YK, Shin DH, et al. Copper oxide nanoparticle induces inflammatory response and mucus production via MAPK signaling in human bronchial epithelial cells. Environ Toxicol Pharmacol. 2016;43:21–6. doi:10.1016/j.etap.2016.02.008. http://www.ncbi.nlm.nih.gov/pubmed/26934431
160. Kim YM, Reed W, Lenz AG, Jaspers I, Silbajoris R, Nick HS, et al. Ultrafine carbon particles induce interleukin-8 gene transcription and p38 MAPK activation in normal human bronchial epithelial cells. Am J Physiol Lung Cell Mol Physiol. 2005;288(3):L432–41. doi:10.1152/ajplung.00285.2004. http://www.ncbi.nlm.nih.gov/pubmed/15695543
161. Val S, Hussain S, Boland S, Hamel R, Baeza-Squiban A, Marano F. Carbon black and titanium dioxide nanoparticles induce pro-inflammatory responses in bronchial epithelial cells: need for multiparametric evaluation due to adsorption artifacts. Inhal Toxicol. 2009;21(Suppl 1):115–22. doi:10.1080/08958370902942533. http://www.ncbi.nlm.nih.gov/pubmed/19558243
162. Ursini CL, Maiello R, Ciervo A, Fresegna AM, Buresti G, Superti F, et al. Evaluation of uptake, cytotoxicity and inflammatory effects in respiratory cells exposed to pristine and -OH and -COOH functionalized multi-wall carbon nanotubes. J Appl Toxicol. 2016;36(3):394–403. doi:10.1002/jat.3228. http://www.ncbi.nlm.nih.gov/pubmed/26370214
163. Frieke Kuper C, Grollers-Mulderij M, Maarschalkerweerd T, Meulendijks NM, Reus A, van Acker F, et al. Toxicity assessment of aggregated/agglomerated cerium oxide nanoparticles in an in vitro 3D airway model: the influence of mucociliary clearance. Toxicol In Vitro. 2015;29(2):389–97. doi:10.1016/j.tiv.2014.10.017. http://www.ncbi.nlm.nih.gov/pubmed/25448805
164. Skuland T, Ovrevik J, Lag M, Schwarze P, Refsnes M. Silica nanoparticles induce cytokine responses in lung epithelial cells through activation of a p38/TACE/TGF-alpha/EGFR-pathway and NF-kappaBeta signalling. Toxicol Appl Pharmacol. 2014;279(1):76–86. doi:10.1016/j.taap.2014.05.006. http://www.ncbi.nlm.nih.gov/pubmed/24844442
165. Verstraelen S, Remy S, Casals E, De Boever P, Witters H, Gatti A, et al. Gene expression profiles reveal distinct immunological responses of cobalt and cerium dioxide nanoparticles in two in vitro lung epithelial cell models. Toxicol Lett. 2014;228(3):157–69. doi:10.1016/j.toxlet.2014.05.006. http://www.ncbi.nlm.nih.gov/pubmed/24821434
166. Jing X, Park JH, Peters TM, Thorne PS. Toxicity of copper oxide nanoparticles in lung epithelial cells exposed at the air-liquid interface compared with in vivo assessment. Toxicol In Vitro. 2015;29(3):502–11. doi:10.1016/j.tiv.2014.12.023. http://www.ncbi.nlm.nih.gov/pubmed/25575782
167. Wu W, Samet JM, Peden DB, Bromberg PA. Phosphorylation of p65 is required for zinc oxide nanoparticle-induced interleukin 8 expression in human bronchial epithelial cells. Environ Health Perspect. 2010;118(7):982–7. doi:10.1289/ehp.0901635. http://www.ncbi.nlm.nih.gov/pubmed/20194077
168. Kraneveld AD, van der Kleij HP, Kool M, van Houwelingen AH, Weitenberg AC, Redegeld FA, et al. Key role for mast cells in nonatopic asthma. J Immunol. 2002;169(4):2044–53. http://www.ncbi.nlm.nih.gov/pubmed/12165531
169. Katwa P, Wang X, Urankar RN, Podila R, Hilderbrand SC, Fick RB, et al. A carbon nanotube toxicity paradigm driven by mast cells and the IL-(3)(3)/ST(2) axis. Small. 2012;8(18):2904–12. doi:10.1002/smll.201200873. http://www.ncbi.nlm.nih.gov/pubmed/22777948
170. Moldaver DM, Larche M, Rudulier CD. An update on lymphocyte subtypes in Asthma and Airway Disease. Chest. 2016; doi:10.1016/j.chest.2016.10.038. http://www.ncbi.nlm.nih.gov/pubmed/27818326
171. Kim HY, Lee HJ, Chang YJ, Pichavant M, Shore SA, Fitzgerald KA, et al. Interleukin-17-producing innate lymphoid cells and the NLRP3 inflammasome facilitate obesity-associated airway hyperreactivity. Nat Med. 2014;20(1):54–61. doi:10.1038/nm.3423. http://www.ncbi.nlm.nih.gov/pubmed/24336249
172. Johnston NW, Sears MR. Asthma exacerbations.1: epidemiology. Thorax. 2006;61(8):722–8. doi:10.1136/thx.2005.045161. http://www.ncbi.nlm.nih.gov/pubmed/16877691
173. Gill MA, Bajwa G, George TA, Dong CC, Dougherty II, Jiang N, et al. Counterregulation between the FcepsilonRI pathway and antiviral responses in human plasmacytoid dendritic cells. J Immunol. 2010;184(11):5999–6006. doi:10.4049/jimmunol.0901194. http://www.ncbi.nlm.nih.gov/pubmed/20410486
174. Durrani SR, Montville DJ, Pratt AS, Sahu S, DeVries MK, Rajamanickam V, et al. Innate immune responses to rhinovirus are reduced by the high-affinity IgE receptor in allergic asthmatic children. J Allergy Clin Immunol. 2012;130(2):489–95. doi:10.1016/j.jaci.2012.05.023. http://www.ncbi.nlm.nih.gov/pubmed/22766097
175. Lambert AL, Trasti FS, Mangum JB, Everitt JI. Effect of preexposure to ultrafine carbon black on respiratory syncytial virus infection in mice. Toxicol Sci. 2003;72(2):331–8. doi:10.1093/toxsci/kfg031. http://www.ncbi.nlm.nih.gov/pubmed/12660365
176. Lambert AL, Mangum JB, DeLorme MP, Everitt JI. Ultrafine carbon black particles enhance respiratory syncytial virus-induced airway reactivity, pulmonary inflammation, and chemokine expression. Toxicol Sci. 2003;72(2):339–46. doi:10.1093/toxsci/kfg032. http://www.ncbi.nlm.nih.gov/pubmed/12655033
177. Hashiguchi S, Yoshida H, Akashi T, Komemoto K, Ueda T, Ikarashi Y, et al. Titanium dioxide nanoparticles exacerbate pneumonia in respiratory syncytial virus (RSV)-infected mice. Environ Toxicol Pharmacol. 2015;39(2):879–86. doi:10.1016/j.etap.2015.02.017. http://www.ncbi.nlm.nih.gov/pubmed/25795424
178. Bawage SS, Tiwari PM, Singh A, Dixit S, Pillai SR, Dennis VA, et al. Gold nanorods inhibit respiratory syncytial virus by stimulating the innate immune response. Nanomedicine. 2016;12(8):2299–310. doi:10.1016/j.nano.2016.06.006. http://www.ncbi.nlm.nih.gov/pubmed/27381068
179. Sanpui P, Zheng X, Loeb JC, Bisesi JH Jr, Khan IA, Afrooz AR, et al. Single-walled carbon nanotubes increase pandemic influenza A H1N1 virus infectivity of lung epithelial cells. Part Fibre Toxicol. 2014;11:66. doi:10.1186/s12989-014-0066-0. http://www.ncbi.nlm.nih.gov/pubmed/25497303
180. Wei L, Lu J, Xu H, Patel A, Chen ZS, Chen G. Silver nanoparticles: synthesis, properties, and therapeutic applications. Drug Discov Today. 2015;20(5):595–601. doi:10.1016/j.drudis.2014.11.014. http://www.ncbi.nlm.nih.gov/pubmed/25543008
181. McKenzie Z, Kendall M, Mackay RM, Tetley TD, Morgan C, Griffiths M, et al. Nanoparticles modulate surfactant protein A and D mediated protection against influenza A infection in vitro. Philos Trans R Soc Lond B Biol Sci. 2015;370(1661):20140049. doi:10.1098/rstb.2014.0049. http://www.ncbi.nlm.nih.gov/pubmed/25533100
182. Blank F, Gerber P, Rothen-Rutishauser B, Sakulkhu U, Salaklang J, De Peyer K, et al. Biomedical nanoparticles modulate specific CD4+ T cell stimulation by inhibition of antigen processing in dendritic cells. Nanotoxicology. 2011;5(4):606–21. doi:10.3109/17435390.2010.541293. http://www.ncbi.nlm.nih.gov/pubmed/21231795
183. Fromen CA, Robbins GR, Shen TW, Kai MP, Ting JP, DeSimone JM. Controlled analysis of nanoparticle charge on mucosal and systemic antibody responses following pulmonary immunization. Proceedings of the National Academy of Sciences of the United States of America. 2015;112(2):488–93. doi:10.1073/pnas.1422923112. http://www.ncbi.nlm.nih.gov/pubmed/25548169
184. Fromen CA, Rahhal TB, Robbins GR, Kai MP, Shen TW, Luft JC, et al. Nanoparticle surface charge impacts distribution, uptake and lymph node trafficking by pulmonary antigen-presenting cells. Nanomedicine. 2016;12(3):677–87. doi:10.1016/j.nano.2015.11.002. http://www.ncbi.nlm.nih.gov/pubmed/26656533
185. Seydoux E, Rodriguez-Lorenzo L, Blom RA, Stumbles PA, Petri-Fink A, Rothen-Rutishauser BM, et al. Pulmonary delivery of cationic gold nanoparticles boost antigen-specific CD4+ T Cell Proliferation.

Nanomedicine. 2016;12(7):1815–26. doi:10.1016/j.nano.2016.02.020. http://www.ncbi.nlm.nih.gov/pubmed/27013126
186. Choi HS, Ashitate Y, Lee JH, Kim SH, Matsui A, Insin N, et al. Rapid translocation of nanoparticles from the lung airspaces to the body. Nat Biotechnol. 2010;28(12):1300–3. doi:10.1038/nbt.1696. http://www.ncbi.nlm.nih.gov/pubmed/21057497
187. Blank F, Stumbles PA, Seydoux E, Holt PG, Fink A, Rothen-Rutishauser B, et al. Size-dependent uptake of particles by pulmonary antigen-presenting cell populations and trafficking to regional lymph nodes. Am J Respir Cell Mol Biol. 2013;49(1):67–77. doi:10.1165/rcmb.2012-0387OC. http://www.ncbi.nlm.nih.gov/pubmed/23492193
188. Stano A, Nembrini C, Swartz MA, Hubbell JA, Simeoni E. Nanoparticle size influences the magnitude and quality of mucosal immune responses after intranasal immunization. Vaccine. 2012;30(52):7541–6. doi:10.1016/j.vaccine.2012.10.050. http://www.ncbi.nlm.nih.gov/pubmed/23103199
189. Mottram PL, Leong D, Crimeen-Irwin B, Gloster S, Xiang SD, Meanger J, et al. Type 1 and 2 immunity following vaccination is influenced by nanoparticle size: formulation of a model vaccine for respiratory syncytial virus. Mol Pharm. 2007;4(1):73–84. doi:10.1021/mp060096p. http://www.ncbi.nlm.nih.gov/pubmed/17274665
190. Kundig TM, Klimek L, Schendzielorz P, Renner WA, Senti G, Bachmann MF. Is The Allergen Really Needed in Allergy Immunotherapy? Curr Treat Options Allergy. 2015;2(1):72–82. doi:10.1007/s40521-014-0038-5. http://www.ncbi.nlm.nih.gov/pubmed/25722959
191. Ballester M, Jeanbart L, de Titta A, Nembrini C, Marsland BJ, Hubbell JA, et al. Nanoparticle conjugation enhances the immunomodulatory effects of intranasally delivered CpG in house dust mite-allergic mice. Sci Rep. 2015;5:14274. doi:10.1038/srep14274. http://www.ncbi.nlm.nih.gov/pubmed/26387548
192. Hirai T, Yoshioka Y, Izumi N, Ichihashi K, Handa T, Nishijima N, et al. Metal nanoparticles in the presence of lipopolysaccharides trigger the onset of metal allergy in mice. Nat Nanotechnol. 2016;11(9):808–16. doi:10.1038/nnano.2016.88. http://www.ncbi.nlm.nih.gov/pubmed/27240418
193. Mano SS, Kanehira K, Taniguchi A. Comparison of cellular uptake and inflammatory response via toll-like receptor 4 to lipopolysaccharide and titanium dioxide nanoparticles. Int J Mol Sci. 2013;14(7):13154–70. doi:10.3390/ijms140713154. http://www.ncbi.nlm.nih.gov/pubmed/23803652
194. Chen JK, Ho CC, Chang H, Lin JF, Yang CS, Tsai MH, et al. Particulate nature of inhaled zinc oxide nanoparticles determines systemic effects and mechanisms of pulmonary inflammation in mice. Nanotoxicol. 2015;9(1):43–53. doi:10.3109/17435390.2014.886740. http://www.ncbi.nlm.nih.gov/pubmed/24559390
195. Lelieveld J, Evans JS, Fnais M, Giannadaki D, Pozzer A. The contribution of outdoor air pollution sources to premature mortality on a global scale. Nat. 2015;525(7569):367–71. doi:10.1038/nature15371. http://www.ncbi.nlm.nih.gov/pubmed/26381985
196. Guarnieri M, Balmes JR. Outdoor air pollution and asthma. Lancet. 2014;383(9928):1581–92. doi:10.1016/S0140-6736(14)60617-6. http://www.ncbi.nlm.nih.gov/pubmed/24792855
197. Khreis H, Kelly C, Tate J, Parslow R, Lucas K, Nieuwenhuijsen M. Exposure to traffic-related air pollution and risk of development of childhood asthma: A systematic review and meta-analysis. Environ Int. 2016; doi:10.1016/j.envint.2016.11.012. http://www.ncbi.nlm.nih.gov/pubmed/27881237
198. Zheng XY, Ding H, Jiang LN, Chen SW, Zheng JP, Qiu M, et al. Association between Air Pollutants and Asthma Emergency Room Visits and Hospital Admissions in Time Series Studies: A Systematic Review and Meta-Analysis. PloS One. 2015;10(9):e0138146. doi:10.1371/journal.pone.0138146. http://www.ncbi.nlm.nih.gov/pubmed/26382947
199. Bowatte G, Lodge C, Lowe AJ, Erbas B, Perret J, Abramson MJ, et al. The influence of childhood traffic-related air pollution exposure on asthma, allergy and sensitization: a systematic review and a meta-analysis of birth cohort studies. Allergy. 2015;70(3):245–56. doi:10.1111/all.12561. http://www.ncbi.nlm.nih.gov/pubmed/25495759
200. Peters A, Wichmann HE, Tuch T, Heinrich J, Heyder J. Respiratory effects are associated with the number of ultrafine particles. Am J Respir Crit Care Med. 1997;155(4):1376–83. doi:10.1164/ajrccm.155.4.9105082. http://www.ncbi.nlm.nih.gov/pubmed/9105082
201. von Klot S, Wolke G, Tuch T, Heinrich J, Dockery DW, Schwartz J, et al. Increased asthma medication use in association with ambient fine and ultrafine particles. Eur Respir J. 2002;20(3):691–702. http://www.ncbi.nlm.nih.gov/pubmed/12358349
202. Lwebuga-Mukasa JS, Oyana TJ, Johnson C. Local ecological factors, ultrafine particulate concentrations, and asthma prevalence rates in Buffalo, New York, neighborhoods. J Asthma. 2005;42(5):337–48. doi:10.1081/JAS-62972. http://www.ncbi.nlm.nih.gov/pubmed/16036408
203. Penttinen P, Timonen KL, Tiittanen P, Mirme A, Ruuskanen J, Pekkanen J. Ultrafine particles in urban air and respiratory health among adult asthmatics. Eur Respir J. 2001;17(3):428–35. http://www.ncbi.nlm.nih.gov/pubmed/11405521
204. Penttinen P, Timonen KL, Tiittanen P, Mirme A, Ruuskanen J, Pekkanen J. Number concentration and size of particles in urban air: effects on spirometric lung function in adult asthmatic subjects. Environ Health Perspect. 2001;109(4):319–23. http://www.ncbi.nlm.nih.gov/pubmed/11335178
205. McCreanor J, Cullinan P, Nieuwenhuijsen MJ, Stewart-Evans J, Malliarou E, Jarup L, et al. Respiratory effects of exposure to diesel traffic in persons with asthma. N Engl J Med. 2007;357(23):2348–58. doi:10.1056/NEJMoa071535. http://www.ncbi.nlm.nih.gov/pubmed/18057337
206. Zhang JJ, McCreanor JE, Cullinan P, Chung KF, Ohman-Strickland P, Han IK, et al. Health effects of real-world exposure to diesel exhaust in persons with asthma. Res Rep Health Eff Inst. 2009;138:5–109. discussion 11–23. http://www.ncbi.nlm.nih.gov/pubmed/19449765
207. Pekkanen J, Timonen KL, Ruuskanen J, Reponen A, Mirme A. Effects of ultrafine and fine particles in urban air on peak expiratory flow among children with asthmatic symptoms. Environ Res. 1997;74(1):24–33. doi:10.1006/enrs.1997.3750. http://www.ncbi.nlm.nih.gov/pubmed/9339211
208. Iskandar A, Andersen ZJ, Bonnelykke K, Ellermann T, Andersen KK, Bisgaard H. Coarse and fine particles but not ultrafine particles in urban air trigger hospital admission for asthma in children. Thorax. 2012;67(3):252–7. doi:10.1136/thoraxjnl-2011-200324. http://www.ncbi.nlm.nih.gov/pubmed/22156960
209. Evans KA, Halterman JS, Hopke PK, Fagnano M, Rich DQ. Increased ultrafine particles and carbon monoxide concentrations are associated with asthma exacerbation among urban children. Environ Res. 2014;129:11–9. doi:10.1016/j.envres.2013.12.001. http://www.ncbi.nlm.nih.gov/pubmed/24528997
210. Andersen ZJ, Wahlin P, Raaschou-Nielsen O, Ketzel M, Scheike T, Loft S. Size distribution and total number concentration of ultrafine and accumulation mode particles and hospital admissions in children and the elderly in Copenhagen, Denmark. Occup Environ Med. 2008;65(7):458–66. doi:10.1136/oem.2007.033290. http://www.ncbi.nlm.nih.gov/pubmed/17989204
211. Andersen ZJ, Loft S, Ketzel M, Stage M, Scheike T, Hermansen MN, et al. Ambient air pollution triggers wheezing symptoms in infants. Thorax. 2008;63(8):710–6. doi:10.1136/thx.2007.085480. http://www.ncbi.nlm.nih.gov/pubmed/18267985
212. Benor S, Alcalay Y, Domany KA, Gut G, Soferman R, Kivity S, et al. Ultrafine particle content in exhaled breath condensate in airways of asthmatic children. J Breath Res. 2015;9(2):026001. doi:10.1088/1752-7155/9/2/026001. http://www.ncbi.nlm.nih.gov/pubmed/25830607
213. Kim JL, Elfman L, Wieslander G, Ferm M, Toren K, Norback D. Respiratory health among Korean pupils in relation to home, school and outdoor environment. J Korean Med Sci. 2011;26(2):166–73. doi:10.3346/jkms.2011.26.2.166. http://www.ncbi.nlm.nih.gov/pubmed/21286005
214. Delfino RJ, Wu J, Tjoa T, Gullesserian SK, Nickerson B, Gillen DL. Asthma morbidity and ambient air pollution: effect modification by residential traffic-related air pollution. Epidemiology. 2014;25(1):48–57. doi:10.1097/EDE.0000000000000016. http://www.ncbi.nlm.nih.gov/pubmed/24240657
215. Newcomb P, Hunt A, Rast P, Cauble D, Rowe N, Li J. Acute effects of walking environment and GSTM1 variants in children with asthma. Biol Res Nurs. 2012;14(1):55–64. doi:10.1177/1099800410389167. http://www.ncbi.nlm.nih.gov/pubmed/21196426
216. Adar SD, D'Souza J, Sheppard L, Kaufman JD, Hallstrand TS, Davey ME, et al. Adopting Clean Fuels and Technologies on School Buses. Pollution and Health Impacts in Children. Am J Respir Crit Care Med. 2015;191(12):1413–21. doi:10.1164/rccm.201410-1924OC. http://www.ncbi.nlm.nih.gov/pubmed/25867003
217. Gong H Jr, Linn WS, Clark KW, Anderson KR, Sioutas C, Alexis NE, et al. Exposures of healthy and asthmatic volunteers to concentrated ambient ultrafine particles in Los Angeles. Inhal Toxicol. 2008;20(6):533–45. https://doi.org/10.1080/08958370801911340. http://www.ncbi.nlm.nih.gov/pubmed/18444007
218. Schaumann F, Fromke C, Dijkstra D, Alessandrini F, Windt H, Karg E, et al. Effects of ultrafine particles on the allergic inflammation in the lung of asthmatics: results of a double-blinded randomized cross-over clinical pilot study. Part Fibre Toxicol. 2014;11:39. doi:10.1186/s12989-014-0039-3. http://www.ncbi.nlm.nih.gov/pubmed/25204642
219. Pietropaoli AP, Frampton MW, Hyde RW, Morrow PE, Oberdorster G, Cox C, et al. Pulmonary function, diffusing capacity, and inflammation in healthy

and asthmatic subjects exposed to ultrafine particles. Inhal Toxicol. 2004; 16(Suppl 1):59–72. doi:10.1080/08958370490443079. http://www.ncbi.nlm.nih.gov/pubmed/15204794
220. Frampton MW, Utell MJ, Zareba W, Oberdorster G, Cox C, Huang LS, et al. Effects of exposure to ultrafine carbon particles in healthy subjects and subjects with asthma. Res Rep Health Eff Inst. 2004;126:1–47. discussion 9–63. http://www.ncbi.nlm.nih.gov/pubmed/15768531
221. Olvera HA, Perez D, Clague JW, Cheng YS, Li WW, Amaya MA, et al. The effect of ventilation, age, and asthmatic condition on ultrafine particle deposition in children. Pulm Med. 2012;2012:736290. doi:10.1155/2012/736290. http://www.ncbi.nlm.nih.gov/pubmed/22848818
222. Chalupa DC, Morrow PE, Oberdorster G, Utell MJ, Frampton MW. Ultrafine particle deposition in subjects with asthma. Environ Health Perspect. 2004; 112(8):879–82. http://www.ncbi.nlm.nih.gov/pubmed/15175176
223. Shannahan JH, Kodavanti UP, Brown JM. Manufactured and airborne nanoparticle cardiopulmonary interactions: a review of mechanisms and the possible contribution of mast cells. Inhalation toxicology. 2012;24(5):320–39. doi: 10.3109/08958378.2012.668229. http://www.ncbi.nlm.nih.gov/pubmed/22486349
224. Samet JM, Rappold A, Graff D, Cascio WE, Berntsen JH, Huang YC, et al. Concentrated ambient ultrafine particle exposure induces cardiac changes in young healthy volunteers. Am J Respir Crit Care Med. 2009;179(11):1034–42. doi:10.1164/rccm.200807-1043OC. http://www.ncbi.nlm.nih.gov/pubmed/19234105
225. Stolzel M, Breitner S, Cyrys J, Pitz M, Wolke G, Kreyling W, et al. Daily mortality and particulate matter in different size classes in Erfurt, Germany. J Expo Sci Environ Epidemiol. 2007;17(5):458–67. doi:10.1038/sj.jes.7500538. http://www.ncbi.nlm.nih.gov/pubmed/17108895
226. Demedts M, Gyselen A. The cobalt lung in diamond cutters: a new disease. Verh K Acad Geneeskd Belg. 1989;51(6):559–81. http://www.ncbi.nlm.nih.gov/pubmed/2561412
227. Journeay WS, Goldman RH. Occupational handling of nickel nanoparticles: a case report. Am J Ind Med. 2014;57(9):1073–6. doi:10.1002/ajim.22344. http://www.ncbi.nlm.nih.gov/pubmed/24809594
228. Li XY, Gilmour PS, Donaldson K, MacNee W. Free radical activity and pro-inflammatory effects of particulate air pollution (PM10) in vivo and in vitro. Thorax. 1996;51(12):1216–22. http://www.ncbi.nlm.nih.gov/pubmed/8994518
229. Carosino CM, Bein KJ, Plummer LE, Castaneda AR, Zhao Y, Wexler AS, et al. Allergic airway inflammation is differentially exacerbated by daytime and nighttime ultrafine and submicron fine ambient particles: heme oxygenase-1 as an indicator of PM-mediated allergic inflammation. J Toxicol Environ Health A. 2015;78(4):254–66. doi:10.1080/15287394.2014.959627. http://www.ncbi.nlm.nih.gov/pubmed/25679046
230. Becker S, Soukup J. Coarse(PM(2.5-10)), fine(PM(2.5)), and ultrafine air pollution particles induce/increase immune costimulatory receptors on human blood-derived monocytes but not on alveolar macrophages. Journal of toxicology and environmental health Part A. 2003;66(9):847–59. doi:10.1080/15287390306381. http://www.ncbi.nlm.nih.gov/pubmed/12746131
231. Li N, Wang M, Bramble LA, Schmitz DA, Schauer JJ, Sioutas C, et al. The adjuvant effect of ambient particulate matter is closely reflected by the particulate oxidant potential. Environ Health Perspect. 2009;117(7):1116–23. doi:10.1289/ehp.0800319. http://www.ncbi.nlm.nih.gov/pubmed/19654922
232. Li N, Wang M, Barajas B, Sioutas C, Williams MA, Nel AE. Nrf2 deficiency in dendritic cells enhances the adjuvant effect of ambient ultrafine particles on allergic sensitization. J Innate Immun. 2013;5(6):543–54. doi:10.1159/000347060. http://www.ncbi.nlm.nih.gov/pubmed/23595026
233. Wang P, You D, Saravia J, Shen H, Cormier SA. Maternal exposure to combustion generated PM inhibits pulmonary Th1 maturation and concomitantly enhances postnatal asthma development in offspring. Part Fibre Toxicol. 2013;10:29. doi:10.1186/1743-8977-10-29. http://www.ncbi.nlm.nih.gov/pubmed/23856009
234. Balakrishna S, Saravia J, Thevenot P, Ahlert T, Lominiki S, Dellinger B, et al. Environmentally persistent free radicals induce airway hyperresponsiveness in neonatal rat lungs. Part Fibre Toxicol. 2011;8:11. doi:10.1186/1743-8977-8-11. http://www.ncbi.nlm.nih.gov/pubmed/21388553
235. Thevenot PT, Saravia J, Jin N, Giaimo JD, Chustz RE, Mahne S, et al. Radical-containing ultrafine particulate matter initiates epithelial-to-mesenchymal transitions in airway epithelial cells. Am J Respir Cell Mol Biol. 2013;48(2):188–97. doi:10.1165/rcmb.2012-0052OC. http://www.ncbi.nlm.nih.gov/pubmed/23087054
236. Chan JK, Fanucchi MV, Anderson DS, Abid AD, Wallis CD, Dickinson DA, et al. Susceptibility to inhaled flame-generated ultrafine soot in neonatal and adult rat lungs. Toxicol Sci. 2011;124(2):472–86. doi:10.1093/toxsci/kfr233. http://www.ncbi.nlm.nih.gov/pubmed/21914721
237. Shukla A, Timblin C, BeruBe K, Gordon T, McKinney W, Driscoll K, et al. Inhaled particulate matter causes expression of nuclear factor (NF)-kappaB-related genes and oxidant-dependent NF-kappaB activation in vitro. Am J Respir Cell Mol Biol. 2000;23(2):182–7. doi:10.1165/ajrcmb.23.2.4035. http://www.ncbi.nlm.nih.gov/pubmed/10919984
238. Layachi S, Rogerieux F, Robidel F, Lacroix G, Bayat S. Effect of combined nitrogen dioxide and carbon nanoparticle exposure on lung function during ovalbumin sensitization in Brown Norway rat. PloS One. 2012;7(9):e45687. doi:10.1371/journal.pone.0045687. http://www.ncbi.nlm.nih.gov/pubmed/23029182
239. Haland G, Carlsen KC, Sandvik L, Devulapalli CS, Munthe-Kaas MC, Pettersen M, et al. Reduced lung function at birth and the risk of asthma at 10 years of age. N Engl J Med. 2006;355(16):1682–9. doi:10.1056/NEJMoa052885. http://www.ncbi.nlm.nih.gov/pubmed/17050892
240. Gauderman WJ, Avol E, Gilliland F, Vora H, Thomas D, Berhane K, et al. The effect of air pollution on lung development from 10 to 18 years of age. N Engl J Med . 2004;351(11):1057–67. doi:10.1056/NEJMoa040610. http://www.ncbi.nlm.nih.gov/pubmed/15356303
241. Gauderman WJ, Vora H, McConnell R, Berhane K, Gilliland F, Thomas D, et al. Effect of exposure to traffic on lung development from 10 to 18 years of age: a cohort study. Lancet. 2007;369(9561):571–7. doi:10.1016/S0140-6736(07)60037-3. http://www.ncbi.nlm.nih.gov/pubmed/17307103
242. Reibman J, Hsu Y, Chen LC, Kumar A, Su WC, Choy W, et al. Size fractions of ambient particulate matter induce granulocyte macrophage colony-stimulating factor in human bronchial epithelial cells by mitogen-activated protein kinase pathways. Am J Respir Cell Mol Biol. 2002;27(4):455–62. doi:10.1165/rcmb.2001-0005OC. http://www.ncbi.nlm.nih.gov/pubmed/12356579
243. Ramgolam K, Chevaillier S, Marano F, Baeza-Squiban A, Martinon L. Proinflammatory effect of fine and ultrafine particulate matter using size-resolved urban aerosols from Paris. Chemosphere. 2008;72(9):1340–6. doi:10.1016/j.chemosphere.2008.04.025. http://www.ncbi.nlm.nih.gov/pubmed/18555515
244. Ramgolam K, Favez O, Cachier H, Gaudichet A, Marano F, Martinon L, et al. Size-partitioning of an urban aerosol to identify particle determinants involved in the proinflammatory response induced in airway epithelial cells. Part Fibre Toxicol. 2009;6:10. doi:10.1186/1743-8977-6-10. http://www.ncbi.nlm.nih.gov/pubmed/19302717
245. Val S, Martinon L, Cachier H, Yahyaoui A, Marfaing H, Baeza-Squiban A. Role of size and composition of traffic and agricultural aerosols in the molecular responses triggered in airway epithelial cells. Inhal Toxicol. 2011;23(11):627–40. doi:10.3109/08958378.2011.599445. http://www.ncbi.nlm.nih.gov/pubmed/21879948
246. Borgie M, Dagher Z, Ledoux F, Verdin A, Cazier F, Martin P, et al. Comparison between ultrafine and fine particulate matter collected in Lebanon: Chemical characterization, in vitro cytotoxic effects and metabolizing enzymes gene expression in human bronchial epithelial cells. Environ Pollut. 2015;205:250–60. doi:10.1016/j.envpol.2015.05.027. http://www.ncbi.nlm.nih.gov/pubmed/26093079
247. Codispoti CD, LeMasters GK, Levin L, Reponen T, Ryan PH, Biagini Myers JM, et al. Traffic pollution is associated with early childhood aeroallergen sensitization. Ann Allergy Asthma Immunol. 2015;114(2):126–33. doi:10.1016/j.anai.2014.10.020. http://www.ncbi.nlm.nih.gov/pubmed/25499550
248. Brandt EB, Biagini Myers JM, Acciani TH, Ryan PH, Sivaprasad U, Ruff B, et al. Exposure to allergen and diesel exhaust particles potentiates secondary allergen-specific memory responses, promoting asthma susceptibility. J Allergy Clin Immunol. 2015;136(2):295–303 e7. doi:10.1016/j.jaci.2014.11.043. http://www.ncbi.nlm.nih.gov/pubmed/25748065
249. Diaz-Sanchez D, Garcia MP, Wang M, Jyrala M, Saxon A. Nasal challenge with diesel exhaust particles can induce sensitization to a neoallergen in the human mucosa. J Allergy Clin Immunol. 1999;104(6):1183–8. http://www.ncbi.nlm.nih.gov/pubmed/10588999
250. Brandt EB, Kovacic MB, Lee GB, Gibson AM, Acciani TH, Le Cras TD, et al. Diesel exhaust particle induction of IL-17A contributes to severe asthma. J Allergy Clin Immunol. 2013;132(5):1194–1204 e2. doi:10.1016/j.jaci.2013.06.048. http://www.ncbi.nlm.nih.gov/pubmed/24060272
251. Stevens T, Cho SH, Linak WP, Gilmour MI. Differential potentiation of allergic lung disease in mice exposed to chemically distinct diesel samples. Toxicol Sci. 2009;107(2):522–34. doi:10.1093/toxsci/kfn248. http://www.ncbi.nlm.nih.gov/pubmed/19074765

252. Tanaka M, Aoki Y, Takano H, Fujitani Y, Hirano S, Nakamura R, et al. Effects of exposure to nanoparticle-rich or -depleted diesel exhaust on allergic pathophysiology in the murine lung. J Toxicol Sci. 2013;38(1):35–48. http://www.ncbi.nlm.nih.gov/pubmed/23358138
253. Alberg T, Nilsen A, Hansen JS, Nygaard UC, Lovik M. Nitrogen dioxide: no influence on allergic sensitization in an intranasal mouse model with ovalbumin and diesel exhaust particles. Inhal Toxicol. 2011;23(5):268–76. doi:10.3109/08958378.2011.566898. http://www.ncbi.nlm.nih.gov/pubmed/21506877
254. Jang AS, Choi IS, Takizawa H, Rhim T, Lee JH, Park SW, et al. Additive effect of diesel exhaust particulates and ozone on airway hyperresponsiveness and inflammation in a mouse model of asthma. J Korean Med Sci. 2005;20(5):759–63. doi:10.3346/jkms.2005.20.5.759. http://www.ncbi.nlm.nih.gov/pubmed/16224148
255. Wang T, Moreno-Vinasco L, Huang Y, Lang GD, Linares JD, Goonewardena SN, et al. Murine lung responses to ambient particulate matter: genomic analysis and influence on airway hyperresponsiveness. Environ Health Perspect. 2008;116(11):1500–8. doi:10.1289/ehp.11229. http://www.ncbi.nlm.nih.gov/pubmed/19057703
256. Kleinman MT, Sioutas C, Froines JR, Fanning E, Hamade A, Mendez L, et al. Inhalation of concentrated ambient particulate matter near a heavily trafficked road stimulates antigen-induced airway responses in mice. Inhal Toxicol. 2007;19(Suppl 1):117–26. doi:10.1080/08958370701495345. http://www.ncbi.nlm.nih.gov/pubmed/17886059
257. McGee MA, Kamal AS, McGee JK, Wood CE, Dye JA, Krantz QT, et al. Differential effects of particulate matter upwind and downwind of an urban freeway in an allergic mouse model. Environ Sci Technol. 2015;49(6):3930–9. doi:10.1021/es506048k. http://www.ncbi.nlm.nih.gov/pubmed/25710269
258. Li N, Harkema JR, Lewandowski RP, Wang M, Bramble LA, Gookin GR, et al. Ambient ultrafine particles provide a strong adjuvant effect in the secondary immune response: implication for traffic-related asthma flares. Am J Physiol Lung Cell Mol Physiol. 2010;299(3):L374–83. doi:10.1152/ajplung.00115.2010. http://www.ncbi.nlm.nih.gov/pubmed/20562226
259. Xia M, Viera-Hutchins L, Garcia-Lloret M, Noval Rivas M, Wise P, McGhee SA, et al. Vehicular exhaust particles promote allergic airway inflammation through an aryl hydrocarbon receptor-notch signaling cascade. J Allergy Clin Immunol. 2015;136(2):441–53. doi:10.1016/j.jaci.2015.02.014. http://www.ncbi.nlm.nih.gov/pubmed/25825216
260. Lundborg M, Dahlen SE, Johard U, Gerde P, Jarstrand C, Camner P, et al. Aggregates of ultrafine particles impair phagocytosis of microorganisms by human alveolar macrophages. Environ Res. 2006;100(2):197–204. doi:10.1016/j.envres.2005.08.007. http://www.ncbi.nlm.nih.gov/pubmed/16171796
261. Lee GI, Saravia J, You D, Shrestha B, Jaligama S, Hebert VY, et al. Exposure to combustion generated environmentally persistent free radicals enhances severity of influenza virus infection. Part Fibre Toxicol. 2014;11:57. doi:10.1186/s12989-014-0057-1. http://www.ncbi.nlm.nih.gov/pubmed/25358535
262. Pettitt ME, Lead JR. Minimum physicochemical characterisation requirements for nanomaterial regulation. Environ Int. 2013;52:41–50. doi:10.1016/j.envint.2012.11.009. http://www.ncbi.nlm.nih.gov/pubmed/23280375
263. Laborda F, Bolea E, Cepria G, Gomez MT, Jimenez MS, Perez-Arantegui J, et al. Detection, characterization and quantification of inorganic engineered nanomaterials: A review of techniques and methodological approaches for the analysis of complex samples. Anal Chim Acta. 2016;904:10–32. doi:10.1016/j.aca.2015.11.008. http://www.ncbi.nlm.nih.gov/pubmed/26724760
264. Monopoli MP, Aberg C, Salvati A, Dawson KA. Biomolecular coronas provide the biological identity of nanosized materials. Nat Nanotechnol. 2012;7(12):779–86. doi:10.1038/nnano.2012.207. http://www.ncbi.nlm.nih.gov/pubmed/23212421
265. Whitwell H, Mackay RM, Elgy C, Morgan C, Griffiths M, Clark H, et al. Nanoparticles in the lung and their protein corona: the few proteins that count. Nanotoxicol. 2016;10(9):1385–94. doi:10.1080/17435390.2016.1218080. http://www.ncbi.nlm.nih.gov/pubmed/27465202
266. Djurisic AB, Leung YH, Ng AM, Xu XY, Lee PK, Degger N, et al. Toxicity of metal oxide nanoparticles: mechanisms, characterization, and avoiding experimental artefacts. Small. 2015;11(1):26–44. doi:10.1002/smll.201303947. https://www.ncbi.nlm.nih.gov/pubmed/25303765
267. Hwang BF, Young LH, Tsai CH, Tung KY, Wang PC, Su MW, et al. Fine particle, ozone exposure, and asthma/wheezing: effect modification by glutathione S-transferase P1 polymorphisms. PloS One. 2013;8(1):e52715. doi:10.1371/journal.pone.0052715. http://www.ncbi.nlm.nih.gov/pubmed/23357926
268. Castro-Giner F, Kunzli N, Jacquemin B, Forsberg B, de Cid R, Sunyer J, et al. Traffic-related air pollution, oxidative stress genes, and asthma (ECHRS). Environ Health Perspect. 2009;117(12):1919–24. doi:10.1289/ehp.0900589. http://www.ncbi.nlm.nih.gov/pubmed/20049212
269. Bowatte G, Lodge CJ, Knibbs LD, Lowe AJ, Erbas B, Dennekamp M, et al. Traffic-related air pollution exposure is associated with allergic sensitization, asthma, and poor lung function in middle age. J Allergy Clin Immunol. 2016; doi:10.1016/j.jaci.2016.05.008. http://www.ncbi.nlm.nih.gov/pubmed/27372567
270. Gordon T, Halzack N, Blaustein M, Galdanes K, Chen L. The toxicity of fresh versus aged nanoparticles.Annual Meeting Abstract Supplement, Society of Toxicology. 2008;Abstract No. 1508.
271. Botta D, Schmuck S, Scoville D, White C, Carosino C, Schaupp C, et al. Nanosilver-Induced Lung Inflammation Is Mouse Strain Dependent. Annual Meeting Abstract Supplement, Society of Toxicology. 2013;Abstract No. 1364.
272. Inoue K, Takano H, Yanagisawa R, Koike E, Shimada A. Size effects of latex nanomaterials on lung inflammation in mice. Toxicol Appl Pharmacol. 2009;234(1):68–76. doi:10.1016/j.taap.2008.09.012. http://www.ncbi.nlm.nih.gov/pubmed/18938192
273. Mishra V, Baranwal V, Mishra RK, Sharma S, Paul B, Pandey AC. Titanium dioxide nanoparticles augment allergic airway inflammation and Socs3 expression via NF-kappaB pathway in murine model of asthma. Biomaterials. 2016;92:90–102. doi:10.1016/j.biomaterials.2016.03.016. http://www.ncbi.nlm.nih.gov/pubmed/27057692
274. Su CL, Chen TT, Chang CC, Chuang KJ, Wu CK, Liu WT, et al. Comparative proteomics of inhaled silver nanoparticles in healthy and allergen provoked mice. Int J Nanomedicine. 2013;8:2783–99. doi:10.2147/IJN.S46997. http://www.ncbi.nlm.nih.gov/pubmed/23946650
275. Gustafsson A, Bergstrom U, Agren L, Osterlund L, Sandstrom T, Bucht A. Differential cellular responses in healthy mice and in mice with established airway inflammation when exposed to hematite nanoparticles. Toxicol Appl Pharmacol. 2015;288(1):1–11. doi:10.1016/j.taap.2015.07.001. http://www.ncbi.nlm.nih.gov/pubmed/26163175
276. Park HJ, Sohn JH, Kim YJ, Park YH, Han H, Park KH, et al. Acute exposure to silica nanoparticles aggravate airway inflammation: different effects according to surface characteristics. Experimental & molecular medicine. 2015;47:e173. doi:10.1038/emm.2015.50. http://www.ncbi.nlm.nih.gov/pubmed/26183169
277. Ganguly K, Upadhyay S, Irmler M, Takenaka S, Pukelsheim K, Beckers J, et al. Impaired resolution of inflammatory response in the lungs of JF1/Msf mice following carbon nanoparticle instillation. Respir Res. 2011;12:94. doi:10.1186/1465-9921-12-94. http://www.ncbi.nlm.nih.gov/pubmed/21756372
278. Park EJ, Cho WS, Jeong J, Yi J, Choi K, Park K. Pro-inflammatory and potential allergic responses resulting from B cell activation in mice treated with multi-walled carbon nanotubes by intratracheal instillation. Toxicology. 2009;259(3):113–21. doi:10.1016/j.tox.2009.02.009. http://www.ncbi.nlm.nih.gov/pubmed/19428951
279. Cho WS, Duffin R, Bradley M, Megson IL, Macnee W, Howie SE, et al. NiO and Co3O4 nanoparticles induce lung DTH-like responses and alveolar lipoproteinosis. Eur Respir J. 2012;39(3):546–57. doi:10.1183/09031936.00047111. http://www.ncbi.nlm.nih.gov/pubmed/21828028
280. Cho WS, Duffin R, Poland CA, Duschl A, Oostingh GJ, Macnee W, et al. Differential pro-inflammatory effects of metal oxide nanoparticles and their soluble ions in vitro and in vivo; zinc and copper nanoparticles, but not their ions, recruit eosinophils to the lungs. Nanotoxicology. 2012;6(1):22–35. doi:10.3109/17435390.2011.552810. http://www.ncbi.nlm.nih.gov/pubmed/21332300
281. Lee S, Hwang SH, Jeong J, Han Y, Kim SH, Lee DK, et al. Nickel oxide nanoparticles can recruit eosinophils in the lungs of rats by the direct release of intracellular eotaxin. Part Fibre Toxicol. 2016;13(1):30. doi:10.1186/s12989-016-0142-8. http://www.ncbi.nlm.nih.gov/pubmed/27283431
282. Morimoto Y, Ogami A, Todoroki M, Yamamoto M, Murakami M, Hirohashi M, et al. Expression of inflammation-related cytokines following intratracheal instillation of nickel oxide nanoparticles. Nanotoxicology. 2010;4(2):161–76. doi:10.3109/17435390903518479. http://www.ncbi.nlm.nih.gov/pubmed/20795893
283. Gustafsson A, Lindstedt E, Elfsmark LS, Bucht A. Lung exposure of titanium dioxide nanoparticles induces innate immune activation and long-lasting lymphocyte response in the Dark Agouti rat. J Immunotoxicol. 2011;8(2):111–21. doi:10.3109/1547691X.2010.546382. http://www.ncbi.nlm.nih.gov/pubmed/21309687

Meldrum et al. Particle and Fibre Toxicology (2018) 15:24
https://doi.org/10.1186/s12989-018-0261-5

Particle and Fibre Toxicology

RESEARCH Open Access

Cerium dioxide nanoparticles exacerbate house dust mite induced type II airway inflammation

Kirsty Meldrum[1,3,4], Sarah B. Robertson[2,4], Isabella Römer[1,4], Tim Marczylo[1,4], Lareb S. N. Dean[3,4], Andrew Rogers[3], Timothy W. Gant[1,4], Rachel Smith[1,4], Terry D. Tetley[3,4] and Martin O. Leonard[1,4*]

Abstract

Background: Nanomaterial inhalation represents a potential hazard for respiratory conditions such as asthma. Cerium dioxide nanoparticles (CeO_2NPs) have the ability to modify disease outcome but have not been investigated for their effect on models of asthma and inflammatory lung disease. The aim of this study was to examine the impact of CeO_2NPs in a house dust mite (HDM) induced murine model of asthma.

Results: Repeated intranasal instillation of CeO_2NPs in the presence of HDM caused the induction of a type II inflammatory response, characterised by increased bronchoalveolar lavage eosinophils, mast cells, total plasma IgE and goblet cell metaplasia. This was accompanied by increases in IL-4, CCL11 and MCPT1 gene expression together with increases in the mucin and inflammatory regulators CLCA1 and SLC26A4. CLCA1 and SLC26A4 were also induced by CeO_2NPs + HDM co-exposure in air liquid interface cultures of human primary bronchial epithelial cells. HDM induced airway hyperresponsiveness and airway remodelling in mice were not altered with CeO_2NPs co-exposure. Repeated HMD instillations followed by a single exposure to CeO_2NPs failed to produce changes in type II inflammatory endpoints but did result in alterations in the neutrophil marker CD177. Treatment of mice with CeO_2NPs in the absence of HDM did not have any significant effects. RNA-SEQ was used to explore early effects 24 h after single treatment exposures. Changes in SAA3 expression paralleled increased neutrophil BAL levels, while no changes in eosinophil or lymphocyte levels were observed. HDM resulted in a strong induction of type I interferon and IRF3 dependent gene expression, which was inhibited with CeO_2NPs co-exposure. Changes in the expression of genes including CCL20, CXCL10, NLRC5, IRF7 and CLEC10A suggest regulation of dendritic cells, macrophage functionality and IRF3 modulation as key early events in how CeO_2NPs may guide pulmonary responses to HDM towards type II inflammation.

Conclusions: CeO_2NPs were observed to modulate the murine pulmonary response to house dust mite allergen exposure towards a type II inflammatory environment. As this type of response is present within asthmatic endotypes this finding may have implications for how occupational or incidental exposure to CeO_2NPs should be considered for those susceptible to disease.

Keywords: Asthma, Lung, Nanomaterial, Transcriptomics

* Correspondence: Martin.Leonard@phe.gov.uk
[1]Toxicology Department, Centre for Radiation, Chemical and Environmental Hazards, Public Health England, Harwell Campus, Chilton OX110RQ, UK
[4]The National Institute for Health Research Health Protection Research Unit (NIHR HPRU), Health Impact of Environmental Hazards at King's College London in partnership with Public Health England (PHE) in collaboration with Imperial College London, London, UK
Full list of author information is available at the end of the article

© The Author(s). 2018 **Open Access** This article is distributed under the terms of the Creative Commons Attribution 4.0 International License (http://creativecommons.org/licenses/by/4.0/), which permits unrestricted use, distribution, and reproduction in any medium, provided you give appropriate credit to the original author(s) and the source, provide a link to the Creative Commons license, and indicate if changes were made. The Creative Commons Public Domain Dedication waiver (http://creativecommons.org/publicdomain/zero/1.0/) applies to the data made available in this article, unless otherwise stated.

Background

CeO_2NPs have been used for many applications including precision polishing materials, oxide based fuel cells [1, 2] and as fuel catalysts [3]. Their unique redox properties have also led to investigation of their therapeutic potential for conditions where oxidative stress is indicated [4]. In the main, systemic or oral administration of CeO_2NPs results in protection against injury in models of disease, including amyotrophic lateral sclerosis [5], Alzheimer's disease [6], hepatic ischemic reperfusion injury [7] and drug induced cardiotoxicity [8]. On the other hand, exposure to CeO_2NPs in the absence of underlying disease processes appears to result in toxicological effects, such as disruption of microvascular smooth muscle signalling [9], systemic organ toxicity [10] and potential genotoxicity [11, 12]. These observations of active biological interaction have led to concerns over whether CeO_2NPs may pose a health hazard as a result of incidental or occupational exposure.

The potential effect on pulmonary health is a particular concern for inadvertent nanoparticulate exposure and CeO_2NPs have been investigated in this context. Acute inhalation exposure of rats to CeO_2NPs causes inflammatory effects, including neutrophil accumulation within the lung, an observation not seen when the CeO_2NPs were coated with SiO_2 [13]. Longer inhalation exposure over 1–4 weeks in rats was also found to induce neutrophil accumulation followed by macrophage dominated pulmonary inflammation. Interestingly, particle surface area rather than mass appeared to be a more appropriate metric of dose for predicting the pulmonary response [14]. However, when CeO_2NPs were compared to larger micron sized CeO_2 particles after 28 day inhalation, little quantitative differences in the pulmonary inflammation between materials was observed [15]. Sub-chronic exposures up to 90 days also resulted in inflammatory cell accumulation in the lung and were associated with impaired particle clearance [16]. While it is clear that CeO_2NPs appear to have a detrimental effect on lung health in healthy animals, little information exists on how CeO_2NPs may influence susceptible lung conditions such as COPD and asthma.

Asthma is an obstructive airway condition typified by airway hyperresponsiveness (AHR), bronchospasm and excessive mucus production [17]. Development of the condition as well as exacerbation events involve inflammatory processes, airway remodelling, smooth muscle effects and goblet cell metaplasia [18–21]. Experimental models have been used to assess the impact of nanomaterial exposure as a potential hazard for asthma and allergic airway disease [22]. These typically involve protocols of repeat exposure to allergens such as house dust mite (HDM) and assessment of inflammation, epithelial dysfunction and airway mechanics [23]. As the most common form of asthma is atopic in nature, models have focussed mainly on endpoints aimed at this endotype of disease [24]. These include increased levels of allergen specific IgE, mast cell activation and CD4+ T-cell patterning towards a type II (T_H2) phenotype. These effects are associated with increases in IL-4, IL-5, IL-13 and CCL11 [25]. Type II inflammation involving innate lymphoid type 2 cells can also occur in the absence of allergic sensitisation and has been described as a contributing factor for other endotypes of disease such as intrinsic asthma [25, 26]. For both these conditions, injury to and activation of the airway epithelial cell layer is a prominent feature of type II mediated responses, with epithelial derived factors including CCL20, IL-33, TSLP, IL-25 and GM-CSF all playing a role in driving inflammatory responses. Phenotypical changes in these cells resulting in excessive mucin production, including mucin 5AC (MUC5AC), also support them as key contributors to the asthmatic phenotype [25].

In the absence of any toxicological information on how respiratory exposure to CeO_2NPs may affect asthma, we set out to examine their effects using an HDM allergen exposure murine model of type II inflammatory lung disease [23]. Exposure to CeO_2NPs and HDM was carried out across 9 separate intranasal exposures over 3 weeks and lung tissue was examined for alterations in inflammatory and mucin related changes as well as respiratory function. Alterations were observed with nanoparticle exposure and attempts were made to investigate the mechanisms involved through RNA-SEQ analysis of lung tissue after acute exposure. We also explored the translational nature of our in vivo observations and the role of the airway epithelium in more detail using in vitro exposures of air-liquid interface (ALI) cultures of the human bronchial airway epithelium.

Results

CeO_2NP characterisation and deposition within the lung

The ability of CeO_2NPs to influence pulmonary responses to HDM allergens was investigated through a series of repeat and single exposure intranasal instillation protocols, as described in Fig. 1. Both repeat and single exposures of HDM and CeO_2NPs, either alone or in combination, for up to 3 weeks were used. CeO_2NPs used in this study have been reported by the manufacturer as having an average primary particle size of < 25 nm. TEM analysis of these particles (Fig. 2a) revealed primary particle size in line with this value. Multiple particle shape types were present. Agglomerate size was also determined in the PBS diluent used for exposure protocols and revealed a mean size of 166.5 nm (Fig. 2b). The mode and standard deviation (SD) values indicate a wide agglomerate size distribution. There was a modest increase in mean agglomerate size when HDM was added to the CeO_2NPs. Surface charge was

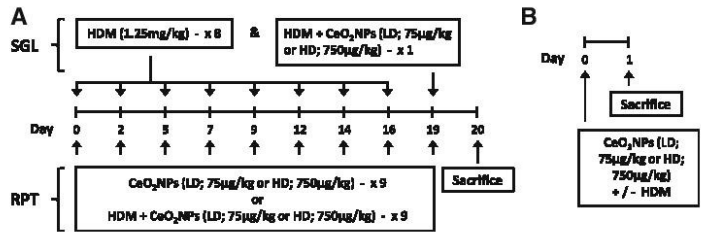
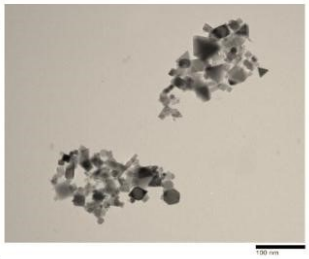


Fig. 1 Experimental protocol for intranasal administration of HDM and nanoparticles. Balb/c mice were exposed through intranasal instillation to cerium dioxide nanoparticles (CeO_2NPs), low dose (LD) (75 μg/kg) or high dose (HD) (750 μg/kg), alone or in combination with house dust mite (HDM) (1.25 mg protein/kg). Three week exposure protocols involved 9 individual instillations on the indicated days (**a**). Specific protocols involved either pre-treatment with HDM for the first 8 instillations followed by a combination of HDM + CeO_2NPs (SGL) or 9 repeat treatments of CeO_2NPs +/− HDM (RPT) as indicated (**a**). Mice were also exposed to a single instillation of CeO_2NPs (LD and HD) +/− HDM (**b**). Sacrifice and collection of tissues was carried out on the days indicated (**a**, **b**)

A



B

Parameter	CeO_2NP	CeO_2NP + HDM
Mean Size (nm)	166.5	263.7
Mode	122.5	193.4
SD	111.7	130.5
ZP (mV)	-8.28 ± 0.37	-10.66 ± 0.57

C

Treatment (24hrs)	Ce µg/g Lung Tissue
CeLD	1.01 ± 0.14
CeHD	1.31 ± 0.08
HDM + CeLD	0.56 ± 0.22
HDM + CeHD	4.38 ± 1.73*

Treatment (3 Weeks)	Ce µg/g Lung Tissue
HDM + CeLD SGL	1.66 ± 0.57
HDM + CeHD SGL	2.78 ± 1.52
CeLD RPT	2.14 ± 0.91
CeHD RPT	24.41 ± 4.85
HDM + CeLD RPT	4.86 ± 2.62
HDM + CeHD RPT	24.39 ± 7.30

D

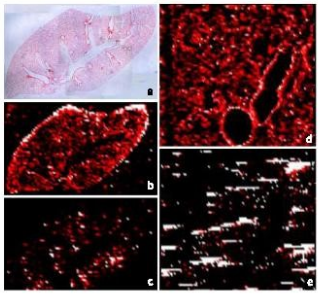


Fig. 2 Nanomaterial characterisation and lung deposition. CeO_2NPs were re-suspended in water, drops dried on TEM grids, and primary size and structure visualised using TEM (**a**). These nanoparticles were also suspended in PBS treatment diluent with and without HDM and agglomerate size was determined using nanoparticle tracking analysis (**b**) with results expressed as mean, mode and standard deviation (SD) of size distribution. Particle charge was also determined as zeta potential (ZP) by dynamic light scattering and expressed in millivolts (mV) mean values ± standard error of the mean (SEM) (**b**). Mice were exposed to CeO_2NPs at either a low dose (CeLD) (75 μg/kg) or high dose (CeHD) (750 μg/kg) with and without HDM (1.25 mg/kg), instillation protocols as described in Fig. 1. After treatment, lung tissue was removed and digested prior to ICP-MS based quantification of elemental ^{140}Ce content. Results are expressed as μg/g lung tissue mean values ± SEM for between 3 and 6 animals (**c**). Statistical significance between all treatments was carried out using one way ANOVA with comparison between CeHD and HDM + CeHD represented as (* $p < 0.05$). Lung tissue from a single exposure to CeHD for 24 h was fixed in 10% formalin and processed for laser ablation ICP-MS detection of ^{63}Cu (b, d) and ^{140}Ce (c, e) tissue distribution (**d**). The elemental distribution in both whole lung (a,b,c) (× 4 magnification) and airway (d,e) (× 100 magnification) was examined. H&E staining was used to visualise general lung structure (a) (**d**)

also assessed for CeO_2NPs alone as a zeta potential of − 8.28 ± 0.37, which increased slightly when HDM was present. Ce elemental content within the lung was assessed using ICP-MS (Fig. 2c). At 24 h, Ce content within the lung after exposure to CeO_2NPs at the lower dose (CeLD) (75 μg/kg) was not significantly different from the high dose (CeHD) (750 μg/kg). HDM (1.25 mg/kg) in combination with CeHD however resulted in a significant increase in Ce levels. At 3 weeks repeat exposure, Ce content within the lung was higher than at 24 h but was not significantly different between CeHD and HDM + CeHD. Ce content for both RPT CeHD treatments were increased above CeLD levels. No Ce was present within the lungs of PBS (CTRL) and HDM exposed mice for either 24 h or 3 week exposure protocols. Spatial distribution of Ce within the lung after instillation was also determined by laser ablation ICP-MS. We found disperse hotspots of cerium throughout the lung with occasional localised patterns around larger airways after 24 h (Fig. 2d) and repeat exposure protocols (data not shown). Spatial distribution was not observed to be different with HDM co-exposure.

Repeat CeO_2NP exposures modify the pulmonary inflammatory response to HDM

BAL cell analysis was carried out to profile the pulmonary inflammatory response to CeO_2NP and HDM after repeat intranasal instillation exposure. Total BAL cell counts were increased with individual CeO_2NP and HDM treatments (Additional file 1: Figure S1A). Co-exposure of CeO_2NPs at the higher particle dose with HDM further increased total BAL cells above HDM induced levels both for SGL and RPT protocols. Differential BAL cell analysis was also assessed (Fig. 3a). HDM exposure caused an increase in neutrophil content, which was not altered by co-exposure with CeHD. It was however reduced by co-exposure to CeLD. Lymphocyte levels in the BAL were also increased by HDM but unmodified by CeO_2NPs co-exposure. The percentage of eosinophils within the BAL was increased by HDM but not to a statistically significant level. This was not modified by CeLD co-exposure, but CeHD co-exposure resulted in a substantial increase in eosinophil levels for the RPT but not SGL exposure protocol (Fig. 3a). CeO_2NP exposure in the absence of HDM did not result in any significant change in any BAL cell type. Mast cell content within the lung was also measured in lung homogenate using the marker MCPT1. Protein levels for this marker were induced by CeLD and HDM alone. HDM levels were further increased by co-exposure with CeHD only with the RPT protocol (Fig. 3b). Total blood plasma immunoglobulin E levels were also examined as an indicator of type II inflammation and revealed increased expression only with HDM + CeHD RPT protocol (Fig. 3c).

The changes in cellular profiles indicated a shift towards type II inflammation. We therefore examined additional markers of this immune profile using analysis of lung tissue gene expression (Fig. 4a). HDM repeat exposure resulted in an increase in IL-4 and CCL11, which was further increased with CeHD RPT co-exposure. IL-5 and IL-13 were also increased with HDM treatment but CeO_2NP exposure had limited effects on these levels. CCL17 and MCPT1 mRNA levels were significantly upregulated only by HDM + CeHD RPT exposure. Protein levels for select type II inflammatory mediators were also examined in BAL fluid (Fig. 4b). Neither HDM nor CeO_2NPs alone resulted in any significant change in protein expression. There was however an increase in CCL11 with HDM + CeHD RPT exposure compared to HDM alone (Fig. 4b). CeO_2NP exposure in the absence of HDM did not result in any significant change in any marker expression. A summary of the impact of different treatment regimens on pulmonary inflammation is provided in Table 1.

Effect of repeat CeO_2NP and HDM exposures on airway remodelling and respiratory function

Goblet cell metaplasia with increased mucin production is one of the hallmark indicators of allergic airway inflammation [27]. PAS histochemical staining can be used to characterise airway structure to determine the extent to which the airway epithelium produces excessive mucin and to determine the extent of goblet cell metaplasia. We identified mucin positive cells in airways between 100 and 250 μm diameter (Fig. 5a; Top panels), and quantified (Fig. 5b). HDM was observed to induce mucin positive cells above CTRL levels, which was further increased by co-exposure to RPT CeHD. MUC5AC is considered a major component of airway mucin and mRNA levels were observed to increase with HDM but not to a significant level (Fig. 5c). HDM + CeHD RPT and SGL treatments caused a significant increase in MUC5AC when compared to HDM alone. CLCA1, which has been closely associated with the regulation of airway mucin [28], was also examined. HDM induced an increase in airway protein levels for CLCA1, which, similar to mucin expression, was exclusively restricted to the airway epithelium of larger airways (Fig. 5a; Bottom panels). CeHD co-exposure with HDM both with RPT and SGL protocol treatments appeared to further increase CLCA1 expression within the airways. Similar effects were observed at the mRNA level for CLCA1, where CeHD co-exposure also significantly increased levels above HDM alone (Fig. 5d). No staining for CLCA1 in lung tissue and very low mRNA levels were observed for CTRL or CeHD RPT alone exposures. SLC26A4 is another bronchial marker protein expressed in asthma and COPD, which has been suggested to

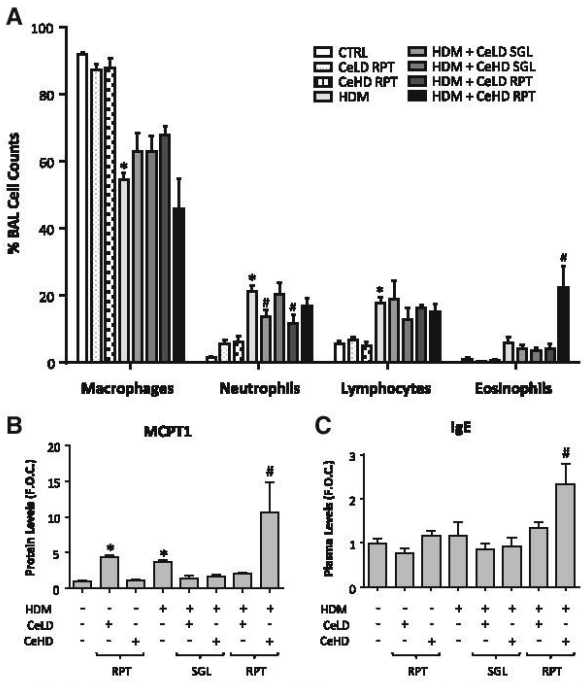


Fig. 3 Inflammatory responses within the lung after repeat CeO_2NPs and HDM exposure. Mice ($n = 5–9$ per treatment group) were exposed to CeO_2NPs at either low dose (CeLD) (75 μg/kg) or high dose (CeHD) (750 μg/kg) with and without HDM (1.25 mg/kg), instillation protocols as described in Fig. 1. After treatment, bronchoalveolar cells were analysed for differential immune cell content. Results are expressed as mean ± SEM % total cells counted (300–500 per animal) (**a**). Lung homogenate was examined for protein levels of the mast cell marker MCPT1 (**b**) and total blood plasma Immunoglobulin E levels (**c**) by ELISA. Results were expressed as mean ± SEM fold over control (F.O.C.) levels. Statistical significance between treatments was carried out by one way ANOVA. Comparisons between particle and HDM treatments alone and control levels are represented as (* $p < 0.05$), while comparisons between particle + HDM combinations and HDM levels are represented as (# $p < 0.05$)

contribute to mucin regulation [29]. Expression levels for SLC26A4 were also found to be significantly upregulated by HDM + CeHD RPT when compared to HDM levels alone (Fig. 5e).

Airway remodelling is a critical component of asthma pathogenesis, underlying airway hyperresponsiveness. Masson's trichrome staining was used to assess peribronchial collagen levels (Fig. 6a; Top panels) and did not reveal any significant difference with treatment. Alpha smooth muscle actin, as a surrogate marker for airway smooth muscle content was also assessed and was demonstrated to have increased levels with HDM RPT treatment, which was not modified by CeHD co-exposure (Fig. 6a; Middle panels). PCNA staining was also examined to assess proliferation, which can accompany airway remodelling (Fig. 6a; Bottom panels). HDM increased PCNA positive cells but CeHD co-exposure did not appear to modify this effect. Respiratory mechanics were also examined as airway responsiveness to increasing concentrations of methacholine. HDM repeat treatment was observed to increase respiratory system resistance and elastance as well as tissue elastance, which was not further modified with co-exposure to CeHD (Fig. 6b-e). A summary of the impact of the different treatment regimens on airway remodelling and respiratory function is provided in Table 1.

Short term effects of airway exposure to CeO_2NP and HDM

To further our understanding of the principal mechanisms involved in the modifying effects of CeO_2NPs in this HDM asthma model, we carried out a series of single instillation exposures for 24 h. Total BAL cell counts were increased with single CeO_2NP and HDM treatments alone (Additional file 1: Figure S1B). Co-exposure of CeO_2NPs at the higher dose with HDM further increased total cells above HDM induced levels. HDM exposure caused an

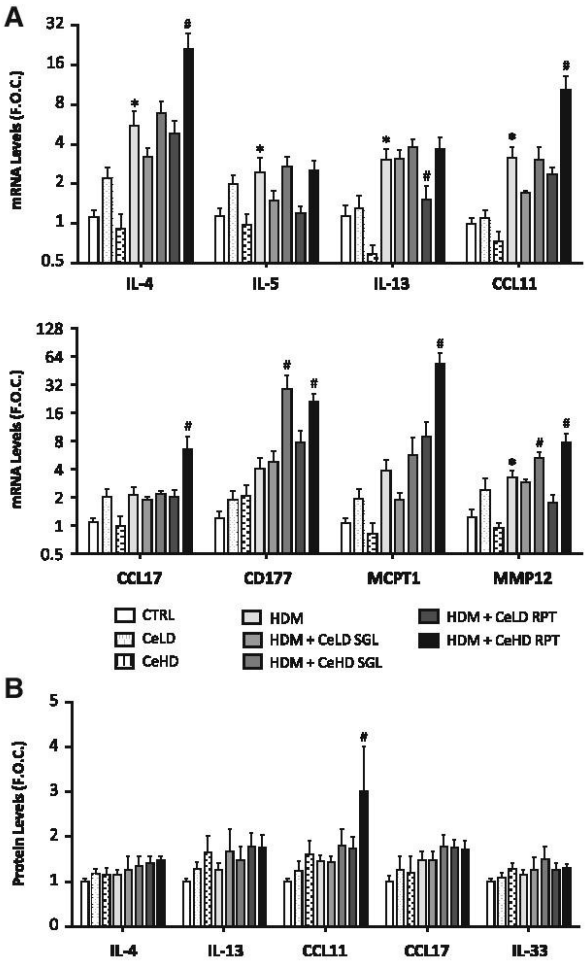


Fig. 4 Inflammatory marker expression within the lung after repeat CeO_2NPs and HDM exposure. Mice ($n = 6–7$ per treatment group) were exposed to CeO_2NPs at either low dose (CeLD) (75 μg/kg) or high dose (CeHD) (750 μg/kg) with and without HDM (1.25 mg/kg), according to instillation protocols described in Fig. 1. After treatment, total lung mRNA was isolated and examined for transcript levels of the indicated inflammatory markers by RT-PCR analysis (**a**). BAL fluid was also examined for protein levels of inflammatory cytokines by ELISA (**b**). Results were expressed as mean ± SEM fold over control (F.O.C.) levels. Statistical significance between treatments was assessed using one way ANOVA. Comparisons between particle and HDM treatments alone and control levels are represented as (* $p < 0.05$), while comparisons between particle + HDM combinations and HDM levels are represented as (# $p < 0.05$)

increase in BAL neutrophil counts, which was further enhanced by both CeLD and CeHD co-exposure (Fig. 7a). CeLD or CeHD alone did not have any effect on BAL cell populations. No effects of any treatment were observed for lymphocyte or eosinophil content within the BAL (Fig. 7a) nor for the mast cell marker MCPT1 (Fig. 7b). Gene expression levels for the neutrophil chemoattractant CXCL5 were increased for HDM and further increased with CeLD co-exposure (Fig. 7b). SLC26A4 mRNA levels were increased with HDM and further increased with CeO_2NP co-exposure. Levels of expression for CCL11 indicated an inhibitory effect for CeO_2NP

Table 1 Summary effect of HDM and CeO_2NP co-exposure on pulmonary inflammation and airway dysfunction

	Bronchoalveolar lavage cells				*Lung inflammatory indicators mRNA (protein)*								*Plasma IgE*	*Airway mucin, structure and mechanics*							
	Total	Neu	Lym	Eos	MCPT1	IL-4	IL-5	IL-13	CCL11	CCL17	CD177	IL33		Mucin	Clca1	Muc5ac	SLC26A4	M.T.	α-sma	PCNA	AHR (Rrs)
CeLD RPT	↑	nc	nc	nc	nc (↑)	nc (nc)	nc	nc (nc)	nc (nc)	nc (nc)	nc	(nc)	nc	nc	nc	nc	nc	nc	nc	nc	nc
CeHD RPT	↑	nc	nc	nc	nc (nc)	nc (nc)	nc	nc (nc)	nc (nc)	nc (nc)	nc	(nc)	nc	nc	nc	nc	nc	nc	nc	nc	nc
HDM	↑	↑	↑	nc	nc (↑)	↑ (nc)	↑	↑ (nc)	↑ (nc)	nc (nc)	nc	(nc)	nc	↑	nc	nc	nc	nc	↑	↑	↑
HDM + CeLD SGL	nc	↓	nc	nc	nc (nc)	nc (nc)	nc	nc (nc)	nc (nc)	nc (nc)	nc	(nc)	nc	nc	nc	nc	nc	nc	nc	nc	nc
HDM + CeHD SGL	↑	nc	nc	nc	nc (nc)	nc (nc)	nc	nc (nc)	nc (nc)	nc (nc)	↑	(nc)	nc	nc	↑	↑	nc	nc	nc	nc	nc
HDM + CeLD RPT	nc	↓	nc	nc	nc (nc)	nc (nc)	nc	↓ (nc)	nc (nc)	nc (nc)	nc	(nc)	nc	nc	nc	nc	nc	nc	nc	nc	nc
HDM + CeHD RPT	↑	nc	nc	↑	↑ (↑)	↑ (nc)	nc	nc (nc)	↑ (↑)	↑ (nc)	↑	(nc)	↑	↑	↑	↑	↑	nc	nc	nc	nc

Pulmonary and systemic responses to intranasal administration of HDM and CeO2NP treatment over 3- week administration regimens is provided as a qualitative metric for cross treatment and protocol comparison purposes. Treatments are indicated within the first column with protocol details as described in Fig. 1. For CeLD RPT, CeHD RPT and HDM treatments, comparison against control animals is represented as an increase (↑), a decrease (↓) or no change (nc) for each measurement. For HDM + CeLD SGL, HDM + CeHD SGL, HDM + CeLD RPT and HDM + CeHD RPT treatments, comparison against HDM treated animals is represented as an increase (↑), a decrease (↓) or no change (nc) for each measurement. Abbreviations used: Neu, neutrophils; Lym, lymphocytes; Eos, eosinophils; M.T., Masson's Trichrome; α-sma, alpha smooth muscle actin; AHR, airway hyperresponsiveness; Rrs, Resistance

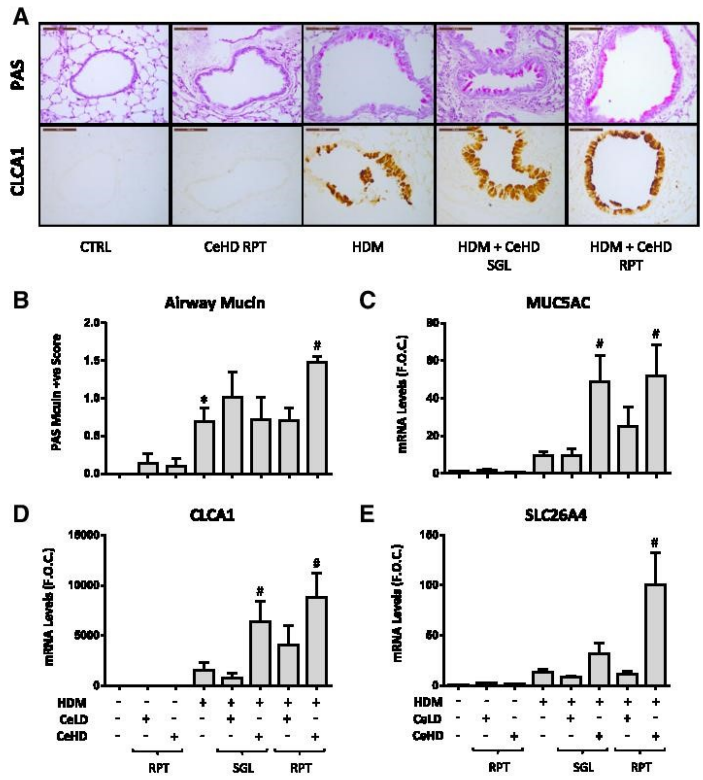


Fig. 5 CeO_2NPs and HDM alter airway mucin and marker expression after repeat exposure. Mice (n = 6–7 per treatment group) were exposed to CeO_2NPs at either low dose (CeLD) (75 μg/kg) or high dose (CeHD) (750 μg/kg) with and without HDM (1.25 mg/kg), according to instillation protocols described in Fig. 1. Lung tissue was fixed and sections processed for PAS staining (**a**; Top panels) or immunohistochemical detection of CLCA1 protein (**a**; Bottom panels). Representative images are displayed with a scale bar of 100 μm. Quantification of airway mucin positive cells was also carried out and displayed as mean ± SEM PAS score (**b**). Total lung mRNA was also examined for mucin related gene expression by RT-PCR analysis (C-E) and results expressed as mean ± SEM fold over control (F.O.C.) levels. Statistical significance between treatments was assessed using one way ANOVA. Comparisons between particle and HDM treatments alone and control levels are represented as (* $p < 0.05$), while comparisons between particle + HDM combinations and HDM levels are represented as (# $p < 0.05$)

co-exposure, while IL-4 and IL-13 levels were not modified. The initiation of type II inflammatory effects and allergic sensitisation in the airways involves the innate immune system including epithelial derived IL-33, TSLP and CCL20, which act to attract and activate dendritic cells. Protein levels of these mediators were examined (Fig. 7c). No statistically different effects were observed for IL-33 and TSLP, although there would appear to be some indication that co-exposure of HDM with CeHD may produce some level of increase. Expression levels however for CCL20 were significantly upregulated for HDM + CeHD as compared to HDM alone (Fig. 7c). IL-1α and IL-4 protein levels in the BAL were also assessed but did not result in any significant alterations (data not shown). PAS staining of lung tissue did not reveal any indication of mucin positive cells within the airways after 24 h exposure (data not shown).

Global gene expression alterations for HDM and HDM + CeHD were also examined using RNA-SEQ (Fig. 8). A heatmap representation of those differentially regulated transcripts is depicted (Fig. 8a) and demonstrates the majority of HDM induced changes to be upregulated. CeHD + HDM also resulted in differential transcript expression independent of HDM regulation. Pathway analysis of those transcripts regulated by HDM alone identified innate immune responses, including granulocyte processes

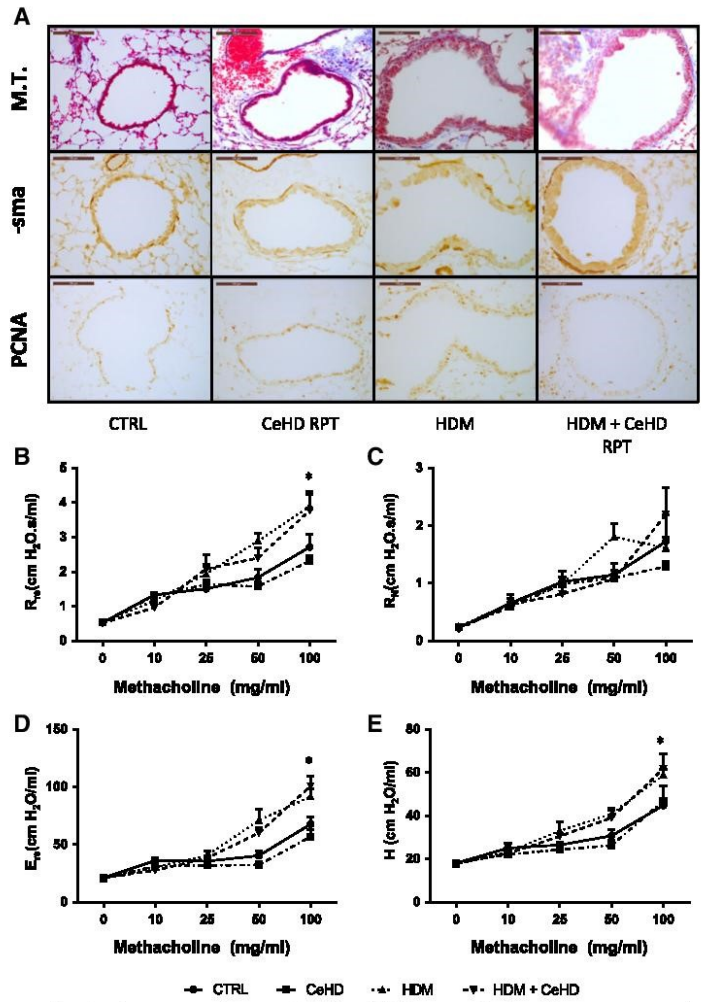


Fig. 6 Airway structure and lung function assessment after repeat CeO_2NPs and HDM exposure. Mice ($n = 6–7$ per treatment group) were exposed to CeO_2NPs at the higher dose (CeHD) (750 μg/kg) with and without HDM (1.25 mg/kg) 9 times over a period of 3 weeks. Lung tissue was fixed and sections processed for Masson's Trichrome (M.T.) staining (**a**; Top panels) and immunohistochemical detection of α-sma (**a**; Middle panels) or PCNA (**a**; Bottom panels). Representative images are displayed with a scale bar of 100 μm. Mice were also assessed for airway hyperresponsiveness to increasing concentrations of inhaled methacholine aerosol (**b**-**d**) using the forced oscillation technique. Respiratory system resistance (Rrs) (**b**), elastance (Ers) (**d**) as well as Newtonian resistance (R_N) (**c**) and tissue elastance (H) (**e**) were calculated within flexivent system software and expressed as mean + SEM cmH_2O. Statistical significance between treatments at each concentration of methacholine was carried out using student t-test (* $p < 0.05$) compared to control group

and interferon signalling, as the most prominent (Fig. 8b). Expression of a selection of genes representative of these pathways and within the top 10 highest regulated genes by HDM, for both HDM and HDM + CeHD are displayed (Fig. 8c). These include CXCL10, IRF7, LY6I and IFIT1, which are upregulated by HDM. Pathway analysis also revealed that IRF3 and IRF7 as the most significant transcriptional regulators responsible for driving HDM induced

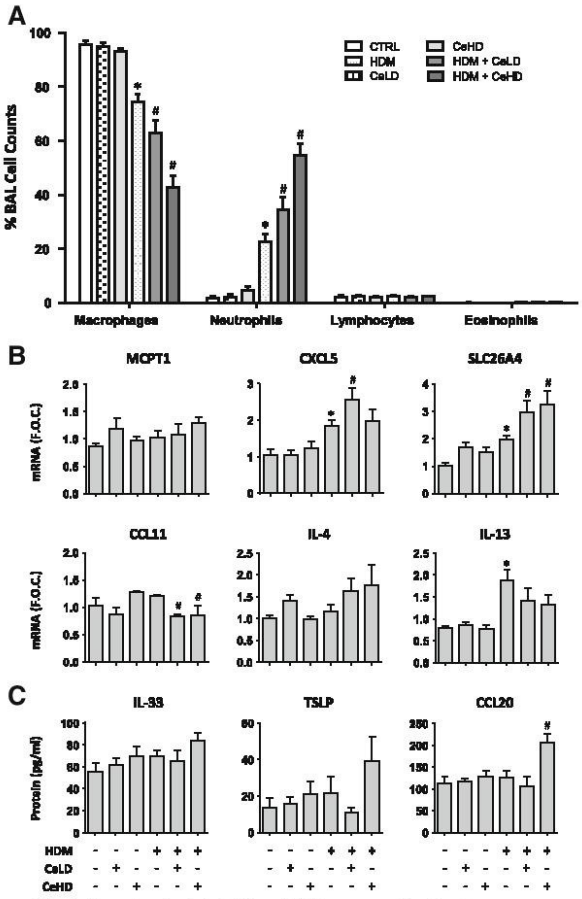


Fig. 7 Inflammatory responses within the lung after single CeO_2NPs and HDM exposure. Mice ($n = 6$ per treatment group) were exposed to CeO_2NPs at either low dose (CeLD) (75 μg/kg) or high dose (CeHD) (750 μg/kg) with and without HDM (1.25 mg/kg) for 24 h. After treatment, bronchoalveolar cells were analysed for differential immune cell content. Results are expressed as mean ± SEM % total cells counted (300–500 per animal) (**a**). After treatment, total lung mRNA was isolated and examined for transcript levels of the indicated inflammatory markers by RT-PCR analysis with results expressed as mean ± SEM fold over control (F.O.C.) levels (**b**). BAL fluid was also examined for protein levels of inflammatory cytokines by ELISA (**c**) and results expressed as mean ± SEM pg/ml. Statistical significance between treatments was assessed using one way ANOVA. Comparisons between particle and HDM treatments alone and control levels are represented as (* $p < 0.05$), while comparisons between particle + HDM combinations and HDM levels are represented as (# $p < 0.05$)

gene expression (data not shown). This level of expression was modified by co-exposure with CeHD to levels significantly lower than HDM alone. Interestingly CeHD was observed to increase expression of SAA3 and CLEC10A above HDM regulated levels. A full list of the most highly regulated transcripts both up and downregulated are displayed in Fig. 8d.

Evidence thus far would indicate a role for the airway epithelium as a central player in the modifying effect of CeO_2NP co-exposure on the HDM response within the lung. To determine whether such observations can be translated to a representative human model, we exposed ALI differentiated cultures of human primary bronchial epithelial cells to HDM and CeO_2NPs. Transcript expression

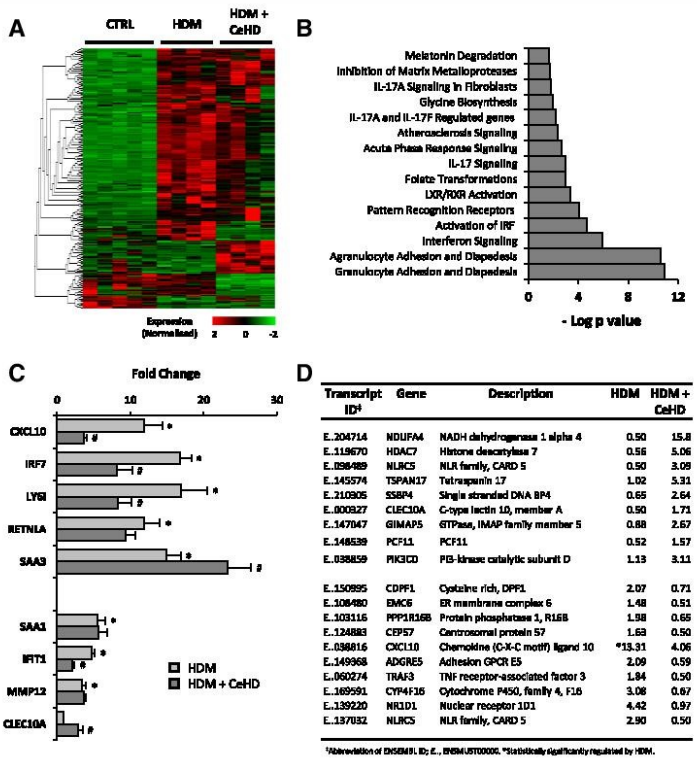


Fig. 8 RNA-Seq analysis after single CeO_2NPs and HDM exposure. Mice ($n = 5$ per treatment group) were exposed to HDM (1.25 mg/kg) alone or in combination with CeO_2NPs at the higher dose (CeHD) (750 μg/kg) for 24 h. Total lung mRNA was isolated and Truseq library prepared prior to 90PE sequencing analysis. RPKM normalised counts were analysed for statistically differentially regulated transcripts between all exposure groups using Qlucore software ($p < 0.005$) using a 2 fold cut-off. Significantly regulated transcripts were visualised as a heatmap of normalised RPKM values (**a**). Regulated transcripts induced by HDM were analysed for pathway association using IPA analysis with results displayed as statistically ranked associations (**b**). Selected transcript expression is shown as mean ± SEM fold over control RPKM values (**c**). Statistical significance between treatments was assessed using one way ANOVA. Comparisons between control (CTRL) and HDM treatments are represented as (* $p < 0.05$), while HDM vs HDM + CeHD are represented as (# $p < 0.05$). The most highly regulated transcripts by HDM + CeHD over HDM levels are displayed (**d**)

levels of epithelial derived inflammatory and mucin related signals were examined and summarised as a heatmap (Additional file 1: Figure S2A). HDM alone produced little effect on gene expression. For the majority of responses to CeO_2NP co-exposure, repeat apical treatments over 1 week produced more significant differences than single exposure for 24 h. Select genes were visualised in greater detail (Additional file 1: Figure S2B). The neutrophil chemoattractant IL-8 displayed significantly higher levels of expression with HDM + ce1340 as compared to HDM alone for 1 week exposure. Similarly, the mucin related genes SLC26A4 and CLCA1 also displayed higher levels of expression with the higher doses of CeO_2NPs at 1 week but not after single exposure. There were no observable alterations in toxicity or cellular dysfunction with any of the treatments, determined as release of LDH and lactate levels into the apical and basolateral compartments (data not shown).

Discussion

Repeat exposure to house dust mite allergens over 3 weeks resulted in pulmonary inflammation, characterised as increases in neutrophils, lymphocytes and mast cells. CeO_2NP co-exposure at the highest dose resulted in eosinophilia, increased plasma IgE as well as enhanced mast cell marker expression. HDM induced increases in the inflammatory cytokines IL-4 and CCL11, which are responsible for B cell class switching to IgE production and

eosinophil recruitment respectively [25], were further increased by CeO_2NP exposure. In addition, goblet cell metaplasia and MUC5AC expression were significantly induced. These observations are consistent with the induction of type II inflammation. The mechanisms involved in driving this type of inflammation could not be specifically attributed, but may involve adaptive immune T_H2 T-cells or non-atopic mechanisms involving ILC2 cells [25, 30]. Lymphocyte levels within the BAL were induced by HDM but remained unaltered by CeO_2NP co-exposure. This does not exclude the possibility of different profiles of lymphocytes with CeO_2NP treatment. Mast cells and basophils can produce mediators and drivers of type II inflammation such as IL-4 [25, 31]. Interestingly, mast cells have been previously observed to control inflammatory processes within the lung in response to CeO_2NP exposure [32] strengthening the possibility that CeO_2NPs exert part of their influence on type II inflammation in our study through mast cell recruitment and activation. CeO_2NP co-exposures were not observed to influence airway hyperresponsiveness over changes induced by HDM alone. As our model design aimed to capture acute responses, it is interesting to speculate whether longer term exposure to CeO_2NPs and HDM together with a persistent type II inflammatory environment would influence airway remodelling and respiratory mechanics.

Pathological alterations in the conducting airway compartment drive asthmatic disease and therefore were the main focus for our study. When compared to inhalation exposure, pulmonary instillation techniques result in greater deposition of material in the bronchial/bronchiolar regions as compared to more distal parts of the lung [33]. Studies have shown that intranasal instillation of a 25 μl volume typically results in approximately 50% deposition of material within the lung [34]. To examine deposition patterns within the lung, we used LA-ICP-MS. 24 h after instillation; cerium was widely distributed throughout the lung with localised hotspots likely representing clearance activity by phagocytes. Given the relatively rapid clearance of particles from the mouse conducting airways [35], cerium levels at times before the 24 h time point would likely reveal widespread conducting airway coverage, before phagocytotic clearance and material redistribution. Interestingly, Ce levels in the presence of HDM were higher than with CeO_2NP treatment alone after 24 h exposure. It could be suggested that the presence of HDM resulted in a slower clearance as a mechanism for increased nanoparticle retention and increased biological impact. However since this effect was not observed with repeat treatments, the contribution to enhanced biological effects is uncertain. The behaviour of CeO_2NPs in the presence of HDM may also be different. CeO_2NPs + HDM produced a larger agglomerate size and altered zeta potential. These were however within the error range and therefore unlikely to explain differences in biological effect. A more likely explanation stems from the ICP-MS measurements. When compared to 24 h single exposure, repeat treatment with CeO_2NPs, either in the presence or absence of HDM resulted, in a substantially greater quantity of Ce within the lung, especially for the CeHD. As no inflammatory responses were observed with repeat exposure to CeO_2NPs in the absence of HDM, we can suggest that a higher dose of CeO_2NPs modifies HDM effects towards type II inflammation. This is also supported by the observations that a single CeO_2NP exposure given after repeated HDM exposure failed to induce type II inflammation, although HDM did appear to prime for some responses including neutrophil effects.

BAL cell analysis 24 h after a single exposure to HDM resulted in significant neutrophil accumulation, which was further enhanced with CeO_2NPs co-exposure. Levels of SAA3, which strongly correlates to neutrophil influx into pulmonary tissue in response to nanoparticle exposure [36], followed the pattern of BAL neutrophil levels with HDM and CeO_2NPs exposures. As serum amyloid A acts as a neutrophil chemoattractant and is released from macrophages [37, 38] we suggest that given the spatial distribution of cerium in lung tissue after 24 h, indicative of phagocytosis, that macrophages are a likely early responder and influence subsequent tissue responses including neutrophil recruitment. CeO_2NPs alone did not induce neutrophil recruitment, with increases in total BAL cells at both 24 h and repeat exposures likely due to increased macrophage content. Neutrophils are active phagocytes and have the potential to ingest particles including nanomaterials to influence their function [39, 40]. They have also been observed to induce type II inflammation through the release of neutrophil extracellular (NET) traps containing genomic DNA, in a mouse model of rhinovirus induced asthma exacerbation [41]. Markers specific to neutrophils include CD177, which when expressed has roles in endothelial migration [42] as well as reactive oxygen species (ROS) production and NET formation [43]. It is interesting to speculate whether the CeO_2NP induced increases in CD177 expression in lung tissue in HDM primed SGL and co-exposed RPT protocols play a role in the induction of type II inflammation, and whether this may involve the regulation of NET formation.

The primary mechanisms by which CeO_2NPs modulate type II inflammation were further investigated. RNA-Seq and pathway analysis of exposure to HDM for 24 h revealed a profile of gene expression within the lung predominantly of granulocyte recruitment to inflamed tissues and fits with our observations of neutrophil accumulation within the lung. Moreover, there was also a significant induction of genes associated with type I interferon

signalling including IRF7, OAS1, IRF9, IFIT3, ISG15 and IFITM3. Prediction software to identify transcriptional regulators responsible for HDM induced gene expression revealed IRF7 and IRF3 as the most significant regulators. Whether IRF3 and the control of interferon type I signalling and related gene expression is involved in the promotion of allergic airway inflammation in response HDM is somewhat unclear. Evidence however, would suggest that gene expression changes in our study support a role for IRF3 and regulation of type I interferon related genes in the early responses to HDM and CeO_2NPs. For example, CeO_2NP co-exposure with HDM inhibited the expression of OAS1G, MX1, MX2, NLRC5, RTP4, LY6I, IRF7, CXCL10, OASL1, OAS3 and CXCL9, all of which were observed as IRF3 dependent in lung DCs [44]. How these early changes may translate to regulation of type II inflammatory effects is unknown but one could consider modulation of dendritic cells and the balance of T-cell differentiation as a component part. Indeed, the involvement of DC recruitment in the responses to HDM and CeO_2NPs co-exposure are indicated from the increased CCL20 protein expression within the lung after 24 h single exposure.

Besides DC and T-cells, other immune cells are likely to play a major role in controlling the type of inflammatory response to CeO_2NPs. CeO_2NP co-exposure with HDM after 24 h resulted in the induction of CLEC10A. This gene is a known marker of M2 macrophage polarisation [45, 46], an important macrophage immunological profile responsible for driving anti-inflammatory/repair processes as well as promoting type II inflammatory tissue responses through the M2a sub-phenotype [40], including allergic airway responses within the asthmatic lung [47]. RETNLA another marker of M2 macrophage polarisation was strongly induced by HDM but unaltered by CeO_2NP co-exposure. Interestingly, CeO_2NPs have been documented to cause a shift in macrophage phenotype in the rat lung towards M2 [48, 49] and this has been suggested as a mechanism through which they promote pro-fibrotic activity within the lung. Polarisation of macrophages towards the M2 phenotype early on in HDM and CeO_2NP co-exposure is therefore likely, but the precise nature and subcategory of M2 profile, as well as the precise role in promoting type II inflammation requires further investigation.

It has been suggested that the unique ability of CeO_2NPs to modify oxidative potential underlies their ability to influence biological processes after cellular exposure [50]. We have previously reported that CeO_2NPs can reduce oxidative stress induced alterations in epithelial injury and transcriptional responses [51]. It has also been reported that the ability of CeO_2NPs to influence DC function towards modulation of T-cells to a T_H2 phenotype was related to their ability to reduce ROS induced inflammasome activation [52]. We investigated whether markers of oxidative stress were altered with HDM and CeO_2NP treatment by PCR analysis of mRNA and found no changes in HMOX1 or NQO1 with any exposure protocol used in this study. It has been demonstrated that HDM repeat pulmonary exposure can produce oxidative damage and DNA double strand breaks in the lungs and is suggested as the driver of asthma pathophysiology [53]. Whether CeO_2NPs are modulating HDM induced oxidative stress and inhibiting Th1 promoting ability of HDM, thus allowing predominant T_H2 responses and type II inflammatory environments to prevail [52] is untested but consistent with observations in our study.

In addition to immune cell activation as a key mediator of CeO_2NPs effects, the epithelial response is also important. HDM has been observed to mediate allergic airway disease through epithelial expression and activation of the PRR TLR4, and downstream DC activation as a consequence of endotoxin present within the HDM [54]. TLR4 mediated airway effects have also been observed to be activated through HDM-induced TLR activation via dual oxidase 2-mediated reactive oxygen species [55] and may represent a target for redox modulating capability of CeO_2NPs. Epithelial specific responses within lung tissue on repeat treatments were observed as increases in airway mucin, MUC5AC and the regulators CLCA1 and SLC26A4. Interestingly these later two proteins have been associated with asthmatic disease and are regulated by type II inflammatory mediators such as IL-13 [28, 56, 57]. The significance of these alterations and the role of the airway epithelium in directing tissue responses were also supported by increased expression of these genes in human bronchial airway epithelial ALI cultures, which also included regulation of CXCL5. Our experimental approach using ALI cultures did not allow for direct aerosol particle exposure but rather application of a nanoparticle suspension to the apical compartment. While we acknowledge differences may arise due to the method of particle application, we believe our observations to be significant in our attempts to develop translational in vitro model testing strategies for pulmonary exposure.

Finally, it is a priority within nanotoxicology research to identify those nanomaterial properties that can be associated with adverse outcome. Toxicological testing to date using models of asthma and AAD, has attempted this but difficulties surrounding diverse model parameters, dosing regimen, exposure types as well as the lack of material characterisation across studies makes extrapolation of reliable hazard information difficult [22]. Apart from the CeO_2NPs used in our current study, testing for nanomaterial effects on HDM induced pulmonary outcomes has only been carried out for carbon nanotubes. MWCNT intranasal

co-administration with HDM produced similar changes in immune cells, select cytokine expression and mucin production when compared to CeO_2NPs used in our study. There did appear to be however greater tissue remodelling and fibrotic changes with MWCNT exposure [58]. Interestingly, the fibrotic effect of MWCNT has also been observed in another model of HDM induced airway inflammation [59]. Model parameter differences preclude direct comparison to CeO_2NP effects in our study but it is interesting to speculate whether properties inherent to MWCNTs such as a fibre-like structure may contribute to fibrotic pathology on pulmonary exposure.

Conclusion

CeO_2NPs were observed to modulate the murine pulmonary response to HDM allergen exposure towards a type II inflammatory environment. This type of response is present within atopic and non-atopic asthmatic endotypes and may have implications for how occupational or incidental exposure to CeO_2NPs should be considered for those susceptible to disease. Through mechanistic investigation we suggest that CeO_2NPs modulate specific interferon signalling events including IRF3 to direct inflammatory responses. Whether such responses are under the control of the redox modifying capabilities of cerium dioxide is unknown but warrants further investigation.

Methods

Nanoparticle preparation and characterisation

CeO_2NPs were obtained from Sigma Aldrich (Dorset, United Kingdom) (cat # 544841). Particles were suspended in distilled H_2O before sonication (QSonica Sonicators, CT, USA) with $4.2x10^5 kJ/m^3$. For transmission electron microscopy (TEM), particles were placed onto Formvar/Carbon 200 Mesh Copper TEM grids and visualized using a JEOL 3000F instrument (JEOL Inc., Tokyo, Japan). CeO_2NPs were also suspended in phosphate buffered saline (PBS) +/− HDM (Greer Laboratories, Lenoir, cat# XPB82D3A25) prior to size and charge characterisation. The particle size distribution was determined by nanoparticle tracking analysis using a NanoSight LM10 instrument (NanoSight, Amesbury, UK). Instrument recordings were at least 60 s and processed using NTA 3.2 Analytical software. Particle charge was determined as zeta potential by dynamic light scattering using a Zetasizer Nano (Malvern, Malvern United Kingdom). Size and zeta potential measurements were carried out for 3 technical replicates across 3 separate samples.

In vivo exposure and tissue collection

Female Balb/c mice between 6 and 8 weeks (Envigo, UK) were anaesthetised with 5% isoflurane in oxygen using a precision vaporizer and intranasally instilled with 25 μl of combinations of CeO_2NPs with and without HDM in different combinations and at different intervals, as described in Fig. 1. Instillation of an equivalent dosing volume of PBS was carried out as the control procedure. After the treatment period, mice were euthanized using an overdose of 0.1 mL sodium pentobarbital (200 μg/mL) by intraperitoneal injection and exsanguination by cardiac puncture. Blood was collected into EDTA coated tubes and plasma was isolated by centrifugation at 1500×g for 15 min at 4 °C. Lung tissue was removed after bronchoalveolar lavage (BAL), washed in sterile PBS and either frozen for later analysis or perfused with 10% formaldehyde solution.

BAL cell analysis

Immediately after sacrifice BAL fluid was collected for assessment of the inflammatory responses in the lungs. Briefly, the trachea was exposed and cannulated allowing the lungs to be lavaged with 500 μl ice-cold sterile PBS. The lungs were gently aspirated and the process repeated a further two times (1.5 ml total). BAL fluid was centrifuged at 1500×g for 10mins at 4 °C and the supernatant from the first lavage was collected for subsequent cytokine enzyme-linked immunosorbent assay (ELISA) analysis. BAL Cells were counted using a haemocytometer and results expressed as total BAL cell counts (Additional file 2). Cells were adjusted to a concentration of 1×10^6 cells/ml, centrifuged using EZ single cytofunnels (Thermo Scientific, cat# 97200125) onto Superfrost™ Plus slides (Menzeil-Gläser Superfrost Plus, Thermo Scientific, cat# 10149870). Cells were then stained for differential immune cell counts using a Wright-Giemsa stain (Kwik Diff, Thermo Scientific, cat# 9990700). Slides were dried overnight before mounting and counting macrophages, lymphocytes, neutrophils and eosinophils across a minimum of 300 cells per sample. Cells were counted for each animal over three different slides.

In vitro culture and exposure

Normal human primary bronchial epithelial cells (HPBEC) from 5 different donors without any reported pathology were obtained from Epithelix Sàrl (Switzerland). Cells were cultured at 37 °C in a 5% CO_2 humidified atmosphere. Cells between passage 2–4 were sub-cultured onto type IV human collagen (Sigma Aldrich, Dorset, UK, Cat# C5533) coated transwell growth supports (Corning, Sigma Aldrich, Dorset, UK, Cat# 3450) to create ALI cultures of epithelial cells. After 4 days of submerged culture in growth media (Epithelix, Cat# EP09AM) to allow cells to reach confluence, apical media was removed from the filter supports. On day 7 after seeding, basolateral media was changed to a differentiation defined media formulation composed of a 50:50 ratio of LHC-9 and DMEM (High Glucose) media, supplemented with bovine serum albumin 1.5 μg/mL, bovine pituitary extract, 180 μg/mL, insulin 0.86 μM,

transferrin 0.125 μM, hydrocortisone 1.38 μM, triiodothyronine 0.01 μM, epinephrine 2.7 μM, epidermal growth factor 0.5 ng/mL, retinoic acid 5×10^{-8} M, penicillin G sulphate 100 U/mL, streptomycin sulphate 100 μg/mL, as described [60]. Media change was carried out every 2–3 days and cells were treated between 7 and 12 days post differentiation. For cell treatment, apical deposition of CeO_2NPs and HDM was carried out in 50 μl of differentiation media.

Elisa

BAL fluid was analysed for cytokine levels of IL-4 (Cat# DY404), IL-13 (Cat# DY413), CCL11 (Cat# DY420), CCL17 (Cat# DY529), IL-33 (Cat# DY3626), TSLP (Cat# DY555) and CCL20 (DY760) using DuoSet kits from R&D systems (Abingdon, UK) according to manufacturer's instructions. For mast cell protease 1 (MCPT1) protein detection, lung tissue was homogenised using MagNa lyser beads (Roche, cat# 03358941001) in HBSS lysis buffer containing 2% Triton-× 100 (Sigma Aldrich, cat# 93426-100ML) and protease inhibitor cocktail (Roche, cat# 05892970001). Protein levels of MCPT1 were detected using ELISA as per manufacturer's instructions (Cat# 88–7503; Invitrogen, VWR Lutterworth, UK). Plasma IgE concentrations were analyzed using a BD OptEIA ELISA kit (cat# 555248; BD Bioscience, Oxford, UK) according to the manufacturer's instructions. Samples were analyzed in duplicate and diluted as appropriate in sample buffer. Absorbance was assessed at 450 nm with background levels at 570 nm using a plate reader (Bio-Tek Synergy HT). Extrapolation of protein levels was carried out from a standard curve of recombinant proteins.

ICP-MS measurements

Lung tissue was microwave digested in 20% nitric acid using an UltraWAVE™ microwave digester. Total Ce content was measured using an iCAP Q ICP-MS (Thermo Fisher Scientific, Hemel Hempstead, UK). The ICP-MS was run in KED mode and the isotopes monitored were ^{140}Ce and ^{63}Cu. Calibration standards (0 – 10 μg/L) were prepared from a Spex CertPrep 50 μg/L stock solution and iridium was used as internal standard. Laser ablation inductively coupled plasma mass spectrometry (LA-ICP-MS) analyses of formalin fixed lung tissue sections was undertaken using a New Wave Research NWR213 laser ablation system (Electro Scientific Industries, Portland, Oregon, USA) linked to the iCAP Q ICP-MS. Laser ablation conditions comprised 5 μm diameter spot size, fluence 10 J/cm^2, 25μms^{-1} scan speed and a repetition rate of 20 Hz. Scan log files of ^{140}Ce and ^{63}Cu track quantities were generated to allow reconstruction of the data into an image using Iolite v3 [61] within Igor Pro 6.36 (Wavemetrics Inc. Oregon, USA).

RNA extraction and PCR analysis

For in vitro gene expression analysis total RNA was isolated using an RNeasy spin column method (Qiagen, Valencia, CA). For in vivo gene expression, lung tissue (post BAL) was initially homogenised using MagNA lyser bead disruption (Roche Diagnostics, West Sussex, UK) prior to RNeasy spin column based RNA isolation. RNA purity was determined using the nanodrop platform (Thermo Scientific) and cDNA was synthesised using a random hexamer based protocol and reverse transcriptase as per manufacturer's instructions (Cat# BIO-27036, Bioline Reagents Ltd., UK). SYBR green based real time PCR (40 cycle) was carried out using the QuantStudio™ 6 Flex Real-Time PCR System. Primers were obtained from the published literature or designed using Primer 3 software and provided by Integrated DNA technologies, UK. Primer sequences are listed in the Additional file 2. Cycle thresholds (Ct values) were quantitatively assessed using the delta-delta Ct method and normalized to B-actin control.

RNA-SEQ and bioinformatic analysis

RNA from lung tissue was analyzed for quality using an Agilent 2100 Bioanalyser and samples with RIN above 8.0 were used for TruSeq™ library preparation (Illumina, San Diego, USA) as previously described [62]. Processing and sequencing was carried out using 90PE sequencing on the Illumina HiSeq™ 2000 platform. Raw sequence data was processed to remove adaptor sequences, contamination and low-quality reads. 20 million clean reads for each sample were brought forward for further processing using CLC Genomics Workbench software (CLCBIO, Aarhus, Denmark). Paired end reads were trimmed to remove remaining adapter and other variable sequences followed by annotation using the GRCm38.p5 mouse reference genome assembly build. For normalization, RPKM (Reads per Kilobase per Million mapped reads) values > 0.5 in at least one treatment condition were selected for differential expression analysis. Further comparative analysis and visualization of differentially regulated transcripts was carried out using Qlucore Omics Explorer software (Qlucore, Lund, Sweden). RNA-SEQ and pathway analysis of differently regulated transcripts was performed using ingenuity pathway analysis (IPA) (Ingenuity Systems, Redwood, CA, USA) and as previously described [62].

Histochemical and immunohistochemical analysis

After tracheal perfusion fixation of the lung in formalin, the left lung was placed into cassettes (Tissue Tek Processing Embedding cassette, Tissue Tek, cat# 4185TT2), dehydrated and embedded in paraffin wax using the Tissue-Tek system (VIP Sakura). Samples were then fixed into moulds, cut into 5 μm serial sections (Accu-Cut SRM, Sakura),

placed onto microscope slides (Menzeil-Gläser Superfrost Plus, Thermo Scientific, Cat# 10149870) before drying overnight at 37 °C. Sections were stained with hematoxylin–eosin (HE) to visualise lung tissue structure and inflammatory infiltrate. Periodic acid–Schiff (PAS) staining was used to determine airway epithelial cell mucin content. Mucin positive cells, identified as pink in colour, were counted in airways of between 100 and 250 μm in diameter. Scoring of airways for mucin positive cells was carried out after counting and expressed as a percentage of total epithelial cells within the airway. A PAS score was then calculated: < 10% = 0 11–20% = 2 21–50% = 3 51–75% = 4 and > 75% = 5. All counts were performed blinded and for 3 airways per individual animal in order to determine a group average. Masson's trichrome staining of lung sections was used to determine collagen content, reflective of airway fibrosis and remodelling. All histochemical stains were performed using a Sakura Tissue Tek Prisma-E2S (Sakura). Immunohistochemical staining was carried out using the VECTASTAIN Elite ABC Kit (Cat#PK-6100, Vector Laboratories) according to the manufacturer's instructions using mouse specific antibodies directed against alpha smooth muscle actin (α-sma) (Cat#ab5694, Abcam, Cambridge, UK), proliferating cell nuclear antigen (PCNA) (Cat#13110, Cell Signalling Technology, Leiden, The Netherlands) and chloride channel accessory 1 (CLCA1) (Cat#ab180851, Abcam, Cambridge, UK), at 1:1000, 1:8000 and 1:250 antibody dilutions respectively. Prior to all staining procedures sections were dewaxed and hydrated. This involved first removing the paraffin wax by clearing 3 times with xylene (5 min each), and then rehydrating through an alcohol series from 100% to distilled water (30 s – 1 min in each concentration). Sections were then mounted and a cover slip applied before being imaged using Leica DM 2000 with images captured using a Leica DFC450C camera (Leica Microsystems Ltd).

Airway mechanics measurements

Mice were anaesthetised by intraperitoneally administration of sodium pentobarbital (90 mg/kg), ensuring the mouse was at surgical levels of anaesthesia throughout the procedure. The mouse was placed under a heat lamp, the trachea exposed and cannulated. Mechanical ventilation was initiated immediately using a computer-controlled piston Flexivent ventilator (Flexivent, Scireq Scientific Respiratory Equipment Inc) system. Prior to airway function measurements, a deep inflation of the lung was performed to recruit closed lung areas and standardize lung volume history. The absence of spontaneous inspiratory efforts was also confirmed using a test pressure volume curve measurement (PVs-V). AHR to inhaled aerosolised methacholine (Acetyl-β-Methylcholine Chloride (cat#A2251-25G, Sigma Aldrich, UK)) (0-100 mg/ml) was then carried out using the forced oscillation technique [63]. All operational scripts for ventilation and force oscillation technique measurements, including data acquisition were handled using Flexiware software (Version 7.6.3).

Statistical analysis

Statistical significance compared to control values was carried out using one way ANOVA and Fisher's LSD Test using Graphpad Prism Software. Results are expressed as mean ± standard error of the mean (SEM) unless otherwise stated. Animal measurements were carried out on a minimum of 6 mice per treatment unless otherwise stated.

Additional files

Additional file 1: Figure S1. Total BAL cell counts after repeat CeO2NPs and HDM exposure. Mice ($n = 5$–9 per treatment group) were exposed to CeO2NPs at either low dose (CeLD) (75 μg/kg) or high dose (CeHD) (750 μg/kg) with and without HDM (1.25 mg/kg) according to instillation protocols as described in Fig. 1. Mice were either exposed 9 times over 3 weeks (A) or a single administration for 24 h (B). After treatment, bronchoalveolar cells were analysed for total immune cell content. Results are expressed as mean ± SEM cells counted per ml of BAL fluid. Statistical significance between treatments was carried out by one way ANOVA. Comparisons between particle and HDM treatments alone over control levels are represented as (* $p < 0.05$), while comparisons between particle + HDM combinations and HDM levels are represented as (# $p < 0.05$). **Figure S2.** Effect of CeO2NPs and HDM exposure on primary human airway epithelial cell gene expression. Human primary bronchial epithelial cells ($n = 5$ different donors) in air-liquid interface culture were apically exposed to HDM (1.1 μg/cm2) alone or in combination with CeO2NPs at either 2.2 ng, 67 ng or 1340 ng per cm2, labelled as Ce2.2, Ce67 or Ce1340 respectively. Cells were treated either once for 24 h or 3 x repeat treatments interspersed over 1 week. mRNA was isolated and examined for transcript levels of inflammatory or mucin related gene expression by RT-PCR analysis with results expressed as mean ± SEM fold over control (F.O.C.) levels (A,B). Results were expressed as a heatmap of normalised values with green down and red upregulated expression, where the intensity of colour is proportional to magnitude of change (A). Selected gene expression was also displayed in more detail (B). Statistical significance between treatments was carried out by one way ANOVA. Comparisons between control (CTRL) and HDM treatments are represented as (* $p < 0.05$), while HDM vs HDM + CeO2NP treatments are represented as (# $p < 0.05$). (PPTX 125 kb)

Additional file 2: Primer Sequences. (DOCX 16 kb)

Abbreviations

α-sma: Alpha smooth muscle actin; AHR: Airway hyperresponsiveness; ALI: Air-liquid interface; BAL: Bronchoalveolar lavage; CeHD: CeO_2NPs at the higher dose (750 μg/kg); CeLD: CeO_2NPs at the lower dose (75 μg/kg); CeO_2NP: Cerium dioxide nanoparticle; CeO_2NPs: Cerium dioxide nanoparticles; CLCA1: Chloride channel accessory 1; Clec10a: C-Type lectin domain containing 10A; CTRL: Control; ELISA: Enzyme-linked immunosorbent assay; HDM: house dust mite; HE: Hematoxylin–eosin; HPBEC: Normal human primary bronchial epithelial cells; Ifit1: Interferon induced protein with tetratricopeptide repeats 1; IL-13: Interleukin-13; IL-25: Interleukin-25; IL-33: Interleukin-33; IL-4: Interleukin-4; IL-5: Interleukin-5; IPA: Ingenuity pathway analysis; Irf7: Interferon Regulatory Factor 7; LA-ICP-MS: Laser ablation inductively coupled plasma mass spectrometry; Ly6i: Lymphocyte antigen 6I; MCPT1: Mast cell protease 1; Muc5AC: Mucin 5AC; PAS: Periodic acid–schiff; PBS: Phosphate buffered saline; Pcna: Proliferating cell nuclear antigen; ROS: Reactive oxygen species; Saa3: Serum Amyloid A3; SD: Standard deviation; SEM: Standard error of the mean; Slc26a4: Solute Carrier Family 26 Member 4; TEM: Transmission electron microscopy; Tslp: Thymic stromal lymphopoietin

Acknowledgements
The authors would like to thank Kevin Whitehill and Chris Ottaway for their assistance with the in vivo studies.

Funding
The in vivo and in vitro aspect of this research was funded through Public Health England Asthma Program and PhD Studentship fund. The in vitro aspect of this research was part funded by the National Institute for Health Research Health Protection Research Unit (NIHR HPRU) in Health Impact of Environmental Hazards at King's College London in partnership with Public Health England. The views expressed are those of the author(s) and not necessarily those of the NHS, the NIHR, the Department of Health or Public Health England.

Availability of data and materials
The datasets used and/or analysed during the current study are available from the corresponding author on reasonable request.

Authors' contributions
KM and MOL designed the experiments and analysed the resulting data. KM, SBR & MOL performed in vivo exposure and tissue collection. KM performed BAL cell, ELISA, PCR and immuno/histochemical analysis. KM & MOL performed AHR measurements and RNA-SEQ analysis. KM, IR & TM performed nanomaterial characterisation and ICP-MS analysis. KM performed in vitro cell experiments. KM, AR & LSND performed transmission electron microscopy. KM, MOL, RS, TWG & TDT all contributed to study design. MOL prepared the manuscript for publication. All authors read, edited and approved the final manuscript.

Ethics approval
All procedures were performed in accordance with the Animals (Scientific Procedures) Act 1986 which complies with EU Directive 2010/63/EU, including review and approval by the local Animal Welfare and Ethical Review Body.

Competing interests
The authors declare that they have no competing interests. The authors alone are responsible for the content and writing of the manuscript.

Publisher's Note

Springer Nature remains neutral with regard to jurisdictional claims in published maps and institutional affiliations.

Author details
[1]Toxicology Department, Centre for Radiation, Chemical and Environmental Hazards, Public Health England, Harwell Campus, Chilton OX110RQ, UK. [2]Environmental Hazards and Emergencies Department, Centre for Radiation, Chemical and Environmental Hazards, Public Health England, Chilton, Harwell Campus, Chilton OX110RQ, UK. [3]Lung Cell Biology, Airways Disease, National Heart & Lung Institute, Imperial College London, London, UK. [4]The National Institute for Health Research Health Protection Research Unit (NIHR HPRU), Health Impact of Environmental Hazards at King's College London in partnership with Public Health England (PHE) in collaboration with Imperial College London, London, UK.

Received: 29 January 2018 Accepted: 15 May 2018
Published online: 23 May 2018

References

1. Qiao ZA, Wu Z, Dai S. Shape-controlled ceria-based nanostructures for catalysis applications. ChemSusChem. 2013;6(10):1821–33. https://doi.org/10.1002/cssc.201300428. https://www.ncbi.nlm.nih.gov/pubmed/24115732
2. Fan L, Wang C, Chen M, Zhu B. Recent development of ceria-based (nano)composite materials for low temperature ceramic fuel cells and electrolyte-free fuel cells. J Power Sources. 2013;234:154–74. https://doi.org/10.1016/j.jpowsour.2013.01.138.
3. Dale JG, Cox SS, Vance ME, Marr LC, Hochella MF Jr. Transformation of cerium oxide nanoparticles from a diesel fuel additive during combustion in a diesel engine. Environ Sci Technol. 2017;51(4):1973–80. https://doi.org/10.1021/acs.est.6b03173. https://www.ncbi.nlm.nih.gov/pubmed/28112928
4. Sims CM, Hanna SK, Heller DA, Horoszko CP, Johnson ME, Montoro Bustos AR, et al. Redox-active nanomaterials for nanomedicine applications. Nano. 2017;9(40):15226–51. https://doi.org/10.1039/c7nr05429g. https://www.ncbi.nlm.nih.gov/pubmed/28991962
5. DeCoteau W, Heckman KL, Estevez AY, Reed KJ, Costanzo W, Sandford D, et al. Cerium oxide nanoparticles with antioxidant properties ameliorate strength and prolong life in mouse model of amyotrophic lateral sclerosis. Nanomedicine. 2016;12(8):2311–20. https://doi.org/10.1016/j.nano.2016.06.009. https://www.ncbi.nlm.nih.gov/pubmed/27389143
6. Kwon HJ, Cha MY, Kim D, Kim DK, Soh M, Shin K, et al. Mitochondria-targeting ceria nanoparticles as antioxidants for Alzheimer's disease. ACS Nano. 2016;10(2):2860–70. https://doi.org/10.1021/acsnano.5b08045. https://www.ncbi.nlm.nih.gov/pubmed/26844592
7. Manne N, Arvapalli R, Graffeo VA, Bandarupalli VVK, Shokuhfar T, Patel S, et al. Prophylactic treatment with cerium oxide nanoparticles attenuate hepatic ischemia reperfusion injury in Sprague Dawley rats. Cell Physiol Biochem. 2017;42(5):1837–46. https://doi.org/10.1159/000479540. https://www.ncbi.nlm.nih.gov/pubmed/28750366
8. El Shaer SS, Salaheldin TA, Saied NM, Abdelazim SM. In vivo ameliorative effect of cerium oxide nanoparticles in isoproterenol-induced cardiac toxicity. Exp Toxicol Pathol. 2017;69(7):435–41. https://doi.org/10.1016/j.etp.2017.03.001. https://www.ncbi.nlm.nih.gov/pubmed/28431810
9. Minarchick VC, Stapleton PA, Fix NR, Leonard SS, Sabolsky EM, Nurkiewicz TR. Intravenous and gastric cerium dioxide nanoparticle exposure disrupts microvascular smooth muscle signaling. Toxicol Sci. 2015;144(1):77–89. https://doi.org/10.1093/toxsci/kfu256. https://www.ncbi.nlm.nih.gov/pubmed/25481005
10. Hardas SS, Butterfield DA, Sultana R, Tseng MT, Dan M, Florence RL, et al. Brain distribution and toxicological evaluation of a systemically delivered engineered nanoscale ceria. Toxicol Sci. 2010;116(2):562–76. https://doi.org/10.1093/toxsci/kfq137. https://www.ncbi.nlm.nih.gov/pubmed/20457660
11. Kumari M, Kumari SI, Kamal SS, Grover P. Genotoxicity assessment of cerium oxide nanoparticles in female Wistar rats after acute oral exposure. Mutat Res Genet Toxicol Environ Mutagen. 2014;775–776:7–19. https://doi.org/10.1016/j.mrgentox.2014.09.009. https://www.ncbi.nlm.nih.gov/pubmed/25435351
12. Kumari M, Kumari SI, Grover P. Genotoxicity analysis of cerium oxide micro and nanoparticles in Wistar rats after 28 days of repeated oral administration. Mutagenesis. 2014;29(6):467–79. https://doi.org/10.1093/mutage/geu038. https://www.ncbi.nlm.nih.gov/pubmed/25209125
13. Demokritou P, Gass S, Pyrgiotakis G, Cohen JM, Goldsmith W, McKinney W, et al. An in vivo and in vitro toxicological characterisation of realistic nanoscale CeO(2) inhalation exposures. Nanotoxicology. 2013;7(8):1338–50. https://doi.org/10.3109/17435390.2012.739665. https://www.ncbi.nlm.nih.gov/pubmed/23061914
14. Keller J, Wohlleben W, Ma-Hock L, Strauss V, Groters S, Kuttler K, et al. Time course of lung retention and toxicity of inhaled particles: short-term exposure to nano-ceria. Arch Toxicol. 2014;88(11):2033–59. https://doi.org/10.1007/s00204-014-1349-9. https://www.ncbi.nlm.nih.gov/pubmed/25273020
15. Gosens I, Mathijssen LE, Bokkers BG, Muijser H, Cassee FR. Comparative hazard identification of nano- and micro-sized cerium oxide particles based on 28-day inhalation studies in rats. Nanotoxicology. 2014;8(6):643–53. https://doi.org/10.3109/17435390.2013.815814. https://www.ncbi.nlm.nih.gov/pubmed/23768316
16. Schwotzer D, Ernst H, Schaudien D, Kock H, Pohlmann G, Dasenbrock C, et al. Effects from a 90-day inhalation toxicity study with cerium oxide and barium sulfate nanoparticles in rats. Part Fibre Toxicol. 2017;14(1):23. https://doi.org/10.1186/s12989-017-0204-6. https://www.ncbi.nlm.nih.gov/pubmed/28701164
17. Murphy DM, O'Byrne PM. Recent advances in the pathophysiology of asthma. Chest. 2010;137(6):1417–26. https://doi.org/10.1378/chest.09-1895. http://www.ncbi.nlm.nih.gov/pubmed/20525652
18. Bergeron C, Tulic MK, Hamid Q. Airway remodelling in asthma: from benchside to clinical practice. Can Respir J. 2010;17(4):e85–93. http://www.ncbi.nlm.nih.gov/pubmed/20808979
19. Folli C, Descalzi D, Scordamaglia F, Riccio AM, Gamalero C, Canonica GW. New insights into airway remodelling in asthma and its possible modulation. Curr Opin Allergy Clin Immunol. 2008;8(5):367–75. https://doi.org/10.1097/ACI.0b013e32830a7086. http://www.ncbi.nlm.nih.gov/pubmed/18769186
20. Walters EH, Soltani A, Reid DW, Ward C. Vascular remodelling in asthma. Curr Opin Allergy Clin Immunol. 2008;8(1):39–43. https://doi.org/10.1097/ACI.0b013e3282f42696. http://www.ncbi.nlm.nih.gov/pubmed/18188016
21. Bara I, Ozier A, Tunon de Lara JM, Marthan R, Berger P. Pathophysiology of bronchial smooth muscle remodelling in asthma. The European respiratory journal : official journal of the European Society for Clinical Respiratory.

Physiology. 2010;36(5):1174–84. https://doi.org/10.1183/09031936.00019810. http://www.ncbi.nlm.nih.gov/pubmed/21037369
22. Meldrum K, Guo C, Marczylo EL, Gant TW, Smith R, Leonard MO. Mechanistic insight into the impact of nanomaterials on asthma and allergic airway disease. Part Fibre Toxicol. 2017;14(1):45. https://doi.org/10.1186/s12989-017-0228-y. https://www.ncbi.nlm.nih.gov/pubmed/29157272
23. Gregory LG, Causton B, Murdoch JR, Mathie SA, O'Donnell V, Thomas CP, et al. Inhaled house dust mite induces pulmonary T helper 2 cytokine production. Clin Exp Allergy. 2009;39(10):1597–610. https://doi.org/10.1111/j.1365-2222.2009.03302.x. https://www.ncbi.nlm.nih.gov/pubmed/19545261
24. Lockey RF. Asthma phenotypes: an approach to the diagnosis and treatment of asthma. J Allergy Clin Immunol Pract. 2014;2(6):682–5. https://doi.org/10.1016/j.jaip.2014.09.008. http://www.ncbi.nlm.nih.gov/pubmed/25439357
25. Lambrecht BN, Hammad H. The immunology of asthma. Nat Immunol. 2015;16(1):45–56. https://doi.org/10.1038/ni.3049. https://www.ncbi.nlm.nih.gov/pubmed/25521684
26. Porter PC, Lim DJ, Maskatia ZK, Mak G, Tsai CL, Citardi MJ, et al. Airway surface mycosis in chronic TH2-associated airway disease. J Allergy Clin Immunol. 2014;134(2):325–31. https://doi.org/10.1016/j.jaci.2014.04.028. http://www.ncbi.nlm.nih.gov/pubmed/24928648
27. Lloyd CM, Hessel EM. Functions of T cells in asthma: more than just T(H)2 cells. Nat Rev Immunol. 2010;10(12):838–48. https://doi.org/10.1038/nri2870. https://www.ncbi.nlm.nih.gov/pubmed/21060320
28. Brett TJ. CLCA1 and TMEM16A: the link towards a potential cure for airway diseases. Expert Rev Respir Med. 2015;9(5):503–6. https://doi.org/10.1586/17476348.2015.1081064. https://www.ncbi.nlm.nih.gov/pubmed/26296094
29. Nofziger C, Dossena S, Suzuki S, Izuhara K, Paulmichl M. Pendrin function in airway epithelia. Cell Physiol Biochem. 2011;28(3):571–8. https://doi.org/10.1159/000335115. https://www.ncbi.nlm.nih.gov/pubmed/22116372
30. Fahy JV. Type 2 inflammation in asthma–present in most, absent in many. Nat Rev Immunol. 2015;15(1):57–65. https://doi.org/10.1038/nri3786. https://www.ncbi.nlm.nih.gov/pubmed/25534623
31. Bradding P, Arthur G. Mast cells in asthma–state of the art. Clin Exp Allergy. 2016;46(2):194–263. https://doi.org/10.1111/cea.12675. https://www.ncbi.nlm.nih.gov/pubmed/26567481
32. Wingard CJ, Walters DM, Cathey BL, Hilderbrand SC, Katwa P, Lin S, et al. Mast cells contribute to altered vascular reactivity and ischemia-reperfusion injury following cerium oxide nanoparticle instillation. Nanotoxicology. 2011;5(4):531–45. https://doi.org/10.3109/17435390.2010.530004. https://www.ncbi.nlm.nih.gov/pubmed/21043986
33. Driscoll KE, Costa DL, Hatch G, Henderson R, Oberdorster G, Salem H, et al. Intratracheal instillation as an exposure technique for the evaluation of respiratory tract toxicity: uses and limitations. Toxicol Sci. 2000;55(1):24–35. https://www.ncbi.nlm.nih.gov/pubmed/10788556
34. Southam DS, Dolovich M, O'Byrne PM, Inman MD. Distribution of intranasal instillations in mice: effects of volume, time, body position, and anesthesia. Am J Physiol Lung Cell Mol Physiol. 2002;282(4):L833–9. https://doi.org/10.1152/ajplung.00173.2001. https://www.ncbi.nlm.nih.gov/pubmed/11880310
35. Sorokin SP, Brain JD. Pathways of clearance in mouse lungs exposed to iron oxide aerosols. Anat Rec. 1975;181(3):581–625. https://doi.org/10.1002/ar.1091810304. https://www.ncbi.nlm.nih.gov/pubmed/1122038
36. Saber AT, Lamson JS, Jacobsen NR, Ravn-Haren G, Hougaard KS, Nyendi AN, et al. Particle-induced pulmonary acute phase response correlates with neutrophil influx linking inhaled particles and cardiovascular risk. PLoS One 2013;8 7:e69020; doi: https://doi.org/10.1371/journal.pone.0069020. https://www.ncbi.nlm.nih.gov/pubmed/23894396.
37. Badolato R, Wang JM, Murphy WJ, Lloyd AR, Michiel DF, Bausserman LL, et al. Serum amyloid a is a chemoattractant: induction of migration, adhesion, and tissue infiltration of monocytes and polymorphonuclear leukocytes. J Exp Med. 1994;180(1):203–9. https://www.ncbi.nlm.nih.gov/pubmed/7516407
38. Meek RL, Eriksen N, Benditt EP. Murine serum amyloid A3 is a high density apolipoprotein and is secreted by macrophages. Proc Natl Acad Sci U S A. 1992;89(17):7949–52. https://www.ncbi.nlm.nih.gov/pubmed/1518819
39. Goncalves DM, de Liz R, Girard D. Activation of neutrophils by nanoparticles. ScientificWorldJournal. 2011;11:1877–85. https://doi.org/10.1100/2011/768350. https://www.ncbi.nlm.nih.gov/pubmed/22125444
40. Boraschi D, Italiani P, Palomba R, Decuzzi P, Duschl A, Fadeel B, et al. Nanoparticles and innate immunity: new perspectives on host defence. Semin Immunol. 2017;34:33–51. https://doi.org/10.1016/j.smim.2017.08.013. https://www.ncbi.nlm.nih.gov/pubmed/28869063
41. Toussaint M, Jackson DJ, Swieboda D, Guedan A, Tsourouktsoglou TD, Ching YM, et al. Host DNA released by NETosis promotes rhinovirus-induced type-2 allergic asthma exacerbation. Nat Med. 2017;23(6):681–91. https://doi.org/10.1038/nm.4332. https://www.ncbi.nlm.nih.gov/pubmed/28459437
42. Sachs UJ, Andrei-Selmer CL, Maniar A, Weiss T, Paddock C, Orlova VV, et al. The neutrophil-specific antigen CD177 is a counter-receptor for platelet endothelial cell adhesion molecule-1 (CD31). J Biol Chem. 2007;282(32):23603–12. https://doi.org/10.1074/jbc.M701120200. https://www.ncbi.nlm.nih.gov/pubmed/17580308
43. Zhou G, Yu L, Fang L, Yang W, Yu T, Miao Y, et al. CD177(+) neutrophils as functionally activated neutrophils negatively regulate IBD. Gut. 2017; https://doi.org/10.1136/gutjnl-2016-313535. https://www.ncbi.nlm.nih.gov/pubmed/28468761
44. Janss T, Mesnil C, Pirottin D, Lemaitre P, Marichal T, Bureau F, et al. Interferon response factor-3 promotes the pro-Th2 activity of mouse lung CD11b(+) conventional dendritic cells in response to house dust mite allergens. Eur J Immunol. 2016;46(11):2614–28. https://doi.org/10.1002/eji.201646513. https://www.ncbi.nlm.nih.gov/pubmed/27546168
45. Ohashi K, Parker JL, Ouchi N, Higuchi A, Vita JA, Gokce N, et al. Adiponectin promotes macrophage polarization toward an anti-inflammatory phenotype. J Biol Chem. 2010;285(9):6153–60. https://doi.org/10.1074/jbc.M109.088708. https://www.ncbi.nlm.nih.gov/pubmed/20028977
46. Mathews JA, Kasahara DI, Ribeiro L, Wurmbrand AP, Ninin FM, Shore SA. Gammadelta T cells are required for M2 macrophage polarization and resolution of ozone-induced pulmonary inflammation in mice. PLoS One. 2015;10(7):e0131236. https://doi.org/10.1371/journal.pone.0131236. https://www.ncbi.nlm.nih.gov/pubmed/26135595
47. Winkler C, Witte L, Moraw N, Faulenbach C, Muller M, Holz O, et al. Impact of endobronchial allergen provocation on macrophage phenotype in asthmatics. BMC Immunol. 2014;15:12. https://doi.org/10.1186/1471-2172-15-12. https://www.ncbi.nlm.nih.gov/pubmed/24612750
48. Ma JY, Mercer RR, Barger M, Schwegler-Berry D, Scabilloni J, Ma JK, et al. Induction of pulmonary fibrosis by cerium oxide nanoparticles. Toxicol Appl Pharmacol. 2012;262(3):255–64. https://doi.org/10.1016/j.taap.2012.05.005. https://www.ncbi.nlm.nih.gov/pubmed/22613087
49. Ma JY, Zhao H, Mercer RR, Barger M, Rao M, Meighan T, et al. Cerium oxide nanoparticle-induced pulmonary inflammation and alveolar macrophage functional change in rats. Nanotoxicology. 2011;5(3):312–25. https://doi.org/10.3109/17435390.2010.519835. https://www.ncbi.nlm.nih.gov/pubmed/20925443
50. Casals E, Gusta MF, Piella J, Casals G, Jimenez W, Intrinsic PV. Extrinsic properties affecting innate immune responses to nanoparticles: the case of cerium oxide. Front Immunol. 2017;8:970. https://doi.org/10.3389/fimmu.2017.00970. https://www.ncbi.nlm.nih.gov/pubmed/28855907
51. Guo C, Smith R, Gant TW, Leonard MO. Cerium dioxide nanoparticles protect against oxidative stress induced injury through modulation of TGF-β signalling. Toxicol Res. 2015;4(2):464–75. https://doi.org/10.1039/c4tx00210e.
52. Schanen BC, Das S, Reilly CM, Warren WL, Self WT, Seal S, et al. Immunomodulation and T helper TH(1)/TH(2) response polarization by CeO(2) and TiO(2) nanoparticles. PLoS One. 2013;8(5):e62816. https://doi.org/10.1371/journal.pone.0062816. https://www.ncbi.nlm.nih.gov/pubmed/23667525
53. Chan TK, Loh XY, Peh HY, Tan WN, Tan WS, Li N, et al. House dust mite-induced asthma causes oxidative damage and DNA double-strand breaks in the lungs. J Allergy Clin Immunol. 2016;138(1):84–96 e1. https://doi.org/10.1016/j.jaci.2016.02.017. https://www.ncbi.nlm.nih.gov/pubmed/27157131
54. Hammad H, Chieppa M, Perros F, Willart MA, Germain RN, Lambrecht BN. House dust mite allergen induces asthma via toll-like receptor 4 triggering of airway structural cells. Nat Med. 2009;15(4):410–6. https://doi.org/10.1038/nm.1946. https://www.ncbi.nlm.nih.gov/pubmed/19330007
55. Ryu JH, Yoo JY, Kim MJ, Hwang SG, Ahn KC, Ryu JC, et al. Distinct TLR-mediated pathways regulate house dust mite-induced allergic disease in the upper and lower airways. J Allergy Clin Immunol. 2013;131(2):549–61. https://doi.org/10.1016/j.jaci.2012.07.050. https://www.ncbi.nlm.nih.gov/pubmed/23036747
56. Nakagami Y, Favoreto S Jr, Zhen G, Park SW, Nguyenvu LT, Kuperman DA, et al. The epithelial anion transporter pendrin is induced by allergy and rhinovirus infection, regulates airway surface liquid, and increases airway reactivity and inflammation in an asthma model. J Immunol. 2008;181(3):2203–10. https://www.ncbi.nlm.nih.gov/pubmed/18641360
57. Nakao I, Kanaji S, Ohta S, Matsushita H, Arima K, Yuyama N, et al. Identification of pendrin as a common mediator for mucus production in bronchial asthma and chronic obstructive pulmonary disease. J Immunol. 2008;180(9):6262–9. https://www.ncbi.nlm.nih.gov/pubmed/18424749

58. Ronzani C, Casset A, Pons F. Exposure to multi-walled carbon nanotubes results in aggravation of airway inflammation and remodeling and in increased production of epithelium-derived innate cytokines in a mouse model of asthma. Arch Toxicol. 2014;88(2):489–99. https://doi.org/10.1007/s00204-013-1116-3. https://www.ncbi.nlm.nih.gov/pubmed/23948970
59. Shipkowski KA, Taylor AJ, Thompson EA, Glista-Baker EE, Sayers BC, Messenger ZJ, et al. An Allergic Lung Microenvironment Suppresses Carbon Nanotube-Induced Inflammasome Activation via STAT6-Dependent Inhibition of Caspase-1. PLoS One. 2015;10(6):e0128888. https://doi.org/10.1371/journal.pone.0128888. https://www.ncbi.nlm.nih.gov/pubmed/26091108
60. Gray TE, Guzman K, Davis CW, Abdullah LH, Nettesheim P. Mucociliary differentiation of serially passaged normal human tracheobronchial epithelial cells. Am J Respir Cell Mol Biol. 1996;14(1):104–12. https://doi.org/10.1165/ajrcmb.14.1.8534481. https://www.ncbi.nlm.nih.gov/pubmed/8534481
61. Paton C, Hellstrom J, Paul B, Woodhead J, Hergt J. Iolite: freeware for the visualisation and processing of mass spectrometric data. J Anal At Spectrom. 2011;26(12):2508–18. https://doi.org/10.1039/C1JA10172B. https://doi.org/10.1039/C1JA10172B
62. Meldrum K, Gant TW, Macchiarulo S, Leonard MO. Bronchial epithelial innate and adaptive immunity signals are induced by polycyclic aromatic hydrocarbons. Toxicol Res. 2016;5(3):816–27.
63. McGovern TK, Robichaud A, Fereydoonzad L, Schuessler TF, Martin JG. Evaluation of respiratory system mechanics in mice using the forced oscillation technique. J Vis Exp. 2013;75:e50172. https://doi.org/10.3791/50172. https://www.ncbi.nlm.nih.gov/pubmed/23711876

Ready to submit your research? Choose BMC and benefit from:

- fast, convenient online submission
- thorough peer review by experienced researchers in your field
- rapid publication on acceptance
- support for research data, including large and complex data types
- gold Open Access which fosters wider collaboration and increased citations
- maximum visibility for your research: over 100M website views per year

At BMC, research is always in progress.

Learn more biomedcentral.com/submissions

BMC